

MULTILAYER NETWORK RELATIONSHIPS AND CULTURE CONTACT IN
MISSISSIPPIAN WEST-CENTRAL ILLINOIS, A.D. 1200 - 1450

By

Andrew James Upton

A DISSERTATION

Submitted to
Michigan State University
in partial fulfillment of the requirements
for the degree of

Anthropology—Doctor of Philosophy

2019

ABSTRACT

MULTILAYER NETWORK RELATIONSHIPS AND CULTURE CONTACT IN MISSISSIPPIAN WEST-CENTRAL ILLINOIS, A.D. 1200 - 1450

By

Andrew James Upton

This dissertation explores the impact of migration on structure and change in human social networks. Prior scholarship on intercultural contacts emphasizes interaction spheres, hybridization, technological transfer, or models of exchange as indicators for constructing borders and defining societal membership. The current study assesses how network relationships among complex and smaller-scale societies structured, and were restructured by, migration. In particular, I address the role of ceramic industry in the transformation of communal-scale interaction and identification networks through culture contact across the middle to late Mississippian transition in the Late Prehistoric central Illinois River valley (ca. 1200 – 1450 A.D.).

In this study, I draw on a body of contemporary social theory focused on parsing social structure across multiple types of interrelationships to investigate how both indigenous societies and migrant peoples approach intercultural social and economic relations. This theoretical framework posits that specific types of relationships act as sensitive features in explanations of group contact, continuity, or change, but that understanding of the entire social system is only approachable through analysis of how individual network layers influence and co-construct each other. Building on a recent formalism, I refer to the superpositioning of individual network layers as a multilayer social network. Through multilayer network analysis, expectations are offered that seek to characterize communal behavioral strategies in the negotiation of a multicultural

social and economic environment following cultural contact. This dissertation thus offers theoretical and methodological means to investigate social settings in which disparate material culture traditions coexist or intermix in time and space through the comparative modeling of various networks of relationships that connect individuals and communities.

Ceramic industry is parsed into three relational dimensions in this study: A model for assessing social interaction via the cultural transmission of ceramic artifact attributes is applied to a database representing technological characterizations of over 1,300 vessels. Networks of social identification are modeled from a database of stylistic designs incised or trailed onto the outflaring rim of over 490 plates primarily used in the serving of food. Networks of economic interactions related to ceramic industry are modeled through the compositional analysis of over 580 ceramic vessels.

Based on a comparative analysis of the structure of multiple network layers, I hypothesize that Oneota in-migration into the Mississippian central Illinois River valley resulted in a period of accommodative intercultural communal coexistence at the macro-regional scale. In social settings following culture contact characterized by accommodative coexistence, relational transaction costs are relatively moderate to low but heterogeneous or exclusive categorical identities delimit the extent of collective action or social movements. A breakdown of economic relationships and reduction in the social scale of shared categorical identities among communities are argued to be clear inflection points in delimiting social transformations to sub-groups of relational networks that did share common categorical identities, identities that may have cross-cut cultural boundaries.

Copyright by
ANDREW JAMES UPTON
2019

For Sarah and my Mom and Dad;
To Grandma and Papa

ACKNOWLEDGEMENTS

This study, I hope, does justice to all those mentors, colleagues, peers, family, and friends who have contributed to my intellectual development and fanned my curiosity and skepticism over the course of my academic career. I am deeply grateful to all of you. I would be remiss to not acknowledge the following individuals and organizations in particular.

First and foremost, I would like to thank my dissertation committee: Drs. Jodie O’Gorman, William Lovis, Lynne Goldstein, Michael Conner, and Susan Sleeper-Smith as well as my outside reader Dr. Matthew Peeples. Each of you have encouraged me to challenge my instincts, to think in a rigorous and skeptical way, and to broaden my theoretical and methodological perspectives. I owe an immense debt of gratitude to my advisor, Dr. Jodie O’Gorman for her unwavering support and her many contributions to my personal and professional development. Dr. Lovis, thank you for developing and reinforcing a scientific mindset in me and for opening the world of statistical analysis to me, for that I will be forever grateful. Dr. Goldstein, thank you for grounding me and for being an inspiring role model. Dr. Conner, thank you for your support and mentoring, and thanks to you and Katie for providing housing for me during my time at Dickson Mounds in Havana – I will remember that time fondly. Dr. Peeples, thank you for paving the way for this study, for reviewing the mountain of code I produced for it, and for being such a positive source of support – I truly could not have made it this far without him.

My dissertation research was funded in part by a National Science Foundation Doctoral Dissertation Improvement Grant (1745150), a Wenner-Foundation Dissertation Fieldwork Grant (Gr. 9479), an individual grant from the Ruth Landes Memorial Research Fund, a program of the

Reed Foundation, the R. Bruce McMillan Museum Internship with the Illinois State Museum at Dickson Mounds, the Graduate School, College of Social Science, and Department of Anthropology at Michigan State University, and the Field Museum of Natural History's Elemental Analysis Facility National Science Foundation subsidy program. Many thanks to the Western Illinois Archaeological Research Center, Western Illinois University, and the Upper Mississippi Valley Archaeological Research Foundation for gracious access to collections used in this research and to Lawrence Conrad for his support of my research and many hours of discussion on Mississippian and Oneota occupations in west-central Illinois. Thanks to the Consortium for Archaeological Research for access to collections at Michigan State University. Thanks to Tom Emerson, Duane Esarey, Kjersti Emerson, Alexy Zelin, and Laura Kozuch for access to reports, photographs, and collections at the Illinois State Archaeological Survey. I owe many thanks to Dee Ann Watt, Alan Harn, Kelvin Sampson, and Drs. Michael Wiant and Bonnie Styles, for facilitating access to materials at the Illinois State Museum system and for assisting with my many destructive and other analysis requests. Many thanks to Dr. Jeremy Wilson and John Flood for their support and for providing access to materials at Indiana University Purdue University Indianapolis.

Drs. Laure Dussubieux and Mark Golitko provided invaluable support in the collection of LA-ICP-MS data at the Field Museum and gave me a crash course on analytical chemistry and the analysis of compositional data. I am grateful to Matthew Peeples, Gianmarco Alberti, Hadley Wickham, Manlio De Domenico, Gábor Csárdi, and Matteo Magnani for creating the open-source programming tools that made this dissertation research possible.

I would like to acknowledge supervisors from the various careers paths I have taken while working on this study. Each of you not only contributed to my personal and professional

development but also supported my research needs in countless ways: James Mack, Yonatan Eyal, Mary Horan, Justine Clark-Lomax, James Robertson, Erik Kreusch, Dan Reeves, Patricia Likins, and Brad Peters.

Moral and academic support was instrumental from my peers at MSU: Frank and Nicole Raslich, Sylvia Galaty, Stefan Johnson, Nikki Klarmann, Jessica Yann, Sean Dunham, Kate Frederick; and from friends beyond Alex Ferko, David Armacost, Chris Robinson, Evan Jones, Emily Repp, Evonne Swallie, Courtney Mills, Rachael Crane, Tommy Hemmer, and scores of others. I offer sincerest apologies to any I have omitted.

My parents, Bill and Joanne Upton, gave me the freedom to follow my dreams and to find my passions – I cannot express in words how grateful I am for that and for their undying love. Thanks to my brother Ian, sister Abby, and brother in-law Scott for everything they have done for me over the years. Many thanks to my grandparents, Jack Upton, Mary Lou Upton, Jean Streb and William Streb for your sacrifices, practical life advice, and support. I wish you all could have been here to see the completion of this work. And thanks to my extended family – to Bill and Annie Jones, the Lightles and the Santalucias, the Snyders (and Tyler), the Dieckmanns, the Permes, the Brezgers, and Jenny and Andy Kranz and Jessica, Jared and Megan Van Vooren. Nothing means more to me than having the love and support of my family.

Finally, and most of all, I am thankful to Sarah for being the love of my life, an ever-present source of inspiration, and for reminding me every day that there are more important things than the Late Prehistoric central Illinois River valley.

TABLE OF CONTENTS

CHAPTER 1	INTRODUCTION	1
1.1	Brief Introduction to the Research Problem.....	1
1.2	Multicultural Social Interrelationships and Multilayer Social Network Analysis ..	2
1.3	The Case Study	5
1.4	Dissertation Organization.....	7
CHAPTER 2	MULTILAYER SOCIAL NETWORKS AND INTERCULTURAL COMMUNAL COEXISTENCE	10
2.1	Introduction	10
2.2	Evolving Perspectives on Social Interaction and Identity Formation.....	10
2.3	Social Systems as Multilayered, Relational Networks	19
2.3.1	Theory in Networks	20
2.3.2	Multilayer Ties in Anthropological Archaeology.....	28
2.3.3	Social Transformation through Relational and Categorical Identification	33
2.4	Intercultural Communal Coexistence – Linking Culture Contact, Multilayer Social Network Analysis, and Archaeological Evidence.....	36
2.4.1	Material Culture Correlates to Intercultural Communal Coexistence	41
CHAPTER 3	REGIONAL AND CULTURAL BACKGROUND: LATE PREHISTORY IN THE CENTRAL ILLINOIS RIVER VALLEY	47
3.1	Introduction	47
3.2	Geographic Setting	48
3.3	The Mississippian Tradition.....	49
3.4	The Upper Mississippian Tradition and the Oneota	54
3.5	The Mississippian Period central Illinois River valley	56
3.6	Eveland Phase (A.D. 1100-1175)	61
3.7	Orendorf Phase (A.D. 1200-1250).....	64
3.8	Larson Phase (A.D. 1250-1300).....	67
3.9	Crabbe Phase (A.D. 1300-1425)	72
3.10	The Bold Counselor Phase Oneota	79
3.11	Regional Abandonment.....	84
CHAPTER 4	METHODOLOGICAL CONSIDERATIONS	86
4.1	Introduction	86
4.2	Data Collection Methods.....	87
4.2.1	Ceramic Vessel Technological Data	87
4.2.2	Ceramic Vessel Stylistic Data	89
4.3	Compositional Analysis of Archaeological Ceramics	91
4.3.1	Compositional Analysis in Archaeology.....	92
4.3.2	Clay: Geological, Chemical and Mineralogical Considerations.....	95
4.3.3	Technological Choice and Pottery Production	97
4.3.4	Use-Wear Effects on Sherd Chemistry	99

4.3.5	Diagenesis and Sherd Chemistry	99
4.4	Compositional Methods: pXRF, XRD, and LA-ICP-MS	100
4.4.1	Portable X-Ray Fluorescence	101
4.4.2	X-Ray Diffraction	101
4.4.3	Laser Ablation-Inductively Coupled Plasma-Mass Spectrometry.....	103
4.5	Analytical Methods for Monoplex Social Networks	104
4.6	Definitions and Methods for Constructing and Analyzing Multilayer Networks	108
4.6.1	Multilayer Network Analysis Measures.....	110
CHAPTER 5	NETWORKS OF INTERACTION THROUGH CULTURAL TRANSMISSION.....	116
5.1	Introduction	116
5.2	Cultural Transmission Theory, Artifact Variation, and Network Ties	119
5.3	Defining the Sample and Assessing Dependencies	124
5.3.1	Assessing Dependencies.....	130
5.3.2	Identifying Social Information Bearing Artifact Type-Attributes from Cultural Transmission	135
5.4	Methodology: Constructing Social Interaction Networks from Social Information Bearing Artifact Type-Attributes	142
5.5	Evaluating the Results: Statistical Interpretation of Ceramic Industry Social Interaction Network Models.....	156
5.5.1	Statistical Analysis of Pre-Migration Interaction Networks, 1200 – 1300 A.D.....	161
5.5.2	Statistical Analysis of Post-Migration Interaction Networks, 1300 – 1450 A.D.....	174
5.5.3	The Role of Geographic Distance.....	190
5.6	Discussion and Visual Interpretation of Ceramic Industry Social Interaction Network Models	194
5.6.1	Pre-Migration Technological Similarity Networks, 1200 – 1300 A.D.....	197
5.6.2	Post-Migration Technological Similarity Networks, 1300 – 1450 A.D.	207
5.6.3	Technological Similarity Networks Across Time, 1200 – 1450 A.D.....	216
5.7	Conclusion.....	225
CHAPTER 6	CERAMIC STYLE AND NETWORKS OF SOCIAL IDENTIFICATION.....	230
6.1	Introduction	230
6.2	Migration and Social Identification	232
6.3	Oneota Migration into West-Central Illinois.....	236
6.3.1	Plates, Ceramic Design, and Sun Symbolism in the CIRV.....	241
6.4	Methodology.....	251
6.5	Results and Discussion: Social Identification in the Late Prehistoric CIRV	262
6.6	Conclusion.....	273
CHAPTER 7	NETWORKS OF ECONOMIC RELATIONSHIPS: RESULTS OF THE CHEMICAL ANALYSES	275
7.1	Introduction	275

7.2	Ceramic Industry Economic Relationships	276
7.3	Central Illinois River valley Geology	279
7.4	The Ceramic and Clay Sample	285
7.5	Ceramic Paste and Clay Chemical Characterization Using LA-ICP-MS	287
7.5.1	Controlling for Shell Tempering	290
7.5.2	Statistical Routines in the Analysis of Geochemical Data	292
7.6	Results of the Clay Analyses	304
7.7	Results of the Ceramic Analyses	309
7.7.1	Compositional Group Identification and Assignment	311
7.7.2	Structure within the Core compositional group	319
7.8	Compositional Groups as Economic Social Networks	330
7.9	Ceramic Industry Economic Network Analysis and Discussion	335
7.10	Conclusion	346
CHAPTER 8	TOWARD EXPLAINING SOCIAL INTERRELATIONSHIPS THROUGH CERAMIC INDUSTRY MULTILAYER SOCIAL NETWORKS	349
8.1	Introduction	349
8.2	Culture Contact and Multi-dimensionality in Archaeological Social Networks	349
8.3	Layers of Evidence – Results of the Individual Network Layers	353
8.3.1	Relational Interaction from Cultural Transmission	354
8.3.2	Categorical Identities from Ceramic Design	357
8.3.3	Economic Relationships as Relational Interaction	359
8.4	Building Late Prehistoric CIRV Ceramic Industry Multilayer Networks	361
8.5	Overlap and Influence among Layers and Communities	370
8.5.1	Layer Interactions	370
8.5.2	Community and Layer Influence	370
8.6	Intercultural Communal Coexistence in the Late Prehistoric CIRV	382
8.7	Contributions of this Research	386
8.7.1	Contributions to Archaeology and CIRV Archaeology	388
8.8	Future Directions	390
APPENDICES	393
APPENDIX A	Coding Sheet	394
APPENDIX B	Ceramic Vessel Measurement Data Availability	404
APPENDIX C	All R Code for Statistical Analyses	405
APPENDIX D	LA-ICP-MS Data and Supplementary Statistical Documentation for Group Assignments	572
APPENDIX E	Plate Stylistic Design Group Sketches	581
APPENDIX F	Jar and Plate Profile Sample	625
APPENDIX G	Mineralogical Analysis Results	643
APPENDIX H	Site Identification Codes and Radiocarbon Probabilities	644
REFERENCES	652

LIST OF TABLES

Table 2.1 Matrix of expectations for intercultural communal coexistence strategies	37
Table 5.1 Expectations for Attributes under Global or Local Functional Control, and Serving as Emblematic and Assertive Markers (Eerkens and Bettinger 2008, p. 25)	122
Table 5.2 Expectations for Attributes under Social or Engineering Constraint	123
Table 5.3 Coding Schema (See Appendix A for Full Coding Sheet)	126
Table 5.4 Count of plate sherds from each site for each continuous variable above n crit.....	128
Table 5.5 Count of burial jar sherds from each site for each continuous variable above n crit..	129
Table 5.6 Count of domestic jar sherds from each site for each continuous variable above n crit.....	129
Table 5.7 Pearson correlation coefficient for pairwise complete burial jar metric observations.....	132
Table 5.8 Pearson correlation coefficient for pairwise complete domestic jar metric observations.....	133
Table 5.9 Pearson correlation coefficient for pairwise complete plate metric observations.....	134
Table 5.10 VOM, AV, and VOV values, scores, and summary data for type attributes	137
Table 5.11 Summation of networks constructed with artifact type-attribute social interaction markers.....	147
Table 5.12 Network Statistics for Ceramic Industry Social Interaction Network Models	189
Table 6.1 Summary of plate sample design techniques by site	253
Table 6.2 Counts of vessels by site and design category; [∨] indicates pre-migration occupation (1200 – 1300 A.D.), [^] indicates post-migration occupation (1300 – 1450 A.D.), ^{<} indicates occupation(s) that span(s) the pre- and post-migration time periods.....	261
Table 6.3 Central Illinois River Valley Social Identification Network Statistics	264
Table 7.1 Distribution of pottery samples by site and vessel type	286
Table 7.2 Elemental summary statistics measured across 131 replicates of New Ohio Red clay	289

Table 7.3 Average chemical concentrations and standard deviations for the two clay groups (ppm).....	308
Table 7.4 Eigen values and percent variance for first 12 principal components on the ceramic data set	313
Table 7.5 Mahalanobis distance based probabilities of group membership in the core and outgroups for the outgroup sherds.....	316
Table 7.6 Mahalanobis distance based probabilities of group membership in the Core A group and Core B and Core C provisional groups	321
Table 7.7 Compositional group assignments by site	329
Table 7.8 Compositional group assignments summarized by site geography and vessel class ..	329
Table 7.9 Central Illinois River Valley Ceramic Industry Economic Network Statistics	338
Table 8.1 Matrix of expectations for intercultural communal coexistence strategies	351
Table 8.2 Network properties for individual undirected network layers	369
Table D.1 Component loadings for the first 12 principal components, accounting for 90.4% of the variance in the 44 element data set.....	572
Table D.2 Posterior classification probabilities based on jackknifed Mahalanobis for Core A1 and Core A2 Sub-Groups	573
Table D.3 Mean and standard deviation values for the ceramic geochemical compositional groups.....	578
Table G.1 X-ray Diffraction Results.....	643
Table H.1 Site IAS and ISM Identification Numbers.....	644
Table H.2 Radiocarbon assay probabilities and results	645

LIST OF FIGURES

Figure 3.1 Lidar map of, and archaeological sites under consideration in the Late Prehistoric central Illinois River valley (circa 1200 – 1450 A.D.)	48
Figure 3.2 Probability distributions of three recalibrated dates for the Eveland site (Bender et al. 1975)	63
Figure 3.3 Probability distributions of five recalibrated dates for the Orendorf site (Bender et al. 1975)	65
Figure 3.4 Probability distributions of four recalibrated dates for the Larson site (Bender, et al. 1975)	68
Figure 3.5 Probability distributions of one recalibrated dates for Walsh Site (Wilson, personal communication 2017).....	71
Figure 3.6 Probability distributions of four recalibrated dates for Ten Mile Creek and Star Bridge sites; dates include DirectAMS Codes D-AMS 020156 – D-AMS 020159 respectively	74
Figure 3.7 Probability distributions of four recalibrated dates for Crable and the Oneota occupation of the C.W. Cooper sites	75
Figure 5.1 Mean-standard deviation relationships for type-attribute variables calculated by material culture class with best-fit regression lines. Log base 10 values reported to account for effects related to different measurement scales.....	127
Figure 5.2 QQplot of domestic jar rim angles showing deviation from normality in Eveland and Kingston Lake	131
Figure 5.3 Scatterplot of Burial Jar Height by Burial Jar Orifice Diameter with best-fit regression line and 0.95 confidence interval shading.....	132
Figure 5.4 VOM, AV, and VOV residual scores for all 15 ceramic vessel type attributes measurements	138
Figure 5.5 Ridgeline plot of domestic jar type-attributes likely constrained by social forces, all measurements are in mm aside from rim angle which is in degrees.....	141
Figure 5.6 Ridgeline plot of plate type-attributes likely constrained by social forces, all measurements are in cm aside from flare angle which is in degrees.....	142
Figure 5.7 Adjacency matrix representation of multilayer social media friendship network.....	153

Figure 5.8 Flattened adjacency matrix representation of multilayer social media friendship network	153
Figure 5.9 Example of multilayer network slicing with networks embedded in geographical regions, showing a network of European airports rendered using MuxViz with each layer representing a different airline and edges representing flights between airports (De Domenico, Porter, et al. 2015)	154
Figure 5.10 Network Randomization Results for Jar Pre-Migration Layer. Observed statistic represents red line. Histogram shows distribution of statistic based on network randomization of 5000 random graphs using the Erdős–Rényi random network modeling technique.	162
Figure 5.11 Network Randomization Results for Plate Pre-Migration Layer. Observed statistic represents red line. Histogram shows distribution of statistic based on network randomization of 5000 random graphs using the Erdős–Rényi random network modeling technique.	163
Figure 5.12 Authorities and Hubs in the Jar and Plate Pre-Migration Period Network Layers. Authority and Hub scores are modeled as node size.....	165
Figure 5.13 Degree distribution of Jar and Plate Pre-Migration networks.	166
Figure 5.14 Edge betweenness community detection in the Jar and Plate Pre-Migration Attribute Networks.....	168
Figure 5.15 Network Randomization Results for Multilayer Pre-Migration Network. Observed statistic represents red line. Histogram shows distribution of statistic based on network randomization of 5000 random graphs using the Erdős–Rényi random network modeling technique.....	169
Figure 5.16 Authorities and Hubs in the Multilayer Pre-Migration Period Network. Authority and Hub scores are modeled as node size.....	170
Figure 5.17 Edge betweenness community detection in the Multilayer Pre-Migration Network	171
Figure 5.18 Network Randomization Results for Post-Migration Jar Attribute Network. Observed statistic represents red line. Histogram shows distribution of statistic based on network randomization of 5000 random graphs using the Erdős–Rényi random network modeling technique.....	177
Figure 5.19 Network Randomization Results for Post-Migration Plate Attribute Network. Observed statistic represents red line. Histogram shows distribution of statistic based on network randomization of 5000 random graphs using the Erdős–Rényi random network modeling technique.....	178

Figure 5.20 Authorities and Hubs in the Jar and Plate Post-Migration Period Network Layers. Authority and Hub scores are modeled as node size.	180
Figure 5.21 Edge betweenness community detection in the Jar and Plate Post-Migration Attribute Networks.....	181
Figure 5.22 Degree Distributions of Jar and Plate Post-Migration Networks.....	182
Figure 5.23 Network Randomization Results for Multilayer Post-Migration Network. Observed statistic represents red line. Histogram shows distribution of statistic based on network randomization of 5000 random graphs using the Erdős–Rényi random network modeling technique.....	183
Figure 5.24 Hubs and Authorities in the Post-Migration Multilayer Attribute Network. Hub and Authority score modeled as node size	185
Figure 5.25 Edge Betweenness Community Detection in the Multilayer Post-Migration Attribute Network	186
Figure 5.26 Distributions of Randomly Sampled Linear Models for Strength of Relational Connection as a Function of Geographic Distance in Multilayer jar and plate attribute networks. Dashed red line indicates linear model for observed data.....	191
Figure 5.27 Distributions of Randomly Sampled Linear Models for Strength of Relational Connection as a Function of Geographic Distance in Jar and Plate Attribute Interaction Networks faceted by time phase designation. Dashed red line indicates linear model for observed data.....	192
Figure 5.28 Yifan Hu multilevel network graph layout of domestic jar technological similarity network for the Pre-Migration Time Period (1200-1300 A.D.); edges are colored by weight; nodes are colored and sized by closeness centrality.....	198
Figure 5.29 Geographic network graph layout of domestic jar technological similarity network for the Pre-Migration Time Period (1200-1300 A.D.); edges are colored by weight; nodes are colored and sized by closeness centrality	199
Figure 5.30 Yifan Hu multilevel network graph layout of plate technological similarity network for the Pre-Migration Time Period (1200-1300 A.D.); edges are colored by weight; nodes are colored and sized by weighted degree	200
Figure 5.31 Geographic network graph layout of plate technological similarity network for the Pre-Migration Time Period (1200-1300 A.D.); edges are colored by weight; nodes are colored and sized by closeness centrality	201
Figure 5.32 Yifan Hu multilevel network graph layout of domestic jar and plate technological similarity flattened multilayer network for the Pre-Migration Time Period (1200-1300 A.D.); edges are colored by weight; nodes are colored and sized by weighted degree.....	202

Figure 5.33 Geographic network graph layout of domestic jar and plate technological similarity flattened multilayer network for the Pre-Migration Time Period (1200-1300 A.D.); edges are colored by weight; nodes are colored and sized by weighted degree	203
Figure 5.34 Geographic network graph layout of domestic jar (left) and plate (right) technological similarity sliced multilayer network for the Pre-Migration Time Period (1200-1300 A.D.); edges are colored by weight; nodes are colored and sized by closeness centrality.....	205
Figure 5.35 Yifan Hu multilevel network graph layout of domestic jar technological similarity network for the Post-Migration Time Period (1300-1450 A.D.); edges are colored by weight; nodes are colored and sized by weighted degree.....	211
Figure 5.36 Geographic network graph layout of domestic jar technological similarity network for the Post-Migration Time Period (1300-1450 A.D.); edges are colored by weight; nodes are colored and sized by closeness centrality	208
Figure 5.37 Yifan Hu multilevel network graph layout of plate technological similarity network for the Post-Migration Time Period (1300-1450 A.D.); edges are colored by weight; nodes are colored and sized by weighted degree	211
Figure 5.38 Geographic network graph layout of domestic plate similarity network for the Post-Migration Time Period (1300-1450 A.D.); edges are colored by weight; nodes are colored and sized by weighted degree.....	212
Figure 5.39 Yifan Hu multilevel network graph layout of domestic jar and plate technological similarity flattened multilayer network for the Post-Migration Time Period (1300-1450 A.D.); edges are colored by weight; nodes are colored and sized by weighted degree.....	213
Figure 5.40 Geographic network graph layout of domestic jar and plate technological similarity flattened multilayer network for the Post-Migration Time Period (1300-1450 A.D.); edges are colored by weight; nodes are colored and sized by weighted degree	214
Figure 5.41 Geographic network graph layout of domestic jar (left) and plate (right) technological similarity sliced multilayer network for the Post-Migration Time Period (1300-1450 A.D.); edges are colored by weight; nodes are colored and sized by closeness centrality for jars (left) and weighted degree for plates (right).....	215
Figure 5.42 Yifan Hu multilevel network graph layout of domestic jar technological similarity network flattened across Time Periods (1200 – 1450 A.D.); edges are colored by weight; nodes are colored and sized by weighted degree score	217

Figure 5.43 Geographic network graph layout of domestic jar technological similarity network flattened across Time Periods (1200 – 1450 A.D.); edges are colored by weight; nodes are colored and sized by weighted degree.....	218
Figure 5.44 Yifan Hu multilevel network graph layout of plate technological similarity network flattened across Time Periods (1200 – 1450 A.D.); edges are colored by weight; nodes are colored and sized by closeness centrality score.....	219
Figure 5.45 Geographic network graph layout of plate technological similarity network flattened across Time Periods (1200 – 1450 A.D.); edges are colored by weight; nodes are colored and sized by weighted degree.....	220
Figure 5.46 Yifan Hu multilevel network graph layout of domestic jar and plate technological similarity multilayer network flattened across Time Periods (1200 – 1450 A.D.); edges are colored by weight; nodes are colored and sized by weighted degree	221
Figure 5.47 Geographic network graph layout of domestic jar and plate technological similarity multilayer network flattened across Time Periods (1200 – 1450 A.D.); edges are colored by weight; nodes are colored and sized by weighted degree	222
Figure 5.48 Geographic network graph layout of domestic jar (left) and plate (right) technological similarity sliced multilayer network flattened across Time Period (1200-1450 A.D.); edges are colored by weight; nodes are colored and sized by weighted degree	224
Figure 6.1 Examples of plate form. Images © Andy Upton 2018, courtesy Western Illinois Archaeological Research Center and Dickson Mounds Museum.....	243
Figure 6.2 Ridgeline density plots for plate continuous attribute measurements at Late Prehistoric CIRV sites	244
Figure 6.3 Plate decoration techniques: trailed (left) and incised (right). Images © Andy Upton 2018, courtesy Western Illinois Archaeological Research Center	246
Figure 6.4 Trailed and punctate impression decoration. Image © Andy Upton 2018, courtesy Western Illinois Archaeological Research Center.....	247
Figure 6.5 Plate sherd showing sun with nested cross motif. Image © Andy Upton 2018, courtesy Western Illinois Archaeological Research Center.....	248
Figure 6.6 Sketch tracings of plate decoration motif emblems	255
Figure 6.7 Distribution of Brainerd-Robinson coefficients for simulated (green) and observed (blue) design category matrices.....	257
Figure 6.8 Correlation Matrix Heat-Map of Rescaled Brainerd-Robinson Coefficients.....	262

Figure 6.9 Yifan Hu multilevel network graph layout for the Pre-Migration Time Period (1200-1300 A.D.; left) and Post-Migration Time Period (1300-1450 A.D.; right) ..	265
Figure 6.10 Geographic network graph layout for the Pre-Migration Time Period (1200-1300 A.D.).....	267
Figure 6.11 Geographic network graph layout for the Post-Migration Time Period (1300-1450 A.D.).....	267
Figure 6.12 Yifan Hu multilevel network graph layout flattened across time (1200 – 1450 A.D)	268
Figure 6.13 Geographic network graph layout flattened across time (1200 – 1450 A.D).....	268
Figure 6.14 Network randomization results for pre-migration social identification network. Observed statistic represents red line. Histogram shows distribution of statistic based on network randomization of 5000 random graphs using the Erdős–Rényi random network modeling technique.....	270
Figure 6.15 Network randomization results for post-migration social identification network. Observed statistic represents red line. Histogram shows distribution of statistic based on network randomization of 5000 random graphs using the Erdős–Rényi random network modeling technique.....	270
Figure 6.16 Histogram showing the range of design categories present at sites in different CIRV time periods	271
Figure 7.1 Bedrock geology map of the CIRV showing locations of archaeological sites and clay samples. Adapted from (adapted from Kolata 2005)	280
Figure 7.2 Surficial deposits of west-central Illinois. Cross-section A-A' shows the increased thickness of the glacial sediments approaching Lake Michigan. Adapted from (Curry, et al. 2011)	282
Figure 7.3 Statistical workflow for the analysis of compositional data.....	296
Figure 7.4 Principal components biplot showing the distinction between the two clay groups identified. Ellipses represent 90% confidence intervals for group membership. The first two principal components account for 66.5% of the variance in the clay data set.	305
Figure 7.5 Bivariate plot of logged (based 10) Beryllium and Lithium showing distinctions between the two clay groups. Ellipses represent 90% confidence intervals for group membership.	306
Figure 7.6 Bivariate plot of logged (based 10) Cesium and Nickel showing further chemical distinctions between the two clay groups. Ellipses represent 90% confidence intervals for group membership.	307

Figure 7.7 Principal components biplot showing elemental enrichment for sherds recovered from sites north of the Spoon/Illinois River confluence in general. Ellipses show 90% confidence intervals. Together, PC 1 and 2 account for 49.99% of variance in the ceramic dataset.....	312
Figure 7.8 3D scattergram of PCs 1, 2, and 3 showing core and non-core compositional groups.....	314
Figure 7.9 Principal components 1 and 5 biplot showing distinctions between the Core group, Outgroup 1, and Outgroup 2. Ellipses demarcate 90% confidence intervals.....	315
Figure 7.10 Bivariate plot of log base 10 magnesium and ytterbium concentrations of Outgroup 1 and 2 and Core sherds with 90% confidence ellipse boundaries	318
Figure 7.11 Principal components 1 and 2 biplot showing distinctions between the Core group, and core provisional groups – Core B and Core C. Ellipses demarcate 90% confidence intervals.	320
Figure 7.12 Principal components 1 and 2 biplot showing distinctions within the Core A group. Ellipses demarcate 90% confidence intervals.....	323
Figure 7.13 Bivariate plot of log base 10 magnesium and nickel concentrations of Core A1 and Core A2 sherds with 90% confidence ellipse boundaries.....	324
Figure 7.14 Principal component 1 and 2 bivariate plot of all group, sub-group, and provisional group assignments with 90% confidence ellipse boundaries.	326
Figure 7.15 Principal component 1 and 2 bivariate plot of all group, sub-group, and provisional group assignments emphasizing component loadings with 90% confidence ellipse boundaries.....	327
Figure 7.16 Bivariate plot of log base 10 magnesium and molybdenum concentrations of all group, sub-group, and provisional group assignments with 90% confidence ellipse boundaries.....	328
Figure 7.17 Distribution of Brainerd-Robinson coefficients for simulated (green) and observed (blue) compositional group membership matrices.....	331
Figure 7.18 Correlation matrix heat-map of rescaled Brainerd-Robinson coefficients.....	337
Figure 7.19 Yifan Hu multilevel network graph layout for the Pre-Migration Time Period (1200-1300 A.D.; left) and Post-Migration Time Period (1300-1450 A.D.; right).	340
Figure 7.20 Geographic network graph layout for the Pre-Migration Time Period (1200-1300 A.D.).....	342

Figure 7.21 Geographic network graph layout for the Post-Migration Time Period (1300-1450A.D.).....	342
Figure 7.22 Yifan Hu multilevel network graph layout flattened across time (1200-1450 A.D.).....	343
Figure 7.23 Geographic network graph layout flattened across time (1200-1450A.D.)	343
Figure 7.24 Network randomization results for pre-migration ceramic industry economic network. Observed statistic represents red line. Histogram shows distribution of statistic based on network randomization of 5000 random graphs using the Erdős–Rényi random network modeling technique.....	344
Figure 7.25 Network randomization results for post-migration ceramic industry economic network. Observed statistic represents red line. Histogram shows distribution of statistic based on network randomization of 5000 random graphs using the Erdős–Rényi random network modeling technique.....	345
Figure 8.1 Pre-migration multilayer network (circa 1200 – 1300 A.D.)	364
Figure 8.2 Post-migration multilayer network (circa 1300 - 1450 A.D.)	365
Figure 8.3 Flattened multilayer network (circa 1200 - 1450 A.D.).....	366
Figure 8.4 Multilevel graph layout for the pre-migration multilayer network (circa 1200 - 1300 A.D.).....	367
Figure 8.5 Multilevel graph layout for the post-migration multilayer network (circa 1300 - 1450 A.D.).....	368
Figure 8.6 Edge overlap for the pre-migration time period	371
Figure 8.7 Edge overlap for the post-migration time period.....	372
Figure 8.8 Node centrality measures for the pre-migration multilayer network.....	377
Figure 8.9 Node centrality measures for the post-migration multilayer network	377
Figure 8.10 Summary of node degree centrality and strength for the pre-migration time period	379
Figure 8.11 Summary of node degree centrality and strength for the post-migration time period	379
Figure 8.12 Site-node degree deviation for the pre-migration CIRV time period; lower scores indicate more even influence across layers	381

Figure 8.13 Site-node degree deviation for the post-migration CIRV time period; lower scores indicate more even influence across layers	381
Figure D.1 Percent variance explained by each principal component for the sherds data set.....	572
Figure H.1 Emmons Lake radiocarbon assay probability.....	646
Figure H.2 Kingston Lake radiocarbon assay probability	646
Figure H.3 Baehr South radiocarbon assay probability	647
Figure H.4 Buckeye Bend radiocarbon assay probability.....	647
Figure H.5 Morton Village radiocarbon assay probability (1).....	648
Figure H.6 Morton Village radiocarbon assay probability (2).....	648
Figure H.7 Morton Village radiocarbon assay probability (3).....	649
Figure H.8 Star Bridge radiocarbon assay probability (1).....	649
Figure H.9 Star Bridge radiocarbon assay probability (2).....	650
Figure H.10 Ten Mile Creek radiocarbon assay probability (1)	650
Figure H.11 Ten Mile Creek radiocarbon assay probability (2)	651

CHAPTER 1 INTRODUCTION

1.1 Brief Introduction to the Research Problem

The story of human kind is, in many ways, one of social relations among groups, among individuals, and among things. For many thousands of years, demographic upheaval and migration have led to social settings in which extant social relationships are challenged, negotiated, or reinforced as a result of the intersection of previously separate network formations. This dissertation offers theoretical and methodological means to investigate social settings in which disparate material culture traditions coexist or intermix in time and space through the comparative modeling of various networks of relationships that connect individuals and communities. Under this model, the structure of network relationships and the structural positioning of actors within the network act as sensitive indicators in the potential for and trajectory of behavioral responses to culture contact at various scales.

Using archaeological data from the Late Prehistoric Period in west central Illinois (circa 1200 – 1450 A.D.), I explore how network relationships among complex and smaller-scale societies structured, and are restructured by, migration. The case study under consideration here is marked by a well-documented in-migration process of a tribal group into a chiefly environment, though the location of origin of the immigrants is unknown (Esarey and Conrad 1998; Santure, et al. 1990; Steadman 1998). In this study, I draw on a body of contemporary social theory focused on parsing social structure across multiple types of interrelationships to investigate questions revolving around how both indigenous societies and migrant peoples approach intercultural social and economic relations.

1.2 Multicultural Social Interrelationships and Multilayer Social Network Analysis

Explaining social interrelationships in settings characterized by coexisting material culture traditions has been of central and continuous concern in archaeology since its first articulation as a discipline (e.g. Childe 1936; Wolfe 1982); in particular, in contexts where differing traditions amalgamate (Frangipane 2015; Liebmann 2013; Stone 2003). Recent archaeological research recognizes the value of incorporating formal network analysis methodologies based on ‘relational’ sociology as theorized by Harrison White to address questions related to coexisting material culture traditions (Borck, et al. 2015; Brughmans 2013; Mills, Roberts Jr., et al. 2013). I employ a theoretical framework that builds on this application of White’s relational theory to archaeological contexts in order to address anthropologically significant issues related to cultural contact, social interaction, identity, and exchange.

This study is specifically focused on examining the structuring and restructuring of social interrelationships following culture contact at geographic and demographic scales above the individual or household (i.e. at the spatially bounded community scale). Prior scholarship on intercultural contacts emphasizes interaction spheres, hybridization, technological transfer, or models of exchange as measures for constructing borders and defining societal membership, often based on anthropological perspectives of social identity or ethnicity (Barth 1969; Bentley 1987; Blanton 2015; Graves 1994; Jones 1997; C. G. Sampson 1988; Shennan 1989). Identity, as rooted in culture or ethnicity, is a foundational variable in guiding both intra- and inter-group social interrelationship formation and maintenance. However, no theoretical consensus has emerged to the anthropological study of identity. This is particularly true in archaeological contexts, where taxonomic distinctions in material culture are traditionally relied upon to model geographic and temporal patterns related to social organization, interaction, identification, and

change. Equating patterns of material culture similarity with traditional anthropological models of identity presupposes the derivation of identity from an archaeological definition of a culture, which often leads to the projection of normative and idealist notions of culture onto past peoples (Shennan 1989). In this dissertation, I argue that cultural or ethnic identity and networks of social interrelationships recursively interplay, and that analyzing social interrelationships across multiple layers in separate and in aggregate provides new insights into regional scale understanding of social interaction and identification among people and the communities in which they are nested in the past and present.

The theoretical perspective I employ in this research builds on the integration of anthropological archaeology and ‘relational’ sociology as theorized Harrison White (Mills, Roberts Jr., et al. 2013; Peeples 2011). In opposition to considering network analysis as a de-contextualized structuralist research strategy, White argues that social networks should be studied in conjunction with cultural systems (Fuhse 2015; Mische 2011; White 1992). That is, social networks are imprinted with culture and therefore serve as a habitat of cultural forms. Therefore, the traditional archaeological hermeneutic to the study of culture is eschewed in favor of a perspective that seeks to model cultural forms through their linkages within a network. Network relationships reflect and build on cultural models such as kinship, gender, heterarchy, and hierarchy. White views interactions and categories used to construct networks as being driven through the inherent uncertainty in the roles of participants (White 2008a). From this uncertainty, White sees identities as a means to ‘gain footing’ in, or to ‘control’, social contexts (White 1992). These control attempts are posited to leave a trace in social space as ‘stories’, or information defining and relating identities to each other. White’s ‘New York School’ of relational sociology (Mische 2011) posits that processes of collective social identification, that

form the empirical basis of ‘stories’, take place in either relational identification or categorical identification.

Relational identification is a process whereby individuals identify with larger collectives through networks of interpersonal interaction (Peeples 2011), whereas *categorical identification* refers to a process whereby individuals identify with collectives based on formal social units such as ethnic groups or genders that are defined outside of the relations among members (Peeples 2011). Networks consist of the traces of meaning from previous interactions based on categorical or relational identification, which become encapsulated in stories that relate identities to one another. As individuals jointly reproduce relational or categorical identities through their mutually patterned actions, they acquire a *style* (White 1993). And “styles must mate to change” (White 1993:163). That is, novelty in stories or identities develops only from the “creative combination of cultural forms at the intersection of previously separate network formations” (Fuhse 2015:19). White’s relational perspective on culture is geared toward empirical applicability wherein social networks act as informal patterns of order that emerge from stories that are built in response to the uncertainty of identities and attempts to control interactions, governed by neo-institutional rules, and jointly reproduced as styles (Fuhse 2015). Because White’s styles are inherently the product of singular institutional frameworks, however, I argue here that investigating culture as networks is enhanced when multiple networks constituting phenomenological realities in distinct cultural spheres are explored simultaneously in separate and in aggregate. Only then may style and story, when mated, be parsed to uncover the constituent components of cultural change. This dissertation is a formal empirical application and expansion of White’s theoretical conception of whether or not, and if so how, novel

interactive frameworks may form because of the intersection of previously separate network formations.

From trends inherent in multiple networks of relational identification and categorical identification, expectations are offered that seek to characterize communal behavioral strategies in the negotiation of a multicultural social and economic environment following cultural contact. These characterizations are referred to as behavioral explanations of patterns of *intercultural communal coexistence*. Through analysis of multiple layers of social interaction and social identification, it is possible to examine and to explain how communities constructed social, economic, and other relational networks before an in-migration and capture communally based responses to multicultural society after cultural contact.

1.3 The Case Study

The focus of this dissertation is the latter portion of the Late Prehistoric Period (circa A.D. 1200 – 1450) of the central Illinois River valley (CIRV) in the North American Midwest. This region spans an approximately 80-mile expanse, as the crow flies, of the Illinois River from Pekin, IL southerly to Meredosia, IL. Publicized reports in newspapers, magazines, and professional journals in the late 19th and early 20th centuries led to the first archaeological field schools in North American being established by Dr. Fay-Cooper Cole of the University of Chicago in 1930-1932 in the Dickson Mounds vicinity near the confluence of the Illinois and Spoon Rivers. The cultural sequence resulting from these investigations is still, by and large, in use today (Cole and Deuel 1937; Harn 1978). Progressive, though at times sporadic, research investigations continued in the region throughout the 20th and 21st centuries (Bardolph 2014; Conrad 1989, 1991; Esarey and Conrad 1981, 1998; Harn 1978:235-237; Hatch 2015, 2017; G.

R. Milner, et al. 1991; Steadman 1998, 2001, 2008; Strezewski 2003; Vanderwarker and Wilson 2016; Vanderwarker, et al. 2013; G. D. Wilson, et al. 2018; J. J. Wilson 2010). Aside from a few notable exceptions, research efforts in the CIRV rarely endeavor toward regional scale issues (Conrad 1991; Harn 1978; J. J. Wilson 2010). Nevertheless, the availability of material culture, and in particular ceramic artifacts, from sites across the geographic and temporal expanse of the Late Prehistoric period lends to the regional scale focus of this dissertation.

Of central concern to the period under consideration in this study is an expansionary process of a distinct Upper Mississippian cultural group, the Oneota, who began pushing out of the western Upper Midwest and into surrounding environs beginning in the 13th and early 14th centuries A.D. (Brown and Sasso 2001; Hollinger 2005; Overstreet 1997). Some characterize the spread of the Oneota cultural tradition throughout the US Midwest and eastern Prairie Plains as an aggressive, rapid territorial expansion (Hollinger 2005). The Oneota expansion coincided with a decline in Middle Mississippian influences across the Upper Midwest region and with the onset of the droughty Pacific climatic episode (Gibbon 1995). While many Late Woodland populations in the riverine Midwest and western Great Lakes were replaced by or integrated into Oneota peoples during this expansion, societies in the ecologically rich CIRV, or northern Middle Mississippian frontier, maintained their positions in fortified temple mound centers, and outlying sites, and entered into a period of regional cohabitation with an intrusive Oneota population (Esarey and Conrad 1998). Recent archaeological inquiry in the Late Prehistoric CIRV has focused on the unprecedented levels of violence seen in burial and cemetery contexts both prior to and following the Oneota in-migration (Hatch 2015; Steadman 2008; Vanderwarker and Wilson 2016; G. D. Wilson 2012). Although the CIRV is remarkable for its levels of sustained violence, evidence indicating the communal cohabitation of these distinct but interrelated

cultural groups is apparent (Esarey and Conrad 1998). Coexisting Oneota and Mississippian material culture at multiple sites at the household level provides the opportunity to examine the various social interrelationships that were present. Instead of focusing on traditional typological cultural classifications, hybridity, or technological transfer, my research examines the ways in which models of network interrelationships between CIRV communities change concomitant with Oneota in-migration. In this study, I argue that multicultural society following migration or population movement can be fruitfully explored by dissecting networks of culture across distinct layers. In particular, I explore networks of categorical social identification, networks of economic interaction, and relational networks of cultural transmission each as evidenced in ceramic industry. Across these multiple network layers, community-scale interrelationships are modeled in separate and in aggregate to assess how immigrant and indigene behavior exposes approaches to intercultural social and economic relations in a Late Prehistoric period central Illinois River valley case study.

1.4 Dissertation Organization

Chapter 2 (“Multilayer Social Networks and Intercultural Communal Coexistence”) of this dissertation provides a necessary historical background to anthropological and archaeological perspectives on social identification and social interaction before developing and adapting a model rooted in a contemporary body of theory on processual social structure in complex systems to the study of cultural contact. This model forms the overall basis of the theoretical framework underlying this study.

Chapter 3 (“Regional and Cultural Background”) introduces the Late Prehistoric central Illinois River valley (or CIRV) as well as the Middle Mississippian and Oneota cultural

traditions through the lens of the settlements whose interrelationships form the focus of interest in this dissertation.

Chapter 4 (“Methodological Consideration”) presents finer grain detail on many of the methodologies employed in this dissertation for data collection and data analysis. While the four chapters that follow each address these areas, a fuller and richer discussion is provided in Chapter 4 in cases that would otherwise detract from the linear arguments made therein.

Chapter 5 (“Networks of Interaction through Cultural Transmission”) develops and applies a model rooted in cultural transmission theory to identify technological artifact attributes constrained by social, as opposed to engineering, forces. These socially-mediated artifact attributes are used to model networks of relational identification through social interaction. This method results in a proportional scale of ceramic technological similarity that represents a proxy measure to model and analyze the strength and directionality of relational connections among communities across the study area through time.

Chapter 6 (“Ceramic Design and Networks of Social Identification”) presents network models of social identification constructed based on patterns of proportional similarity in designs incised or trailed on the interior outflaring rims of ceramic plates.

Chapter 7 (“Networks of Economic Relationships – Results of the Chemical Analyses”) presents the results of laser ablation inductively coupled plasma mass spectrometry (LA-ICP-MS) analysis of clay samples and Mississippian and Oneota pottery. The resulting chemical compositional groups form the basis of models of economic interaction related to ceramic industry.

Chapter 8 (“Toward Explaining Social Interrelationships through a Ceramic Industry Multilayer Network”) draws together each of the unique relational perspectives on ceramic

industry discussed in Chapters 5 - 7 into synthetic multilayer networks. Through analysis of the different layers in the multilayer networks, it is possible to access the influence and overlap of each individual network in structuring and being restructured by migration-induced culture contact in a Late Prehistoric west-central Illinois case study region. From these trends, patterns of *intercultural communal coexistence* are revealed. Finally, contributions of the study and future directions are offered.

CHAPTER 2 MULTILAYER SOCIAL NETWORKS AND INTERCULTURAL COMMUNAL COEXISTENCE

2.1 Introduction

Although parsimony is often stated to be desirable when constructing scientific theories, theoretical economy is self-defeating if it ignores the diversity and complexity of what is being explained (Trigger 2006, p. 498)

This chapter provides a detailed overview of the theoretical framework underlying this study. The discussion is divided into three broad sections. To provide a necessary background, initially discussed are traditional anthropological perspectives, and their evolution, on two key components of culture contact in non-state societies: social interaction and social identification. Focus is placed on models that endeavor to explain social interrelationships and social structure in settings characterized by the presence of multiple, distinct social groups or where culture contact has otherwise occurred. I then discuss key concepts and terms derived from a contemporary body of theory on processual social structure in complex systems. This body of theory is then adapted into a model of intercultural communal coexistence, which is argued to offer new insights into the study of culture contact based on enhanced understanding of the transmutability and multi-dimensionality of social structure both preceding and postdating a migration process in a Late Prehistoric period central Illinois River valley case study and beyond. Finally, I discuss the methods and techniques used to link this body of theory with the archaeological data considered in this dissertation.

2.2 Evolving Perspectives on Social Interaction and Identity Formation

Archaeologists have long placed an analytical focus on identifying cultural or social groups, exploring group organization, and understanding how these groups interact and change

over time in prehistory. Over the last century, the theoretical perspectives and methodological tools to accomplish these goals have changed in dramatic fashion. Nascent archaeological studies of the late nineteenth and early twentieth centuries rooted their knowledge and inquiry of prehistoric human society in identifying archaeological cultures. Distributions of shared material culture were used to define discrete territories of peoples with an oft stated or unstated objective being the creation of an historical and pre-historical lineage tracing contemporary national or ethnic populations to antecedents in the distant past (Jones 1997:1-14; Peeples 2011:8-10; Shennan 1989). In connecting prehistory to history, the archaeological record could be linked with a present ethnic variant (Kossinna 1911). Culture, language, and ethnicity were therefore thought to be directly linkable to the past, and the archaeological record became a tool with which to detect the history of a politically expressed ethnic identity (i.e. the nation state) (Trigger 2006). These efforts often resulted in furthering nationalistic political agendas or in delegitimizing various contemporary peoples by denying them a prehistoric past or ethnic identity. Thus, identity and in particular ethnicity, was a critical analytical component of early archaeological inquiry. While the focus of this dissertation is not ethnicity or identity per se, the role of ethnic identity in shaping archaeological and anthropological thought necessitates a brief historical overview of the use of these concepts as they relate to culture contact, migration, and social structure.

The culture-historical paradigm of early archaeologists such as V. Gordon Childe is an out-growth of analytical focus on archaeological cultures based on patterned variation of idealist-types in material culture (Shennan 1989). The idealist tendencies of culture-historians meant that they favored uniformity as opposed to variation in studying material culture, and as a result, many of the cultural groups they defined are not representative of the full gamut of the material

expressions of individuals and groups within those cultures. These monolithic cultural entities are based on normative and idealist conceptions of culture (Jones 1997). That is, as opposed to being discovered through a combination of deductive and inductive methods, archaeologists were responsible for constructing a type, rooted in ancient Greek artistic notions of the ideal, and therefore a cultural social entity. Cultures were thought of as homogenous entities whose histories unfolded in a coherent, linear narrative towards increasing complexity and resulting in the nations and ethnic groups that dominated European academic and political discourse (Jones 1997). Further, cultures remained relatively static until diffusion or migration events catalyzed rapid change.

Following the instability of World War I, Childe was instrumental in sparking a trend to divest archaeology of its role in furthering nationalistic agendas and expanding upon the definition of archaeological cultures. Childe placed an emphasis on people as the producers of material culture and society as the object of focus in archaeological investigations based on a concern with systematically describing distinctions and interactions among cultures based on functional traits (Childe 1936; Veit 1989). Childe further placed emphasis on diffusion as a means for the spread of techno-functional enhancement or stylistic innovation in contrast to migration as a means for cultural replacement or mixing (Trigger 2006). This shift in emphasis toward diffusion and migration made cultural continuities of ethnic identity tenuous at best, gave archaeologists a working tool – the archaeological culture, and a sense of theoretical purpose – the posing of particularistic, historical questions.

In Eastern North America, two taxonomic systems influenced by European culture-historian archaeologists emerged and continue to form the foundation on which modern Eastern North American archaeology is built: the Midwestern and the Willey and Phillips Taxonomic

Systems. While archaeologists in the United States were not utilizing the archaeological record to promote a nationalistic agenda, by and large, the methods used for this purpose in Europe were borrowed and adapted to aid in describing the vastness of the American archaeological record. Chiefly among these tools was that of the analysis of style. Variation in artifact style provided culture-historical archaeologists the ability to assign groups of artifacts into distinct cultural units. In addition, style enabled these cultural units to be contextualized both spatially, and more importantly at the time, chronologically. While these new cultural units were constructed using European assumptions about ethnic identity, Eastern North American archaeologists had, for the first time, broad generalizations about the distinct peoples that initially populated the area that were able to apply form to both space and time.

Preoccupation with the creation of typologies of artifacts and the development of cultural chronologies, however, led American archaeologists to relegate to mere speculation the “reconstruction of prehistoric patterns of life” (Trigger 2006:288), any attempts to understand cultural change beyond migration and diffusion, and the linking of ethnology and modern North American Indians with archaeology. The grouping of archaeological data based on idealist types enables the efficient assignation of spatial and temporal units. Though in lacking any functional correlate to these categorizations, it meant that culture-historical archaeologists were often unable or unwilling to extend their analyses beyond that of taxonomy. To align itself with a scientific endeavor, the Midwestern and Willey and Phillips Taxonomic systems allowed artifacts to be divorced from the people who were responsible for their creation. While this fundamentally delimited the scope of American archaeology at the time, it did allow for the production of numerous regional chronologies of spatially bounded cultural entities that are largely still in use today, including in this study.

The development of the New Archaeology in the 1960s heralded a shift in attention away from defining idealist and normative archaeological cultures to identifications of cultures as expressed by individuals and groups themselves. Clarke (1968), for example, argued for a polythetic definition of culture. Further, Binford (1962) argued that cultural variation results from a multitude of factors, not just culture or ethnicity, and that archaeological data must therefore be subjected to a process of analysis – the foundational assumption of processualism. However, both culture-historians and processual archaeologists “regarded the results of their process of definition as entities representing the cultural traditions of human groups. Both adopted classificatory expedients to remove the untidiness in the cross-cutting distributions rather than taking the more radical step of recognizing that this untidiness is, in fact, the essence of the situation” (Shennan 1989:13). The shift of focus in archaeology by processualists towards systematics and general processes resulted in a de-emphasis on studies of identity and ethnicity as it relates to archaeological cultures.

At the same time processualism re-focused American archaeological attention away from ethnic identity, anthropological perspectives on these dimensions to the study of people in the past changed. Ethnicity first became a studied phenomenon in its own right when it was dichotomized from culture in the 1950s (Bentley 1987). Debate followed as to the nature of ethnicity based on two camps: primordialists and instrumentalists. Primordialists viewed ethnicity as a means to seek refuge from disorienting change in those aspects of individual’s lives that most fundamentally define who they are based on a deep psychological and emotional sense of shared heritage that varies little through time (Geertz 1963; Jones 1997; Peeples 2011:10). Social groups were therefore based on relatively static concepts of discrete and well-bounded collective identities (Wolf 1982). Distinct ethnic identities and the boundaries that

separate them exist because of structural oppositions between groups. As a result, primordialists espoused that assimilation or other forms of social integration can only occur when structural oppositions between ethnic groups are removed (Keyes 1979). On the other hand, instrumentalists view ethnicity as a mechanism in pursuit of shared objective interests, primarily economic and political. Instrumentalists such as Barth (1969), Moerman (1965), and others consider ethnicity as processes, or instruments, of social categorization and interaction wherein members create we/they distinctions that guide inter- and intra-group interaction in situational contexts. These relational processes of inclusion and exclusion form identity, according to instrumentalists. Dynamic and fluid social organizations result wherein membership is constantly being negotiated and reified (Barth 1969; Stone 2003). More recent research on ethnic identity grapples with these two extremes: ethnic identity as being simultaneously situational and the product of a shared heritage (Geary 1983; Jenkins 2000, 2004; Snead and Preucel 1999; Stone 2003; D. Upton 1996).

Many researchers studying identity and ethnicity and their relationship to material culture have found Bourdieu's practice theory and the concept of habitus to be theoretically productive constructs that bridge the key insights of both instrumentalists and primordialists (Bentley 1987; Bourdieu 1977, 1990; Conkey 1990; Lightfoot, et al. 1998; Shennan 1989), especially in multi-ethnic or culture contact contexts (Lightfoot and Martinez 1995; D. Upton 1996). In particular, Bourdieu's theory of practice is argued by Bentley (1987) to bridge the situational nature of identity favored by instrumentalists with the enduring shared heritage of identity favored by primordialists. Practice theory contends that individual habitus act to guide the fluid and contextual nature of cultural identity wherein cultural differences are objectified vis-à-vis others in the context of social interaction (Jones 1997). Individuals "enact and construct their

underlying organizational principles, worldviews, and social identities in the ordering of everyday life” or habitual routines (Lightfoot, et al. 1998:199). However, Bourdieu’s concept of habitus emphasizes cultural content within a given ethnic group as opposed to interaction between groups. Behavioral change is rare, in that it only occurs through encountering and interacting with different habitus (Bentley 1987; Stone 2003). Thus, there is a contrast between the primordialist camp, which sees ethnicity as a conscious construct, and the use of the concept of habitus necessitating ethnicity to be an unconscious construct.

Stone (2003) details theoretical advances drawn from practice theory and posits two competing schools of thought guiding studies of ethnicity in the late twentieth century: interactionist and enculturationist approaches. Proponents of the interactionist approach view ethnicity and group spatial boundedness as resulting from social interaction between socially distinct groups (Braun and Plog 1982; Emberling 1997). As the moniker implies, the general impetus of the interactionist approach is that groups can be most readily distinguished based on the differences between them vis-à-vis their interactions. For example, distributions of stylistically distinct artifacts between sites, within site zones, or individual households may be used to infer exchange relationships or boundaries between distinct social groups at various scales (Bardolph 2014; Cook 2007; Cook and Fargher 2007; Friberg 2018; Rowe 2016; Schneider 2015; Wallis, et al. 2010; Wallis, et al. 2016; Zvelebil 2006). Style is seen as an active means of non-verbally communicating social differences and as a marker of social boundaries (Hegmon, et al. 1997; C. G. Sampson 1988; Wiessner 1983, 1990; Wobst 1977). On the other hand, the enculturationist approach focuses on ethnic identity as a set of shared norms of habitual practice (Bourdieu’s habitus) resulting from processes of enculturation (Dietler and Herbich 1998; Jones 1997; Shennan 1989; Stark, et al. 1998). Thus, shared processes of enculturation or

social learning are sought to define spatial boundedness to groups in archaeological contexts. Through the theoretical guidance of habitus, these processes are thought to be unconscious and therefore suggest common enculturative backgrounds, where divergent learning frameworks or contexts imply distinct ancestry or habitual routine and therefore infer social boundedness (Lightfoot and Martinez 1995; Lightfoot, et al. 1998; VanPool 2008).

Although enculturationist and interactionist approaches have provided valuable insights to understanding social identity, both often struggle to offer nuanced perspectives in broad regional contexts where multiple traditions merge, blend, or otherwise amalgamate such as the case study region that is the focus this study. That is, enculturation approaches generally require a social context where multiple groups are sufficiently distinct to identify different enculturative backgrounds, while interactionist approaches focus on modelling the boundaries between ethnic or other groups (Stone 2003).

Multiple alternative perspectives, divorced from ethnic identity, have emerged to explain the process of “creation through recombination” or the “combination or convergence of two or more existing forms to create something different” in archaeological contexts (Liebmann 2013:27). Terms such as acculturation, syncretism, bricolage, creolization, mestizaje, and hybridity each carry unique definitions and characteristics to describe and explain social processes of cultural amalgamation. However, each term also carries the baggage of those definitions and respective case study applications. For example, acculturation, which parallels enculturationist perspectives on ethnicity, seeks to measure transitions from one cultural pattern to another and therefore seeks assess the progress of assimilation. Acculturation has been criticized for issues of uni-directionality and lack of agency. Acculturation also acts to ‘other’ subaltern, often non-Western groups by casting them as passive, subordinate receptors of cultural

forms supplied by more complex, colonial, or hegemonic societies who remain unchanged during the process of amalgamation (Liebmann 2013). The more recent term hybridity carries less baggage and stresses ambivalence, resistance, and agency. Hybridity emphasizes disjuncture and the forcing together of unlike things. Yet, like the study of social identity through ethnicity, hybridity and other concepts to explain social identity in multicultural archaeological contexts continue to represent cultures as bounded wholes, marked by a preexisting purity in social formations that are combined at some later time. Indeed, in archaeological contexts, the study of social identity and interaction as interpreted via material culture through theoretical lenses such as hybridity and cultural contact are fundamentally issues of taxonomy, where the underlying question of analysis is really at what spatial and social scales may groups be defined (Burmeister 2000; Liebmann 2013:32; Parkinson 2006; Renfrew 1994; Rice 1998; Trubowitz 1992).

Traditional studies of social identity therefore rely heavily on traditional perspectives on ethnicity, and in archaeological contexts continue to rely heavily on taxonomic correlates to the nature of spatial and temporal social group boundedness. Given this pervasive focus on the process of social or ethnic group identification, these models may not be appropriate for addressing questions related to behavioral relationships at broad regional and temporal scales that are not necessarily driven by ethnic or cultural amalgamation. However, because North American archaeology's general foundations are built upon these concepts, it is difficult if not impossible to fully separate out current archaeological inquiry from them. Nevertheless, the discussion below builds on a model from an alternative perspective on social identity that is explicitly focused on society as a dynamic multilayered system of relational interaction and categorical identification.

2.3 Social Systems as Multilayered, Relational Networks

Contemporary and historical social relationships have been studied by social scientists through quite different theoretical lenses than the anthropological perspectives on identity and ethnicity discussed above. While anthropological perspectives have been influential to these studies, very different kinds of research questions generally prompt a very different approach. For example, while some anthropological archaeologists may have been more concerned with identifying a culturally metaphorical 'index fossil' to denote group or population boundaries (e.g. Goodby 1998; Graves 1994; C. M. Milner and Stark 1999; C. G. Sampson 1988; Stark, et al. 1998), social scientists studying social identity and social change in modern contexts have often been more concerned with identifying a few generalized, essential features that govern social reality (Azarian 2005:33-34; Mische 2011; Tilly 2001a, 2004; White 2008a). Like many archaeologists, however, sociologists and other social scientists working under this paradigm argue that these conceptual models that govern social reality should be mined empirically as opposed to being rooted in theoretical abstraction. Derived out of this empirical rigor was a focus on social networks.

Under the relational paradigm, social ties and the networks they form among actors are argued to constitute the fundamental conditions of human social existence. Networks are viewed as process based on the continual making and un-making of ties. Society as stratification is cast aside as well as the notion of static social structures or static actor identities (White 1992, 2008a). Social identification is therefore understood within this framework as operating in terms of two related processes known as relational identification and categorical identification. Ties that form relationships through social identification are therefore multiplex, or constituted by different sorts of connections, and individuals must contend with inherent uncertainty in

information flows through connections that may converge or diverge. Viewing social actors as dynamic as opposed to static and social identification along multiple processual dimensions necessitates an approach to the study of the culture contact that can capture a complex, realistic social framework. Relational and categorical identification, as complex analytical dimensions, have been recently argued to be critical conduits through which collective action and social transformation may be viewed, understood, and predicted in archaeological contexts (Borck, et al. 2015; Mills, Clark, et al. 2013; Mills, Roberts Jr., et al. 2013; Peeples 2018). I employ a theoretical framework that builds on this application of relational sociological theory to archaeological contexts in order to address anthropologically significant issues. To this end, a multilayer network approach is drawn upon to underlie the study of culture contact that is the focus of this dissertation.

In this section, I present a discussion of concepts drawn from social science that ground the analyses that follow within a theoretical corpus. A model is presented that captures society as multiple relational networks to understand the structuring and restructuring of economic, cultural, and identity politic interactions following migration and culture contact.

2.3.1 Theory in Networks

Much of the theoretical component of the application of relational methodologies in archaeology is drawn from the works of Harrison C. White, as well as and Charles Tilly and students of theirs such as Mark Granovetter and Barry Wellman. Harrison White is a theoretical physicist turned sociologist turned anthropologist turned structural sociologist (Azarian 2005; Santoro 2008). I argue that it is the melding of these unique and seemingly chaotic backgrounds that resulted in the primary lasting impact of White on the social sciences more broadly. Namely,

the study of the social world as networks of relationships that interplay with cultural forms. The root ideas related to this approach were initially presented in the unpublished release of ‘Notes on the Constituents of Social Structure’ in 1966 and influenced a generation of social scientists to expand upon White’s idea to bring together notions of the network (or net) and categories (or cat) into a new concept, the catnet (Santoro 2008; White 1992, 2008a, 2008b, 2008c). Quite different from rigid social structures, catnets consider any set of individuals comprising both a category (cat) and a network (net). Sociologists at the time saw this as an opportunity to fundamentally re-think approaches to individuals and their relationship to society and societal structures. Problematically for anthropologists at the time, White and his protégé’s soon left behind the concept of culture to focus instead on the methodological nature of network analysis, or the mathematical analysis of social structure. Beginning in the 1990s, however, White and many of his students endeavored to reintroduce the role of culture into the study of networks (Mische 2011). The following discussion traces social network analysis as a theoretical paradigm through descriptions of key concepts before exploring the intertwining of social networks and culture.

Social network analysis (SNA) provides a body of theory and techniques for visualizing and measuring relationships among social entities (Brughmans 2010; Knappett 2013). SNA “is a comprehensive paradigmatic way of taking social structure seriously by studying directly how patterns of ties allocate resources in a social system” (Wellman 1988:20). As a theoretical paradigm, four concepts are integral to social network analysis, and generally agreed upon by network analysts:

1. Actors and their behaviors are interdependent rather than independent, functionally autonomous units;

2. Social ties, or social or relational transactions (Tilly 2002), between transmutable social actors or social entities are channels for the transfer of resources of various kinds;
3. Social structures are conceptualized as durable, lasting patterns of relations among actors; and
4. The structural position of a node has important perceptual, attitudinal, and behavioral implications and has significant enabling, as well as constraining, bearings on its social action. (Azarian 2005:35; Berkowitz 1982; Emirbayer and Goodwin 1994; Knoke and Kuklinski 1982; Scott 2000; Wasserman and Faust 1994; Wasserman and Galaskiewicz 1994; Wellman 1983).

The basal units of network analysis are actors, ties, and the networks they form together.

Actors are social units. Actors may be individual human beings, informal groups, formal organizations, or palimpsests of individuals, groups, and scalar organizations among them.

Actors are defined as discrete analytical units by the researcher. Actors are often referred to as nodes or vertices in the terminology of SNA, depending upon whether the researcher is inclined more toward the social or physical sciences respectively. In archaeology, actors are typically defined as either households or spatially discrete communities or settlements.

Ties are formed through processes of social interaction among at least two actors. A succinct definition of a tie is as a quantification of a relationship (Östborn and Gerding 2014). However, ties are a theoretical construct with significant theoretical depth (White 1992). They are also defined by the analyst, but instead of scale being a primary concern as with actors, ties must be defined as an abstraction to wade through the total, erratic confrontations of a dyad of actors in all their contexts (White 1992). Ties are thus ambiguous until defined, with its basic parameters including timing, intensity, symmetry, and topic (Azarian 2005). Through their

ambiguous nature, ties may be applied to any relational or categorical experience and be able to account for diachronic changes therein. For example, ties may include familial or friendship relationships, exchange relationships such as gifts or physical coercion, economic transactions, romantic interactions, teaching-learning interactions, mentorship interactions, and so on (Nexon 2009). Ties may represent cooperation or love as well as competition, conflict, or outright hostility (White and Lorrain 1971). Ties may be direct, or the result of face-to-face relations, such as the co-presence of individuals at conference sessions or tribal council meetings, or individuals engaged in a fist-fight. They may also be indirect through a third party or a physical communicative or non-communicative medium such as the adoption of common ideologies or methodologies through interaction with text, the exchange of information through a khipu record or a cuneiform tablet, or through the emulation of projectile points, pottery, or other artifacts. No physical presence of interaction is therefore required to define a tie. The ties of most concern to archaeologists are those with cultural implications that may be significant at multiple scalar levels (Mills, et al. 2015).

Ties are also referred to as relationships, links, or edges again reflecting the inclinations of the researcher from social science toward more physical science orientations respectively. Interactions defined as ties can be ‘weighted’, for example the number of times two authors shared co-authorship roles on research papers. Other interactions can be ‘unweighted’, or binary, such as the presence or absence of a researcher at a conference symposium. Ties may be directed, originating with a source actor and reaching a target actor, where the relationships is not necessarily mutual such as advice seeking, learning, or antagonism (Knoke and Kuklinski 1982). On the other hand, ties may be undirected and therefore do not distinguish between

senders and receivers. Undirected ties can be constructed based on marriage, alliance, or kinship relationships, for example.

Ties may be ephemeral and persist only for a brief moment, such as a chance encounter during a sporting match or ritualistic gathering. Other ties, however, may be of sufficient depth or of sufficient repetition such that they become durable. As ties blend into the routine, it is argued that they tend to acquire understandings, practices, commitments, and cultural standings that are at least partially autonomous from the initial motivations and interests that led to their production in the first place (Nexon 2004). For example, religious or political movements cannot outlive the death of their founder(s) unless a transformation to routine, durable ties takes place among followers. In this way, a lasting network is formed.

Networks are spatio-temporal patterns of durable ties and are a ubiquitous feature of social life. When ties become routine and therefore become durable, the presence or absence of specific actors may no longer be essential to the maintenance of the network. Social structure is therefore observed through the identification and mapping of the form and content of social networks (Nexon 2004:27). For many years after White sparked a relational revolution with ‘Notes on the Constituents of Social Structure’, many social scientists were dismayed by network analyst’s focus on the methodological and mathematical formulations of networks and network structure. Within network analysis itself, the primary focus of analysis shifted from that of the individual actor and their cultural milieu to that of the entirety of network structure, prompting the need for new mathematical models to aid in interpretation. Cultural theorists saw network analysis, as a result, as positivistic and reductionist, decomposing cultural richness to 1s, 0s, and graph objects (Mische 2011). A paradigm shift in sociology, however, heralded change. The increasing popularity of cultural sociology, and the maturing of the sub-field of SNA

practitioners, during the 1990s led to a convergence of scholars studying networks, culture, and historical analysis. A primary figure involved in this exchange of information was again Harrison White.

“In short, the New York area in the 1990s and 2000s was a rich hub of conversation that contributed to a reformulation of the link between networks, culture and social interaction”

(Mische 2011:8). Out of this reformulation emerged four key tenets that returned social network analysis to its roots, roots where network and culture should be studied in conjunction. These four tenets include:

1. Networks are conduits for culture;
2. Networks shape culture (or vice versa);
3. Culture itself is organized into networks of cultural forms; and
4. Networks are composed of cultural processes of communicative interaction (Mische 2011).

In opposition to considering network analysis as a de-contextualized structuralist research strategy, White argues that social networks should be studied in conjunction with cultural systems (Fuhse 2015; White 1992). That is, culture and network structure are argued to interplay in a recursive manner as opposed to being abstractions of each other. Social networks are imprinted with culture and therefore serve as a habitat of cultural forms. Network relationships build on cultural models such as kinship, gender, heterarchy, and hierarchy. However, White views interactions as being driven through the inherent uncertainty in the roles of participants, harkening back to the classical structural-functionalism tradition in sociology of Parsons, Luhmann, and others. From the inherent uncertainty in the roles of participants, White sees identities as a means to ‘gain footing’ in, or to ‘control’, social contexts (White 1992). Control

“boils down to handling one’s relationships, with the primary aim of reducing uncertainties as far as possible” (Azarian 2005:66). In other words, control is a term used to describe tie management, in consideration of the fact that an actor is embedded at the intersection of multiple social networks that often lack clear definitions and conditions on how to conduct life. These control attempts are posited to leave a trace in social space as ‘stories’, or information defining and relating identities to each other. Stories invoke a subjective dimension based on an actor’s interpretations of a tie, thereby providing a rationale for expectations and claims related to a dyadic relationship. Stories report on the synchronic and diachronic nature of the relationship – friendship or enmity, attraction or repulsion, cooperation or competition, etc. From stories, ties, and networks social landscapes appear as a “huge and dense texture of interlocking and overlapping networks, without any clear-cut boundaries...ties of various kinds concatenate into numerous strings, which evolve into a complex and multi-layered texture of endless networks, intertwining and weaving together in such intricate ways that it is practically impossible to keep track of the individuality of any of them” (Azarian 2005:54).

White made a point of contention, in regard to the web of interlocking social ties, between contemporary society and societies traditionally in the domain of anthropological research. He argued that intensifying interaction among the various spheres of modern society have resulted in social actors becoming a nodal point of inflection between many, often divergent social groups. Social actors take on a plurality of roles in these many social groups, which may have contrasting expectations and behavioral profiles. Constant switching is therefore required, a concept referred to as *embeddedness* (Granovetter 2001; White 1992). However, I argue that many such forces exist(ed) in anthropological contexts among bands, tribes, and chiefdoms. Multiple social groups with often diverging norms and behavioral profiles are no

doubt present in networks in non-state societies. Furthermore, social actors in pre-modern social settings are each uniquely situated within different social spheres that fundamentally constrain their ability to comprehend the social landscape beyond their individual spheres, despite any increases in overlap in their social networks relative to those in a contemporary setting. As a result, I argue that it would be no easier for an actor in a social context that is traditionally within the domain of anthropological inquiry to be able to predict or fathom the outcome of their actions just a few removes away than it is for individuals in contemporary society (contra White 1973). In this way I extend White's concept of embeddedness, or individual social actors being embedded as a nodal inflection point within multiple, often contrasting networks, to the anthropological cultural world.

White's relational perspective on culture is geared toward empirical applicability wherein social networks act as informal patterns of order that emerge from stories built in response to the uncertainty of identities and attempts to control interactions (Fuhse 2015). Networks consist of the traces of meaning from previous interactions encapsulated in stories that relate identities to one another. For White, novelty in stories or identities develops from the creative combination of cultural forms at the intersection of previously separate network formations. That is, while they "mate to change", such "change comes only through messes and fights, and emerges out of chaos" (White 1993:77-78). This is a product of both direct interaction and structural equivalence, or actors occupying similar positions in a network. That is, novelty occurs when previously separate network formations converge in both repeated directed action and in similarity in identities in a superposition of overlap and interpenetration around themes or topics.

Because of the inherent embeddedness of individual actors in a multitude of networks, multiple networks are required to understand change in both micro- and macro-cultural and

network structure. Problematically, however, many SNA practitioners today continue to construct models that decompose networks of networks into static, one-dimensional models. For example, political scientists may model voting interactions among politicians or economists model trade interactions among countries in isolation from other interactive dimensions among actors. The following section thus returns to the concept of ties and how and why change in networks of social and cultural systems is best modeled along multi-dimensional, comparative continua, setting the stage for a novel approach to the study of social structure in anthropological archaeology.

2.3.2 Multilayer Ties in Anthropological Archaeology

More often than not, individual social ties span across multiple dimensions in a complex overlay. Many ties that are initially one-dimensional generate depth as new layers or dimensions are appended to them. Dimensions may belong to separate, or specialized, spheres of life. “Often having a greater strength, a many-stranded tie represents the extent to which the connected parties are bound to each other in different social arenas and with a multiplicity of interests” (Azarian 2005:50). The anthropologist Max Gluckman (1967) is regarded as the first to diagnose the presence of an all-embracing kind of connection between two actors, where multiple dimensions blur. In his study of Lozi society, Gluckman (1967) identified that village and kinship groupings overlap but have a distinctive character. That is, an individual Lozi actor is simultaneously embedded as a member in different types of groupings. Relationships extended to neighbors, blood-brothers, friends, political allies and foes, members of the royal family, and with fellow-tribesmen. “This multiple membership of diverse groups and in diverse relationships is an important source of quarrels and conflict; but it is equally the basis of internal cohesion in

any society” (Gluckman 1967: 20). Thus, while individual actors in modern contexts must contend with membership in groups that often are partially or wholly separate (Granovetter 2001; White and Lorrain 1971), actors in non-state contexts more typically are embedded in networks that are somewhat or highly intersecting. As Gluckman (1967:19-20) pointed out in this regard, “Lozi social structure is uncomplicated when compared to our own; but it is complicated compared with, say, Andamanese or Bushman structure. Degree of complication therefore defines relatively the degree of congruence in the links between the positions of persons in various systems of ties which make up the total social system.” Yet, regardless of societal complexity, networks of networks constitute the fundamental conditions of social reality. Here, I argue that rather than concatenating multiple relational layers into a single, all-encompassing multiplex tie, it is more theoretically economical to parse ties into individual network layers. Each type of tie may therefore span a distinct social network of its own. Understanding of the entire social system is only approachable through analysis of how the network layers influence and co-construct each other (Szell, et al. 2010). As a result, society may be characterized by the superpositioning of its constitutive network layers. Building on a recent formalism, I refer to this superpositioning as a multilayer social network (Kivelä, et al. 2014).

The fundamental basis of a multilayer network approach is that it is implausible to consider a dyadic tie in isolation. The implication of this is that social relationships are embedded within a larger system made of similar ties, meaning that actions that occur in one relationship may affect, or be dependent upon, other relationships within the larger network system. In other words, the relationships between two focal nodes is not independent from the actor’s ties to other actors. This is more so true in anthropological contexts primarily because of the presence of fewer social categories and perhaps fewer hierarchical classes as a result of a

reduction in the scale of the social system in comparison to modern social systems. According to Breiger (1975:9), “it has for long been a basic assumption of anthropology that where relations are multiplex, that is where the relations between two persons derive from their activities in several institutional fields, the different types of relations impinge on and influence that actors in the various roles they play. Indeed, it is a basic assumption of those subscribing to the network approach that behavior cannot be explained in terms of any one single activity field.”

Multilayer networks constitute a social network where different layers may represent different types of social relationships. For example, nuclear family ties, friendship ties, clan ties, activity party ties, and economic ties may all be modeled in different layers. In instances where the actors are identical across each layer, the network may be referred to as a multiplex network (Kivelä, et al. 2014). Whereas if actors are differentially represented across the layers, the network may be referred to as a node-disjoint multilayer network. In either case, the multi-relational nature of these networks is thought to play an important role in the organization of large-scale networks (Szell, et al. 2010), and to illuminate political and social change in middle range and early state societies (Mills, Clark, et al. 2013; Munson and Macri 2009; Scholnick, et al. 2013).

Multilayer network methodology begins analysis by exploring the structure of different network model layers as separate entities. Key insights are then able to be mined through the comparisons of network layers. There are three primary analytical dimensions able to be explored across the different layers. First, it is possible to examine the degree of overlap among layers. Overlap is a quantification of similarities across the layers, or how often the different layers are characterized by common connections among nodes. For example, in anthropological contexts, a family network layer and feasting network layer may overlap significantly whereas a

friendship network and antagonism network may overlap very little, presenting implications for understanding multilayer network structure as a whole. Second, it is possible to explore the structural positioning of actors within each network layer. Actors may be centrally located in information or interaction flows in certain layers and quite isolated in other layers. For example, a market-hub may be of central importance to an economic network layer but have little importance to a religious network layer. Finally, it is possible to investigate the influence each layer has on the structure of the full multilayer network. Influence, in this regard, considers how many actors and ties are present in a given network layer relative to other layers. Certain network layers may be considerably more influential than others. For example, a multilayer transportation network may have a highly influential road network layer in an in-land context or a multilayer economic network may have a highly influential cash transaction network layer in a pre-information technology market economy.

This study represents the first application of a multilayer network approach applied in anthropological archaeology. A multilayer network approach is argued to be particularly instructive in contexts where more than one archaeologically or anthropologically defined cultural group is present. In other words, a multilayer network approach may provide a deeper understanding of multi-cultural social contexts because of the focus on parsing social ties regardless of the taxonomic placement of actors (whether actors may be individuals, households, or communities). From a normative point of view, the blurring of cultural or other group boundaries invariably invokes the theoretical baggage inherent in concepts such as hybridity, acculturation, syncretism, or creolization, ultimately being cast as an issue that is fundamentally related to taxonomic distinctions (Liebmann 2013). Beginning with social relationships that span multiple networks and defining social actors based on their membership and roles in various

networks, on the other hand, provides a means of penetrating how individuals from the different groups may cross-cut or blur social boundaries. In turn, this theoretical underpinning may lead to greater insight into the individual and collective role of various networks in structuring multicultural relationships, reflecting and being reflective of cultural milieu, and providing deeper understanding of taxonomically defined groups themselves. That is, a multilayer social network approach applied in archaeological domains need not supplant or disregard taxonomic groups. Instead, multilayer networks and taxonomic cultural groups are argued to recursively interplay. In archaeological contexts, a multilayer network approach is ultimately reliant on taxonomic groups to facilitate communication of findings and to provide meaning to the scientific community and the public at large beyond the relational. Inherently, this is because archaeological multilayer social networks must be constructed from the same kinds of material culture that were used to construct taxonomic cultural entities. However, unlike taxonomic groups, networks can cross scales, recast boundaries as being both relational and spatial, and avoid social determinism (Knappett 2013).

Because material culture remains and traces must be used to construct social networks, the scale at which actors can be defined in archaeological contexts is often delimited to individual households, spatially bounded household groups, sites, or site clusters. As a result, archaeologists often spend substantial amounts of time on the construction of ties and networks from often incomplete data, delimiting analytical scales to that of the regional or inter-regional (Sindbæk 2013). Out of this primary analytical scale has come a particular interest in understanding processes of collective action and social transformations (Gjesfjeld 2015; Mills, Clark, et al. 2013; Mizoguchi 2009). Tilly (1978, 1998a, 2002), in building on the catnet concept, posits that two analytical dimensions are particularly apt for studying the organization of

collective action and social transformations at broad geographic and demographic scales. Tilly recasts the ‘cat’ component of catnet as categorical identification and the ‘net’ component as relational identification. The next section discusses these uniquely relational analytical dimensions.

2.3.3 Social Transformation through Relational and Categorical Identification

Harrison White has made a powerful distillate of the most insipid wines in the sociological cellar – group taxonomies. There we find only two elements. There are categories of people who share some characteristic...A full-fledged category contains people all of whom recognize their common characteristic, and whom everyone else recognizes as having that characteristic. There are also networks of people who are linked to each other, directly or indirectly, by a specific kind of interpersonal bond (Tilly 1978:62)

If the networks present in a social system are nearly endless, how does one wade through such a morass to define specific network layers that might be sensitive features in explanations of group contact, continuity, or change? Here, I follow Peebles (2011, 2018) in turning to a theoretical perspective that builds on the work of historical sociologists and political scientists studying collective action and social movements among large groups of people – many of whom are related in academic genealogy to Harrison White (Diani 2007; Emirbayer and Goodwin 1994; Fuhse 2012, 2015; Nexon 2004, 2009; Stokke and Tjomsland 1996; Tilly 1978, 2001a, 2002, 2004; White 1992, 1993, 2008a, 2008c; White and Lorrain 1971). For collective social action, or the converging of large numbers of individuals toward a common outcome, to occur it must be organized. Organization refers to the extent of common identity and unifying structure among the individuals in a population (Tilly 1978). Through the catnet concept, organization can be thought of as operating primarily along two analytical dimensions: relational identification

and categorical identification. These concepts are discussed at length by Peeples (2011:17-38; 2018:24-39) and as a result are only presented in abridged form here.

Relational identification refers to a process through which individuals identify themselves and others with larger social groups based on their positions within networks of interpersonal interaction and are forged out of direct and indirect connections among people (Peeples 2018). Routine social ties in this regard may be formed through co-residence, co-activity in work parties, kinship obligations, or friendships, for example. Activities such as exchange or sport contests that are more limited in frequency may be less influential in forming relational ties, but are important because they connect distinct social settings that may otherwise be partially or wholly separate, forming ‘weak tie’ relationships (Granovetter 1973; Peeples 2018).

Categorical identification, on the other hand, is a process through which individuals identify themselves and others with larger groups based on perceived similarities with socially defined categories or social roles to which one can belong (Peeples 2018). Categories are usually named social entities that are not built out of direct or indirect relations. As a result, symbols are used in order to facilitate recognition (Calhoun 1993). Formal categories might include political organizations, religious affiliation, genders, artisanship craft, clan or moiety, and the like. Categorical identities are not a simple extension of relational ties because they are defined without direct reference to the internal relations among individuals (Peeples 2018; Stokke and Tjomsland 1996). Categories may therefore be manipulated and used strategically by individuals. Competition, stress, or conflict may lead to increasing pronouncement of categorical identities at multiple scalar levels. Some categories may be resistant to change as a result of being rooted in acculturation, socialization, and learning (Jenkins 2000, 2004).

Through explicit consideration of the interplay between relations and categories, it is possible to understand how social transformations originate and spread (Mills, Clark, et al. 2013; Nexon 2009; Peeples 2011; Tilly 1978; White 2008a). Proponents of the relational/categorical identification distinction argue that social transformation only occurs through social movements resulting from sustained collective action, or when there is parity in the scale of relational and categorical identification among individuals across broad demographic and geographic scales. That is, the extent to which a group is characterized by both strong relational networks and a high degree of categorical homogeneity provides a means of assessing the potential for larger scale collective action, the formation of social movements, and the enacting of social transformation (Peeples 2011, 2018; Tilly 1978:62-69). Collective action may be rooted in an evolutionary perspective, where individuals overcome rational economic obstacles to cooperation through repeated relational interaction (Blanton 2010, 2011; Blanton and Fargher 2009). However, social movements also depend on groups that share common identities that extend beyond any specific action or protest (Tilly 1978). In leading to social transformation, social movements “invoke new or altered social identities while at the same time reconfiguring the social, economic, and political relationships among people” (Peeples 2011:25). Such social transformations are one possible outcome following culture contact.

The relational/categorical distinction to the analysis of social change presupposes the presence of multiple, often overlapping networks as being necessary to any understanding of social structure or socio-cultural systems more broadly. Because the end goal of any social transformation is to reconfigure multiple extant relationships, a multilayer network approach is a particularly apt at not only determining if a social transformation did or did not occur but also the particular relational dimensions that may have been motivating or delimiting factors. As a result,

defining individual networks as contributing toward either categorical identification or relational identification provides a firm theoretical grounding to the application of multilayer network analysis methodology.

2.4 Intercultural Communal Coexistence – Linking Culture Contact, Multilayer Social Network Analysis, and Archaeological Evidence

In archaeological contexts, material culture represents a physical manifestation of the stories from which social identity and relational interactions can be gleaned and network relationships can be modeled. Migration represents a critical social context in which to observe the creative refashioning of cultural forms resulting from the intersection of previously separate social networks. As a process, migrations are often guided by networks formed in a stepwise fashion through connections based in kinship, exchange, or other social ties (Mills, et al. 2016). This has led to the use of “network-mediated migration theory” by many anthropologists and sociologists as an alternative to the “rational choice and decision making models” used in other social science disciplines (Brettell 2000:107). A network approach replaces predetermined categories with explicitly defined ties that allow groups to be defined based on social relationships. Social networks are of paramount importance for navigating culture contact during communal migrations. Migrants must adapt to a new cultural and natural landscape where information and interaction with existing groups can ease or antagonize settlement. Interaction networks and identification networks are sensitive indicators of the negotiation of social and economic systems by indigenous and migrant peoples (Rockman 2003). Differential positions of influence within a network can be elucidated through this approach by analyzing the locations of individual, household, or community nodes with respect to each other. In this way, networks may reveal the nature of *intercultural communal coexistence* between cultural groups. Intercultural

communal coexistence, as used here, refers to the synchronous habitation of lineally asymmetrical groups in proximity. It is not deterministic of peaceful or tolerant relations. Following culture contact, individuals, communities, and households pursue various relational and identification strategies in multicultural environments (Lightfoot 1995). Due to archaeology’s focus on material culture remains, attempts to elucidate ideological strategies of multicultural coexistence are eschewed in favor of elucidating behavioral strategies of multicultural coexistence at the regional scale. That is, expectations are offered here that seek to characterize communal behavioral strategies in the negotiation of a multicultural social and economic environment following cultural contact. More specifically, a multicultural environment is argued here to manifest in four general forms based on the expectations in Table 2.1. These general forms of intercultural communal coexistence are drawn heavily from Peoples’ (2011, 2018) reformulation of Tilly’s (Nexon 2004, 2009; 1978) insights regarding collective action and social transformation processes.

<i>Communal Coexistence Trend</i>	<i>Depth of Relational Interaction</i>	<i>Categorical Identities Similarity</i>
Pluralistic Coexistence	Absent or Limited	Low
Accommodative Coexistence	Moderate to High	Low
Integrative Coexistence	Absent or Limited	Moderate to High
Ethnogenesis	Moderate to High	Moderate to High

Table 2.1 Matrix of expectations for intercultural communal coexistence strategies

Expectations for communal social trends are based on whether or not social and economic relational interaction between communities occurs more often than not and whether categorical identities between communities are more similar than they are different. Depth of relational interaction is linked to the concept of relational identification. Because of the focus on eliciting behavioral strategies in the negotiation of a multicultural social environment, relational interaction captures networks of direct or indirect interpersonal interaction. Relational

identification is then inferred. Categorical identities similarity is linked to the concept of categorical identification and seeks to assess the behavior of indexing extant social categories. Relational interaction and categorical identity similarities are assessed through an analysis of the positioning of a community node in individual network layers. That is, two communities would be considered to have absent or limited relational interaction if a proportional majority of proxy evidence for interaction suggests that communities are divergent as opposed to convergent. Low categorical identity similarity would be assessed if proxy evidence for the presence of social categories among two sites are proportionally more different than they are similar.

Among large groups of individuals who engage in direct or indirect interaction infrequently or never and who maintain categorical distinctions, collective action or social movements are likely to be rare if not non-existent. Such social settings following culture contact would therefore be characterized by *pluralistic communal coexistence*. A modern correlate to a pluralistic social setting following culture contact would be a ghetto, migrant camp, enclave or the establishment of a commune. With an absence of either shared identification categories or routine pathways of interaction, individuals in these circumstances will tend to be focused on their own or their group's interests, with little desire to engage in inter-cultural dialogue or categorical identities (Nexon 2009). An archaeological correlate to pluralistic coexistence is the Tiwanaku colonial expansion into the Middle Moquegua Valley sector of the Osmore drainage between the 7th and 11th centuries A.D. Tiwanaku occupations in the region were restricted to four large town sites, "suggesting insularity and separation from the valley's indigenous inhabitants in the surrounding countryside. Like present-day diaspora communities, Tiwanaku colonists looked homeward and avoided transculturation with peoples of the local indigenous

tradition, and local peoples likewise did not adopt Tiwanaku cultural practices nor, it appears, live or intermarry with Tiwanaku settlers” (P. S. Goldstein 2015:9204).

On the opposite end of the intercultural communal coexistence spectrum is *ethnogenesis*, or the refashioning of traditions between communities to form a durable group identity, which is marked by both engagement in relational interaction more often than not and a proportional similarity of categorical identities among cultural groups (Hill 2013). The cost of cooperation in these circumstances is low due to the strength of overlapping network ties. Any tendencies for sub-divisions to form within relational networks is also low as a result of the high degree of categorical commonality (Peeples 2011). Examples of ethnogenesis in communal coexistence following cultural contact include resettled farmers forming the Cahokia polity (Alt 2006; Pauketat 2003; Pauketat and Emerson 1999), the polyethnic community formed by immigrants from the South Sulawesi mainland and indigenous peoples on the island of Bonerate, Indonesia (Broch 1987), and in aggregated communities during the Linden and Pinedale phases (1200 – 1325 A.D.) of the Silver Creek Area among the Western Pueblos (Mills 1999; Stone 2003).

Intercultural settings characterized by sparse social ties but strong similarities in categorical identities following culture contact are referred to here as instances of *integrative communal coexistence*. While common categorical identities may lead to rapid, intercultural joint-action, a lack of clearly defined pathways for relational ties beyond normal daily social and economic routines result in challenges to sustaining collective action that act to prohibit social transformation or ethnogenesis. Such settings may be characterized by a downplaying of categorical distinctions in public settings, but a maintenance of those distinctions in private social settings, and a lack of routinized direct or indirect relational interaction. Symbols can be used in a manipulative framework by elites to encourage integrative communal coexistence

among heterogeneous populations. For example, elites may use symbols to incite shared feelings of belonging but by otherwise maintain the status quo. Such a strategy was employed by elites in the Naco region and La Sierra polity of Prehispanic Southeastern Mesoamerica and likewise by elites during the Uruk expansion in Early Mesopotamia (Emberling 1997, 1999; Schortman and Urban 1992; Schortman, et al. 2001).

A fourth and final manifestation of intercultural communal coexistence occurs in social settings following culture contact where relational transaction costs are relatively low but where heterogeneous or exclusive categorial identities delimit the extent of collective action or social movements. These settings are characterized as *accommodative coexistence*. Collective action may be limited to sub-divisions within densely relational networks that do share common categorial identities as opposed to spreading across a broader array of actors (Peeples 2018). Examples of social contexts similar in nature to accommodative coexistence include Native Alaskan men and Native Californian women intermarrying and living side-by-side at historic Fort Ross yet maintaining distinct categorial identities as seen in evidence from their habitual daily routines (Lightfoot, et al. 1998). Another example of accommodative coexistence is the reincorporation of Paleoeskimo Frobisher Bay Dorset peoples into interaction networks with other Dorset peoples in the eastern Arctic. Despite increasing interaction with far-flung interaction networks after more than 200 years of apparent isolation, Frobisher Bay Dorset peoples maintained a distinctive stylistic material culture, and therefore categorial, identity (Odess 1998). Finally, Grasshopper Pueblo witnessed an in-migration event wherein migrants maintained categorial distinctions as seen in architectural and pottery style despite living side-by-side and participating in the construction of new room blocks and pit structures (Stone 2003).

An intercultural communal coexistence framework is therefore grounded in the analysis of multiple layers of network relationships. In particular, categorical and relational layers are argued to be critical lenses with which to model behavioral response trends to multicultural regional cohabitation, thereby necessitating a multilayer network analytical framework. Traditional attempts in this regard using concepts such as assimilation or hybridity are generally ill-suited to grasp the complex dynamics of multicultural social settings (Kent 2002; Rumbaut 2015). By instead focusing on relations and categories, it is possible to both problematize the interplay of multiple lines of evidence as well as parse the complexity of multicultural social contexts. Archaeological settings in particular are uniquely suited to explore long-term trends in networks of social interaction and categorical identification, majority-minority power dynamics, and negotiations of identity politics. It is therefore possible to examine how communities constructed social, economic, and other relational networks before an in-migration and capture communally based responses to multicultural society after cultural contact.

2.4.1 Material Culture Correlates to Intercultural Communal Coexistence

If intercultural communal coexistence consists of behavioral response trends to multicultural regional cohabitation following culture contact as diagnosed through a multilayer network analysis of relational and categorical similarities, what specific lines of evidence are able to be used to identify such trends in the archaeological record? As discussed in the preceding section, many such trends have been identified already. Each of the anthropological or archaeological examples for the various communal coexistence trends discussed previously rely on multiple lines of evidence to identify both categorical and relational lines of evidence. Here, I discuss lines of evidence that may be used in a multilayer network analysis of intercultural

communal coexistence as well as introduce the specific lines of evidence used in this dissertation in a Late Prehistoric central Illinois River valley archaeological case study.

A common theme in archaeological examples discussed in the previous section is using stylistic and technological dimensions of material culture to infer the presence of migrants or heterogeneous populations and therefore the occurrence of culture contact. The presence of a migrant population is often bolstered with osteological evidence such as analysis of cranial morphology, mitochondrial DNA, or dental strontium signatures. From these lines of evidence, it is possible to model host and migrant populations as lineally distinct. Material culture style may then be used to model categorical identities, and technological choices related to material culture may be used to model relational identification and interaction. Exchange of material culture as assessed via style, technological choices, or geo-chemical patterning is another tool with which to model relational interaction. In each of these cases, it is assumed that as different layers of data converge among communities, so does the likelihood that individuals from those different communities engaged in more frequent relational interaction and were characterized by a higher degree of categorical similarity.

The key principals discussed in this chapter are applied in the rest of this dissertation to an archaeological case study across the Middle to Late Mississippian transition in an archaeological region known as the central Illinois River valley (or CIRV; circa 1200 – 1450 A.D.), which is briefly summarized here. The CIRV is characterized by a suite of large, mounded and often palisaded towns, smaller villages, and outlying sites that are primarily dotted along the western bluff edge of the Illinois River valley expanse. *In situ* social dynamics are argued to be largely responsible for the Mississippianization of the region beginning circa 1050 – 1100 A.D. (Bardolph 2014; Bardolph and Wilson 2015; Friberg 2018; Steadman 1998; G. D. Wilson, et al.

2018). Beginning in the late 13th century, Oneota peoples began an expansionary process out of an upper midwest core and into the lower and midwest and central plains (Hollinger 2005; Pugh 2010). Mississippian peoples in the CIRV, which represents the northern frontier of contiguous Mississippian territorial expansion, maintained their positions in fortified temple mound centers and outlying sites and entered into a period of regional cohabitation with an intrusive Oneota population. Available data from CIRV settlements exhibit varying degrees of intermixing between Mississippian and Oneota material culture, intermixing that has had proved to be a quandary to the taxonomic models that define these distinct cultural groups. Tantalizing evidence for cultural mixing is most readily apparent in the mixing of ceramic traits. Because of the availability of an array of ceramic data from sites across the geographic and temporal expanse of the CIRV, ceramic industry is the focus of modeling relational and categorical similarity among sites.

In assessing intercultural communal coexistence in a Late Prehistoric CIRV case study region, connections indicative of three types of relationships gleaned from ceramic industry are considered here: i) exchange relations, overlapping resource exploitation zones, or raw material acquisition information sharing indicated by geochemical source groups (Gjesfjeld 2015, 2018; Golitko and Feinman 2014); ii) shared categorical identities as evidenced by proportions of stylistic decoration similarity (Borck, et al. 2015; Mills, Clark, et al. 2013; Mills, Roberts Jr., et al. 2013) and iii) relationships of descent or shared learning mechanisms based on relative technological similarity in type-attributes constrained by social, as opposed to engineering, forces (Eerkens and Bettinger 2008; Peeples 2011). All three network models chosen for this research constitute frameworks for constructing relationships between humans, wherein edges between sites act as statements of probability that a relationship existed. Pottery exchange,

overlapping resource exploitation areas, or raw material source location information sharing indicate episodes of direct or indirect economic relational interaction (Brose 1994; Brown 2004; Zvelebil 2006). Repeated relational interaction leads to pathways for relational identification. Categorical identities are mechanisms for people to index ascription to common social units, express solidarity, and nonverbally communicate social information (Braun 1985; Wiessner 1990). Distinctive combinations of technological characteristics indicate shared relationships of learning and the expression of social information (Herbich 1987; Stark, et al. 1998).

Because each of the different network layers utilizes a distinct theoretical bridge in linking archaeological evidence to either relational or categorical identity, a more thorough discussion of those theoretical bridges is provided in each individual chapter. A brief description is provided for each here, however. Relational identification through social interaction is assessed across three distinct analytical layers. The first two layers are assessed by using technological characteristics of two distinct vessel classes – domestic cooking jars and plates primarily used in the serving of food. By drawing on a theory of cultural transmission, it is possible to differentiate between variation in vessel technological attributes mainly affected by engineering constraints from that affected mainly by social constraints (Eerkens and Bettinger 2008). Commonality between site assemblages in technological attributes of pottery is therefore argued to be indicative of either historical relations of descent or shared learning mechanisms (VanPool 2008). This ensures that similarities in relational social ties are not confused with similarities caused by engineering constraints in the execution of a given artifact attribute. The resulting networks of interaction through cultural transmission are discussed in Chapter 5. Another means of establishing relational identities is through compositional analysis. Proportional similarity among sites of membership in geo-chemical compositional groups may

show that potters and potter communities not only resided within a particular geographic location, and perhaps engaged in exchange relationships, but also shared specific information about how to procure and prepare their raw materials. Thus, compositional analysis provides an essential additional objective measure to assess not only variation in the transmission of information related to pottery making but also to model economic relationships of exchange. Network models of economic interaction are discussed in Chapter 7. Finally, categorical identities as assessed via stylistic designs incised or trailed on the outflaring rim of the plate vessel class are analyzed in Chapter 6. As primarily serving vessels, plates are often used in highly visible contexts. Stylistic design groups are therefore argued to be reflective of social roles or social groups to which individuals may index belonging because the process of symbolization must be used to facilitate the recognition of members compared to non-members.

Comparing models of communal coexistence against network models of exchange, interaction, and identification enables economic, social, and identity politic relationships to be contextualized relative to one another. A multilayer perspective allows these relationships to then be explored in aggregate and is the topic of Chapter 8. In this way models of human behavioral relationships can lead to a systemic understanding of the impact of a migration process on a whole society by understanding individual networks and how they influence and co-construct each other (Szell, et al. 2010).

On a regional level, this research contributes to an understanding of social structure during the Late Prehistoric period in the U.S. Eastern Woodlands. This critical period in American prehistory preceded the collapse and abandonment of fifteenth century chiefly polities in the central Illinois River valley (Esarey and Conrad 1998), the American Bottom (Cobb and Butler 2002, 2006), the lower Ohio valley and central Mississippi valley (Cobb 2005), and the

lower Savannah River drainage (Anderson, et al. 1995). While many analyses of societal collapse focus on environmental factors (Bird, et al. 2017; Weiss and Bradley 2001) this research offers an alternative perspective by analyzing network models of social relations prior to abandonment and population displacement (Borck, et al. 2015). Problematizing and integrating social interaction and categorical identification with larger-scale political and social change is fundamental for understanding how culture is created, continued, and contested by people in the past and the present.

CHAPTER 3 REGIONAL AND CULTURAL BACKGROUND: LATE PREHISTORY IN THE CENTRAL ILLINOIS RIVER VALLEY

3.1 Introduction

Exploring social relationships between communities presupposed a basic knowledge of those communities themselves. Since potter communities are used here as a proxy measure for the larger, spatially bounded settlements within which they were nested, it is necessary to provide a proper context and association. This chapter presents an overview of the Middle Mississippian and Oneota cultural traditions more generally as well as the occupation of the central Illinois River valley by these societies primarily through the lens of the settlements whose interrelationships form the focus of interest in this dissertation. The archaeological and cultural background of this region has been discussed from a number of vantages previously. These include, but are not limited to, considerations of bioarchaeology (Bengtson 2012; Hatch 2015; Steadman 1998, 2001, 2008; Strezewski 2003; J. J. Wilson 2010), subsistence patterns (Tubbs 2013; Vanderwarker and Wilson 2016; Vanderwarker, et al. 2013), residence patterns (Painter 2014), settlement patterns (Harn 1978, 1994), chronology (G. D. Wilson, et al. 2018), or in general taxonomic definitions and descriptions of Middle Mississippian and Oneota central Illinois River valley expressions (Cole and Deuel 1937; Conrad 1989, 1991; Esarey and Conrad 1998; Santure, et al. 1990). This chapter endeavors to synthesize much of this information to enable a contextualized interpretation of the results of this study. All radiocarbon assay calibrations are presented courtesy of OxCal 4.3 (Reimer, et al. 2013).

Because this study focuses on relational connections among communities, environmental factors are generally de-emphasized in the succeeding substantive analytical chapters.

3.2 Geographic Setting

The archaeological region known as the central Illinois River valley (hereafter CIRV; Figure 3.1) encompasses a 210 km stretch of the Illinois River extending approximately from the modern village of Hennepin, IL southerly to the village of Meredosia, IL (Harn 1994:4-9); though the Late Prehistoric CIRV is centralized in an approximately 137 km stretch of the Illinois River from the present town of Peoria, IL southerly to the unincorporated village of Chambersburg, IL. This archaeologically defined region has been referred to in the past as the Central Illinois Valley (Conrad 1991:120), but has more recently referenced to by the moniker used herein. Modern topography, surficial geology, and hydrology is largely a product of

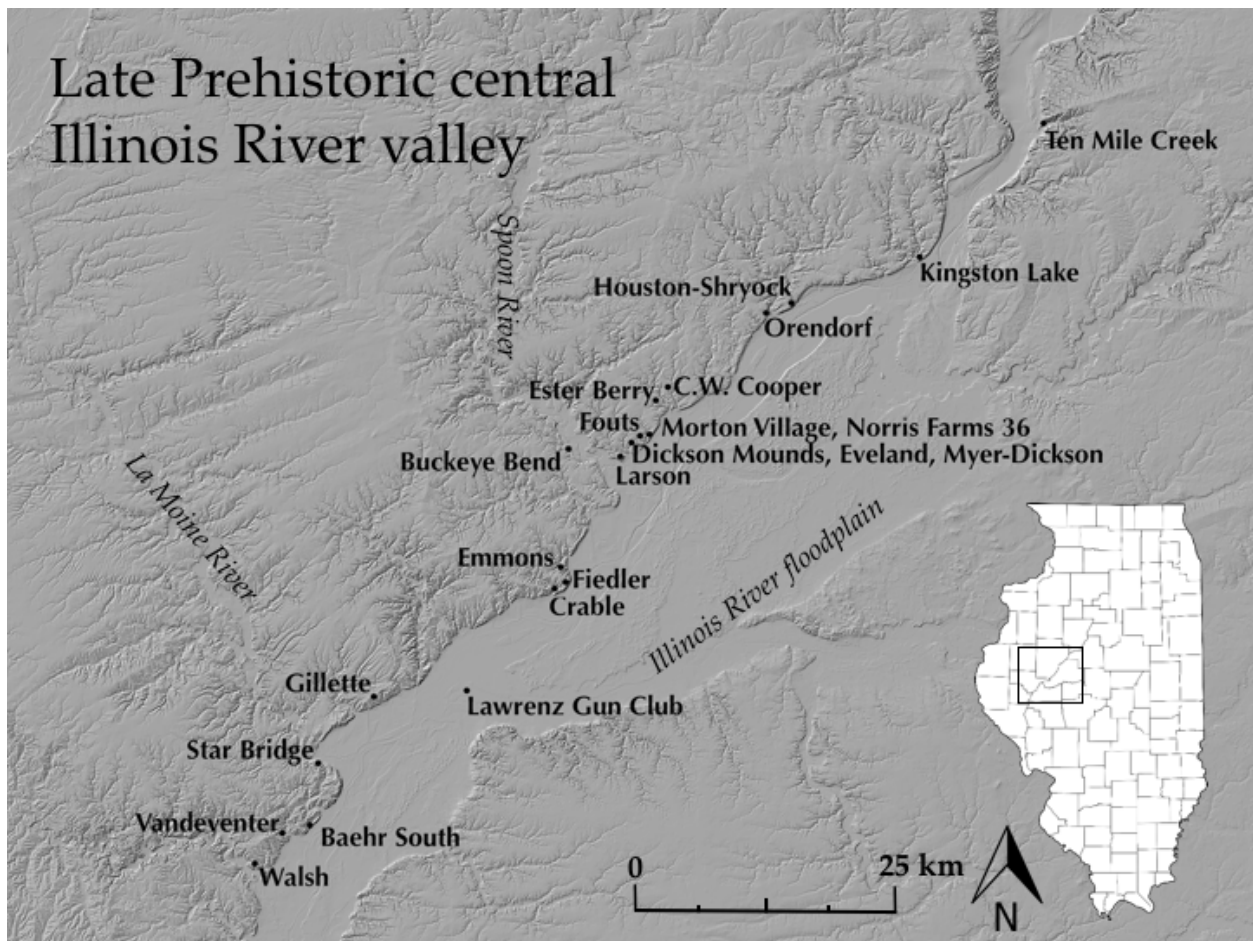


Figure 3.1 Lidar map of, and archaeological sites under consideration in the Late Prehistoric central Illinois River valley (circa 1200 – 1450 A.D.)

Illinoisan and Wisconsin glaciation, which spanned in varying levels of intensity from approximately 250,000 to 13,600 years before present (Wiggers 1997). The CIRV is the southeastern part of the Galesburg Plain, which encompasses a 20,700 km² landform including the central Illinois and Mississippi River valleys from the beginning of the lower Illinois River valley northward to the Green River drainage system (Leighton, et al. 1948). The Illinois River and associated tributaries in the CIRV, including the Spoon and La Moine Rivers, are characterized by a relatively slow current, with an expansive Illinois River floodplain distinguishing the physiographic region from northerly, southerly, and easterly environs.

Climatic conditions in the CIR during the Late Prehistoric period were largely similar to the climate at the turn of the 2nd millennium A.D., indicating that a wide variety of floral and faunal resources were available to support human occupations (F. B. King 1990). Harn (1978:237-241) and Harn (1994:4-9) provide a rich description of the physiology and natural history of the region. The following two sections describe the Mississippian and Oneota archaeological traditions more broadly before returning to the central Illinois River valley case study in Section 3.4.

3.3 The Mississippian Tradition

Different, yet linked, societies bearing traits such as intensified maize horticulture and agriculture, fortified communities with large earthen mounds, social ranking, and a set of rituals and symbols concerned with fertility, ancestors, and war largely characterizes the Mississippian cultural development (Blitz 2010). Extending from central Illinois and Wisconsin to the Gulf coast and east to Florida and North Carolina and dating to approximately AD 1000-1550, the Mississippian phenomenon constitutes the social melding and integration of different groups

through contact, coalescence, and population movement that supported newly formed elite hierarchies. Archaeologically, variation in Mississippian complexity is manifest in polity scales, settlement tiers and the built and perceived landscape, the organization of labor, mortuary ritual and ideology, and tribute and feasting (Cobb 2003). Elites are thought to have attained and maintained their largely knowledge based authority through warfare related activities, ritual feasting, ceremonial smoking, and public display of goods that imbue prestige, with ethnographic accounts explaining a duality of conception in the political sphere of Mississippian society between war and peace (Dye 2013). Significant Mississippian communities are often marked by large earthen mounds, an open plaza around which structures were arranged, and likely dominated regional or local settlement hierarchies. Household arrangement around plazas is also featured prominently in many non-mounded, secondary communities. While smaller communities and individual households may have been dispersed across the landscape for economic reasons, members of each community are thought to have engaged in the same basic subsistence and household activities (Schroeder 2004). Architectural variation encompasses wall trench and occasionally individual post structures, smaller functionally distinct structures such as sweat lodges or storage facilities, and prominent mound-top structures. Migration, warfare, exchange, and the movement of exotic raw materials, finished artifacts, ideas and even subsistence items structure the succeeding discussion of Mississippian societies.

An order of magnitude larger than any other Mississippian society, Cahokia represents not only the beginning but can also be argued to be the apogee of Mississippian society. Research amongst Mississippian societies often implicates Cahokia due to its early emergence, size, and complexity (Benson, et al. 2009; Emerson 2012; Emerson and Lewis 1991; G. R. Milner 1990; Pauketat 1994, 2003; Pauketat and Emerson 1991, 1997; Schroeder 2004). The

founding of Cahokia catalyzed, or was catalyzed by, large scale population movement within the American Bottom region and an influx of indigenous and migrant peoples to Cahokia itself. Large numbers of kin groups became attached to Cahokia and began a dynamic period of cultural negotiation wherein the greatest public works in eastern North America were constructed in this planned but accretional site (Alt 2006; Pauketat 2003). Outside of Cahokia proper, the American Bottom region witnessed the large scale abandonment of pre-Mississippian villages and the appearance of dispersed Mississippian farmsteads, lower level mound centers and an upland farming community known as the Richland Complex whose culturally pluralistic immigrants negotiated with Cahokians and defined Mississippianism in their own practical terms (Pauketat 2003). Cahokia likely dominated the American Bottom region politically and economically, however relatively autonomous mound centers and their respective territories were perhaps present throughout the Mississippian period (G. R. Milner 1990). While authoritative power presided at Cahokia, rich grave offerings in Mound 72 are considered by Brown (2006) to represent collective, ritual performance with allegorical implications wherein structural power disregards any notions of individual hierarchy in favor of communal celebration of Mississippian ideology. Symbols of prestige seem to have increased in importance at Cahokia over time. Kelly (1991a) explains that Cahokia emerged as a major trade hub as a result of the lack of high quality raw materials in the American Bottom floodplain and that population increases led to mechanisms wherein non-elite were able to obtain chert and salt, thereby circumventing elite control, playing a role in the de-emphasis of utilitarian good exchange overtime, and likely contributing to the increase in exchange of prestige-imbuing goods. Increasing interaction with southern Mississippian groups also occurred overtime at Cahokia according to Kelly and is seen in a strong congruence of ceramic style and in ceremonial ware.

Brown and Kelly (2000) posit Cahokia as a foundational nexus in the formative processes of the Southeastern Ceremonial Complex, a continuity in belief systems and iconography in the Mississippian Period, and a Copper-Dominated Horizon between 1250 and 1350 A.D. as seen at Etowah, Moundville, and Spiro. Together, this indicates the material and ideological interconnectedness of Mississippian societies as emanating from an incipient American Bottom region.

Hierarchical relationships and cultural complexity were not uniform amongst Mississippian societies, and the nature of that variation has fundamental ramifications for understanding social interaction, organization, and identity formation at vertical and horizontal levels. Beck (2003) offers a model of Mississippian chiefly variability wherein chiefdoms form through hierarchically organized staple finance consolidation via either coercive expansion or persuasive aggregation. The directionality of power is either Constituent (lower level leaders toward higher) or Apical (higher level leader(s) toward lower). Power is often thought to be wrested at either one or two levels above the household or community in Mississippian societies, forming a simple or complex chiefdom with paramount chiefs presiding over complex chiefdoms (Blitz 1999; Earle 1989; Pauketat 1994). Chiefdoms, furthermore, are considered a highly unstable and dynamic form of political organization. Blitz (1999) proposes that this political dynamic consisted of oscillations between dispersed and concentrated regional power centers, where mound-affiliated political units assembled and disassembled to create polities of different size and complexity in a fission- fusion process. An important component of chiefdoms, or middle complex societies in general, is their kin-based organization. Knight (1986, 1990) argues that this feature of ethnographic and ethnohistoric descendants of Mississippian chiefdoms in the southeast resulted from an aristocratic organization likely evolving out of a uniform base of

ranked exogamous matrilineal moiety systems. As such, kin relationships were a fundamental guiding agent to not only inter-group but also intra-group political, economic, and social interactions in Mississippian societies.

Variation is inherent in Mississippian groups both inter- and intra-regionally. Mississippian mound centers vary not only in size and political economy but also in specific functionality. Some mound centers hosted large swaths of the population while others were primarily ceremonial in nature and show evidence of only limited occupation (Anderson 1991; Brown 1996; Conrad 1991; G. R. Milner 1986). Regardless, these mound centers played host to large gatherings of otherwise dispersed Mississippian peoples wherein elite and non-elite alike interacted and negotiated an ever changing dynamic of local Mississippian ideology (Sullivan and Harle 2009). One unique Mississippian site at the far northern fringes of the Mississippian sphere, Aztalan, may have functioned as a conduit through which both material goods and information were directed to elites in the American Bottom, as an outpost for Mississippianization, a trade hub, a successful proselytization of indigenous Woodland peoples, a movement/expansion of already Mississippianized Woodland peoples from Northern Illinois or as a hybrid resulting from Middle Mississippian and Effigy Mound peoples (L. G. Goldstein and Richards 1991). The case of Aztalan illustrates the importance of understanding local and regional contexts in investigations of the nature of any specific Mississippian center and the locality under its purview.

While much focus has been placed on the major Mississippian centers, the bulk of the Mississippian population and mainstay of local Mississippianism, as an ideology, was housed in the peripheries in the form of small communities or farmsteads. The Mississippians who lived at these sites are known to have assisted through labor and goods in mound construction,

communal hunting forays, agricultural field preparation, and cultivation of community fields whose products fed the disadvantaged in society in addition to those of a high social standing (Scarry 1999). Elite influence did not penetrate into these peripheral areas evenly. In a case study of Mill Creek chert hoe production and exchange, Cobb (2000) shows that while elites may have exerted some influence on the distribution of these tools in their respective areas of purview, that influence did not penetrate the southwestern Illinois locus of their production. Smith (1995) contextualizes Mississippian household studies by explaining five pertinent levels of analysis: seasonality, activities, size/composition, duration and context and provides a case study at the single household Gypsy joint site. Finally, Pauketat (1989) offers a model of ceramic refuse formation processes in order to determine the duration of small habitation sites during the Lohmann and Stirling phases of the American Bottom region, and then uses the model to test the economic integration of these largely self-sufficient homesteads within a larger Cahokia centered settlement hierarchy.

3.4 The Upper Mississippian Tradition and the Oneota

The upper Mississippi watershed, or Prairie Peninsula, that encompasses parts of the present day states of Minnesota, Wisconsin, Iowa, Illinois, Indiana, Missouri, Kansas and Michigan, was once home to a suite of peoples who, by virtue of shared cultural elements such as shell-tempered and wet-paste decorated globular pottery, a diversified economic regime incorporating maize, beans and squash agriculture, and an adherence to broad symbolic activities, have been established by archaeologists as Upper Mississippian peoples (Fisher 1997; McKern 1939; Swartz 1996). More specifically, archaeologists refer to the subset of peoples living in the Prairie Peninsula from approximately A.D. 1000 – 1700 as the Oneota. Various

accounts have been developed that attempt to account for the emergence of these peoples from the materially, economically, and ideologically different Late Woodland peoples who preceded the Oneota occupation of the region (Benn 1995; Gibbon 1972; Griffin 1960; Theler and Boszhardt 2006), however, little consensus is generally agreed upon.

Twenty years after W.C. McKern (1945) used his Midwestern Taxonomic System to define Upper Mississippian peoples based on similarities in pottery style and form, Brown (1965) examined the cultural development and diversity of the peoples of the Prairie Peninsula, suggesting an assignation of this area as an interaction zone with variations in material culture and subsistence practices being the result of adaptation to various ecological niches. These Culture-Historical and early Processual definitions are, largely, still the basis for classifications of archaeologically recovered materials from the Late Prehistoric period in the Prairie Peninsula today, with the focus on ceramic assemblages produced by the peoples of this region leading to the moniker 'pottery culture' for the Oneota in general (Berres 2001). Based largely on changes in ceramic decoration, Overstreet (1997) distinguishes four Oneota Horizons: Emergent (A.D. 950 – 1150), Developmental (A.D. 1150 – 1350), Classic (A. D. 1350 – 1650), and Historic (post A.D. 1650). Brown and Sasso (2001) posit a basic continuity of subsistence and settlement patterns overtime, a distinctive shift to the ethnohistorically known lifeway pattern occurring around A.D. 1450, and a relative uniformity in material culture following the circa A.D. 1500 disappearance of Mississippian culture in the eastern prairie region. In focusing specifically on changing architectural patterns, Hollinger (1995) hypothesizes a relationship between Oneota architecture and post-marital residence patterns wherein a shift from patrilocal to matrilocality residence occurred during the Classic Horizon and a reversion to patrilocality during the turmoil

following European contact. This shift residence patterns has been accepted by other Oneota scholars (Schneider 2015).

Inter- and intra-group interaction patterns are fundamental components not only to the nature of Oneota variation but also to the appearance of the Oneota lifeway in various regions and localities. Emerson (1999) models a process of tribalization in northern Illinois based on asymmetrical interaction with chiefly groups in the region producing the rapid expansion and correspondingly rapid collapse of the Langford tradition. Gibbon (1995) argues against a single Oneota mode of exchange because exchange in tribal societies plays simultaneous social, political, ideological, and economic roles and shifts in sometimes subtle and sometimes dramatic ways with the vicissitudes of broader social and natural environments. O'Gorman (2010) outlines the interweaving relationship between community, identity, and dwelling based on the presence of longhouses in the La Crosse locality during Oneota occupation (circa A.D. 1300-1650). While the Oneota expression in the central Illinois River valley has gained a reputation for experiencing significant rates of violence and trauma (Hatch 2015; G. R. Milner, et al. 1991; Vanderwarker and Wilson 2016; G. D. Wilson 2012, 2013), recent examination from Oneota skeletal remains from Winnebago phase Wisconsin suggest that violence may have been the norm among Oneota peoples as opposed to anomalously intensive in Late Prehistoric west-central Illinois (Oemig 2016).

3.5 The Mississippian Period central Illinois River valley

The central Illinois River valley's position at the eastern edge of the Prairie Peninsula and proximity to the Mississippian cultural core in the American Bottom situated this archaeological region at the intersection of Plains-Prairie-Woodland lifeways and booming agricultural

complexes during the beginning of the first millennium of the common age. A host of contact scenarios have emerged to explain the Mississippianization process in the CIRV and the Midwest more broadly. These scenarios include *in situ* emulation based on limited direct engagement, proselytization by small cadres of Mississippian emissaries or missionaries, or whole-scale movements of Mississippian peoples from Cahokia and other American Bottom sites (Bardolph 2014; Conrad 1991; Delaney-Rivera 2007; Emerson and Lewis 1991; Harn 1978; Pauketat and Emerson 1997; Steadman 2001; Stoltman 1991, 2000). While no general consensus exists, there is little doubt that this process is fundamentally related to entanglements among polity, cultural contact, frontier, and expansion.

Extant Late Woodland groups in the CIRV prior to the Mississippianization are posited to have comprised two contemporaneous group: Bauer Branch in the south and Maples Milles in the north (Esarey 2000; W. Green and Nolan 2000). Biodistance indicators suggest that it is these Late Woodland peoples in the CIRV that adopted a maize intensive agricultural subsistence base, new forms of architecture, new ceramic technology and decoration, and new socio-political-religious beliefs and practices to form a unique expression of Middle Mississippian culture (Bardolph 2014; Bardolph and Wilson 2015; Conrad 1991; Steadman 1998, 2001; Vanderwarker, et al. 2013). This cultural expression would thrive in the region from approximately A.D.1100 to perhaps as late as A.D. 1450. The 210 km stretch of the CIRV contains the remains of at least seven fortified Mississippian temple towns and numerous smaller villages and farming hamlets with an hypothesized distinction between Mississippian peoples in the upper portion of the CIRV near the Spoon River and those inhabiting the lower portion of the valley near the La Moine River (Conrad 1989, 1991; Harn 1978, 1994).

The Spoon River Mississippian manifestation is comprised of four well defined phases: Eveland (1100-1150 AD); Orendorf (1150-1250 AD); Larson (1250-1300 AD); and the Marbletown Complex (1300-1400? AD). However, multiple culture-history models have been developed with these dates shifting somewhat overtime (J. J. Wilson 2010:54). The earliest Mississippian phase, the Eveland phase, is marked by the Mississippianization of local Late Woodland Maple Mills peoples, with material culture similar to the Lohmann Phase of the American Bottom (Bardolph 2014; Conrad 1991; Esarey 2000). The type site of the period, Eveland, is believed to have served “as a centralized cemetery linking numerous habitation sites”, and is marked by finely crafted Cahokia-style material culture alongside a minor admixture representative of local Maple Mills ware (Conrad 1989:102). The following phase, Orendorf, is marked by the appearance of the first substantial Mississippian town in the CIRV, the Orendorf site, which underwent repeated episodes of rebuilding and renewal (Conrad 1989:107). Fortifications first appear during the Orendorf phase, suggesting regional strife or the threat of violence. Large platform mounds represent the most obvious difference between the Orendorf phase and the subsequent Larson phase (Conrad 1991; Harn 1994). At least two or three contemporary Mississippian towns existed during the Larson phase, though much of the population resided in dispersed hamlets and farmsteads, some of which had large council houses and mounds of their own. The final Spoon River Mississippian occupation in the CIRV is marked by regional cohabitation with Bold Counselor Oneota peoples, and is referred to as the Marbletown Complex or Bold Counselor phase (Conrad 1991; Esarey and Conrad 1998).

The La Moine River Mississippian expression is poorly studied compared to the Spoon River manifestation and is not as rigidly demarcated into phases as a result (Conrad 1989, 1991; Harn 1978, 1994). The general developmental trajectory, however, mirrors that of the northerly

Spoon River expression and as a result it is the Spoon River phases that will be discussed in more detail below, subsuming a general CIRV culture-history model as presented herein. Conrad (1989, 1991) divides the La Moine River culture into four phases: Gillette (1050-1150 A.D.), Orendorf and Larson contemporary (1150-1300? A.D.), Crabtree (1300-1375 A.D.), and Crable (1375-1450 A.D.). Like the Spoon River variant, the earliest phase, Gillette, is marked by the Mississippianization of local Late Woodland peoples, known as Bauer Branch (Bardolph 2014; Green and Nolan 2000). The following phase is marked by overlapping but contemporary occupations with Orendorf and Larson phase sites to the north, known primarily from a minor occupation of the Lawrenz Gun Club town center and the Star Bridge site (Conrad 1991). While A.D. 1300 marked the appearance of the Bold Counselor Oneota in the Spoon River area, La Moine River Mississippian sites during the coeval Crabtree phase do not show evidence of site level integration until the proceeding Crable phase.

The historical trajectory of Middle Mississippian populations in general in the CIRV is argued to be one of increasing population aggregation and conflict (G. R. Milner, et al. 1991; Steadman 2008; G. D. Wilson 2012). Less important than the elusive causes of the increasing hostilities in the region are the effects of those hostilities on the Mississippians themselves. At least sixteen percent of adults over the age of fifteen years at the large village site Orendorf suffered warfare-related trauma, including scalping, decapitation, inflicted projectile points, and antemortem cranial depression fractures (Steadman 2008:58). Perhaps thirty percent of adult individuals in the Norris Farms #36 cemetery died a violent death (G. R. Milner, et al. 1991). Palisades at numerous sites in the region indicate high levels of endogamous or exogenous threats, as does evidence of a number of burned villages and outlying farmsteads (G. D. Wilson 2012, 2013). Given the widespread evidence for conflict in the region, many scholars have

proposed a socio-ideological system of warriors gaining prestige at all levels of the social scale through warfare and battle; a hypothesis bolstered by widespread evidence for ritual weaponry, iconographic depictions of violence, and human sacrifice seen in Middle Mississippian contexts in the CIRV and elsewhere (Dye 2013; Knight Jr 1986; Maschner and Reedy-Maschner 1998; G. D. Wilson 2012).

Biodistance studies further suggest that social dynamics during the Mississippian periods in the region were most likely the result of *in situ* social and demographic processes as opposed to being the result of gene flow from major centers in the nearby American Bottom (Steadman 2001). Yet, exotic material culture such as marine shell gorgets and Upper Great Lakes copper hairpins and pendants indicate that these populations were very much a part of the widespread exchange network characteristic of Mississippians in other contexts (Brown 2004; Conrad 1989, 1991; Kelly 1991a). As a result, the Mississippian periods of the CIRV are generally characterized by increasing factionalism, conflict, and violence under the auspices of chiefly cycling and power based on *in situ* social processes.

Sometime in the early to mid-14th century, an Oneota group from the north migrated into the CIRV and fundamentally changed the social dynamics of the region (Esarey and Conrad 1998; O'Gorman and Conner 2016; Santure, et al. 1990; Steadman 1998). Known by only five habitation sites and one cemetery, the Bold Counselor Oneota's immigration into the CIRV offers an unparalleled opportunity to study inter-group social interaction within the context of small scale warfare and social stress. Based on biodistance studies comparing the Oneota population interred at the Norris Farms #36 cemetery and CIRV Middle Mississippian burial assemblages, Steadman (1998) concluded that the Oneota group contributed marked variation to the regional gene pool. Coupled with distinct differences in ceramic decoration, architectural,

and certain lithic tool patterns, there is little doubt to the non-local origins of this unique expression of the Oneota lifeway.

For the purposes of this dissertation, time-space systematics will be bifurcated between the phases prior to the in-migration of Oneota peoples into the CIRV (e.g. the Eveland, Orendorf and Larson phases of the Spoon River variant and the Gillete, Orendorf and Larson contemporary, Crabtree of the La Moine variant) and the phase following this in-migration process (Marbletown complex of the Spoon River variant and the Crable phase of the La Moine River variant). This is primarily an effort to best fit models of changing social interrelationships concomitant with the in-migration process and recognizes that prior efforts to classify time-space systematics lack “grounding in empirical data...[and are characterized by a] conflicting series of radiometric dates, which both Harn and Conrad have noted” (Conrad 1991; Harn 1994; J. J. Wilson 2010:53-54). Further, the discussion below follows the culture-history sequence of the Spoon River variant alone, subsuming the evidence from the La Moine River variant. This is partially an effort to present the culture-history of the region as a unified Mississippian sequence despite marked evidence for perhaps competing polities, which is characteristic of Mississippian society in other contexts (Blitz 1999), to situate and contextualize the results and interpretation sections and recognize the efforts of prior archaeological research in the region.

3.6 Eveland Phase (A.D. 1100-1175)

The Eveland Phase marks the beginning of strong Mississippian influence in the CIRV and is named after the Eveland Site (11F353), where those influences are most acute. Quite detailed overviews of the Eveland phase and its sister phase in the La Moine River region, the Gillette phase, are found in Conrad (1991:124-132) and Harn (1991). As a result, an abridged

discussion will be provided here. Eveland is marked by an arrangement of “four elaborate ceremonial buildings and two habitation structures located at the base of the western Illinois River bluff” (Bardolph and Wilson 2015:143). The ceremonial buildings have been interpreted as a council house or earthen lodges and are architecturally characteristic of Middle Mississippian norms in the American Bottom and Lower Illinois River, in stark contrast to local Late Woodland architectural styles (Conrad 1991). Perhaps the most striking evidence of the ceremonial nature of these buildings is a cross-shaped building, which is posited to perhaps have served as a “fire temple” (Conrad 1991:124). Ceramic vessels recovered from Eveland include finely crafted Ramey Incised and Powell Plain jars that date to the Stirling phase component in the American Bottom (Vogel 1975). While the Stirling phase saw the beginnings of massive public works in the form of monumental architecture and infrastructure in the American Bottom, there are no known Mississippian towns occupied during the Eveland phase or Gillette phase. However, the Cahokian florescence in the American Bottom likely accelerated the readiness of local Late Woodland peoples to acculturate to the Mississippian lifeway. The alignment of Eveland phase ceramics with Stirling phase material culture in the American Bottom coupled with recent excavations by the University of California Santa Barbara have led to a revision of the timeline for the Eveland phase from an initial beginning at A.D. 1050 to A.D. 1100 and an ending around A.D. 1200; though the occupational sequence at Eveland may be further refined given the large probability distributions for radiocarbon assays from the site, see Figure 3.2 (Bardolph 2014; Bardolph and Wilson 2015; G. D. Wilson, et al. 2018). As a result of these past and potential future revisions, the socio-interrelationships between the Eveland site and other CIRV sites are considered in this dissertation, despite the general focus here on the later Mississippian phases in the CIRV.

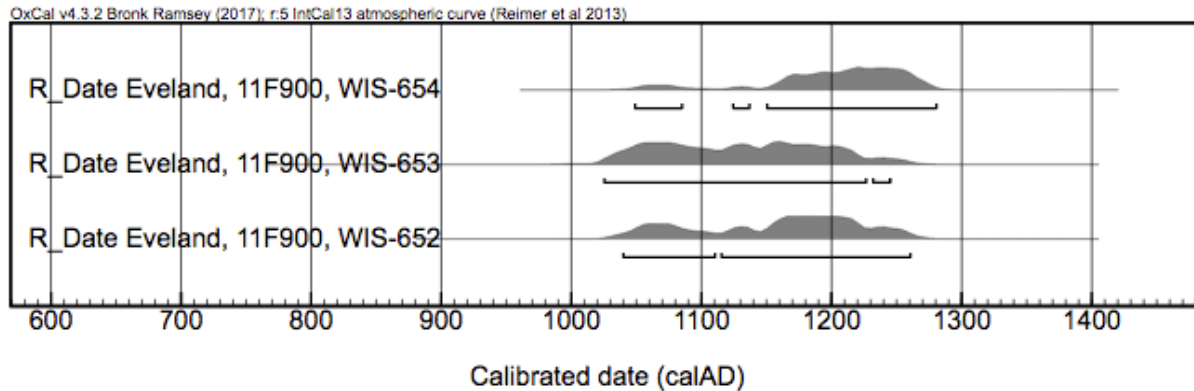


Figure 3.2 Probability distributions of three recalibrated dates for the Eveland site (Bender et al. 1975)

Including the Eveland site, approximately thirteen other sites have been identified by Harn (1991) that date to the Eveland phase. Most of these sites were small homesteads, less than one hectare in size, with a limited number of structures that bear no evidence of rebuilding or extensive occupation (Harn 1991; J. J. Wilson 2010). Much of the material culture remains from these sites, such as Ramey Incised and Powell Plain jars, are quite similar to their American Bottom analogs, but with some deviation in stylistic decoration (Harn 1994). This suggests that perhaps either local potters were expressing and non-verbally communicating local socio-religious symbols onto non-local pottery designs as a means to amalgamate the known with the unknown, or that Cahokian potters were actively negotiating the transmission of culture by conforming to those local socio-religious conventions. Thin section analysis indicates that these vessels were made from locally available clays (Harn 1991:143). Pottery morphology in the region became progressively dissimilar to analogs in the American Bottom overtime, suggesting the increasing importance of local social dynamics and/or waning Cahokian influences overtime.

Recent evidence suggests that the Eveland phase was a “context of converging but still very much entangled Woodland and Mississippian traditions” (Bardolph and Wilson 2015:144). Late Woodland peoples were selectively adopting or emulating aspects of Mississippian

traditions to the south but maintained certain Bauer Branch ceramic traditions at the Lamb site for example; a process that is mirrored among Maples Mills traditions at the Gillette site (Bardolph 2014). This indicates that the Mississippianization process during the Eveland phase was a selective, intentional, and measured process at different sites in the CIRV and that the local social dynamics took early precedence (Friberg 2018). These local preferences in material culture and later mortuary expressions are the basis for an interrelated but perhaps also divergent evolution of the Spoon and La Moine River Mississippian traditions from their humble beginnings (Harn 1994).

3.7 Orendorf Phase (A.D. 1200-1250)

The revision of the Eveland phase timeline to an A.D. 1200 end frame resulted in the concurrent revision of the Orendorf phase to begin at A.D. 1200, though it is possible that the initial development of full-fledged Mississippian culture began during the latter half of the 12th century A.D. based on radiocarbon assays from the Orendorf site in Figure 3.3 (Bardolph 2014; Esarey and Conrad 1998; G. D. Wilson, et al. 2018). The Orendorf phase is known primarily from the type site, the Orendorf site and its adjacent cemetery (Conrad 1991; Esarey and Conrad 1981; Steadman 2008). Orendorf is characterized by a series of four to five distinct settlements that appear to have been constructed over the perhaps 100 year history of the site's occupation (Esarey and Conrad 1981; J. J. Wilson 2010). Information on two of these settlements are of particular importance to this dissertation, Orendorf Settlements C and D. Settlement C forms the primary focus of the unpublished working papers organized by Esarey and Conrad (1981), which is chiefly responsible for information on the phase in general. A report summarizing the Settlement D occupation is as yet forthcoming from the Illinois State Archaeological Survey.

The Orendorf phase marks a number of important distinctions in the Mississippian history of the CIRV. First, the Orendorf site is likely the first Mississippian habitation that conforms to the general expectations of a classic Mississippian town. Settlement D, which is believed to be the earliest occupation, is marked by a distinctive plaza with nearly 100 domestic structures arranged around this central feature of the site (Esarey and Conrad 1981). In addition to the central plaza, Settlements C and D both are enclosed by extensive palisades. Coupled with skeletal trauma and other evidence such as burned structures with intact household assemblages, this suggests that the threat of attack during this phase was very real (Steadman 2008).

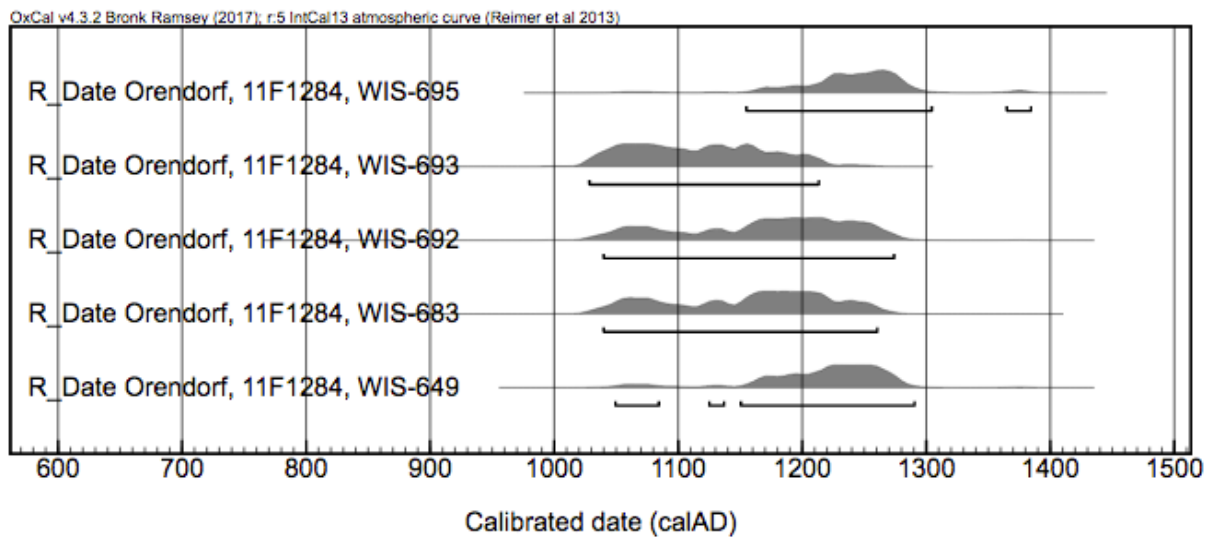


Figure 3.3 Probability distributions of five recalibrated dates for the Orendorf site (Bender et al. 1975)

The shift to a Mississippian lifestyle included a shift to an economic base primarily centered around maize agriculture, deer, fish, waterfowl, and local cultigens to a lesser extent (Tubbs 2013; Vanderwarker and Wilson 2016; Vanderwarker, et al. 2013). Larger populations were able to be supported based on this subsistence regime, with Orendorf Settlements C and D estimated at population figures in the 400-500 range at any given time, making them perhaps two to three times larger than any previous settlement in the CIRV (Esarey and Conrad 1981). Larger

populations, however, often result in increased economic stress risk factors and perhaps more difficulty or increased competition in climbing social ladders of Mississippian defined success factors. The susceptibility to drought coupled with success in war as a means for prestige building, coalesced into an increasingly hostile Mississippian occupation throughout the CIRV following the relatively peaceful Eveland phase, with some sixteen percent of adults at Orendorf being directly affected by interpersonal trauma such as scalping, decapitation, inflicted projectile points, and antemortem cranial depression fractures (Steadman 2008; G. D. Wilson 2012).

Ceramics in the CIRV increasingly diversified from their American Bottom counterparts beginning in the Orendorf and later phases, indicating a distinct cultural trajectory based primarily on *in situ* social dynamics (Conrad 1991; Harn 1994; Strezewski 2003). While calibrated radiometric dates (n=11; see Figure 3.3 for a subset) places the Orendorf site between A.D. 1149 to 1320, it is generally agreed upon by Harn (1991) and Conrad (1991) that Orendorf predated the later, but overlapping, Larson phase based on the inferred evolution of Mississippian ceramic styles and forms local to the CIRV (J. J. Wilson 2010). While Cahokia-style Ramey and Powell Plain jars gave way to more distinctively local vessels at Orendorf, the scrolled and curvilinear designs that form the hallmark of the Ramey tradition often adorn the minority of jars that are decorated from Orendorf Settlement assemblages (Conrad 1991). Jars and a ceramic vessel class new to the region in the Orendorf phase, a class variously referred to as plates or broad-rimmed bowls, are often smoothed over and plain. However, decorations characterized by sun-motifs or sun-emulations also seen in other Mississippian regions does occur (Conrad 1991; Hilgeman 2000; Vogel 1975).

Several other, perhaps rival, settlements appear to be occupied alongside Orendorf during the Orendorf phase. These include Kingston Lake, Emmons Village, Weaver-Betts, and Ten

Mile Creek (Conrad 1991). Recently obtained radiocarbon dates from the Ten Mile Creek site, however, place the occupation of this site almost entirely within the 14th century A.D., some 50 years after the supposed end of the Orendorf phase (see Figure 3.6). Although the possibility of a limited earlier occupation of the site remains plausible, the primary occupation of Ten Mile Creek (also known as Hildemeyer), however, is likely to have post-dated the Orendorf phase. Regardless, the Orendorf phase certainly represents the beginnings of Mississippian florescence in the central Illinois River valley, with the introduction of classic Mississippian-style sites, material culture reminiscent of the American Bottom but with a distinctive local flair, and artifacts bearing socio-religious themes associated with the Southeastern Ceremonial complex including the forked-eye motif, short- and long-nosed maskettes, and distinctive beakers, among other examples of upper and lower Mississippian world symbolism (Brown and Kelly 2000; Conrad 1989; Emerson 2012; Kelly 1991a; Pauketat and Emerson 1991, 1997).

3.8 Larson Phase (A.D. 1250-1300)

While both Conrad (1991, p. 141) and Harn (1994, p. 26) suggest that the inhabitants of Orendorf may have abandoned the site in the middle of the 13th century A.D. to found a new Mississippian town, Larson, in the south-central portion of the region, it is plausible based on overlapping radiocarbon dates and distinctive ceramic differences between these sites that they may have been contemporaneous for a generation or more. Nevertheless, considerable effort both in the field and in the lab has resulted in the assignation of the Larson phase, Larson settlement system, and a general definition of the Spoon River Mississippian apogee as thriving during the latter half of the 13th century A.D. (Harn 1978, 1994). Because of the nature of the salvage excavations at Orendorf in comparison to the more dispersed focus on archaeological resources

in the vicinity of the Larson site, more is known about the Larson community and the relationship between a central town and its supposed subsidiary sites during the Larson phase than during the preceding Orendorf phase, which is largely defined based on the Orendorf site itself (Conrad 1991). Though forty years of excavations have indeed produced a bounty of knowledge about the Larson phase type site, the Larson town.

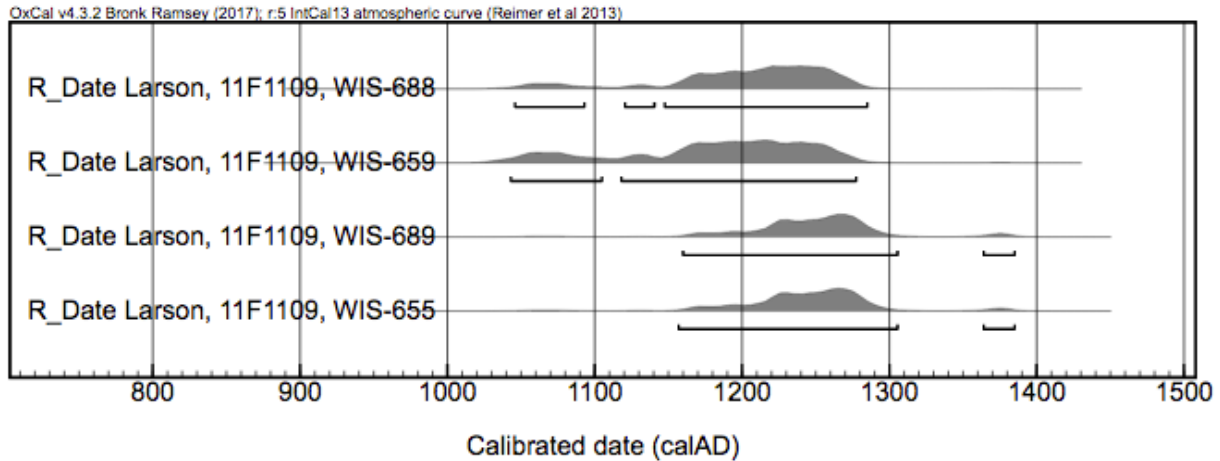


Figure 3.4 Probability distributions of four recalibrated dates for the Larson site (Bender, et al. 1975)

The Larson phase saw a manifestation of Mississippian culture that mirrors the settlement hierarchies of other Mississippian regions in the American southeast (Blitz 1999; Cobb 2003; A. King 2002). As a result, Harn (1978, 1994) endeavored to apply the multi-tiered Mississippian “settlement system” model used to define this archaeological culture in those other regions (Fowler 1974; B. D. Smith 1978). This model presupposes an apical primary site supported by progressively smaller subsidiary settlements located in key resource exploitation zones. Harn (1994:16-17) envisions a four-tiered system for the Larson phase CIRV that includes the central Larson town, several primary villages (e.g., Myer-Dickson, FV66), intermediate settlements (e.g., Fouts Village, Buckeye Bend, M.S.D. 1), and subsidiary settlements (e.g., Norris Farms 1 and 24). Each of the lower tiered settlements lies within a 25 km radius of the central town. Beyond

this Larson nucleus, Harn (1994) identifies Kingston Lake, Lawrenz Gun Club, and Walsh as central town present during the Larson phase (Harn also identified Hildemeyer or Ten Mile Creek, though recent dating by the author suggests a predominant occupation in the succeeding Crable phase, see Figure 3.6). Conner (2016) suggests at least two temporally and spatially distinct Larson phase occupations at Myer-Dickson whose proximity to the regionally important Dickson Mounds mortuary center, presence of a plaza, and presence of one of the largest buildings known in prehistoric Illinois make this a unique non-nuclear settlement habitation site.

Situated atop a cornering bluff overlooking the confluence of the Spoon and Illinois River valleys, Larson is centrally positioned in the CIRV from both ecological and geographic perspectives. Larson is a stockade settlement marked by a single stage, truncated pyramidal platform mound measuring some 60 x 60 meters and perhaps 3-5 meters high with a ramp abutting a 150 sq. meter plaza, which is in turn flanked by domestic structures on three sides (Conrad 1991; Harn 1994). No evidence for bastions is present along the stockade. Portions of the site were at times burned, perhaps on more than one occasion. Relatively scant remains from the floors of the structures in these burned portions suggest that the site was still occupied at the time of burning. This observation is buttressed by comparison to structures burned with entire suites of artifacts related to a variety of economic and artistic pursuits seen at Myer-Dickson and Orendorf Settlement D (Conrad 1991). The presence of maize in most storage/refuse pits as well as within the domestic structures speaks to the importance of this subsistence resource to the Larson population (Harn 1994). In addition to maize, large quantities of fall-ripening nuts and seeds as well as large mammals, migratory fowl, and other aquatic resources indicates a broad subsistence system focusing on maize agriculture supported by hunting, gardening, gathering, fishing, and perhaps limited scavenging. Harn (1994:48) views the Larson settlement system as

an “integral series of procurement subsystems whereby the seasonal cycles of the local population and those of their target resources intersect”. That is, primary villages, intermediate settlements, and subsidiary sites were positioned strategically around the central town at locations allowing for the maximal exploitation of the surrounding plains-prairie-woodland-riparian-lacustrine subsistence offerings but at such distance as to prohibit over exploitation of any particular resource zone. An estimated 450 – 1,175 individuals may have populated the central Larson town at any given time with another perhaps 1,000 – 1,500 individuals spread across the primary villages and intermediate settlements according to Harn (1994:53).

The primary point of contention in arguing for a separation between the Orendorf and Larson phases are the differences in ceramic assemblages from these sites. The Larson phase saw the emergence of the Dickson series of jars, which are differentiated primarily by cord-marked lower hemispheres of the globular vessels with plain or sometimes trailed/incised line-filled triangle motif adorned shoulders. The line-filled triangle designs, when viewed from above, mimic sun rays. This upper-world symbolism indicates some connection to socio-politico-religious themes of the Southeastern ceremonial complex (Brown and Kelly 2000; Griffin 1949; Hally 2006; Pauketat and Emerson 1991). Larson jars are marked by increases in the height and width of jar rims with more rounded shoulders, increased occurrence of cord-marking, and a general increase in the presence of stylistic decorations when compared to the Orendorf and Eveland phases. However, there is considerable overlap in these trends among the phases. Dickson style jars are present at both Kingston Lake and Ten Mile Creek, indicating perhaps incipient occupations at these sites at the extreme northern extent of the CIRV (Conrad 1991).

Population aggregation in the Larson site vicinity suggests spatial emphasis in the CIRV shifting to the central-south portion of the valley. However, the Larson phase also may be

characterized by multiple, contemporaneous Mississippian town sites, perhaps for the first time. Walsh, Kingston Lake, and Lawrenz Gun Club each appear to be coeval based on radiocarbon assays as well as ceramic forms and surface finishes, though with some stylistic variation present between them (Harn 1994:21-22). Conrad (1991) views the southern cadre of towns, Walsh and Lawrenz Gun Club, as perhaps representing a different polity developed locally to the extreme southern portion of the valley, which he refers to as the Crabtree phase. Jeremy Wilson of Indiana University Purdue University Indianapolis has recently obtained dates from both Walsh and Lawrenz Gun Club, placing both of these sites within the Larson phase, though Lawrenz Gun Club does appear to be marked by an earlier occupation as well (see Figure 3.5). Harn (1994:25) explains that the “difficulty in proposing a single comprehensive occupation of the entire study area by each or any of the phases of the Spoon River tradition is that the various local artifact assemblages considered representative of a particular phase disclose a great degree of stylistic variability. It seems that each town and related nucleus of sites retained its

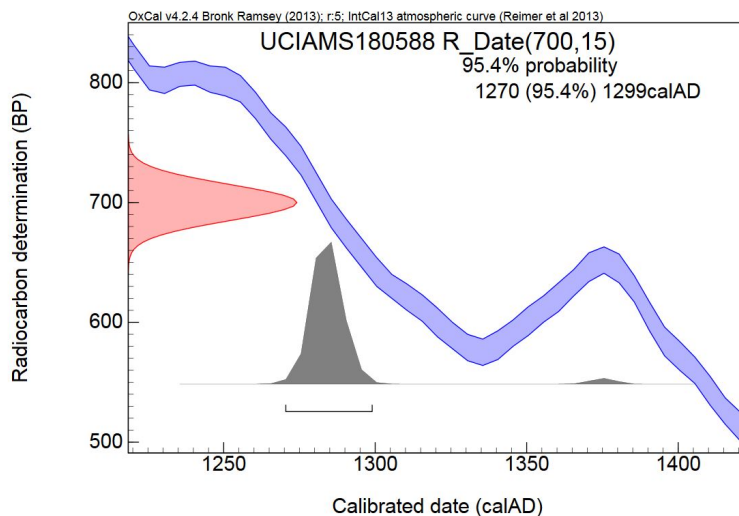


Figure 3.5 Probability distributions of one recalibrated dates for Walsh Site (Wilson, personal communication 2017)

individuality, whether intentionally for sociopolitical reasons or incidentally because no competing settlement systems were simultaneously functioning nearby”. Whether the individuality argued for in each town’s ceramic assemblage is related to contemporaneous polities operating in restricted areas or the evolution of ceramic technology and style based on the progressive founding of new towns is certainly a matter of unresolved debate.

3.9 Crable Phase (A.D. 1300-1425)

Sometime in the late 13th or early 14th century A.D., an Oneota group from the north migrated into the CIRV and fundamentally changed the social dynamics of the region (Esarey and Conrad 1998; O’Gorman and Conner 2016; Santure, et al. 1990). Some characterize this immigration as part of an aggressive territorial expansion of the Oneota cultural tradition leading to intrusion, replacement, or displacement of peoples across US Midwest and eastern Prairie Plains (Hollinger 2005). Oneota expansion coincided with a rapid decline in Middle Mississippian influences in these regions and with the onset of the droughty Pacific climatic episode (Gibbon 1995). While many Late Woodland populations in the riverine Midwest and western Great Lakes were replaced by or integrated into Oneota peoples during this expansion, CIRV societies on northern Middle Mississippian frontier, maintained their positions in fortified temple mound centers, and outlying sites, and entered into a period of coexistence with an intrusive Oneota population. At the regional level, the sudden appearance of five Oneota components along a 27 km stretch of the Illinois River circa A.D. 1300 and biodistance indicators in the Norris Farms #36 cemetery population attests to the occurrence of a migration process in the CIRV, though the location of origin of the Oneota immigrants is unknown (Esarey and Conrad 1998; Santure, et al. 1990; Steadman 1998). Recent archaeological inquiry in the Late Prehistoric CIRV has focused

on the unprecedented levels of violence seen in burial and cemetery contexts both prior to and following the Oneota in-migration that catalyzed the Crable phase assignment (Bengtson and O'Gorman 2017; Emerson 1999; Hatch 2015, 2017; G. R. Milner 1999; G. R. Milner, et al. 1991; Steadman 2008; Vanderwarker and Wilson 2016; Vanderwarker, et al. 2013; G. D. Wilson 2012). Conflict and warfare, as an analytical topic, has featured prominently in discussions of cultural and biological evolution more broadly but more especially in regard to interactions among and between middle complex societies such as Mississippian and Oneota peoples (Carneiro 1970; Dye 2013; Golitko 2010; Keeley 2014; Maschner and Reedy-Maschner 1998; G. R. Milner 1999). Although the CIRV is remarkable within the corpus of eastern North American prehistory for its evidence of levels of interpersonal violence, evidence indicating the community scale coexistence of these distinct but interrelated cultural groups is also apparent. This is not to say that warfare was not in-grained in both Mississippian and Oneota culture and society; it no doubt was. However, ethnographic accounts of societies likely descendent from various Oneota and Mississippian peoples suggest strongly that both war and peace structured both intra- and inter-group interactions in a perhaps cyclical nature (Dye 2013; Landes 1959). Coexisting Oneota and Mississippian material culture at multiple sites at the household level provides the opportunity to examine the various social interrelationships that were present during the Crable phase and to perhaps better understand the preceding Mississippian phases of the CIRV (Esarey and Conrad 1998). It is my contention here that extant definitions of CIRV peoples, especially during the Crable phase, may place too great an emphasis on conflict at the expense of understanding and attempting to explain more nuanced relationships between these peoples.

While both Conrad (1991) and Harn (1994) have previously parsed the Crable phase into two separate phases (the Crabtree (A.D. 1300-1375) and Crable (A.D. 1375-1450) phases), the

most recent phase assignation is followed here (Esarey and Conrad 1998). At or immediately prior to the Oneota in-migration, there appears to be a consolidation of Mississippian sites and peoples in the Anderson Lake and La Moine River mouth areas, but with one extreme northerly outlier in the form of the Ten Mile Creek site. Radiocarbon assays performed as part of this dissertation place two previously undated sites, Ten Mile Creek (11T2) and Star Bridge (11Br105), definitively within the Crable phase (see figure 3.6).

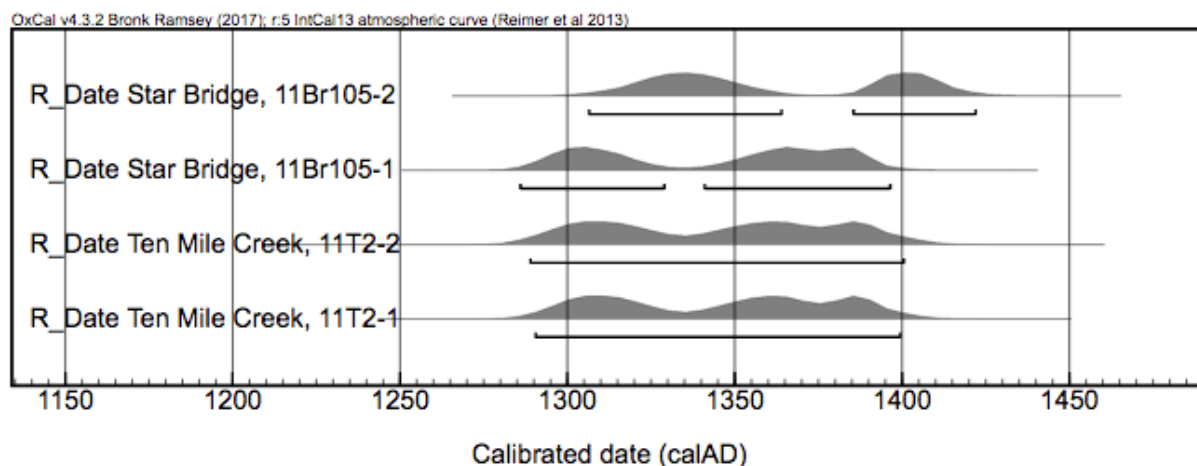


Figure 3.6 Probability distributions of four recalibrated dates for Ten Mile Creek and Star Bridge sites; dates include DirectAMS Codes D-AMS 020156 – D-AMS 020159 respectively

Most of the evidence used to define the Crable phase is derived from the phases' type site, Crable. The Crable site is located in southern Fulton County on narrow strip of bluff edge overlooking the Anderson Lake Conservation Area. Archaeological research at the site has been a mixture of amateur and pot hunting efforts dating back to at least 1879 and professional excavations stretching back to the early 1930s; though no known professional excavation has taken place at the site since the 1970s (K. Sampson 2000). The Crable site constellation consists of a village area, the remains of a platform mound that was bulldozed by the landowner following a soured land deal, a ridge of smaller mounds, and at least four cemeteries (Painter 2014; K. Sampson 2000). Given amateur and illicit archaeological interest in entire vessels, pot

hunting in the cemetery was extensive. Unfortunately, these amateur and illicit efforts left little behind to aid in understanding the nature of the occupation at Crable aside from the equally extensive collections of artifacts from grave goods and a handful of excavation photographs (H. G. Smith 1951). Radiocarbon assays from the village area date to the 14th and early 15th centuries A.D. (see Figure 3.7).

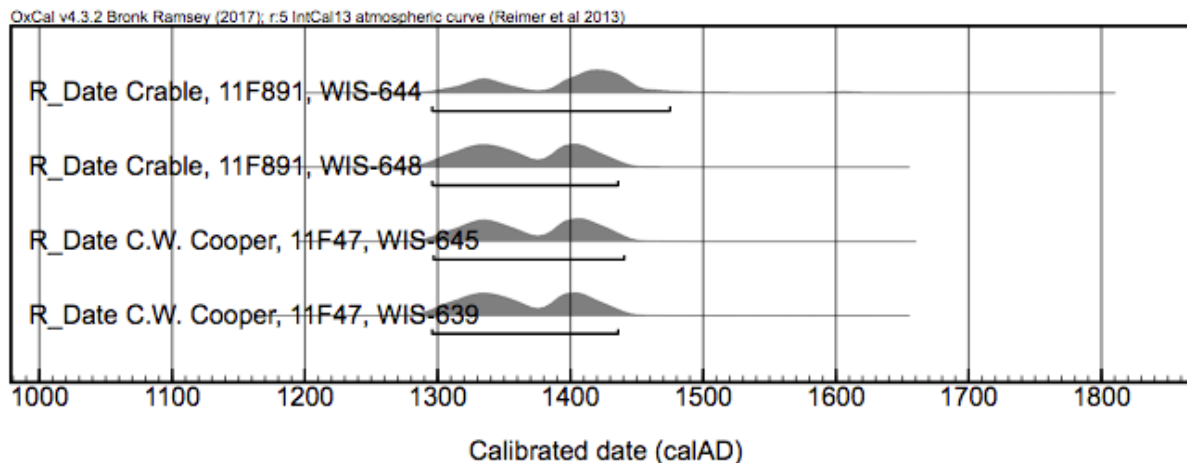


Figure 3.7 Probability distributions of four recalibrated dates for Crable and the Oneota occupation of the C.W. Cooper sites

Evidence of Crable’s connection to the Mississippian Southeastern ceremonial complex include conch-shell masks marked with the weeping-eye motif, copper and shell pendants with repousse circles and crosses, shell gorgets with incised spiders, rattlesnakes, and avian figures, pottery decorated with the cross-in-circle motif, and a chipped flint mace (H. G. Smith 1951). Crable, however, posed quite the challenge to researchers when originally described as a result of the mixed Oneota and Mississippian assemblage, which was deciphered to be contemporary in an early publication describing the site based in part on an inventory of artifacts from Glenn McGirr’s collection from the site (K. Sampson 2000). While the culture-historian perspective of early to mid-20th century archaeology typically endeavored to separate out material culture based on decoration and form in order to define time-space systematics, Hale Smith noted that “if one

is to obtain a valid conception of the site, the culture complex must be viewed as a cultural whole...where mixture occurs, it is unwise to make a marked distinction in cultural items as many traits are co-existent in both the Middle and Upper Mississippi phases” (H. G. Smith 1951:32).

Unclear mixing between Oneota and Mississippian peoples in the Crable phase is not unique to the Crable site alone. Of the five known Bold Counselor sites in the CIRV, there is a spectrum of inter-group social interaction patterns with their local Mississippian neighbors exhibited based on currently available data. From the assemblage at the C.W. Cooper (see Figure 3.7) site that is characterized solely by Oneota ceramic decoration and vessel forms, to evidence of cohabitation and at least some integration of Oneota and Mississippian peoples at the household level at both Morton Village and the Crable site (Esarey and Conrad 1998; Santure, et al. 1990; H. G. Smith 1951), the Bold Counselor occupation of the CIRV during the Crable phase indicates that cooperative strategies must be considered alongside evidence of endemic hostilities in the region. For example, while the Crable site exhibits the hallmarks of a Mississippian regional center such as a pyramidal mound and adjacent plaza, some 15% of ceramic artifacts recovered from the site have decoration that has been ascribed to the Oneota tradition (Esarey and Conrad 1998). Further, every feature excavated at Crable thus far shows a minor amount of Oneota ceramic vessels alongside a predominantly Mississippian admixture (Painter 2014). In remarking on the presence of Oneota decoration found on an otherwise uniquely Mississippian vessel type, the shallow or deep rimmed plate, Smith (1951:28) “infers that a transference of technique has taken place, probably indicating a culture fusion from two separate sources.” On the other hand, that Ten Mile Creek, Star Bridge, and Lawrenz Gun Club each have occupation components that date unambiguously to the Crable phase and are

characterized by non-existent or an extremely minor admixture of Oneota ceramic decoration indicates that Mississippian chiefly societies were not uniform in their attitudes toward the community scale cohabitation of Oneota immigrants. That is, while Mississippian peoples lived alongside Oneota peoples quite unambiguously at both Crable and Morton Village (O'Gorman and Conner 2016; H. G. Smith 1951), there is no evidence of such community scale cohabitation at Star Bridge or Ten Mile Creek based on the ceramic assemblages analyzed as part of this dissertation. Ceramics with distinctly Oneota decoration are present at the Lawrenz Gun Club site, though it is presently inconclusive as to whether the site was characterized by cohabitation of Mississippian and Oneota peoples during the Crable phase (Lawrence Conrad 2017, personal communication). Bold Counselor Oneota peoples appear to have not been uniform in their attitude toward local Mississippian peoples either, with distinctly homogenous Oneota assemblages at C.W. Cooper and limited surface scatter recovered from the Otter Creek site as well. That is, while Oneota decoration is present on plates, a Mississippian ceramic form, at Morton Village and Crable, there are no known examples of plates recovered from either C.W. Cooper's or Otter Creek's Oneota occupations (Esarey and Conrad 1998; H. G. Smith 1951).

These observations presuppose the contemporaneity of each of these sites, which is a matter of debate. However, this discussion should make it apparent that explaining patterns of social interaction in the Late Prehistoric CIRV through the lens of warfare as a 'prime mover' is entirely insufficient. That is, the Oneota presence alongside Mississippian peoples during the Crable phase provides a setting wherein nuanced evidence may support the sentiment that social interaction, "trade and exchange are as likely to breed conflict as cooperation and understanding" (Emerson 1999:38). That is, material remains from the Crable phase suggest a duality of social structure between cooperation and conflict, with a high likelihood that social institutions were

enacted to at times prioritize war and at times counterbalance war with peace, and that conflict was likely pursued between sites or communities ascribing to the same supra-group to a greater or lesser frequency as conflict being pursued between sites or communities ascribing to different supra-groups or polities (Landes 1959). The proximity of Mississippian chiefly societies to Oneota tribal peoples at times resulted in population aggregation, increasing centralized leadership, escalated levels of violence, and increased territorial boundedness (Emerson 1999). Yet, at other times, and perhaps in response to that escalation in violence, Oneota and Mississippian peoples endeavored to overcome their differences and engage in direct interaction based on economic, social, political, and perhaps religious impetuses, leading to the hybridization of ceramic vessel forms and decoration, perhaps intermarriage, and certainly household scale cohabitation. It is argued here that this duality should play a more prominent role in discussions of social dynamics in the CIRV in the Crable and preceding phases as opposed to a focus on warfare alone.

As part of their designation of the Bold Counselor taxonomic phase, Esarey and Conrad (1998:53-54) remark that:

Group continuity in the form of retained and progressively evolving traditional cultural elements is apparently maintained through this local sequence. Bold Counselor phase [or Crable phase] is simply the addition of an extraneous cultural unit that interacts with the contemporary local inhabitants differentially on a site by site basis.

We have seen that the Crable and household ceramic assemblages include Bold Counselor and Late Mississippian vessels. It would not be difficult to imagine that vessels would be exchanged in a cohabitation setting. Yet at Crable, not only were both household assemblages mixed, but the fill of every pit feature and every house basin yet examined has contained both Bold Counselor and Late Mississippian pottery.

It may be that for the Crable site, the minority Bold Counselor population was integrated not as a political unit, but as marriage partners, individual refugees, or captives. The subtle implications of these various scenarios are brought out when it is seen that, at other sites with Bold Counselor and Late Mississippian cohabitation, the relative proportion of each group present is highly varied...Even more than usual, interpretation rests heavily on chronology.

These potential interaction scenarios between Mississippian and Oneota peoples at Crable are thus numerous and unclear based on present evidence. Painter (2014:96-105) outlines and further discusses these scenarios as raised by Esarey and Conrad, but ultimately finds a lack of strong evidence to support one hypothesized scenario over the others. The most intriguing aspect of the occupation of Crable is that Oneota peoples were able to produce numerous artifacts at the site that are quite unambiguously characteristic of Oneota peoples in other contexts. These include pottery with wet paste trailed designs typical of Oneota peoples, 'snub' edge scrapers, grooved maul, tanged shell spoon, and certain copper implements (H. G. Smith 1951:33-34). Without extensive professional excavation data, and perhaps even despite it should it become available at a future date, the nature of the Crable occupation by Bold Counselor and Late Mississippian peoples may never be clear.

Chronological precision alone at a scale refined enough to provide disambiguation between site occupations during the Crable phase is as yet untenable. In lieu of advancements in dating technology and continued professional excavation at Crable and other Late Mississippian and Bold Counselor phase sites, this dissertation seeks to further examine the nature of social, economic, and identity politic interactions between the taxonomically distinct, but socially interrelated, Mississippian and Oneota peoples that lived side by side during the Late Prehistoric CIRV.

3.10 The Bold Counselor Phase Oneota

While the Bold Counselor Oneota have been discussed in detail in the preceding Crable phase section, some treatment of Bold Counselor peoples is warranted. While Esarey and Conrad (1998) defined a Bold Counselor phase as a taxonomic entity, given the entanglements between

Late Mississippians and Oneota peoples in the CIRV this discussion will focus on the Bold Counselor phase as a cultural expression of the Oneota archaeological tradition. The origins of Bold Counselor Oneota peoples is unknown prior to their emergence in the 14th century A.D. CIRV. Similar to other Oneota expressions, Bold Counselor phase peoples have been interpreted as tribal-scale sedentary villagers who practiced a mixed subsistence strategy including the cultivation of crops such as maize, hunting, fishing, and gathering of an array of locally available floral and faunal resources (Henning 1995; G. R. Milner, et al. 1991; Overstreet 1997). Ceramic stylistic similarities have been noted between Bold Counselor phase sites in the CIRV and Oneota sites in the Red Wing and Apple River areas (Conrad and Esarey 1983; Emerson and Brown 1992; Hollinger 2005; Santure, et al. 1990:154). Bold Counselor phase ceramics have been recovered from the Wever Terrace Village of Iowa, the Lima Lake locality, the Kingston locality, the Sponemann site in the American Bottom, and perhaps the McKinney Oneota village (Benn 1998; Henning 1995; Hollinger 2005; Jackson 1992; Nolan and Conrad 1993). Bold Counselor phase ceramic assemblages consist predominantly of jars and bowls with a minor admixture of deep-rimmed plates. Domestic jars are globular vessels characterized by high, everted rims (or long lip lengths), shoulder decorations consisting of horizontal or zig-zag lines with punctate borders and “stab and drag” vertical decorations trailed onto wet paste (Esarey and Conrad 1998). The most common jar shoulder decoration motif consists of three to five trailed horizontal lines bordered by punctates above vertical stab and drag trailing. Bowls are common and typically plain, though many borrow the Crable deep-rimmed plate design, utilizing the plate flare to trail chevron and zig-zag lines with zoned or bordering punctates, even occasionally borrowing stylistic norms seen on incised Mississippian plates (Vogel 1975). Aside from

ceramic style and technology, it is the unique relationship Bold Counselor phase peoples shared with Mississippian peoples that distinguishes them from other Oneota groups.

A plethora of speculative scenarios have been proposed to account for the presence of Bold Counselor phase peoples in the CIRV. These include motivations of conflict between Mississippian peoples in the CIRV and another Upper Mississippian group, the Langford tradition of the Apple River region (Emerson 1999); a product of intrusion or alliance building between Oneota and CIRV Mississippian peoples (G. D. Wilson 2012); as one of a series of repeated southerly migrations of northern groups that would continue into the proto-Historic period Illinois (H. G. Smith 1951); an intrusion at the front of a cultural expansion of Oneota groups (Henning 2005; J. J. Wilson 2010); or that “Bold Counselor phase Oneota may have originated among the earlier Oneota of the Apple River region and may have moved into the Central Illinois River valley at the invitation of the local Spoon River Mississippians [and] may have formed an alliance...against a third group” (Hollinger 2005, p. 160). It seems unlikely that ‘smoking gun’ evidence will ever be found to accurately identify the location of origin of Bold Counselor phase Oneota peoples. However, the most plausible speculative scenario for their presence in the CIRV is one of Oneota cultural expansion motivated in part by a waning Mississippian hegemonic frontier, climatic conditions that saw increases in drought and difficulty in maintaining horticultural/incipient agricultural productivity in northerly latitudes, and perhaps Oneota socio-economic reorganization that favored densely occupied communities adjacent to habitats most favorable for maize horticulture/incipient agriculture (Gibbon 1972; O’Gorman 2010; Overstreet 1997).

Available data from CIRV settlements (Figure 3.1) exhibit varying degrees of intermixing between Mississippian and Oneota material culture. From the Oneota assemblage at

C.W. Cooper that “shows almost no evidence of any influence or actual presence by the Late Mississippians” (Esarey and Conrad 1998:41) and the ‘purely’ Late Mississippian assemblages at the fortified Ten Mile Creek and Star Bridge Mississippian mound centers (Conrad 1991), to evidence “probably indicating a cultural fusion from two separate sources” at the Crable mound center (H. G. Smith 1951:28), no discernible pattern emerges as to the nature of cultural interrelationships in the Late Prehistoric CIRV. Tantalizing evidence for cultural mixing between Oneota and Mississippian peoples is most readily apparent in the mixing of ceramic traits. For example, the use of deep-rimmed plates by Oneota peoples is apparent at several sites in the CIRV, but virtually absent in Oneota contexts outside this region. In fact, the presence of Crable plates at Oneota sites outside the CIRV is a common indicator for the potentiality of a Bold Counselor phase presence (Benn 1998; Henning 1995). At the Crable Mississippian mound center itself, some 14% of vessels from a sample of pit features were ascribed to Oneota, leading Esarey and Conrad (1998:46) to suggest that “the most likely explanation for these assemblages is that Bold Counselor people were present (in one social context or another) as a minority admixture to Crable’s overwhelmingly Mississippian-derived population. Furthermore, this admixture seems to represent social integration at the household level.” The Morton Village site appears to indicate the inverse: an Oneota village with an admixture of Late Mississippian people (O’Gorman and Conner 2016). Trends in technological distinctions suggest possible interaction-based transmission processes from Oneota and perhaps other Upper Mississippian peoples as possibly being influential in type-attribute trends seen on distinctly Mississippian ceramics. Specifically, domestic jar rim heights (or lip lengths) and plate flare angles are known qualitatively to increase overtime in the CIRV (Harn 1978). Analyzing these trends quantitatively reveals that sites with an Oneota presence, which are also the most recent pre-

Columbian sites in the region, show the highest values for these metrics, while earlier Mississippian sites show the lowest values. Perhaps interaction based transmission processes from Oneota and other Upper Mississippian peoples were influential in the morphological changes demonstrated in these type-attributes (A. J. Upton 2016).

Aside from Bold Counselor habitation sites, the Norris Farms #36 cemetery provides key data about these peoples themselves. The Norris Farms #36 cemetery represents the largest Oneota burial sample presently available, with some 264 burials assigned to the Bold Counselor phase (Santure, et al. 1990; Tubbs 2013). The cemetery is a modest “D”-shaped mound situated on a bluff edge overlooking the Illinois River valley and is immediately adjacent to the Morton Village habitation site. As is typical of Oneota mortuary treatment elsewhere, the majority of burials were single individuals, extended, and elliptical in shape (Foley-Winkler 2011; Kreisa 1993; O’Gorman 1996). Fully one-third of adult burials in the Norris Farms #36 cemetery died a violent death, though this seemingly high rate of trauma may not be unique to the Bold Counselor phase (G. R. Milner 1999; G. R. Milner, et al. 1991; Santure, et al. 1990), as Oneota in Wisconsin appear to be characterized by similar rates of violence (Oemig 2016). Many individuals were likely interred in open graves, with evidence suggesting that some of which were covered by a pole roof prior to being filled (Santure, et al. 1990:72). Non-celestial orientation of the graves is apparent. From a comparative mortuary perspective (Bengtson 2012; L. G. Goldstein 1981, 2006), both similarities and differences exist between Norris Farms #36 and nearly Mississippian mortuary sites that may be related to ethnic identity. Differences such as the covered graves, artifact styles, and non-celestial orientation of the graves suggest a distinctly Oneota ethnic identity at Morton Village (Tubbs 2013). However, similarities such as a preponderance of single-internment burials, occasional instances of post-internment additions, a

wide range of burial furniture with primarily utilitarian objects accompany male internments, and a positive linear relationship between age and burial furniture density suggest some degree of permeability of ethnic identity among Bold Counselor peoples in the CIRV (L. G. Goldstein 2000; Santure, et al. 1990; Tubbs 2013).

3.11 Regional Abandonment

After an approximately 250 year history of occupation by Late Prehistoric peoples, the central Illinois River valley witnessed complete regional abandonment circa 1425 – 1450 A.D. (Esarey and Conrad 1998; Santure, et al. 1990). In fact, there were no substantial occupations until the late 17th century A.D. when Illiniwek from northern Ohio took refuge in the region while fleeing from Iroquoian aggression further to the east (Ethridge 2009a; Hollinger 2005). Regional abandonment was not unique to the CIRV during the mid-15th century A.D.: the American Bottom, the lower Ohio Valley, interior western Kentucky, lower Savannah River Valley, and Upper Susquehanna drainage all witnessed wholesale depopulation and abandonment (Cobb and Butler 2002). Explanations of abandonment often incorporate deteriorating or changing climate as a primary contributing factor, however social stresses and the responses of social leaders to climatic conditions were no doubt critical factors as well. Hollinger (2005:162) posits a scattering of Bold Counselor peoples to the Lima Lake locality and other portions of the Mississippi Alluvial Plains region where they would have been absorbed by local Oneota groups; and likewise posits a merging of Mississippian peoples in the CIRV with Angel phase Mississippians to perhaps form the Caborn-Welborn phase of Mississippian peoples at the mouth of the Wabash River.

Regardless of the outcome, the CIRV represents a significant contribution to understanding social structure during the Late Prehistoric period in the U.S. Eastern Woodlands. This regional case study will be the backdrop for exploring long-term trends in networks of social interaction and categorical identification, majority-minority power dynamics, and negotiations of identity politics. In particular, this regional and cultural backdrop will be the focus of an examination of how communities of ceramic artisans constructed social and economic relations before and after an intrusive migration process to better understand the ways humans navigate cultural contact and multicultural community scale interrelationships.

CHAPTER 4 METHODOLOGICAL CONSIDERATIONS

4.1 Introduction

An essential component to any scientific endeavor is a series of systematic and reproducible protocols for the collection and analysis of data. Collecting data from archaeological contexts poses a number of challenges toward this end. For example, random sampling is often impractical due to limitations on data availability and the expense and time horizons required for excavation or survey. Furthermore, archaeological artifacts or features available in museum or private collections are often fragmentary and incomplete. From an analytical perspective, new methodologies have burgeoned at an unprecedented rate in the latter half of the 20th and early 21st centuries. These issues therefore require some treatment regarding the methodologies employed in this dissertation for data collection and data analysis in particular. In this chapter, I provide such treatment.

Unlike many anthropological archaeological dissertations which separate theory, methodology, analysis, results, and interpretations into separate chapters, the four chapters that follow this contain each of these pieces as a bounded whole, much like an academic journal article. In order not to detract from the linear arguments made in Chapters 5 – 8, this chapter incorporates a rich discussion of many methodological considerations including descriptions of statistical measures for social network analysis, data collection routines, and intricacies related to the collection of mineralogical and geochemical data from sediments and archaeological ceramics. This chapter therefore ‘fills in the gap’ in those cases where it was not deemed essential to provide an extended treatment of methodology or analytical protocol in the chapter itself.

4.2 Data Collection Methods

Discussed here the methodologies for data collection used in Chapters 5 and 6 at greater length. Specifically, this discussion considers how continuous type-attributes were measured and how stylistic decorations were identified and categorized. In this way, it is hoped that this study may be seen as systematic in approach and the methodologies reproducible inasmuch as possible in other archaeological contexts.

4.2.1 *Ceramic Vessel Technological Data*

In Chapter 5, I introduce a model adapted from cultural transmission theory designed to differentiate between artifact attributes that are likely constrained by social forces from those constrained by engineering forces. To apply this model, continuous artifact attribute measurements were taken from three distinct vessel classes: domestic jars, burial jars, and plates. Specific guidelines for each of the continuous artifact attributes are provided in the coding sheet in Appendix A. I provide additional detail here as to how each measurement was systematically collected.

Analog calipers were used to measure eight type attributes on jars, seven type attributes on plates, and four type attributes on burial jars. Because these vessels were made by hand in a non-standardized production context, it was necessary to take multiple measurements on each vessel. For each continuous attribute measurement, the maximal observation that was not an outlier was recorded. An outlier was assessed as being greater than or equal to twice that of any other measurement.

Domestic jars are characterized by a globular shape with an everted rim (see Appendix F for jar profile samples). As a result, it was possible to assess up to eight attribute measurements on a continuous scale for each sherd. Jar orifice diameter was measured using an orifice diameter

chart. Because of the everted rim, the orifice diameter measures the greatest extent of vessel opening (i.e. as opposed to the restricted opening below the everted rim). In cases where an insufficient amount of the jar rim was present to discern an accurate diameter, no measurement was recorded. Jar lip thickness refers to the extruded edge or margin of the orifice of the vessel and measures the distance from the interior of the everted rim lip to its exterior. Measurements for domestic jar shoulder thickness were taken above where the vessel wall angle is 90° perpendicular to the vessel opening. In other words, the shoulder is maximal measurement observed between the point of everted rim attachment and where the vessel wall angle is perpendicular to the vessel opening plane. Domestic jar wall thickness was measured within a cm of the equator of the globular jar (or where the vessel wall angle is 90° perpendicular to the vessel opening plane, and as a result was often not present). Jar rim height measures the area between the lip and neck of the vessel. Finally, domestic jar rim angle was measured using a protractor where a measurement of 90° equates to a completely vertical rim, a measurement less than 90° equates to an in-slanting rim, and a measurement of 360° equates to a completely unrestricted vessel opening. A flat plane such as the underside of a desk was used to determine the opening plane of the jar prior to recording the rim angle measurement.

Burial jars are typically intact due to the great care taken in the positioning and entombing of them alongside deceased individuals. As a result, measurements were constrained to four features. Of the four, three were measured following the same criteria as for domestic jars and include orifice diameter, lip thickness, and rim height. The fourth attribute measures burial jar height, or the vertical distance between the base of the vessel and its opening plane.

Plates are used to primarily serve food and are characterized by an outflaring rim attached to a globular body (see Appendix F for plate profile samples). This enables seven

measurements to be observed. Plate diameter refers to the circumference of the opening plane of the plate, or where the plate touches a surface when flipped upside-down, and was assessed using a rim diameter chart. The plate flare is used to refer to the outflaring rim and was assessed in length, or the distance from the opening of the globular plate well to the plate lip, as well as in angle. Plate flare angle measures the degree of eversion of the outflaring rim above the globular well of the plate. Plate lip thickness measures the margin of the plate rim prior to any tapering. Plate thickness below lip measures the attachment point of the flare to the well or the maximal thickness of the outflaring rim, whichever was found to be thicker.

Both domestic jars and serving plates were often adorned with stylistic decoration. These decorations were either incised into a dry paste or trailed into a malleably damp paste. In either case, incising thickness or trailing thickness measure the maximal observed thickness of these decorative elements.

A host of other features were collected for domestic jars, burial jars, and plates that were not included in any analysis presented in this dissertation. These features are described in the Coding Sheet in Appendix A and will be made available in a tDAR archive at the following static link: <https://core.tdar.org/project/447475>

4.2.2 Ceramic Vessel Stylistic Data

Chapter 6 explores networks of social identification based on proportional similarities among sites in decoration grouping categories derived from stylistic decoration present on plates. A linear sequence was used to arrive at decoration grouping category assignments. The author alone is solely responsible for category assignments in order to avoid inter-observer inconsistencies. The first step in this process was the identification of wholly unique design features, which encompass both design techniques and decoration motifs. A design technique

refers to the technique used to decorate the vessel – whether incised, trailed, or trail-impressed. A decoration motif, on the other hand, refers to the specific shape and form of elements comprising the decoration. It was necessary to make such a distinction because of the different methodological processes required to apply decorations in these ways. Incised decorations necessitate a dry paste while trailed or trail-impressed decorations necessitate a wet paste. All plates were assessed for the combination of these features and a unique type number was assigned. For example, an identical decoration motif applied using distinct design techniques would be assigned different unique type numbers. These unique types are described in Appendix A. It is often difficult to determine if a design was unique based on a narrative description of a unique type decoration and as a result high-resolution photographs of each sherd were taken and repeatedly referenced during this process. Unique decoration type-categories totaled 94 across the 429 vessels with designs present.

Since the goal of Chapter 6 was to explore social identities through symbolic communication, the next step in the linear sequence of category assignments was to group the unique types into decoration grouping categories based on perceived similarities in decoration motifs alone (i.e. disregarding design technique). This emphasized symbolism alone as opposed to technique. To accomplish this in a systematic way, photographs of plates were traced, in order of unique decoration motif type, using an old computer monitor that was setup flat on a desk. Tracing the actual designs, as opposed to appealing to the artistic intent of the decoration and embellishing any imperfections, enables focus to be placed on overall presentation and execution of the motifs present and aided in identification of other similar designs as a result. In each case, photographs of all plates with decorations that were previously categorized as belonging to the unique type were referenced during the sketching process and the most emblematic was chosen

for sketching. Photographs of each plate lacking a decoration grouping category assignment were then meticulously inspected to determine whether or not they might also share the symbolism present in the decoration grouping category in question. This process was iterated until all decorated plates were assigned to a decoration grouping category, determined to be wholly unique, or indeterminate in category assignment. It was often necessary to assign plates to a decoration category based on incomplete or partial decoration motifs present. In these cases, license was not taken beyond what was present on the plate. In other words, no assumptions were made about what other motifs might be present based on the co-presence of two motifs on other plates. Instead, decoration motif categories were assigned often based on potentially incomplete motifs. Nevertheless, because the potentially incomplete motifs were deemed similar in the actual motifs present, the decoration motif categories assigned should be considered fairly robust. This process resulted in 29 decoration grouping categories used in Chapter 6. Sketch tracings are provided in Appendix E. Photographs may be requested from the author for research or teaching purposes.

4.3 Compositional Analysis of Archaeological Ceramics

Following the development of effective methodology in the elemental, mineralogical, and compositional characterization from the mid-20th century to the present, identifying shared source information for artifacts has become a well-established and common research tool in archaeological studies (Glascok 2016; Neff 1993). Compositional analysis in archaeology explores human behavior through chemical fingerprints obtained from archaeological materials. Information from those chemical fingerprints is used to discern the location of raw material sources, identify production sites, investigate production or manufacturing technology, or trace

the movement or circulation of artifacts between different regions or production locales. The basic assumption underlying this methodology is that compositional variability in archaeological artifacts will arise from the geological forces responsible for the production of the raw materials used to create the artifacts, often in conjunction with technological choices made by the manufacturer. Studying human behavior from this evidence is a complex endeavor, especially when considering ceramic artifacts given the heterogeneous nature of clay and the multitude of factors that may influence the final measured composition of a pottery vessel (Neff 2003).

The following discussion provides an overview of central concepts related to the compositional analysis of ceramic artifacts in particular as they relate to the compositional analyses presented in Chapter 7. The objective is to provide a discussion of many of the issues inherent in compositional analysis techniques more broadly and their application to anthropological archaeological research contexts more specifically.

4.3.1 Compositional Analysis in Archaeology

At the most basic level, compositional analysis in archaeology is a means to identify groups of similar objects. The most commonly addressed research goal built on group identification is the movement of objects in the past (Golitzko 2010; Speakman, et al. 2007). Analyzing the movement of objects is theoretically grounded in the concept of the “provenience postulate”, which proposes “that there exists differences in chemical composition between different natural sources that exceed, in some recognizable way, the differences observed within a given source” (Weigand, et al. 1977:24). Because each source location is produced as a result of context-specific geological forces, the provenience postulate applies in unique ways to different classes of raw materials. Sourcing ceramic artifacts in particular requires a variety of

unique considerations compared to other inorganic materials. For example, while virtually every obsidian flow on earth is chemically distinct (Glascock 2002), raw clay resources are often multitudinous throughout the landscape and found in often large and diverse outcrops that are formed and transported through an array of geological forces that may lead to a blending of clay particles (Eerkens, et al. 2002; Gjesfjeld 2014). Nevertheless, the ubiquity of clay resources and ceramic artifacts in prehistoric contexts lends to the advantageous nature of compositional analysis to answer a host of behavioral questions despite these and other challenges. For example, while obsidian or glass artifacts can often only answer questions related to long-distance exchange as a result of the vast distances between production or outcrop locales, pottery sourcing studies can often provide more informative results when examining exchange relationships at intra-regional or inter-regional scales (Dussubieux and Oliver 2016; Falabella, et al. 2013; Fowles, et al. 2007; Pearce and Moutsiou 2014; Zvelebil 2006). This is particularly relevant in the case of archaeological cultures such as the Oneota, which are often only able to be differentiated internally based on distinctions in ceramic artifacts and are therefore often recognized as a ‘pottery culture’ (Henning 1998; Hollinger 2005; Overstreet 1997).

A number of methods exist for the chemical or compositional measurement of ceramics. The earliest such method used in archaeology was neutron activation analysis (NAA), following the suggestion of renowned physicist J. Robert Oppenheimer (Harbottle 1976; Sayre, et al. 1957). Since then, many other analytical techniques from the physical sciences have been applied to archaeological studies for the purposes of compositional analysis. These include X-ray fluorescence (XRF), portable XRF (pXRF), particle-induced X-ray emission (PIXE), Scanning Electron Microscopy with Energy Dispersive Spectra/Wavelength Dispersive Spectra (SEM-EDS/EDX), electron probe microanalysis (EPMA), inductively coupled plasma-mass

spectrometry (ICP-MS), and laser ablation ICP-MS (LA-ICP-MS) (Glascock 2016; Golitko 2010:216). For many years, instrumental neutron activation analysis (INAA) was the method of choice for archaeological composition analysis due to the presence of numerous first and second generation dedicated research reactors at national laboratories, museums, and major universities (Glascock 2002; Neff 1993, 2003). Though LA-ICP-MS has increased ‘market share’ relative to INAA in recent years largely due to the waning of available research reactors for INAA and due to the lower detection limits, higher range of elements able to be characterized, and rapid ability to analyze many samples by LA-ICP-MS (Dussubieux and Oliver 2016; Glascock 2016).

Neff and colleagues (Golitko 2010:216-217; Neff 2002:202) detail five hypotheses that should be considered when analyzing the chemical composition of pottery:

- 1) Chemical patterning is a reflection of differences in elemental concentrations present in the source clay(s) and is therefore a function of local geological variability,
- 2) The composition as measured principally reflects technological choices made by potters in paste preparation, such as the mixing of clays or additions of aplastic, thereby modifying the compositional signature of the elemental fingerprints of the clay resources used,
- 3) The use-life of the ceramic objects has modified the chemical patterning of the paste as a result of the leaching of organic or inorganic compounds into the ceramic matrix,
- 4) The raw clay chemical composition is altered as a result of diagenesis, or post-depositional changes to the chemical profile of the ceramic objects,

- 5) Some combination of the four factors above has resulted in the chemical composition readings.

Controlling for the five factors above requires knowledge about local geological variability regarding raw clay resources, knowledge about cultural practices related to vessel production such as clay preparation and tempering additions, knowledge about the chemical profiles of any tempering additions, potential effects caused by the use-life of the ceramic vessels under consideration, and knowledge about soil chemistry in the location(s) where the ceramic vessels were recovered. The following sections provide a brief discussion of these factors, particularly as they relate to shell-tempered ceramics from the Late Prehistoric period of the central Illinois River valley.

4.3.2 Clay: Geological, Chemical and Mineralogical Considerations

Clays are complex materials from a variety of perspectives, but it is precisely this complexity which lends to their value as an adaptable raw material in many applications both in pre-modern and industrial contexts. At the most basic level, clays may be defined as a very fine-grained earthy material that, when moistened, becomes plastic or malleable (Rice 2005). Clays result from the weathering of silicate rocks, which are formed via igneous, metamorphic or sedimentary forces, and clays reflect the original compositional profile of the specific rocks which weathered to form them following the removal of large particles (sands), oxides, and mobile cations (Golitzko 2010; Keller 1964). Primary, or residual, clays are those that form in the same location as their geological parent source. Hydrological, aeolian, glacial, erosional, or other forces may transport clays (or their initial parent source material) to a different location. These are referred to as secondary, transported, or sedimentary clays and are most often the product of

marine, riverine, or lacustrine forces. This often leads to a higher organic content present in secondary clays but also a finer-grained and well-sorted substrate. In addition to their depositional nature, clays may be described in terms of their granular, chemical, or mineralogical properties. The following discussion will briefly touch on these descriptive lenses.

Particle-size is an oft-used quantitative measure used in defining clays. Granulometry, or the measurement of the distribution of particle sizes, has been applied to distinguish between the individual mineral grains of sediments based on their diameter. The International Organization for Standardization (ISO) 14688-1:2002 establishes a scale of soil sediment particle diameter sizes where clays are the smallest in size at less than 2 μm (or 0.002 mm). While this standard is used by geologists and soil scientists, different scales for the definition of clays based on particle size are often considered by sedimentologists, colloid chemists, or geotechnical engineers. Nevertheless, it is the remarkably small particle size of clay minerals that enables the highly desirable characteristic of plasticity.

Clays are composed of a number of different kinds of minerals, each falling within the less than 2 μm size range, but no consensus exists to impose order on or classify the minerals into discrete categories (Rice 2005). While mineralogists and soil scientists continue to examine and detangle the evolving nature of clay mineralogy, often as a lens to access the principles of mineralogical evolution more broadly (Hazen, et al. 2013), it is known that the multitudinous minute minerals that compose clay are arranged in a crystalline structure which results in certain chemical properties (Golitsko 2010:218; Rice 2005:31-53; Velde and Druc 1999:35-38). Clay minerals are composed of flat sheets of aluminum and silica atoms that may be arranged in different layer combinations, or more rarely as lath or chain structures. Alumina and silica are the two chemical elements most resistive to the weathering forces that result in clay. As part of

the form of the crystalline structure, the aluminum and silica cations are strongly bound in two dimensions but weakly bound in a third direction. Within the lattice structure of layered silica and alumina, these bonding arrangements result from the interplay of dominant cations and the anions (most often oxygen) to which they become linked (though it should be noted that other major cations such as calcium, magnesium, sodium, titanium, iron, and potassium may link together layers). Clay plasticity arises from the ‘sliding’ of various sheets of silica-aluminum-oxygen across one another along hydroxol bonds. When heated, hydrogen ions bond with oxygen anions to form water and are driven off as vapor. This leaves behind the silica-aluminum layers, which fuse together from the artificial metamorphic reaction. Once these layers are fused, clay takes on the solid and water impervious properties sought after in use as serving, storing, or artistic objects. If sufficient heat is applied during this process, the internal crystalline structure is destroyed. The very high refractoriness (or ability to maintain chemical and physical robustness when exposed to temperatures above 1,000 °F) enables fired clay to serve as a cooking vessel.

4.3.3 Technological Choice and Pottery Production

Technological choices and pottery production techniques may alter baseline clay compositions primarily through the addition of tempers and the mixing of different clay resources. When considering pottery for compositional analysis, the most significant confounding factor is the presence of non-plastic materials embedded in the ceramic paste matrix. As a result of these inclusions, bulk compositional profiles of ceramic artifacts reflect not only the geochemistry of the clay resource(s) used, but also any other ingredients used in pottery manufacture (such as tempering) or inorganic material inclusions that were not removed from the raw clay material (such as small pebbles) in addition to changes that result from use and

diagenesis (or the absorption of chemicals from the soil in which the sherds were deposited) (Gjesfjeld 2014; Stoltman, et al. 2005). The influence of added tempering on compositional readings and paste behavior in particular has been a source of debate (Boulangier and Glascock 2015; Neff 2008; Peacock, et al. 2007; Stoner and Glascock 2012; Tite, et al. 2001; A. J. Upton, et al. 2015). However, given the often elementally restricted profiles of materials used in tempering (e.g., volcanic ash, mollusk shell, limestone) it has been demonstrated that tempering is likely to only modestly influence the identification of chemical source groups unless it is present in remarkably high (>80%) proportions relative to clay in the paste matrix (Eerkens, et al. 2002; Neff 2002; Neff, et al. 1989). Mathematical corrections and/or the removal of tempering-abundant elements from analyses are common strategies employed to control for the presence of tempering in compositional studies of ceramics (Cogswell, et al. 2015; Peacock, et al. 2007).

Because the LA-ICP-MS technique used in this dissertation allows the researcher to sample specific locations on a pottery vessel, as opposed to a bulk sampling technique such as INAA that analyzes the entire sherd, the effect of tempering on vessel chemical composition are often able to be controlled for, but highly tempered pastes often require alternate means of dealing with the impacts of temper on chemical compositions. A mathematical method to control for the presence of shell tempering in vessels used in this dissertation was used and is discussed in detail in Chapter 7.

Clay mixing, or the use of bits of discarded pottery as temper – known as grog, can be a more impactful issue, particularly for studies aiming to determine potential geologic resource exploitation areas as opposed to production locales of pottery. That is, the mixing of clays may obfuscate the final chemical composition of a vessel such that neither constituent clay may be

differentiated. However, since most studies of ceramic provenance are primarily interested in the circulation of ceramic vessels out of a production locale, as opposed to a geological source area, these factors are generally of minor hindrance.

4.3.4 Use-Wear Effects on Sherd Chemistry

Ceramic vessels are highly versatile tools, and with that versatility comes the potential for use-wear effects on sherd chemistry. Since the primary uses of ceramic vessels in prehistoric eastern North America involve organic materials and because elements present in organic materials are not typically measured in provenience studies, however, use-wear effects are generally negligible for impacting chemical concentrations (Golitzko 2010). Examples of use-wear effects that might result in a significant impact to sherd chemistry include the storing of metal coins or other metal objects.

4.3.5 Diagenesis and Sherd Chemistry

Perhaps the most impactful factor effecting sherd chemistry is that of post-burial alteration. A number of factors impact the role of taphonomy in changing sherd chemistry, such as the temperature to which a vessel was fired, the mineralogical and chemical composition of the sherd in question, and the burial environment of the vessel. These effects are thoroughly discussed by Golitzko (2010:224-226). For the case of Native American pottery produced in eastern North America, the simple leaching of mobile elements is the most probably form of diagenetic alteration. This is due to the fact that Late Prehistoric pottery was open or pit fired to a maximum of some 700 °C due to constraints imposed by mollusc shell tempering and a lack of evidence for forced-air firing methods (A. J. Upton, et al. 2015).

4.4 Compositional Methods: pXRF, XRD, and LA-ICP-MS

In order to look holistically at the chemical composition of ceramics in this dissertation, three different methods were used to explore chemical and mineralogical characterizations. The bulk of analysis was performed using LA-ICP-MS, which is discussed at length in Chapter 7. However, two other methods were employed toward different ends. First, due to the catastrophic burning of a number of sites incorporated in the analysis, some sherds were re-fired to significant temperatures (G. D. Wilson 2013). As a result, it was hypothesized that the chemical composition of those vessels may have been impacted. In order to test for potential changes due to re-firing, x-ray diffraction was employed. X-ray diffraction assesses the crystalline structure, or mineralogical makeup, of ceramic vessels and was used to determine whether or not sherds from sites that were incinerated have distinct mineralogical profiles from sherds recovered from sites that were not burned. X-ray diffraction methods and results are presented below and the raw data is provided in Appendix G.

A recent technology, portable x-ray fluorescence (pXRF), allows for quite rapid and quite inexpensive characterization of a subset of chemical concentrations compared to LA-ICP-MS. However, pXRF is entirely non-destructive, highly portable, and much more affordable than LA-ICP-MS. While the data produced by LA-ICP-MS and pXRF differ in many important ways, funding was obtained to collect pXRF data from a subset of vessels to determine if analytical results might be comparable to those obtained from LA-ICP-MS analysis of the same vessels. Work in this regard is on-going and as a result no pXRF analytical results are provided in this dissertation. However, the raw data will be curated alongside raw LA-ICP-MS data in a tDAR archive at the following static link <https://core.tdar.org/project/447475>

4.4.1 Portable X-Ray Fluorescence

Portable X-Ray Fluorescence (pXRF) spectrometry, performed at Michigan State University, was used to analyze the elemental composition of a sub-sample of 30 ceramic artifacts with an objective to enhance understanding of the raw material prehistoric populations selected for ceramic production. The first group of artifacts were selected from a previously analyzed sample from Morton Village (11F2) while the second group was derived from Crable (11F249). Random proveniences were selected to reflect the compositional diversity that may be present within each site. The goal of this effort was to provide raw count data that may potentially be used to determine the range of compositional variation detectable through the use of handheld spectrometry.

Analysis was performed using a Bruker Tracer SD-III with a 10 mm² X-Flash SDD, peltier cooled, detector with a typical resolution of 145 eV at 100,000 cps. An x-ray tube Rh target was used with a max voltage of 40 kV. pXRF settings were set to 300 second timed assays at 40 kV 30 μ A using a green filter (12 mil Al = 1 mil Ti + 6 mil Cu). Data were collected and analyzed using the S1PXRF and ARTAX software.

Results of pXRF analysis are available via a permanent web link provided in Appendix B.

4.4.2 X-Ray Diffraction

X-Ray diffraction analysis was performed on all collected material at the Advanced Materials Characterization Center at the University of Cincinnati College of Engineering and Applied Science. Samples include 9 sherds, 9 outcrop localities, and 4 core samples. Diffractograms were collected on a Phillips X-Pert diffractometer operating with Cu-K α

radiation at 45Kv and 40Ma. The samples were prepared for both bulk mineralogical quantification and clay speciation in order to acquire the full mineralogical dataset. Bulk mineral analysis was scanned from 5-70° 2θ, with a step size of 0.02° scanning at 0.5 seconds/step. Clay analysis was scanned from 5-32° 2θ, with a step size of 0.02° scanning at 0.5 seconds/step. A 1° divergence slit, 2° anti-scatter slit, and a programmable receiving slit set to 2mm were used for all analyses.

Bulk samples were crushed in a mortar and pestle to a fine powder and top-loaded into an aluminum holder for analysis. Clay preparation follows the pipette procedure of Moore and Reynolds (1997) in order to separate the clays from solution. Bulk samples were placed into distilled water and repeatedly agitated until a visible suspension was sustained. The <2μ fraction was isolated from gravity sedimentation, and a small amount was pipetted onto a glass slide and allowed to dry for 24 hours. The clay slides were scanned as air-dried isolates, and then glycolated to expand any swelling clays present in the samples. For glycolation, samples were placed in a dessication bowl over ethylene glycol and cooked at 60 °C for approximately 12 hours. Individual samples remained in the glycol bowl at room temperature until ready for analysis.

Quantification of bulk samples was performed using the reference intensity ratio method (RIR), a comparative method that scales peaks to an internal spike. Since quartz is abundant in most natural rock and soil samples, it provides an effective natural internal spike to reference other peaks to. The method follows the equation, $\left(\frac{A(x)/RIR(x)}{\sum_{i=1}^n A/RIR} \right) * 100$, where A is the area under the 100% peak of the identified phase, RIR is the reference intensity ratio obtained from the ICDD PDF-4+ database, and x is each phase included in the quantification. This provides a weight percentage for each mineral phase identified in the sample. Clay quantification was done

using the same equation, but RIRs were calculated using NEWMOD modeling software (see website below for citation). The quantification of all mineral phases is assumed to be semi-quantitative, with a general margin of error of approximately $\pm 5\%$ for the bulk minerals and $\pm 10\%$ for the clay species.

Bulk mineralogical analysis of the sherds reveals a silicate-rich mineralogy, with abundant quartz (32-74%), feldspar (5-20%), and total clay (29-60%) in all samples. Calcite was present in sample 766 (9%) and 844 (30%), most likely due to carbonate filler used in the production of the pottery. The sherd clay mineralogy is comprised entirely of illite with no evidence of swelling clays present. This is a result of the high temperature firing causing the destruction of swelling smectite and kaolinite, and the subsequent enhancement of the dehydrated 10Å illite phase. The bulk mineralogy of samples collected from outcrop and core are very similar to the sherds. The silicates include quartz (25-64%), feldspars (3-19%), and total clay (25-68%). Sample 38 is the notable exception and is composed almost entirely of calcite (85%). Some minor dolomite is found in several samples, as well as lesser amounts of calcite. The clay mineralogy is more diverse than the sherds, which includes mostly illite and kaolinite, with one sample (KMM-01) containing 20% mixed layer swelling illite/smectite. The observed bulk mineralogy is to be expected from glacial till outwash sediments, and also explains the abundance of clay sized particles. The anomalously high dolomite and calcite outcrop material could be a result of carbonate enrichment from bedrock pore fluids interacting with surficial deposits.

4.4.3 Laser Ablation-Inductively Coupled Plasma-Mass Spectrometry

See Chapter 7, section 7.5, for a detailed description of LA-ICP-MS as used in this dissertation.

4.5 Analytical Methods for Monoplex Social Networks

Chapters 5 – 8 each incorporate the analysis of monoplex, or single-layer, social networks that model a single type of tie. Numerous measures exist for the statistical analysis of monoplex network graph properties. Monoplex network measures used in this study focus broadly on those that describe network structure. These include degree distribution, centrality (with a particular emphasis on closeness centrality), centralization, edge weights, network diameter, network density, average clustering coefficient, and average path length (or distance). A general discussion of each of these measures is presented here. However, no mathematical formulae will be provided for graph measure application as all measures were implemented using the igraph package (Kolaczyk and Csárdi 2014), which contains detailed documentation and references regarding their implementation.

Social networks are mathematically formulated as graph objects, which consist of a set of nodes (or vertices) and a set of edges (or links) that connect them. The number of nodes in a network, in this case spatially bounded archaeological communities, is referred to as network order. The number of edges in a network is referred to as network size. The degree of a node captures the number of edges that are connected to, or incident to, that node. In the case of directed networks, where edges are characterized by directionality, in-degree refers to the number of edges pointing in toward a node and out-degree refers to the number of edges emanating from a particular node out toward another node. When aggregated and rescaled, the degrees of individual nodes are studied by looking at the distribution of their frequencies, a concept referred to as degree distribution. In graph objects where edges carry a weight, such as the flow of goods in a shipping trade network or the number of passengers on individual flights

in an air transportation network, degree is the sum of a node's edges. By extension, the weighted degree distribution considers the frequency of various weighted degrees and is referred to as strength. A related measure, density, considers the frequency of realized edges relative to the potential maximal number of edges possible given a set of nodes.

Often, questions arise as to the flow of information in a graph object. One way to examine information flow is through understanding of the paths within a network. A common notion in this regard is to determine the distance between any two nodes, or the shortest path between them. Distance is often referred to as geodesic distance or simply geodesic. The average path length considers how many nodes must information travel through, on average, to reach a target destination node. The diameter of a graph is the value of the longest distance among nodes within it. Diameter captures the notion of how many nodes must information travel from the two most distance nodes in a graph.

Social relationships are often reciprocal, and it is common for friends of friends to also be friends for example. The notion of whether or not two individuals who are friends with the same person are also friends corresponds to the concept of network transitivity. Transitivity is often referred to as the global clustering coefficient, which considers the proportion of transitive triads in a graph – or where two nodes who share a relationship with a third node also share a relationship. This may also be considered the proportion of triadic closure. Thus, transitivity considers a specific case of clustering – the proportion of three nodes all sharing a relationship together in a graph – and as a result care must be taken such that one does not confuse the global clustering coefficient based on triadic transitivity to be confused with statistical clustering measures applied to non-graph data. Graph transitivity is therefore a global measure in that it considers all triads within a graph object.

A local clustering coefficient is also used in network analysis. The local clustering coefficient extends beyond the concept of triadic transitivity and instead considers whether all nodes in a node's neighborhood, or all nodes connected to a single node, are in turn completely connected to each other (Watts and Strogatz 1998). The average of each node's local clustering coefficient is therefore able to assess the average completeness of node neighborhoods. Thus, the local clustering coefficient is again distinct from statistical clustering methods applied to non-graph data.

A common research aim in social network analysis is to determine the role of individual nodes in the network. For example, the unique role of the Medici family in various networks is hypothesized to be of importance to the family's rise to power, prestige, and great wealth in the early Florentine Renaissance (Padgett and Ansell 1993). The 'importance' of individual nodes is captured in measures of node centrality, of which there are many (Scott 2000; Scott and Carrington 2016; Wasserman and Faust 1994). Because the research questions in this study are generally restricted to identifying changes in overall network structure, as opposed to an analysis of the role(s) that specific site-nodes may have played in the Late Prehistoric period central Illinois River valley, centrality measures are downplayed in favor of a set of centralization measures, which extend the concepts inherent in individual centrality measures to that of the graph object as a whole. In other words, centralization describes the extent to which information flow (as captured in corresponding measures of centrality) is organized around particular focal points. Centralization therefore assesses the likelihood that a single actor, or sub-group of actors, plays an outsized role in the network.

As degree centrality considers the degree (as defined above) of individual nodes, degree centralization considers the variation in individual node degrees divided by the maximum degree

that is possible in a network of the same size (Scott 2000). A high degree centralization score therefore indicates that all nodes are primarily connected to one central node, while a low degree centralization score indicates the inverse – nodes connections are more evenly distributed. Another measure of centralization is rooted in the concept of betweenness. Betweenness centrality describes the extent to which a node is located between other pairs of nodes and is rooted in the idea that node ‘importance’ relates to where a node is located with respect to the paths between nodes in a network (Kolaczyk and Csárdi 2014). Betweenness centralization considers the extent to which all nodes are equally connected *through* one central node. In a graph with high betweenness centralization, the only way for information to travel from one node to another is through one central node. Betweenness centralization differs from degree centralization in that betweenness is rooted in analysis of paths while degree is rooted in the analysis of node connectivity.

Related to measures of degree and betweenness is that of closeness. In cases where it may not be as relevant to have many relationships, nor to be between many nodes, it is possible to assess whether or not a node is still ‘close’ to the middle of information flows. Closeness centrality is related to the average shortest path length and describes the extent to which an individual node is close, on average, to other nodes (Wasserman and Faust 1994). Extending this concept to that of a graph as a whole, closeness centralization describes the extent to which all nodes are able to reach a central node in only one step. That is, a high closeness centralization score would indicate that one central node is only one step away from, or ‘close’, all other nodes. While a low centralization score would indicate that no one node is only one step away from all other nodes.

A somewhat more complex notion of centrality is that of eigenvector centrality, which defines a node as central based on its relationships to other central nodes. This definition is therefore recursive. A high eigenvector centralization score may therefore indicate that a network is composed of a sub-group of highly interconnected nodes and a sub-group of nodes that are weakly integrated into the highly interconnected sub-group, much like a core and periphery might be modeled.

Because graph centralization measures are standardized between 0 and 1, their interpretation is often straightforward. For most other network statistical measures, however, it is often difficult to discern whether a score is unusually high or low. Statistical hypothesis testing may be used in these cases to hold certain network features constant while simulating different network formulations. This approach is taken here using the Erdős-Rényi graph randomization technique (Erdős and Rényi 1959). Erdős-Rényi graph models place equal probability on all graphs of a given order and size. That is, a collection of graphs are considered based on the provided order and size and a probability is assigned to each, where the total number of distinct node pairs are considered (Kolaczyk and Csárdi 2014). An extension provided by Gilbert (1959) enables the random graph concept to be extended to graphs of a fixed order but where each pair of distinct nodes are independently assigned based on a given probability.

4.6 Definitions and Methods for Constructing and Analyzing Multilayer Networks

In order to quantify and analyze each of the distinct ceramic industry social networks as a cohesive whole, it is necessary to construct a formal multilayer network. In this section, I briefly discuss the methods used to perceive and construct multilayer networks following De Domenico et al. (2013), Kivelä et al. (2014), Boccaletti et al. (2014), and Dickison et al. (2016) as well as

methods for multilayer network analysis using two different analytical platforms: MuxViz and multinet (De Domenico, Porter, et al. 2015; Magnani 2017).

Single-layer networks, or graphs, are considered a tuple $G = (V, E)$, where V is the set of nodes (or vertices) and $E \subseteq V \times V$ is the set of edges (or links) that connect pairs of nodes. Nodes connected by an edge are said to be adjacent to one another. A multilayer network has a set of nodes, V , similar to a normal network graph, but is also comprised of a set of individual layers that are each composed of their own nodes. As a result, a multilayer network is defined as a quadruplet $M = (V_M, E_M, V, \mathbf{L})$. Each distinct layer is composed of a node set V_M and edge set E_M . Elementary layers may be a specific interaction type or a time stamp, and a layer (\mathbf{L}) consists of the combination of both a specific interaction type *and* a time stamp. A multilayer network may be node-aligned when all layers contain all of the nodes, or layer-disjoint if each node exists in at most one layer.

A multilayer adjacency tensor is a data object used to store and manipulate both multilayer and multiplex networks (De Domenico, Solé-Ribalta, Cozzo, et al. 2013:3). A multiplex network is a specific type of multilayer network in which the only possible types of connections across different layers are ones in which a given node is connected to its counterpart nodes in the other layers (De Domenico, Solé-Ribalta, Cozzo, et al. 2013). Great care must be taken when performing multilayer network analysis in cases where nodes are not identical across the layers because the tensorial approach requires any missing nodes to be present on each layer but without edges (or empty) on layers where the node is otherwise absent. This can result in misleading network statistics such as mean degree or clustering coefficients (Cozzo, et al. 2013; De Domenico, Solé-Ribalta, Cozzo, et al. 2013; Kivelä, et al. 2014).

Because of the multilayer adjacency tensorial approach, tabular (or rectangular) data structures alone are unable to be used to store multilayer network. There are thus two general approaches used to format multilayer networks. I refer to these as either a split file approach or a complex file approach. A split file approach is used by MuxViz (De Domenico, Porter, et al. 2015) and requires a master configuration text file that specifies the locations of separate text files that contain node and edge information. Node information is contained in a layout file, specifying a distinct number for each node and any other ancillary information. Edge information is contained within a distinct file for each layer and is formatted as an edge list. A complex file approach, such as that used in multinet (Dickison, et al. 2016; Magnani 2017), combines node, edge, and layer information into a single, complexly formatted file.

4.6.1 Multilayer Network Analysis Measures

This section details the specific multilayer network analysis metrics used in this research. There are two overarching trends that these metrics are designed to assess – influence and overlap in multilayer networks. Within a multilayer network, influence and overlap may be applied to the actors across the network layers, the edges that connect actors across the layers, or some combination of these features. Metrics falling under the concept of influence seek to ascertain the impact of individual network layer properties on structuring the entire multilayer network. While metrics falling under the concept of overlap seek to assess the different network layer properties relative to one another. In these ways, both overlaps and influences in multilayer network analysis are specifically designed to compare the different layers to one another in order to arrive at a richer interpretation of the full multilayer network and to aid in causal inference.

Multilayer network analysis was carried out in two distinct platforms – MuxViz 2.0 and multinet 1.1.5 (De Domenico, Porter, et al. 2015; Dickison, et al. 2016; Magnani 2017), both

using the R statistical programming language. All R code for the multinet analysis is provided in Appendix C. No code is provided for the analyses performed using MuxViz, as it is a graphical user interface driven program. However, as it is open source, all code for the analytical measures is freely accessible.

The concept of graph centrality is applied throughout the individual layer analyses (Chapter 5 – 7) but must be extended to account for the presence of multiple network layers in a multilayer network. Node centrality was analyzed using MuxViz 2.0 for the multilayer network and a number of different centrality measures are considered in Chapter 8. Node centrality measures are designed to identify the most important nodes in a graph (Scott 2000; Wasserman and Faust 1994). However, the concept of importance can take many forms. In the multilayer network analysis presented in Chapter 8, three kinds of centrality are analyzed: degree, eigenvector, and strength.

Perhaps the most straightforward centrality measures are that of degree centrality and strength, which are simply the sum of all edges that a given node is characterized by or the sum of all edge weights that a given node is characterized by respectively (Opsahl, et al. 2010). In the parlance of network analysis, this is the sum of edges or edge weights *incident* to a node. Extending degree centrality and strength to multilayer networks is quite simple – one sums the number of edges or edge weights incident to a given node across each of the different layers, which can include edges that span across different layers in a multiplex network. Thus, degree centrality and strength quantify the number of edges or depth of edge relationships a node has across the different layers, which can have far-reaching consequences for the role that each node plays in full multilayer network.

Somewhat less straightforward, eigenvector centrality characterizes nodes based on their connectiveness to other well-connected nodes. The basic idea is that important actors are likely well-connected and as a result are more likely to be connected to other well-connected nodes. A given node therefore has high eigenvector centrality if its neighbors also have high eigenvector centrality, and the recursive nature of this notion results in a vector of centralities that satisfies an eigenvalue problem (De Domenico, Solé-Ribalta, Omodei, et al. 2013). Using the rank-4 multilayer adjacency tensor formulation of multilayer networks, it is naïve to simply aggregate all network layers and then compute eigenvector centrality or to compute eigenvector centrality across the layers individually and aggregating the results (De Domenico, Solé-Ribalta, Cozzo, et al. 2013). By simply aggregating the layers, information across the layers is intermixed with uncontrollable effects. While calculating individual layer eigenvector centralities would require that a heuristic aggregation metric (say mean or median of individual layer eigenvector centralities) be applied, which disregards the solution of unique eigenvalues problems that each individual layer metric is designed to answer. Instead, an eigentensor is used to encode the centrality of each node in each layer in due consideration of the whole interconnected network structure (De Domenico, Solé-Ribalta, Omodei, et al. 2013).

A metric from multinet, degree deviation, is used to provide additional meaning and insight to the calculation of a given node's degree by recasting degree centrality as discussed above. Degree deviation is defined as the standard deviation of the degree of an actor on the input layers. Much like degree centrality, degree deviation does not consider the weight of an edge, only its presence or absence. An actor with the same degree on all layers will have a deviation of 0, while an actor with many neighbors on one layer and just a few on another layer will have a high degree deviation, which indicates an uneven usage of the layers (or layers with

different densities) (Dickison, et al. 2016; Magnani 2017). Thus, degree deviation is a measure that quantifies the inter-layer overlap of individual nodes and can therefore aid in interpretations about the role that individual nodes play across the different layers of the network and in the full multilayer network as a cohesive whole.

Related to both degree centrality and degree deviation is another metric from multinet that assesses information about the multiplexity of actors in a network – connective redundancy. One may ask, to what extent does an actors' relationships on one layer hold true on other layers in a multilayer network? Connective redundancy answers this question by assessing each actors' neighborhood (or the total number of actors incident to a given actor on specified layers) and degree (or the total number of edges incident to a given node on those same specified layers). The formal equation is one minus neighborhood divided by degree (Magnani 2017). Thus, high connective redundancy occurs when the actors are connected to the same neighbors on multiple layers (Dickison, et al. 2016).

Additional methods for the comparative analysis of edges across different network layers is that of mean global edge overlapping and layer edge overlapping from MuxViz. The mean global edge overlap measures the fraction of edges which are common to all layers and can be applied to either unweighted or weighted multilayer networks (De Domenico, Porter, et al. 2015). This acts as a measure of comparative similarity between all layers but may also be applied on a layer by layer basis to measure similarity of any two given layers in the case of layer edge overlapping. A method is also able to be applied that hierarchically clusters layers to determine which layers are most similar in terms of the edges present within them. Edge overlapping is valuable for weighted networks because the weight of each edge is factored into the inter-layer comparison.

As individual networks are constructed as edge lists and converted into adjacency matrices in MuxViz, it is also possible to explore each of the matrices and their aggregate as heatmaps. This is referred to as a matrix explorer in MuxViz and is an easy way to gain intuition about how the different network layers are similar and different with respect to the presence of actors and edges. Aggregating the individual network layers together through a process of layer flattening (or forming new edge weights between each actor-actor combination by summing all edges across all layers), also provides insight as to the structure of the full multilayer network. It is also possible to apply clustering to both the multilayer adjacency matrices and aggregate adjacency matrix to identify structurally similar actors or groups of actors.

The final multilayer measures utilized in Chapter 8 are a class of layer comparisons from multinet. These measures compare each pair of layers based on common statistical measures of overlap, distribution dissimilarity, or correlation (Dickison, et al. 2016; Magnani 2017). In the analyses presented in Chapter 8, two measures of overlap in particular are used: Jaccard edge overlap and Simple Matching overlap. Jaccard edge overlap follows the Jaccard index, which is defined as the intersection divided by the union of layer edges. Simple Matching acts just as one would expect based on its name and assesses whether or not an edge between a pair of nodes present in one layer is also present in another layer, providing a return value of the percentage of such matching edges. Unlike the edge overlapping measure from MuxViz, edge weight is disregarded in the multinet implementations of both Jaccard and Simple Matching overlap. The Jaccard edge overlap and Simple Matching coefficients therefore quantify the interaction between two network layers by measuring the tendency that links are simultaneously present in both networks. Whereas the Jaccard coefficient considers the presence of a link as a function of

all links present, the Simple Matching coefficient simply quantifies the degree to which there are overlapping links.

CHAPTER 5 NETWORKS OF INTERACTION THROUGH CULTURAL TRANSMISSION

5.1 Introduction

Explaining similarity, variation, and change in material culture is a critical and long-standing research objective for archaeologists. It is particularly important and challenging in contexts where differing material culture traditions merge, blend, or otherwise amalgamate (Frangipane 2015; Liebmann 2013; Stone 2003). Culture historians initially used assemblage similarities as a proxy measure for historical relatedness and artifact typologies as a means of telling time to discern *how* sequences varied from place to place and over time (Eerkens and Lipo 2005:240). These cultural sequences and boundaries largely persist as the foundation of American archaeological inquiry today (Lyman, et al. 1997). More recent trends in the measurement of artifact assemblage attributes focus on interpreting variation among and between individuals and communities as opposed to between archaeological cultures (Goodby 1998; Rowe 2016). A key interpretive outcome of these studies is to evaluate networks of relational connections among individuals and larger social groups. Problematically, many technological characterization studies make *a priori* assumptions about which artifact attributes contribute to relational or social connections (Dietler and Herbich 1998; Stark, et al. 1998). For example, ethnoarchaeological surveys suggest that low visibility attributes act as indicators of shared contexts of learning (Carr 1995b; Clark 2001; Peeples 2011:173), or that high visible attributes express emblematic information (Eerkens and Bettinger 2008:22). I argue here that while the study of material culture type-attributes is a productive avenue for discerning relational interaction between communities of artisans (Herbich 1987; VanPool 2008), the forces acting on the execution of a given artifact attribute must be problematized as opposed to assumed. That is, to

interpret attribute-based technological similarity as evidence of face-to-face interaction through shared learning mechanisms or historical relationships of descent (Peeples 2011), similarities affected by social processes must be differentiated from those affected by physical or engineering forces constraining the execution of a given artifact attribute.

This research presented below draws from an established evolutionary approach to quantitatively explore which attributes are more likely to be constrained by social or engineering forces before modelling social relationships via network analysis techniques. In particular, I describe and adapt a model developed by Eerkens and Bettinger (2008). The model is explicitly concerned with differentiating between variation in artifact traits mainly affected by physical, or engineering, constraints and variation mainly affected by social constraints. Eerkens and Bettinger (2008) refer to physical or engineering constraints based on raw material type or other factors as ‘function,’ and social constraints as ‘markers,’ which operate in many ways similar to ‘style’ as defined by Wiessner (1983, 1984, 1990). The Eerkens and Bettinger model is applied here as a means to determine which type-attributes across three ceramic vessel classes behave more or less in accord with predictions for empirical patterning in artifacts to diagnose the operation of different transmission processes. These type-attributes constrained by social processes will then be used to construct networks of relational interaction vis-à-vis cultural transmission. This method results in a proportional scale of ceramic technological similarity that represents a proxy measure to model the strength and directionality of relational connections among communities across the study area through time. The resulting interaction networks are examined on their own terms here before being used in Chapter 8 as one component of a model focused on interpreting the nature of communal coexistence in multicultural social environments using archaeological data across the Middle to Late Mississippian transition in the Late

Prehistoric central Illinois River valley (ca. A.D. 1200-1450; CIRV). While the presence of Oneota peoples following a *circa* 1300 A.D. migration into west-central Illinois has been demonstrated, the nature of intercultural relationships with indigenous Middle Mississippian peoples is unclear. It is argued that these networks provide insight into patterns of frequent interaction or homologous relationships between communities of ceramic artisans to better understand both indigenous and migrant community-based behavioral responses to multicultural regional and communal coexistence. In particular, four general questions are considered:

- 1) Are changes in the structure of interaction network patterns inherent across time, and how might the *circa* 1300 A.D. in-migration of an exogenous Oneota group be related to those changes?
- 2) Do interaction patterns support an hypothesized taxonomic distinction of Mississippian into La Moine and Spoon River cultural variants (Conrad 1989, 1991)?
- 3) It has been postulated that the onset of the Mississippian period *circa* 1200 A.D. was paralleled by the emergence of chronic, internecine violence and warfare (G. R. Milner 1999; G. R. Milner, et al. 1991). The threat of warfare is argued to have transformed both settlement and subsistence practices such that, among other things, “families coalesced into large communities behind defensive walls...limiting foraging and fishing trips” and “women became increasingly sequestered behind village walls” (Vanderwarker and Wilson 2016:98-100). Given that ethnographic accounts indicate that when pottery manufacture is done by hand, it is typically done by women (Rice 2005), it is possible to test whether sufficient variation in pottery attributes characterize different communities such that it can be reasonably assumed that potters were

geographically circumscribed in the cultural transmission of artifact attribute social information primarily as a result the threat of violence and warfare?

- 4) Given that the plate vessel class is absent or extremely rare in Oneota contexts outside the CIRV (Esarey and Conrad 1998), do imitations/emulations of serving plates by Oneota peoples inject sufficient variation to suggest that the adoption of this vessel class was made at a distance, or are the imitations/emulations technologically similar enough for there to be a higher likelihood that direct cultural transmission of ceramic technology between Mississippian and Oneota potters occurred?

Network models of interaction through cultural transmission provide robust answers to these questions and shed new light on archaeological understanding of the Late Prehistoric period CIRV more broadly.

5.2 Cultural Transmission Theory, Artifact Variation, and Network Ties

Cultural transmission theory offers a means to link “artifact variation to different ways in which cultural information is transmitted through space and time” (Eerkens and Bettinger 2008:22). The basic premise underlying this study is the supposition that different processes guiding the transmission of cultural traits will result in distinct patterns in measures of artifact variation (Eerkens and Lipo 2007; Lipo 2001). That is, artifacts or attributes should pattern differently if they were used to mark group identity (also referred to as “emblemic markers” (*sensu* Wiessner 1983), individual identity (also referred to as “assertive markers” (*sensu* Wiessner 1983)), or were constrained by engineering principles depending on whether they are context dependent. This model is designed to allow for the quantitative testing of otherwise qualitative assumptions about the nature of artifact attribute variation.

This model is applicable to any attribute measured on a continuous scale and involves the analysis of measurements of central tendency and dispersion. Attribute means and standard deviations are obtained for each site-based assemblage. From the mean and standard deviation, the coefficient of variation (CV) can be derived. The CV is a standardized measure that shows the extent of variability in relation to the mean of the sample or population. CVs are “appropriate to the study of variation in [archaeological] collections because it corrects for a near-universal scalar relationship between mean and standard deviation that prevents comparison between variables with different means using standard deviation alone” (Eerkens, et al. 2013:1135). Since statistical populations are rarely available in archaeological contexts, an unbiased estimator is used here for normally distributed data to calculate the coefficient of variation based on moderately sized samples. These metrics are used to derive three measures designed to “capture different aspects of the strength of the forces that produced variation” in the given attribute (Eerkens and Bettinger 2008:22).

The first metric, “variation of the mean” (VOM) is obtained by calculating the coefficient of variation of sample means, or the standard deviation of sample means divided by their average. VOM indicates whether a given attribute is under global or local control; local control refers to assemblage-specific control (Eerkens and Bettinger 2008:23). Low VOM suggests global control in that design constraints on an attribute are arguably severe enough for local contexts to be inconsequential – the mean of the attribute will be roughly the same from assemblage to assemblage. High VOM results from substantial variability in the mean of an attribute from assemblage to assemblage, and infers that variability in local control matters, resulting from local social forces or context specific engineering constraints.

The second metric, “average variation” (AV) indicates the strength of global or local control. AV is obtained by calculating the average of the assemblage coefficients of variation and records the average amount of variation around the mean disregarding the location of the mean. Low AV suggests strong control in that variation around the mean is generally small (less latitude is taken when executing the artifact attribute). High AV infers weak global control because variation around the mean is generally large (more latitude is taken when executing the artifact attribute). That is, AV assesses the degree of type-attribute variation within the assemblages and is suited to assess whether control is driven primarily by individuals (high AV) or by the group (low AV).

The third and final metric, “variation of variation” (VOV) “indicates the degree to which an attribute is homogenous with respect to strength of control and, by implication, kind of control” (Eerkens and Bettinger 2008:23). VOV is obtained by calculating the coefficient of variation of assemblage coefficients of variation. VOV assess between-assemblage differences in attribute variability. Low VOV suggests global homogeneity in strength and kind of control because variation around the mean is roughly the same from site to site. Whereas high VOV indicates global heterogeneity in strength and kind of control because of substantial local variation around the mean from assemblage to assemblage.

In order to remove scalar effects, the final VOM, AV, and VOV scores are obtained by standardizing their raw values (rescaling to produce attribute distributions with a mean of 0.0 and standard deviation of 1.0).

From these three metrics, functional (or selective) and social (or selectively neutral) dimensions of artifact variation can be explored in due consideration of demographic context. Eerkens and Bettinger (2008:25) summarize expectations for attributes under different forces

based on the three metrics in Table 5.1. At the most general level, the model differentiates between global functional control, which is characterized by relatively low VOM, and local or site-specific control, which is characterized by relative high VOM. Further, the signature of emblematic and assertive markers should be high VOV, with low AV indicating emblematic markers and high AV indicating assertive markers within a high VOV attribute. Though I must emphasize the acknowledgement by Eerkens and Bettinger (2008, p. 26) that while many complex factors contribute to artifact variability, much of the objective of their model is to simplify those complexities “in the sense that many can be regarded as local functional constraints”.

Force	VOM	AV	VOV
Strong global function	Low	Low	Low
Moderate global function	Intermediate	Intermediate	Low
Neutral (afunctional)	High	High	Low
Variable strength global function	Undefined	Undefined	High
Strong local function	Intermediate–high	Low	Low
Moderate local function	High	Intermediate	Low
Emblematic style, universal attribute	High	Low	Low
Emblematic style, local attributes	Undefined	Undefined	High
Assertive style, universal attribute	Intermediate–high	High	Low
Assertive style, local attributes	Undefined	Undefined	High

Table 5.1 Expectations for Attributes under Global or Local Functional Control, and Serving as Emblematic and Assertive Markers (Eerkens and Bettinger 2008, p. 25)

The concerns of the current analysis are not to characterize specific social forces as assertive or emblematic style nor to parse the nature of attribute function. Rather, the focus here is to identify artifact type-attributes that are free to vary from site to site, which is argued to indicate that social forces are more likely to be a contributing factor to that variation. As a result, interpretive guidelines for the current analysis are presented in Table 5.2.

The guiding assumption behind each of the expectations in Table 5.2 is that moderate to significant variation in type-attribute measurements between site assemblages is more likely to

be related to social forces guiding the execution of a given type-attribute rather than engineering constraints. Because evolutionary forces tend to favor social transmission (as opposed to individual learning and experimentation) for complex technologies where the cost of experimentation is high (Eerkens and Lipo 2007:259-260), such as in the case of cooking vessels, variation in a given attribute from assemblage to assemblage is therefore more likely to

Force	VOM	AV	VOV
Social Constraint (local control)	Undefined	Undefined	Moderate - High
Engineering Constraint (global control)	Low – Intermediate	Low – Intermediate	Low

Table 5.2 Expectations for Attributes under Social or Engineering Constraint

result from the expression of assertive style or community-specific social information. Spencer (1993) argues that frequent and unpredictable warfare may further contribute to the favorability of social learning to acquire information, which is argued to be rampant in the case study region (G. R. Milner, et al. 1991; Steadman 2008; Vanderwarker and Wilson 2016; G. D. Wilson 2012, 2013), though not ubiquitous (Hatch 2015, 2017). Confounding factors including context-specific constraints such as raw material availability, however, may impact in these local dependencies.

In a separate article, (Bettinger and Eerkens 2008) argue that variation “should decrease as cultural/technical complexity and population density cause transmission systems to shift emphasis from” models of cultural transmission favoring experimentation such as guided variation to models that are variation reducing such as direct bias and frequency dependent (Boyd and Richerson 1985, 1987; McElreath, et al. 1993). That is, the expectations in Table 5.2 do not preconceive a specific content, context, or mode of cultural transmission (Eerkens and

Lipo 2007). Instead, these expectations are predicated upon the argument that complexity and risk tolerance are inversely related in the production of material culture type-attributes. As a result, moderate to high variation in an attribute associated with a technologically complex artifact class, such as shell tempered ceramics (Feathers 2006), suggests that social forces are more likely to have resulted in that observed variation. In sum, as proportional similarities based on pairwise comparisons of type-attributes between two assemblages increases, so does the probability that social interaction resulting from shared learning mechanisms or homologous relationships between those sites increases. Network ties, representing statements of probability that a relationship existed between two communities, will be modeled on only the type-attributes where moderate to high variation is observed across all communities relative to the amount of variation observed across all type-attributes. Thus, social information as opposed to engineering factors that delimit the range of variation in a given artifact attribute will contribute to the network ties.

5.3 Defining the Sample and Assessing Dependencies

The model is operationalized here on a database of measurements from over 1,300 ceramic vessels belonging to three major types represented in twenty-two different central Illinois River valley (CIRV) site assemblages for the Late Prehistoric period of A.D. 1200-1450. All data, aside from three assemblages, were recorded by the author to minimize measurement error between individual observers. It is important to note that there is significant variability in the amount of data that was able to be recorded from each archaeological site. The sampling of sites chosen does not reflect a probabilistic survey. Further, the amount of excavation or other data collection from each site varies significantly. Some sites were completely excavated, while

others only saw minimal sub-surface sampling. As a result, the procedure outlined below, and the interpretations that follow, should be considered foundational as opposed to definitive in the analysis of the nature of relationships between Late Prehistoric CIRV sites.

The ceramic vessel types under consideration – likely serving plates, domestic jars, and burial jars – were chosen to explore whether different spheres of society (e.g., public, private, and ritual respectively) were more utilized to exhibit the loading of social information in comparison to others. The term plate is used here to refer to a class of ceramics referred to in other contexts as “broad-rimmed bowls” or “deep-rimmed plates” to emphasize their likely function as serving vessels primarily used in more public social contexts (Esarey and Conrad 1998; Hilgeman 2000; K. E. Smith, et al. 2004; Vogel 1975). While, domestic jars and plates are characterized by complex and multifaceted use-lives (Appadurai 1986), the public-private-ritual distinction is a generalization made to capture the primary social locus of vessel use. Table 5.3 lists all of the variables recorded along with the type of variable and the range of levels or measurements used in assessing each variable. Appendix A contains the Coding Sheet, which describes the specific guidelines and procedures used to systematically code or measure each attribute. Factor and ordinal data were collected alongside continuous attribute measurements in order to aid in potential future analyses and are not examined as part of this dissertation aside from the analysis of style based on decoration, which is discussed in Chapter 6.

Domestic jars were measured for eight type attributes across seventeen sites. Plates were measured for seven type attributes across sixteen sites. The largely intact nature of burial jars constrained measurements to four type attributes across six sites. Attempts to characterize the site-wide diversity of ceramics were made in sample selection. That is, samples were chosen from different site-contexts and from multiple repositories. A total of nineteen type-attributes are

Table 5.3 Coding Schema (See Appendix A for Full Coding Sheet)

	<i>Variable</i>	<i>Variable Type</i>	<i>Levels</i> <i>Measurement</i>
All Vessels	Unique Sherd I.D. Number	Factor	1 – 1,308
	Site	Factor	1 – 25
	Institutional Holding	Factor	1 – 5
	Provenience Sphere	Factor	1 – 4
	Specific Provenience	Factor	1 – 8
	Sherd Type General	Factor	1 – 3
	Traditional Taxonomic Type	Factor	1 – 20
	Residue	Factor	0 – 3
	Tempering Agent	Factor	1 – 4
	Tempering Max Grain Size	Ordinal	1 – 7
	Percent Temper Occurrence	Ordinal	1 – 3
Jars (both domestic* and mortuary^) *Domestic Jar variables included in analysis ^Mortuary Jar variables included in analysis	Lip Decoration	Factor	1 – 2
	Handle Decoration	Factor	1 – 3
	Orifice Diameter*^	Continuous	cm
	Height^	Continuous	cm
	Max Lip Thickness*^	Continuous	mm
	Max Shoulder Thickness*	Continuous	mm
	Max Wall Thickness*	Continuous	mm
	Rim Height*^	Continuous	mm
	Rim Angle*	Continuous	degrees
	Primary Design Technique	Factor	0 – 6
	Max Cord-marking Thickness*	Continuous	mm
	Max Incising Thickness	Continuous	mm
	Max Trailing Thickness*	Continuous	mm
	Shape of Elements	Factor	-1 – 8
	Shoulder Decoration	Factor	-1 – 79
	BR Design Group	Factor	-1 – 7
	Shoulder Type	Factor	-1 – 4
Slip/Paint	Factor	0 – 5	
Lip Shape	Factor	0 – 9	
Plates# #Plate variables included in analysis	Max Diameter#	Continuous	cm
	Height	Continuous	mm
	Depth	Continuous	mm
	Flare Length#	Continuous	mm
	Flare Angle#	Continuous	mm
	Max Rim Thickness#	Continuous	mm
	Max Thickness Below Lip#	Continuous	mm
	Max Incising Thickness#	Continuous	mm
	Max Trailing Thickness#	Continuous	mm
	Primary Design Technique	Factor	0 – 3
	Decoration	Factor	0 – 95
	BR Design Group	Factor	-1 – 29
Lip Shape	Factor	0 – 9	

reported here. These data sets represent over 1,300 unique ceramic vessels or vessel fragments and over 5,500 individual type-attribute measurements. All values reported are the maximum value of the attribute present on the vessel or sherd.

A primary statistical problem associated with investigating central tendency and dispersion in continuous attributes is sample size. Put another way, how many ceramic vessels are needed to meaningfully represent a population such that social relationships between communities may be modeled? A crucial decision for the model is therefore the selection of a critical sample size, which will act as a threshold at which site-specific samples may be included for study. Following Eerkens and Bettinger (2008:28), visual inspection and correlation of means and standard deviation across all variables were used to assess the critical sample size. Firstly,

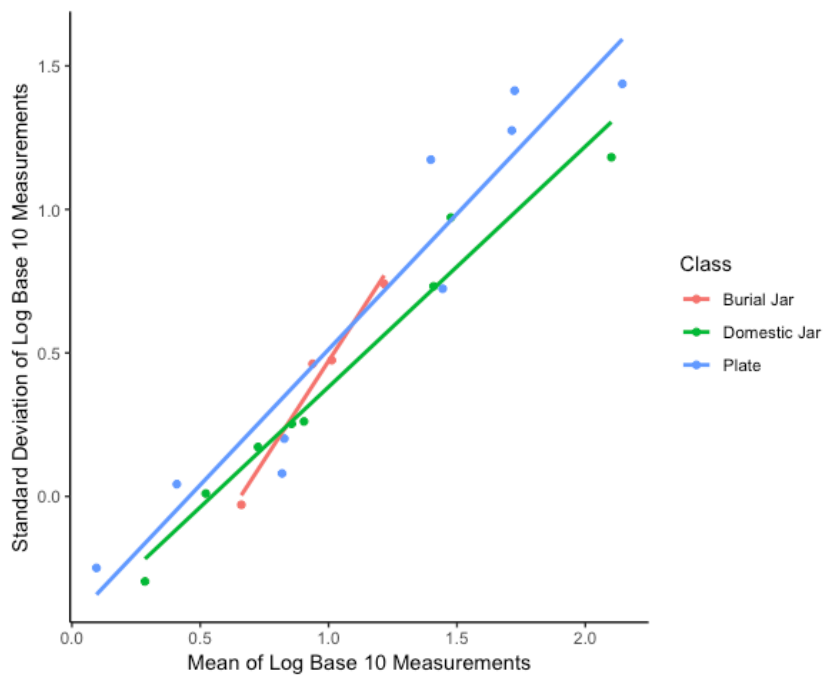


Figure 5.1 Mean-standard deviation relationships for type-attribute variables calculated by material culture class with best-fit regression lines. Log base 10 values reported to account for effects related to different measurement scales

the correlation between the mean and standard deviation of attributes across each ceramic vessel type was assessed to be quite high ($r = 0.822$; see Figure 5.1 for correlations across each vessel

type). This indicates that the standard deviation of any given variable can be reasonably predicted based on its mean alone. Given the similarity in correlation between mean and standard deviation in the current data to the projectile point data used in Eerkens and Bettinger's (2008) study, the critical sample size of six (6) or greater is used. This *n crit* is one less than that used by Eerkens and Bettinger and takes into account the need to maximize the number assemblages used in the analysis while also minimizing errors in estimating individual sample means and standard deviations. While several other established methods for determining critical sample size using observed mean, standard deviation, and sample size exist, these methods act to exclude values with high sample standard deviations. Using these methods would bias the current evaluation

Site Name	Diameter	Flare Length	Lip Thickness	Thickness Below Flare	Flare Angle	Incising	Trailing
Orendorf Settlement C	18	25	31	24	20	8	10
Crabbe	45	59	74	36	32	60	13
Walsh	6	7	20			16	
Lawrenz Gun Club	22	27	36	26	15	34	
Emmons	11	16	21	16	6	15	
Baehr South	8		11			11	
Myer-Dickson	10	10	14	13		13	
Star Bridge	49	43	73	44	27	74	
Ten Mile Creek	7	7	13	8		13	
Kingston Lake	36	42	47	35	25	29	10
Buckeye Bend	6	6	10	8		12	
Fouts Village			9			10	
Larson	34	40	42	37	25	34	
Morton Village	32	23	33	13	26	18	11
Houston-Shryock	8	15	25	15	8	22	
Orendorf Settlement D	16	15	16		11		
Total	308	335	475	275	195	369	44

Table 5.4 Count of plate sherds from each site for each continuous variable above *n crit*

Site	Orifice Diameter	Height	Lip Thickness	Rim Height
Crable	31	28	32	32
Ester Berry	15	12	16	16
Houston-Shryock	30	30	31	31
Vandeventer	47	47	47	47
Norris Farms #36	30	29	30	30
Total	153	146	156	156

Table 5.5 Count of burial jar sherds from each site for each continuous variable above n crit

Site	Orifice Diameter	Lip Thickness	Shoulder Thickness	Wall Thickness	Rim Height	Rim Angle	CM Thickness	Trailing Thickness
Orendorf Settlement C	43	47	47	20	47	46	10	35
Crable	44	60	60	29	59	55	49	13
Walsh		10	10		10	7	10	
Lawrenz Gun Club	30	49	51	15	50	38	48	
C.W. Cooper	23	28	32	18	29	30		29
Emmons	16	25	26		25	21	18	7
Baehr South		6	6		6		6	
Myer-Dickson	14	19	19	6	19	16	8	
Star Bridge	38	51	51	9	51	40	44	
Ten Mile Creek	34	41	41	14	42	37	36	
Eveland	23	33	32	10	33	29		15
Kingston Lake	39	46	48	14	47	44	24	20
Buckeye Bend	7	8	8		8	7		
Fouts Village	7	9	9		8	7	8	
Larson	37	42	42	25	42	37	37	6
Morton Village	39	46	48	33	46	42	16	32
Houston-Shryock	10	13	13		13	12	9	
Orendorf Settlement D	47	46	45		44	37		
Total	451	579	588	193	579	505	328	157

Table 5.6 Count of domestic jar sherds from each site for each continuous variable above n crit

because the values that are free to vary from assemblage to assemblage are actively being sought out by the routine used in the current study. Using this fixed sample size allows all samples above the critical sample size to be included regardless of observed variation.

Due to the fragmentary nature of most archaeological ceramics, not all of the twenty-two site assemblages contained every attribute in sufficient quantity to be considered by the study ($n_{crit} = 6$). Tables 5.4, 5.5, and 5.6 display the total number of vessels observed from each site and a breakdown of the number of vessels included for each continuous attribute. Indeed, only two sites considered in this analysis, Crable and Morton Village and its associated Norris Farms #36 cemetery, contain sufficient quantities of vessels from each vessel class to include observations above the critical sample size number for each variable considered in the analysis. Efforts to account for the presence of missing data and unequal samples sizes are further discussed below.

5.3.1 *Assessing Dependencies*

Prior to the implementation of the model, exploratory data analysis is necessary to assess the distributions of each artifact attribute as well as the degree of correlation between them. Gaussian distributions are required for the use of the unbiased CV estimator and ensure that assemblage samples are sufficiently random, often despite small sample sizes. Exploring correlations is used to assess whether or not different metric attributes are free to vary independent of one another. High correlation between attributes indicates that all attributes within a given type will behave in the same manner. Ensuring the independence of each attribute allows for the analysis of variation between type-attributes as opposed to simply comparing different vessel classes only (Eerkens and Bettinger 2008:27). Given the large number of distributions that were inspected (plate = 112 distributions; burial jar = 20 distributions; domestic jar = 144 distributions), only distributions that do not conform to expectations for normality are displayed here. Figure 5.2 shows deviation from normality in the distributions of rim angles on domestic jars from Eveland and Kingston Lake. Inspection of the data indicates that the

deviation is caused by a preponderance of jars with a vertical rim angle (recorded as 90 degrees from the jar opening plane) at both sites. Density plots of these two sites show bimodal distributions given the 90-degree preponderance. As a result, the unbiased estimator was not applied to these type-attributes. No other sample distribution deviated significantly from normality. Thus, the unbiased estimator for the coefficient of variation was applied to every variable aside from the domestic jar rim angle variable at Eveland and Kingston Lake, where a biased coefficient of variation estimator (sample standard deviation/sample mean) was used.

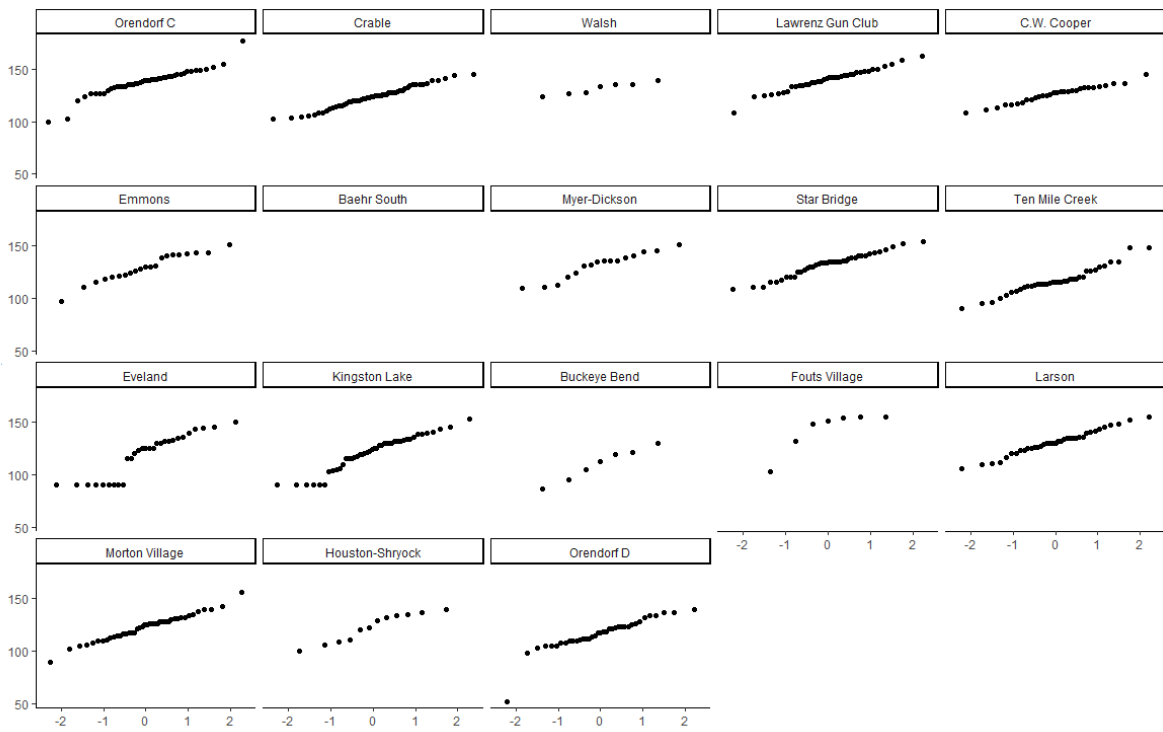


Figure 5.2 QQplot of domestic jar rim angles showing deviation from normality in Eveland and Kingston Lake

Problematically for the current analysis, burial jars show unusually strong positive linear relationships across the four continuous values under consideration. As shown in Table 5.7, each of the burial jar metrics are characterized by either moderately ($r > 0.5$) or strongly ($r > 0.70$) positive linear relationships to one another based on pairwise complete Pearson correlation computations. A particularly strong positive linear relationship exists between burial jar orifice

diameter and burial jar vessel height ($r = 0.869$; Figure 5.3). This finding suggests that the continuous burial jar type-attributes measured in this analysis are not free to vary independent of one another on a single vessel. As a result, any analysis of these burial jar type-attributes will actually consider the entire vessel itself as opposed to any singular attribute metric. This suggests that burial jars in the Late Prehistoric central Illinois River valley may be constructed based on a relatively standardized form where varying size in a single attribute results in concurrent size changes in every other attribute measured here.

	Orifice Diameter	Vessel Height	Lip Thickness	Rim Height
Orifice Diameter	1			
Vessel Height	0.869	1		
Lip Thickness	0.659	0.570	1	
Rim Height	0.664	0.777	0.477	1

Table 5.7 Pearson correlation coefficient for pairwise complete burial jar metric observations

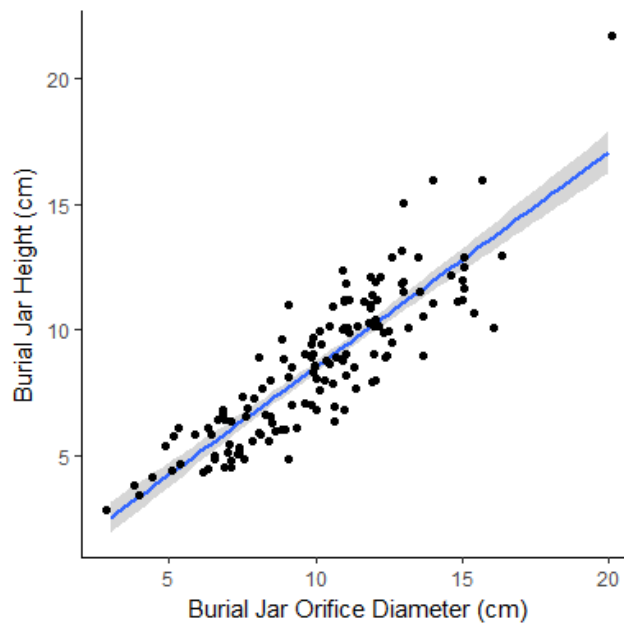


Figure 5.3 Scatterplot of Burial Jar Height by Burial Jar Orifice Diameter with best-fit regression line and 0.95 confidence interval shading

This lends to potentially fruitful hypothesis generation concerning the relationship between the size of burial jars and the social or demographic profiles of the individuals that were accompanied by those jars in mortuary contexts more broadly. Perhaps the size of the burial jar may be related to the social position of the individual in life – their age, sex, gender, or relationship to the potter community (Binford 1971; Brown 1995; L. G. Goldstein 2006; Saxe 1970). Regretfully, however, because of this high level of observed correlation among burial jar attributes, the burial jar class is not considered in the remainder of the analysis presented herein.

Jar and plate continuous metrics (Tables 5.8 and 5.9 respectively) are characterized by non-linear or weak linear relationships to one another, with one exception. A nearly moderately negative linear relationship exists between the plate attributes Flare Length and Trailing Thickness ($r = - 0.453$). That is, as the length of plate flares increases, the thickness of trailed

	Orifice Diameter	Lip Thickness	Shoulder Thickness	Wall Thickness	Rim Height	Rim Angle	Cord Marking	Trailing
Orifice Diameter	1.000							
Lip Thickness	0.397	1.000						
Shoulder Thickness	0.334	0.215	1.000					
Wall Thickness	0.190	0.140	0.399	1.000				
Rim Height	0.325	-0.024	0.349	0.311	1.000			
Rim Angle	0.204	0.055	0.097	0.003	-0.113	1.000		
Cord Marking	0.073	0.093	0.022	-0.024	0.146	0.023	1.000	
Trailing	0.374	0.154	0.027	0.042	-0.139	0.190	NA	1.000

Table 5.8 Pearson correlation coefficient for pairwise complete domestic jar metric observations decorations tends to moderately decrease. This correlation may be related to technological considerations such as the tool used to create the trailed decorations or perhaps to social

considerations such as plate flares acting as a canvas onto which symbol is used as non-verbal communication of social identification. The latter hypothesis is considered in Chapter 7.

It is worth noting at this point in the analysis that the methods used here are exploratory, as opposed to explanatory, in nature. As noted by Herbich (1987), ‘micro-styles’ or distinctive combinations of decorative, formal and technological features may characterize different potter communities within a society. Variation within components of decoration, decorative aspects such as organization of the decorative field, aspects of form, and details of workmanship all contribute to these distinctions in micro-styles. However, “no single aspect will be sufficient to distinguish between the work of two given communities; the micro-styles are polythetic sets...Luo potters are clearly attuned to the combinations of variables which distinguish the work of their community from that of others” (Herbich 1987:196). This analysis of type-attribute

	Diameter	Flare Length	Rim Thickness	Thickness Below Flare	Flare Angle	Incising	Trailing
Diameter	1.000						
Flare Length	0.179	1.000					
Rim Thickness	0.298	0.187	1.000				
Thickness Below Flare	-0.013	-0.026	0.296	1.000			
Flare Angle	-0.127	0.026	0.017	0.129	1.000		
Incising	0.027	-0.229	-0.017	0.067	0.085	1.000	
Trailing	0.233	-0.453	-0.065	0.115	0.300	NA	1.000

Table 5.9 Pearson correlation coefficient for pairwise complete plate metric observations

variation based on continuous metrics should not be considered an effort to uncover the complete polythetic sets responsible for distinguishing potter communities. Rather, the objective here is to identify which continuous type-attributes may vary between communities such that it is likely that they were used in such a capacity either overtly and consciously or as an unconscious by-product of cultural evolution. Additionally, there is no attempt made to calculate the statistical significance between any of the given attributes based on the VOM, AV, or VOV statistics.

In review, the steps followed to obtain the VOM, AV, and VOV values used in this analysis include: 1) measure continuous type-attributes and calculate assemblage-specific means and coefficients of variation for type-attributes represented by six or more observations; 2) assess sample distributions and dependencies to determine if type-attributes are free to vary independent of one another and form normal distributions; 3) compute raw VOM, AV, and VOV statistical measurements for each type-attribute; and 4) standardize the raw values. The standardized VOM, AV, and VOV values are then compared against the expectations in provided in Table 5.2.

5.3.2 Identifying Social Information Bearing Artifact Type-Attributes from Cultural Transmission

Because the model assumes that each statistical metric is free to vary independent of each other, it is first necessary to assess the coefficient of determination, or the square of the correlation between each metric. The interactions between AV and VOM ($r^2 = 0.006$) and between VOV and AV ($r^2 = 0.032$) are quite minor, which indicates that these variables are fully independent of each other. That is, as the average variation around sample means increases (as AV increases), there is no associated tendency for the mean of an attribute itself to vary more (or less) from sample to sample (a stepwise increase or decrease in VOM), nor is there an associated

tendency for the magnitude of variability around the mean to vary more (or less) from sample to sample (a stepwise increase or decrease in VOV) (Eerkens and Bettinger 2008:30).

A somewhat higher positive correlation is present between VOM and VOV ($r^2 = 0.205$). That is, as domestic jar and plate attributes tend to vary widely in mean from site to site (as VOM increases), there is a tendency for the magnitude of variability around the means of those attributes to slightly increase (increasing VOV). The inverse is also true in a general sense – as domestic jar and plate attributes tend to have the same mean from site to site (as VOM decreases), there is a tendency for the magnitude of variability around the means of those attributes to vary somewhat less from site to site. Put another way, for attributes that are free to vary in mean from site to site, inter-assemblage differences in not only the location of the mean but also the range of variability around the mean become more apparent. Domestic jars and plates in the Late Prehistoric central Illinois River valley appear to be less constrained by global control in determining these specific attributes. This finding supports the hypothesis that certain type attributes on these vessels are constrained by social forces, or local afunctional control, as opposed to engineering constraint and therefore may contribute to the polythetic sets of micro-styles that characterize different potter communities. Attributes that tend to have similar means from site to site (low VOM) tend to have low between-assemblage differences in the magnitude of attribute variability relative to the mean (low VOV). This suggests that these attributes are more likely to be constrained by moderate or strong global function across the geographic and temporal expanse of the Late Prehistoric central Illinois River valley. In kind, attributes that tend to vary widely in mean from site to site (high VOM) tend to have high between-assemblage differences in the magnitude of attribute variability relative to the mean (high VOV). This suggests that attributes with means that are free to vary from site to site are likely to be loci for

the loading of social information or are driven by context specific engineering constraints such as local clay characteristics.

The critical statistical observation for the purposes of this analysis is the variation of variation (VOV). The slightly positive correlation between VOV and VOM supports the underlying assumption that modelling social interaction based on artifact attributes is fruitful. However, that the coefficient of determination between VOM and VOV, as a measure of the goodness of fit of a linear relationship, is only somewhat moderately positive is therefore only indicative of a weak positive linear relationship between the metrics.

Vessel Type	Attribute	# of Sites	#of Vessels	VOM	VOM Score	AV	AV Score	VOV	VOV Score
Jar	Orifice Diameter	16	451		0.079	Low	-0.712		-0.773
Jar	Lip Thickness	18	579		0.377	Low	-0.674		-0.480
Jar	Shoulder Thickness	18	588		0.235	Low	-0.716		-1.323
Jar	Wall Thickness	11	193	High	0.579		-0.362	Medium	0.329
Jar	Rim Height	18	579	High	0.766		0.221	Medium	0.488
Jar	Rim Angle	18	505	Low	-1.252	Low	-0.980	Medium	0.651
Jar	Cord-marking Thickness	14	328	High	0.724	Low	-1.069		-0.276
Jar	Trailing Thickness	8	157	High	1.428		-0.331	Medium	0.519
Plate	Diameter	15	308	Low	-1.432		-0.160	Medium	0.107
Plate	Flare Length	15	335		0.319	High	1.213		-0.402
Plate	Rim Thickness	16	475	Low	-1.769		-0.015		-1.088
Plate	Thickness Below Flare	13	275	Low	-1.450		0.611		-1.633
Plate	Flare Angle	11	195	High	1.116	Low	-0.857	High	1.842
Plate	Incising Thickness	15	369		-0.056	High	1.608	Medium	0.382
Plate	Trailing Thickness	4	44		0.335	High	2.223	High	1.656

Table 5.10 VOM, AV, and VOV values, scores, and summary data for type attributes

Turning to the standardized values (or rescaled values that form distributions with a mean of 0.0 and standard deviation or 1.0) of VOM, AV, and VOV themselves Table 5.10 presents the values, metric scores, and associated site and sherd data for each of the 15 type-attribute combinations. Values for each of the statistics were identified by ordering the VOM, AV, and

VOV residual scores separately and visually inspecting their distributions and associated probabilities for discontinuities suggestive of natural divisions from all attributes within a given

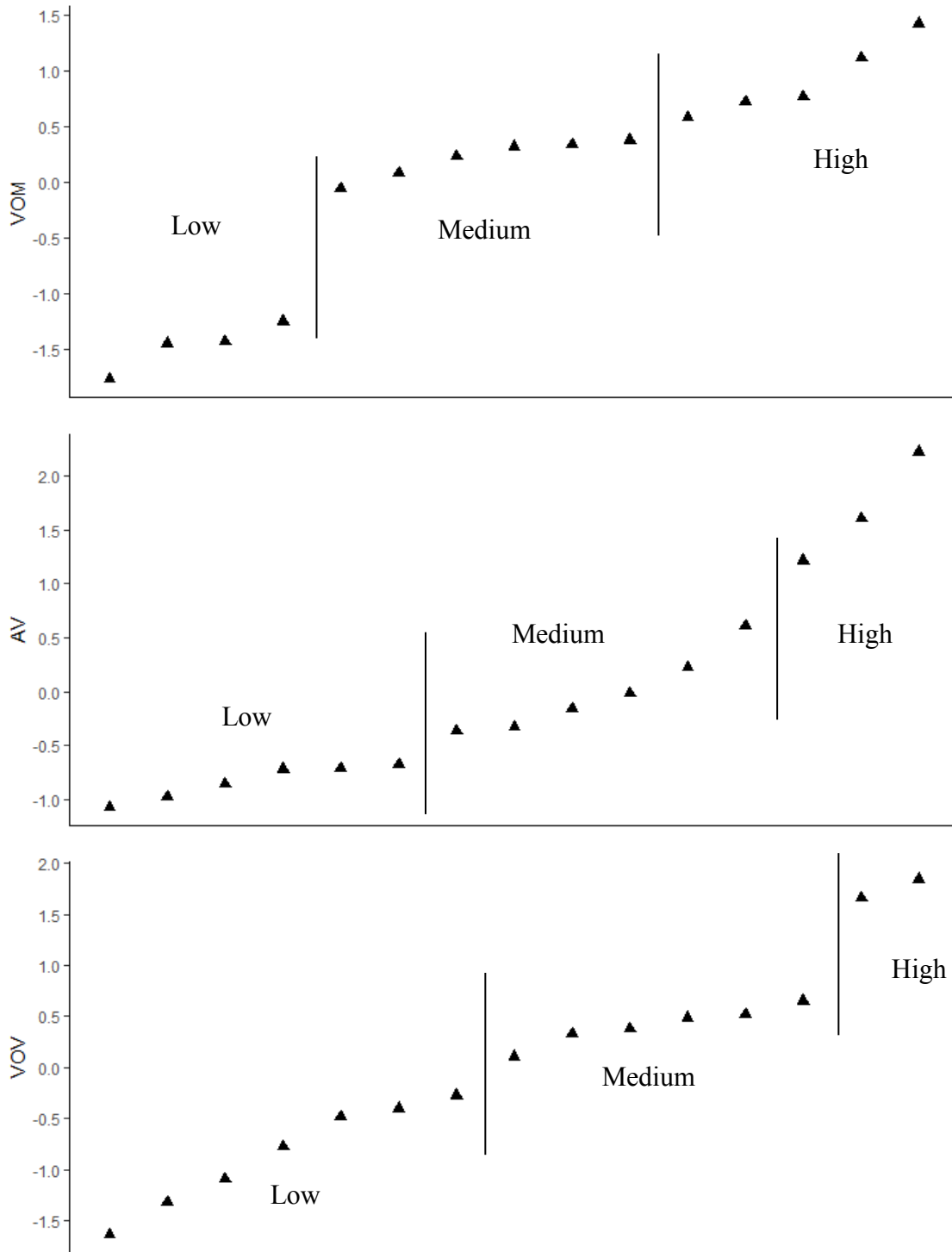


Figure 5.4 VOM, AV, and VOV residual scores for all 15 ceramic vessel type attributes measurements

statistic. These cutoffs are reported in Figure 5.4. A clear natural division between outlying low scores and medium scores is apparent in the ordered distribution of VOM (< -1.0 , $n = 4$), a subtle division is present between medium scores and high scores (> 0.40 , $n = 5$), with medium scores in between (< -1.0 to > 0.40 , $n = 6$). The ordered distribution of AV scores also shows relatively clear break for outlying high scores (> 0.7 , $n = 3$), a slight break for low scores (< -0.6 , $n = 6$), with medium scores falling in between (< -0.6 to > 0.7 , $n = 6$). VOV showed a very clear break for outlying high scores (> 0.75 , $n = 2$), a slighter break for low scores (< 0.0 , $n = 7$), with medium scores falling in between (< 0.0 to > 0.75 , $n = 6$). Given that VOV is the primary statistic of interest for this analysis, High and Medium values are reported in Table 5.10, while High and Low value assignments are reported for VOM and AV.

Returning to the expectations summarized in Table 5.2, I argue here that eight of the fifteen type-attributes with medium or high VOV are likely to be social information bearing as opposed to be constrained by engineering forces. VOV is designed as a statistic to highlight variation expressed in individual assemblages. In exploring individual assemblage CV values for the eight socially influenced variables, two general patterns are present that lead to the medium or high VOV values. The first pattern is that of tightly constrained CV distributions with one or two high outlying assemblage values pushing the spread of the CV values beyond the norm witnessed among other vessel attributes. Plate flare angle, diameter, trailing thickness, and incising thickness are characterized by the trend of tight distribution with one or two high outliers. The second pattern is that of CV distributions with very high interquartile ranges and outlying values on the upper and lower ends, which characterizes jar trailing thickness, rim angle, rim height, and wall thickness. That these trends are dichotomized by vessel class speaks to the differences in function and perhaps production techniques between them.

Figures 5.5 and 5.6 display ridgeline plots of the distributions of the eight type-attributes constrained by social forces for jars and plates respectively. These ridgeline plots visualize the variation in attribute distributions and show which sites are driving variation as well as significant distinctions between the pre- and post-migration time periods. For example, Eveland domestic jars have very short rim heights and are much more likely to have vertical (90 degree) rim angles, two characteristics in contrast to most other assemblages. Additionally, positive skew appears to be driving the variation between assemblages in plate incising, suggesting that incising thick lines into a dry paste on plates was likely controlled by social forces such as the selection and transmission of incising tool norms or non-verbal communication of perhaps assertive style.

It is argued here that as proportional similarity in type-attributes with medium or high VOV values increases, so does the likelihood that that similarity is related to shared learning mechanisms or historical relationships between groups. Moreover, it is argued that shared learning mechanisms or historical relationships between sites is a key indicator of increased social interaction between them.

This analysis shows that the following variables in the Late Prehistoric central Illinois River valley are likely to be markers suggesting the degree of social interaction between potter communities: plate trailing thickness, flare angle, diameter, and incising thickness; and domestic jar rim angle, wall thickness, rim height, and trailing thickness.

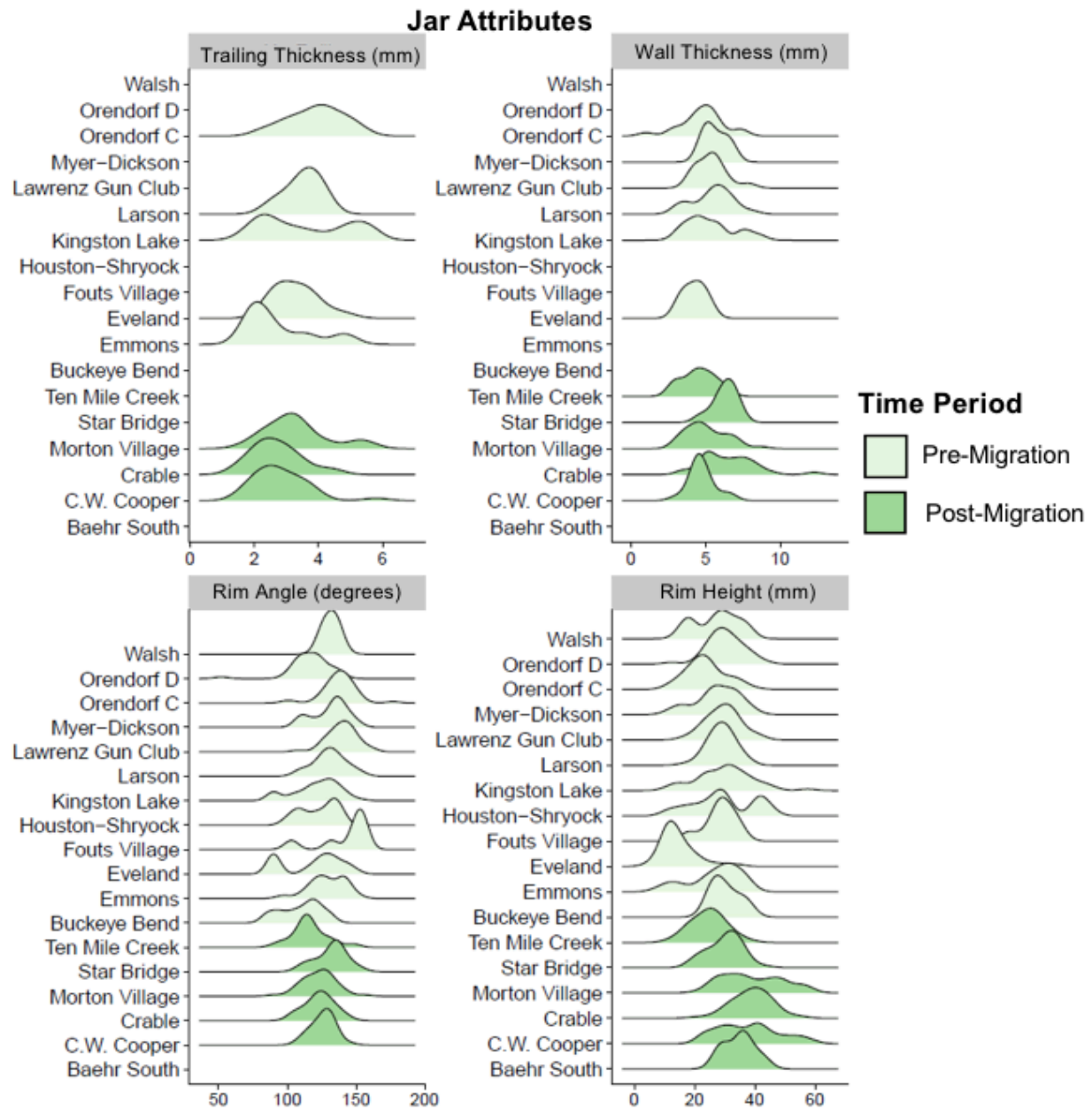


Figure 5.5 Ridgeline plot of domestic jar type-attributes likely constrained by social forces, all measurements are in mm aside from rim angle which is in degrees

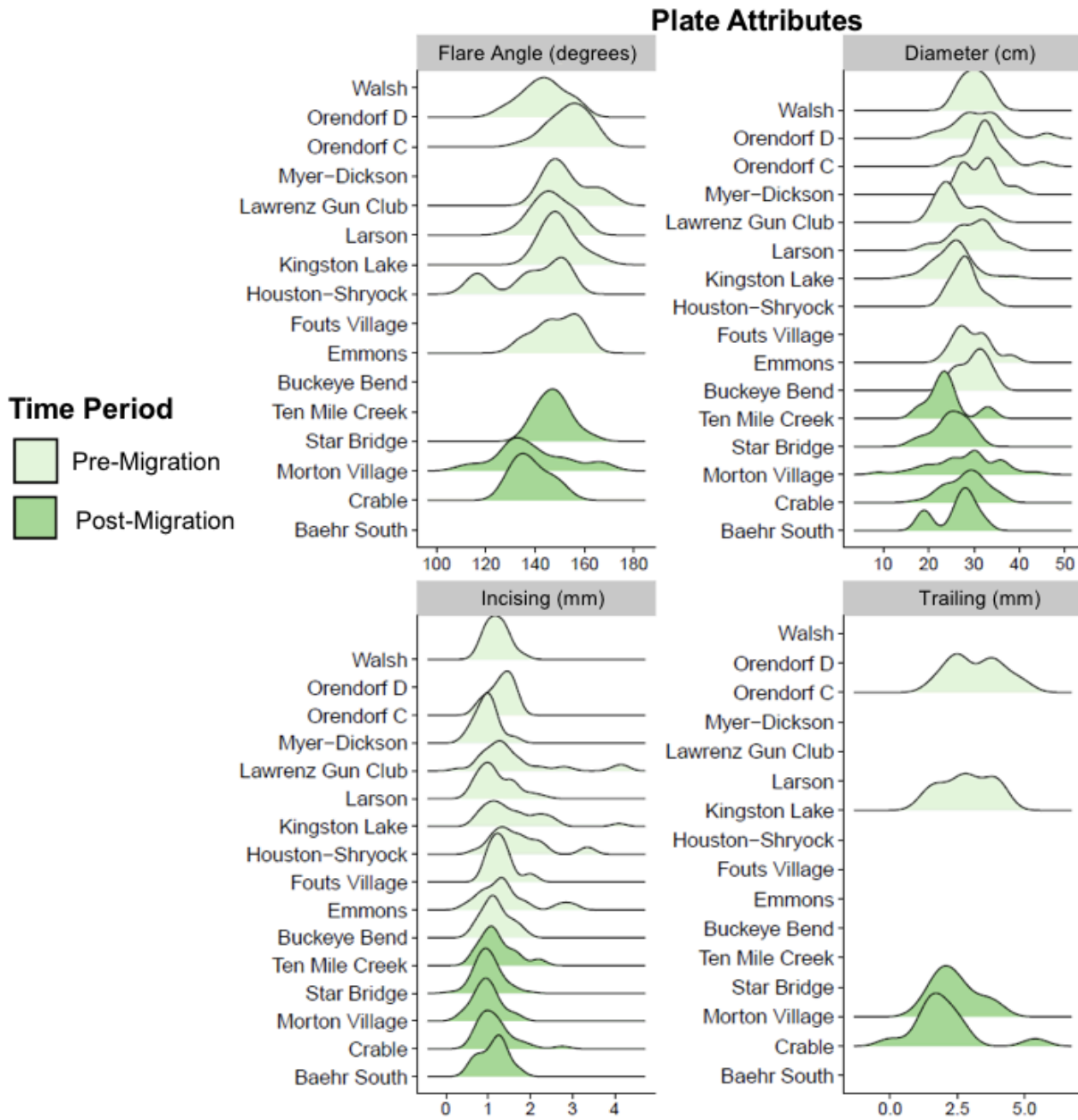


Figure 5.6 Ridgeline plot of plate type-attributes likely constrained by social forces, all measurements are in cm aside from flare angle which is in degrees

5.4 Methodology: Constructing Social Interaction Networks from Social Information Bearing Artifact Type-Attributes

The theoretical basis for the use of social network analysis is discussed in detail in Chapter 2. As a result, only a brief overview will be outlined here. A network constitutes a

graphical representation of a set of actors (“nodes”) and the relationships or connections (“edges” or “links”) between them (Borgatti, et al. 2009; Brughmans 2013; Collar, et al. 2015; Golitko and Feinman 2014; Peebles, et al. 2016; Scott 2000; Wasserman and Faust 1994). Nodes may represent actors at almost any scale, from neurons in the brain up to individual human or non-human actors, communities, cities, or even entire nations. Edges may be assigned between nodes based on nearly any conceivable index of similarity or contact, such as the presence of two individuals at a conference session, marriage relationships, website links, the volume of international trade relationships, or flights between airports. The directionality of edges may be considered. Edges may be undirected, such as the representation of familial ties, or they may be directed, such as individualistic notions of friendship within a high school clique. Furthermore, the intensity of the edge may be characterized. Edges may carry a weight, such as the volume of trade in a particular commodity between nation states or the amount of traffic flowing along connections in a transportation model. Alternatively, edges may be unweighted, such as a network of a nation states’ power grid connections, social circles from social media platforms, or models of hyperlinks shared between websites.

Renewed interest in network analysis methods in archaeology has led to a number of applications in a host of geographic and temporal contexts including exchange relationships based on procurement and distribution of obsidian across pre-Hispanic Mesoamerica (Golitko and Feinman 2014), hierarchization and state formation based on prestige good exchange and monumental architecture in Japan (Mizoguchi 2009), regionalization of Clovis hunter-gatherers based on lithic distributions in late Pleistocene North America (B. Buchanan, et al. 2016), regional shifts in economy and society based on ceramic cultural markers in the mid-Holocene Sudan (Garcea and Hildebrand 2009), and ceramic and lithic evidence for collective action and

social transformation in the United States Southwest (Borck, et al. 2015; Mills, et al. 2016; Mills, Clark, et al. 2013; Peeples and Roberts Jr. 2013).

As opposed to placing explanatory emphasis on culture, community, society, or agents themselves, archaeological applications of social network analysis instead focus on the relationships between these entities. In addition, network analysis does not place *a priori* definition on analytical constructs such as spatial structures, social organization, or economic systems in order to interpret network structure. As a result, network approaches can simultaneously incorporate multiple scales of analysis into global analytical constructs (Golitko and Feinman 2014). While applications of network analysis methodologies, in archaeology and other disciplines, typically focus on constructing a single global analytical graph, the approach taken here instead advocates for parsing graphs into different analytical dimensions, or layers, to discern how they may converge or diverge when explored independent of one another and in aggregate. As a result, edges may be structurally different from one another, such as a co-authorship network separated by layers of professors and students or economic links between nation states separated by layers of different commodities such as foodstuffs or manufactured goods. This is particularly instructive in archaeology given that archaeologists “cannot directly observe or quantify either edges or vertices of human relations in the past, they must deduce, or derive, both from the observable attributes of the residual evidence available to them” (Terrell 2013:22). For example, traditional models of social identification, organized conflict, exchange, and social organization may not be evident in singular network structures identified archaeologically (Brughmans 2010; Phillips and Gjesfjeld 2013). As a result, new models may need to be generated within the archaeological community that place greater emphasis not only on the role of network relationships, but also on the roles that the particular material culture

class(es) and traditional model(s) being tested may play in these and other processes. Multiple relations, or *multilayer*, network methodology seeks to parse the overlap and influence of different social and economic relationship layers on individual nodes and the combined network as a whole (Mucha, et al. 2010; Preiser-Kapeller 2011; Scholnick, et al. 2013). Multilayer network methodology begins analysis by exploring the structure of different network model layers as separate entities. It then progresses to explore i) how the different layers overlap among one another (or share common connections); ii) how nodes are positioned within each network layer; and iii) what influence each layer has on the structure of the total network (or how many connections a given network layer contributes to the multilayer network as a whole) (Kivelä, et al. 2014; Szell, et al. 2010). As a result, different models of social behavior and the corresponding material classes used to construct distinct network layers can be investigated separately and together in order to provide insight on their individual and collective role in structuring the interrelationships between nodes under analysis. This chapter focuses on the strength or degree of relationships of social interaction based on the cultural transmission of ceramic technological information. Economic relationships of exchange or shared raw material source information are discussed in Chapter 7 and social identification relationships based on shared categorical identities are discussed in Chapter 6. From these three distinct networks, a ceramic industry multilayer network is constructed in Chapter 8 toward explaining social interrelationships in multicultural social environments following migration, as in the Late Prehistoric central Illinois River valley case study region.

The approach taken here considers proportional similarities in material culture as a proxy measure for the strength, or degree, of connectedness between past communities. Other researchers have demonstrated the utility of this approach in a variety of contexts (Gjesfeld

2014; Golitko and Feinman 2014; Mills, Roberts Jr., et al. 2013; Shaw, et al. 2016). Nodes represent different potter communities and are presumed to be representative of spatially discrete pre-Columbian settlements populated by Ancestors of Native American peoples. Edges represent probabilistic relationships between those communities and the larger settlements within which they are nested. The weight of an edge represents the probabilistic strength or degree of that relationship. Edges are directed, meaning that they consider the degree of a relationship from one node directed toward another. Given that many of the Late pre-Columbian central Illinois River valley site assemblages considered here were recovered via surface survey, illicit excavation, or other non-professional archaeological excavation techniques where internal provenience of vessels is lacking, analyzing intra-community scale variability is not currently possible based on available data. Thus, the scalar focus of this investigation is explicitly regional. Analysis at the household or site sector scale may be an area of potential research at some sites in the future, however (see Chapter 5).

In order to model social interaction between sites using the eight artifact type-attributes that have been found to be more likely to bear social information, it is necessary to develop a procedure to assess relative technological similarity across each of these attributes simultaneously respective to each material culture class. A total of four ‘monoplex’ or single-layer networks and five multilayer networks are constructed: two from each vessel class during each time period under consideration, one multilayer network for each time period, one multilayer network for each vessel class across time periods, and one multilayer network for both vessel classes across time (Table 5.11). The methods developed for this study are based in part on techniques for measuring technological similarity in archaeological ceramics borrowed from quantitative morphology and genetics by Peeples (2011:185). All analyses were performed using

the R statistical package with network graphs generated using open-source software including the R statistical language and environment; Gephi, an open source graph visualization platform; and the vector graphics editor Inkscape.

Type of Network	Vessel Class(es)	Time-Period	Calendar Date
Monoplex	Domestic Jar	Pre-Migration	1200 – 1300 A.D.
Monoplex	Plate	Pre-Migration	1200 – 1300 A.D.
Monoplex	Domestic Jar	Post-Migration	1300 – 1450 A.D.
Monoplex	Plate	Post-Migration	1300 – 1450 A.D.
Multilayer	Jar and Plate	Pre-Migration	1200 – 1300 A.D.
Multilayer	Jar and Plate	Post-Migration	1300 – 1450 A.D.
Multilayer	Jar	Across Time	1200 – 1450 A.D.
Multilayer	Plate	Across Time	1200 – 1450 A.D.
Multilayer	Jar and Plate	Across Time	1200 – 1450 A.D.

Table 5.11 Summation of networks constructed with artifact type-attribute social interaction markers

The analysis performed can be summarized in six general steps. 1) First, the social information bearing type-attributes are converted into a symmetrical matrix of pairwise distances between sherds. 2) Next, the distance matrix is converted into a symmetrical similarity matrix between sherds. 3) The similarity matrix is then converted into a directed, weighted edge list of individual sherd to sherd similarities. 4) Proportional pairwise similarity is then calculated between each site based on individual sherd to sherd similarity scores. 5) The resulting proportional similarity list is then normalized by site for scores between 0 and 1, or a list of weighted, directed similarity between each site using a threshold value of > 0.5 , to allow for the production of each of the individual ceramic industry social interaction networks listed in Table 5.11. 6) Finally, domestic jar and plate networks are flattened and sliced into five multilayer networks that consider the roles of each vessel class and time period(s) under consideration. Each of these steps is applied to both material culture classes under consideration here (domestic

jars and serving plates) separately and described in detail below. All R code is provided in Appendix C for these operations.

(1) & (2) The first step in this analytical procedure is the construction of a symmetrical matrix of relative distances of every sherd against every other sherd of the same vessel class in the sample for the type-attributes discerned to be likely bearing of social information. That is, each domestic jar attribute is compared to every other domestic jar attribute and each plate attribute is compared to every other plate attribute to assess the dissimilarity between them. In this way, social interaction may be modelled for each vessel class independently based on individual attributes. Gower's coefficient of similarity was selected for this analysis because it incorporates cases with missing data handily and computes a distance score between 0, indicating complete dissimilarity, and 1, indicating perfect similarity (Gower 1971). For each continuous type-attribute, Gower's coefficient is defined as:

$$G_{ijk} = G(i, j)_{(k)} = 1 - \frac{|x_{ik} - x_{jk}|}{R_k}$$

Equation 5.1 Gower's coefficient

where (R_k) denotes the absolute range of the values for the k th variable. When all variables are quantitative, as in the case here, the Gower coefficient is a range-normalized Euclidean coefficient, which is quite similar to the Brainerd-Robinson coefficient of similarity used in archaeological statistics (Brainerd 1951; Robinson 1951). Implementation of Gower's similarity coefficient in the R cluster package (L. Kaufman and Rousseeuw 1990a) is focused on obtaining a *dissimilarity* coefficient as opposed to a similarity coefficient, and is commonly used in clustering procedures such as those used in machine learning (Lesmeister 2015). As a result, statistical packages using the Gower coefficient calculate a dissimilarity score by subtracting the

similarity score from one (i.e., $(1 - G_{ijk})$). This process is reversed by subtracting the distance score from one (i.e., $(1 - (1 - G_{ijk}))$).

(3) Because the matrix produced from the procedures above is symmetrical and therefore equal to its transpose, it is easier to handle and manipulate the data in edge list format. This is especially true given the large number of sherd to sherd comparisons, which makes for very large matrices (n plate comparisons = 256,032; n jar comparisons = 354,025). Edge lists are a data class amenable to the production of network graphs, the others being adjacency lists and adjacency matrices (Kolaczyk and Csárdi 2014). Edge lists are composed of a two-column list of all vertex pairs connected by an edge, with ancillary columns indicating the weight of the edge, directionality of the edge relationships, data layer, or other information such as geospatial positioning, time period of the edge relationships, and the like.

(4 & 5) Proportional pairwise similarity is then calculated between site assemblages for each material culture class separately. The coefficient developed to accomplish this is a natural extension of the Gower coefficient of similarity, where a proportional similarity coefficient (PS_{ijk}) between sites i and j is assessed by taking the sum of pairwise similarities based on the Gower coefficient (G_{ij}) and dividing by the total number of pairwise comparisons between two site assemblages (n_{ij}) based on the k th variable:

$$PS_{ijk} = PS(i, j)_{(k)} = \frac{\sum_k G_{ijk}}{n_{ijk}}$$

Equation 5.2 Proportional similarity coefficient

To allow for network graph construction, the proportional similarity coefficient scores for each site are then normalized between 0 and 1, and act as the weight of an edge between two sites. Through normalization, these weights represent the probabilistic strength of a directed relationship from one site to another, relative to one site's relationships to every other site. That

is, the weights of each site's respective relationships to every other site are normalized relative to each other with the strongest relationship represented by 1, the weakest relationship represented by 0, and relationships in between scaled proportionally. Each site thus forms their own, *directed*, ties to other sites such that the tie from actor l to k is differentiated from the tie from actor k to actor l . This is done for a number of reasons. First, it enables an analysis of reciprocity of ties. In other words, one may ask whether the tie modeled from a given site is reciprocated and to what degree. Furthermore, the use of directed ties enables an acknowledgement of the internal variation and potential obfuscation of individual potter to individual potter relationships when using settlements as nodes. A simple heuristic to understand directionality is the concept of following in the Twitter™ social network platform. *User a* may follow *user b*, but *user b* may or may not reciprocate and follow *user a* back. Directed networks therefore allow for the capturing of both agent-scale complexity in a community-scale focus and for the analysis of reciprocity in social interrelationships. This ensures the maximal representation of community-scale relationships among potters relative to each other. The weights act as statements of probability of the strength of relative social interaction between two sites based on the similarity of socially mediated artifact type-attributes. In order to model particularly strong relationships only, a threshold value of > 0.5 is used as a cut-off value in graph construction. That is, all edges lower than 0.5 are not considered when constructing network graphs.

(6) Whereas the single-layer networks can be represented by a graph as a tuple (e.g. $G = (V, E)$ where V is a set of nodes and $E \subseteq V \times V$ is the set of edges that connects pairs of nodes), a multilayer network constitutes a quadruplet (e.g. $M = (V_M, E_M, V, L)$ where the first two elements in a multilayer network M yield a graph $G_M = (V_M, E_M)$, that has a set of global nodes V , and a set of layers L (Dickison, et al. 2016; Kivelä, et al. 2014). In layman's terms, a

multilayer network is a set of actors connected through multiple types of relationships. Those relationships span different layers and the nodes in different layers can correspond to the same actor. In this chapter, the relationships between any two given spatially bounded archaeological sites span two layers: technological similarity in domestic cooking jars and similarity in likely serving plates. Because not all nodes occur within each network under consideration here (i.e. some sites do not have ceramic assemblages that include plates and all sites aside from one have occupations limited to one of the two time periods under consideration), these networks are considered node-colored-network representations based on layer-disjoint node sets. Further, because couplings between nodes are not diagonal, and therefore do not link nodes from different layers, the network is considered multilayer only and not multiplex.

It should be noted at this point in the analysis that network graph production and visualization is simply an efficient means to convey information about the complex relationships among the Late Prehistoric central Illinois River valley settlements included in this study. The lack of an edge or tie, as modelled based on thresholds chosen, should not be interpreted as a statement that a particular kind of social relationship was absent between two settlements. However, by applying common threshold criteria, it does allow the most potentially meaningful relationships to be modelled and therefore increases the interpretability of patterns of network relationships. Network graphs distill an enormous amount of information, and the application of a common threshold allows the visualization to alert the viewer to the most pertinent or relevant information in each model (Weidele, et al. 2016). Furthermore, applying thresholds allows for the application of additional community detection algorithms otherwise not available for weighted networks due to the complexities of handling weights in multilayer networks (Magnani 2017, personal communication). That is, most algorithms designed to detect communities within,

or otherwise analyze, multilayer networks are not yet capable of supporting weights, directionality, or other edge attributes. Only unweighted, undirected networks are generally supported at this time, however some exceptions are available (Edler and Rosvall 2014).

Multilayer graphs are constructed in two ways for visual representation and network metric generalization: flattening and slicing. The first method is via flattening. Flattening is perhaps best illustrated with a toy example. A typical way to mathematically represent a multilayer network is with a set of adjacency matrices. Each matrix corresponds to a particular type of edge, with one row/column for each node and element (i, j) indicating actors i and j are connected by an edge of the corresponding type (Dickison, et al. 2016). Figure 5.7 illustrates a very simple representation of a multilayer network with relationships formed by friendships on different social media platforms. The various matrixes constitute an adjacency list of tables. To flatten this adjacency list of tables, it is transformed by combing all aspects i and j into a new aspect h . That is, a multilayer network is defined by summing all the binary friendship relationships between actors to emphasize the weight of a friendship across different social media platform layers. While the toy example shown here uses a network of binary (e.g. presence/absence) relationships, this process holds true for networks where the relationship is modeled by a weight as well. Each of the relationship layer weights are summed to create a flattened representation of the multilayer network. This is a method of simplification that can aid in the detection of cohesive subgroups using community detection algorithms, for example. Flattening can be problematic due to its relative simplicity, however. For example, a particularly dense network layer, or a layer with many edges between nodes, may reduce the ability for interesting patterns to be revealed in the multilayer network. That is, an excessive amount of edges in one layer may mask the ability of algorithms to detect meaningful.

$$\begin{array}{c}
 \text{Bob Pat Jon Cici Jill Phil} \\
 \text{Bob} \\
 \text{Pat} \\
 \text{Jon} \\
 \text{Cici} \\
 \text{Jill} \\
 \text{Phil}
 \end{array}
 \begin{pmatrix}
 0 & 1 & 1 & 1 & 0 & 0 \\
 1 & 0 & 0 & 0 & 0 & 1 \\
 1 & 0 & 0 & 1 & 1 & 0 \\
 1 & 0 & 1 & 0 & 0 & 1 \\
 0 & 0 & 1 & 0 & 0 & 1 \\
 0 & 1 & 0 & 1 & 1 & 0
 \end{pmatrix}$$

Friendship on Facebook™

$$\begin{array}{c}
 \text{Bob} \\
 \text{Pat} \\
 \text{Jon} \\
 \text{Cici} \\
 \text{Jill} \\
 \text{Phil}
 \end{array}
 \begin{pmatrix}
 0 & 1 & 1 & 1 & 1 & 1 \\
 1 & 0 & 1 & 0 & 0 & 1 \\
 1 & 1 & 0 & 1 & 1 & 0 \\
 1 & 0 & 1 & 0 & 1 & 1 \\
 1 & 0 & 1 & 1 & 0 & 1 \\
 1 & 1 & 0 & 1 & 1 & 0
 \end{pmatrix}$$

Friendship on Twitter™

$$\begin{array}{c}
 \text{Bob} \\
 \text{Pat} \\
 \text{Jon} \\
 \text{Cici} \\
 \text{Jill} \\
 \text{Phil}
 \end{array}
 \begin{pmatrix}
 0 & 0 & 0 & 0 & 0 & 0 \\
 0 & 0 & 0 & 0 & 0 & 1 \\
 0 & 0 & 0 & 1 & 1 & 0 \\
 0 & 0 & 1 & 0 & 0 & 1 \\
 0 & 0 & 1 & 0 & 0 & 1 \\
 0 & 1 & 0 & 1 & 1 & 0
 \end{pmatrix}$$

Bob Pat Jon Cici Jill Phil

Friendship on Snapchat™

Figure 5.7 Adjacency matrix representation of multilayer social media friendship network

$$\begin{array}{c}
 \text{Bob Pat Jon Cici Jill Phil} \\
 \text{Bob} \\
 \text{Pat} \\
 \text{Jon} \\
 \text{Cici} \\
 \text{Jill} \\
 \text{Phil}
 \end{array}
 \begin{pmatrix}
 0 & 2 & 2 & 2 & 1 & 1 \\
 2 & 0 & 1 & 0 & 0 & 3 \\
 2 & 1 & 0 & 3 & 3 & 0 \\
 2 & 0 & 3 & 0 & 1 & 3 \\
 1 & 0 & 3 & 1 & 0 & 3 \\
 1 & 3 & 0 & 3 & 3 & 0
 \end{pmatrix}$$

Figure 5.8 Flattened adjacency matrix representation of multilayer social media friendship network

communities or community relationships based on information from other, sparser layers. Furthermore, different combinations of layers may show different group configurations. If we only flattened the Facebook™ and Snapchat™ network layers in the example above, it would produce different results than the network based on all three social media platform friendship layers. Thus, flattening is a useful technique for simplifying the different network layers but can often mask potential insights as a result of the reduction of layer information.

Another means of visualizing a multilayer network is through layer slicing. The idea of layer slicing is to visualize each layer in what is called a 2.5-dimensional representation (De Domenico, Nicosia, et al. 2015; De Domenico, Solé-Ribalta, Cozzo, et al. 2013). While each layer is made of 2-dimensional planes, in visualizing them in proximity to one another, preferably using the same layout, it is possible to interactively explore the multilayer structure. This allows for visual interpretation and appreciation of the structure of each layer and how they contribute to the multilayer network as a whole, but at the expense of reducing the ability to

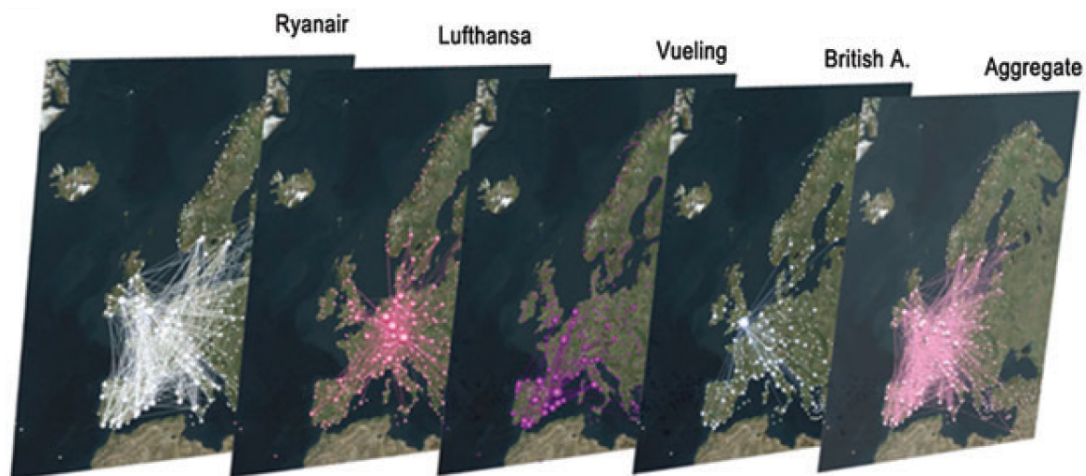


Figure 5.9 Example of multilayer network slicing with networks embedded in geographical regions, showing a network of European airports rendered using MuxViz with each layer representing a different airline and edges representing flights between airports (De Domenico, Porter, et al. 2015)

detect network structure developing over multiple layers. An example of layer slicing is shown in Figure 5.9.

Layer slicing and layer flattening provide complementary means to visually interpret and statistically analyze multiple relations networks. Both produce sociograms, which have become the hallmark visualization technique of social network analysis. Other visualization methods are available but are not presented here. However, visualization of graph structure will be augmented in the succeeding sections using network measures such as degree, closeness centrality, and edge weight to ease visual interpretation of the role of individual nodes and network structure as a whole. Other methods for network graph visualization not used here include annular graphs, histograms of degree distributions, cognitive social structures, heatmaps, dendrograms, and hierarchical clustering, among others (De Domenico, Porter, et al. 2015; Dickison, et al. 2016; Kivelä, et al. 2014). However, contingencies related to network structure will be analyzed using both traditional and multilayer network statistics as well as linear models and other traditional statistical techniques for the analysis of relational data.

Numerous statistical metrics have been developed for monoplex networks (Scott 2000; Wasserman and Faust 1994). In many cases, these metrics can be generalized to work with multilayer networks, especially if a network aggregation technique such as flattening has been applied to the network turning the multilayer network into a monoplex network. However, it is often more constructive to apply monoplex metrics to individual network layers and aggregate the results in order to facilitate comparison of network structure across the different layers, and then to further compare those individual layer results to the aggregated network as a whole. This is the general approach taken here: each layer will be visually presented such as to highlight certain structural features and monoplex network statistics will be presented and discussed before

moving on to present multilayer measures designed for implementation for networks without inter-layer edges.

Monoplex network measures will focus on those that describe network structure, and include degree distribution, centrality (with a particular emphasis on closeness centrality), edge weights, network diameter, network density, average clustering coefficient, and average path length (or distance) (Brughmans 2013; Knox, et al. 2006; Kolaczyk and Csárdi 2014; Scott 2000). These metrics will be computed for each individual network layer and for the flattened multilayer network.

Multilayer network measures will focus on describing the relationships between network layers. These multilayer metrics include multilayer average degree, multilayer degree deviation, multilayer connective redundancy, simple matching multilayer edge comparison, Jaccard index multilayer edge comparison and overlapping community detection (based on the clique percolation method) (Afsarmanesh and Magnani 2016; Cozzo, et al. 2013; Dickison, et al. 2016; Kivelä, et al. 2014; Magnani 2017). These multilayer, and the prior monoplex, network metrics are described in Chapter 4.

5.5 Evaluating the Results: Statistical Interpretation of Ceramic Industry Social Interaction Network Models

The procedures outlined in the preceding section allow for the creation and statistical analysis of network graph models based on similarities between pairs of settlements, which act as proxy measures for the relative degree of social interaction through cultural transmission or homologous interrelationships between groups of potters and other groups at different spatial and social scales. For a given settlement to settlement comparison, a higher edge weight suggests more frequent interaction, stronger relational connections, and/or a higher degree of homology in

evolutionary relationships among the inhabitants of those sites. As a result, the degree of technological similarity may provide insight into the nature and structure of social interrelationships between settlements in the Late Prehistoric central Illinois River valley (CIRV) case study region. Patterns of social interaction and relational connections among settlements across the study area are visually and statistically explored via social network graphing and analysis techniques. Because network models are such a rich source of information beyond what can be presented in static visualizations, it is necessary to preface interpretations based on visual features with statistical analyses. In particular, this section presents a statistical analysis of the structural nature of pre- and post-migration interaction patterns through cultural transmission of ceramic attributes in the Late Prehistoric CIRV based on measurements and concepts used in formal social network analysis and in multilayer social network analysis (Dickison, et al. 2016; Scott 2000; Wasserman and Faust 1994). Given the regional scale of this analysis, interpretations focus on a top-down perspective to inferentially predict the dynamics of social structure in the CIRV. Additionally, because distance has been shown to play an important role in network dynamics in other archaeological contexts (Golitzko and Feinman 2014; Mizoguchi 2009; Peoples 2011), this section specifically discusses the role of geographic distance on the structure of network relationships in the Late Prehistoric CIRV case study region. These analyses both inform and are informed by the visual interpretation and discussion provided in the subsequent section.

It is important to again emphasize that there is considerable variability in the amount of data from each site in the analyses that form the basis of the succeeding interpretations. Quantitative archaeological analysis is often an endeavor conducted on datasets wherein considerable data are missing, and this dissertation research is no exception. Given the regional

scale of this project, and the resulting reliance on extant collections, the interpretations below are not based on a probabilistic survey nor is there perfect comparability between any two given sites. Thus, the relationships modeled between sites may be negatively impacted by issues of sampling. Nevertheless, since the interpretations are based on comparisons between artifact attributes, as opposed to vessels themselves, and because the relationships modeled below conform to the n-critical for each attribute comparison, the interpretations should be considered as robustly laying the foundation for exploring the nature of site to site relationships in the Late Prehistoric CIRV.

In examining the networks constructed here, several structural components are considered and evaluated across space and overtime. First, it is anticipated that changes in network structure overtime are related in some capacity to the in-migration of Oneota peoples into the CIRV circa 1300 A.D. This migration process represents the basis for the temporal partitioning of network graph models. One may ask whether there are changes in network structure across time, and how might the in-migration of an exogenous tribal group be related to those changes? Second, Mississippian peoples in the CIRV have been taxonomically defined as likely representing two distinct chiefly polities – the La Moine River and the Spoon River Mississippian variants (Conrad 1991). As a result, and more especially in the pre-migration context of the CIRV, network topological statistics such as the clustering coefficient and community detection algorithms are analyzed to determine how strongly settlement nodes form ties in dense, relatively unconnected (between group) groups and if those groups are geographically aligned with the hypothesized La Moine and Spoon River Mississippian variants. While many other factors aside from domestic jar and plate technological characteristics were used to differentiate between these variants, it is possible to ascertain here whether or not

ceramic technology may be a contributing or delimiting factor to the proposed taxonomic distinction. Thirdly, given that the serving plate ceramic vessel class is absent or extremely rare in Oneota contexts outside the CIRV (Esarey and Conrad 1998), particular attention is given to this class in the post-migration CIRV. That is, do imitations/emulations of serving plates by Oneota peoples inject sufficient variation to suggest that the adoption of this vessel class was made at a distance, or are the imitations/emulations technologically similar enough for there to be a higher likelihood that direct cultural transmission of ceramic technology between Mississippian and Oneota potters occurred? Additionally, it has been postulated that the onset of the Mississippian period circa 1200 A.D. was paralleled by the emergence of chronic, internecine violence and warfare (G. R. Milner 1999; Wilson, 2012 #1667). The threat of warfare is argued to have transformed both settlement and subsistence practices such that, among other things, “families coalesced into large communities behind defensive walls...limiting foraging and fishing trips” and “women became increasingly sequestered behind village walls” (Vanderwarker and Wilson 2016:98-100). Given that ethnographic accounts indicate that when pottery manufacture is done by hand, it is typically done by women (Rice 2005), it is possible to test whether the Mississippian CIRV is characterized by geographically circumscribed potter communities. That is, does sufficient variation in pottery attributes characterize different communities such that it can be reasonably assumed that potters were geographically circumscribed in the cultural transmission of artifact attribute social information primarily as a result the threat of violence and warfare?

In addition to relying on formal methods in the statistical analysis of monoplex and multilayer network data, which are discussed at length in Chapter 4, interpretations are based in part on conditional uniform graph tests through Monte Carlo simulation. Each observed network

statistic was compared against the distribution of that statistic generated from 5,000 random graphs of the same order (number of nodes) and probability of an edge being given between any two nodes (based on the observed graph's density) or size (number of edges) using the Erdős-Rényi graph randomization technique (Erdős and Rényi 1959). Network randomization simulation enables formal hypothesis testing of whether the observed network statistics are unusually high or low given what might be expected if the same probability of edges (or number of edges) were connected to the same number of nodes as the observed network based on random chance alone.

Erdős-Rényi random graph models place equal probability on all graphs of a given order and size. That is, a collection of graphs are considered based on the provided order and size (number of nodes and edges) and a probability is assigned to each, where the total number of distinct node pairs are considered (Kolaczyk and Csárdi 2014). As a result, each permutation of a network of a particular order and size is able to be drawn upon to simulate graph models uniformly at random. An extension provided by Gilbert (1959) enables the random graph concept to be extended to graphs of a fixed order but where each pair of distinct nodes are independently assigned based on a given probability. This is often referred to as a Bernoulli random graph model, but will be subsumed here under the Erdős-Rényi framework (Kolaczyk and Csárdi 2014). Erdős-Rényi random graph models were chosen for statistical comparison because they most closely resemble the topology of the networks generated using the procedure described above. As further described below, the networks do not appear to conform to properties expected of small-world or scale-free/preferential attachment models that often characterize large-scale networks observed in many real-world networks (Barabási and Albert 1999; Watts and Strogatz 1998).

5.5.1 *Statistical Analysis of Pre-Migration Interaction Networks, 1200 – 1300 A.D.*

Because networks are defined by their actors and the connections among them, in this case spatially bounded archaeological sites and the degree of similarity in socially mediated artifact attributes, a useful starting point in statistical network analysis is examination of these properties. Table 5.12 displays network summary and analytical statistics, including network order (number of nodes), size (number of connections or edges), and mean weighted degree (or average total strength of connections) for each network under consideration. In examining these measures for the jar and plate interaction networks for the pre-migration period, some important distinctions are apparent. For example, the jar attribute network includes many more edges (or connections) than the plate attribute network for the pre-migration period (81 edges compared to 63 edges). While one additional site-node in the jar layer (Eveland) compared to the plate layer may account for the discrepancy in edges, the mean weighted degree further hints at important structural distinctions between the two layers. The jar attribute pre-migration network layer is composed of significantly stronger connections between sites on average than the plate pre-migration layer (mean weighted degree of 5.117 compared to 3.994). Thus, in terms of simple summary statistics, the jar attribute layer contributes many more and many stronger connections in the pre-migration interaction networks than does the plate attribute layer.

In network terminology, both layers in the pre-migration period conform to an expected connectedness (referred to as density), or proportionality of present ties compared to the possible number of ties (see Table 5.12; Figures 5.10 and 5.11), based on a Monte Carlo simulation of 5,000 random graphs of the same number of nodes and probability of edge creation using the Erdős–Rényi random graph modeling technique (Erdős and Rényi, 1959). That is, pre-migration

networks conform to random expectations for density. Additionally, both the jar and plate pre-migration networks consist of many hubs, as shown in Figure 5.12. In fact, nearly every site displays the behavior associated with hubs. The concept of hubs and authorities, based on the HITS algorithm (Kleinberg 1999), considers the importance of hub-nodes based on how many authorities-nodes they point to, and authority-nodes based on how many hub-nodes point to them. In other words, hubs advertise or distill information gathered from authority nodes. Because every site in the pre-migration time period has a high hub score, information is not hierarchically restricted nor restricted to site clusters. At a minimum, density and hub measures imply that the ceramic vessel attributes argued here to be socially mediated indicate shared

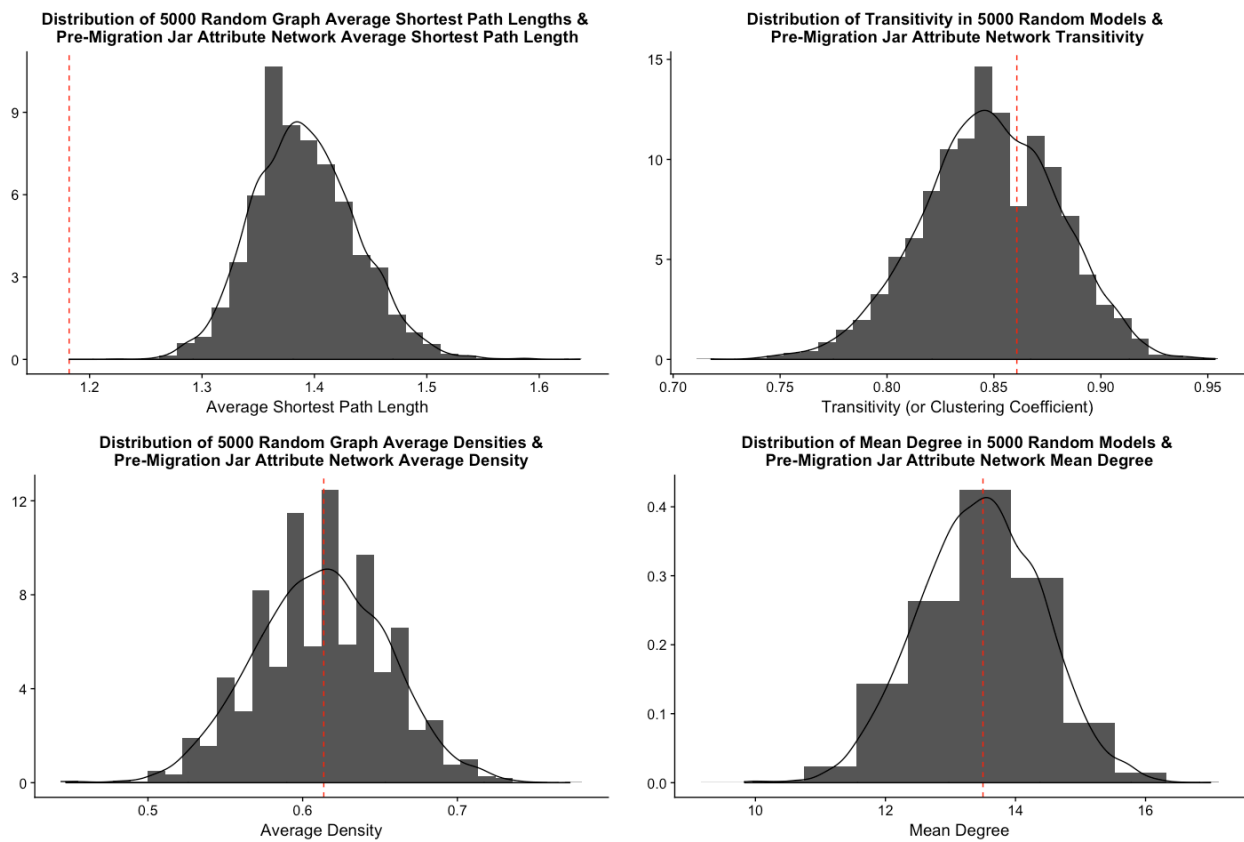


Figure 5.10 Network Randomization Results for Jar Pre-Migration Layer. Observed statistic represents red line. Histogram shows distribution of statistic based on network randomization of 5000 random graphs using the Erdős–Rényi random network modeling technique.

contexts of learning and homologous relationships across sites and a capacity for site actors to inter-operate. That is, the interaction cost in both jar and plate attribute networks is low enough to suggest that on average there is a tendency for information to flow broadly and frequently throughout the networks in the pre-migration period (Borgatti, et al. 2009).

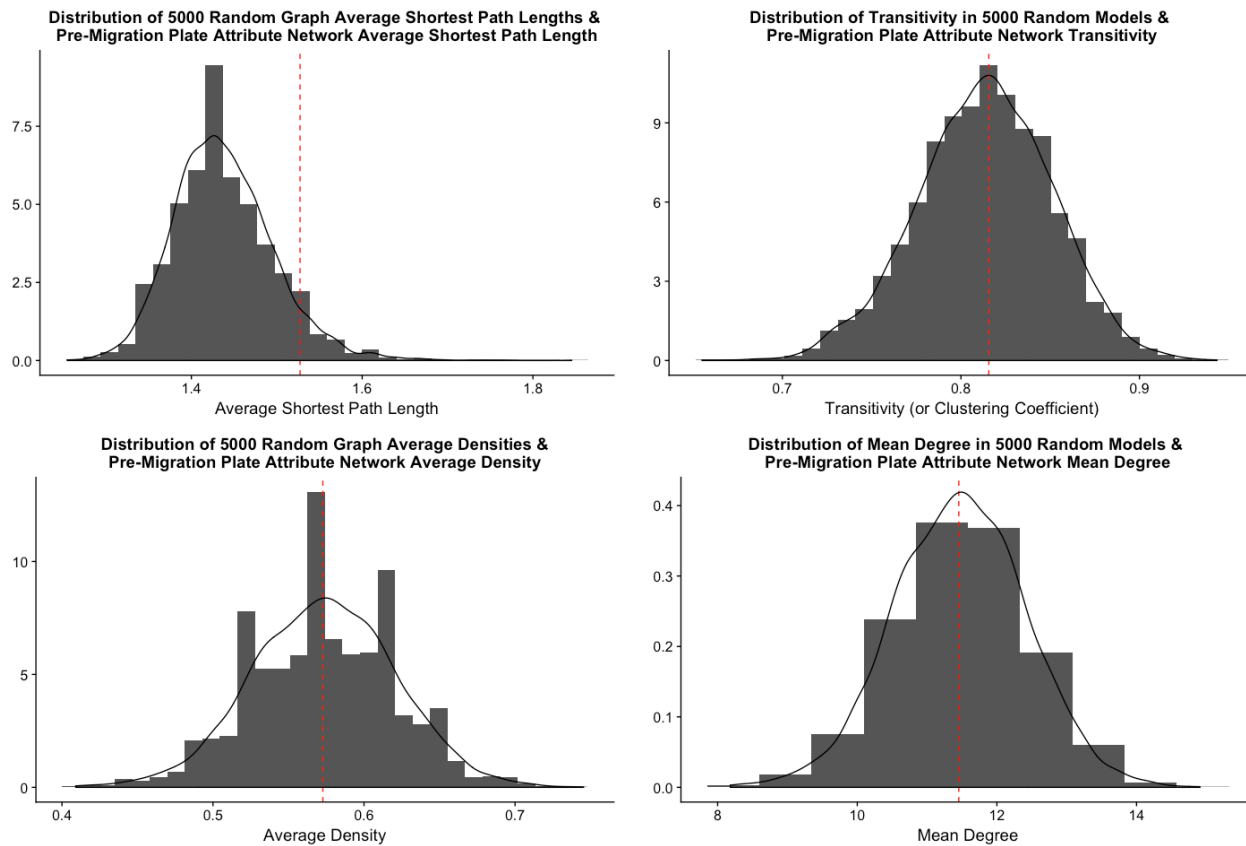


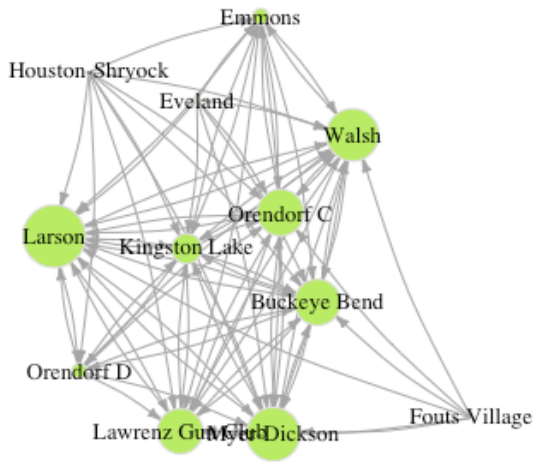
Figure 5.11 Network Randomization Results for Plate Pre-Migration Layer. Observed statistic represents red line. Histogram shows distribution of statistic based on network randomization of 5000 random graphs using the Erdős–Rényi random network modeling technique.

On the other hand, a more interconnected domestic jar network is supported by the average shortest path length, or average number of nodes in between any two given nodes, which is just 1.182 for the domestic jar layer but a much higher 1.527 for the plate layer. In fact, none of the random graph models for the pre-migration jar network reported a lower average shortest path length than the observed network (Figure 5.10), but some 92% of 5,000 random graph

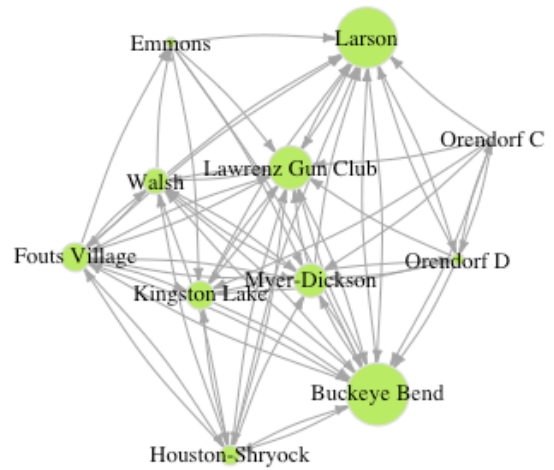
models based on the plate pre-migration network reported shorter average path lengths (Figure 5.11). The unusually low average shortest path length for the jars suggests widespread and efficient transmission about socio-cultural information embedded in jar attributes, while the unusually high average shortest path length for the plates indicates the inverse – less efficient or restricted transmission about cultural information related to plate attributes. An alternative, and perhaps more plausible, interpretation of the high average shortest path length for the plate pre-migration network is that plate attributes were more a product of adaptation to the local social environment whereas socially mediated jar attributes appear to have been perhaps more globally adapted. The diameter, or longest shortest path, which is just two for the jar layer but three for the plate layer further substantiates the difference in network topology between the layers in the pre-migration CIRV. These observations suggest that the jar attributes not constrained by engineering forces may have contributed more to signaling global social relationships among potter communities in the pre-migration CIRV or were perhaps more resistant to change given the presumed functional importance of cooking facilitated by domestic jars. Furthermore, since plates emerge as a distinct vessel class only after the occupation of the Eveland site, plate attributes may be characterized by a greater degree of variation in general than jars as a result of the novelty of the vessel class, and perhaps accompanying changes in foodways, in the increased situational usage of a presumed serving vessel.

A low average shortest path length, such as that observed in the jar pre-migration network, is often accompanied by a high transitivity (or clustering coefficient) score in real-world networks. This combination of structural features has been identified as a ‘small-world network’ where most nodes are not neighbors of each other, but information easily passes through the network in a relatively small number of steps (Watts and Strogatz 1998). The pre-

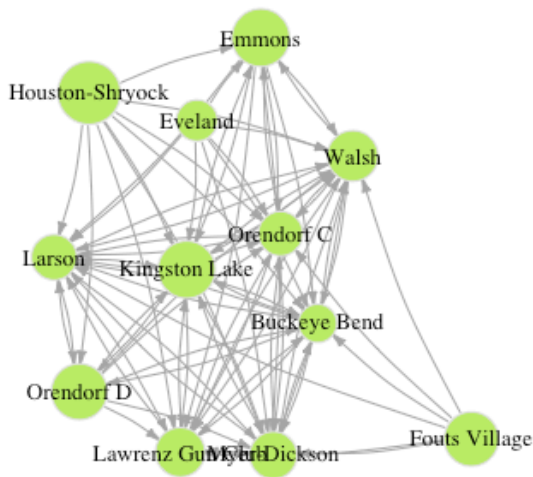
Authorities in the Jar Pre-Migration Network



Authorities in the Plate Pre-Migration Network



Hubs in the Jar Pre-Migration Network



Hubs in the Plate Pre-Migration Network

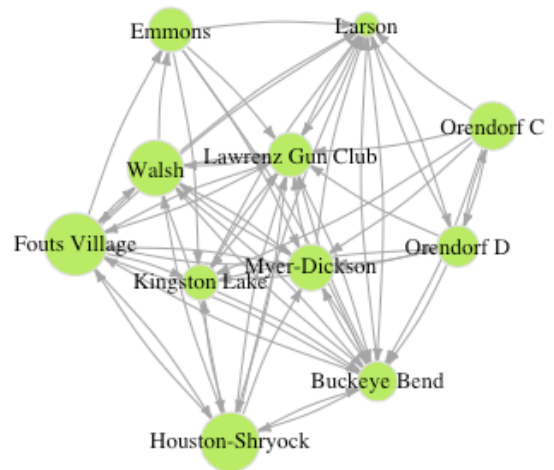


Figure 5.5.12 Authorities and Hubs in the Jar and Plate Pre-Migration Period Network Layers. Authority and Hub scores are modeled as node size.

migration jar attribute network, however, is characterized by a transitivity (or clustering coefficient) score only moderately above what might be expected based on chance alone (65% of 5,000 random graph simulations report a transitivity lower than the observed jar pre-migration layer). The pre-migration plate attribute network is neither characterized by a low average shortest path length nor an unusually high clustering coefficient score. As a result, both the jar and plate pre-migration attribute networks do not support a small-world network model for the pre-migration period.

Based on the degree distributions, or frequencies of the total connectedness of nodes in the network, it can be affirmed that the jar and plate pre-migration attribute networks do not display characteristics associated with a scale-free network using a preferential attachment mechanism, also known as the Barabási-Albert model (Albert and Barabási 2002; Barabási and Albert 1999). Figure 5.13 displays the degree distributions of the jar and plate pre-migration

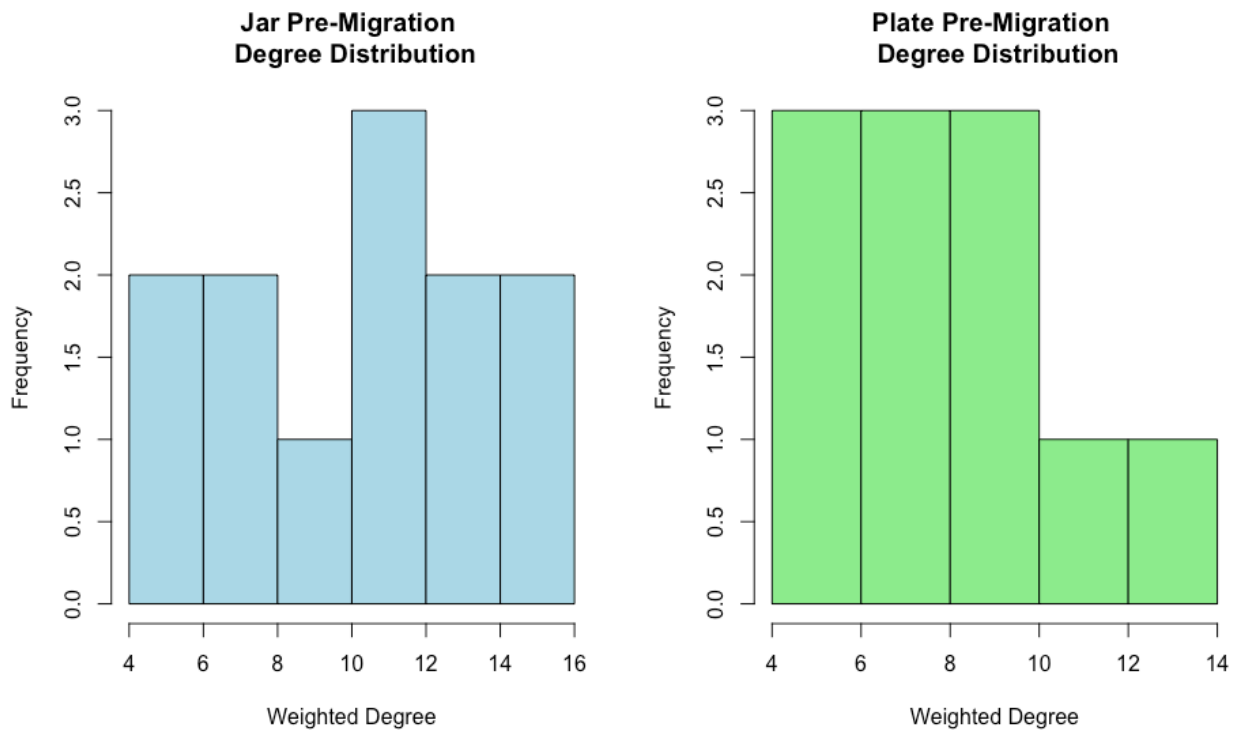


Figure 5.5.13 Degree distribution of Jar and Plate Pre-Migration networks.

networks. Under the Barabási-Albert model preferential attachment model, the distributions would be highly right skewed showing that many nodes have few connections and just a few nodes have many connections, which is often referred to as the ‘rich get richer’ postulate of node creation overtime. Such a model would suggest that ‘child’ nodes would splinter off of ‘parent’ nodes, with few parents connected to many budding children nodes. The incongruence of the jar and plate networks with the Barabási-Albert model indicates that the settlements considered here were likely not hierarchically organized in the Late Prehistoric CIRV.

Both pre-migration period networks lack a central actor or actor-clique with significantly higher degrees of connectivity than others as indicated by low degree, betweenness, closeness, and eigenvector centralization scores (Table 5.12). Centralization scores address inequality in node interconnectedness, or if one or a few nodes are more central to the network than others in certain ways (Scott 2000:Wasserman, 1994 #329). The low centralization scores observed in the pre-migration networks indicate that node importance is relatively evenly distributed across the entire network. However, certain sites do appear to be more authoritative, in terms of their connections to other sites, based on the HITS algorithm (Kleinberg 1999). In other words, some sites are significantly more connected than others, suggesting that these sites were likely loci of information, regional events, or producers of exogamous offspring to other sites that would account for the many strong connections to these sites in terms of social interaction through cultural transmission. The Larson site in particular plays an authoritative role in both the jar and plate pre-migration networks, as do Lawrenz Gun Club, Buckeye Bend, Myer-Dickson, Kingston Lake, and Walsh to a lesser extent (Figure 5.12). However, the combination of low centralization scores, the presence of multiple authorities, and the ubiquity of hubs in the pre-migration period indicates that no one site-actor dominated regional interaction or information flow as might be

expected in a hierarchical regional settlement system as seen in other Mississippian contexts such as the American Bottom (Fowler 1974), at least at the unrefined scale of the entire pre-migration period (~1200 – 1300 A.D.) considered in this analysis.

In attempting to identify communities, or modules that form dense connections among themselves and sparser connections to nodes outside the module, a diverging trend is apparent between the jar and plate pre-migration attribute networks. A particularly instructive community structure detection technique for the weighted and directed networks considered here is edge betweenness, which maps a value to each edge (or link) in the network based on how many shortest paths traverse through it (Kolaczyk and Csárdi 2014; Newman and Girvan 2004). Edges that connect separate modules, or individual communities within a network, have high edge betweenness values. By gradually removing these edges with high betweenness values, a hierarchical map is created similar to a network dendrogram. Clusters can therefore be identified in the same way that clusters might be identified via hierarchical clustering techniques, for

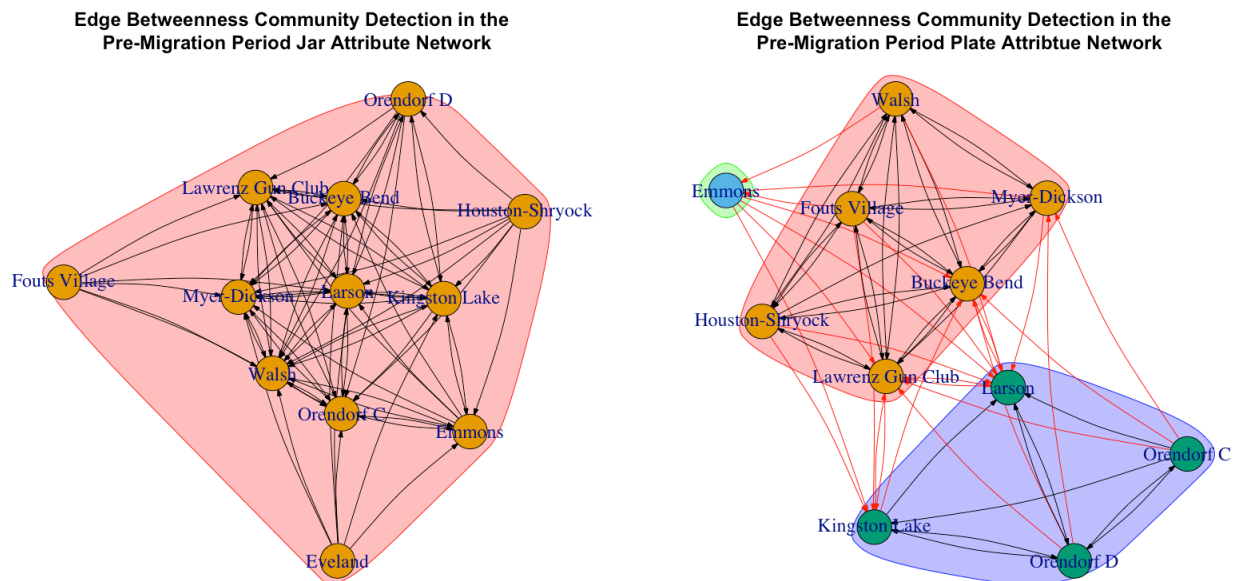


Figure 5.5.14 Edge betweenness community detection in the Jar and Plate Pre-Migration Attribute Networks

example. Figure 5.14 shows that no meaningful community structure is able to be identified based on edge betweenness in the pre-migration jar attribute network whereas three distinct modules are identified in the pre-migration plate attribute network. This finding aligns with interpretations from other network statistics indicating important structural differences between the layers where jar attributes reflect a global pattern of interaction and information flow and plate attributes are more so the product of localized or nuanced social interaction through cultural transmission.

The multilayer network combining both jar and plate networks in the pre-migration period is characterized by a significantly increased mean weighted degree of 7.917 as a result of

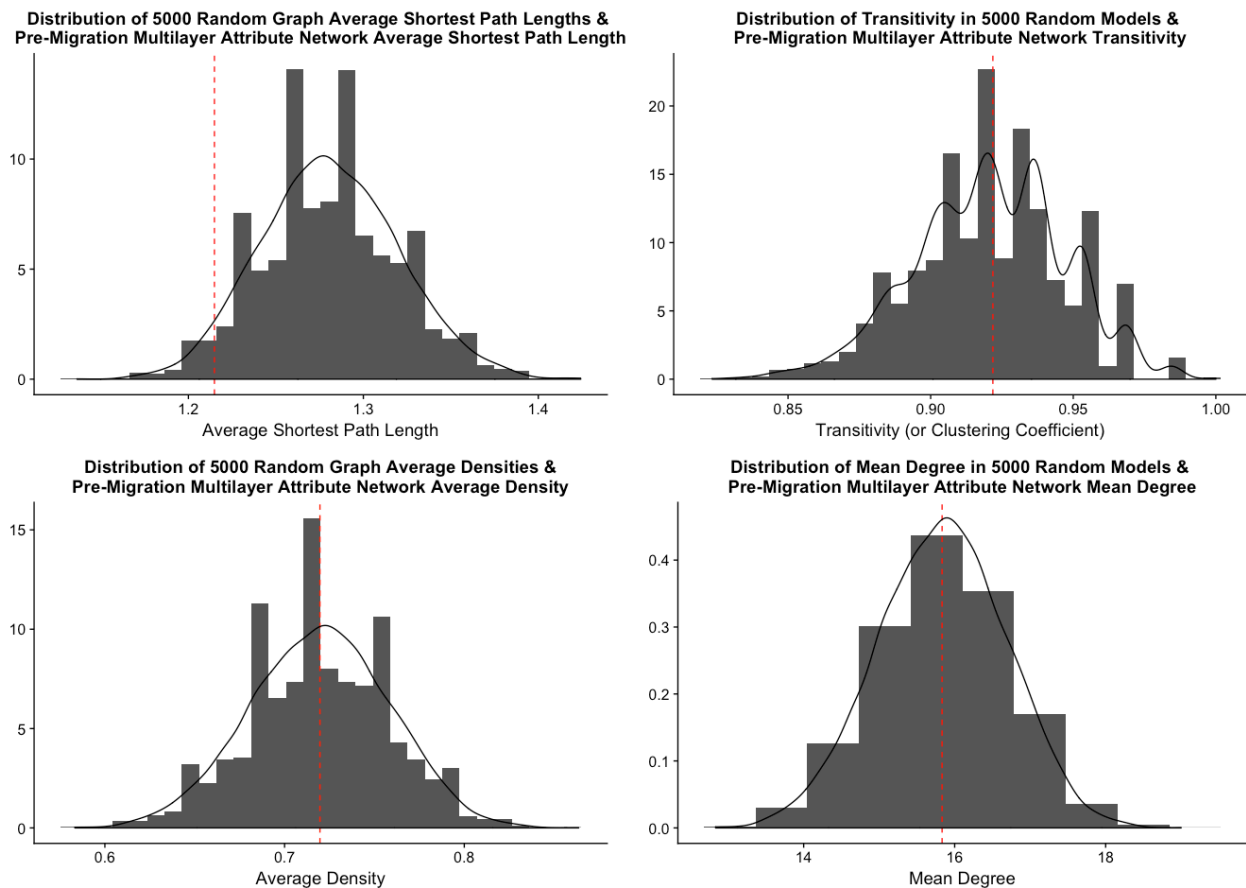


Figure 5.15 Network Randomization Results for Multilayer Pre-Migration Network. Observed statistic represents red line. Histogram shows distribution of statistic based on network randomization of 5000 random graphs using the Erdős–Rényi random network modeling technique.

the concatenation of the two layers together. Both density and transitivity (or mean clustering coefficient) also increase in the flattened multilayer pre-migration attribute network in comparison to that of the individual jar or plate layers. Though none of these figures are significant relative to network randomizations for the pre-migration multilayer network as shown in Figure 5.15. However, despite the high average shortest path length in the pre-migration plate layer, the multilayer network follows the very low average shortest path of the domestic jar pre-migration layer, with a low score of 1.215, or 1.215 steps in between any two given nodes in the network on average. No doubt, the higher edge weights in the jar layer contribute to this trend. The increased number of edges and stronger edge weights in the pre-migration jar attribute network also obfuscate the nuances of authorities across the jar and plate attribute layers. In general, trends of authority in the pre-migration jar attribute layer supersede those in the plate layer when modeled as a singular multilayer network (Figure 5.16). This trend holds true in

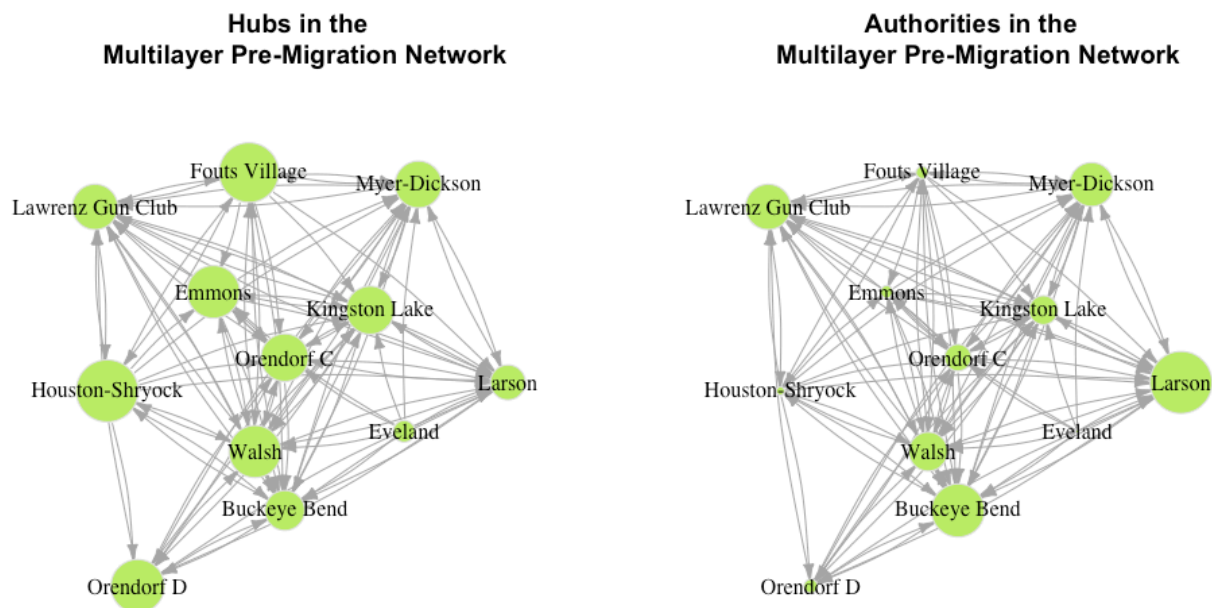


Figure 5.5.16 Authorities and Hubs in the Multilayer Pre-Migration Period Network. Authority and Hub scores are modeled as node size.

community detection, where no community structures are able to be identified in the multilayer network as in the jar pre-migration layer (Figure 5.17). The ability to identify that 1) increased jar edge weights obfuscate the much higher average shortest path length of the plate layer in the pre-migration period, and 2) the nuanced nature of authorities and community structures across the jar and plate networks further substantiates the value of the multilayer network analysis methodology.

In examining the multilayer network for the pre-migration period using formal techniques from multilayer social network analysis, Eveland shows the highest degree deviation, or standard deviation of an actor’s degree over the different layers. Degree deviation shows which actors are unevenly represented on different layers (Dickison, et al. 2016). All other sites are characterized by low degree deviations indicating that their presence in the jar and plate network layers is

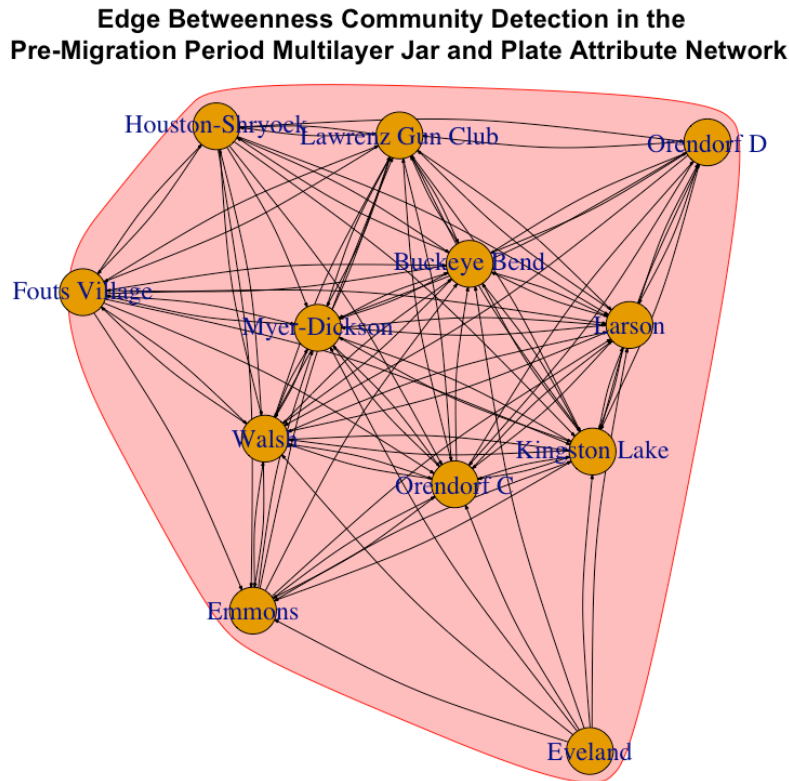


Figure 5.17 Edge betweenness community detection in the Multilayer Pre-Migration Network

comparable aside from Walsh and Orendorf C, which also have high degree deviations indicating an uneven presence in the jar and plate layers. Perhaps this is an indication that Walsh and Orendorf C were both occupied early in the occupational sequence of the pre-migration CIRV during the initial introduction of the plate vessel class.

With an average connective redundancy of 0.375, the jar and plate networks are characterized by a fairly high degree of multiplexity. Average connective redundancy between the pre-migration layers is a measure that considers how often actors are connected to the same neighbors across multiple layers (Dickison, et al. 2016). However connective redundancy does not consider the weight of an edge, only its presence or absence across layers as weight and directionality have yet to be implemented in many multilayer network analysis algorithms (Matteo Magnani personal communication, 2017).

Despite the many structural differences discussed above, the jar and plate pre-migration attribute network layers do share much in common. A simple matching coefficient considering common edges across the multiple layers shows that they share nearly 87% of edges in common when directionality and weight are not factored into the comparison. A more nuanced comparison using the Jaccard measure of similarity, which is computed as the amount of common edges between the layers divided by the union of all edges for pairs of layers (Dickison, et al. 2016), shows that the jar and plate attribute networks in the pre-migration period are 67% similar. Again, this metric is only able to consider deprecated edges by disregarding weight and directionality.

In summary, when considering formal statistical measures for the analysis of monoplex and multilayer social networks, the jar and plate attribute networks in the pre-migration period are largely similar but with some very important distinctions. The most instructive measures

evidencing the distinctions between the layers are the average shortest path, HITS algorithm, and edge betweenness community detection. In general, these metrics indicate that the interactions through cultural transmission based on the sharing of jar attribute information represent connectivity among sites at a regional scale, whereas the sharing of plate attribute information represents connectivity at a more localized or nuanced scale. These scalar differences suggest distinctions in the production and likely situational usage of these vessel types in the pre-migration period and speaks to the complexity of modeling social interrelationships between archaeological sites using artifactual data. Numerous authorities are modeled in the jar attribute network layer, but the Larson site plays a particularly authoritative role in this layer. Perhaps the emergence of the Dickson series of plain, cord-marked, or trailed jars at Larson, representing a fundamentally CIRV innovation to the production of Mississippian domestic jars, in addition to the central location of Larson geographically and its proximity to the Dickson Mounds mortuary ceremonial center are responsible for this authoritative distinction (Harn 1971, 1980, 1991, 1994; Strezewski 2003; J. J. Wilson 2010).

Pre-migration CIRV interaction networks can overall be described as distributed, or lacking any central actor or actor-cliques, and highly cohesive, or generally lacking any structural evidence for distinct communities, modules, or cliques within the individual or multilayer networks, save those identified in the plate pre-migration attribute network layer. These interpretations, which are further discussed and expanded upon in the discussion in Section 6.6.1, indicate that social networks of interaction through cultural transmission of socially mediated jar and plate attributes in the pre-migration period do not support an hypothesized cultural distinction of CIRV Mississippian peoples into a La Moine and Spoon River variants (Conrad 1991), nor do they provide support for a model of delimited mobility as a

result of the threat of warfare (Vanderwarker and Wilson 2016). Were there to be intensive cultural distinctions between Mississippian peoples in different portions of the CIRV, it would be expected that those distinctions would be reflected in separate communities, cliques, or modules forming sub-networks of interaction through information sharing, imitation, and cultural transmission of ceramic artifact attributes. While some distinctions do exist in the plate vessel class, they do not follow a geographic divide based on the Spoon and La Moine River Valleys. Furthermore, were there to have been a marked curtailment in mobility patterns due to chronic or structural violence patterns, it would be expected again that interaction through information sharing, imitation, and cultural transmission of ceramic artifact attributes would be bifurcated along alliance lines or otherwise restricted to site or site-cluster scale patterns. Because these patterns of bifurcation or community structure do not exist across the network layers, it is established here that patterns of violence seen in skeletal data, the presence of fortifications, and ritual weaponry (Steadman 2008; Vanderwarker and Wilson 2016; G. D. Wilson 2012, 2013) did not inhibit interaction patterns in the Mississippian CIRV in a structural way. Rather, and perhaps despite the high levels of inter-personal violence, Mississippian peoples appear to have sustained widespread social interaction in the sharing and cultural transmission of information related to jar and plate ceramic industry.

5.5.2 Statistical Analysis of Post-Migration Interaction Networks, 1300 – 1450 A.D.

Sometime in the late thirteenth or early fourteenth century, an expansionary process of Oneota peoples began out of an upper Midwest and eastern Prairie Plains core territory (Gibbon 2002; Henning 1998). Some characterize the Oneota expansionary process as aggressive and warlike (Hollinger 2005). While many Late Woodland populations in the riverine Midwest and

western Great Lakes were replaced by or integrated into Oneota peoples during this expansion, Mississippian peoples in the central Illinois River valley, or northern Middle Mississippian frontier, maintained their positions in fortified temple mound centers, and outlying sites, and entered into a period of regional multicultural coexistence (Esarey and Conrad 1998; O'Gorman and Conner 2016; Painter 2014).

The post-migration period Late Prehistoric CIRV is comprised of many fewer sites than were occupied during preceding phases in the region, suggesting that a consolidation process, population upheaval, or other demographic change seen in Mississippian contexts in other regions was likely also being grappled with in the CIRV based on local conditions (Benson, et al. 2009; Blitz 2010; Cobb 2005; Cobb and Butler 2002). That is, compared to the 11 or 12 town and village sites modeled in the pre-migration period attribute network layers, only some 7 or 8 sites are able to be examined following the circa 1300 A.D. Oneota in-migration, depending on the layer. As in the pre-migration period, the different artifact attribute network layers are node-disjoint as a result of one additional site in the jar layer compared to the plate layer. That is, the C.W. Cooper Oneota habitation site lacks any presence of the plate vessel class and as such was not able to be modeled in the post-migration plate layer. Thus, analysis of the post-migration period factors in the reduced network sizes as potentially confounding network statistics given the very small number of nodes.

Despite a decrease in the number of nodes in the post-migration network, the mean weighted degree in the plate attribute network layer actually increases compared to the pre-migration period (from 3.994 to 4.406). However, the mean weighted degree for the jar attribute network layer falls precipitously in the post-migration period (from 5.117 to 3.962). Furthermore, the diameter (or longest shortest path in the network) in the plate attribute network

drops from 3 to 2 while the diameter in the jar attribute network layer increases dramatically from 2 to 4 in the post-migration period. More striking is the mean path length, which is only 1.048 for the plate layer, indicating that actors need only move between 1.048 sites on average to reach a destination node. These simple summary statistics imply significant structural changes in networks of interaction through cultural transmission occurring alongside Oneota in-migration into the region.

The significance of the shift in structure of both jar and plate attribute networks is apparent when examining the results of Monte Carlo network randomizations using the Erdős–Rényi random network modeling technique (Figures 5.18 – 5.19). In particular, the average shortest path length for the jar attribute network shifts from being lower than any value measured in network randomizations for the pre-migration jar attribute network to being higher than some 94.9% of average shortest path lengths in the 5,000 randomized networks for the post-migration jar attribute network based on the Erdős–Rényi random network modeling technique. Furthermore, the average shortest path in the plate attribute network shifts from being higher than some 92.4% of randomly generated networks of the same order and size as the plate attribute pre-migration network layer, to being higher than only 42.7% of randomly generated networks based on the plate attribute post-migration network. In other words, the scalar pattern at which the different vessel classes were used in forming strong relational connections changed from the pre-migration period to the post-migration period in the Late Prehistoric CIRV. Whereas the jar attribute network formed strong relational connections among sites at a regional scale in the pre-migration, relational connections in the jar attribute network altered to form strong relational connections only at a reduced or nuanced scale in the post-migration period. The infusion of Oneota domestic jar technological choices undoubtedly contributed to this scalar

shift in relational connections. However, while the infusion of distinctly Oneota designs on jars is readily apparent, the infusion of distinct technological choices in jar manufacture by Oneota peoples is less obvious without using formal quantitative methods such as those used in this dissertation. What’s more, that Oneota peoples maintained not only distinctive stylistic but also technological choices in the manufacture of domestic jars speaks to the cultural maintenance of an importance facet of domestic life – cooking technology. Perhaps there was broad appeal to an Oneota heritage and the formation of bonding ties in the domestic sphere of life by Oneota potters (Crowe 2007).

On the other hand, interactions with local Mississippian peoples did result in the adoption

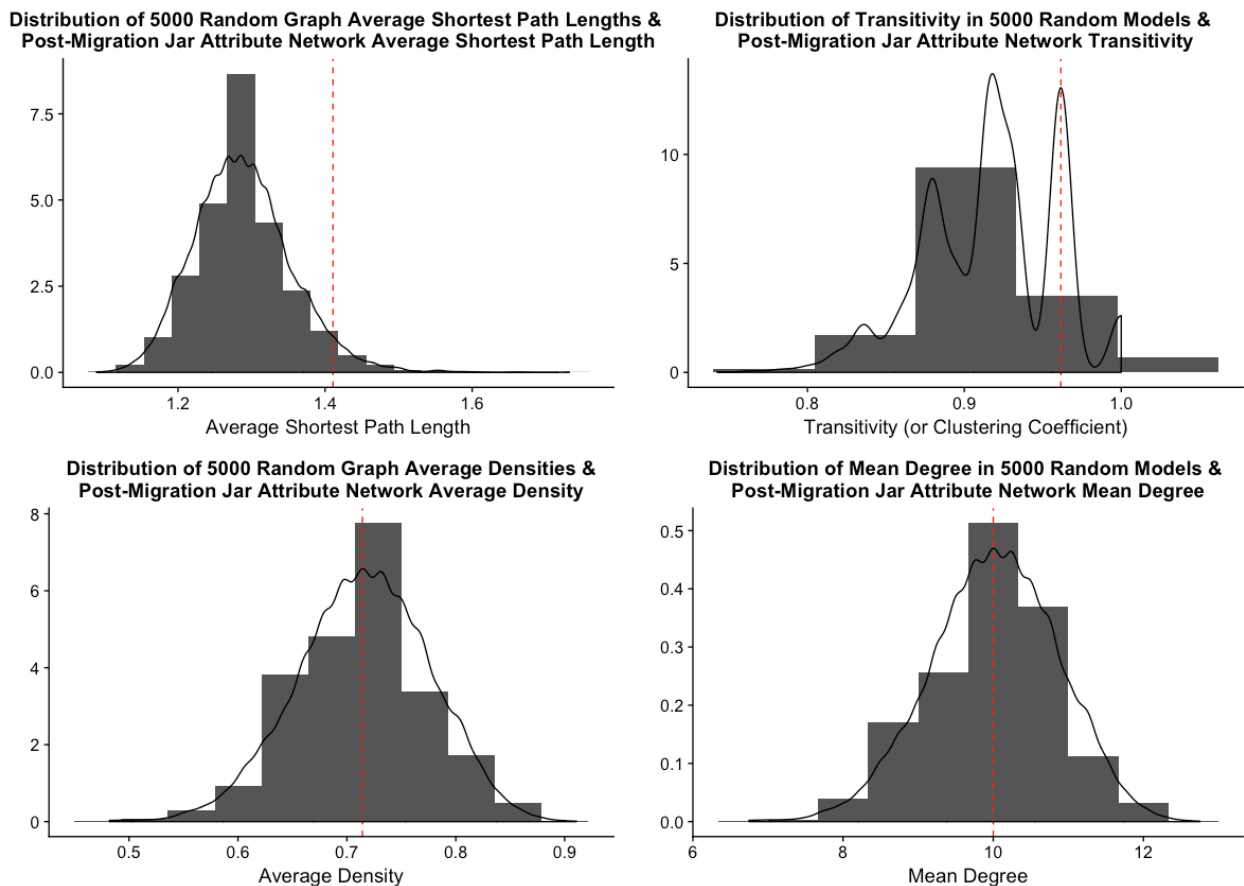


Figure 5.5.18 Network Randomization Results for Post-Migration Jar Attribute Network. Observed statistic represents red line. Histogram shows distribution of statistic based on network randomization of 5000 random graphs using the Erdős–Rényi random network modeling technique.

of a unique vessel form by Oneota peoples, the plate – a vessel ostensibly used primarily as a food serving tool. While not all Oneota immigrants in the CIRV adopted the plate into their ceramic repertoire, as no plates have yet been recovered from the Oneota occupation at C.W. Cooper (Esarey and Conrad 1998), examination of the post-migration plate attribute network suggests an impetus for cultural integration or mediation by Oneota peoples in actively choosing to utilize the plate vessel class. The post-migration plate attribute network shows a high mean weighted degree, low average shortest path length, low diameter, higher density and low centralization scores comparable only to the pre-migration jar attribute network (Table 5.12). In

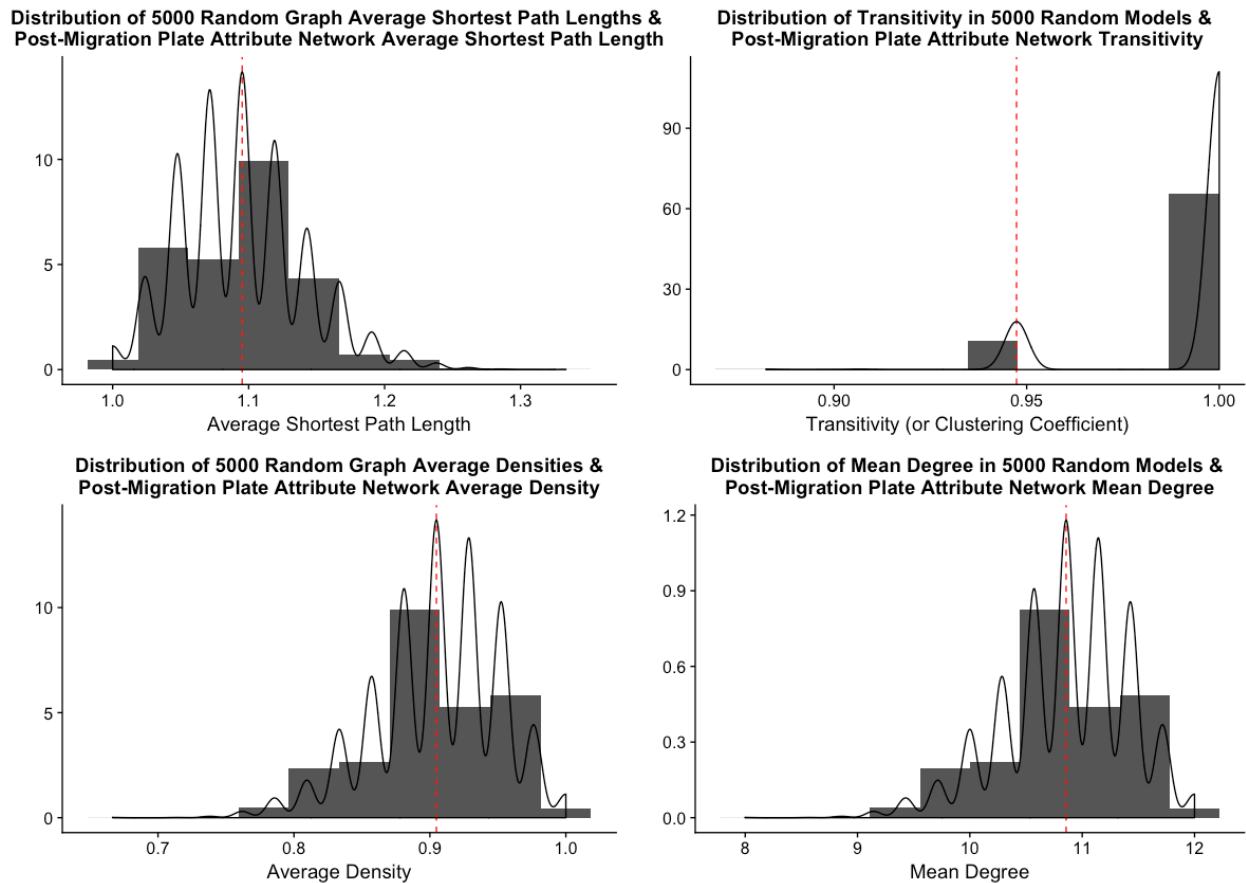


Figure 5.5.19 Network Randomization Results for Post-Migration Plate Attribute Network. Observed statistic represents red line. Histogram shows distribution of statistic based on network randomization of 5000 random graphs using the Erdős–Rényi random network modeling technique.

other words, the scale at which strong connections were formed increased dramatically from the pre-migration to post-migration periods in plate attribute networks at the same time that the scale at which strong connections were formed in the jar attribute networks decreased dramatically.

No site with an Oneota presence – Crable, Morton Village, C.W. Cooper – is characterized as an authority when analyzing the post-migration period jar attribute network using the HITS algorithm (Kleinberg 1999) (Figure 5.20). This indicates that, in terms of jar attributes, sites with an Oneota presence retained pluralistic distinctions from their Mississippian peers, perhaps straining the formation and maintenance of regional relational connections given that jars were previously a source of widespread relational interaction through cultural transmission. However, because the sites with an Oneota presence do act as hubs in the post-migration period jar attribute network, mediation was perhaps pursued but not reciprocated or there was a concerted effort by post-migration Mississippian sites to distinguish their own domestic jar technological communities of practice from Oneota immigrant jar technology (D. Upton 1996; VanPool 2008). In other words, the post-migration jar attribute network suggests that inter-cultural pluralism in the domestic sphere of life likely characterized the Late Prehistoric Period Crable and Crabtree phases of the CIRV.

While pluralism may have been present in the domestic sphere of life based on the domestic jar network, the public sphere of life appears to have been in part an arena of inter-cultural accommodation, integration, or other mediation between Oneota and Mississippian peoples as modeled by the post-migration plate attribute interaction network. Because every site in the plate attribute network post-migration time period has a high hub score, information regarding plate manufacture was decidedly not hierarchically restricted nor restricted to site clusters. This implies that the plate attributes argued here to be socially mediated indicate shared

contexts of learning and homologous relationships across sites occupied during the post-migration period and a capacity for site actors to inter-operate – at least in the public sphere of life that a presumed serving vessel would primarily function within. That is, the interaction cost in plate attribute networks is low enough to suggest that on average there is a tendency for

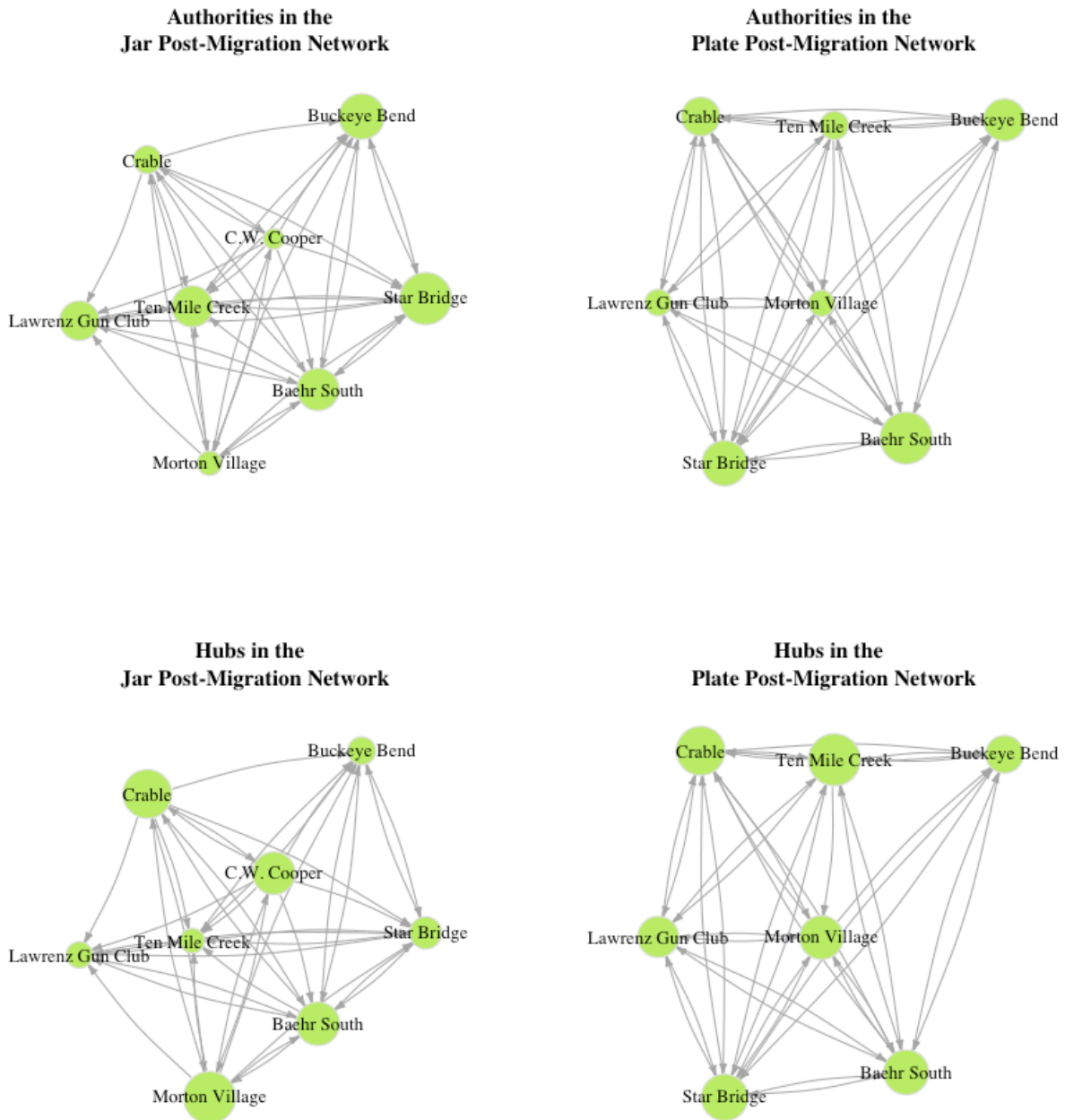


Figure 5.20 Authorities and Hubs in the Jar and Plate Post-Migration Period Network Layers. Authority and Hub scores are modeled as node size.

information to flow broadly and frequently throughout the plate attribute network in the post-migration period (Borgatti, et al. 2009).

This duality in the scale of relational connection formation between the artifact classes is best illustrated in community structure detection using edge betweenness (Figure 5.21). Whereas the pre-migration plate attribute network is characterized by a single, region-wide community, three distinct communities are detected in the post-migration plate attribute network. Of the three distinct communities, one is comprised of sites with an Oneota presence in addition to the Lawrenz Gun Club site – a site marked by a modest and unclear Oneota presence. A separate community structure is detected that comprises three Mississippian sites with no evidence of a multicultural occupations between Oneota and Mississippian peoples. Finally, Baehr South, a modest Mississippian village site appears to straddle these distinct communities and as a result forms a community unto itself. Thus, according to community structure, regional scale cultural

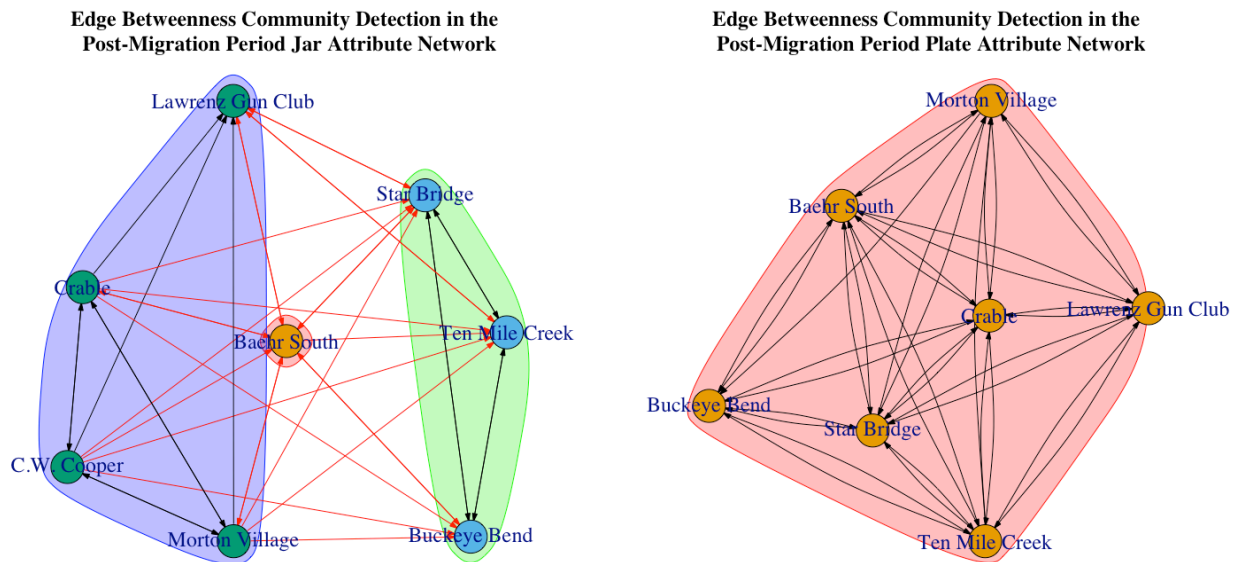


Figure 5.5.21 Edge betweenness community detection in the Jar and Plate Post-Migration Attribute Networks

pluralism was largely maintained by Oneota and Mississippian peoples in the domestic or private sphere of life with some public deemphasis of inter-cultural differences. The multi-cultural occupations at Crable and Morton Village, however, do show that limited domestic scale inter-cultural mediation did occur. This pattern of nuanced multi-cultural public-private distinction has precedent in other archaeological contexts (Stone 2003).

Similar to the pre-migration period attribute networks, neither the jar nor plate attribute networks in the post-migration period exhibit characteristics associated with small world or scale free preferential attachment network models. Figure 5.22 shows that both post-migration networks are characterized by degree distributions with quite high values at the low end of the distribution (e.g. degrees of 6+) and a lack of extensive kurtosis that would suggest a log-log

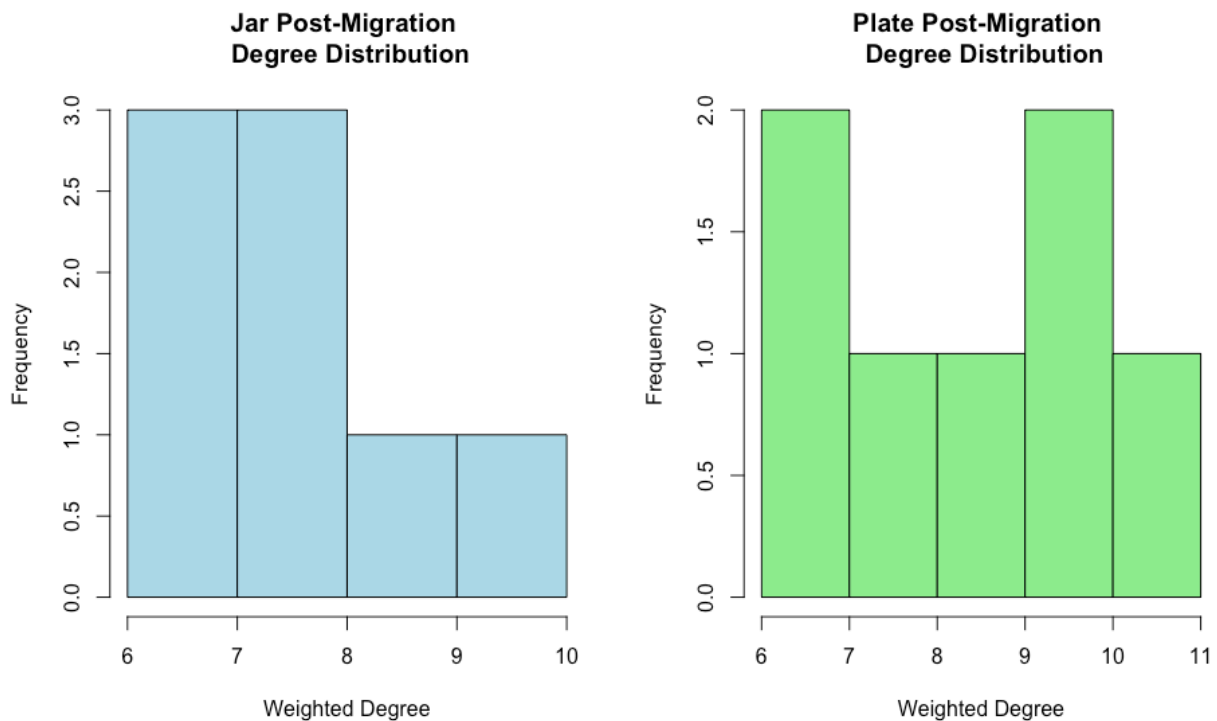


Figure 5.5.22 Degree Distributions of Jar and Plate Post-Migration Networks

power law distribution typical of scale-free preferential attachment models (Barabási and Albert 1999). Furthermore, low centralization scores (Table 5.12) reported for the post-migration

attribute networks indicate a lack of hierarchization in information flow, another characteristic element of preferential attachment. While both the jar and plate post-migration networks have very high mean clustering coefficient scores, the clustering comprises the entire networks as opposed to distinct cliques that are otherwise weakly integrated with the larger network. Therefore, these networks continue to exhibit a unique pattern separate from the kinds of graphs models that are oft used in explaining modern social interaction patterns (Albert and Barabási 2002; Barabási and Albert 1999; Wasserman and Faust 1994; Watts and Strogatz 1998).

In concatenating the post-migration jar and plate attribute networks into a single multilayer network it is apparent that the more influential network based on edge weights, in this

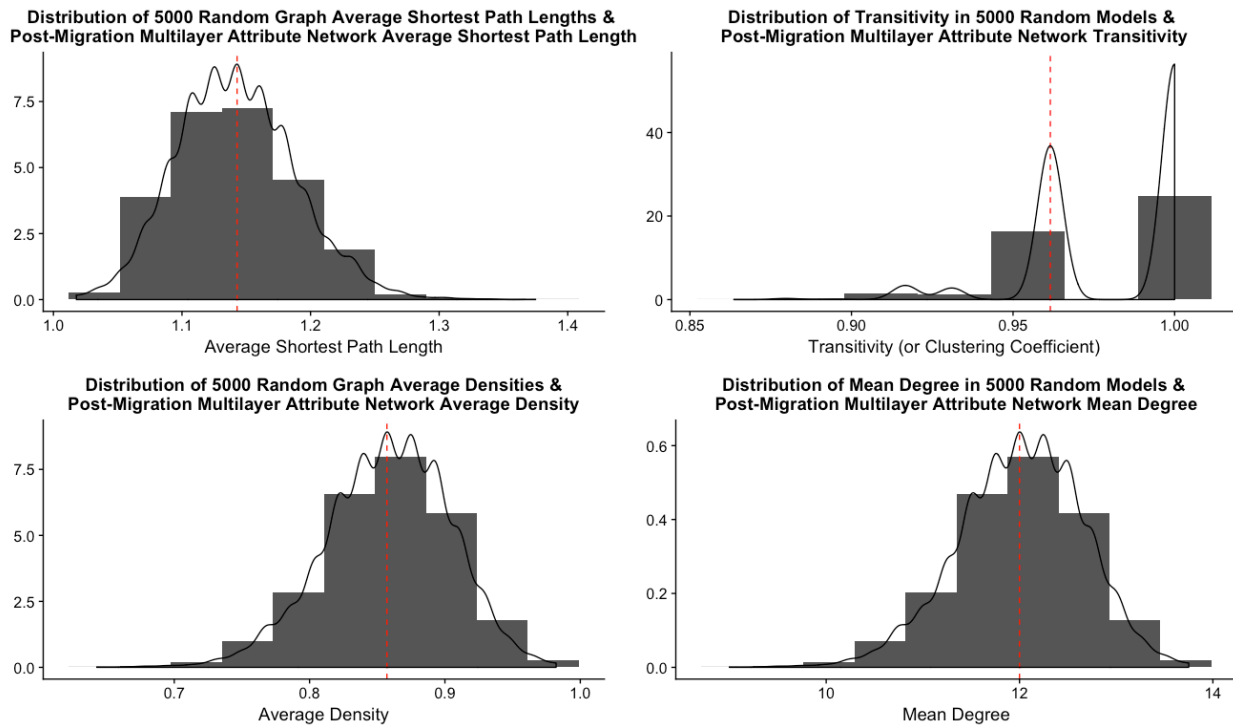


Figure 5.23 Network Randomization Results for Multilayer Post-Migration Network. Observed statistic represents red line. Histogram shows distribution of statistic based on network randomization of 5000 random graphs using the Erdős–Rényi random network modeling technique.

case the plate network, takes precedence in summary network statistics. That is, the diameter, average shortest path length, degree, centralization scores, and average clustering coefficient

score more closely follows that of the plate attribute network layer than the jar attribute network layer in the post-migration period. However, network randomizations of the post-migration multilayer attribute network show that none of the four network summary statistics are unusually high or low compared to 5,000 random graphs of the same order and size (or probability of edge creation) using the Erdős–Rényi random network modeling technique. Significantly, the increased average shortest path length in the aggregated multilayer attribute network does indicate that interaction through cultural transmission decreased in frequency or scale following the in-migration of Oneota peoples into the Late Prehistoric CIRV, suggesting perhaps heightened inter-regional tensions or an increase in regional hostility that may have cross-cut cultural lines. Hub and authority analysis of the post-migration multilayer attribute network indicates that nearly every site operates as a strong hub based on connections to authority nodes. The sole exception is the C.W. Cooper Oneota habitation site, which is connected reciprocally only to other sites with an Oneota presence. As in the hub and authority analysis of individual attribute network layers for the post-migration period, none of the three sites with an Oneota presence are modeled as operating as authorities. This perhaps indicates an unwillingness on the part of the local Mississippian population to engage with these sites as frequently as with each other or wherein interaction through cultural transmission was otherwise limited to specific spheres of daily life. On the other hand, since no distinct communities are able to be modeled via edge betweenness in the multilayer post-migration attribute network (Figure 5.25) both positive and negative inter-cultural interactions between Mississippian and Oneota peoples are likely to have occurred in some context beyond the sites with unequivocal evidence for household scale inter-cultural interaction – Morton Village and Crable (Bengtson and O'Gorman 2017; Conrad and Esarey 1983; Esarey and Conrad 1998; O'Gorman and Conner 2016; Painter 2014; K. Sampson

2000; Santure, et al. 1990; H. G. Smith 1951).

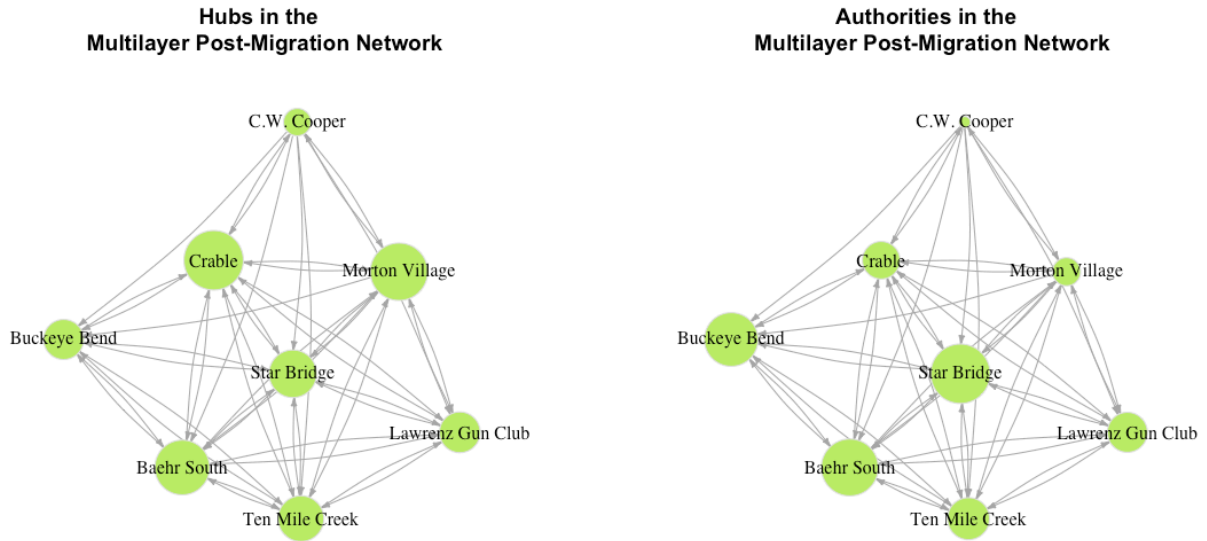


Figure 5.5.24 Hubs and Authorities in the Post-Migration Multilayer Attribute Network. Hub and Authority score modeled as node size

Turning to formal multilayer network analysis measures for the post-migration period, all sites share identical degree deviation scores (or deviation across the network layers) aside from the C.W. Cooper site, which lacks any plates, and therefore has a very high degree deviation score. This indicates remarkable consistency across the layers in the presence of edges (Dickison, et al. 2016). However, this measure lacks the nuance of weight and directionality and simply indicates that each site has roughly the same number of neighbors on each layer aside from C.W. Cooper in the post-migration period when weight and directionality of edges are ignored.

With an average connectivity redundancy of 0.402, the post-migration multilayer attribute network is characterized by a slightly higher degree of multiplexity than the pre-migration period. Connective redundancy provides a more nuanced look at the co-presence of edges among the same node across different network layers. This higher score indicates slightly increased consistency in connections among nodes across different layers in the post-migration

period compared to the pre-migration period. A likely driving force behind the higher connective redundancy score is the high density (or total number of edges observed out of the total possible number of edges) for each of the post-migration attribute network layers.

Despite the many structural difference discussed above, the jar and plate post-migration attribute network layers do share much in common with each other. A simple matching coefficient across the multiple layers shows that the two networks share over 95% of edge-node connections in common when directionality and weight are not factored into the comparison for the post-migration period. A more nuanced comparison using the Jaccard measure of similarity, which is computed as the amount of common edges between the layers divided by the union of all edges for pairs of layers, indicates that the jar and plate attribute networks in the post-migration period are 74% similar. Again, this metric is only able to consider deprecated edges by disregarding weight and directionality. That these two measures of layer comparison are so high

Edge Betweenness Community Detection in the Post-Migration Period Multilayer Jar and Plate Attribute Network

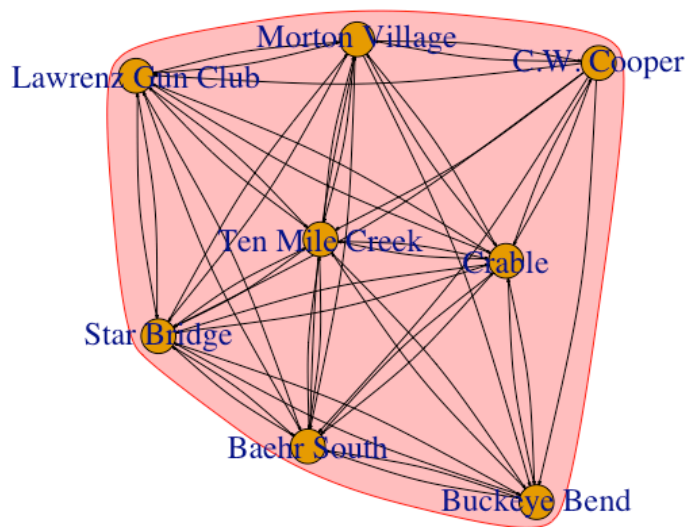


Figure 5.5.25 Edge Betweenness Community Detection in the Multilayer Post-Migration Attribute Network

is an indication that there is overall more consistency in connections among sites in the post-migration period CIRV compared to the pre-migration period. Fewer sites and overall more dense networks likely contribute to this trend in the post-migration period.

To summarize, important structural changes occur in networks of interaction through cultural transmission across the Middle to Late Mississippian transition in the Late Prehistoric CIRV. In particular, the post-migration plates attribute network exhibits a pattern of creating regional scale relational connections whereas jar attribute network in the post-migration period saw the infusion of significant variation from the Oneota in-migration and altered to only form strong connections at a reduced or nuanced scale relative to the pre-migration period. In general, post-migration period interaction networks are characterized by attempts at inter-cultural mediation in the public sphere but with retention of cultural differences in the private, or domestic, sphere of life. Oneota immigrants into the CIRV actively chose to incorporate a new vessel class into their ceramic inventory, and likely accompanying foodway patterns, but retained distinct stylistic and technological features in cooking jars. The tensions inherent in a public de-emphasis but private retention of inter-cultural differences no doubt contributed in some way to the pattern of increasing violence and aggression in the post-migration period (G. R. Milner, et al. 1991; Stone 2003). Though such patterns of violence were certainly nothing new to Oneota peoples (Hollinger 2005; Oemig 2016). Sites with an Oneota presence in particular appear to be weakly integrated into post-migration interaction networks. However, since two of these sites are marked by a significant presence of Mississippian peoples and one shows no evidence of inter-cultural interaction at the site level, divergence among both indigenous and migrant peoples characterizes interactions patterns in the post-migration period Late Prehistoric CIRV. Yet,

interact these peoples did, as shown in the very dense networks of interaction through cultural transmission for the post-migration period.

The post-migration period CIRV can overall be described as distributed, or lacking a central actor or actor-cliques, and cohesive but with evidence for structurally distinct communities in at least one interpretive layer – jar attribute networks of interaction through cultural transmission. Post-migration attribute networks continue to lack support for an hypothesized cultural distinction between Mississippian peoples into Spoon and La Moine River variants. Distinct community structures along geographic lines among Mississippian sites in these areas are not able to be modeled. Delimited mobility along cultural lines, however, is supported in at least one network layer – the post-migration jar attribute network – in addition to the geographic layout of immigrant Oneota or multi-cultural sites in a restricted portion of the region. Nevertheless, an active and concerted attempt at inter-cultural mediation or accommodation was made by Mississippian and Oneota peoples in the transference of plate technological characteristics and likely accompanying foodway patterns. These interpretations are further expanded upon in Section 6.6.2 when considering analysis of sociograms for the post-migration period. However, because geographic distance can play a foundational role in interaction patterns, the following section discusses the impact of geographic distance on networks of interaction through cultural transmission in the Late Prehistoric CIRV.

	Plate Attributes			Jar Attributes			Multilayer - Jar and Plate		
	Pre-Migration	Post-Migration	Flattened Across Time	Pre-Migration	Post-Migration	Flattened Across Time	Pre-Migration	Post-Migration	Flattened Across Time
<u>Summary Statistics</u>									
Nodes	11	7	16	12	8	18	12	8	18
Edges	63	40	101	81	42	121	95	50	143
Mean Weighted Degree	3.994	4.406	4.578	5.117	3.962	6.722	7.917	7.817	9.17
<u>Network Size Measures</u>									
Diameter	3	2	4	2	4	4	2	2	3
Mean Path Length	1.527	1.048	1.708	1.182	1.375	1.733	1.215	1.107	1.564
<u>Network Topology Measures</u>									
Network Density	57.3%	95.20%	42.10%	61.4%	75.00%	39.50%	72.0%	89.30%	46.70%
Mean Clustering Coefficient	62.6%	95.20%	70.80%	69.0%	75.00%	68.40%	76.8%	89.30%	77.60%
Degree Centralization	0.250	0.111	0.476	0.223	0.163	0.359	0.207	0.163	0.408
Betweenness Centralization	0.133	0.104	0.179	0.086	0.303	0.058	0.299	0.146	0.199
Closeness Centralization	0.063	0.013	0.259	0.026	0.266	0.171	0.034	0.073	0.216
Eigenvector Centralization	0.320	0.105	0.507	0.266	0.192	0.464	0.217	0.151	0.446

Table 5.12 Network Statistics for Ceramic Industry Social Interaction Network Models

5.5.3 *The Role of Geographic Distance*

A potentially confounding variable to the formation of strong ties of social interaction through cultural transmission between settlements is that of the physical distance between them. In evaluating the role of distance in the strength of relational connections, linear regression models are fit to network model data to investigate whether closer physical proximity is associated with a higher degree of relational interaction among sites. That is, do sites that are closer together share stronger relational connections than sites that are far apart on average, and as such is geographic distance a primary factor in delimiting patterns of social interaction?

Figure 5.26 displays a scatter plot and linear models of the strength of relational connections in multilayer jar and plate attribute networks flattened across time as a function of distance in kilometers. Across each network, 100 random samples of 50 each are drawn from the population to inform heuristic understanding of the sampling distribution on the slope coefficient. A moderately negative linear relationship between the degree of relational interaction among sites and geographic distance characterizes these multilayer interaction networks. However, there is a high degree of residual variation and heteroscedasticity in the strength of relational connections variable. That is, a subtle distance-decay effect is seen in interaction networks where the strength of relational connections somewhat decreases on average across the entire temporal expanse of the Late Prehistoric CIRV. This is a natural, though not statistically significant, finding considering that sites within a day's walk or canoe ride from each other are much more likely to sustain strong relational interaction patterns through cultural transmission. However, following Simpson's Paradox (Simpson 1951), this trend is significantly more nuanced and even reversed when models are fit to individual network layers as opposed to the entire regional sequence in the Late Prehistoric CIRV.

Distribution of Linear Regression Lines of 100 random samples from the Multilayer Jar and Plate Attribute Networks Flattened Across Time

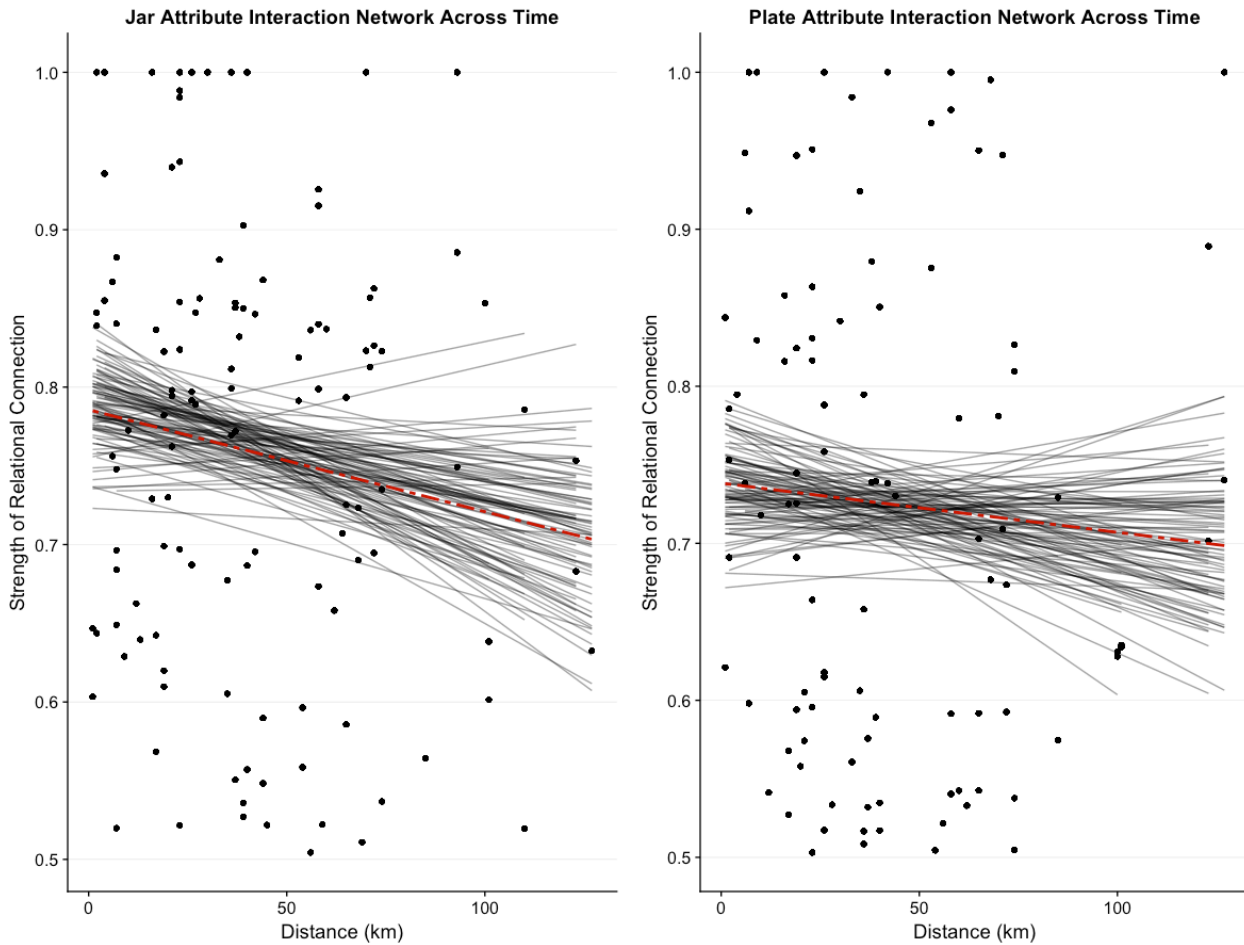


Figure 5.5.26 Distributions of Randomly Sampled Linear Models for Strength of Relational Connection as a Function of Geographic Distance in Multilayer jar and plate attribute networks. Dashed red line indicates linear model for observed data

As shown in Figure 5.27, structural differences exist in artifact attribute networks when the strength of relational connection among sites is modeled as a function of geographic distance across the individual vessel-class layers. During the pre-migration period Eveland, Orendorf and Larson Phases, the previously discussed trend of jar artifact attribute networks operating at a regionally inclusive scale is bolstered based on the failure to reject the null hypothesis that distance shows no linear relationship to the strength of relational connection. On the other hand, the plate attribute interaction network for the pre-migration period shows a strong negative

Distribution of Linear Regression Lines of 100 random samples from the Jar and Plate Attribute Networks

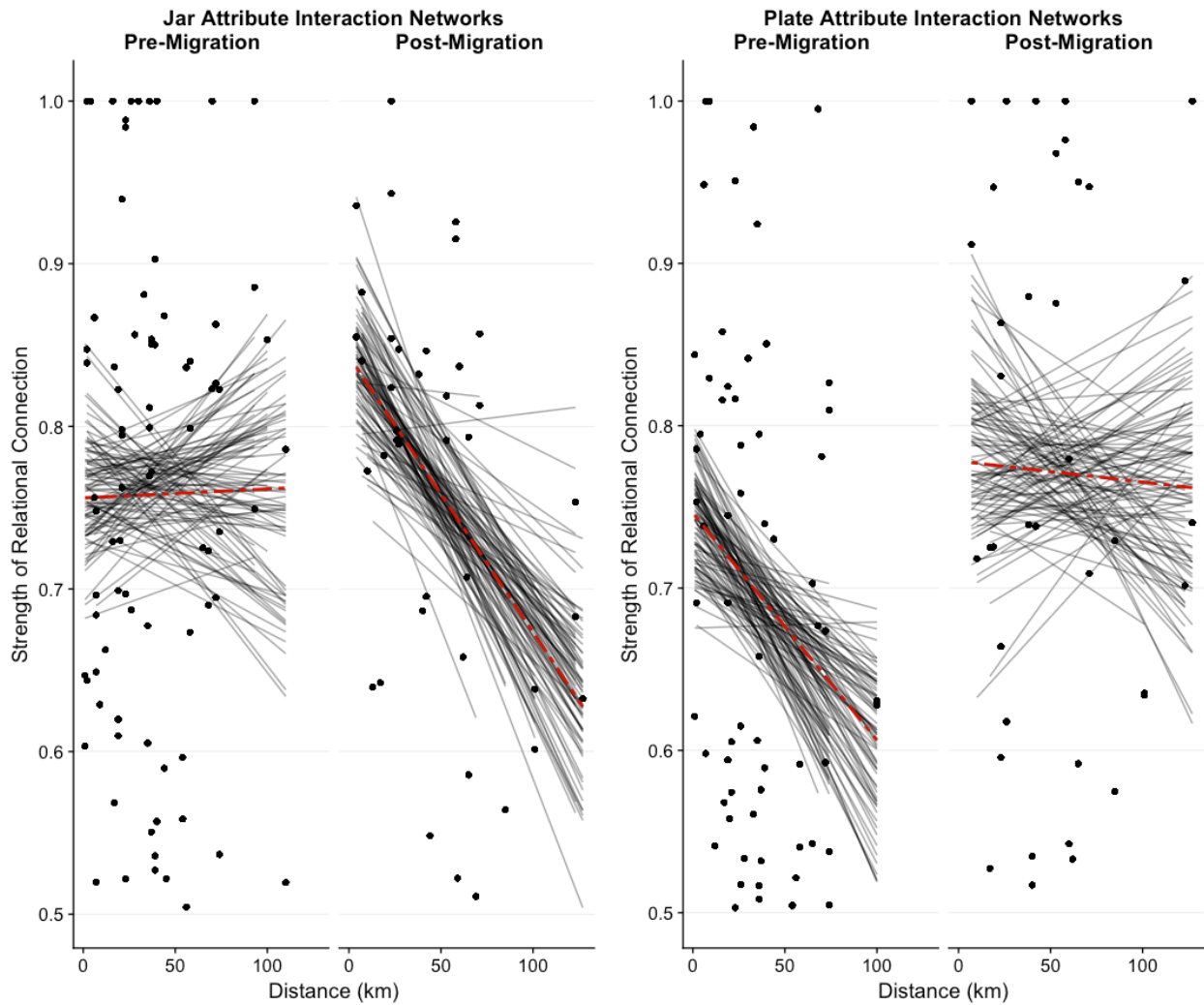


Figure 5.27 Distributions of Randomly Sampled Linear Models for Strength of Relational Connection as a Function of Geographic Distance in Jar and Plate Attribute Interaction Networks faceted by time phase designation. Dashed red line indicates linear model for observed data

linear relationship between strength of relational connection and geographic distance. The role of geographic distance on the strength of relational connection for plate attribute pre-migration interaction networks is statistically significant at an alpha of 0.06 ($p\text{-value} = 0.05796$) and shows a Pearson's correlation coefficient of $r = -0.24$. As a result, in the pre-migration context, information regarding plates was less apt to be shared at a regional scale among Mississippian peoples. In other words, strong relational connections were formed among more localized

communities of practice on average when considering the transmission of information related to plate attributes in the pre-migration CIRV. At the same time, geographic distance plays no discernible role in the strength of relational connections based on linear models from jar attributes in the pre-migration period.

This trend reverses in the post-migration period, where the infusion of technological variation from Oneota immigrant-potters likely impacted the scale at which information spread among communities regarding jar attributes. As shown in Figure 5.27, a strong negative linear relationship exists between the degree of relational connection and geographic distance in the post-migration jar attribute interaction network. This trend is significant at an alpha of 0.01 (p-value = 0.0032) and shows a Pearson's correlation coefficient of $r = -0.45$. Geographic distance, therefore, plays a significant role in structuring relational connections in the post-migration jar attribute interaction network. At the same time, the null hypothesis cannot be rejected for the plate post-migration attribute network. In other words, no discernible linear relationship exists between the strength of relational connections among sites and the geographic distance between them as modeled in the plate attribute interaction network for the post-migration period. This further lends support for the presence of a public-private distinction in structuring interaction patterns in the post-migration CIRV.

Linear models show that geographic distance influences artifact attribute interaction networks in nuanced ways in the Late Prehistoric CIRV. During Mississippian phases, jar attributes break with expectations and show no influence from geographic distance on the strength of relational connections among sites. This finding indicates a willingness on the part of Mississippian potters to share information regarding the production of domestic jars at a regional scale. However, the plate attribute network indicates that networks of interaction among

Mississippian peoples prior to Oneota in-migration in the CIRV were not entirely fluid. Geographic distance was shown to negatively impact the strength of relational connections among Mississippian peoples, suggesting that information regarding plate production was transmitted in nuanced ways across the geographic expanse of the Mississippian CIRV.

Following the in-migration of Bold Counselor Phase Oneota peoples, this trend shifted – Oneota jar technology was maintained to a large degree and as a result impacted the scale at which information was shared regarding domestic jar technology. Jar technology became increasingly the product of the local social environment and precipitously drops in similarity across geographic distance. However, plate technology was shared broadly across the post-migration CIRV as geographic distance has been shown to play no role in the cultural transmission of information related to plate production through networks of interaction.

During both the pre- and post-migration contexts in the CIRV, one vessel class operated at a regional level while the other has been shown to be the product of interaction at a more nuanced scale. This interpretation portends the complexity networks of interaction during the Late Prehistoric Period in the central Illinois River valley – different forces in society likely operated to promote high levels of interaction and others likely operated to curtail such interactions to a more localized scale.

5.6 Discussion and Visual Interpretation of Ceramic Industry Social Interaction Network Models

Given that the primary interest here is the flow of information between communities of practice that may not follow the most efficient delivery process, as a proxy measure of the degree of social interaction or homologous relationships between sites, two node level statistics are emphasized in visualizing networks as sociogram: weighted degree and closeness centrality.

Weighted degree is equal to the sum of all edge weights connected to a given node and is indicative of the relative similarity of a particular node's ceramic vessel technological characteristics when considering every other node. A high weighted degree indicates that the ceramic assemblage from a given node is more similar to other nodes' assemblages based on the attributes considered, and therefore suggests that perhaps the node was more influential in being a locus of ceramic manufacturing technology or has more shared ancestry (homology) with other nodes. A low weighted degree does not necessarily indicate that a particular node is less important, populous, or influential, but rather it indicates that a particular node's ceramic assemblage is less similar to other nodes based on the vessel attributes under consideration.

Closeness centrality considers how near all other individual nodes are in a network to a given site-node in question. Closeness centrality is defined as the normalized average distance (or number of steps between each node based on existing links) between the node and every other node in the network and is therefore more pertinent to graphs constructed from one particular ceramic vessel class and time period. A high closeness centrality score indicates that a particular site may be more directly accessible to other potter communities or may be a locus from which innovation (information) appears and spreads, while a low closeness centrality score indicates that the site is either isolated, inaccessible, or embedded in a cluster that is separate, from the rest of the network in terms of ceramic technology. These metrics, as well as others presented in this section, are more fully described and defined in Chapter 4.

A final note about how the networks are presented below is that of network topology. Network topology is the arrangement and interrelationships of the constituent parts (i.e. nodes, edges) of a computer network and is used here in a metaphorical sense (Scott 2000; Wasserman and Faust 1994). Network topology can be thought of in two ways: the physical topology of the

network and the logical topology of the network. Physical topology refers to the actual layout of the physical nodes, for example computer servers and the cables that connect them. While logical topology refers to the ways that the computer signals act in the network, or the way that data passes through the cables from one node-device to another. Graphs presented here attempt to account for this metaphorical duality by utilizing different layout methodologies. A geographic layout methodology is used to capture the metaphorical physical topology of the ceramic technology networks, while the Yifan Hu multilevel network graph layout is used to capture the metaphorical logical topology of the network (Hu 2005). As a force-directed algorithm, the Yifan Hu multilevel graph layout places the node-bodies in the graph by minimizing the energy of the system but uses a multilevel approach to allow spring and repulsion energy flows to be applied to local as well as community levels to find a global optimal layout combined with an otree technique to approximate short- and long-range forces.

Network graphs have been developed to be as interpretable as possible, even to individuals without network analysis experience. This is accomplished by visualizing network structure in conjunction with the numerical properties that describe the network. This allows information about nodes, edges, and the structure of the network to be embedded within visualizations simultaneously. All graphs, or sociograms, presented below are both weighted and directed. Directionality is expressed in a clockwise fashion. That is, an edge emanating from a node in a clockwise direction indicates that node's relationship directed toward another node. An edge emanating into a node that is counter-clockwise indicates another node's relationships with the node in question. Weight of an edge is visualized in two specific ways. The first is color. A warm color palette is used to enable strong relationships (warmer in color) to be distinguished from weaker relationships (less warm in color), as modelled by the numerical weight of an edge

between two nodes. That is, the warmer or redder an edge is, the stronger the modelled relationship. The second is size. A warm color palette is combined with size to show either the strength of the node's weighted degree or the strength of a node's closeness centrality score. These metrics are used to show either the degree of similarity of one node to all other nodes (weighted degree) or to show the relative influence of one node relative to other nodes in their ability to form relationships with all other neighbor-nodes in the network in question (closeness centrality).

Following multilayer network methodology, individual network layers are presented and discussed prior to the joint analysis of multiple layers. The value of this approach is to discern the topology, or structural nature, of individual network layers initially before aggregating layers together. For the purposes of the case study presented here, it allows the role of domestic jars and plates to be visualized and interpreted for each time period separately, which then provides a more nuanced engagement with the multidimensional chains of social relationships in the multilayer networks that follow.

5.6.1 Pre-Migration Technological Similarity Networks, 1200 – 1300 A.D.

While the occupational sequence of the Mississippian central Illinois River valley began sometime in the early 11th or 12th century A.D., the analyses presented here consider only the Mississippian occupation from A.D. 1200 – 1300 A.D. (Bardolph 2014; Conrad 1991). The first four sociograms presented are models of technological similarity for each vessel class separately before they are presented as flattened and sliced models for the Mississippian CIRV prior to Oneota in-migration.

A number of interpretations are immediately apparent, while others less so, when visually examining the domestic jar and plate technological attribute network graph models for the pre-migration period. Both network layers conform to a structural interpretation of a distributed and highly interconnected Mississippian central Illinois River valley (CIRV). Both networks lack a central hub or hubs. In other words, in neither the jar nor plate pre-migration networks are all sites connected to a singular, central site or site cluster. Furthermore, distinct coalitions, or

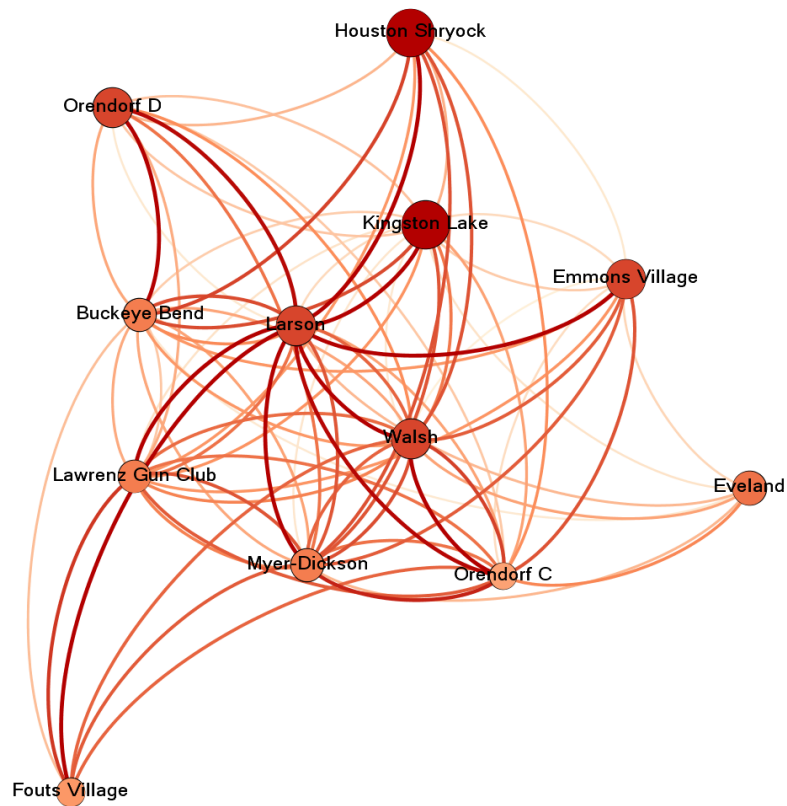


Figure 5.28 Yifan Hu multilevel network graph layout of domestic jar technological similarity network for the Pre-Migration Time Period (1200-1300 A.D.); edges are colored by weight; nodes are colored and sized by closeness centrality

clusters of sites more connected to each other than sites exogenous to the cluster, are not apparent. This suggests a distributed structure of information flow within the networks as opposed to a hierarchical, coalitional, or broker-bridging model of information flow (Scott 2000). However, both the domestic jar and plate networks appear to support a significant

presence located at the mouth of the Spoon River consistent with Harn's Larson Settlement System (Harn 1978, 1994), or densely occupied central position within the geographic renderings. The central Larson town figures prominently in the jar network with many sites showing strong interactions based on the transmission of socially-mediated jar attributes with Larson (Figures 5.28 – 5.29). A presumed primary village within the Larson Settlement System, Buckeye Bend, figures prominently in the plate network (Figures 5.30 – 5.31). That a modestly sized site such as Buckeye Bend could figure so prominently in the plate attribute network is

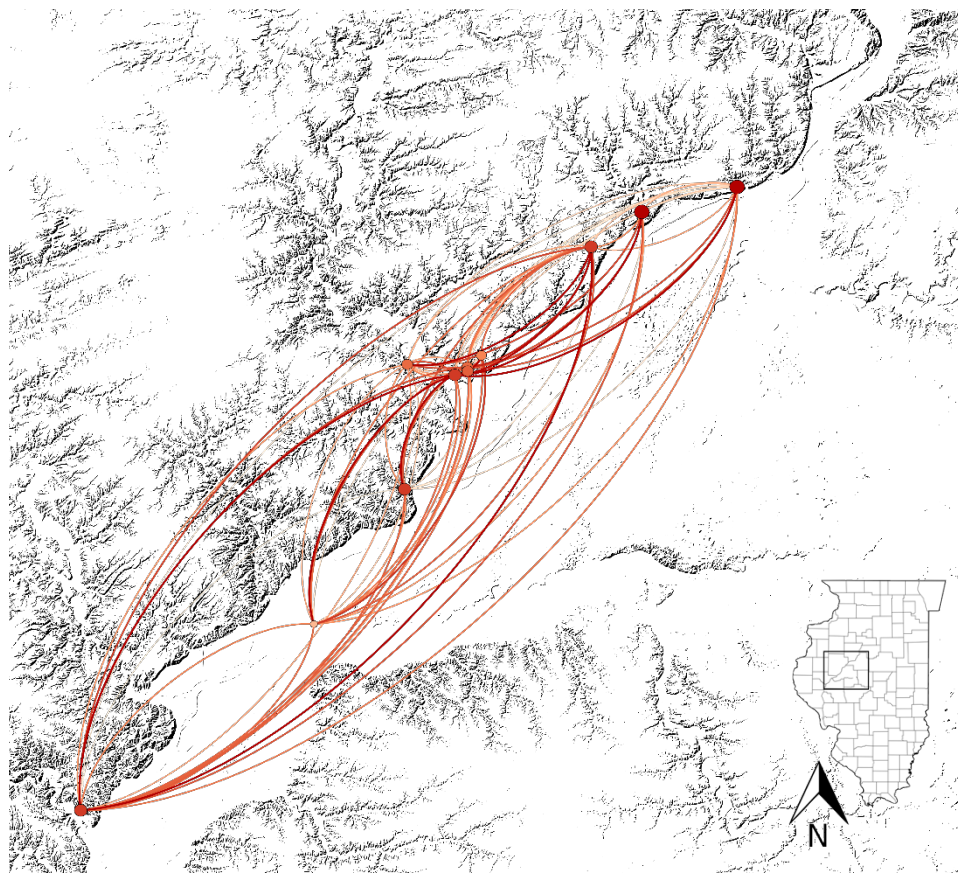


Figure 5.29 Geographic network graph layout of domestic jar technological similarity network for the Pre-Migration Time Period (1200-1300 A.D.); edges are colored by weight; nodes are colored and sized by closeness centrality

surprising, and perhaps suggests that novelty in several key attributes (e.g. plate diameter and incising thickness) may have emerged at, and spread from, Buckeye Bend. Alternatively, the

prominent role Buckeye Bend plays in the pre-migration network may be owed to its long or intermittent occupation span that straddles both the pre- and post-migration time periods (see Chapter 3).

The more numerous edges and stronger (i.e. warmer) edge weights on average in the domestic jar layer in comparison to the plate layer do indicate topological difference between the layers. Interestingly, while no site in the plate pre-migration layer is without at least one reciprocal relationship, three sites in the domestic jar layer only direct relationships outwards.

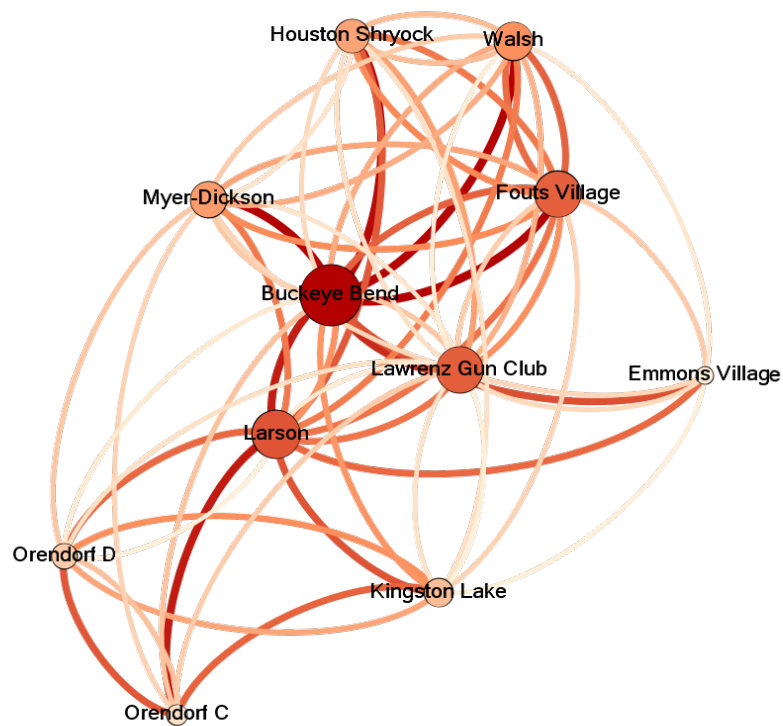


Figure 5.30 Yifan Hu multilevel network graph layout of plate technological similarity network for the Pre-Migration Time Period (1200-1300 A.D.); edges are colored by weight; nodes are colored and sized by weighted degree

That is, Fouts Village, Houston-Shryock, and Eveland only direct relationships to other sites as opposed to having any relationships reciprocally directed toward them in the pre-migration domestic jar layer. This does not mean that these sites were isolated but does suggest that in terms of interactions with other sites through the cultural transmission of socially-

mediated jar attributes, these sites were perhaps more imitative or had more homologous descendants from other sites as opposed to being a locus of imitation or producers of exogenous offspring.

As seen in the network models laid out based on energy flows in the system, a distinct lack of site clustering is apparent in either the jar or plate pre-migration technological similarity networks. That is, neither network in the pre-migration period shows strong support for the presence of a clique or cliques. In order to form a clique, a group of sites would need to be more connected to each other than the rest of the nodes in the network. This lack of settlement

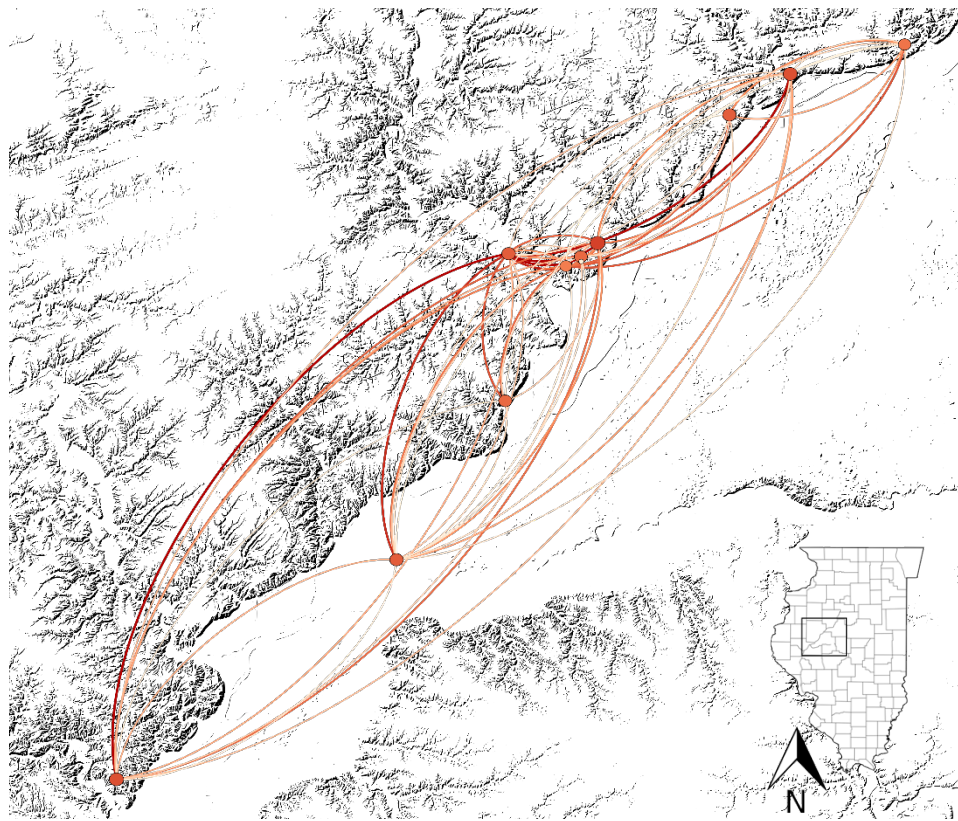


Figure 5.31 Geographic network graph layout of plate technological similarity network for the Pre-Migration Time Period (1200-1300 A.D.); edges are colored by weight; nodes are colored and sized by closeness centrality

clustering in both jar and plate attribute networks contrasts with expectations related to the widespread appearance of evidence for inter-personal violence and conflict during the

Mississippian period. These expectations include intensive population aggregation, migration events, boundary formation, and alliance-based site clusters such as those observed in the pre-Hispanic American Southwest (Fowles, et al. 2007; LeBlanc 2000). That is, despite increasing evidence for violence that has led to comparisons with warfare (G. R. Milner, et al. 1991; Steadman 2008; Vanderwarker and Wilson 2016; G. D. Wilson 2012), Mississippian potters appear to have been interacting, intermarrying, or otherwise engaging with individuals and their wares at

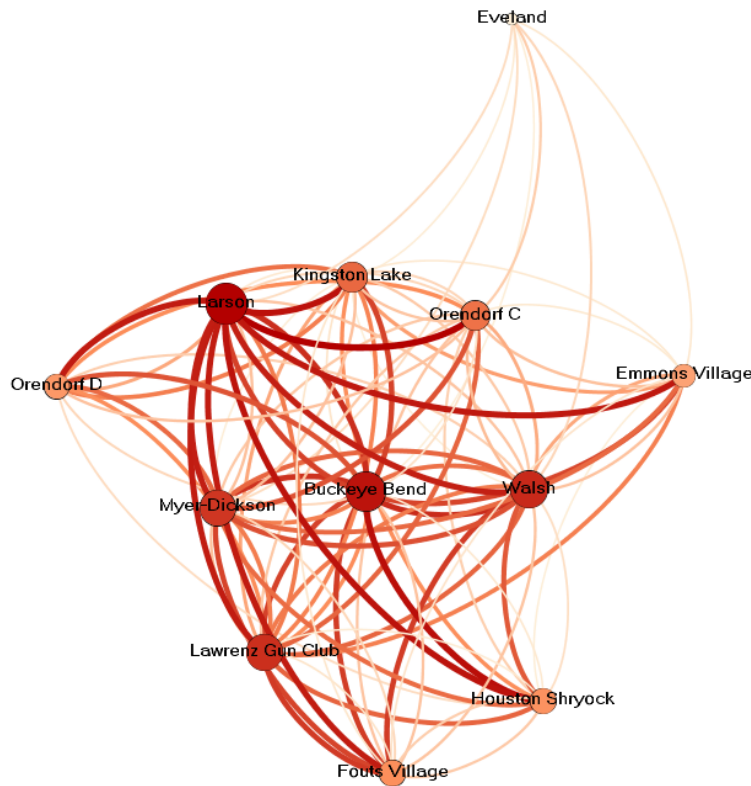


Figure 5.32 Yifan Hu multilevel network graph layout of domestic jar and plate technological similarity flattened multilayer network for the Pre-Migration Time Period (1200-1300 A.D.); edges are colored by weight; nodes are colored and sized by weighted degree

settlements across the geographic expanse of the CIRV frequently enough to transmit social information in the production of ceramic vessels. Perhaps this is an indication that conflicts were

seasonal or episodic as opposed to chronic in impacting mobility and interaction patterns. This interpretation is consistent with findings from a recent analysis of skeletal evidence at many pre-migration Mississippian sites that indicated conflict and violence “was not ubiquitous” (Hatch 2015:208).

High density of connections and low clustering seen in both jar and plate attribute networks also suggests that an hypothesized distinction between Mississippian sites in the vicinity of the Spoon River from those near the La Moine River is not supported by ceramic

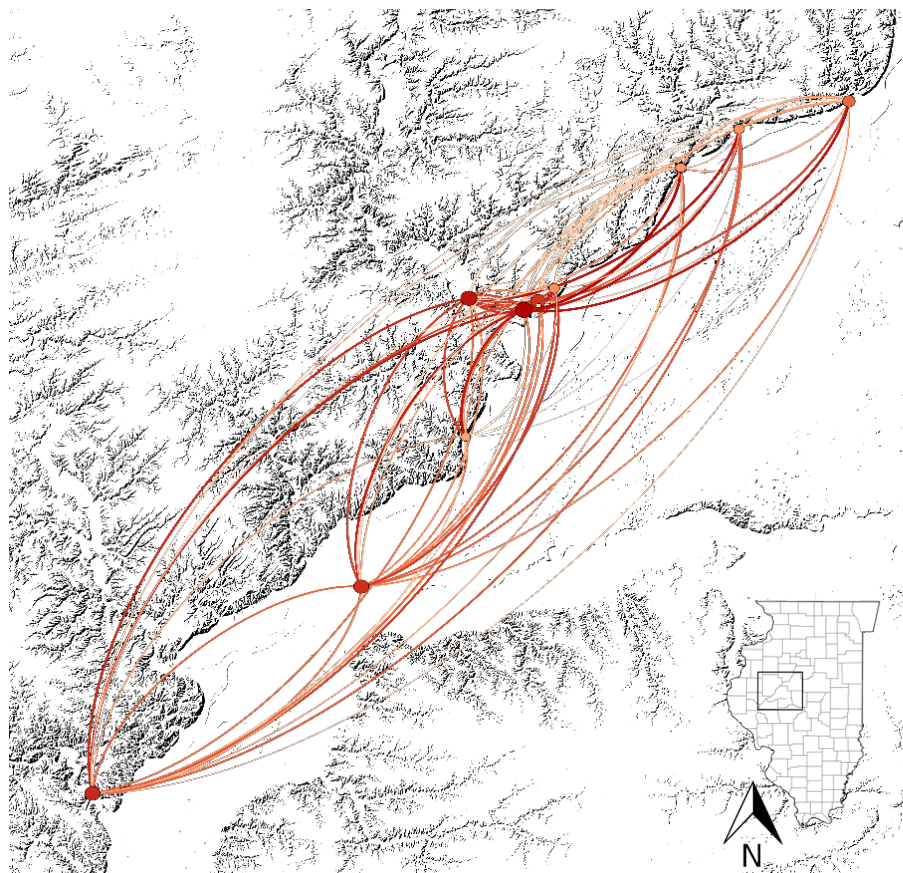


Figure 5.33 Geographic network graph layout of domestic jar and plate technological similarity flattened multilayer network for the Pre-Migration Time Period (1200-1300 A.D.); edges are colored by weight; nodes are colored and sized by weighted degree

attribute data in the Mississippian CIRV (Conrad 1991). That is, there is a marked lack of a strongly connected settlement cluster geographically positioned near the La Moine River that is

weakly integrated with settlements further to the north near the Spoon River. Though only a few southerly sites (Walsh, Lawrenz Gun Club) were able to be considered in this analysis for the pre-migration period as less professional archaeological excavation has occurred near the La Moine River in comparison to the Spoon River vicinity.

Trends indicating a lack of support for reduced mobility and a lack of support for a Spoon-La Moine River Mississippian distinction based on jar and plate technological attributes is further substantiated in the flattened pre-migration network where both jar and plate network layers are combined into a single network for the pre-migration time period (Figures 5.32 - 5.33). That is, the multilayer network continues to exhibit a distributed and highly cohesive network topology similar to both individual network layers. In other words, shared contexts of learning, homologous interrelationships, and strong relationships based on frequent social interaction generally characterizes potter communities at settlements in the pre-migration CIRV as seen in socially mediated jar and plate ceramic attributes.

With its central positioning both geographically at the Spoon-Illinois River confluence area and temporally in the pre-migration period, the Larson site does exhibit a higher degree of proportional similarity in socially mediated jar and plate attributes to other sites in the flattened multilayer network. Figure 5.33 shows many strong links from four sites to the north to Larson that are weakly reciprocated. These include Orendorf Settlements C and D, Houston-Shryock, and Kingston Lake. Perhaps information regarding ceramic attribute production or individuals flowed from these northerly sites to Larson.

The Eveland site, on the other hand, is a significant outlier in that it is weakly integrated into the flattened multilayer pre-migration technology network. This is owed to three factors. The first is its occupational sequence very early in the pre-migration period (Bardolph 2014;

Conrad 1989, 1991; Harn 1991). Though more recent chronological calibrations suggest an early 13th century A.D. occupation at the site (G. D. Wilson, et al. 2018). The second is the likely ceremonial, as opposed to domestic, nature at Eveland given the unique architectural patterns present at the site including a cross-shaped structure and extensive burial furniture including Mississippian prestige items accompanying Eveland Phase burials interred at Dickson Mounds (Conrad 1989; Harn 1991). Finally, and most importantly, plates emerge as a distinct vessel class in the CIRV only after the occupation of the Eveland site. Without any connections in the pre-migration plate attribute network layer, relationships to and from the Eveland site can only be considered based on the presence of domestic jars. This is nevertheless instructive in that the connections from Eveland hint at which other sites may have been occupied during this early

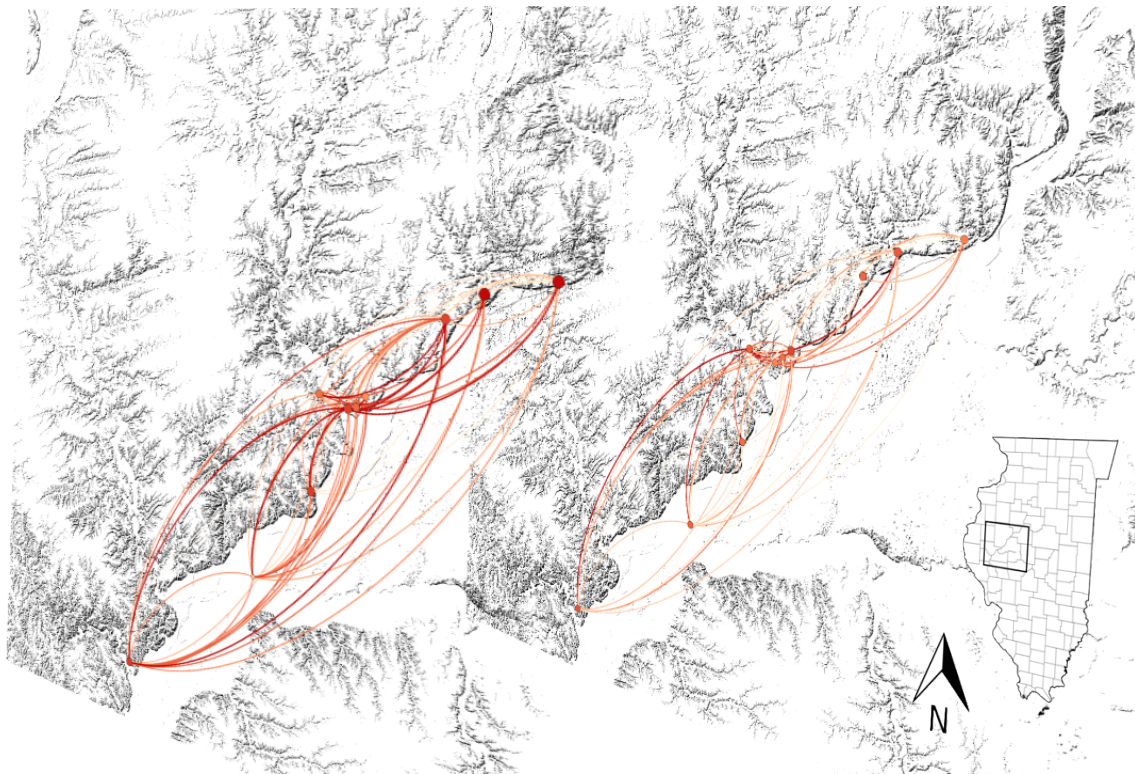


Figure 5.34 Geographic network graph layout of domestic jar (left) and plate (right) technological similarity sliced multilayer network for the Pre-Migration Time Period (1200-1300 A.D.); edges are colored by weight; nodes are colored and sized by closeness centrality

1200s A.D. timeframe.

In sum, the overall topological structure of interaction patterns in the central Illinois River valley as gleaned from the cultural transmission of ceramic attributes prior to Oneota immigration can be characterized as highly interconnected and distributed. The analysis of distinct network layers in the pre-migration period suggests some important differences between the cultural transmission of information related to socially mediated jar attributes compared to plate attributes. In particular, information related to jar attributes is shared, or appealed to, globally much more so than information related to plate attributes. In terms of social signaling (Birch and Hart 2018; Bliege Bird and Smith 2005), it can be inferred that potters likely formed bonding ties to reinforce dense social relationships based on global Mississippian interaction patterns across the geographic expanse of the Eveland, Orendorf, and Larson phases of the Late Prehistoric central Illinois River valley through interactions regarding domestic jar attribute technology (Conrad 1991; Esarey and Conrad 1998). On the other hand, plate attributes seem to reflect adaptation to more localized social environments, which suggests nuanced interaction and foodway patterns.

There is a marked lack of meaningful clustering in both the jar and plate network layers as well as in the flattened multilayer attribute network. As a result, ceramic attribute networks do not support curtailed or reduced interaction patterns posited based on a reduction in intra-regional mobility due to increasing conflict and violence (Vanderwarker and Wilson 2016), nor do the attribute networks support an hypothesized taxonomic distinction between Spoon and La Moine River Mississippians in the pre-migration period (Conrad 1989, 1991). It is worth noting, however, that not all sites modeled in this pre-migration period were occupied simultaneously and thus these interpretations are both a product of spatial and temporal processes at relatively

unrefined scales and based entirely on interaction patterns gleaned from a subset of ceramic industry in the Late Prehistoric CIRV. Increased resolution in occupational sequences at sites in the Mississippian CIRV would greatly enhance the interpretability of these models of interaction through cultural transmission of ceramic technological attributes.

5.6.2 Post-Migration Technological Similarity Networks, 1300 – 1450 A.D.

In visually examining ceramic artifact attribute networks models for the post-migration period, it is apparent that significant changes in the structure of interaction through cultural transmission occurred just prior to, following, or concomitant with Oneota in-migration. In

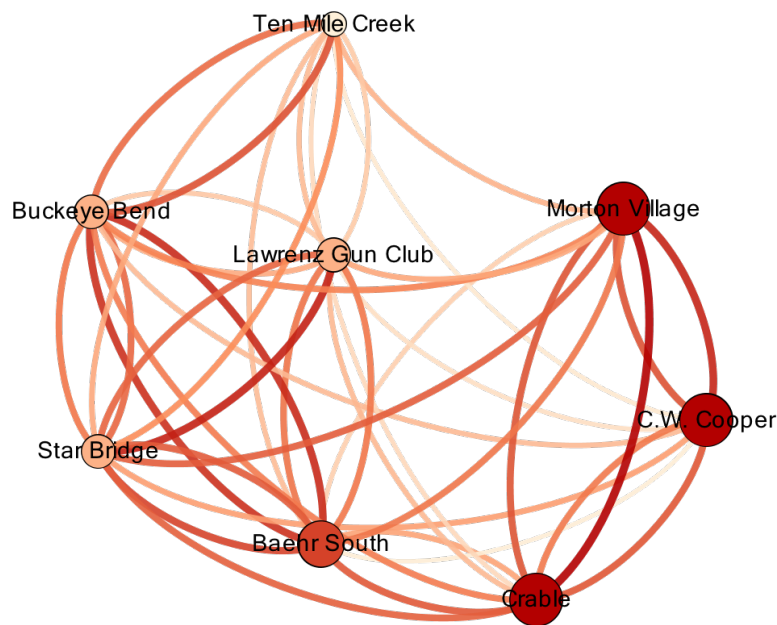


Figure 5.35 Yifan Hu multilevel network graph layout of domestic jar technological similarity network for the Post-Migration Time Period (1300-1450 A.D.); edges are colored by weight; nodes are colored and sized by closeness centrality

particular, a significant reduction in the scale of interaction based on the sharing of information related to socially-mediated jar attributes and a significant expansion of interaction based on the sharing of information related to plate attributes characterizes the post-migration period CIRV.

This is in stark contrast to the pre-migration period where information related to socially mediated jar attributes was likely shared at a regional Mississippian scale and plate attribute information transmission more conformed to local scale social interaction processes. Prior to the in-migration of Oneota peoples, however, a marked aggregation process is evident among indigenous Mississippian peoples. Many fewer Mississippian sites were occupied during, and following, the circa 1300 A.D. Oneota in-migration. It can therefore be posited based on

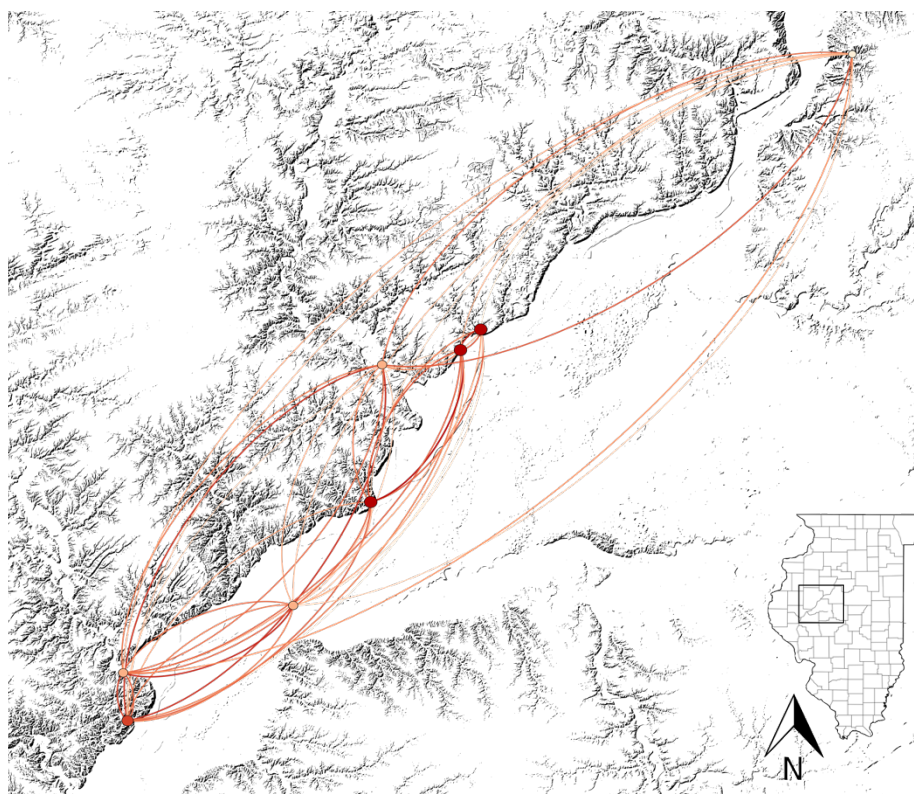


Figure 5.36 Geographic network graph layout of domestic jar technological similarity network for the Post-Migration Time Period (1300-1450 A.D.); edges are colored by weight; nodes are colored and sized by closeness centrality

network models from the current analysis that Oneota immigration into the Mississippian CIRV may have been facilitated, or otherwise structurally guided, by two important factors. The first factor is the structure of Mississippian relationships and interaction patterns in the pre-migration

CIRV as seen in ceramic industry social interaction network models. While at times violent and warlike, Mississippian potters show fluidity and mobility in interaction based on the transmission of information related to ceramic industry, and likely the movement of individuals, between sites. The second is the apparent near abandonment of the Spoon and Illinois River confluence area by Mississippian peoples. Only one modest Mississippian site, Buckeye Bend, appears to have been occupied in the vicinity of the Spoon and Illinois confluence following the circa 1300 A.D. in-migration of Oneota peoples. While Buckeye Bend has been characterized as an intermediate village in the Larson settlement system (Harn 1994), a radiocarbon assay produced for this research indicates an occupation at the site during the post-migration period (see chapter 3). Perhaps the Spoon-Illinois confluence area's ecological resources were exhausted or heavily strained as a result of intensive occupation and utilization over an approximately 100-year span, especially as related to agricultural pursuits. The Spoon-Illinois River confluence may have therefore been an attractive settlement region to Oneota peoples, who were arguably less reliant, in comparison to Mississippian peoples in general, on agricultural pursuits for their subsistence needs and were in the process of expanding out of an upper Midwest and eastern Prairie Plains core region (Blitz 2010; Hart 1990; Tubbs 2013; Tubbs and O'Gorman 2005).

While distinctly Oneota material culture has been recovered from five known CIRV sites, only three of those sites have extant collections of ceramic artifacts of sufficient sample sizes to be included in this study: Crable, Morton Village, and C.W. Cooper (Esarey and Conrad 1998). Of these five sites, two are located just north of the Spoon-Illinois River confluence area – Morton Village and C.W. Cooper. Both of these sites were also previously occupied by Mississippian peoples during the Early Mississippian period in the CIRV (Bardolph 2014; Bardolph and Wilson 2015; Santure, et al. 1990; Strezewski 2003; G. D. Wilson, et al. 2018).

Although Morton Village shows a distinct household-scale multi-cultural occupation, evidence for site-level interaction between Oneota and Mississippian peoples is presently lacking at C.W. Cooper (Conrad and Esarey 1983; O'Gorman and Conner 2016). Household-scale interaction between Oneota and Mississippian peoples is also present at Crable, though the nature of the Oneota presence at this Mississippian town is unclear (Esarey and Conrad 1998; Painter 2014; K. Sampson 2000; H. G. Smith 1951).

The robust relationships between the three sites with an Oneota presence as modeled in the post-migration jar attribute sociograms is unmistakable. In addition to being strategically close to one another geographically (three centrally located red nodes in Figure 5.36), these sites are also strategically close to one another socially according to the jar attribute post-migration network modeled based on information flows in the system (Figure 5.35). Thus, the global scale interaction patterns seen in domestic jar attributes in the Mississippian CIRV, and the likely accompanying bonding ties that such a global pattern would ostensibly foster (Birch and Hart 2018; Crowe 2007), were starkly interrupted by the in-migration of Oneota peoples. Furthermore, Oneota potters in multi-cultural contexts such as Crable and Morton Village appear to have been free to exercise autonomy in the production and cultural transmission of technological information related to domestic jar attributes. Such autonomy would likely reinforce bonding ties to an Oneota heritage among the immigrant population in the production of wares used in cooking. At the same time, interaction relationships between Mississippian sites in the post-migration period domestic jar networks appear less intensive, active, or otherwise more constrained. Perhaps this resulted from differences in how to engage with Oneota immigrants. A strategy of cultural accommodation or perhaps integration of Oneota jar-producing potters was pursued by at least one Mississippian site, Crable. However, the coeval

Ten Mile Creek, Star Bridge, Buckeye Bend, and Baehr South sites show no indication that multi-cultural accommodation took place. Instead cultural pluralism was pursued by peoples at these Mississippian sites.

In the same way that a dramatic shift characterized the role of socially mediated jar attributes in the post-migration CIRV, plates attributes also formed distinct structural interaction patterns through cultural transmission following in the in-migration of Oneota peoples. While the domestic jar attribute network largely indicates that pluralistic tendencies with some cultural accommodation or integration in interaction through cultural transmission in the post-migration CIRV, network models based on socially mediated plate attributes suggest that attempts at

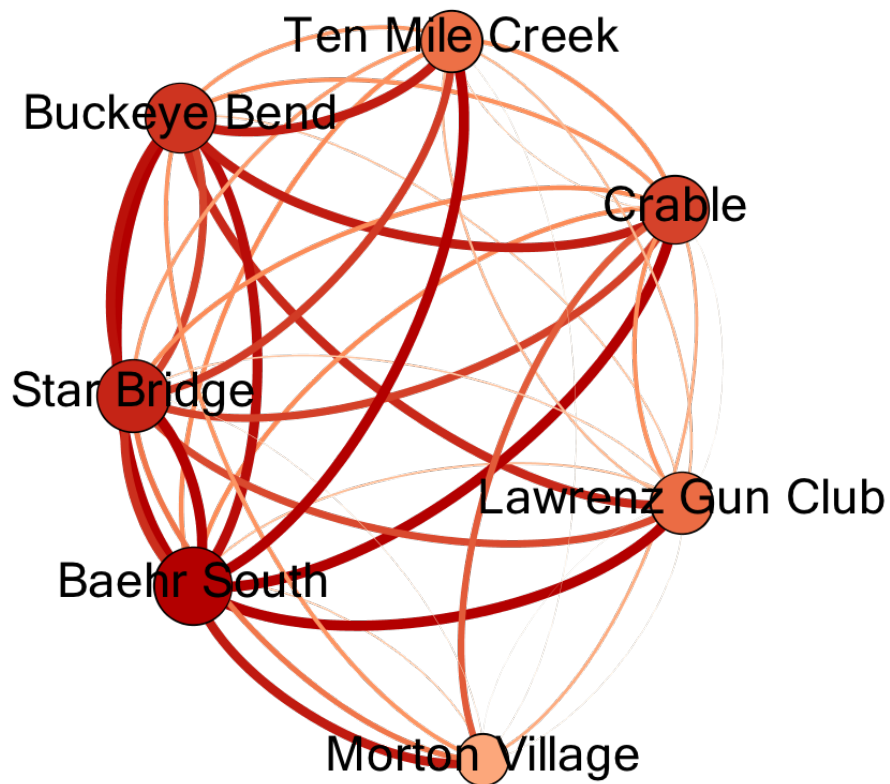


Figure 5.37 Yifan Hu multilevel network graph layout of plate technological similarity network for the Post-Migration Time Period (1300-1450 A.D.); edges are colored by weight; nodes are colored and sized by weighted degree

integration between Oneota and Mississippian peoples were at times pursued. Figures 5.37 and 5.38 show that at the sites where Oneota peoples endeavored to adopt the plate ceramic vessel type, a type absent or rare to Oneota in other contexts (Esarey and Conrad 1998; Overstreet 1997), they likely did so based on direct interactions with Mississippian potters.

The clique-like cluster of Mississippian sites without an Oneota presence as seen in Figure 5.37 suggests that cultural transmission of plate attributes perhaps fostered bonding ties in the consolidation process among Mississippian peoples, who became clustered together in many fewer sites and where public interactions in the form of the serving and sharing food likely took on increased importance in daily habitual routines or during seasonal or episodic feasting events.

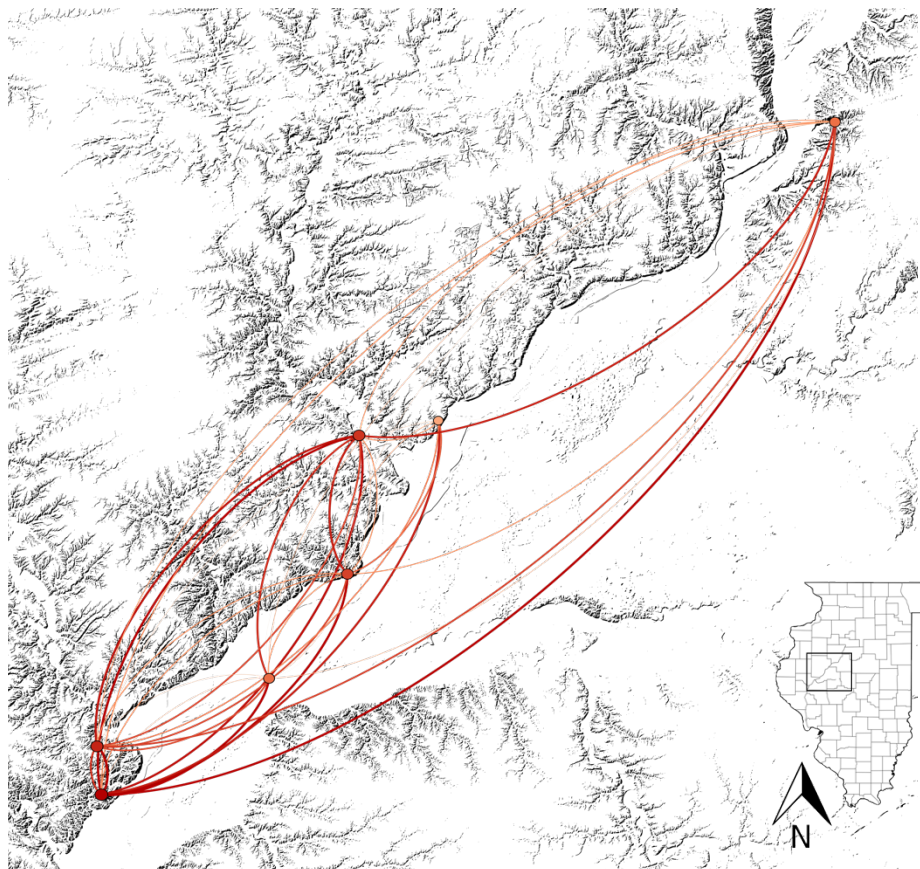


Figure 5.38 Geographic network graph layout of domestic plate similarity network for the Post-Migration Time Period (1300-1450 A.D.); edges are colored by weight; nodes are colored and sized by weighted degree

By adopting a vessel type that perhaps evinces bonding ties and likely played an important role in foodways, Oneota potters show a marked attempt to bridge extant cultural distinctions with indigenous Mississippian peoples. Likewise, Mississippian potters were likely engaging in direct interaction with Oneota potters by integrating them into the communities of practice where cultural transmission related to plate raw material acquisition and/or manufacture took place. This affirms Hale Smith's (1951:28) notion in examining the material remains from Crable that "a transference of technique has taken place, probably indicating a culture fusion from two separate sources." Such transference, however, seems limited only to the multi-cultural settlements, Crable and Morton Village, as no plates have yet been recovered from the C.W. Cooper Oneota habitation site nor is there evidence of Oneota material culture at the coeval Ten Mile Creek, Star Bridge, Buckeye Bend, and Baehr South Mississippian towns and habitation

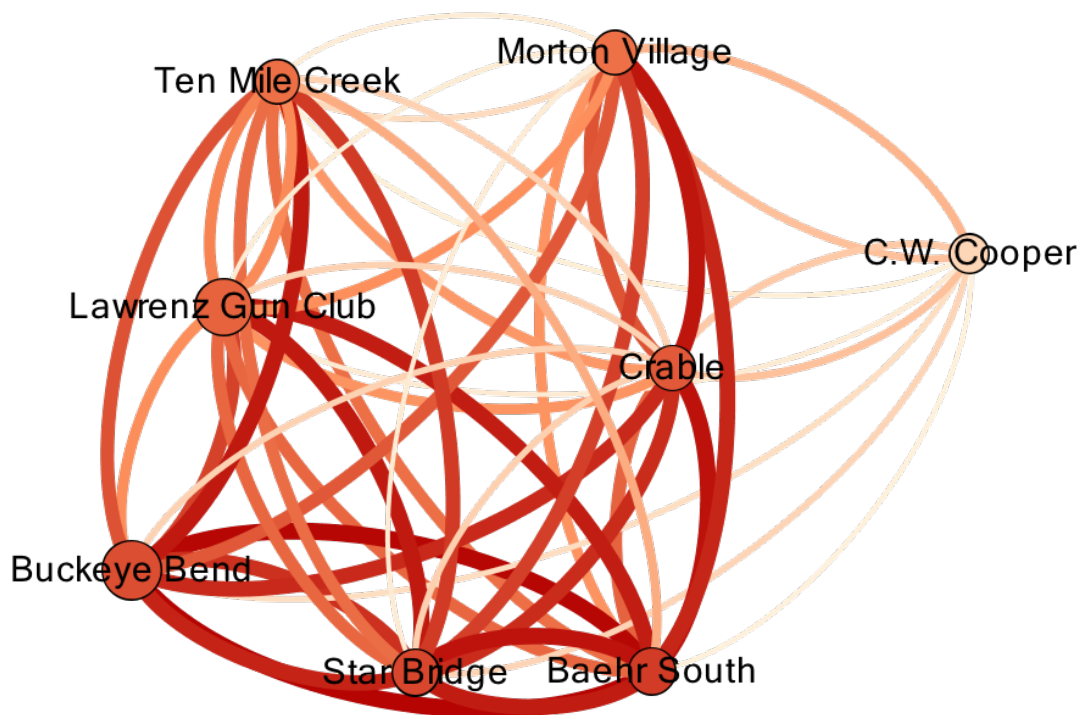


Figure 5.39 Yifan Hu multilevel network graph layout of domestic jar and plate technological similarity flattened multilayer network for the Post-Migration Time Period (1300-1450 A.D.); edges are colored by weight; nodes are colored and sized by weighted degree

sites. A very minor admixture of Oneota material culture, including pottery, has been recovered from Lawrenz Gun Club (Lawrence Conrad personal communication, 2017), though these materials were too fragmentary and too few to be included in this analysis.

When considering the flattened and sliced multilayer socially mediated attribute networks in the post-migration period (Figures 5.39 - 5.41), it is further apparent that structural changes indeed characterize interaction patterns concomitant with and following Oneota in-migration. However, based on the aggregation of Mississippian peoples into many fewer sites, it is more plausible that Oneota in-migration simply exacerbated structural changes in interactions patterns that were already ongoing among indigenous Mississippian peoples as opposed to being the

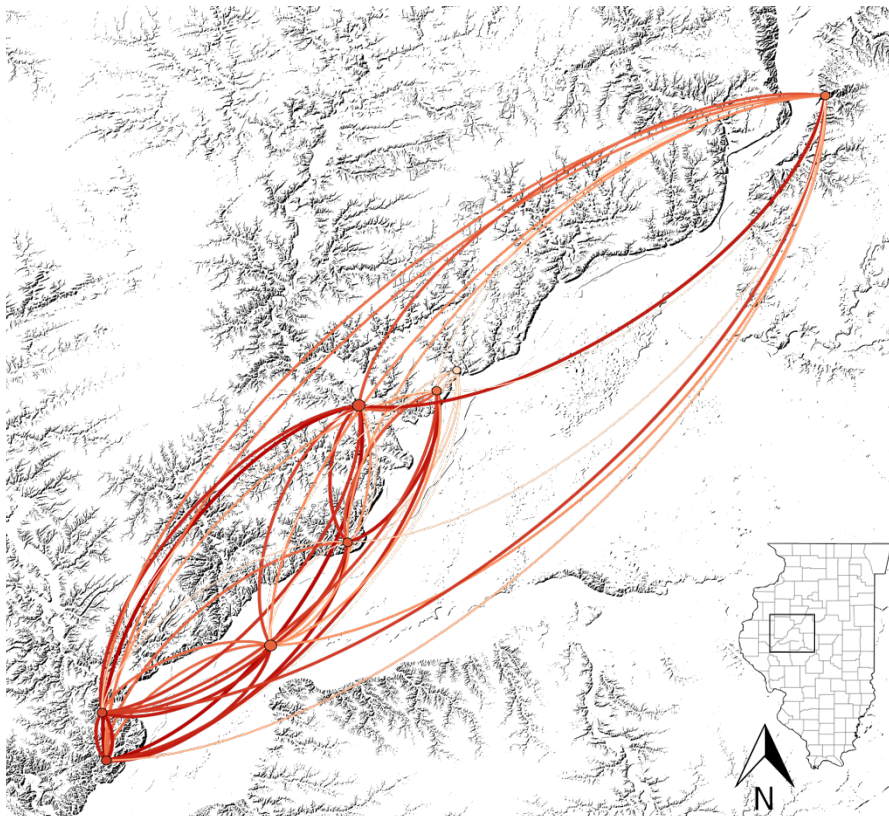


Figure 5.40 Geographic network graph layout of domestic jar and plate technological similarity flattened multilayer network for the Post-Migration Time Period (1300-1450 A.D.); edges are colored by weight; nodes are colored and sized by weighted degree

primary factor responsible for those changes.

Oneota infusion of variation related to jar attribute production was likely a significant disruption to communities of practice and interaction patterns among indigenous Mississippian potters. The shift from global to local scale transmission of socially mediated jar attributes, and the inverse for socially mediated plate attributes, suggests that significant changes occurred in the transmission of cultural information related to ceramic industry *writ large* following Oneota in-migration. These changes undoubtedly impacted the interaction patterns of the communities of



Figure 5.41 Geographic network graph layout of domestic jar (left) and plate (right) technological similarity sliced multilayer network for the Post-Migration Time Period (1300-1450 A.D.); edges are colored by weight; nodes are colored and sized by closeness centrality for jars (left) and weighted degree for plates (right)

practice responsible for vessel production and use. That both Oneota and Mississippian peoples maintained distinct jar production techniques as seen in socially mediated attributes but did transmit and share information related to plate production techniques in limited contexts is perhaps an indication that cultural transmission patterns were restricted to certain spheres of

material culture or daily life only, while cultural pluralism between Mississippian and Oneota peoples was otherwise maintained. As a result, mobility to reinforce networks of interaction that would foster the maintenance of social ties at a regional scale was likely disrupted, an interpretation commensurate with evidence for increasing violence and threats to mobile work-parties as seen in the Norris Farms #36 cemetery associated with the Morton Village site (G. R. Milner, et al. 1991; Santure, et al. 1990). On the other hand, the expansion of the scale of interaction through cultural transmission of plate attributes suggests that at least in the public sphere of life in some Mississippian or multi-cultural contexts, perhaps during seasonal or episodic ceremonies or ritual, attempts at inter-cultural mediation, integration, or accommodation did take place among Oneota and Mississippian potters.

5.6.3 Technological Similarity Networks Across Time, 1200 – 1450 A.D.

The preceding sections describe frameworks for social interaction through cultural transmission with different architectures based on material cultural class within time periods. That is, the different social rules, motivations, and purposes of interaction within the transmission of technological information related to socially-mediated jar and plate attributes influence both network topology and the resulting interpretations about the nature of interaction patterns based on visually examining model characteristics. A key value in using the multilayer network analysis approach taken here is to observe the combined effects of distinct networks – as aggregations of different spheres of interaction and different timeframes – wherein the resulting multilayer “framework may be more than only the combination of its parts” (Preiser-Kapeller 2011:391). The multilayer networks presented here are produced by flattening, or concatenating, distinct network layers together. Though a simple procedure, the resulting models form new

topological patterns with which to draw insight about the broader social milieu, both temporally and materially, of which each individual settlement is a part. This section describes visual interpretations of the various multilayer network configurations across the Late Prehistoric CIRV in order to approach the actual complexity of human networks of social interaction through cultural transmission.

Figures 5.42 and 5.44 provide the most readily visually interpretable models when considering the fundamental question of whether changes in patterns of interactions occurred following Oneota in-migration into the CIRV. In both the jar and plate networks, which are

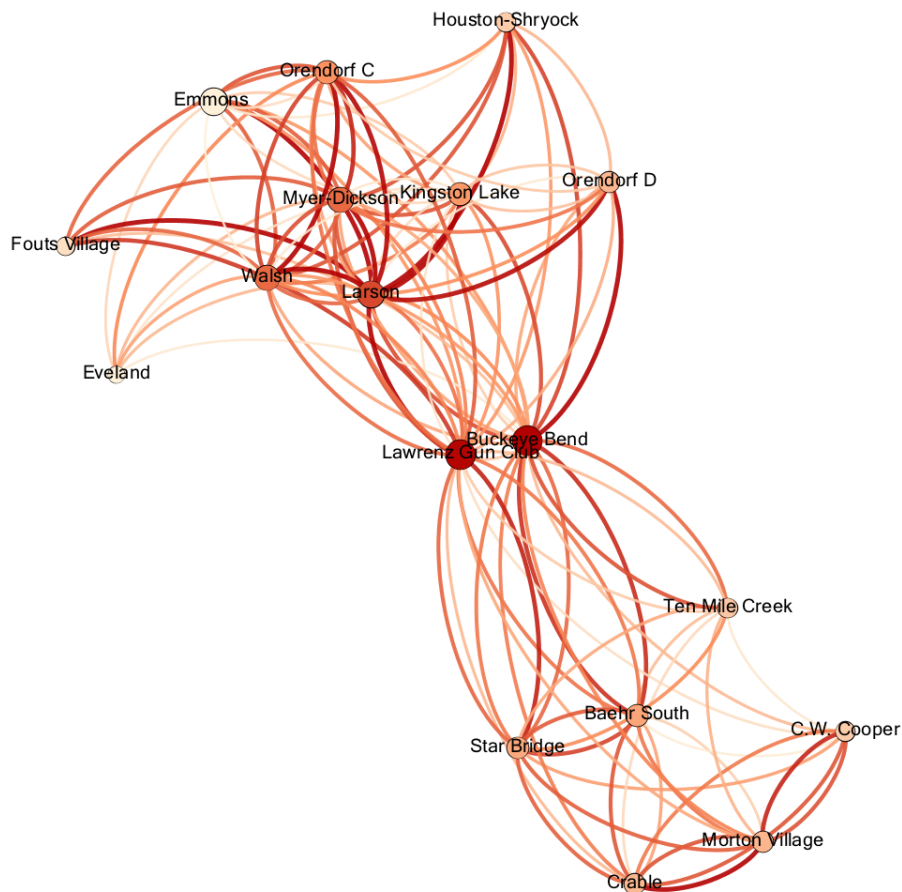


Figure 5.42 Yifan Hu multilevel network graph layout of domestic jar technological similarity network flattened across Time Periods (1200 – 1450 A.D.); edges are colored by weight; nodes are colored and sized by weighted degree score

connected across time through the long occupation span at Lawrenz Gun Club (Jeremy Wilson personal communication, 2018) and the extended or perhaps intermittent occupation at Buckeye Bend (see Chapter 3), distinct patterns of interactions are evident in the pre-migration CIRV (which is laid out in the upper portion of each multilayer sociogram model) compared to the post-migration CIRV (which is laid out in the lower portion of each model). Furthermore, trends discussed in the preceding sections are perhaps brought to bear in a more straightforward way based on the multilayer models presented in Figures 5.42 and 5.44. That is, the Yifan Hu algorithm lays out each site based on the energy flow in the system, with sites sharing strong ties being placed in closer proximity to each other and sites with weaker ties being placed further

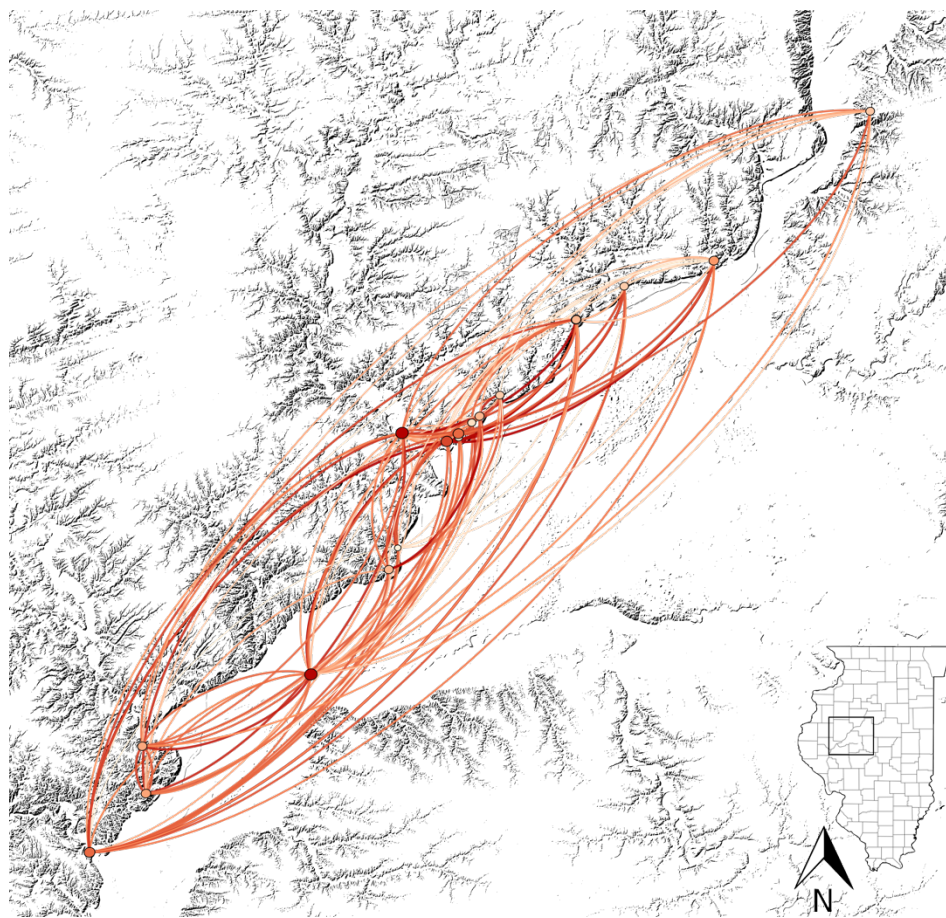


Figure 5.43 Geographic network graph layout of domestic jar technological similarity network flattened across Time Periods (1200 – 1450 A.D.); edges are colored by weight; nodes are colored and sized by weighted degree

apart from one another (Hu 2005). Changes in the structure of interaction based on socially mediated domestic jar attributes is apparent in Figure 5.42. That interaction through the transmission of socially mediated jar attributes likely formed bonding ties at a global scale is evidenced in the many strong links between sites occupied across much of the pre-migration time period, in particular from connections emanating out of or to the centrally located Larson town. Furthermore, the infusion of variation by Oneota peoples and a pattern of more localized or infrequent interaction through transmission of socially mediated jar attributes is seen in the portion of the model showing sites occupied during the post-migration period. Sites with an

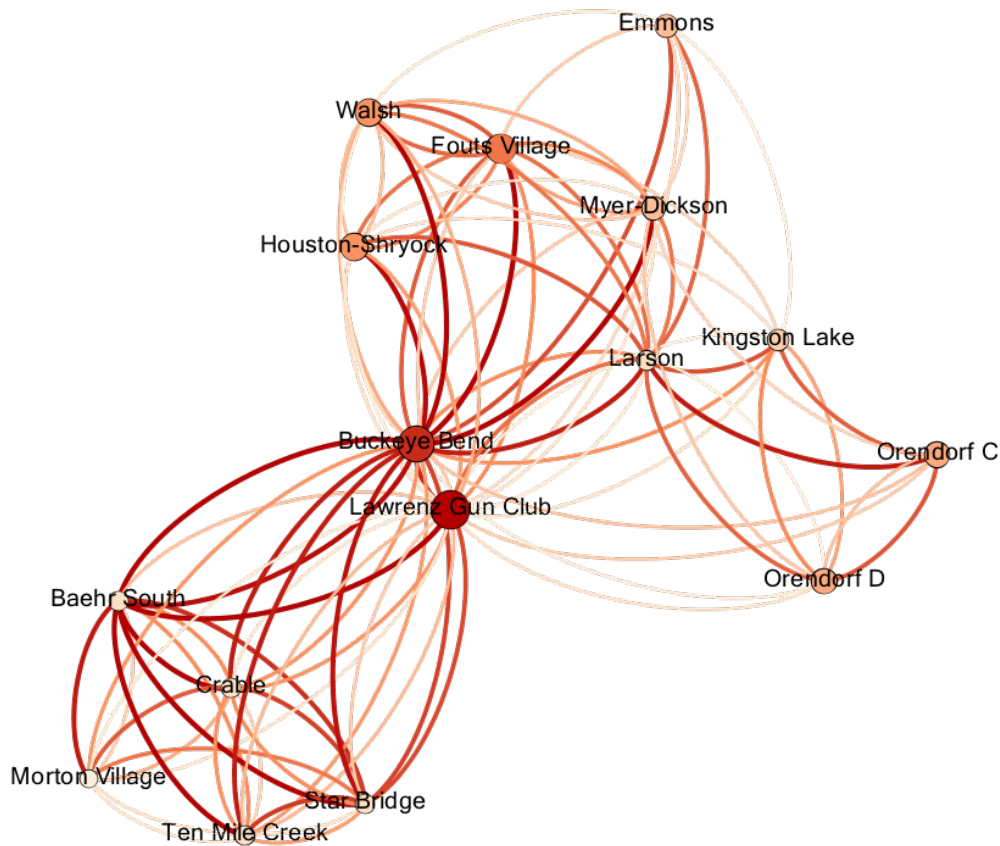


Figure 5.44 Yifan Hu multilevel network graph layout of plate technological similarity network flattened across Time Periods (1200 – 1450 A.D.); edges are colored by weight; nodes are colored and sized by closeness centrality score

Oneota presence are strongly connected to one another and form a distinct clique-like configuration at the bottom portion of Figure 5.42, likely as a result of the presence of trailed designs and very tall rims on jars that are unique to these sites in the post-migration period (see Figure 5.5). While Mississippian sites that lack any evidence of a multi-cultural occupation are generally more weakly connected to sites with an Oneota presence overall, it is important to note that many such connections do exist, suggesting that pluralistic tendencies were perhaps at times offset by some form of accommodation or other interaction through cultural transmission between Mississippian and Oneota jar-producing potters.

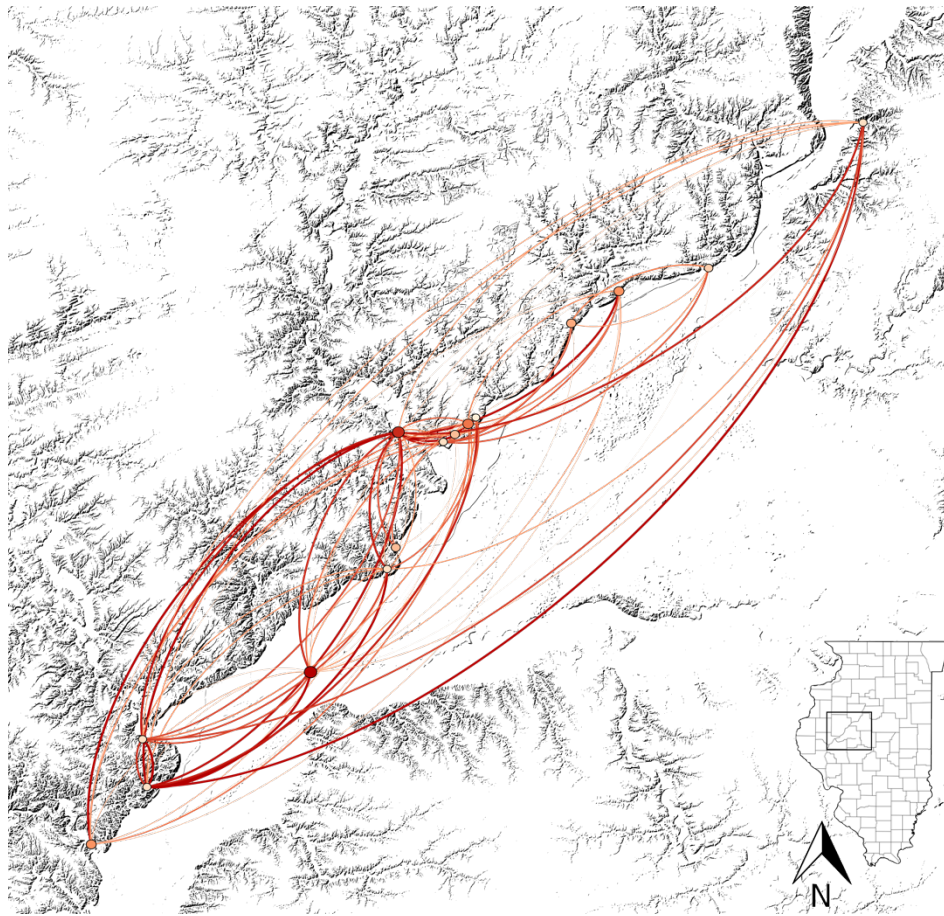


Figure 5.45 Geographic network graph layout of plate technological similarity network flattened across Time Periods (1200 – 1450 A.D.); edges are colored by weight; nodes are colored and sized by weighted degree

A pattern of more localized interaction through socially-mediated plate attribute cultural transmission is seen in sites occupied during the pre-migration period in Figure 5.44. Unlike the multilayer jar attribute network, however, a distinction in topological patterns between the time periods is less apparent in the plate multilayer attribute network. Although, stronger connections overall between sites with a distinctly Mississippian presence in the post-migration CIRV does affirm that more global scale interaction through cultural transmission of socially mediated plate attributes occurred – in particular strong paths from Ten Mile Creek in the north to Star Bridge and to Baehr South near the La Moine River in the south. As do the ties emanating from and to Morton Village and Crable, which are both characterized by a multi-cultural occupation with household scale cohabitation between Mississippian and Oneota peoples.

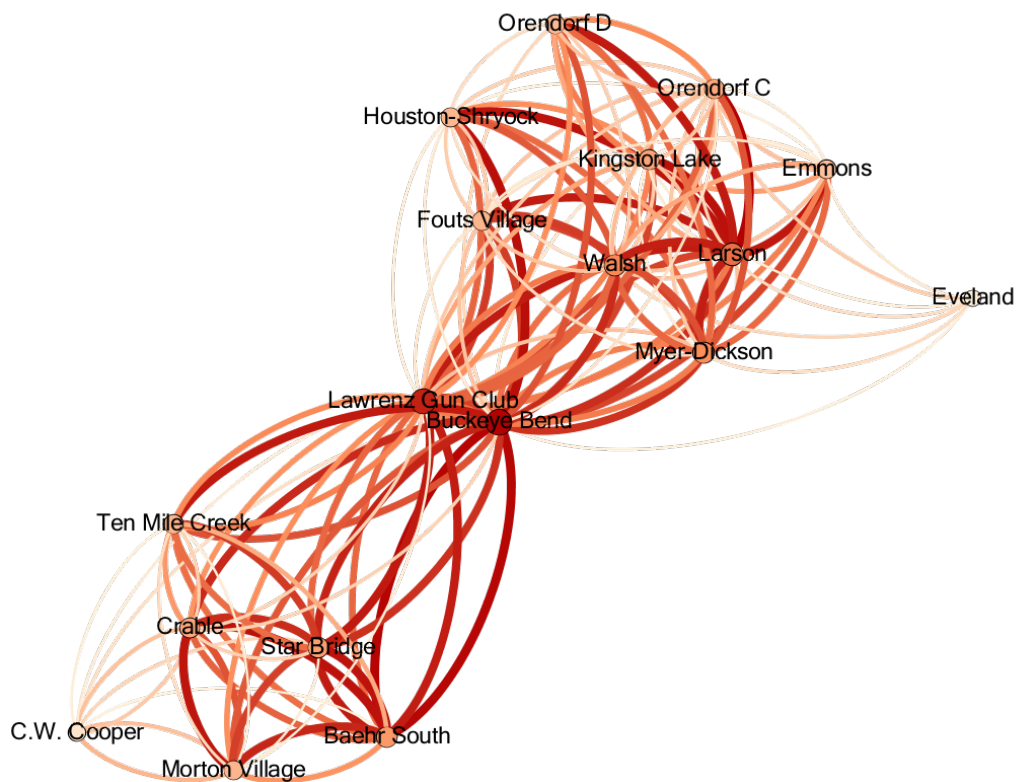


Figure 5.46 Yifan Hu multilevel network graph layout of domestic jar and plate technological similarity multilayer network flattened across Time Periods (1200 – 1450 A.D.); edges are colored by weight; nodes are colored and sized by weighted degree

When both time periods and both material culture classes are flattened into a single multilayer network model, as shown in Figures 5.46 – 5.47, regional scale interaction patterns encompassing the breadth of the Late Prehistoric CIRV are able to be considered. In many ways, these models coincide with known information about sites drawn from qualitative analyses of material cultural remains and traces beyond simply the continuous jar and plate attributes considered here. For example, Eveland, which has been described as a likely ceremonial site wherein local Bauer Branch and Maple Mills Late Woodland groups were proselytized into the

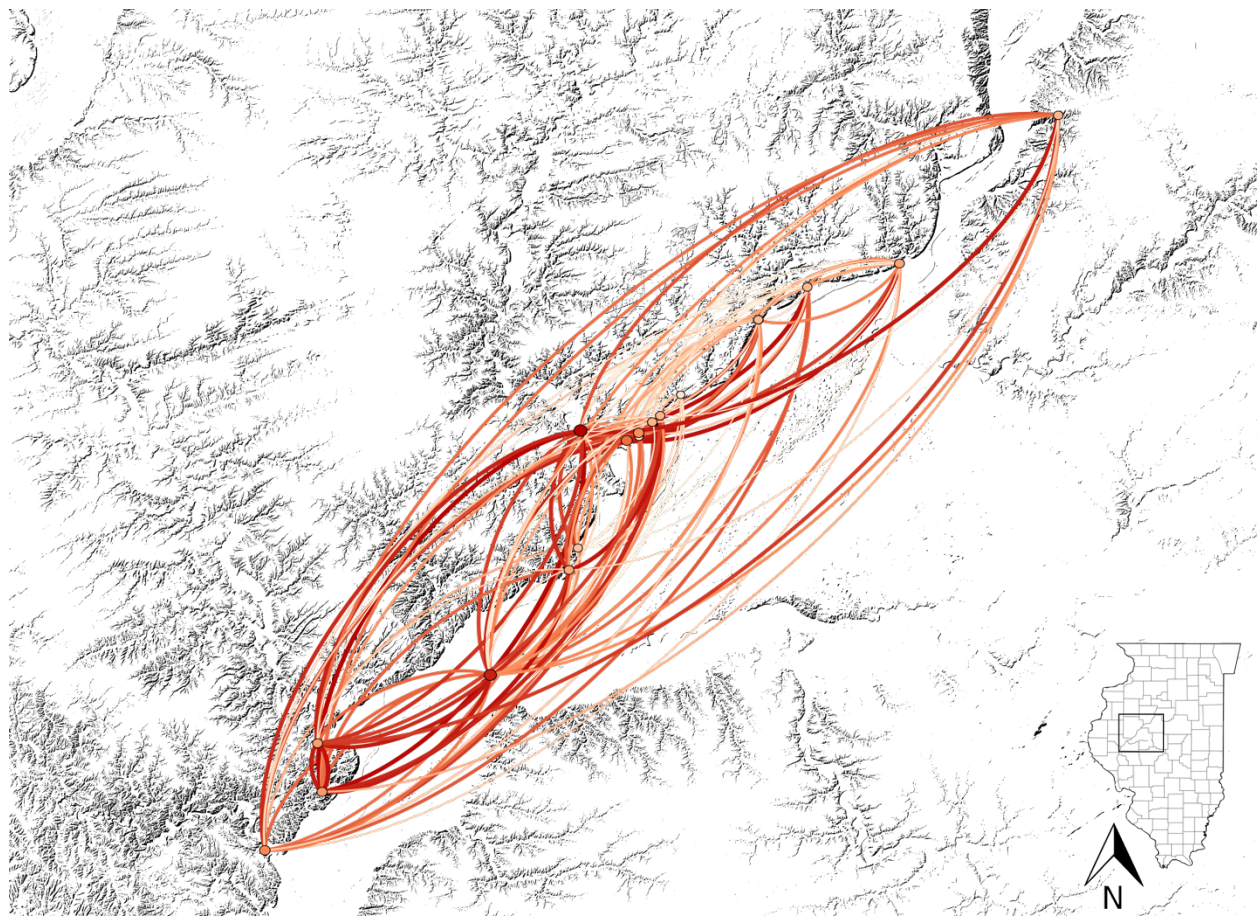


Figure 5.47 Geographic network graph layout of domestic jar and plate technological similarity multilayer network flattened across Time Periods (1200 – 1450 A.D.); edges are colored by weight; nodes are colored and sized by weighted degree

Mississippian lifeway perhaps by missionaries or other emissaries from the Cahokia-dominated American Bottom region (Conrad 1989), is modeled as being quite loosely connected to other Mississippian sites. Furthermore, Eveland is modeled as having the strongest degree of interaction with other sites known to be quite early in the regional sequence of the Late Prehistoric CIRV such as at Orendorf Settlement C and Kingston Lake (Conrad 1991). On the opposite end of both the multilayer network model and the time sequence of the CIRV, is C.W. Cooper. Esarey and Conrad (1998) have described C.W. Cooper as an Oneota habitation site with no evidence of a Mississippian presence in the post-migration period. Indeed, C.W. Cooper is modeled as having very limited interaction with all sites aside from other sites with an Oneota presence – Crable and Morton Village. In fact, no other site shares a reciprocal connection to C.W. Cooper aside from Crable and Morton Village. Nevertheless, that the three sites with an Oneota presence cluster together in the multilayer model but with stark distinctions between how each site is connected to the broader post-migration milieu evidences the close relationships maintained by Oneota peoples following in-migration but perhaps diverging strategies on how to engage with local Mississippian peoples. If these sites were sequentially occupied as opposed to being coeval, the differing relationships suggest evolving strategies of multi-cultural interactions pursued by both Oneota and Mississippian peoples.

Lawrenz Gun Club and Buckeye Bend, the two sites with occupational sequences that span both the pre- and post-migration periods, are placed much closer to the pre-migration sites in both the jar and plate Yifan Hu network layouts. This strongly suggests that the primary occupations at each site were during the pre-migration period, a notion supported by placement of these sites in pre-migration phases by both Conrad (1991) and Harn (1994). Because these sites straddle both time periods under consideration in this analysis, and because it is not known

whether these occupations were intermittent or continuous, the role they played in regional networks of interaction may be overemphasized. Better chronological precision for these and other sites would allow for testing of whether or not the experimental procedure used in this analysis to construct network models of social interaction through cultural transmission contributed to a false-positive overemphasis or if these two sites indeed played a unique role in brokering the pre- and post-migration social milieus of the Late Prehistoric CIRV.

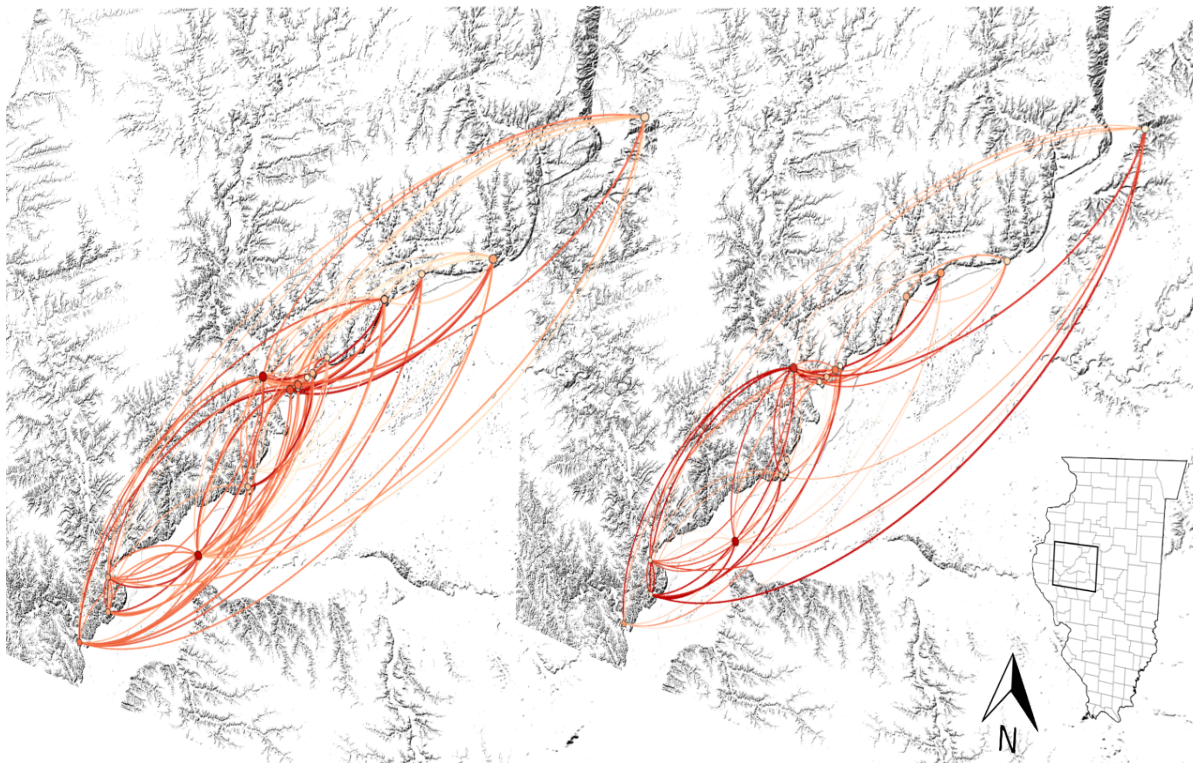


Figure 5.48 Geographic network graph layout of domestic jar (left) and plate (right) technological similarity sliced multilayer network flattened across Time Period (1200-1450 A.D.); edges are colored by weight; nodes are colored and sized by weighted degree

When considering the multilayer network model flattened to include both material classes and time periods with a geographic layout (Figure 5.47), two overarching trends emerge. First, the two most outlying sites in the region – Ten Mile Creek to the north and Walsh to the south – overall tend to be weakly integrated into the regional network. Second, the four sites just to the north of the Spoon-Illinois confluence area – Orendorf Settlements C and D, Houston-Shryock

and Kingston Lake – show strong connections to sites in the Spoon-Illinois confluence area that are not reciprocated as strongly. These one-sided interactions indicate that cultural transmission of information or perhaps populations flowed from these sites to sites in the Spoon-Illinois confluence, likely attesting to the regional importance of this area in regional dynamics during the Mississippian pre-migration period. Mortuary ceremonialism at Dickson Mounds and the may help to explain this trend (Harn 1971, 1980).

5.7 Conclusion

In this chapter, I have described and employed a quantitative method for assessing regional scale networks of interaction through cultural transmission based on ceramic technological similarity. As the discussion above illustrates, the differentiating of networks into distinct layers and considering the ways those different layers interact with each other provides a means of accessing the complexity of human social networks in archaeological contexts – information that is often lost when relying on qualitative or taxonomic methods that consider singular lines of evidence. In this concluding section, I briefly review the principal results of the analytical procedure described above and link these results with the broader research context of this study.

In creating and analyzing networks of interaction through cultural transmission, four main research questions were posed for the Late Prehistoric Period central Illinois River valley (CIRV) case study region:

- 1) Are changes in the structure of interaction network patterns inherent across time, and how might the circa 1300 A.D. in-migration of an exogenous Oneota group be related to those changes?
- 2) Do interaction patterns support an hypothesized taxonomic distinction of Mississippian into La Moine and Spoon River cultural variants (Conrad 1989, 1991)?

- 3) It has been postulated that the onset of the Mississippian period circa 1200 A.D. was paralleled by the emergence of chronic, internecine violence and warfare (G. R. Milner 1999). The threat of warfare is argued to have transformed both settlement and subsistence practices such that, among other things, “families coalesced into large communities behind defensive walls...limiting foraging and fishing trips” and “women became increasingly sequestered behind village walls” (Vanderwarker and Wilson 2016:98-100). Given that ethnographic accounts indicate that when pottery manufacture is done by hand, it is typically done by women (Rice 2005), it is possible to test whether sufficient variation in pottery attributes characterize different communities such that it can be reasonably assumed that potters were geographically circumscribed in the cultural transmission of artifact attribute social information primarily as a result the threat of violence and warfare?
- 4) Given that the plate vessel class is absent or extremely rare in Oneota contexts outside the CIRV (Esarey and Conrad 1998), do imitations/emulations of serving plates by Oneota peoples inject sufficient variation to suggest that the adoption of this vessel class was made at a distance, or are the imitations/emulations technologically similar enough for there to be a higher likelihood that direct cultural transmission of ceramic technology between Mississippian and Oneota potters occurred?

The statistical and visual interpretations of attribute interaction networks provide robust answers to each of the questions above.

Significant structural changes indeed occur in networks of interaction across the Middle to Late Mississippian transition concomitant with the circa 1300 A.D. in-migration of Oneota peoples into the CIRV. In particular, the scale at which attribute interaction networks form

relational connections changes across time. In the pre-migration context, technological similarity in jar attributes suggests cultural transmission across a regional interaction network. At the same time, spatial distance acted as a major factor in influencing the degree of technological similarity in plate attributes, suggesting cultural transmission at a more nuanced scale of interaction. This trend inverses following Oneota in-migration and infusion of significant variation in jar technological norms by Oneota peoples, leading to networks of cultural transmission of jar attributes at reduced or nuanced scales of interaction largely based on spatial proximity. However, technological similarity in plate technology exhibits a pattern of creating regional scale relational connections among post-migration sites. Thus, neither the pre- nor post-migration CIRV is characterized by parity in the scale at which networks of interaction through cultural transmission formed strong relational connections across the different vessel classes under consideration.

Both the pre- and post-migration contexts of the CIRV are characterized by densely connected (or highly cohesive) and distributed (or lacking any primary central actor or actor-clique) network models across each of the vessel classes. While distinct communities were found in the plate attribute pre-migration interaction network and the jar attribute post-migration interaction network, these community structures do not align in spatial proximity to the major river tributaries flowing into the Illinois River – the Spoon and La Moine. As a result, network models of interaction through cultural transmission in jar and plate attribute technology do not support an hypothesized taxonomic distinction of Mississippian cultures into Spoon and La Moine River cultural variants (Conrad 1989, 1991).

Likewise, because the pre-migration period is characterized by densely connected and distributed networks of interaction through cultural transmission, a model of delimited intra-

regional mobility as a result of the threat of structural violence or warfare is not supported (Vanderwarker and Wilson 2016). Again, distinct community structures were able to be detected for the pre-migration plate attribute network layer, however these distinctions are not consistent across the different interaction network layers in the pre-migration CIRV context and do not follow a geographic pattern that would indicate reduced mobility due to the threat of warfare or violence. No doubt, violence was ingrained into the cultural fabric of Mississippian peoples during the Orendorf and Larson phases (Conrad 1989, 1991; Steadman 2008; G. D. Wilson 2012, 2013). Network models among sites occupied during these phases, however, indicate that despite the high levels of inter-personal violence, Mississippian peoples sustained widespread interaction patterns through information sharing and cultural transmission related to ceramic industry.

The post-migration CIRV saw significant infusion of variation related to jar attribute technology by Oneota peoples. That variation interrupted the structurally regional scale relational interaction pattern seen in the pre-migration jar attribute interaction network. As a consequence, sites with an Oneota presence are weakly integrated into the post-migration jar attribute interaction network. On the other hand, Oneota peoples did adopt the plate vessel class at two multi-cultural sites, Morton Village and Crable, likely as a result of the regional scale at which plate technological information spread in the post-migration CIRV. This suggests that the plate vessel class was adopted by Oneota peoples based on direct interaction through cultural transmission with Mississippian potters, and likely as a means to bridge extant cultural distinctions in the public sphere of life where a serving plate is most likely to have been utilized.

Since both Oneota and Mississippian peoples maintained culturally distinct jar production technology as seen in socially mediated attributes but did share information related to plate production techniques in limited contexts is an indication that cultural transmission patterns were

restricted to certain spheres of material culture or daily life only, while cultural pluralism between Mississippian and Oneota peoples was otherwise maintained. As a result, mobility to reinforce networks of interaction that would foster the maintenance of social ties at a regionalscale was likely disrupted. On the other hand, the expansion of the scale of interaction through cultural transmission of plate attributes suggests that at least in the public sphere of life in some Mississippian or multi-cultural contexts, perhaps during seasonal or episodic ceremonies or ritual, attempts at inter-cultural mediation, integration, or accommodation did occur among Oneota and Mississippian potters.

CHAPTER 6 CERAMIC STYLE AND NETWORKS OF SOCIAL IDENTIFICATION

6.1 Introduction

There is a long and storied history on the use of style to explain group formation and interaction processes in archaeology. Style was used by classical archaeologists such as Gerhard, Beazley, Furtwängler and others in the latter half of the 19th century as a replacement over an earlier interest in artifactual and cultural beauty in order to systematically categorize artifacts chronologically, determine where they were made, and try to ascertain who might have made them (Trigger 2006:65-66). A similar technique was used by prehistoric archaeologists on both sides of the Atlantic under the Culture-Historical paradigm of the early 20th century. Variation in artifact style provided a bridge to artifact classification and the defining of distinct archaeological cultures. That is, culture-historical archaeologists assigned groups of stylistically similar artifacts into distinct cultural units. In addition, style enabled these cultural units to be contextualized both spatially, and more importantly, chronologically (Childe 1936; Cole and Deuel 1937; McKern 1939). The specific nature of artifact stylistic differences often provided a means to assign a relatively brief chronology onto cultural units, and as a result, prehistoric archaeologists had for the first time broad generalizations about the distinct peoples who came before us along spatial and chronological dimensions. Both of these dimensions are necessary to model group identification and interaction processes in the archaeological record.

In the latter half of the 20th century, following the shift toward a nomothetic and scientific New Archaeology (Binford 1962), stylistic variation was used to search for analogous traits which in turn would lead to analogous inference and reveal adaptive cultural systems (Flannery 1968). Style, therefore, could lead to the uncovering of social grouping, interaction, information exchange, and social units in prehistoric contexts at fine grained scales heretofore thought

unknowable. Efforts in this regard are abundant (Braun 1985; Goodby 1998; Hargrave, et al. 1991; Hegmon, et al. 1997; C. M. Milner and Stark 1999; Odess 1998; C. G. Sampson 1988; Schortman and Urban 1992; Schortman, et al. 2001; Stark Miriam, et al. 2000; Stark, et al. 1995, 1998). These studies are often influenced by ethnoarchaeological research indicating an active use of style as a form of non-verbal communication to express social identities (Bowser 2000; Carr 1995a; Graves 1981, 1994; Hegmon 2000; Herbich 1987; Kramer 1985; Longacre 1991; Skibo, et al. 1989; Wiessner 1983, 1984, 1990; Wobst 1977).

A recent trend in American prehistoric archaeology and beyond focuses on a particular aspect of style – pottery decoration – as a means to access patterns of shared categorical identities at various social and spatial scales (Birch and Hart 2018; Hart and Engelbrecht 2012; Mills, Clark, et al. 2013; Mills, et al. 2015; Mizoguchi 2009; Peeples 2011, 2018). Due to its highly visible and often symbolic nature, pottery decoration is posited as being an integral part of an active process to signal group membership and individual skill under this paradigm. Categories of group membership may be related to ethnicity, gender, political status, religious affiliation, labor or craft expertise, or other social units at both hierarchical and heterarchical levels. Because “categorical distinctions are not necessarily built out of direct and frequent interactions among people, such identities must be symbolized in order to facilitate recognition among members and non-members of categorical social groups” (Peeples 2011:261-262). Regardless of the specific social grouping, symbolic communication and social identity are argued to interplay recursively. Active expression of identity is therefore intricately linked to the process of symbolization, a process also referred to in other contexts as emblematic style (Wiessner 1983, 1984, 1985, 1990). Consequently, it is argued here that stylistic patterns gleaned from symbolic decoration on pottery vessels may reveal networks of shared categorical identities

among groups of people in archaeological contexts.

This chapter presents an analysis of Mississippian and Oneota pottery that draws on theories of pottery style, social signaling (Birch and Hart 2018; Bliege Bird and Smith 2005; Hart and Engelbrecht 2012), and categorical identification (Azarian 2005; Fuhse 2012; Mills, Clark, et al. 2013; Mische 2011; Peeples 2011, 2018; Tilly 2004; White 1992, 2008a). In particular, social network analysis models are used to assess patterns of similarities in social identification across the middle to late Mississippian transition in the Late Prehistoric central Illinois River valley (ca. A.D. 1200- 1450; CIRV). The objective is to reveal the ways in which migration was structured by, and restructured, networks of social identification. Network models are constructed based on patterns of proportional similarity in designs incised or trailed on the interior outflaring rims of ceramic plates on either side of a circa 1300 A.D. in-migration of Oneota peoples into the region. Plates were used primarily as serving or presentation pieces (Hilgeman 2000). Plate designs are a highly visible decorative component during quotidian or ritualistic public gatherings. Results indicate that intra-regional mobility and shifting patterns in the scale of parity in networks of social identification during the Middle to Late Mississippian transition resulted in the formation of a spatial and social internal frontier that in many ways structured the in-migration of Bold Counselor Oneota peoples into the CIRV. In turn, Oneota peoples likely contributed to increasing diversity in common categories of social identification, thereby acting to disrupt and exacerbate ongoing restructuring of regional social identification networks.

6.2 Migration and Social Identification

Explaining variability in communal interrelationships within multicultural social environments is a key research aim for archaeologists and anthropologists. Establishing and maintaining intercultural relationships is one way for migrant groups to adapt to a novel social environments (Burmeister 2000), or for societies to respond to severe pressure and threat from external (Kowalewski 2006) or internal forces (Birch 2010). Social diversity based on the intersection of migrant and indigenous peoples can be critical to the process of social change (Alt 2006). However, differential patterns of interactions in multicultural contexts may be pursued by communities of social actors, from factionalism and conflict along culturally pluralistic lines, to private retention of cultural or ethnic distinctions with public de-emphasis and cultural accommodation, to hybridity and cross-cultural mediation or integration and ethnogenesis (Broch 1987; Liebmann 2013; Pugh 2010; Stone 2003). That is, a spectrum of internally motivated processes leads to the selective adoption of technology, social identities, and individuals (Frangipane 2015; Pollack, et al. 2002; Schwartz and Green 2013; Trubowitz 1992).

Indexing common social identities represents a primary mechanism visible in archaeological contexts that creates and sustains intercultural network relationships (Bowser 2000). Other mechanisms include engaging in direct relational interaction through cultural transmission or exchange and overlapping resource exploitation areas. These processes are often more overt on the spatial frontiers of polities due to the waning influence of cultural cores over geographic distance (Rice 1998). The goal of this chapter is to explore the role of a theoretically justified ceramic stylistic trait, plate design motifs, in evidencing patterns of similarities in categorical identification and discern how those patterns might change contemporaneous with the in-migration of a tribal Oneota group into a chiefly Mississippian environment late in the prehistory of west-central Illinois.

Recent archaeological research recognizes the value of incorporating formal network analysis methodologies based on the relational sociology of Harrison White, Charles Tilly, and others to address questions related to coexisting material culture traditions (Azarian 2005; Borck, et al. 2015; Collar, et al. 2015; Fuhse 2012, 2015; Mills, et al. 2016; Mills, Clark, et al. 2013; Mills, et al. 2015; Mills, Roberts Jr., et al. 2013; Mische 2011; Peeples, et al. 2016; Tilly 1978, 2001b; White 1992, 2008a; White and Godart 2007). Here, I employ a theoretical framework that builds on this application of relational theory to archaeological contexts in order to address anthropologically significant issues related to processes of social identification.

Because relational theory is examined at length in Chapter 2, only a brief discussion is presented here. White argues that social networks must be studied in conjunction with cultural systems (Fuhse 2015; White 1992). That is, cultural and network structure are argued to interplay in a recursive manner as opposed to being abstractions of each other. Network relationships build on cultural models such as kinship, gender, heterarchy, and hierarchy. White views interactions as being driven through the inherent uncertainty in the roles of participants. From this uncertainty, White sees social identities as a means to ‘gain footing’ in, or to ‘control’, social contexts (White 1992). These control attempts are posited to leave a trace in social space as ‘stories’ or information defining and relating identities to each other. Identities in this way are mobilized as process and often codified by symbolic representation. For White, novelty in stories or identities develops from the “creative combination of cultural forms at the intersection of previously separate network formations” (White 1993:77).

The ‘New York School’ of relational sociology (Mische 2011), building upon the theoretical work of White and others (Azarian 2005), posits that processes of collective social identification take place in either relational identification or categorical identification. Relational

identification is a process whereby individuals identify with larger collectives based on their position within networks of interpersonal interaction (Peeples 2011:18-19; 2018). Strong ties in this regard are based on interactions rooted in kinship, communities of practice, or shared historical origin, and are discussed in Chapter 5. Relations forged through more limited contexts such as the exchange of material goods or information exchange based on shared resource exploitation areas are discussed in Chapter 7. Such “weak ties” generated from more limited contexts of interaction often play an important role in connecting social contexts that would often otherwise be completely separate (Granovetter 1973). The focus of this chapter is categorical identification, which refers to a process whereby individuals identify with larger collectives based on perceptions of belonging to formal social units such as ethnic groups, genders, political affiliations, religious affiliations, or other units at various scales (Peeples 2011:20-23; 2018). Categorical identification need not be coupled with direct social interaction. That is, two individuals may perceive belonging in the same formal social unit irrespective of familial or interactional relationships.

Migration represents a critical social context in which to observe the creative refashioning of cultural forms resulting from the intersection of previously separate social networks. As a process, migrations are often guided by networks formed in a stepwise fashion through connections based in kinship, exchange, or other social ties (Mills, et al. 2016). This has led to the use of “network-mediated migration theory” by many anthropologists and sociologists as an alternative to the “rational choice and decision-making models” used in other social science disciplines (Brettell 2000:107; Mills, et al. 2016). A network approach replaces predetermined typologies with explicitly defined ties that allow groups to be described based on social relationships of interaction or shared categorical identity ascription.

Social networks are of paramount importance for communal migrations. Migrants must adapt to a new cultural and natural landscape where information and interaction with existing groups can ease or antagonize settlement. Migration is a vehicle for cultural maintenance or change based on the clash between public and private, adaptation and tradition, and external and internal cultural transfer (Anthony 1990; Burmeister 2000; Stone 2003). Identification networks are sensitive indicators of the negotiation of social and economic systems by indigenous and migrant groups (Rockman 2003). Individuals, communities, and households pursue various social identification strategies in multicultural environments resulting from migration. Due to archaeology's focus on material culture remains, attempts to elucidate ideological strategies in multicultural contexts are eschewed here in favor of elucidating behavioral strategies in multicultural contexts at the community scale. In particular, the analysis presented here is focused on ascertaining the geographic and demographic scale at which categorical identities were expressed on serving wares and how those scales might change concomitant with the immigration of an exogenous group in a non-state archaeological setting.

6.3 Oneota Migration into West-Central Illinois

During the twelfth and thirteenth centuries a large-scale movement of Oneota peoples out of an Upper Midwest core region and into the lower and eastern Midwest was ongoing. This population movement has been described as an aggressive territorial expansion (Hollinger 2005). Oneota expansion coincided with a rapid decline in Middle Mississippian influences in these regions and with the onset of the droughty Pacific climatic episode (Gibbon 1995). While many Late Woodland populations in the riverine Midwest and western Great Lakes were replaced by or integrated into Oneota peoples during this expansion process, societies in the ecologically rich

central Illinois River valley (or CIRV), or northern Middle Mississippian frontier, maintained their positions in fortified temple mound centers and outlying sites, and entered into a period of regional coexistence with an intrusive Oneota population known archaeologically as the Bold Counselor (Esarey and Conrad 1998). The sudden appearance of characteristically Oneota material culture at five sites circa 1300 A.D. and biodistance indicators in the Norris Farms #36 cemetery population attests to the occurrence of a migration process in the CIRV, though the specific location of origin of the Oneota immigrants is unknown (Esarey and Conrad 1998; Santure, et al. 1990; Steadman 1998). Recent archaeological inquiry in the Late Prehistoric CIRV has focused on the unprecedented levels of violence seen in burial and cemetery contexts both prior to and following Oneota in-migration (Hatch 2015, 2017; G. R. Milner, et al. 1991; Steadman 2008; Vanderwarker and Wilson 2016; G. D. Wilson 2012, 2013). Although the CIRV is remarkable for its levels of sustained inter-personal violence, evidence indicating the communal coexistence of these distinct but interrelated cultural groups is apparent. Coexisting Oneota and Mississippian material culture at multiple sites at the household level provides the opportunity to examine the various social interrelationships that were present.

A discussion of the Mississippian CIRV is warranted in order to provide a baseline for network restructuring concomitant with Oneota in-migration. The archaeological region known as the CIRV encompasses a 210 km stretch of the Illinois River extending approximately from the modern village of Hennepin, IL southerly to the village of Meredosia, IL (Harn 1994:4-9); though the Late Prehistoric CIRV is centralized in an approximately 137 km stretch of the Illinois River from the present town of Peoria, IL southerly to the unincorporated village of Chambersburg, IL. The Mississippian phases of the CIRV have been defined largely based on reference to material cultural correlates in the American Bottom, a few hundred river kilometers

to the south along the Illinois River (Conrad 1991). During the approximately 350-year span of Mississippian occupation, the CIRV housed at least seven fortified Mississippian temple towns and numerous smaller villages and farming hamlets. Subtle trends in material culture based on geographic location have led to a hypothesized cultural distinction between Mississippian peoples in the upper portion of the CIRV near the Spoon River and those inhabiting the lower portion of the valley near the La Moine River (Conrad 1991; Harn 1978, 1994).

The central Illinois River valley's position at the eastern edge of the Prairie Peninsula and proximity to the Mississippian cultural core in the American Bottom situated this archaeological region at the intersection of Plains-Prairie-Woodland lifeways and booming agricultural complexes during the beginning of the first millennium of the common age. The immense population size and political and artifactual complexity at the American Bottom site Cahokia have led to models that view the site as the *axis mundi* for Mississippian culture in eastern North America (Pauketat 1994; Pauketat and Emerson 1997). However, recent research challenges the intensity of Cahokian influence on both demographic and cultural transformations in comparison to *in situ* processes in the CIRV (Bardolph 2014; Bardolph and Wilson 2015; Friberg 2018; Steadman 1998, 2001). That is, far from being passively colonized or demographically replaced by Mississippian peoples from the American Bottom, Late Woodland peoples local to the CIRV were “selectively adopting or emulating aspects of Mississippian lifeways, while maintaining certain [local] traditions” (Bardolph and Wilson 2015:138). Nevertheless, the Mississippianization process promoted increasing regional interconnectedness through cultural realignment among dispersed Late Woodland peoples. This resulted in profound changes to settlement, subsistence, architectural, ceramic, and socio-politico-religious systems in the CIRV and a distinct expression of the Mississippian lifeway at the northern fringe of its expansion in

the American midcontinent, save a few relatively short-lived outposts at Aztalan (L. G. Goldstein and Richards 1991), in the Apple River valley (Emerson 1991), and in the Trempealeau region of Wisconsin (W. B. Green and Rodell 1994; Pauketat, et al. 2015).

The historical trajectory of Middle Mississippian populations in general in the CIRV is argued to be one of increasing population aggregation, factionalism, and conflict (Steadman 2008; Vanderwarker and Wilson 2016; G. D. Wilson 2012, 2013; J. J. Wilson 2010). Around 1200 A.D., Mississippian communities began to aggregate into fewer and larger settlements – a trend that would only intensify over time in the region. These settlements could best be described as nucleated towns, which were often coupled with a mound-fronted plaza surrounded by domestic structures and often fortifications. Some towns, such as Orendorf and Lawrenz Gun Club, were rebuilt numerous times over successive occupations that spanned many generations, while others such as Larson were perhaps only occupied for a generation or two. Numerous villages, intermediate settlements, hamlets, and single-family farms were occupied alongside towns (Conrad 1989, 1991; Esarey and Conrad 1998; Harn 1978, 1994).

Material culture, and in particular burial goods, shows clear connections between Mississippian peoples in the CIRV and symbolically adorned exotic items characteristic of the so-called Southern Cult, or pan-Mississippian cosmological symbolism. These include but are not limited to shell gorgets, Ramey knives, copper pendants, engraved marine shell, flint clay effigy and figurine pipes, stone discoidals, and copper-coated earplugs (Brown and Kelly 2000; Conrad 1989, 1991; Harn 1971, 1980, 1991; Knight Jr 1986). Evidence for interpersonal violence in the region has been shown to increase overtime (G. R. Milner, et al. 1991; Steadman 2008), however it was not a ubiquitous phenomenon (Hatch 2015). An analysis of ceramic technology in this dissertation (Chapter 5) indicates that sites across the Mississippian CIRV

were interacting extensively despite the high levels of violence, suggesting that the threat of violence was perhaps episodic as opposed to chronic in delimiting regional mobility.

Paleodemographic analyses suggest that the emergence of palisaded towns was accompanied by a high-pressure system of elevated fertility and mortality (J. J. Wilson 2010).

Sometime in the early to mid-14th century, an Oneota group from the north migrated into the CIRV and fundamentally changed the social dynamics of the region (Esarey and Conrad 1998; O'Gorman and Conner 2016). Available data from CIRV settlements exhibit varying degrees of intermixing between Mississippian and Oneota material culture. Because intermixing occurs in simultaneous occupations, it has caused a quandary in attempts to taxonomically differentiate Bold Counselor Oneota from their Late Mississippian contemporaries and *vice versa* (Conrad 1991; Esarey and Conrad 1998; H. G. Smith 1951). From the Oneota assemblage at C.W. Cooper that is suggestive of a site-unit intrusion because it “shows almost no evidence of any influence or actual presence by the Late Mississippians” (Esarey and Conrad 1998:41), to evidence “probably indicating a cultural fusion from two separate sources” at the Crable mound center (H. G. Smith 1951:28), to the ‘purely’ Late Mississippian assemblages at the fortified Ten Mile Creek and Star Bridge towns (Conrad 1991), no discernible pattern emerges using traditional taxonomic methods as to the nature of cultural interrelationships in the Late Prehistoric CIRV. Tantalizing evidence for cultural mixing between Oneota and Mississippian peoples is most readily apparent in the intermingling of ceramic traits. For example, the use of plates by Oneota peoples is apparent at several sites in the CIRV, but virtually absent in Oneota contexts outside the region. At the Crable Mississippian mound center, some 14% of vessels from a sample of pit features were ascribed to Oneota, leading Esarey and Conrad (1998:46) to suggest that “the most likely explanation for these assemblages is that Bold Counselor peoples

were present (in one social context or another) as a minority admixture to Crable's overwhelmingly Mississippian-derived population. Furthermore, this admixture seems to represent social integration at the household level." The Morton Village site appears to indicate the inverse: an Oneota village with a minor admixture of Late Mississippian peoples (O'Gorman and Conner 2016).

Given these taxonomic quandaries, an alternative perspective is warranted. In order to access patterns of similarities in social identification processes, a high-visibility stylistic material culture trait is needed. In the CIRV, stylistic traits are abundant, but the most commonly recovered material culture class with stylistic treatment used in high-visibility contexts is pottery and in particular the plate vessel class. As a result, the Late Prehistoric CIRV is an appropriate context, and ceramic plates are an apt material cultural class, with which to apply network-mediated methodologies to explore community scale structuring of, and responses to, cultural contact.

6.3.1 Plates, Ceramic Design, and Sun Symbolism in the CIRV

Pottery assemblages in the Late Prehistoric central Illinois River valley (CIRV) consist of five basic vessel forms – plates, jars, bowls, bottles, and pans. Symbolic motifs are widely adorned on many of these vessel forms, and sub-variants of these forms, but occur in greatest frequencies on plates, effigy bowls, beakers (a specialized bowl form), and jars (Conrad 1991; Esarey and Conrad 1998; Harn 1994). Of these vessels, the most commonly recovered across the geographic and temporal expanse of the CIRV with largely intact symbolic decoration motifs are plates. Where site level data is available, plates comprise on order of 2.5 – 10% of vessel assemblages and are thus not overly common across domestic contexts (Conrad 1991; Esarey and Conrad 1998; Harn 1994). Mississippian and Oneota plates are similar in shape and form to

circular dinner plates you might find in your kitchen cabinet or the kind you might have your dinner served in at a fine-dining restaurant. Based on the high frequency of often finely crafted decorative motifs on the interior outflaring rims of plates and the unrestricted access to their contents, plates likely functioned primarily as serving vessels (Hilgeman 2000; Lieto and O’Gorman 2014).

As a vessel form, plates are common at Mississippian sites in the American Bottom and surrounding regions along the Illinois and Ohio River valleys. Plates comprise a significant proportion of decorated vessels at major Mississippian mound centers such as Cahokia (Griffin 1949; Vogel 1975), Kincaid (Orr 1951), Angel (Hilgeman 2000), Common Field (M. Buchanan 2014), and town sites in the CIRV such as Larson, Crable, Star Bridge, Lawrenz Gun Club, Orendorf, Walsh, and Ten Mile Creek (Conrad 1991; Esarey and Conrad 1998; Harn 1994; Painter 2014; K. Sampson 2000; H. G. Smith 1951), as well as at village and subsidiary sites such as Morton Village, Fouts Village, and Buckeye Bend among many others (Cole and Deuel 1937; Conrad 1991; Harn 1994; Lieto and O’Gorman 2014; Santure, et al. 1990). There is a minor occurrence of plates found at Mississippian period sites in present-day western Kentucky, the Nashville Basin, and the Tennessee-Cumberland region (K. E. Smith, et al. 2004). Despite the widespread adoption of Mississippian cultural characteristics across the late Precolumbian American southeast, however, plates are generally rare in Mississippian period assemblages in areas south and east of present-day Tennessee.

Plates are characterized by a complex profile that includes a flattened, outflaring rim and a distinctive concave well (Hilgeman 2000:36-40). The morphology of plates is chronologically significant across the Mississippian regions wherein these vessels have been recovered (Clay 1976:47; Conrad 1991:148; Hilgeman 2000:42; Kelly 1984, 1991b; Orr 1951:339; K. E. Smith,

et al. 2004:50-51). In particular, plate rims increase in size overtime (e.g. Figure 6.1 C.) and

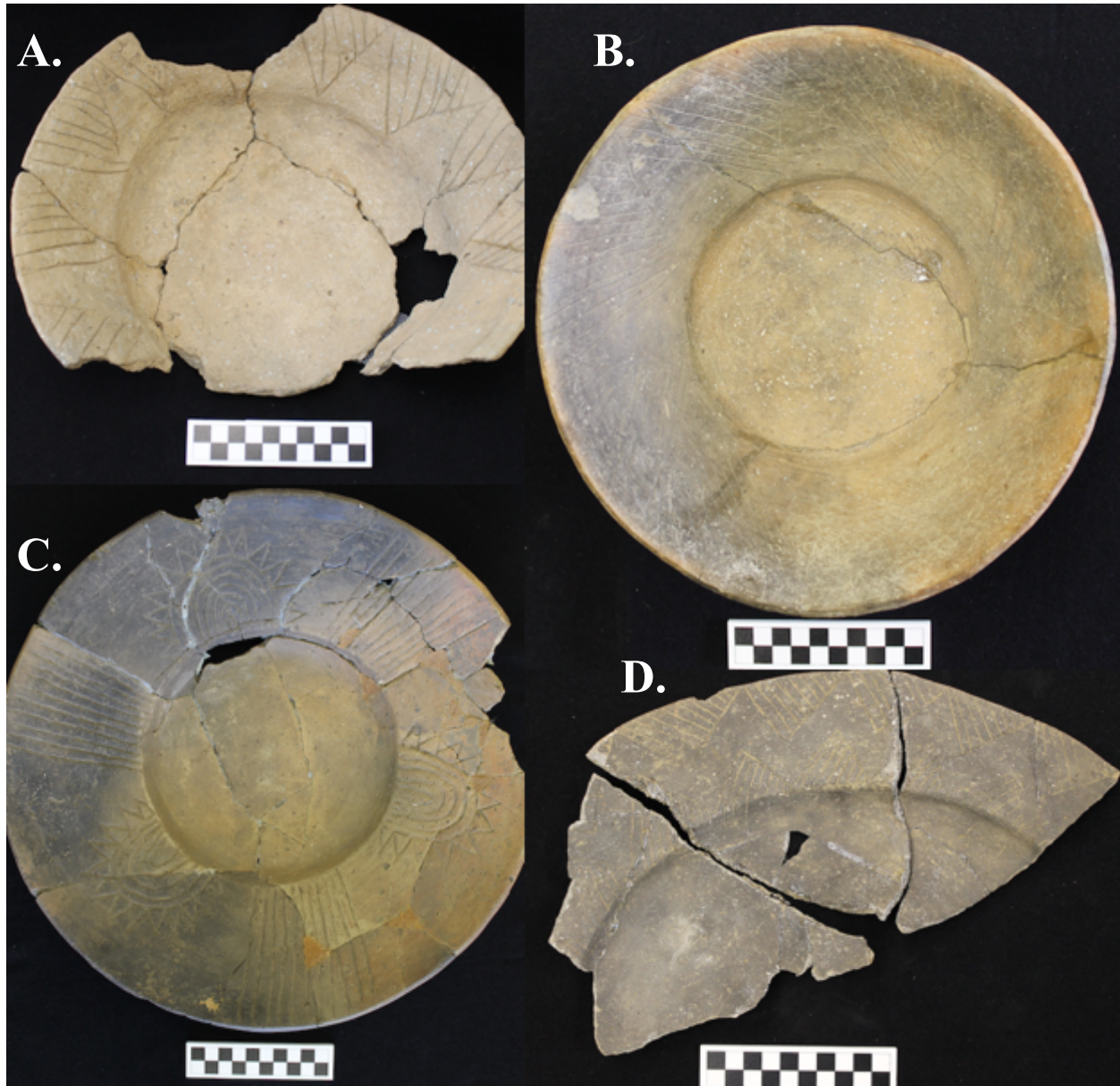


Figure 6.1 Examples of plate form. Images © Andy Upton 2018, courtesy Western Illinois Archaeological Research Center and Dickson Mounds Museum

become more concave toward the well (e.g. Figure 6.1 B.). As a result, plates become more bowl-like overtime. However, this is a very general trend and older plate forms (i.e. with shorter rims and a flatter profile) persist alongside the later, more bowl-like vessels. Figure 6.2 shows continuous attribute metric trends for plates in the CIRV showing these trends quantitatively. In

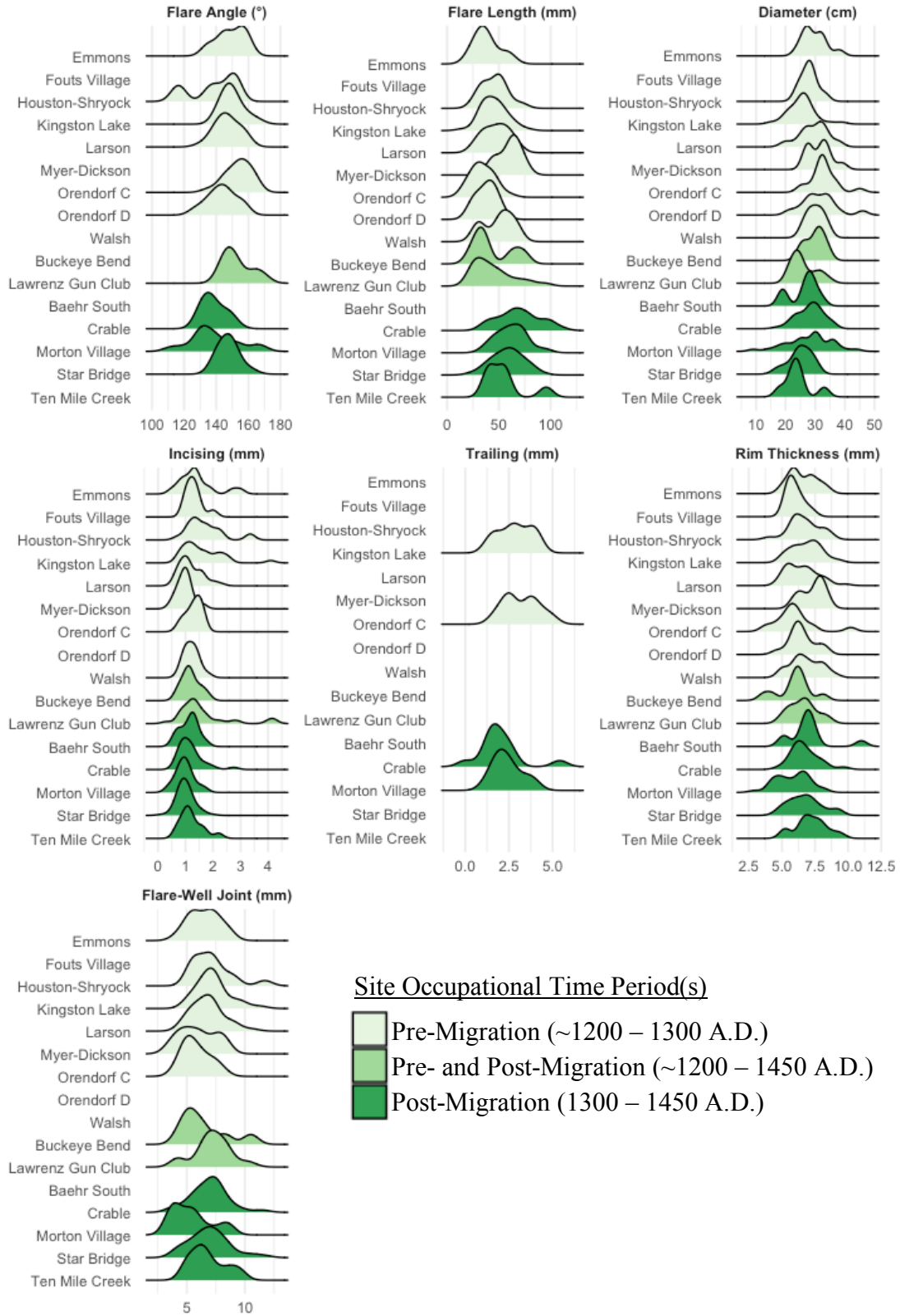


Figure 6.2 Ridgeline density plots for plate continuous attribute measurements at Late Prehistoric CIRV sites

general, the flare angle of plates decreases overtime (where a 90° angle is vertical) and plate flare length increases overtime. However, there is considerable overlap between time periods. This has led to a myriad of ambiguous typological classifications for plates across the different Mississippian contexts of recovery such as ‘Wells incised, ‘O’Byam incised’, ‘Crable deep-rimmed plate’, and ‘O’Byam incised variety Wells’. In addition, a plethora of terms are used in the literature to denote or sub-divide the vessel class, including ‘broad-rimmed bowls’, ‘broad-rimmed plate’, ‘deep-rimmed plate’, ‘deep rim plate’, ‘short rim plate’, ‘standard plate’, and ‘broad shallow bowls’, among others. For ease and consistency, I use the term ‘plate’ to refer to this class of vessel, despite the more bowl-like shape of the vessel class overtime. This signals the primary serving function of the vessel class and disambiguates the likely more utilitarian bowls which are characterized by rounded, as opposed to flattened, rims. Furthermore, since the focus of this research is to consider alternative perspectives to artifact classification, no attempt is made here to assign plates to a taxonomic type nor to refine any sort of typology. Instead, this research focuses on using proportions of similarities in decorative motifs used on the plate serving vessel class as a means to model changes in networks of shared categorical ascription concomitant with demographic change in a multicultural context.

Plates in the CIRV are almost ubiquitously burnished or polished to a soft luster (Conrad 1991). Decoration occurs only on the interior surface of the outflaring rim. As a result, prepared foodstuffs served in the well of plates would leave any decorative motifs clearly visible when used in a public context. Plates tend to break along the joint between the inner lip and the outflaring rim, often leaving a significant portion of the outflaring rim and any accompanying decorative motifs present (Hilgeman 2000). Decoration technique on plates in the CIRV can be characterized in one of two forms: incising or trailing. Incised decorations are sliced into a

leather hard or semi-dried paste and generally form a “V” shape in profile as a result of the cutting motion. A fine pointed or edged, sharp, and sturdy tool would be required to execute plate incising. Possible tools such as a lithic points, flake-tools or drills, porcupine quills, or other faunal implements such as an awl could perhaps be used. Much less common is the scratching of designs onto a dry paste with a wider tool such as a pebble or scraper resulting in thicker but shallower incision lines. Trailed decorations, on the other hand, are drawn into a malleably damp or moist paste and as a result generally form a “U” shape in profile. Tools for



Figure 6.3 Plate decoration techniques: trailed (left) and incised (right). Images © Andy Upton 2018, courtesy Western Illinois Archaeological Research Center

trailing designs would be characterized by a blunted tip – sticks, reeds, rounded-tip river pebbles, cylindrical pottery sherds, or polished faunal long bones might make good tools for this purpose. Quite rare are trailed lines wide enough to suggest a human finger was used as the implement responsible for decoration. Different tools and production sequences would therefore be required

to trail decorations rather than incise them. However, plates with trailed designs typically co-occur as an outlying minor admixture (i.e. < 15% trailed plates) alongside an overwhelming majority of plates with incised designs at CIRV sites (See Table 6.1). This suggests some level of experimentation or perhaps assertive style (Wiessner 1990) in plate decoration by potters across the geographic and temporal expanse of the Mississippian CIRV. A very minor admixture of plates are both trailed and impressed with punctate design motifs characteristic of Oneota peoples, showing an incipient hybridization of Oneota decoration and a Mississippian vessel form (Esarey and Conrad 1998; Lieto and O’Gorman 2014). The only definitive trend regarding plate decoration is that plates with decorative motifs characteristic of Oneota peoples are always



Figure 6.4 Trailed and punctate impression decoration. Image © Andy Upton 2018, courtesy Western Illinois Archaeological Research Center

trailed and never incised (e.g. Figure 6.4).

Motifs present on CIRV plates almost entirely depict Upper World Symbolism and in particular the sun. Line-filled triangular designs use positive and negative space to form sun rays emanating out of the vessel well (e.g. Figure 6.1A & B, Figure 6.4). Zig-zag designs are often formed by the presence of multiple line-filled triangular designs on the upper and lower portions of the outflaring rims (e.g. Figure 6.1D). Finely incised variants of the line-filled triangular designs have been referred to as Wells Incised in the CIRV and American Bottom (Harn 1994; Vogel 1975). Fewer line-filled triangular designs are present at sites with earlier occupations in



Figure 6.5 Plate sherd showing sun with nested cross motif. Image © Andy Upton 2018, courtesy Western Illinois Archaeological Research Center

the CIRV such as Orendorf and Kingston Lake in favor of simpler curvilinear or rectilinear line-based designs (Conrad 1991:138). On the other hand, sites with occupations extending into the

14th century A.D., such as Lawrenz Gun Club, Crable, and Star Bridge, often depict a half-risen sun itself using curvilinear arc lines flanked on all sides by triangles (e.g. Figure 6.1C; Figure 6.3). Rare is a complete circular sun with nested cross motif surrounded by triangular sun-rays (Figure 6.5).

In the American Bottom region, individual design motifs and entire pot symbolism of Ramey Incised vessels are argued “to have been an active element of elite-commoner socio-ideological discourse” in hierarchical Mississippian society and to have relayed information about the Cahokian-style cosmos (Pauketat and Emerson 1991:920). Upper world symbolism appears on Ramey incised vessels dominated by unambiguous sun motifs. Ramey incised pottery spread into the CIRV during the early Mississippian period along with other facets of the Mississippian lifeway (Bardolph 2014; Friberg 2018; Harn 1991). However, both the form of execution and symbols present on Ramey incised pottery in the CIRV are distinct from counterparts in the American Bottom. If Ramey incised pottery does reflect cosmology as practiced by Cahokians and other Mississippian peoples in the American Bottom region, the selective adoption of decorative motifs suggests that peoples in the CIRV “did not adopt Mississippian religion wholesale, but rather made sense of the changing cultural climate within their own worldviews, renegotiating their identities and social relationships in the process, and bundling these spheres of interaction into the products of their daily practice” (Friberg 2018:53). While the Ramey incised vessel type did not persist into the Middle and Late Mississippian CIRV phases (1200 – 1450 A.D.) that are the focus of this research, certain Ramey incised design motifs do – concentric arcs, nested chevrons, and line-filled triangles unmistakably interpretable as sun (or fire) Upper World symbolism. In many ways, plate design motifs depicting Upper World symbolism can be seen as an outgrowth of Ramey incised symbolism. It

can therefore be inferred that the sun and Upper World symbolism adorning plates in the Middle and Late Mississippian phases of the CIRV likely reflect a complex interplay between cosmological and religious themes that relay social identification to a broader Mississippian world but within distinct, localized worldviews.

The sun was intertwined into the cultural fabric of most, if not all, Native American Tribes in the southeast, midwest, and plains regions during the protohistoric period. Ethnographic accounts of the descendants of Mississippian peoples in the southeastern United States indicate a cosmos that consists of three worlds: This World, an Upper World, and an Under World. The Upper World epitomized perfect order and consistency, where things existed in a grander and purer form than in This World (Hudson 1976:122-183). The sun, as the source of all light, warmth, and life, was one of the principal gods and often at the center of Upper World ceremonialism. Among some Tribes, the sun was referred to as ‘our grandparent’ – terminology rooted in the same respect and affection afforded to the Ancestors (Hudson 1976:127). Whereas among other Tribes, the leading family were known as the Suns and the primary chief was called the Great Sun (Lankford 2011:54-55). Such was the integration of solar reverence among the Natchez that Swanton (1928:206) remarked that the “Natchez state was thus to all intents and purposes a solar theocracy.” The sun’s gender was not fixed among Tribes and was sometimes male and sometimes female. For example, the “Cherokees believed that sacred fire, like the Sun, was an old woman. Out of respect, they fed her a portion of each meal” (Hudson 1976:126). The sun dance was, and is, practiced by Tribes in the plains region. Descriptions of the sun dance among the Arapaho, Arikara, Blackfeet, Cheyenne, Crow, Hidatsa, Kiowa, Mandans, Ojibway, Omaha, Sioux, and Ute indicate that the sun, as a manifestation of a deity, was vital in reaffirming Tribal membership and cultural identity (Spier 1921). The sun was

a central manitous, or other-than-human spirit, among the Illinois, Miami, Potawatomi, and Ojibwa (Thwaites 1897). Upon contact with Jesuit missionaries, the Illinois “linked their sun god Manitoua assouv with the Christian God...which literally meant ‘Great Spirit’” (Bilodeau 2001:358, 362). While the role of the sun and Upper World cosmology among Mississippian and Oneota peoples will always be a source of debate, the near ubiquity of solar reverence among the likely descendants of these peoples in the southeastern, midwestern, and plains regions of the United States suggests that the adorning of sun symbolism on plates was likely interwoven into socio-politico-religious beliefs. As a result, the plate vessel class and the symbolic decorative motifs emblazoned upon them are theoretically justified as a good proxy for active expressions of categorical commonality at a region scale because they were likely produced with a concern for visual communication regarding social categorical identification.

6.4 Methodology

Social network analysis provides a body of theory and techniques for visualizing and measuring patterns of shared categorical identities between social entities (Scott 2000; Scott and Carrington 2016; Wasserman and Faust 1994). The application of network analysis techniques in archaeology is contingent upon the basic theoretical argument that similarities in material culture used and discarded at different sites can act as a proxy measure for the degree of social connectedness between them, whether direct or indirect, material or informational (Brughmans 2013; Peeples, et al. 2016:61). The network models of social identification chosen for this research constitute a framework for constructing bonds of shared categorical identification between individuals and communities, wherein ties between sites in network models act as statements of probability that a relationship existed (Matthew Peeples personal communication,

2017). Expressed in stylistic decoration, categorical identities are mechanisms for people to index ascription to common social units, express solidarity, and nonverbally communicate social information related to group membership (Braun 1985; Wiessner 1990).

While Mississippian plates have been explored from a variety of typological perspectives (Conrad 1991; Hilgeman 2000; Vogel 1975), this research represents the first coding scheme devised for Mississippian plate decoration in the CIRV. Each plate sherd was assessed for the presence of a design technique and decoration motif. A design technique, as used here, refers to the technique used to decorate the vessel – whether incised, trailed, or trail-impressed. Whereas a decoration motif refers to the specific shape and form of elements comprising the decoration. A sampling of 490 plates from 15 Late Prehistoric CIRV sites was assessed for this analysis. All samples were assessed solely by the author to minimize inter-observer inaccuracies in design technique and decoration motif characterization. Among the sample of 490 vessel observations, 74 percent ($n = 364$) have incised decoration, 11 percent ($n = 53$) have trailed decoration, 2 percent ($n = 12$) have both trailed and impressed (punctate) decorations, and 12 percent ($n = 61$) are plain with no decoration present. Plates with no decoration motif present are considered in the analysis because the absence of a motif may be symbolically charged given the majority of plates with decorations. However, plates with indeterminate or isolate decoration motifs are not considered. A decoration category was assigned to each unique combination of design technique and decoration motifs present. These unique decoration categories total 94 across the 429 vessels with design techniques present. Descriptions of each unique decoration motif category are provided in the Coding Sheet in Appendix A. Of the decorated vessels, two decorative motif categories are wholly unique with no duplicates. Removing these isolate motifs as well as the vessels with indeterminate motifs results in a sampling universe of some 411 vessels across 15

Site	Plates (<i>n</i>)	Plain	Incised	Trailed	Trailed- Impressed	Time Period
Baehr South	11	-	100% (11)	-	-	Post-Migration
Buckeye Bend	12	-	100% (12)	-	-	Pre- and Post-Migration
Crabbe	74	2.7% (2)	81.9% (59)	13.9% (10)	4.2% (3)	Post-Migration
Emmons	24	29.2% (7)	82.4% (14)	17.6% (3)	-	Pre-Migration
Fouts Village	11	9.1% (1)	100% (10)	-	-	Pre-Migration
Houston-Shryock	27	11.1% (3)	91.7% (22)	8.3% (2)	-	Pre-Migration
Kingston Lake	47	17% (8)	71.8% (28)	28.2% (11)	-	Pre-Migration
Larson	42	14.3% (6)	94.4% (34)	5.6% (2)	-	Pre-Migration
Lawrenz Gun Club	42	9.5% (4)	89.5% (34)	10.5% (4)	-	Pre- and Post-Migration
Morton Village	34	11.8% (4)	60% (18)	10% (3)	30% (9)	Post-Migration
Myer-Dickson	17	11.8% (2)	86.7% (13)	13.3% (2)	-	Pre-Migration
Orendorf C	32	43.8% (14)	38.9% (7)	61.1% (11)	-	Pre-Migration
Star Bridge	81	7.4% (6)	97.3% (73)	2.7% (2)	-	Post-Migration
Ten Mile Creek	16	12.5% (2)	92.9% (13)	7.1% (1)	-	Post-Migration
Walsh	20	10% (2)	88.9% (16)	11.1% (2)	-	Pre-Migration
Total	490	61	364	53	12	

Table 6.1 Summary of plate sample design techniques by site

sites from which to model networks of social identification. The unique decoration motif categories were distilled into 29 decoration grouping categories based on perceived similarities in decoration motifs alone (i.e. disregarding design technique) in order to focus solely on symbolism. A vessel with decorations emblematic of the decoration grouping category was then sketch-traced and shared unique decoration categories noted and subsumed. The full sketches are provided in Appendix E. Design group counts are summarized in Table 6.2, and decoration motif grouping category emblems provided in Figure 6.6.

It is important to note that there is significant variability in the amount of plate decoration data that was able to be recorded from each archaeological site. Given the regional scale of this project, and the resulting reliance on extant collections, the sampling of sites and vessels chosen does not reflect a probabilistic survey. Further, the amount of excavation or other data collection

from each site varies significantly. Some sites were almost completely excavated, while others only saw minimal sub-surface testing. Decorations themselves are also often incomplete or only partially present, potentially obfuscating accurate decoration motif grouping categorizations. Inasmuch as possible, the entire vessel was considered when decorations were assessed. However, complete plate vessels are quite rare. Plates were seldom used as burial furniture, where they might be recovered intact, aside from at the Crable site, for example (H. G. Smith 1951). Thus, in some cases, only individual decoration motif elements might be present. In these cases, decoration motif categorizations were made based on perceived similarities in possibly incomplete decoration elements (e.g. decoration groupings 7 and 13, Figure 6.6). Furthermore, a regression of the number of decoration category groupings as a function of vessel sample size from each site indicates that a significant portion of variation in the number of design category groupings is explained by sample size ($r = 0.85$, $R^2 = 0.71$). Thus, the patterns of shared categorical identification modeled between sites may be negatively impacted by the vagaries of sampling. The interpretations that follow should therefore be considered as foundational as opposed to definitive in the analysis of the nature of social identification processes among Late Prehistoric CIRV sites.

Categorical social identification is explored across the 29 plate decoration motif groupings observed using the Brainerd-Robinson coefficient of similarity, which is commonly used in archaeological analysis as a means to explore relative frequencies, whether counts or percentages, of proportional similarity (Brainerd 1951; Robinson 1951; Shennan 1997:233-234). This measure is a form of city block metric that ranges from a score of 0, indicating no similarity, to a score of 200, indicating complete similarity in terms of the proportions of plate motif groupings present between two sites. For the present purposes, Brainerd-Robinson

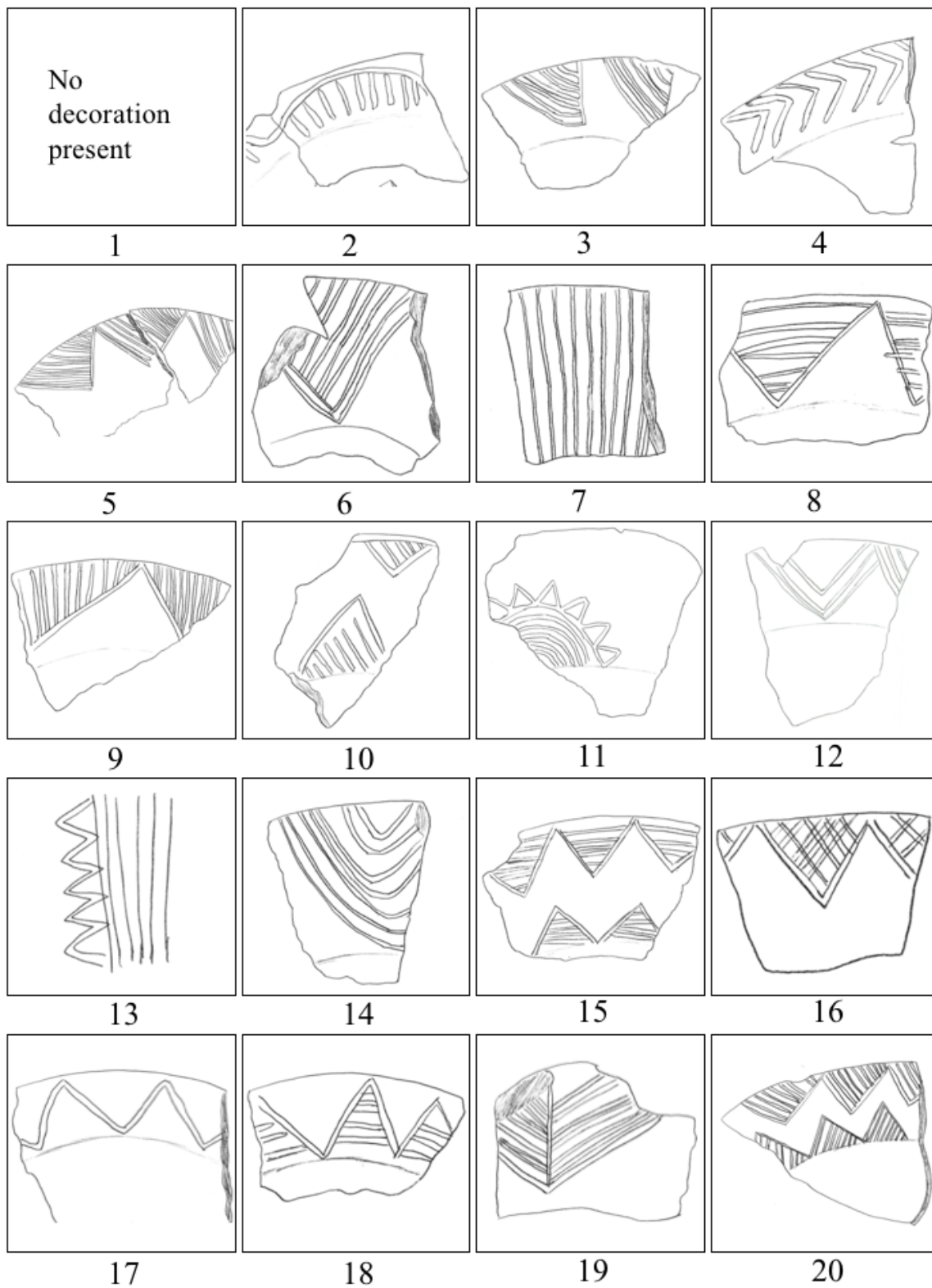
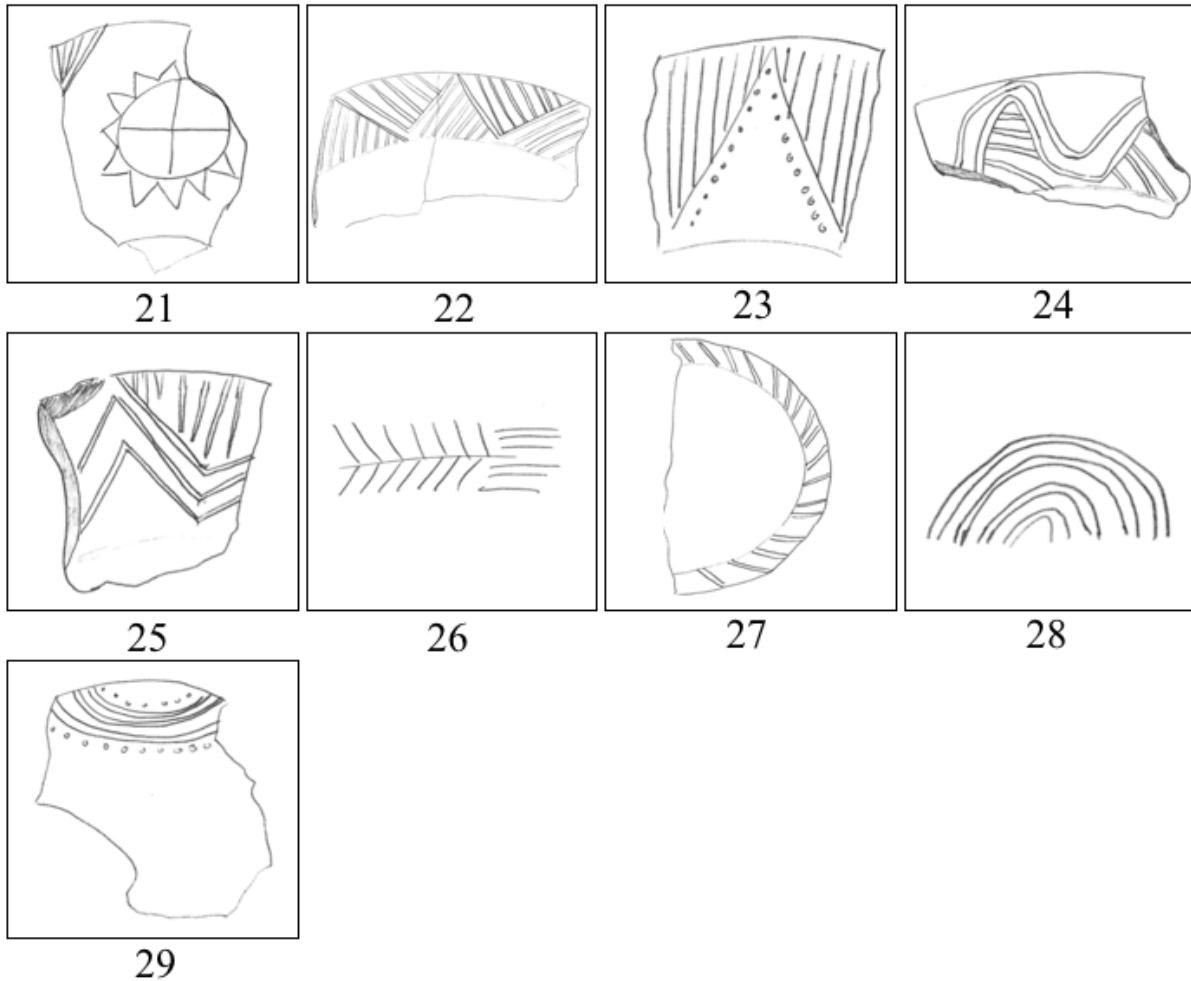


Figure 6.6 Sketch tracings of plate decoration motif emblems

Figure 6.6 (cont.)



coefficients were calculated using scripts written by Matthew Peeples and Gianmarco Alberti in the R statistical platform that were edited by the author (see Appendix C for the relevant code). These scripts calculate raw and rescaled BR coefficients as well as a Monte Carlo procedure to assess differences among samples that are likely the result of sampling error (DeBoer, et al. 1996).

The most important aspects of a particular network model are the definition of nodes and the types of tie used to construct relationships between the nodes. Spatially bounded archaeological sites represent nodes in this study. Shared categorical identities as evidenced by

proportional similarity in stylistic decoration on serving plates among sites is the type of network tie considered. Ties were assigned by defining a threshold similarity value for the Brainerd-Robinson (BR) coefficient scores. The threshold value was chosen through an evaluative framework that considers a Monte Carlo procedure that simulates BR scores from randomly generated matrices based on the actual proportions of design group categories present at each site. That is, the matrix in Table 6.2 was column and row randomized with replacement 10,000 times. The distribution of the BR coefficient values for the randomized matrices provides an estimate of the overall range and frequency of BR scores that might be expected by chance given the number of sites and relative counts for each design category. The random distribution and observed distribution of rescaled BR coefficients are shown in Figure 6.7. While neither the

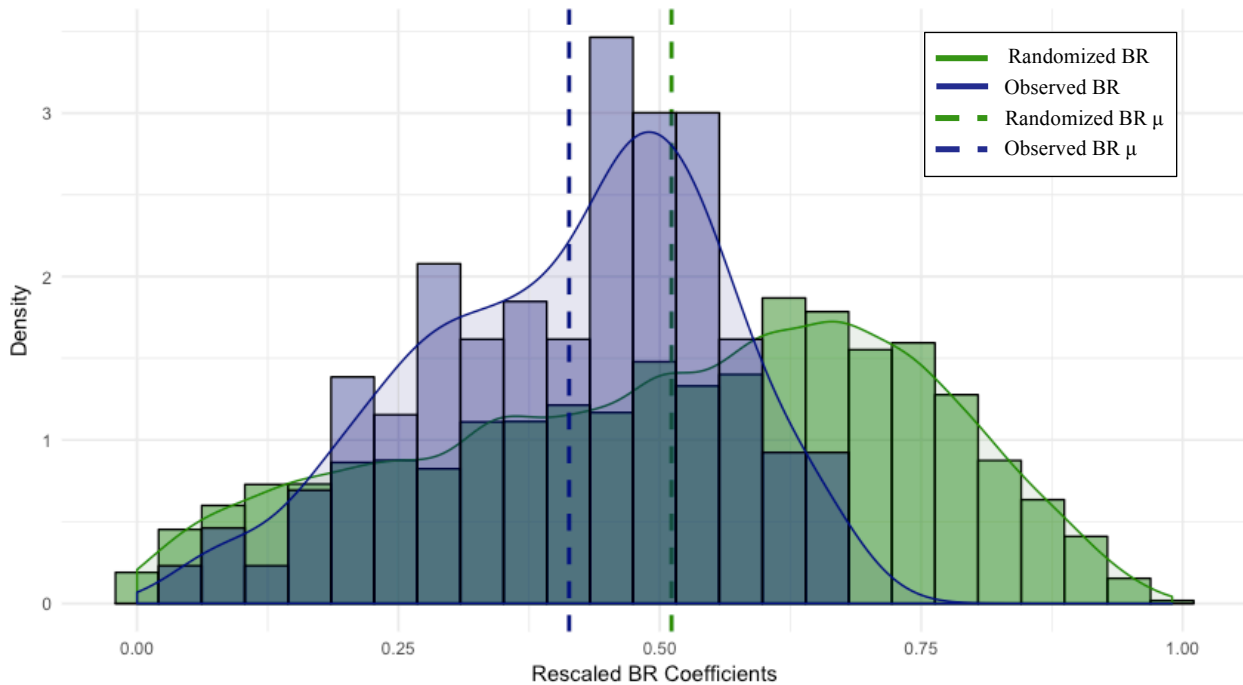


Figure 6.7 Distribution of Brainerd-Robinson coefficients for simulated (green) and observed (blue) design category matrices

simulated nor observed BR coefficient distributions are characterized by a normal distribution, the simulated data set does show a closer approximation and wider range of BR values overall. This indicates that the underlying structure of relationships among archaeological site-nodes is markedly different from what might be expected by chance. Ties between site-nodes are given for all rescaled BR coefficient scores greater than the mean BR value for the observed data set. This is an arbitrary value ($BR > 0.4$) but follows the heuristic of giving a tie between two site-nodes when categorical identities among them are more similar than they are different based on the range and frequency of observed similarity scores. Further, this allows the most robust relationships among site-nodes to be modeled and evaluated using network graphs. Network data was handled in the R statistical package and exported to Gephi 0.9.2 (Bastian, et al. 2009) for visualization. Geographic network visualizations were rendered in Gephi and overlain on vectorized LiDAR maps using the open-source Inkscape program, version 0.92.2. Slight jittering of site geographic coordinates was applied to protect site locations. LiDAR maps are provided courtesy of the Illinois Geospatial Data Clearinghouse and the University of Illinois at Urbana Champaign. Network statistics were calculated using Gephi 0.9.2 and the R tidyverse and igraph package suites (Kolaczyk and Csárdi 2014; Wickham and Grolemund 2017).

Network statistical measures provide insight into the nature of network topology, or overall structure. Network statistical measures assessed here include mean degree, or average number of edges among nodes in the network; mean weighted degree, or the average of the sum of edge weights among nodes in the network; diameter, or number of steps in the longest path from one node to another; mean path length, or average number of steps for each node to reach every other node; density, or proportion of observed ties compared to the number of possible ties; transitivity, which is also known as the global clustering coefficient, or proportion of

transitive triples wherein all three nodes in a triad are connected (Wasserman and Faust 1994). Degree, betweenness, closeness, and eigenvector centralization indices quantify the range or variability of individual actor indices. Centralization indices extend the concept of individual node centrality to the entire network. Degree centralization assesses whether or not all nodes are only connected to a singular central node. Betweenness centralization evaluates the extent to which an individual actor is located ‘between’ other actor pairs – actors in this ‘between’ space for many actor pairs are likely more critical information conduits. Closeness centralization considers how many actors are within one step, or are ‘close’, to a central node. Finally, eigenvector centralization gauges the degree to which central actors are connected to all other central actors.

In addition to relying on formal methods in the statistical analysis of network data, interpretations are based in part on conditional uniform graph tests through Monte Carlo simulation. Each observed network statistic was compared against the distribution of that statistic generated from 5,000 random graphs of the same order (or number of nodes) and probability of an edge being given between any two nodes (based on the observed graph’s density) or size (number of edges) using the Erdős-Rényi graph randomization technique (Erdős and Rényi 1959). Network randomization simulation enables formal hypothesis testing of whether the observed network statistics are unusually high or low given what might be expected if the same probability of edges (or number of edges) were connected to the same number of nodes as the observed network based on random chance alone.

Erdős-Rényi graph models place equal probability on all graphs of a given order and size. That is, a collection of graphs are considered based on the provided order and size and a probability is assigned to each, where the total number of distinct node pairs are considered

(Kolaczyk and Csárdi 2014). An extension provided by Gilbert (1959) enables the random graph concept to be extended to graphs of a fixed order but where each pair of distinct nodes are independently assigned based on a given probability.

Site	Design Group Category																													
	1	2	3	4	5	6	7	8	9	10	11	12	13	14	15	16	17	18	19	20	21	22	23	24	25	26	27	28	29	
Baehr South [^]	0	0	0	0	3	0	2	0	0	0	0	0	0	0	0	0	0	0	0	2	2	0	0	0	0	0	0	0	0	0
Buckeye Bend ^{<}	0	0	0	0	4	0	0	1	1	0	0	0	0	0	0	1	0	1	0	1	0	0	0	0	0	0	0	0	1	0
Crabble [^]	2	0	0	1	23	2	3	2	3	8	10	1	1	1	1	1	0	0	0	1	0	0	4	0	0	0	0	1	1	
Emmons [∨]	7	0	0	0	5	1	0	1	0	0	0	1	0	0	1	0	2	1	0	0	0	0	0	0	0	0	0	0	0	
Houston-Shryock [∨]	3	0	0	0	9	0	0	0	0	0	0	1	0	0	0	0	0	1	1	0	0	0	0	0	0	0	0	3	0	
Kingston Lake [∨]	8	1	0	0	21	0	1	2	2	0	0	1	0	0	0	0	1	0	0	0	0	5	0	0	0	2	1	0	0	
Larson [∨]	6	0	0	1	13	0	0	4	2	1	0	2	0	0	2	0	0	1	0	4	0	1	0	0	0	0	0	1	0	
Lawrenz Gun Club ^{<}	5	1	0	0	5	0	0	1	1	1	3	2	0	0	0	1	5	0	1	1	0	1	0	1	0	0	1	1	0	
Morton Village [^]	4	0	0	0	4	0	0	0	0	0	0	0	0	0	7	0	1	0	0	3	0	1	2	0	1	0	0	1	2	
Myer-Dickson [∨]	1	0	0	0	8	0	0	0	1	0	0	0	0	0	3	0	0	0	0	0	0	1	0	0	0	0	0	0	0	
Orendorf C [∨]	14	4	3	2	2	0	0	0	0	0	0	0	0	0	0	0	0	0	0	0	0	0	0	0	0	0	0	0	0	
Star Bridge [^]	7	0	0	0	21	1	1	3	1	0	10	1	0	1	7	2	0	1	0	13	2	2	0	2	1	0	0	0	0	
Ten Mile Creek [^]	2	0	0	0	4	0	0	0	0	0	0	1	1	0	0	1	0	1	0	1	0	0	0	0	0	0	0	0	1	
Walsh [∨]	2	0	0	0	4	0	1	0	1	0	1	1	0	0	3	0	1	1	1	0	0	0	0	0	0	0	0	0	0	
Total	62	7	3	4	126	4	8	14	12	10	24	11	2	2	26	6	10	8	3	27	4	11	6	3	2	2	5	5	4	

Table 6.2 Counts of vessels by site and design category; ∨ indicates pre-migration occupation (1200 – 1300 A.D.), ^ indicates post-migration occupation (1300 – 1450 A.D.), < indicates occupation(s) that span(s) the pre- and post-migration time periods

6.5 Results and Discussion: Social Identification in the Late Prehistoric CIRV

A correlation matrix of all rescaled Brainerd-Robinson coefficients is shown in Figure 6.8. As was apparent based on the histogram representation of the BR coefficients in Figure 6.7, there is a complete lack of coefficient values above 0.70, which corresponds to a raw BR value of 140. This result is in line with prior work in the region which indicates that town and village sites generally exhibit ceramic individuality (Conrad 1991; Harn 1994). Nevertheless, there is

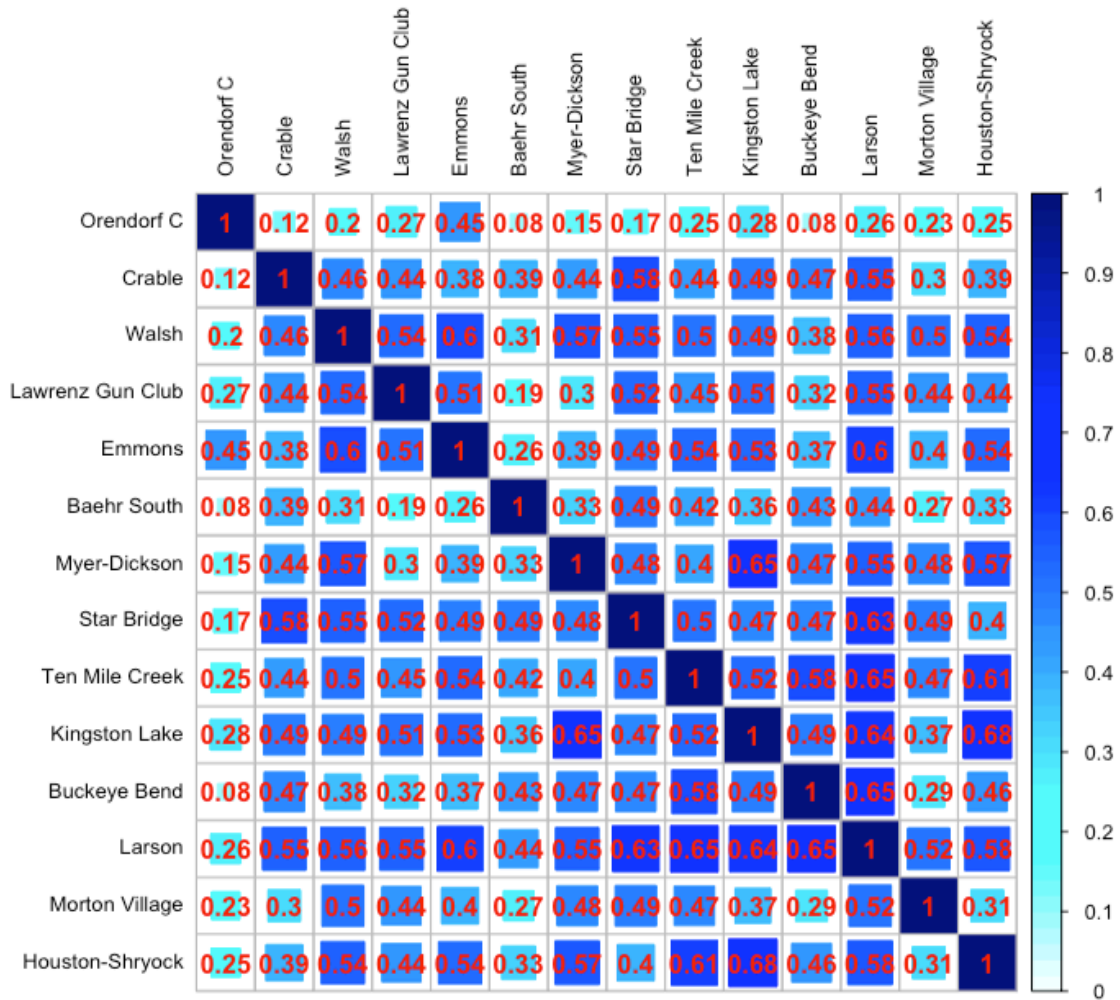


Figure 6.8 Correlation Matrix Heat-Map of Rescaled Brainerd-Robinson Coefficients

a strong cluster of BR coefficient values between the threshold of $BR > 0.40$ and $BR < 0.68$ with which to model networks of social categorical identification on either side of a circa A.D. 1300 in-migration of Bold Counselor phase Oneota peoples into the Mississippian CIRV.

Network visualizations are presented in Figures 6.9 – 6.14. Visualizations are presented in one of two ways. First is through the use of a multilevel layout algorithm that finds a global optimal layout while approximating short and long-range forces (Hu 2005). In other words, site-nodes with strong similarities are laid out in closer proximity in consideration of all site-to-site relationships. The second layout method uses randomly jittered, or modified, geographic coordinates of sites in a geographic network rendering. In each visualization, site-nodes are colored and sized based on weighted degree, which is the sum of relationship (edge) weights. The edges connecting nodes are colored and sized by weight, or the strength of similarity in social identities. That is, edges that are darker green and larger reflect stronger similarities in categorical identification among sites, and darker green and larger site-nodes indicate that a given site is characterized by a high degree of proportional similarities in categorical identification on plates to many other sites.

Several key changes are evident in central Illinois River valley network graphs as well as in their associated network statistical measures (Table 6.3). Perhaps the most significant change to network topology from the pre-migration to the post-migration CIRV is in transitivity, or the global clustering coefficient. As shown in the results of Erdős-Rényi random graph models for the Mississippian period (Figure 6.14), the transitivity value is significantly higher than what might be expected based on chance. In fact, transitivity in the pre-migration CIRV is higher than 99.94% of random graphs constructed based on the same number of nodes and edges as the pre-migration network. Transitivity is a measure of network cohesion and assesses the proportion of

	Pre-Migration	Post-Migration	Flattened Across Time
<u>Summary Statistics</u>			
Nodes	9	7	14
Edges	24	15	39
Mean Degree	5.333	4.286	5.571
Mean Weighted Degree	2.922	2.057	2.907
<u>Network Size Measures</u>			
Diameter	3	2	4
Mean Path Length	1.389	1.286	1.692
<u>Network Topology Measures</u>			
Network Density	66.7%	71.4%	42.9%
Transitivity	80.7%	72.2%	64.6%
Degree Centralization	0.208	0.286	0.264
Betweenness Centralization	0.219	0.128	0.237
Closeness Centralization	0.336	0.519	0.299
Eigenvector Centralization	0.277	0.299	0.386

Table 6.3 Central Illinois River Valley Social Identification Network Statistics

node triads in which all three nodes are connected (Scott and Carrington 2016), capturing the notion that a ‘friend of a friend is a friend’ (Collar, et al. 2015). In the pre-migration CIRV, this notion holds true some 80.7% of the time, indicating an unusually highly interconnected network based on shared ascription to common social categories. This is perhaps best illustrated in Figure 6.9, which shows one large cluster of highly interconnected sites with a single outlying site, Orendorf’s Settlement C. Orendorf is a multi-component site and one of the earliest occupied Mississippian town sites in the CIRV (Conrad 1991; Esarey and Conrad 1981). The dearth of edges to Orendorf Settlement C in the pre-migration network suggests that it may have been occupied prior to the regional scale expression of categorical identities on plates, especially given the preponderance of plates with no decoration present at the site (Table 6.2, Design Group Category 1).

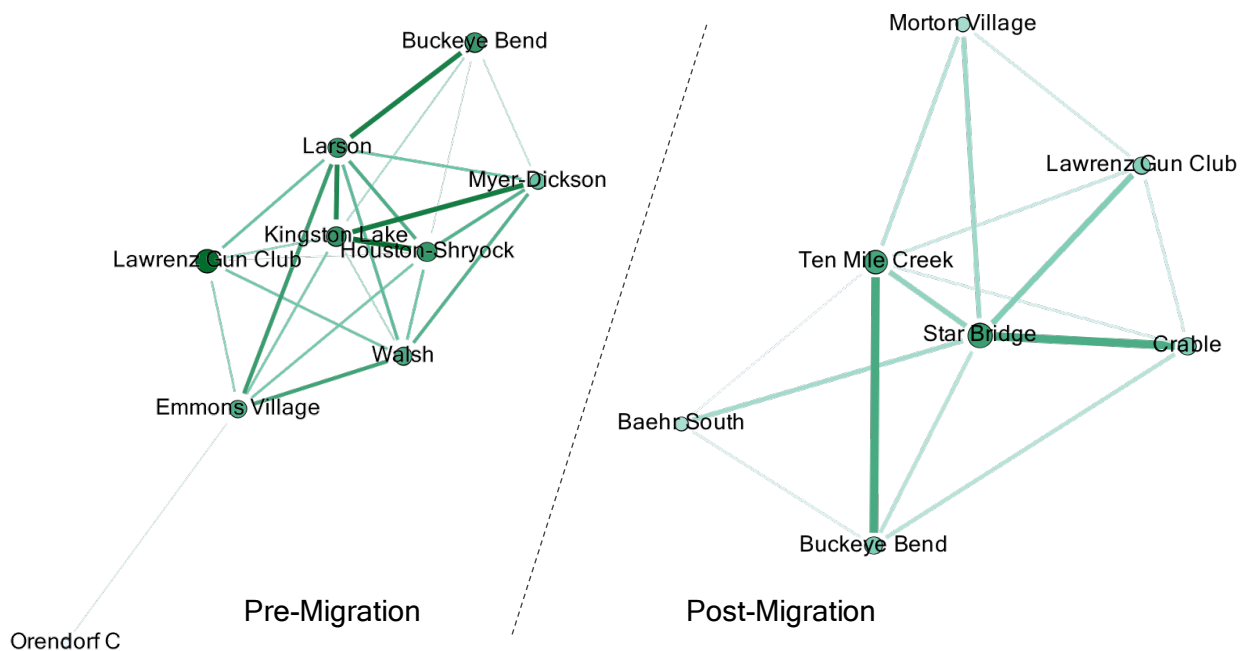


Figure 6.9 Yifan Hu multilevel network graph layout for the Pre-Migration Time Period (1200-1300 A.D.; left) and Post-Migration Time Period (1300-1450 A.D.; right)

Following Oneota in-migration, transitivity is no longer statistically significant (see Figure 6.15), indicating a reduction in the scale at which there is parity in ascription to categorical identities. That is, the strong tendency for triads of site-actors in the Mississippian phases who shared connections based on similarities in ascription to common social categories to become fully connected no longer held true in the post-migration CIRV. Thus, global scale ascription to categorical identities in the Mississippian CIRV gave way to ascription to categorical identities at a reduced social scale. This can be interpreted as a reduction in homophily, or the tendency of socially similar actors to interact more frequently than socially dissimilar actors, and an indication of greater regional variability in ascription to common social categories in the post-migration time period (McPherson, et al. 2001). Indeed, the range of the number of design categories present at sites sharply increases from the pre-migration to post-

migration time periods, with the two sites that straddle both time periods showing an intermediary number of design categories present (Figure 6.17).

Reduced homophily and/or greater regional variability in ascription to common social categories in the post-migration CIRV is further supported by a significant reduction in the mean weighted degree, or the average of the sum of all edge weights among nodes, from 2.922 to 2.057. That is, the average similarity in social identification among sites in the post-migration CIRV reduces by 30% from the pre-migration Mississippian period. While the number of site-nodes decreases overtime, the proportion of site-node connectedness actually increases relative to the number of sites present. Thus, while the post-migration CIRV can be characterized as a dense network with many transitive triads, the degree of similarity in social identities is on average significantly reduced from that of the Mississippian period.

In considering the role of network relationships in structuring Oneota in-migration, comparing the geographic network renderings in Figures 6.10 and 6.11 provides key insight. A spatial aggregation process is evident in the post-migration CIRV, wherein regional emphasis in social identification processes shifted away from the Spoon and Illinois River confluence, to Ten Mile Creek in the north and Star Bridge in the south. Only one modest Mississippian site in the Spoon-Illinois confluence area, Buckeye Bend, remained occupied or saw a sequential occupation in the post-migration time period. The sudden depopulation of the Spoon-Illinois confluence suggests the formation of an internal frontier, or unoccupied interstice between settlements (Kopytoff 1987). The internal CIRV frontier was apparently attractive to Oneota migrants as the only other sites occupied in the area are multi-cultural sites marked by the cohabitation of Mississippian and Oneota peoples, such as Morton Village, as well as three modest Oneota habitation sites not able to be included in this analysis due to a paucity of plates

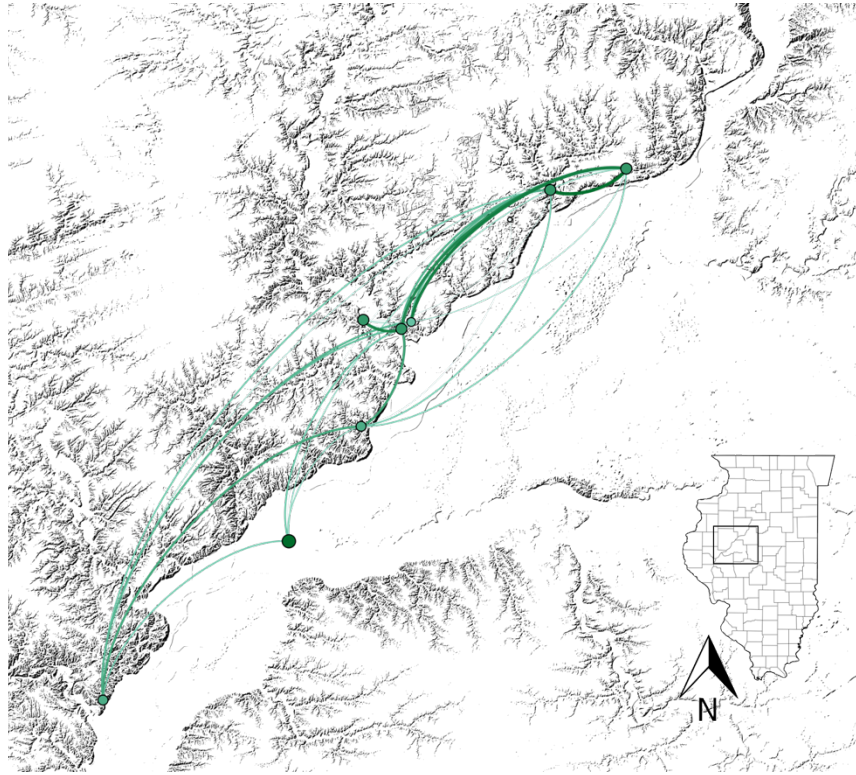


Figure 6.10 Geographic network graph layout for the Pre-Migration Time Period (1200-1300 A.D.)

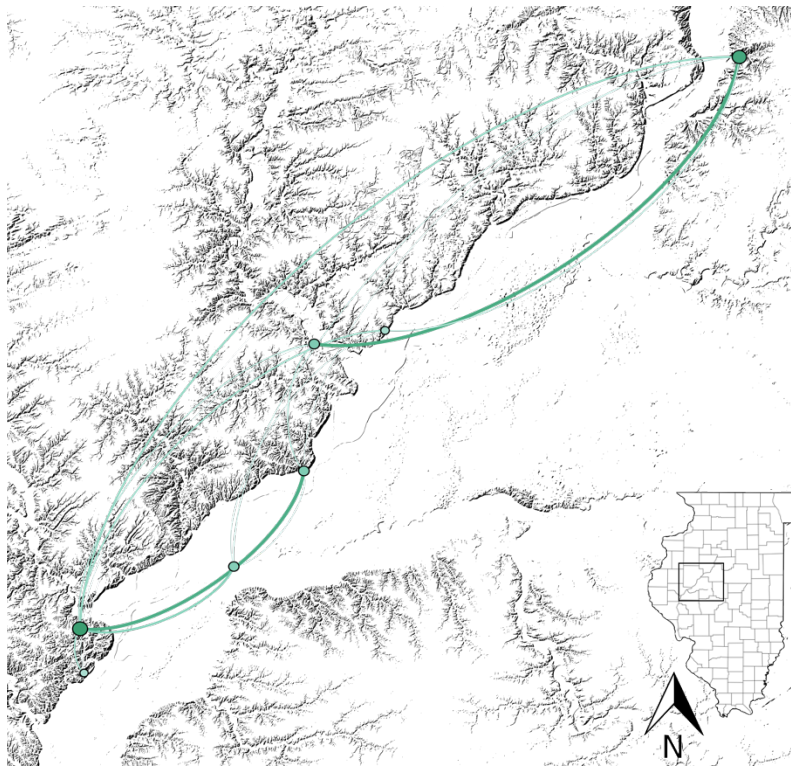


Figure 6.11 Geographic network graph layout for the Post-Migration Time Period (1300-1450 A.D.)

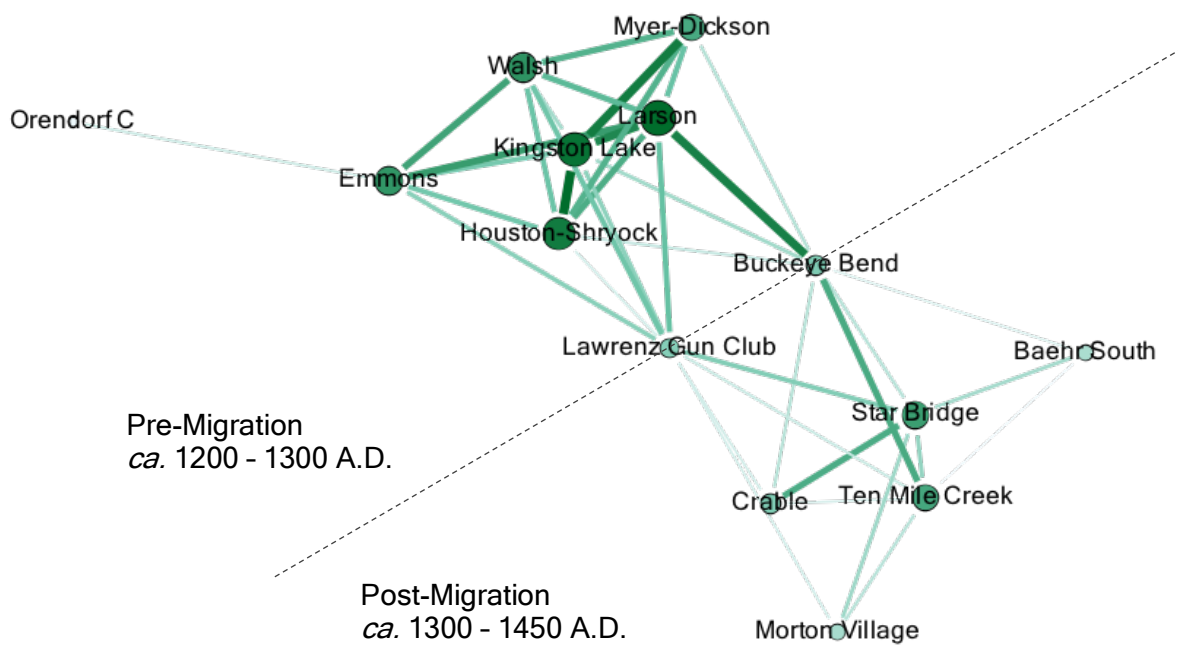


Figure 6.12 Yifan Hu multilevel network graph layout flattened across time (1200 – 1450 A.D)

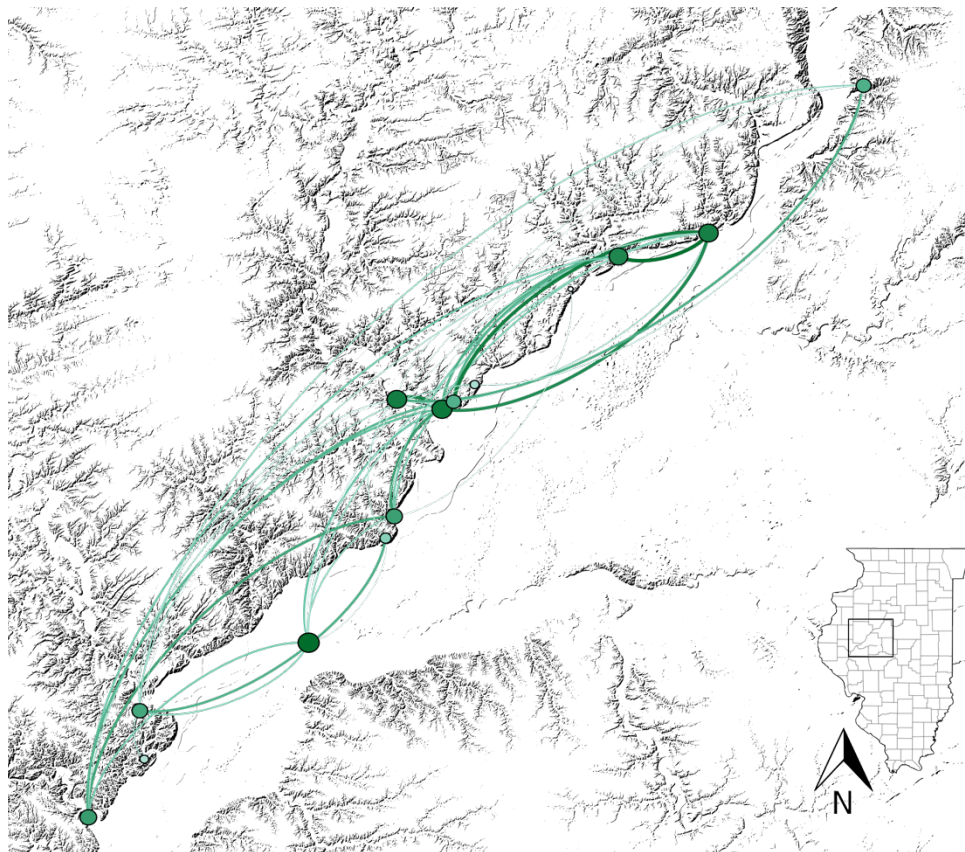


Figure 6.13 Geographic network graph layout flattened across time (1200 – 1450 A.D)

present (Esarey and Conrad 1998). In other words, Oneota migrants followed the tendency of migrant peoples seen in other archaeological contexts, such as the American Southwest, to move into areas that were less densely settled (Mills, et al. 2016; Peeples and Haas Jr. 2013). Oneota in-migration therefore coincided with, and was likely in some way structured by, increasing regional diversity in social identification categories and a reduction in the scale of parity in social identification network relationships among Mississippian peoples in the CIRV.

Internal frontiers offer many advantages for both migrant and indigenous peoples (Kopytoff 1987; Mills 2011). For example, Kopytoff (1987:14) emphasizes the unfolding of social processes occurring in internal frontiers due to its nature as an institutional vacuum. The low centralization scores, which assess the range of relations in social networks directed toward central nodes, attests to a lack of centralized authorities in either the pre- or post-migration time periods. From a relational perspective, densely connected and highly identity-conformist insular areas such as the Mississippian CIRV present significant challenges for the establishment of novel relationships with exogenous groups. Internal frontiers characterized by low population densities and a lack of central authority, on the other hand, offer opportunities for network-mediated migration where migrants and host peoples initially form weak, or bridging, ties before forming stronger bonding ties based on a high-degree of within group cohesion (Granovetter 1973; Mills, et al. 2016). However, unlike the model for ethnogenesis occurring out of this growth of immigrant-host settlement relationships proposed by Kopytoff (1987:6), the frontier internal to the post-migration late prehistoric CIRV was less likely a locus of integrative social capital and more likely a locus of cultural pluralism. The preponderance of weak ties formed by the multi-cultural populations at Morton Village and Crable as shown in Figures 6.9 and 6.11 (i.e. ties not modeled or modeled as thin, light-green ties) suggests that the social diversity

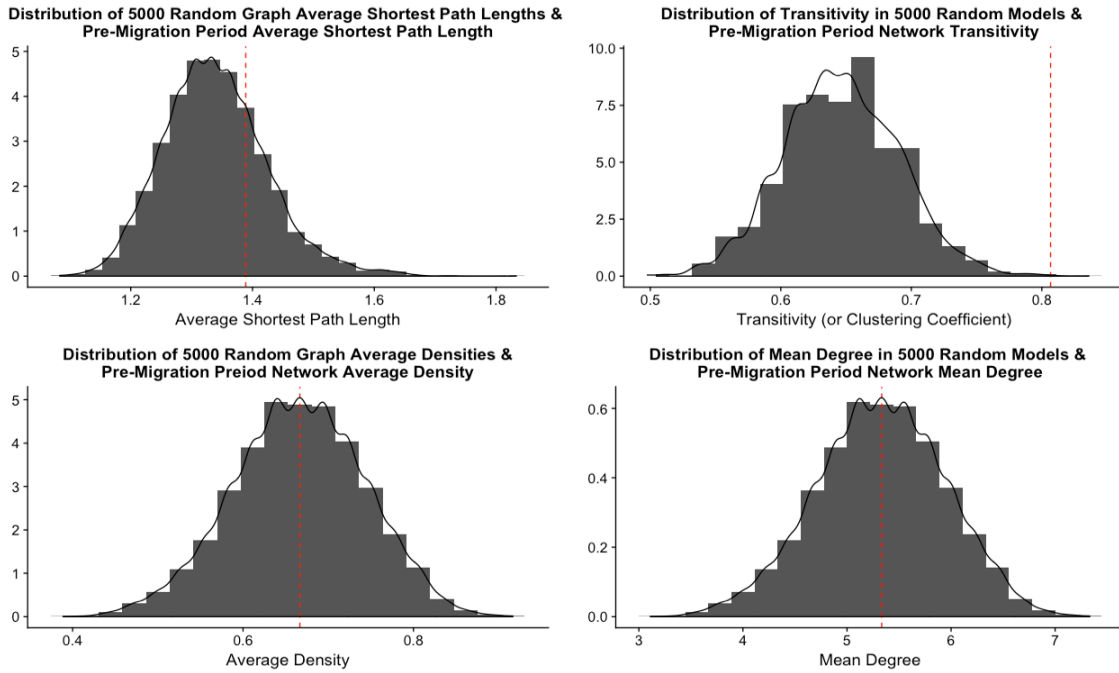


Figure 6.14 Network randomization results for pre-migration social identification network. Observed statistic represents red line. Histogram shows distribution of statistic based on network randomization of 5000 random graphs using the Erdős–Rényi random network modeling technique.

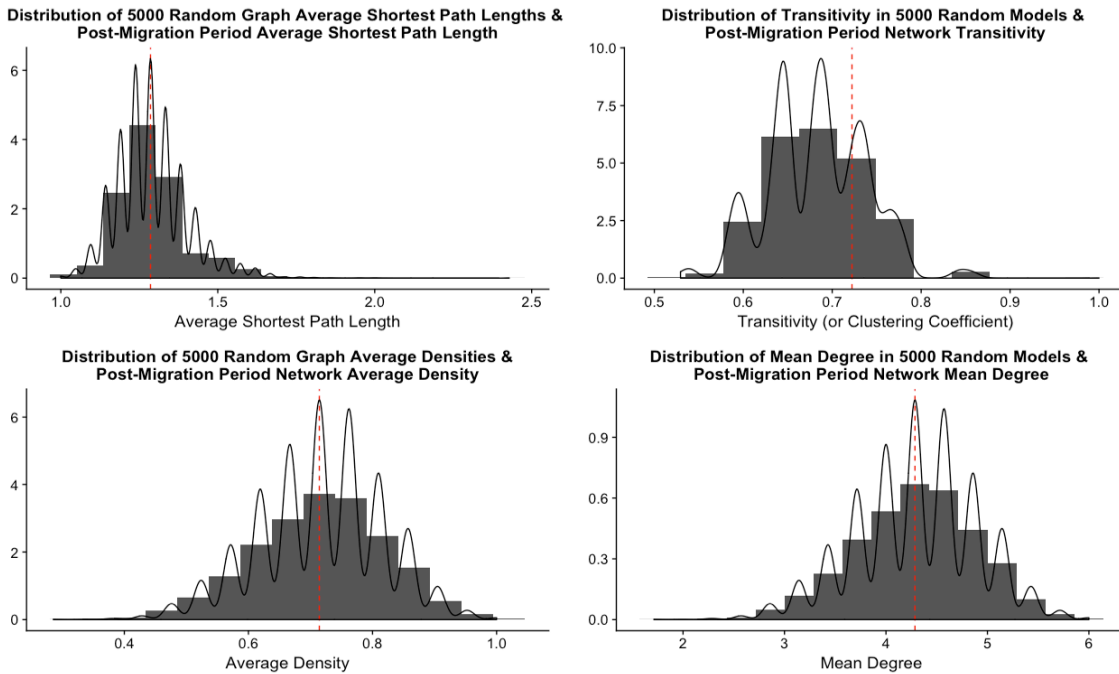


Figure 6.15 Network randomization results for post-migration social identification network. Observed statistic represents red line. Histogram shows distribution of statistic based on network randomization of 5000 random graphs using the Erdős–Rényi random network modeling technique.

imbued by Oneota peoples into the region perhaps exacerbated on-going trends toward regional non-conformity in social identities among Mississippian peoples. Furthermore, non-conformity in social identification is argued to be a delimiting factor in processes of collective social action, processes that can otherwise lead to social transformation at broad geographic and demographic scales (Mills, Clark, et al. 2013; Nelson, et al. 2011; Peeples 2011, 2018). As a result, any disruption to regional similarities in social identification by Bold Counselor phase Oneota peoples likely contributed to decreased cooperation and increased social stresses and conflict (Bengtson and O’Gorman 2017; G. R. Milner, et al. 1991; J. J. Wilson 2010).

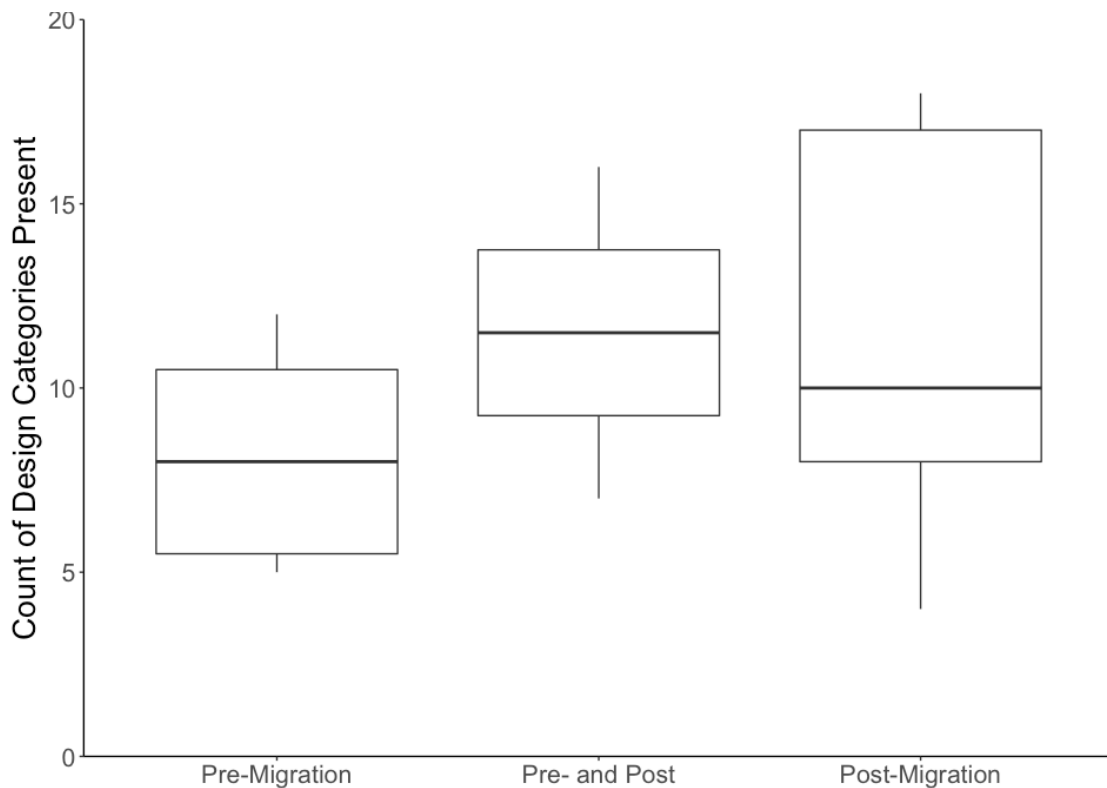


Figure 6.16 Histogram showing the range of design categories present at sites in different CIRV time periods

Significant intra-regional mobility evidenced by the movement Late Mississippian peoples away from the Spoon-Illinois River confluence is posited here to have created a point of cultural inflection, wherein “new practices or beliefs may be adopted or when old ideas may be

more readily challenged” (Cobb and Butler 2006:334). As likely potters (Rice 2005), Mississippian women were active participants in the process of both expanding the range of social categories and challenging prior regional conformity in networks of social identification across the Middle to Late Mississippian transition. The introduction of design categories with distinctly Oneota characteristics, such as wet-paste trailed *and* punctate decorations, indicates some localized inclusivity among potter communities in indexing social identification. However only two sites, Crable and Morton Village, show marked evidence for this sort of inclusivity. A dearth or complete lack of characteristically Oneota decoration motifs at the other five town and village sites occupied in the post-migration time period indicates that cultural pluralism was largely pursued by Late Mississippian peoples in the CIRV. Perhaps it is these forces that intensified regional societal strife as there is no evidence, radiocarbon or otherwise, of any substantial settlement in the central Illinois River valley succeeding the post-migration time period until the proto-historic period (Esarey and Conrad 1998:52-53).

In discussing macro-scale regional population movement during the 15th century in the American midcontinent, Cobb and Butler (2002:638) remark that “the diffusion of Oneota groups southward toward the Mississippian world appears to have been met with some violence (e.g., Milner et al. 1991), and Mississippian communities in the Illinois Valley and the American Bottom may have been rousted or integrated against their will.” By focusing on networks relationships of social identification, this research has shown that Mississippian communities were far from being passively rousted or integrated into Oneota communities. In fact, a much more nuanced cultural contact scenario is more in line with the empirical evidence presented here. Oneota peoples were indeed integrated in select inclusive Mississippian social contexts and appear to be integrative of Mississippian peoples in some of their own communities, but the

majority Mississippian population in the region largely maintained cultural pluralism while they perhaps grappled with internal flux in both social and demographic processes.

6.6 Conclusion

Movement of Oneota peoples into the Mississippian central Illinois River valley provides a unique window into the role of networks of social identification in structuring, and being restructured by, migration. In this regional, or micro-scale (Mills, et al. 2015), application of social network analyses in archaeology I have argued that Oneota in-migration coincided with increasing regional diversity in social identification categories, a reduction in the scale of parity in social identification network relationships, and intra-regional mobility toward consolidation among Mississippian peoples. Through the formation of a spatial and social internal frontier, these processes likely structured Oneota in-migration.

Oneota social identification processes in-turn appear to have restructured Mississippian network relationships. The permeation of distinctly Oneota design motif categories into the region resulted in weak integration of multi-cultural Oneota and Mississippian sites into the larger post-migration identification network, perhaps exacerbated on-going trends toward regional variation and non-conformity in social identities among Mississippian peoples.

Ultimately, the cultural contact between Mississippian and Oneota peoples is an example of unsuccessful longevity in a multi-cultural social environment. After only two or three generations, the CIRV was abandoned by Late Prehistoric peoples. However, the CIRV was not the only region in the midcontinent to witness regional depopulation in the fifteenth century. Coeval chiefly polities in the American Bottom, lower Ohio valley, and central Mississippi valley each collapsed and were abandoned during this tumultuous period (Cobb and Butler 2002). While many analyses of societal collapse focus on environmental factors (Bird, et al.

2017; Weiss and Bradley 2001) this research offers an alternative perspective by showing changes in networks of social identification preceding abandonment and population displacement.

Accepting the women were potters responsible for the plate decorations that form the basis of network models of social identification presented here, it can be concluded that women were active participants in the process of ascribing regional scale conformity to CIRV Mississippian social categories in the pre-migration period and then in asserting increasing variability overtime based on both a proliferation of social categories and decrease in proportional similarity among settlements in the post-migration CIRV. Bold Counselor phase women were likewise active in indexing ascription to distinctly CIRV Oneota social categories on a uniquely Mississippian ceramic vessel form. These results attest to the value of an inductively empirical relational perspective on processes of social identification in the past.

CHAPTER 7 NETWORKS OF ECONOMIC RELATIONSHIPS: RESULTS OF THE CHEMICAL ANALYSES

7.1 Introduction

This chapter presents the results of laser ablation inductively coupled plasma mass spectrometry (LA-ICP-MS) analysis of clay samples and Mississippian and Oneota pottery from west-central Illinois. This archaeological context, also referred to as the central Illinois River valley (or CIRV), is particularly apt for investigating social interactions through provenance studies as a result of a circa 1300 A.D. in-migration of Oneota peoples into a Mississippian chiefly environment and the compelling evidence for regional, and in places household, scale multicultural cohabitation among these peoples. Explaining social interrelationships in settings characterized by coexisting material culture traditions has been a critical concern in archaeology, particularly in settings where differing traditions merge, blend, or otherwise amalgamate (Frangipane 2015; Liebmann 2013; Stone 2003). By using ceramic chemical compositional data, this chapter assesses changes in patterns of economic interactions related to ceramic industry prior to and succeeding an in-migration in order to better understand behavioral response trends by both indigenous and migrant peoples to multi-cultural regional cohabitation. That is, it is argued that increasing parallels of membership in chemical compositional groups reflect increasing economic relationships among sites. Addressing direct or indirect economic relational interaction through the exchange of finished vessels, the sharing of raw source material location information, or involvement in similar ceramic production processes provides a complementary perspective to recent trends in archaeological network science that emphasize relationships modeled by technological or stylistic similarities in material culture (Birch and Hart 2018; Borck, et al. 2015; Hart and Engelbrecht 2012; Mills, Clark, et al. 2013; Mizoguchi 2009).

Results of network analysis and simulation indicate that the Mississippian CIRV was characterized by economic network interrelationships related to ceramic industry of an unusually cohesive nature, supporting an interpretation of regional scale economic interaction patterns. This pattern changed dramatically in concert with a circa 1300 A.D. in-migration of an Oneota tribal group into the region. The succeeding analysis indicates that post-migration ceramic industry economic network structure is characterized as highly dispersed with many fewer and weaker relationships, suggesting a reduction in the spatial and social scale at which economic relationships related to ceramic industry were pursued. Furthermore, network structure in the post-migration period is argued to be reflective of the presence of a social and spatial internal frontier, which was a possible outgrowth of buffer zone or other territorial boundary changes among Mississippian peoples in the CIRV and was likely impactful in structuring Oneota in-migration. Finally, Mississippian and Oneota pottery were chemically indistinguishable, indicating that potters from both cultural groups in the Late Prehistoric period CIRV were utilizing similar or identical raw clay sources, engaging in similar paste preparation and ceramic production regimes, and discarding vessels in ways that did not result in diagenetic differentiation.

7.2 Ceramic Industry Economic Relationships

Addressing direct or indirect economic interaction related to ceramic industry is a vital third line of evidence to compare to network models that capture categorical identification and social interaction. Leveraging the criterion of abundance and circa 7 km radius ethnographic catchment zone for the procurement of raw clay materials (Arnold 1985; Bishop, et al. 1982), it is argued that as similarities of membership in different compositional groups converge between

archaeological communities, so does the likelihood that individuals from those communities engaged in more frequent direct or indirect economic interaction. As used here, economic network relationships related to ceramic industry are built around the concept of ‘weak ties’ (Granovetter 1973). In contrast to ties that are built on deep affinity such as family or marriage relationships, weak ties might be formed with acquaintances or strangers with a common cultural background. That is, weak ties are fertile grounds for connecting individuals within communities or segments of society that otherwise may not frequently interact, “providing contexts where categorical identities could have been expressed and contested” (Peeples 2018:64).

Because quality clay resources are not ubiquitously available and seldom overtly visible in the densely vegetated central Illinois River valley, shared membership between two sites in groups identified through the geo-chemical compositional analysis of ceramic artifacts is therefore likely to be an indicator of economic interaction through behaviors reflective of weak ties. Direct economic interaction related to ceramic industry may take the form of behaviors such as the exchange of vessels or resource outcrop information sharing. While indirect interaction may occur through overlapping resource exploitation areas or shared paste preparation and ceramic production regimes. Each of these behaviors may have somewhat less influence in forming network relationships than other social interactions but, again, are important because they can connect distinct social milieu that might otherwise be partially or wholly separate.

While exchange relationships often may be rooted in close personal relationships that are passed down through the generations, they are also often sporadic and unpredictable depending on the geographic scale at which goods were moved (Brose 1994; Ford 1972; Zvelebil 2006). At the inter-regional scale, material culture, and in particular burial goods, shows clear connections between Mississippian peoples in the CIRV and symbolically adorned exotic items characteristic

of the Southern Cult, or pan-Mississippian cosmological symbolism. These include but are not limited to shell gorgets, Ramey knives, copper pendants, engraved marine shell, flint clay effigy and figurine pipes, stone discoidals, and copper-coated earplugs (Brown and Kelly 2000; Conrad 1989, 1991; Harn 1971, 1980, 1991; Knight Jr 1986). However, there is no currently robust evidence of intra-regional exchange during Late Prehistoric period CIRV. The intra-regional movement of ceramic vessels in particular is often rooted in ritual more so than routine (Fie 2006; Wallis, et al. 2016). However, intra- and inter-regional quotidian ceramic vessel movement, and therefore the likely exchange of domestic goods or movement of individuals, is increasingly being recognized in the archaeological record (Gjesfjeld 2018; Golitko and Terrell 2012; Niziolek 2013; Peebles 2018; Stoner and Glascock 2012; Stoner, et al. 2008).

Exchange and other economic relationships are posited to primarily act to develop or reinforce social relationships between individuals or groups in non-state societies (Renfrew 1984). From a cultural transmission perspective, economic relationships modeled based on geochemical compositional groups may show that potters and potter communities not only resided within a particular geographic location, and perhaps engaged in exchange relationships, but also shared specific information about how to procure and prepare their raw materials (Neff 1993). This perspective expands upon stylistic and technological perspectives of pottery production because ethnographic accounts indicate that, in non-state and non-market contexts, while women are typically responsible for the production of vessels it is often men that are responsible for digging out and gathering raw clay (Rice 2005; Skibo and Schiffer 1995).

Referring to these types of tie as economic in nature is not meant to reify or place *a priori* value upon ceramic vessels (Wallis 2009:48-54), but is rather meant to signify the transmutability of ceramic vessels themselves and emphasize an alternative perspective to how

relationships among individuals can be (re-)constructed in archaeological settings. Because ceramic vessel chemical compositions are the product of much more than simply the composition of raw materials, an approach is warranted that considers how a predominance of shared membership in chemical compositional groups may reflect behavioral interactions in an archaeological context. Here, I argue that an approach rooted in social network analysis (Scott 2000) is an apt methodology for providing interpretive utility to the compositional analysis of ceramic artifacts. That is, social network analysis is well suited to extracting broader understanding from variation in compositional group membership among archaeological settlements because network analysis is explicitly concerned with modeling relationships and overall network structure. The following sections apply this approach with the goal of identifying behavioral nuances regarding the economic nature of ceramic industry prior to and following the circa 1300 A.D. in-migration of Oneota peoples into the central Illinois River valley.

7.3 Central Illinois River valley Geology

This section discusses the geological backdrop of the central Illinois River valley, particularly as it relates to the distribution of clay resources that may have been utilized by Late Prehistoric potters. Potential clay sources include clay or shale weathered from bedrock deposits, clay from alluvium and lacustrine deposits, and clay from modern soil profiles developed into the Peoria loess. Due to the overall trend in bedrock geological variation and available alluvium and lacustrine deposits as one moves from northeast to southwest along the Illinois River and its primary tributaries, it is hypothesized that chemical differences may characterize clay resources. As a result of the potential variability of the locations of usable clay resources accessible to prehistoric potters, chemical differences may therefore be reflected in archaeological ceramics.

Pertinent to the availability of clay for Late Prehistoric potters in the CIRV are bedrock features of Mississippian and Pennsylvanian geologic age that underlie much of the Late Pleistocene and Holocene aeolian loess deposits in the bluffs of the western Illinois Valley. Regionally, bedrock strata are flat-lying to gently sloping on the western margin of the Illinois Basin. These massive bedrock structural features follow a general northeast to southwest orientation. Pennsylvanian sediments underlie most of the study area, except for outcrops along valley walls where the Illinois River and the La Moine River cut through them and expose rocks of the older Mississippian system (see Figure 7.1) (Kolata 2005; Wanless 1957). Pennsylvanian rocks rest unconformably on strata belonging to the Burlington, Keokuk, Warsaw, Salem, and St. Louis formations of the Mississippian system with the resistant St. Louis limestone likely

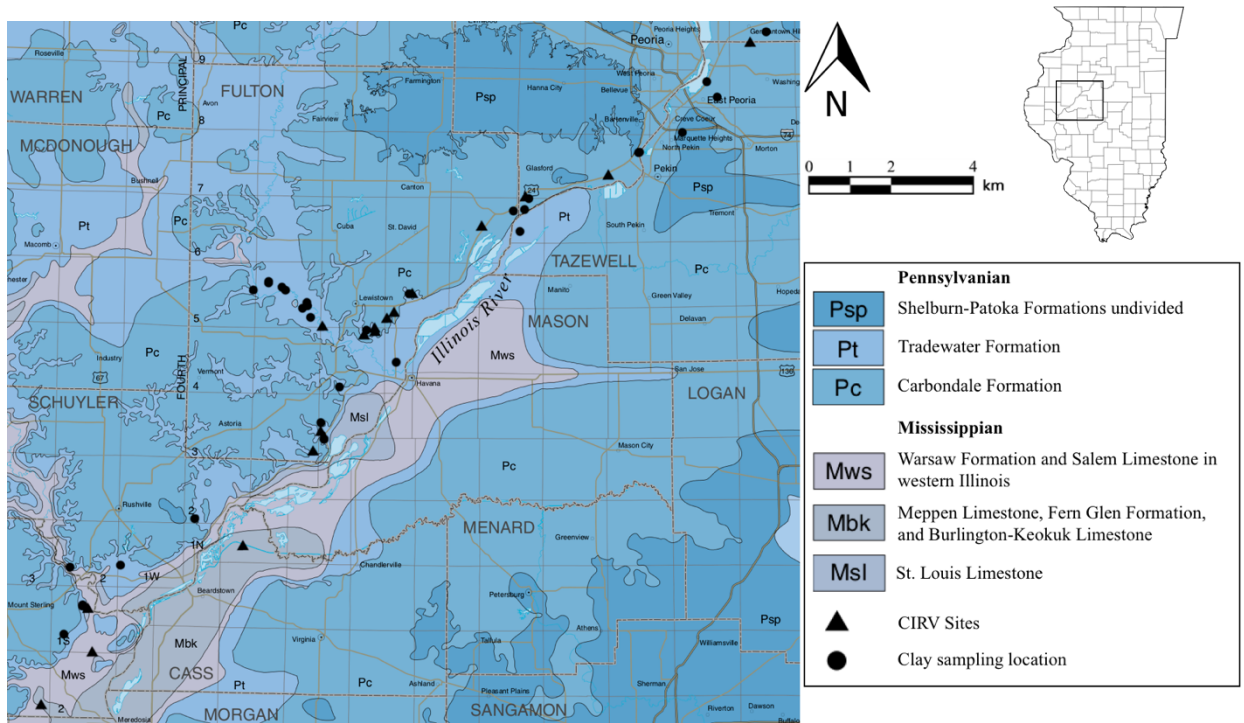


Figure 7.1 Bedrock geology map of the CIRV showing locations of archaeological sites and clay samples. (adapted from Kolata 2005)

forming much of the uplands and the soft Warsaw shale the lowlands (Wanless 1957). Clayey shale with ironstone concretions overlies marine limestone in the uppermost layers of

Pennsylvanian cyclothems, or cyclical repetitions of beds. The shales in these cyclothems, as well as coals and sandstones appear to thin and disappear toward the southwest, with much of the thinning occurring within the Tradewater group (Horberg 1950). While the Spoon River eroded Pennsylvanian strata down to the Tradewater group, the more southerly La Moine River (also known as Crooked Creek) eroded completely through Pennsylvanian strata such that Mississippian strata are continuously exposed along it. Mississippian strata exposed by fluvial erosion from the La Moine primarily consist of limestones and thin beds of shale of the Valmeyer series.

The uplands and lowlands were subsequently mantled with aeolian loess during the Pleistocene burying the bedrock surface. The mantling reaches 80 ft thick or more on the western bluffs of the Illinois Valley. The loess mantling consists of Late Wisconsin age till that extends southward to the Bloomington Moraine in eastern Peoria and Tazewell counties and Illinoisan till plain and morainal ridges that extend from the Bloomington Moraine westerly to the Mississippian River Valley (Figure 7.2) (Curry, et al. 2011). A final mantle of loess and Sangamon Geosol developed in till and pre-Wisconsin loess, mostly preserved only south of the Wisconsin till limit (Edwin Hajic, personal communication 2018).

Loess would make an unlikely candidate for clay used in prehistoric pottery. As a result, clay would more likely be sourced from bedrock outcrops, alluvium and lacustrine deposits, or modern soil profiles developed in loess. This would inherently delimit the availability of potential clay sources to a certain extent, particularly for clay weathered from bedrock strata to locations along valley walls where alluvial or other forces expose otherwise deeply buried outcrops (Figure 7.1; Figure 7.2 A-A').

The availability of alluvial and lacustrine clay deposits is largely related to fluvial action along the Illinois River, whose course and valley extent is largely the result of a single event (or events) known as the Kankakee Torrent. It is worth noting, however, that prior to the Kankakee Torrent late Wisconsin outwash aggraded the Illinois Valley floodplain, which remodeled

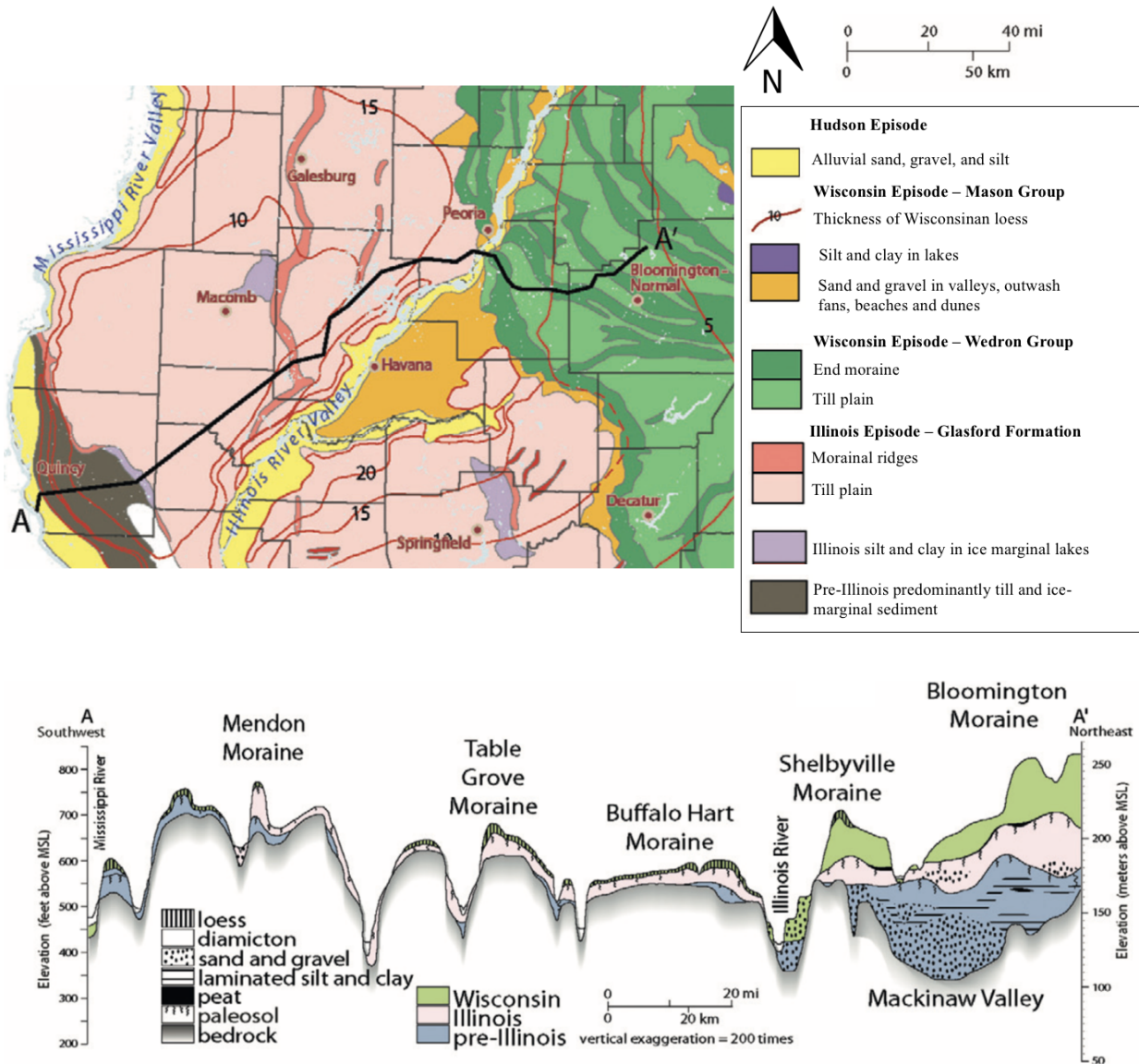


Figure 7.2 Surfacial deposits of west-central Illinois. Cross-section A-A' shows the increased thickness of the glacial sediments approaching Lake Michigan. Adapted from (Curry, et al. 2011)

outwash terrace remnants remain but decrease in percent of valley area as one moves southerly down the valley (Hajic 1990).

The Illinois River Valley is a dynamic fluvial system largely defined in the Pleistocene and Holocene by fluvial response to glaciation, deglaciation, and the ensuing interglacial conditions. Other significant factors influencing landscape evolution include climate and base level fluctuations in the Mississippi Valley. To a lesser extent, glacio-static and tectonic adjustments were likely impactful as well (Hajic 1990). A sequence of three depositional subsystem processes in the late Quaternary acted as controlling factors. First, is a Late Wisconsin Glacial Stage catastrophic flood subsystem. Glaciation in the upper Mississippi Valley resulted in early aggradation on the order of 20-25 m between 26,000 and 19,500 C¹⁴ year B.P. At the end of this aggradation, the Mississippian River drainage diverted from its course in the modern Illinois Valley to its present valley, leading to a reworking and net incision of the valley train in the Illinois Valley as the Lake Michigan Lobe downwasted and retreated (Hajic 1990).

Beginning circa 19,000 cal year B.P., catastrophic glacial lake outburst floods known as the Kankakee Torrent were catalyzed by a large influx of meltwater into proglacial lakes from a subglacial reservoir in the Lake Michigan Basin during the Haeger glacial phase of the Lake Michigan Lobe and unleashed immense volumes of melt-water into the Illinois floodplain (Curry, et al. 2014; Hajic 1990). Glacial dam breaches in the vicinity of Marseilles, IL circa 15,500 C¹⁴ year B.P. (19,000 cal year BP) scoured the Illinois floodplain into bedrock, resulting in the 26-mile expanse of the Illinois River floodplain and cutting and exposure of the valley walls seen in the Late Prehistoric period and today. Thick sand, gravel, and sediment accumulation followed in the wake of the torrent. A lacustrine subsystem existed in the Illinois valley following Kankakee scouring. The Illinois River then developed a series of natural levees

at approximately the altitude of modern natural levees. These levees were the result of Holocene (9,800 – 9,700 C¹⁴ year B.P.) discharge from Lake Agassiz and an initial phase of lacustrine sedimentation that caused incision and terrace formation in the adjacent Mississippi Valley (Hajic 1990). Much of the remaining thick deposition lying at the bottom of the Illinois Valley lacustrine subsystem deposited by the Kankakee Torrent was then re-scoured by the Flag Lake paleochannel as early as or before 9,180 C¹⁴ year B.P. in the Emiquon and surrounding vicinities (Hajic 2006:71; Harn and McClure 2012). Over the next 3,000 – 6,000 years, the major lacustrine basins in the Illinois Floodplain were remodeled by fluvial action before conditions stabilized to those seen in the Late Prehistoric archaeological period (Harn and McClure 2012). During this period of major lacustrine basin stabilization, deep perennial lateral lakes evolved into emergent floodplains as a result of extensive erosion of loess off the surrounding uplands, which was deposited in valley lakes and alluvial fans (Hajic 1990).

Subsequent post-Kankakee Torrent history of the Illinois River Valley is one of fine aggradation. This infers that little has changed regarding the bedrock valley wall outcrops since the Kankakee Torrent (circa 19,000 cal year BP) aside from the accumulation of colluvium at their base.

The preceding discussion suggests an overarching regional trend of increasing variability in the location of accessible usable clay resources as one moves down the central Illinois Valley. In particular, shale or clay deposits of sufficient quality to produce pottery of Mississippian geologic age would likely only be accessible to potters in the south and central-south portions of the CIRV. While quality clay deposits of Pennsylvanian and Pleistocene age would be available across the valley, Pennsylvanian bedrock sediments and Pleistocene glacial till outwash sediments would be more abundant in the north and central-north portions of the valley. Thus,

subtle northeast-southwest chemical distinctions are hypothesized to characterize available clay resources and therefore sherd chemistry at different sites in the Late Prehistoric CIRV.

7.4 The Ceramic and Clay Sample

The present study intends to compositionally compare CIRV ceramics prior to and following Oneota in-migration in order to investigate potential changes in patterns of economic network relationships related to ceramic industry in the valley overtime. The sampling strategy employed four primary goals toward this end. First, I sought to examine pottery from major population centers and smaller outlying sites across the geographic and temporal expanse of the Late Prehistoric period CIRV (~1200 – 1450 A.D.). Second, inasmuch as possible I attempted to sample sherds from different contexts within a single site. Third, sherd samples were selected from two distinct vessel classes: domestic cooking jars and plates (or broad-rimmed bowls) (Conrad 1991; Harn 1994). And, fourth, for sites exhibiting ceramics with both Mississippian and Oneota characteristics at the household level, a representative sample of vessels with design elements characteristic of both cultural groups was analyzed (Esarey and Conrad 1998). This strategy allows estimation of variability between sites, within sites (where possible), between vessel classes primarily used in different social contexts (cooking/storing compared to serving/eating), and between cultural groups. A total of 34 clay samples were also analyzed in order to attempt to link patterns in raw material sources to patterns in sherd chemistry (Figure 7.1). Finally, three shell tempering samples were analyzed as well to aid in correcting for the abundance of aplastic tempering material. In total, 620 samples were analyzed: 583 ceramic, 34 clay, and 3 shell tempering. Table 7.1 provides summary information on the number and type of ceramic samples analyzed from each of the 18 sites included.

Due to the regional scale focus of this study in discerning patterns of economic relationships prior to and following an intrusive in-migration, it was necessary to sample ceramics from existing archaeological site-assemblages. Many assemblages derive from surface, amateur, or illicit collection activities such as the unfortunate whole-sale deep plowing of sites. This often precludes analysis of contextual within-site variation and the inclusion of other lines of evidence such as architectural patterns or other ancillary evidence as potential explanatory variables.

Site	Jars	Plates	Total
Baehr South	6	9	15
Buckeye Bend	8	12	20
C.W. Cooper	28		28
Crabbe	26	29	55
Emmons	15	15	30
Eveland	30		30
Fouts Village	9	11	20
Houston-Shryock	14	16	30
Kingston Lake	20	20	40
Larson	20	20	40
Lawrenz Gun Club	19	21	40
Morton Village	29	29	58
Myer-Dickson	13	16	29
Orendorf C	15	15	30
Orendorf D	21	9	30
Star Bridge	13	16	29
Ten Mile Creek	24	5	29
Walsh	10	20	30
Total Ceramic Samples	320	263	583

Table 7.1 Distribution of pottery samples by site and vessel type

7.5 Ceramic Paste and Clay Chemical Characterization Using LA-ICP-MS

Laser ablation inductively coupled plasma mass spectrometry (LA-ICP-MS) and multivariate statistical techniques for the handling of compositional data have been described at length elsewhere and as a result are summarized here in truncated form (Baxter 2008, 2015; Bishop and Neff 1989; Dussubieux, et al. 2007; Glascock 2016; Neff 1993, 1994, 2012; Sharratt, et al. 2009; Speakman, et al. 2007). LA-ICP-MS was conducted at the Field Museum of Natural History Elemental Analysis Facility using an Analytik Jena (formerly Varian) quadrupole ICP-MS (Elliot, et al. 2004) coupled to a NewWave UP213 laser ablation system (helium carrier gas, 213 nm laser operated at 0.2 mJ and a pulse frequency of 15 Hz) (Dussubieux, et al. 2007).

The clay samples collected during field survey were cleaned of visible organic and inorganic debris, dried in an oven set to 100 °C for four hours, and subsequently left to completely dry out over several weeks. Clay samples were then pulverized using a mortar and pestle, rehydrated with ultra-pure de-ionized water, and formed into discs. The clay discs were fired up to 600 °C using a Paragon Viking High Fire Kiln™ with a Sentry 2.0 Controller™. Several studies suggest that firing temperature has no appreciable effect on chemical composition of clays (Sharratt, et al. 2009:799), however this method was followed to ensure consistency in pre-treatment of all clay samples.

Ceramic sample preparation consisted of the production of a small sherd fragment by using channel locks to make a controlled break off a larger sherd (usually about 1-2 cm²). Ceramic samples were arranged in the ablation chamber perpendicular to the shell tempering present in order to avoid temper grains or other aplastic inclusions. Ablation was constrained to the center portion of each sherd so that analysis concentrated on pastes as opposed to slips, paints, or other surface contamination on the exterior or interior of the sample sherds.

Protocols established for the Field Museum's Elemental Analysis Facility were followed for LA-ICP-MS analysis (Dussubieux, et al. 2007; Golitko 2010; Golitko and Terrell 2012; Niziolek 2013; Vaughn, et al. 2011). Clay and ceramic samples were subjected to laser ablation with a spot size of 150 μm . Every effort was made to avoid temper grains or other aplastic inclusions during ablation location selection. A blank measurement and National Institute of Standards and Technology (NIST) standards n610, n612, and Brick Clay (n679) were run at the beginning of the day and after every five or six samples to aid in concentration calculations and control for any drift in accuracy or precision of measurement. Error values were established through the analyses of New Ohio Red clay, which was subjected to the same protocols as the standard samples (Sharratt, et al. 2015).

Using silica (^{29}Si) as an internal standard to control for the time variability in ablation efficiency and resulting signal strength, each sample was ablated in 10 distinct locations and each standard ablated in 5 distinct locations. Each sample ablation measurement consists of nine replicates (scans of the entire elemental mass range of measured elements). The first three of the replicates are removed during data processing to account for any potential surface contamination and to allow the signal time to stabilize. The remaining replicates are averaged to produce raw count-per-second signal strengths for each ablation location. Concentrations were then calculated by subtracting blank measurement values and internal standardization of elemental signals using silica. The resulting signals were averaged after the deletion of extreme outlier values on an element-wise basis. Outlier measurements often result from the accidental targeting of temper and other aplastic inclusions or occasional large influxes of trace element ions into the detector relative to silica. Concentrations were then calculated using a linear least-squares fit regression

line derived from the silica-normalized signals for the standard reference materials (Golitzko 2010; Gratuze, et al. 2001).

Isotopes of 60 major, minor, and trace elements were measured (⁷Li, ⁹Be, ¹¹B, ²³Na, ²⁴Mg, ²⁷Al, ²⁹Si, ³¹P, ³⁵Cl, ³⁹K, ⁴⁴Ca, ⁴⁵Sc, ⁴⁹Ti, ⁵¹V, ⁵³Cr, ⁵⁵Mn, ⁵⁷Fe, ⁵⁹Co, ⁶⁰Ni, ⁶⁵Cu, ⁶⁶Zn, ⁷⁵As, ⁸²Se, ⁸⁵Rb, ⁸⁸Sr, ⁸⁹Y, ⁹⁰Zr, ⁹³Nb, ⁹⁵Mo, ¹⁰⁷Ag, ¹¹¹Cd, ¹¹⁵In, ¹¹⁸Sn, ¹²¹Sb, ¹³³Cs, ¹³⁷Ba, ¹³⁹La, ¹⁴⁰Ce, ¹⁴¹Pr, ¹⁴⁶Nd, ¹⁴⁷Sm, ¹⁵³Eu, ¹⁵⁷Gd, ¹⁵⁹Tb, ¹⁶³Dy, ¹⁶⁵Ho, ¹⁶⁶Er, ¹⁶⁹Tm, ¹⁷²Yb, ¹⁷⁵Lu, ¹⁷⁸Hf, ¹⁸¹Ta, ¹⁸²W, ¹⁹⁷Au, ^{206,207,208}Pb, ²⁰⁹Bi, ²³²Th, ²³⁸U). A number of elements have been observed as being

	Average	SD	%RSD		Average	SD	%RSD
Li	130.196 ±	14.13	11%	Ba	582.686 ±	73.60	13%
Be	3.157 ±	0.31	10%	La	46.084 ±	14.68	32%
B	136.131 ±	28.26	21%	Ce	106.478 ±	29.23	27%
P	327.149 ±	241.26	74%	Pr	12.119 ±	4.04	33%
Cl	286.325 ±	334.25	117%	Ta	1.799 ±	0.34	19%
Sc	21.596 ±	4.08	19%	Au	0.037 ±	0.08	212%
Ti	5488.957 ±	1316.82	24%	Y	32.090 ±	9.79	31%
V	213.309 ±	23.90	11%	Pb	17.892 ±	4.14	23%
Cr	88.854 ±	8.00	9%	Bi	0.676 ±	0.52	77%
Mn	256.581 ±	30.86	12%	U	3.289 ±	0.80	24%
Fe	28174.564 ±	10405.83	37%	W	2.959 ±	0.54	18%
Ni	77.784 ±	8.25	11%	Mo	1.240 ±	0.20	16%
Co	23.067 ±	2.97	13%	Nd	37.954 ±	13.02	34%
Cu	30.542 ±	57.26	187%	Sm	7.465 ±	2.60	35%
Zn	116.666 ±	17.05	15%	Eu	1.596 ±	0.52	32%
As	16.550 ±	4.55	28%	Gd	6.112 ±	2.17	36%
Rb	195.345 ±	24.66	13%	Tb	0.993 ±	0.28	28%
Sr	73.393 ±	16.43	22%	Dy	5.359 ±	1.35	25%
Zr	146.909 ±	47.59	32%	Ho	1.211 ±	0.34	28%
Nb	24.565 ±	3.86	16%	Er	3.131 ±	0.74	24%
Ag	0.213 ±	0.32	150%	Tm	0.515 ±	0.15	29%
In	0.132 ±	0.03	21%	Yb	3.218 ±	0.80	25%
Sn	4.162 ±	1.06	26%	Lu	0.559 ±	0.16	29%
Sb	1.828 ±	1.92	105%	Hf	5.238 ±	2.92	56%
Cs	11.352 ±	1.75	15%	Th	16.214 ±	3.79	23%

Table 7.2 Elemental summary statistics measured across 131 replicates of New Ohio Red clay

unreliably measured overtime at the EAF laboratory due to such factors as oxide interferences, high ionization energies, or measurements close to instrumental detection limits, and as such were removed from statistical analysis (^{35}Cl , ^{75}As , ^{82}Se , ^{107}Ag , ^{178}Hf , ^{197}Au , ^{209}Bi). New Ohio Red clay standards indicate that additional elements display consistent differences across analyses and were also removed from statistical analysis as a result (^{31}P , ^{65}Cu , ^{121}Sb). New Ohio Red clay was analyzed using the same protocol as the NIST standards and provides a means to assess error values associated with analysis and to maintain consistency between analyses. Table 7.2 lists these approximated error values as average elemental concentration in ppm, standard deviation, and percent relative standard deviation. Relative standard deviations are a reflection of the heterogeneity inherent in clay (Neff 2003) as well as the large number of New Ohio Red clay standard runs ($n = 131$) over the course of many years of analysis (2015 – 2018). In addition, ^{137}Ba was shown to have markedly increased values in ceramic samples compared to clay samples, likely as a result of post-burial absorption of mobile cations in the presence of zeolite formation (Golitzko 2010), and was subsequently removed from analysis.

7.5.1 Controlling for Shell Tempering

Both Oneota and Mississippian potters in the Late Prehistoric period CIRV almost exclusively used burned and crushed mollusc shell as an aplastic inclusion to improve performance characteristics of pottery (Conrad 1991). These benefits include improved workability of clay during the vessel formation process (Feathers 2006), increased strength and toughness (Feathers 1989), and increased thermal shock resistance of the finished vessel (Steponaitis 1983, 1984; Tite, et al. 2001). Shell tempering was shown to have no discernible ‘leachate’ effect as alkali processor of maize (A. J. Upton, et al. 2015). However, improved

workability and performance characteristics provide clear advantages to the use of shell tempering over prior grog, sand, or limestone tempers based on increased demands of food processing and production among maize horticulturalists and agriculturalists.

To understand localized geochemical patterning in mollusc shell, three samples of shell temper grains were subjected to LA-ICP-MS. Tempering samples derived from sherds recovered from three sites that span the geographic expanse of the CIRV – one sample from Kingston Lake in the northerly portion of the valley, one sample from Myer-Dickson in the center of the valley at the Spoon and Illinois River confluence area, and one sample from Lawrenz Gun Club in the southerly portion of the valley. Calcium comprises 96-97% of the geochemical composition of shell and as a result was removed from statistical analysis. For the minor and trace elements, only Strontium and Barium register a noticeable chemical presence in shell and as a result were also removed from statistical analysis. A further mathematical correction was applied to account for the presence of shell-temper derived calcium for ceramic samples.

Despite my best efforts, shell tempering embedded in the ceramic matrix was frequently ablated during sample analysis. These sampling errors were straightforward to detect when examining individual ablation ICP-MS assessments, which showed high calcium and strontium values in particular relative to other ablation assessments. Given this differential impact of shell tempering on sample chemical compositions, a mathematical correction was applied to remove the impacts of shell tempering on compositional measurements. The mathematical correction used here differs from that applied by scholars working with INAA data from shell tempered ceramics due to the fact that LA-ICP-MS is not a bulk compositional analysis technique when analyzing an inherently heterogenous material such as ceramic matrix (Cogswell, et al. 2015). While there is a degree of error related to the spot-sampling procedure of LA-ICP-MS based on

inherent sample variability, a number of studies demonstrate that this loss of precision does not prohibit an adequate characterization of the clay fraction of ceramic samples and generally replicates the results of INAA (Cochrane and Neff 2006; Dussubieux, et al. 2007; Golitko 2010; Wallis and Kamenov 2013).

In LA-ICP-MS analysis, constituent atoms are measured directly, but the use of silica as an internal standard results in raw measurements as ratios of elements to silica. As a result, a means of independently calculating silica concentrations is needed, the customary approach of which is to sum all element signals and assume that these account for approximately 100% of the sample matrix. Because all major oxides can be quantified directly aside from oxygen, oxide multipliers are used to account for its otherwise unmeasured contribution to the sample and the remaining portion is assumed to be accounted for by silica. Parts per million or oxide percentage concentrations for all elements are then calculated by multiplying through the resulting silica concentrations (Golitko 2010; Gratuze, et al. 2001). As a result, to mathematically correct for the differential presence of calcium, which is measured as an oxide, all other elements measured as an oxide percentage are summed aside from calcium for each sample. The elemental or percent oxide signature of every other element is then divided by this amount on a sample by sample basis. Thus, for samples that were not negatively impacted by erroneous ablations of shell tempering (i.e. low calcium concentrations), little to no correction is applied to measured elemental concentrations, while the inverse is true for samples highly negatively impacted by erroneous shell ablations.

7.5.2 *Statistical Routines in the Analysis of Geochemical Data*

The statistical approach taken here mirrors an approach that has become somewhat standardized in the analysis of chemical compositional data in archaeology (Baxter and Buck 2000; Bishop and Neff 1989; Glascock 1992, 2016; Harbottle 1976; Neff 1994). The following discussion provides an overview of these methods in general but with a particular focus on the analysis of ceramic artifacts. Originally developed by Sayre and colleagues during the 1970s at Brookhaven National Laboratory, the primary goal of multivariate statistical analysis routines is the identification of compositionally homogenous groups among observed samples and to link those groups to a source location. Depending on the type of artifact, however, compositional groups may reflect different ‘sources’. That is, a source of origin may refer to a circumscribed exposure of geologic raw material or to a production locale or workshop. In other words, samples derived from different raw materials necessitate different provenance determination strategies. Here, I refer to these distinct methods as ‘natural source’ and ‘production source’ methodologies.

‘Natural source’ grouping methodologies are used for non-chemically altered artifacts such as obsidian, gemstones, flint, basalt and the like. Raw materials from various outcrop locations are collected, analyzed, and used to create statistically valid compositional groups. Artifacts are then compared to these natural source reference groups in order to identify the most likely geologic source of origin for each artifact (Glascock 2016). This method follows the provenance postulate, which states that chemical variation between raw material source locations must surpass variation with a single source (Weigand, et al. 1977). On the other hand, because raw material processing and production systems can alter the chemical composition of artifacts such as pottery, glass, coins, smelted copper, or bricks, a different approach is required. Statistically valid compositional groups are constructed from the elemental profiles of artifacts

themselves. Different production sites are then inferred based on the criterion of abundance, which assumes that if a majority of samples in a statistical cluster originate from the same archaeological site or area, then the raw material source is likely in proximity to that site or area (Bishop, et al. 1982; Gjesfjeld 2014; Rice 2005). In the case of pottery, the criterion of abundance is often coupled with ethnographic data suggesting that a vast majority of potters obtain clay from sources within seven kilometers of their settlements (Arnold 1985). I refer to this as a ‘production source’ methodology.

In either methodology, the end result are statistically valid “reference groups” that are expected to represent the limits of chemical variability associated with artifact production in a given location or region (Bishop, et al. 1988:318; Speakman, et al. 2008). In the present research, both of these approaches are followed to a certain extent, however a ‘production source’ methodology is primarily employed. That is, a clay survey was undertaken to provide a baseline for statistical patterning in raw clay materials in order to inform statistical grouping of ceramic artifacts.

Geographic spatial resolution in interpretations of compositional clustering is entirely a function of geological variability in the study area and, for pottery, the extent to which potters systematically altered baseline clay chemical composition through paste preparation techniques or ‘recipes’. Nearly all clays are characterized by a narrow range of geochemical variability, and the near ubiquity of clay on the landscape often complicates the scale at which reference groups may be defined (Golitzko 2010). Fine grained resolution is possible. For example, a study from Luzon in the Philippines identified both community scale as well as regional scale geochemical patterning, shedding light on a factionalized pottery industry enveloped in elite competition (Neupert 2000). In archaeological contexts that lack ethnographic insight regarding production

systems and source material locations, regional scale chemical patterning that follows such geographic features as river drainages, valleys, lower and higher elevations in mountainous regions, or islands is more often observed (Cochrane and Neff 2006; Emberling and Minc 2016; Golitko 2010; Lazzari, et al. 2017; Peeples 2018; Sharratt, et al. 2009; Sharratt, et al. 2015). Equivocal results can be observed in cases of small sample sizes and substantial geological complexity (Fitzpatrick, et al. 2006)

The statistical workflow utilized for compositional analysis in archaeology is displayed in Figure 7.2. In particular, this workflow includes: 1) data pre-treatment that involves normalization or standardization of elemental values and missing data imputation, 2) visualization and statistical exploration of the data set to assess patterning amenable to group formation, 3) preliminary reference group construction, 4) statistical assessment of group membership probabilities and an iterative process of sample reassignment, 5) formation of core groups, outgroups, and attribution of unassigned samples, and 6) sub-group refinement where possible (Gjesfjeld 2014; Golitko 2010; Peeples 2011). A suite of statistical methods referred to as *supervised* and *unsupervised learning* are used in these processes. Supervised learning techniques are used in ‘natural source’ grouping methodologies because the raw material source locations are already known, providing an inherent structure to the data. With unsupervised learning techniques, which are used in ‘production source’ grouping methodologies, the model or structure of the data is not known in advanced. As such, all variables are treated as equally potential sources for patterned variation. Within that patterning groups are formed. For the present analysis on clay sediments and archaeological ceramics, unsupervised learning techniques are used within a production source group recognition methodology. Formal

multivariate statistical analysis was carried out in the R statistical platform, version 3.3.2, with some data handling in Excel. All R code is provided in Appendix C.

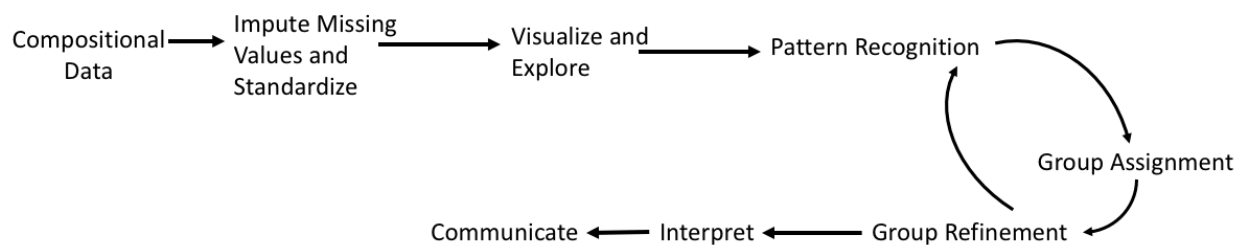


Figure 7.3 Statistical workflow for the analysis of compositional data

Beginning with retained chemical measurements, which are expressed as parts per million values, any missing values are first imputed using a variety of imputation methods such as random forest or predictive mean matching. Missing values often arise for particular elements when they are close to the detection limits of the analytical technique employed. For the present analysis using LA-ICP-MS elemental readings, these elements were removed from consideration and as a result no imputation was necessary. Retained chemical measurements are then converted to base-10 logarithms in order to account for scalar effects related to the orders of magnitude differences in concentrations across the different elements. Once data have been scaled appropriately and contain no missing values, the next step is exploratory visual analysis to search for potential patterning and begin forming exploratory chemical groupings. For this purpose, histograms, bivariate plots, compositional profile plots, and 3D scattergrams provide apt visualizations for inspection. Histograms might show multimodality, bivariate plots or 3D scattergrams might show patterning in sample densities, and compositional profile plots might show deviations from centroid masses. This process can be time consuming and show little in the way of recognizable patterning, however. For example, when analyzing biplots, there are $p(p-1)/2$ possible plots to analyze, where p is the number of elements. In the present analysis, where

44 elements are retained, that equates to some 946 biplots to investigate. As a result, a statistical means of dimensionality reduction is necessary in order to express patterned variation along multivariate dimensions in a visually interpretable format in at most two or three dimensions. Collectively referred to as ‘ordination’ or ‘gradient analysis’, these methods order similar objects near each other and dissimilar objects further away. Similarity and dissimilarity in ordination takes into account relationships across the multiple variables observed.

The primary ordination technique used in archaeological compositional analysis is principal components analysis (PCA). Because many elements have positive correlations with one another, PCA is an apt technique for compositional analysis in archaeology. That is, if any two given elements are highly correlated, they can be expressed by a single variable without a significant loss of information (Golitzko 2010). In this way, PCA acts to reduce the number of variables in the data set and therefore simplify the structure of compositional data.

In short, the goal of PCA is to transform the original multivariate data into a new representative dataset that explain as much of the variance as possible in the original data in a minimum number of variables. Orthogonal transformations convert potentially correlated variables into a set of linearly uncorrelated variables referred to as principal components (Baxter 1995; Glascock 2016; Shennan 1997). Transformations proceed in such a way that the first principal component accounts for the largest possible variance (or variability in the data). Each successive principal component has the highest possible variance orthogonal (or perpendicular) to each preceding component. Components are calculated in this way until the number of components matches the original number of variables. This necessitates that there are at least as many observations as variables when conducting PCA, though many more observations than variables are necessary to obtain robust results.

In addition to providing principal components that contain maximal data set variation in a minimum number of variables, PCA provides a matrix of eigenvalues that express the total amount of original variance explained by each component and an indication of the original variables responsible for that variation (or component loadings that show how strongly correlated each original variable is to each principal component). This gives an indication of the amount of variance accounted for by each principal component, individually and cumulatively. Variance explained is often visualized using a scree plot. For most applications in archaeology, principal components should be retained until they reach 90% of cumulative variance explained, which is often along many fewer dimensions than in the original data set. PCA therefore allows for investigation of the chemical compositional structure in the data, in the absence of information known *a priori*.

Simultaneous R-Q Mode Factor Analysis extends the functionality of PCA by allowing component loadings and sample scores to be visualized on a single biplot. By reducing the dimensionality of the data while maximizing the variance retained in each dimension and providing a sense of original variable component loadings, it is possible to visualize a significant amount of information that would otherwise be spread across multiple plots. Not only is it possible to test hypothetical group separation across multiple dimensions in a single plot, but it is also straightforward to determine which elements (or original variables) are most responsible for any observed group separation and how elements are correlated with one another. While it is tempting to assume that the first principal component, which expresses the largest amount of correlated variability in the dataset, is the most influential in contributing to group patterning, this is not always the case. Loadings on the second, third, fourth and so on principal components may in fact contribute more to patterning that is significant to anthropological, archaeological, or

geological research questions. At the same time, clear group separation may not be evident in principal components, even if they are well separated in multivariate space.

With either scaled elemental data or principal components, the next step is to begin statistical classification of observations into separate groups. It is often instructive to use *a priori* information about sample observations to inform the validity of statistical group formation. Information in this regard might include archaeological site of origin, river drainage of origin, bedrock parent material, artifact type, artifact chronological positioning, type of temper or surface treatment, or a host of other potential grouping features. These features can be incorporated into biplot visualizations of principal components or scaled elemental data to gain insight into potentially statistically meaningful clustering, much in the same way that a machine learning engineer seeks out sensitive features for training artificial intelligence algorithms. Once assumptions or hypotheses are formed as to the role of individual features in group separation, they can be tested using statistical clustering methods. A variety of unsupervised classification methods are available to form initial compositional clusters, which can then be refined into statistically robust groups. Common classification methods include hierarchical cluster analysis, hierarchical divisive clustering, k-means clustering, and k-medoids clustering (Leonard Kaufman and Rousseeuw 1990b; Shennan 1997). Neff (2002) recommends applying multiple methods and treating the resulting groups as hypotheses to be evaluated using additional statistical testing. Groups of samples that are consistently grouped across multiple methods are most likely to stand up to statistical group refinement.

Hierarchical cluster analysis (or HCA) models hierarchical relationships between samples based on a linkage criterion. A measurement of statistical similarity is required to provide a sense of the relative distance between pairs of observations and guide hierarchical classification.

Similarity measures assess the relative distance between samples across multivariate hyperspace, and include such metrics as Euclidean distance, squared Euclidean distance, Manhattan distance, Minkowski distance, Mahalanobis distance, or Brainerd-Robinson distance (Leonard Kaufman and Rousseeuw 1990b). A linkage criterion is then used model heterarchical and hierarchical relationships in the data based on algorithmic interpretations of pairwise distances between observations. Linkage criterion include complete-linkage clustering, average linkage clustering, Ward's Method, or Ward's Square Method (Leonard Kaufman and Rousseeuw 1990b). Average-linkage and Ward's Method are the most commonly employed in archaeological compositional analysis. Average-linkage merges the pair of samples with the highest cohesion and defines similarity between clusters as the average distance between all possible pairs of cases, one from each cluster (Baxter 2015). While Ward's method attempts to minimize the error sum of squares when joining individuals or groups in the clustering process in order to ensure that groups remain as homogenous as possible (Shennan 1997:241-245).

Regardless of the technique employed, the results of clustering analysis can be considered as an additional feature in the data set alongside any previously known information about the samples. The next steps in the statistical procedure is to statistically assign sample observations to preliminary compositional groups and refine them into statistically robust compositional groups. The basic idea is to analyze group members to determine if they are more similar to each other than they are to samples in other chemical groups. A two-step procedure is followed in archaeological compositional analysis to assess and refine group membership.

Mahalanobis distance is first calculated for each sample. "Mahalanobis distance is effectively comparing samples to sample groupings by converting these to standard distributions (i.e. multivariate normal) by dividing the multivariate mean (centroid) by the multivariate

standard deviation (variance-covariance matrix)” (Golitko 2010:243-244; Harbottle 1976:57). In other words, Mahalanobis distance is equivalent to measuring the number of standard deviations and the group mean along each principal component axis (Glascock 2016). Hotelling’s T^2 statistic, which is the multivariate equivalent to a Student’s t-test, is then employed to calculate the probabilities of membership of each sample to every group (Shennan 1997). That is, the Hotelling’s T^2 statistic is transformed into the related F value and compared to the F-distribution. Confidence intervals can then determine a given level of statistical probability that an unassigned sample is derived from the same underlying population as the reference group to which it is being compared (Bishop and Neff 1989; Golitko 2010). A jackknife procedure is employed in the process whereby each sample is removed from the group before being assessed for its own probability of group membership. While the jackknife procedure aids in avoiding bias, it does come with some drawbacks in that the groups being evaluated must contain at least two more members than the number of variables included in the dataset (Neff 2002). In the present analysis with 44 elements, the minimum group size for statistical evaluation using multivariate elemental concentration data would be 46 samples. Groups with too few samples to achieve this threshold for elemental data can be compared against principal component data. This is often used to assess the presence of subgroups within larger groups. As a general rule of thumb, “groups are most robust when the number of members included substantially exceeds the number of elements or principal components considered” (Peeples 2011:112). Multivariate probabilities using the jackknife procedure therefore provides a robust method for comparing a sample to potential chemical or principal component groups because the probabilities simultaneously take into account all, or most, features in a data set.

Assigning samples to core reference groups in this way is fundamentally a means of constructing statistically valid groupings. However, there are no set cutoffs for probability values that are systematically employed in archaeological compositional analysis for assigning samples to groups. There are, however, two heuristics that can be used when deciding upon group membership criteria. The first is a consideration of the probability that a sample is a member of the group to which it has been assigned initially. The second is a consideration that a sample is *not* a member of the group to which it has been assigned initially, or the probability of membership in any other group. It is best to apply both of these heuristic criteria at the same time. For example, applying a common threshold minimum for probability of in-group membership while also applying a common threshold maximum for probability of out-group membership. All samples that fail to meet both thresholds become unassigned. This process is iterated until no additional samples need to be unassigned. It is often customary to visualize the core group samples with unassigned samples projected in the same visualization. Should any unassigned samples merit inclusion in a core group, they may be incorporated and the process continue until group membership is sufficiently stabilized.

An alternative heuristic in determining group membership probability using Mahalanobis distance and the Hotelling's T^2 statistic that is often employed is to initially treat the entire sample as a single group. Probabilities of group membership are assessed and any samples with less than a 1% probability of membership in the single group cluster are removed. This process is then iterated until no additional samples warrant removal. Retained samples are then considered to comprise a statistically robust core group with similar chemical compositions and can typically be related to a ceramic production system at some geographic scale. Unassigned

samples are projected against the core group to determine if any warrant inclusion in the core. This process iterates until group membership is stabilized.

Unassigned samples, which often comprise 30 – 60% of samples in a production source grouping methodology (Neff 2002; Peeples 2011:114), can be assessed for statistical assignment beyond the core groups. Since non-core group sizes rarely reach the amount necessary for using the Hotelling's T^2 statistic on elemental data, principal component data accounting for at least 90% of the observed variability in the elemental data are used. There are several potential interpretations for samples left unassigned: "they may be derived from sources not represented among the defined groups; they may be statistical outliers from one of the identified groups; or they may represent anomalous paste preparation or diagenetic effects" (Neff 2002:33).

With core and unassigned groups defined, analysis proceeds by using the aforementioned statistical clustering methodologies and *a priori* information about samples to find additional structure within the core and unassigned samples.

Another method for non-core assignment, or for the testing of core group separation, is canonical discriminant function analysis (or CDA). With CDA, the analyst imposes group patterning on the dataset. CDA assumes groups to be discrete and that all samples are members of those discrete groups. CDA then identifies axes of maximal separation between the groups, which are based on a number of linear functions (Shennan 1997:350-351). Probabilities for group membership can then be assessed for unassigned samples. However, group assignments made using CDA are less statistically rigorous than assignments made using elemental concentrations or principal components analysis (Bernardini 2005; Neff 2002).

7.6 Results of the Clay Analyses

Samples of clay were gathered from deposits along the central Illinois River and its tributary streams and backwater lakes as well as a handful of roadcuts and small subset of core samples. Bulk mineralogical assessment and clay speciation using x-ray diffraction performed by the Advanced Materials Characterization Center at the University of Cincinnati on a subset of samples confirmed that the majority of samples were consistent with clay minerals (see Appendix G). The bulk mineralogical profile of clay samples collected from both outcrop and core contexts are very similar to sherd mineralogy aside from the lack of measurable swelling smectite and kaolinite due to the ceramic firing process. However, a number of samples were removed from the dataset because of high calcite content. The results presented below refer to 32 clay samples.

The objective for statistical analysis of clays was to provide a baseline of clay heterogeneity in the study region and to provide exploratory insights for the statistical analysis of a much larger sample of ceramic artifacts. While analysis of the compositional data from such a small sample size prohibits statistically robust groupings, some general trends are notable. General patterning suggests the presence of two clay profiles, with some evident overlap between them. Because clay samples were collected primarily from fluvially eroded lithographic profiles below aeolian Quaternary deposits, I propose that the groups result from hypothesized northeast-southwest chemical distinctions in available clay resources eroded from geologic bedrock parent materials. That is, clays from Mississippian formations would like only be available for extraction in the southern portion of the central Illinois River valley while Pennsylvanian formation and Pleistocene glacial till outwash clays would be present in higher concentrations in the northern portion of the central Illinois River valley (see Figure 7.1). The

Spoon and Illinois River confluence, or approximately 40°18'14.7" N latitude, was identified as the most notable line of demarcation between the clay compositional profiles. However, it is important to again emphasize that this is an exploratory hypothesis and not a statistically or geologically significant proposition.

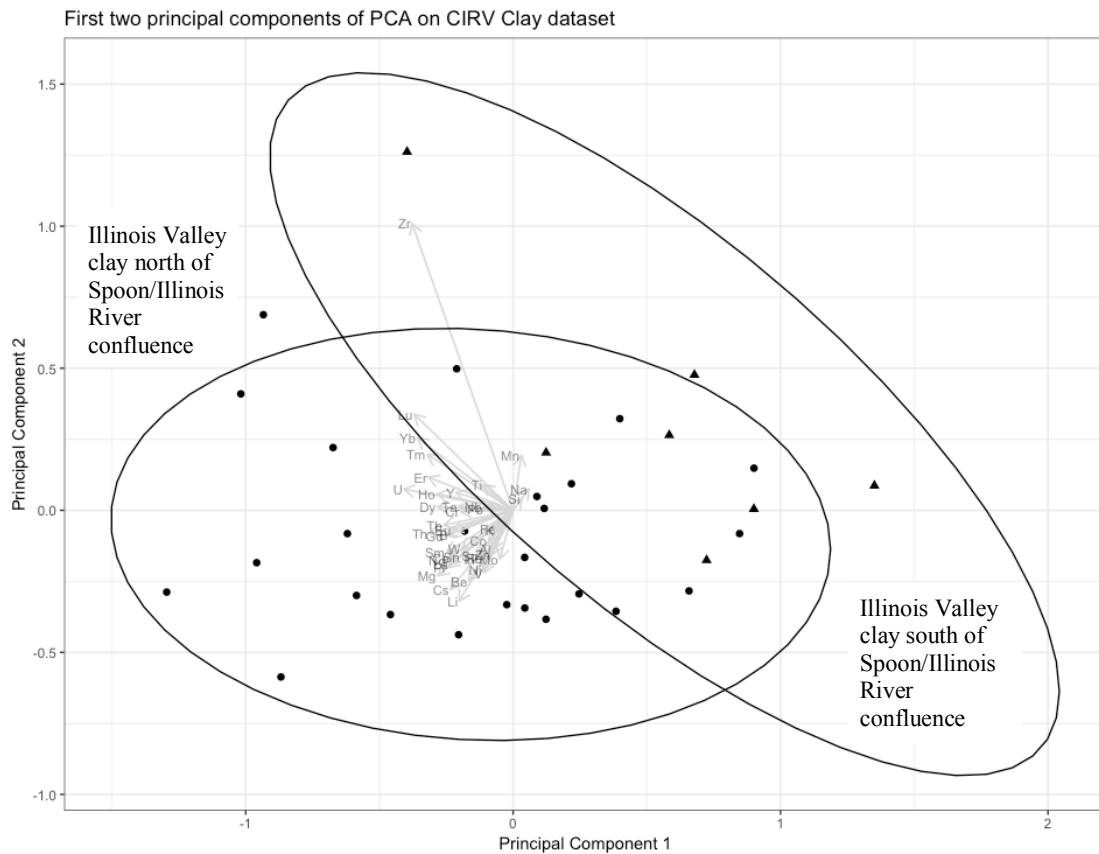


Figure 7.4 Principal components biplot showing the distinction between the two clay groups identified. Ellipses represent 90% confidence intervals for group membership. The first two principal components account for 66.5% of the variance in the clay data set.

A biplot of principal components scores and loadings on the first two principal components, accounting for 66.5% of the total variance in the clay data set (Figure 7.4), shows the distinction between clays from north of the Spoon and Illinois River confluence and clays from south of the Spoon-Illinois confluence. Enrichment in most elements characterizes the

northerly clays, while southerly clays show relative depletion in most elements but a slight enrichment in Mo, Na, and Si relative to the northerly clays.

Bivariate plots comparing individual elements better demonstrate group separation between the northerly and southerly clays analyzed in the central Illinois River valley. Southerly clays have low Be, Li, Cs, and Ni values compared to clays collected in and to the north of the vicinity of the Spoon-Illinois River confluence. Some overlap is present as a result of the demarcation of a latitudinal boundary in a dynamic fluvial environment. The positive linear

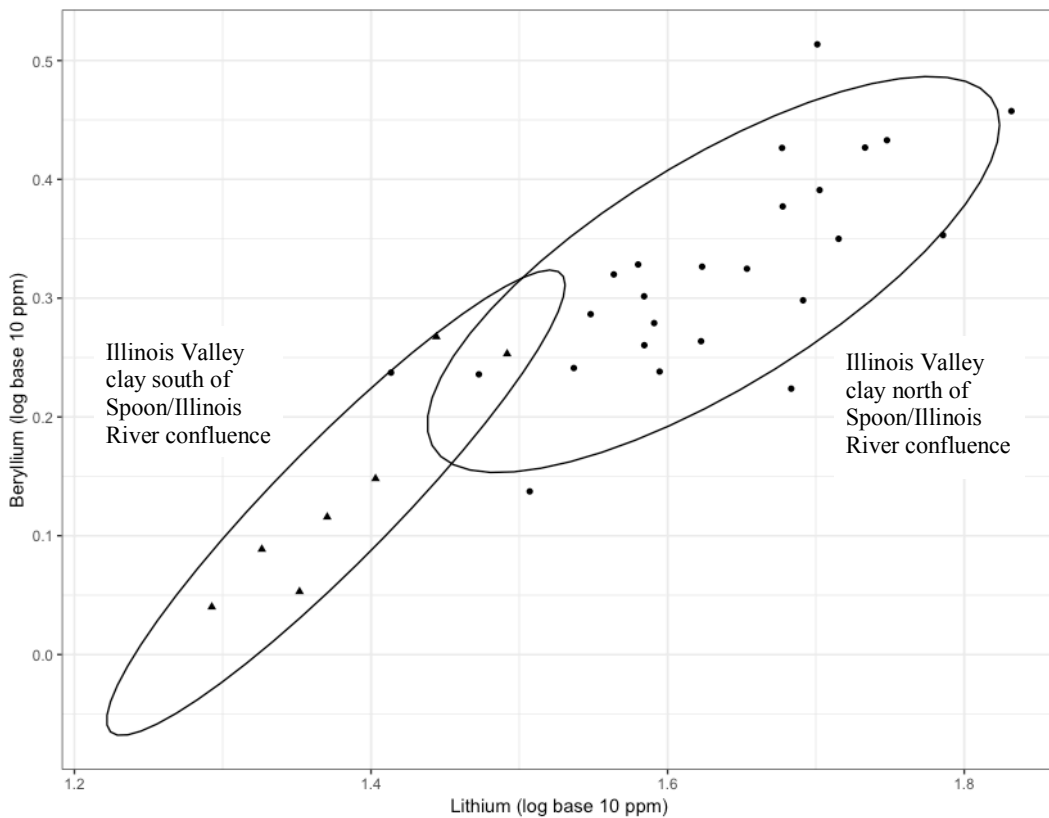


Figure 7.5 Bivariate plot of logged (based 10) Beryllium and Lithium showing distinctions between the two clay groups. Ellipses represent 90% confidence intervals for group membership.

relationship between Li and Be shows a general pattern of decreasing enrichment in these elements as one moves down valley in general from the northeast portion of the CIRV to the

southwest. A positive linear relationship also holds true for Nickel and Cesium, though with significant heteroscedasticity.

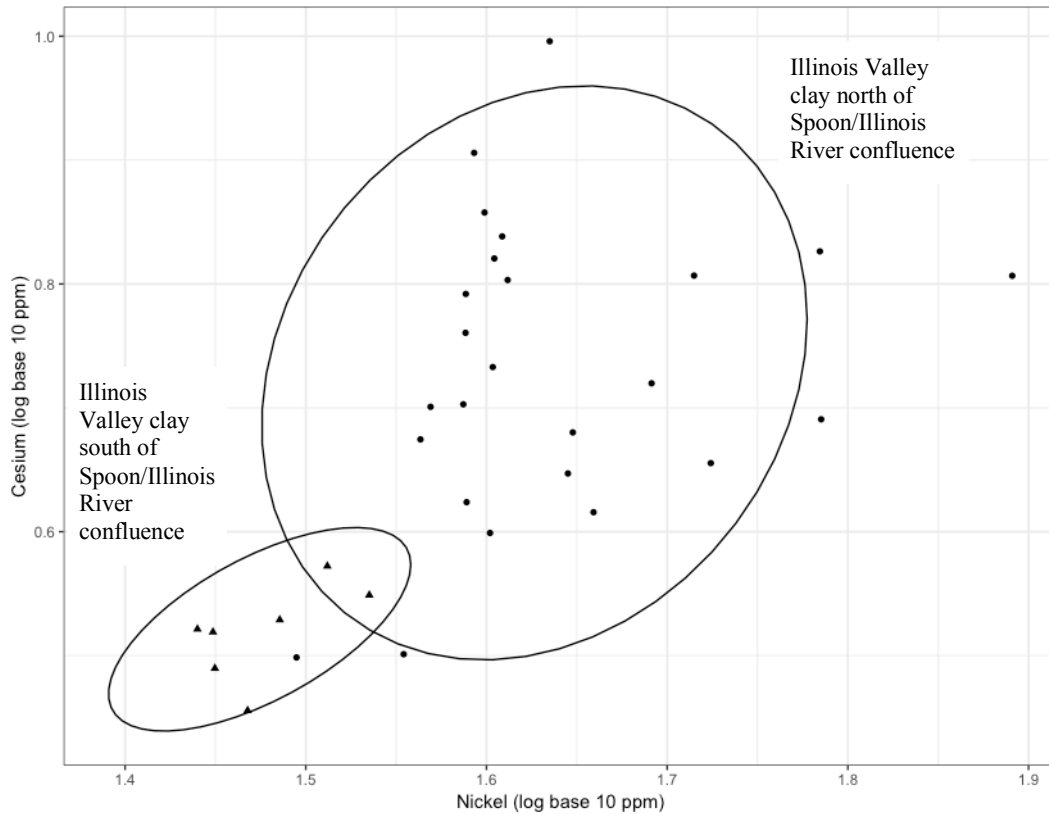


Figure 7.6 Bivariate plot of logged (based 10) Cesium and Nickel showing further chemical distinctions between the two clay groups. Ellipses represent 90% confidence intervals for group membership.

Calculation of statistical probabilities of group membership with such small sample sizes would be unreliable at best and misleading at worst. It is important to again emphasize that the analysis on a small sample of clay sediments is exploratory in nature and designed to provide insight to guide statistical analysis on a much larger sample of ceramic artifacts. Indeed, a general trend of decreasing enrichment in most elements as one moves from the northeast to southwest Illinois River valley is noted. This trend is shown visually in Figures 7.4 – 7.6 and numerically in Table 7.3

Northerly Illinois Valley Clay (<i>n</i> = 25)			Southerly Illinois Valley Clay (<i>n</i> = 7)		
	Average	Std Dev		Average	Std Dev
Al	68495.2	± 9681.7	Al	55977.5	± 3976.5
B	67.3	± 25.0	B	48.1	± 24.8
Be	2.1	± 0.4	Be	1.4	± 0.3
Ce	72.4	± 20.0	Ce	51.1	± 9.5
Co	18.8	± 6.3	Co	14.5	± 1.7
Cr	99.5	± 109.8	Cr	58.5	± 14.3
Cs	5.6	± 1.5	Cs	3.3	± 0.3
Dy	5.1	± 1.6	Dy	3.6	± 1.0
Er	3.0	± 1.0	Er	2.3	± 0.9
Eu	1.4	± 0.4	Eu	1.1	± 0.2
Fe	51040.2	± 7488.0	Fe	44564.0	± 5349.1
Gd	5.4	± 1.5	Gd	3.9	± 0.9
Ho	1.1	± 0.3	Ho	0.8	± 0.2
In	0.1	± 0.0	In	0.1	± 0.0
K	20202.9	± 4362.4	K	18794.3	± 3789.6
La	33.5	± 9.4	La	23.3	± 4.9
Li	44.0	± 9.9	Li	24.4	± 4.0
Lu	0.5	± 0.2	Lu	0.4	± 0.3
Mg	14125.1	± 9630.8	Mg	7107.1	± 778.2
Mn	996.5	± 365.1	Mn	957.5	± 191.7
Mo	1.7	± 0.7	Mo	1.4	± 0.2
Na	7768.3	± 2073.5	Na	8402.4	± 1113.4
Nb	21.2	± 6.4	Nb	16.8	± 2.4
Nd	31.8	± 8.7	Nd	21.4	± 4.3
Ni	44.3	± 10.1	Ni	30.1	± 2.5
Pb	24.7	± 6.7	Pb	24.5	± 5.3
Pr	9.6	± 2.6	Pr	6.3	± 1.2
Rb	124.4	± 19.5	Rb	97.4	± 20.3
Sc	13.9	± 2.5	Sc	10.2	± 1.5
Si	340711.5	± 18112.9	Si	362261.3	± 7687.7
Sm	6.5	± 1.8	Sm	4.5	± 0.9
Sn	2.3	± 0.5	Sn	1.5	± 0.2
Ta	1.3	± 0.3	Ta	1.0	± 0.2
Tb	0.8	± 0.2	Tb	0.6	± 0.1
Th	11.0	± 4.2	Th	8.0	± 1.9
Ti	5075.4	± 1188.7	Ti	4722.3	± 1131.7
Tm	0.5	± 0.2	Tm	0.4	± 0.2
U	4.4	± 2.5	U	3.0	± 1.3
V	126.4	± 24.4	V	89.1	± 8.0
W	1.7	± 0.5	W	1.4	± 0.2
Y	29.9	± 7.2	Y	22.9	± 7.4
Yb	3.2	± 1.3	Yb	2.6	± 1.7
Zn	139.2	± 27.6	Zn	99.0	± 19.2
Zr	220.9	± 201.3	Zr	361.3	± 571.5

Table 7.3 Average chemical concentrations and standard deviations for the two clay groups (ppm)

7.7 Results of the Ceramic Analyses

Using the workflow and statistical methods discussed above, 543 ceramic samples were placed into a number of compositional groups and sub-groups. The ceramic sample consists of one primary, or core, compositional group (Core A) in addition to two outlier groups (Outgroup 1 and Outgroup 2) and two provisional groups (Core B and Core C). Within the Core A group, two sub-groups are evident (Core A1 and Core A2). Among pottery samples, Core A is comprised of 380 samples. Within the Core A group, 133 ceramic samples were assigned to Core A1, 88 ceramic samples were assigned to Core A2 and 161 samples were assigned only to the Core A group and no sub-group. Outgroup 1 and Outgroup 2 (which are comprised of 39 and 20 samples respectively) are likely statistical outliers of the core compositional group, and are therefore likely outliers of, or distinct from, the range of clay sources sampled based on ceramic paste compositional profiles. Core B and Core C (21 and 13 ceramic samples respectively) are probable statistical outliers of the Core A group. A further 68 samples (or 12.5% of the ceramic compositional data set) were unable to be assigned to any group based on equivocal membership probabilities.

In the discussion that follows, attempts are made to relate these compositional groups to various production areas. It is important to emphasize that the identification of chemical compositional groups using elemental concentrations does not equate with the identification of discrete production sources. Paste preparation regimes including the mixing of clays or additions of aplastic materials, use-life alterations, diagenesis (or post-depositional changes to the chemical profile of ceramic objects), or some combination of these factors can contribute to the chemical profile of archaeological ceramics and therefore to the compositional groups defined based on elemental data (Golitzko 2010; Gosselain and Livingstone Smith 2005; Neff, et al. 2003;

Peeples 2011). In addition to insights gained from analysis of the chemical composition of a sample of CIRV clays and an understanding of CIRV geology, this research leverages two general principals to define the likely geographic production areas associated with compositional groups. The first is the criterion of abundance (Bishop, et al. 1982), which proposes that ceramics will be the most common in proximity to their production source. This allows compositional groups to be inferentially related to a production area based on the geographic distribution of group members. The second is the maximal range of raw material source areas known to be utilized in ethnographic contexts (or a ca. 7 km radius) (Arnold 1985). Potters living in nearby settlements could therefore overlap in resource exploitation zones. Support for a geographic production area for a given compositional group is therefore strongest when multiple settlements within a particular geological area have high proportions of that compositional group.

In general, there is support for the hypothesized down valley (or northeast – southwest) ceramic paste chemical distinctions in the Core A CIRV ceramic sample. That is, the Core A1 compositional sub-group is dominated by sherds recovered from sites north of, or in proximity to, the Spoon/Illinois River confluence (82% or $n = 109$). Greater geological source material variation is evident in the Core A2 sub-group, which is only predominantly comprised of sherds recovered from sites south of the Spoon/Illinois River confluence (58% or $n = 51$). A number of sherds were unable to be assigned to either the Core A1 or Core A2 sub-groups ($n = 161$).

The following section discusses the partitioning of ceramic samples into statistically robust compositional groups in a linear fashion. The linear sequence of compositional group identification and refinement is presented in its entirety in Appendix C, as the procedure was entirely implemented in the R statistical platform. Results were cross-referenced using the

MURRAP GAUSS routines developed by Hector Neff for accuracy. Additional support for the chemical compositional reference group assignments is supplied in Appendix D. In the succeeding section, compositional groups are used to construct networks of economic relationships based on overlapping resource exploitation areas, the exchange of finished vessels, or similar paste preparation regimes.

7.7.1 Compositional Group Identification and Assignment

After taking the log base 10 of all elemental concentration values, initial inspection of bivariate plots and exploratory R-Q mode factor analysis was carried out. A similar trend of elemental enrichment in clays north of the Spoon/Illinois River confluence is observed in general among ceramic vessels based on the location of the site of recovery on principal component 1 (Figure 7.7). Principal component 1 is equally enriched in nearly every element. While principal component 2 shows a dominant contribution from molybdenum (Mo) and depletions in magnesium (Mg) and sodium (Na), manganese (Mn), and cobalt (Co) to a lesser extent. However, significant overlap between these hypothetical groups based on the geographic location of sherd recovery indicates that they are likely not statistically robust, an intuition confirmed by equivocal membership probabilities between the samples using jackknifed Mahalanobis distance and the Hotelling's T^2 statistic.

Analysis proceeded using cluster analysis and other exploratory methods to identify potential compositional groupings. R-Q mode factor analysis resulted in 12 significant components. No single eigenvalue is above one, indicating that no principal components have high correlations with particular elements, complicating efforts to define statistically robust compositional groups (Table 7.4). As a result, for the remainder of the analysis, principal

components 1 through 12 (accounting for 90.4% of cumulative variance) are used to calculate group membership probabilities. This minimizes the sample size of the smallest potential group

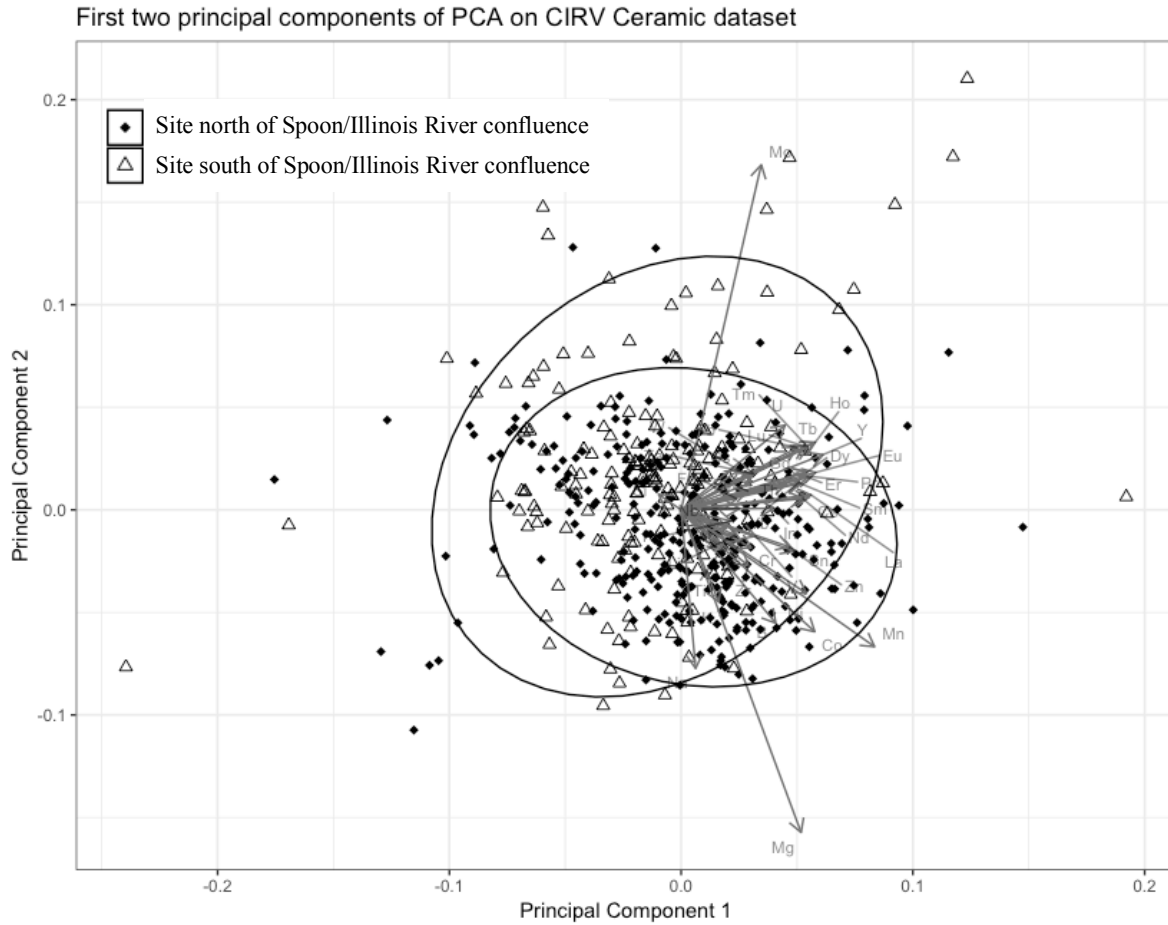


Figure 7.7 Principal components biplot showing elemental enrichment for sherds recovered from sites north of the Spoon/Illinois River confluence in general. Ellipses show 90% confidence intervals. Together, PC 1 and 2 account for 49.99% of variance in the ceramic dataset.

for group membership probability calculations (>14) while maximizing the amount of variation drawn from the original dataset of 44 elements.

Cluster analysis of the full elemental data set resulted in between two and eight optimal clusters depending on the method employed (see Appendix C for the relevant code). However, each of the statistical methods failed to produce statistically robust clusters when group

membership probabilities were assessed using Mahalanobis distances and the Hotelling's T^2 statistic. Anywhere from 75% to 95% of samples were left unassigned to the hypothetical group they were assigned to by statistical clustering methods using a threshold of greater than 10% probability of membership in the assigned group and less than 10% probability of membership in any other group. That is, cluster analysis methods reliably produced equivocal group membership probabilities when assessed for statistically significant of group separation.

Principal Component	Eigenvalue	% Variance	Cumulative % Variance
1	0.206	34.845	34.845
2	0.090	15.143	49.988
3	0.066	11.153	61.141
4	0.044	7.438	68.579
5	0.028	4.724	73.303
6	0.023	3.887	77.190
7	0.019	3.210	80.400
8	0.016	2.715	83.115
9	0.014	2.280	85.395
10	0.011	1.827	87.222
11	0.010	1.620	88.841
12	0.009	1.526	90.367

Table 7.4 Eigen values and percent variance for first 12 principal components on the ceramic data set

As a result of the lack of any evident groups as defined by statistical clustering methods on either the full elemental data set or using principal components 1 through 12, analysis proceeded by initially treating the entire ceramic data set as a single compositional group and assessing group probabilities using jackknifed Mahalanobis distance. After each iteration, samples falling below a 1% membership probability cutoff were removed and the membership probabilities were re-calculated. Samples left unassigned were projected against the retained samples at each step. This process was iterated nine times until groups stabilized and resulted in the identification of a “core” statistical group comprised of 416 samples (76.6%) and the removal

of 127 “non-core” samples (23.4%). Figure 7.7 visualizes the retained core group and non-core group along the first three principal components (61.14% of cumulative variance in the ceramic dataset).

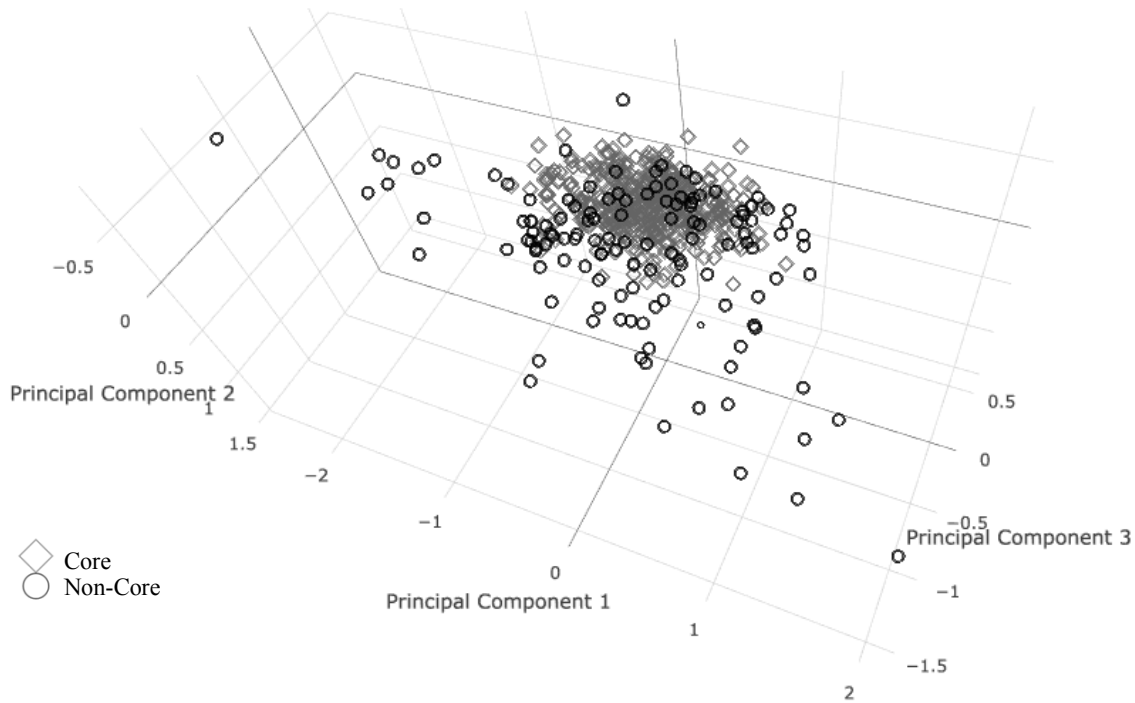


Figure 7.8 3D scattergram of PCs 1, 2, and 3 showing core and non-core compositional groups

Unassigned “non-core” samples were inspected for meaningful group structuring using a combination of bivariate plots (both of logged elemental concentrations and principal components) as well as statistical clustering methods. Broad agreement between k-means and k-medoids cluster analysis for the presence of two groups among the non-core sherds was confirmed using jackknifed Mahalanobis and Hotelling’s T^2 group membership probability assessment. Using a somewhat different cutoff threshold of greater than 2.5% probability of membership in the statistical cluster and less than 10% probability of membership in any other group and at least four times higher likelihood of membership in the assigned group than any other group resulted in the placement of 59 sherds in two non-core outgroups (Figure 7.9; Table

7.5). The other 68 non-core sherds remained unassigned due to ambiguous group membership probabilities.

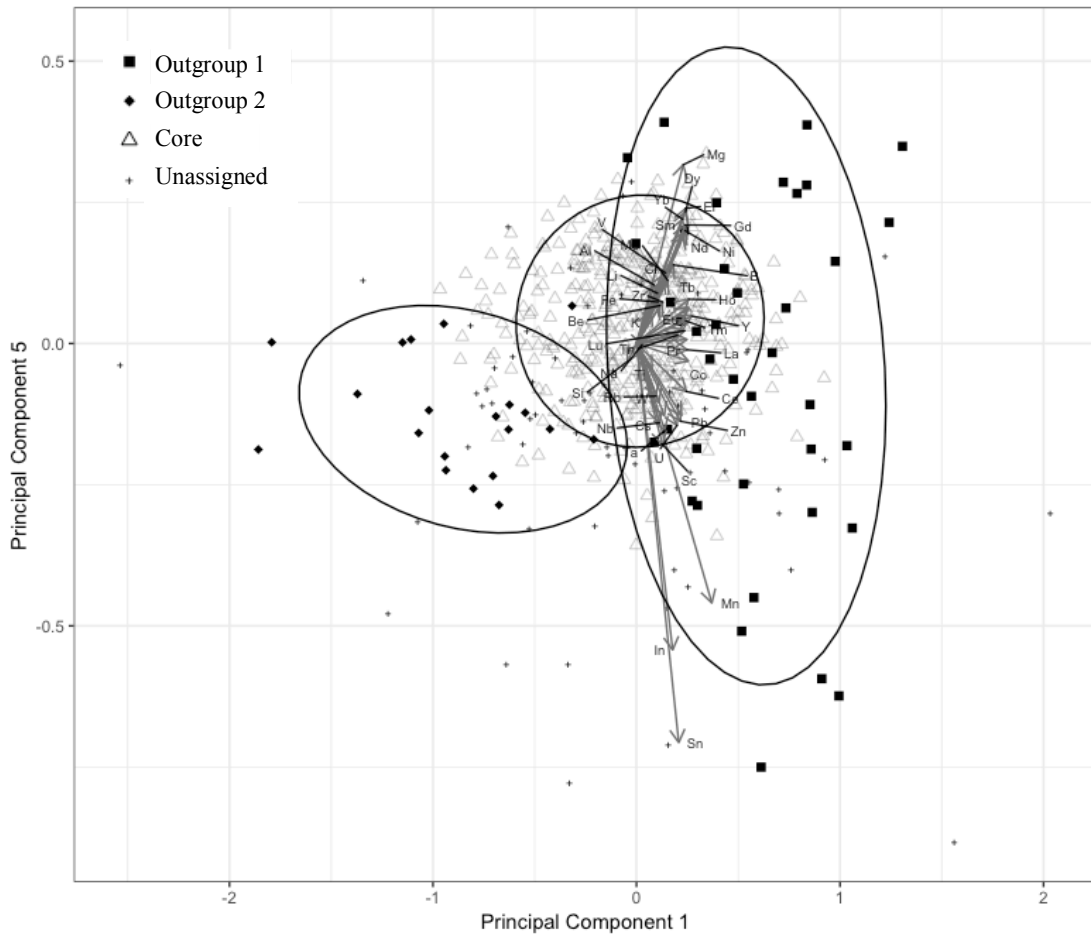


Figure 7.9 Principal components 1 and 5 biplot showing distinctions between the Core group, Outgroup 1, and Outgroup 2. Ellipses demarcate 90% confidence intervals.

The identification of a core group and several outgroups indicates that the entire set of geochemically analyzed ceramic samples cannot be treated as a single, normally distributed chemical group. Given that a number of the unassigned sherds fall within the 90% confidence intervals of the core and outgroups on principal component bivariate plots, it is possible that they may be statistical outliers of one of these groups. However, equivocal membership probabilities

Sample #	Site	Assigned Group	Membership Probability		
			Core	Outgroup 1	Outgroup 2
4	Orendorf C	Outgroup 1	0.000	96.833	0.034
7	Orendorf C	Outgroup 1	0.000	64.239	0.004
11	Orendorf C	Outgroup 1	0.000	75.526	0.017
12	Orendorf C	Outgroup 1	0.000	8.044	0.010
14	Orendorf C	Outgroup 1	0.005	73.011	0.058
15	Orendorf C	Outgroup 1	0.072	21.910	5.172
198	Walsh	Outgroup 1	0.000	17.853	0.000
207	Walsh	Outgroup 1	0.000	22.171	0.000
208	Walsh	Outgroup 1	0.000	56.352	0.002
210	Walsh	Outgroup 1	0.000	27.594	0.000
213	Walsh	Outgroup 1	0.000	19.716	0.001
217	Walsh	Outgroup 1	0.000	76.619	0.290
282	Emmons	Outgroup 1	0.000	81.022	0.001
284	Emmons	Outgroup 1	0.000	9.155	1.414
296	Baehr South	Outgroup 1	0.000	94.941	0.037
297	Baehr South	Outgroup 1	0.000	24.738	0.053
308	Baehr South	Outgroup 1	0.000	75.722	0.000
309	Baehr South	Outgroup 1	0.000	97.236	0.003
497	Ten Mile Creek	Outgroup 1	0.002	79.610	0.009
532	Ten Mile Creek	Outgroup 1	0.000	48.350	0.000
536	Eveland	Outgroup 1	0.001	28.261	0.000
599	Kingston Lake	Outgroup 1	0.155	2.707	0.006
672	Lawrenz Gun Club	Outgroup 1	0.000	11.242	0.023
674	Lawrenz Gun Club	Outgroup 1	0.440	7.224	1.446
726	Buckeye Bend	Outgroup 1	0.003	20.583	0.294
753	Fouts Village	Outgroup 1	0.891	41.847	0.059
754	Fouts Village	Outgroup 1	0.179	78.897	0.612
787	Larson	Outgroup 1	0.000	48.380	0.020
798	Larson	Outgroup 1	0.144	31.056	0.377
872	Morton Village	Outgroup 1	0.000	90.606	0.004
873	Morton Village	Outgroup 1	0.000	13.973	0.003
874	Morton Village	Outgroup 1	0.001	91.443	0.038
911	Houston-Shryock	Outgroup 1	0.002	53.835	0.860
916	Houston-Shryock	Outgroup 1	0.001	49.253	0.001
922	Houston-Shryock	Outgroup 1	0.001	31.838	0.009
1221	Orendorf D	Outgroup 1	0.000	95.673	0.000
1237	Orendorf D	Outgroup 1	0.000	34.230	0.000
1287	C.W. Cooper	Outgroup 1	0.005	71.064	0.149
1300	Crabble	Outgroup 1	0.029	47.899	0.010
56	Orendorf C	Outgroup 2	0.000	0.000	61.760
86	Crabble	Outgroup 2	0.006	0.312	44.854
87	Crabble	Outgroup 2	0.000	0.040	89.296
122	Crabble	Outgroup 2	0.000	0.002	52.612
131	Crabble	Outgroup 2	0.000	0.376	90.177
132	Crabble	Outgroup 2	0.000	0.083	38.189
153	Crabble	Outgroup 2	0.000	0.119	58.474
161	Crabble	Outgroup 2	0.000	0.013	98.434
167	Crabble	Outgroup 2	0.000	0.142	71.598
174	Crabble	Outgroup 2	0.052	0.351	89.258
175	Crabble	Outgroup 2	0.020	0.179	88.492
190	Walsh	Outgroup 2	0.054	2.032	15.133
200	Walsh	Outgroup 2	0.000	0.159	6.678
527	Ten Mile Creek	Outgroup 2	0.000	0.590	24.341
534	Eveland	Outgroup 2	0.000	0.008	6.168
539	Eveland	Outgroup 2	0.214	1.965	8.336
875	Ten Mile Creek	Outgroup 2	0.000	0.000	4.648
1066	Crabble	Outgroup 2	0.000	0.000	9.860
1190	Morton Village	Outgroup 2	0.000	0.000	94.696
1192	Morton Village	Outgroup 2	0.000	0.000	23.712

Table 7.5 Mahalanobis distance based probabilities of group membership in the core and outgroups for the outgroup sherds

across the different groups as identified precludes statistically sound group assignment for the 68 non-core unassigned sherds.

Outgroup 1 sherds differ from Core and Outgroup 2 sherds primarily because of low concentrations of the heavy rare earth elements (HREEs; Eu - Lu) and light rare earth elements (LREEs; La - Sm). While Outgroup 2 is differentiated primarily based on enrichment in HREEs and LREEs as well as enrichment in molybdenum (Mo) relative to Core and Outgroup 1 sherds. However, Outgroup 2 sherds are more difficult to distinguish on an elemental basis (e.g. Figure 7.9). Significant overlap exists between Outgroup 1 and 2 sherds and the Core chemical group on most elemental bivariate plots. Non-trivial multivariate group membership probabilities, on the other hand, affirm the statistical validity of the core and non-core sub-group separation (Table 7.5).

Given the broad-spectrum elemental enrichment of Outgroup 1 sherds and clays recovered in northerly portions of the CIRV, it would be expected that Outgroup 1 sherds would primarily be recovered from sites north of the Spoon/Illinois River confluence. Indeed, some 61.5% of vessels assigned to Outgroup 1 ($n = 24$) were recovered from sites in proximity to or north of the Spoon/Illinois River confluence. No single site comprises a majority of sherds in Outgroup 1. However, Orendorf Settlement C and Walsh are both represented by six vessels each. That a number of sherds in Outgroup 1 emanated from Walsh, the most southerly site in the Late Prehistoric CIRV analyzed for this research, indicates that the geographic location of parent clay material alone may not be the sole explanation for separation of this group. Perhaps Outgroup 1 is demarcated by a distinct production methodology based on the mixing of clays or perhaps elementally enriched clays were available to potters south of the Spoon/Illinois River confluence. On the other hand, one cannot discount the movement of vessels given that all sites

are connected to each other by a relatively short canoe ride on the Illinois River. That some 74.4% ($n = 29$) of the vessels in Outgroup 1 are jars lends credence to the supposition that Outgroup 1 sherds may be the product of intra-regional exchange or vessel movement between

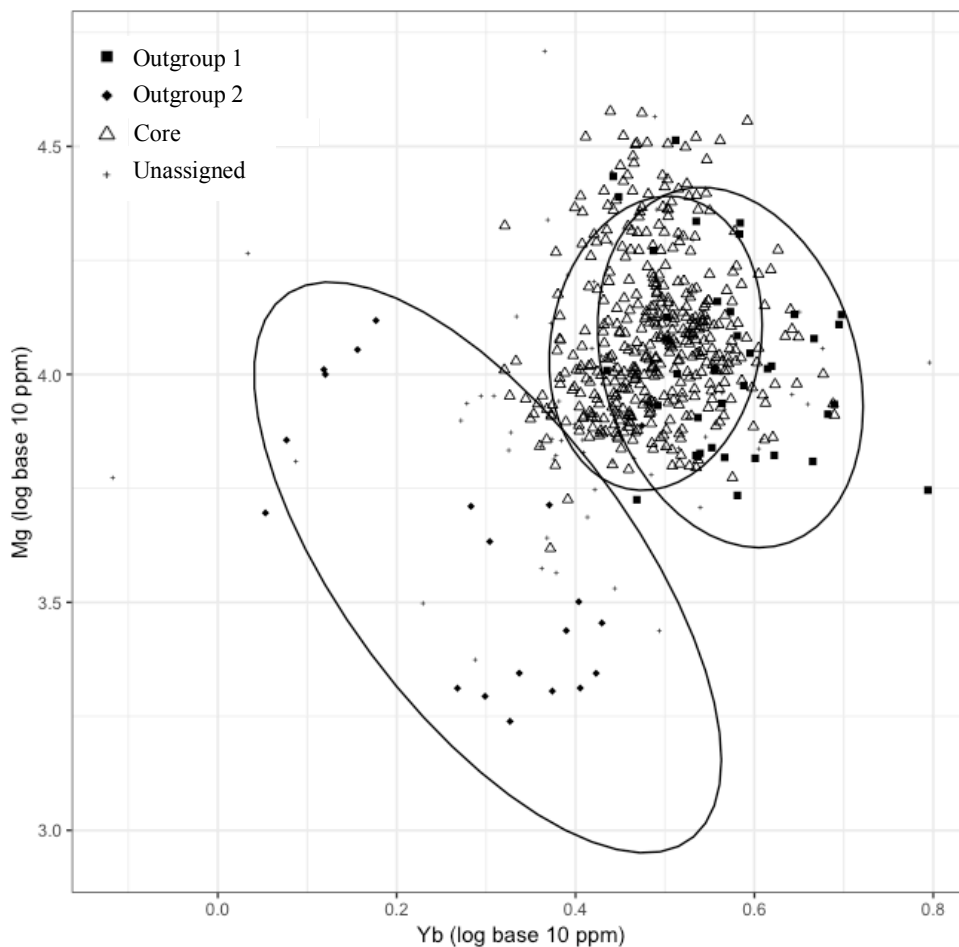


Figure 7.10 Bivariate plot of log base 10 magnesium and ytterbium concentrations of Outgroup 1 and 2 and Core sherds with 90% confidence ellipse boundaries

sites. As domestic cooking and storage vessels with restricted access to their contents, jars are more likely to have been used to transport foodstuffs, seeds, or other goods between sites than a presumed serving vessel such as the plate that has less utility for transport of material goods.

Given the reduced elemental concentrations in Outgroup 2 sherds and the similarly reduced elemental profile of southerly CIRV clays, it would be expected that a majority of Outgroup 2 sherds were recovered from sites south of the Spoon/Illinois River confluence.

Indeed, Outgroup 2 is dominated by sherds from Crable. Some 65% ($n = 11$) of Outgroup 2 sherds are from Crable alone and the vast majority of those vessels are plates. In addition, the vast majority of vessels in Outgroup 2 were recovered from sites dating to the post-migration time period (75%). This would suggest the possible presence of a unique production system in addition to the use of less elementally enriched clay likely emanating from contexts south of the Spoon/Illinois River confluence as being primarily responsible for the compositional profile of Outgroup 2 vessels relative to Core or Outgroup 1 vessels.

7.7.2 Structure within the Core compositional group

With non-core groups identified, attention was turned to the core statistical group. Again, statistical cluster methods and R-Q mode factor analysis were carried out to identify potentially meaningful structuring with the exception that the core group was treated independently of other samples. This approach is warranted because the core group is demonstrably distinct from the non-core group and non-core sub-groups.

As with the prior complete dataset, cluster methods failed to produce compositional groups that held up to statistical rigor using membership probability assessment. Thus, the core group was further refined by identification and removal of two core statistical outlier, or provisional, groups – Core B and Core C. That is, after creating hypothetical two-group assignments using k-means and k-medoids clustering, samples were assessed for group membership probabilities using a threshold of greater than 2.5% probability in the assigned group and less than 1% probability of membership in any other group for the first iteration. This acted to identify likely outliers to the core group. This process was iterated with less conservative membership probabilities (less than 10% membership probability in any other group and greater

than 10% within group) as groups likely to be statistical outliers of the core group were identified and refined. Figure 7.11 shows the separation of the Core A group and Core B and Core C

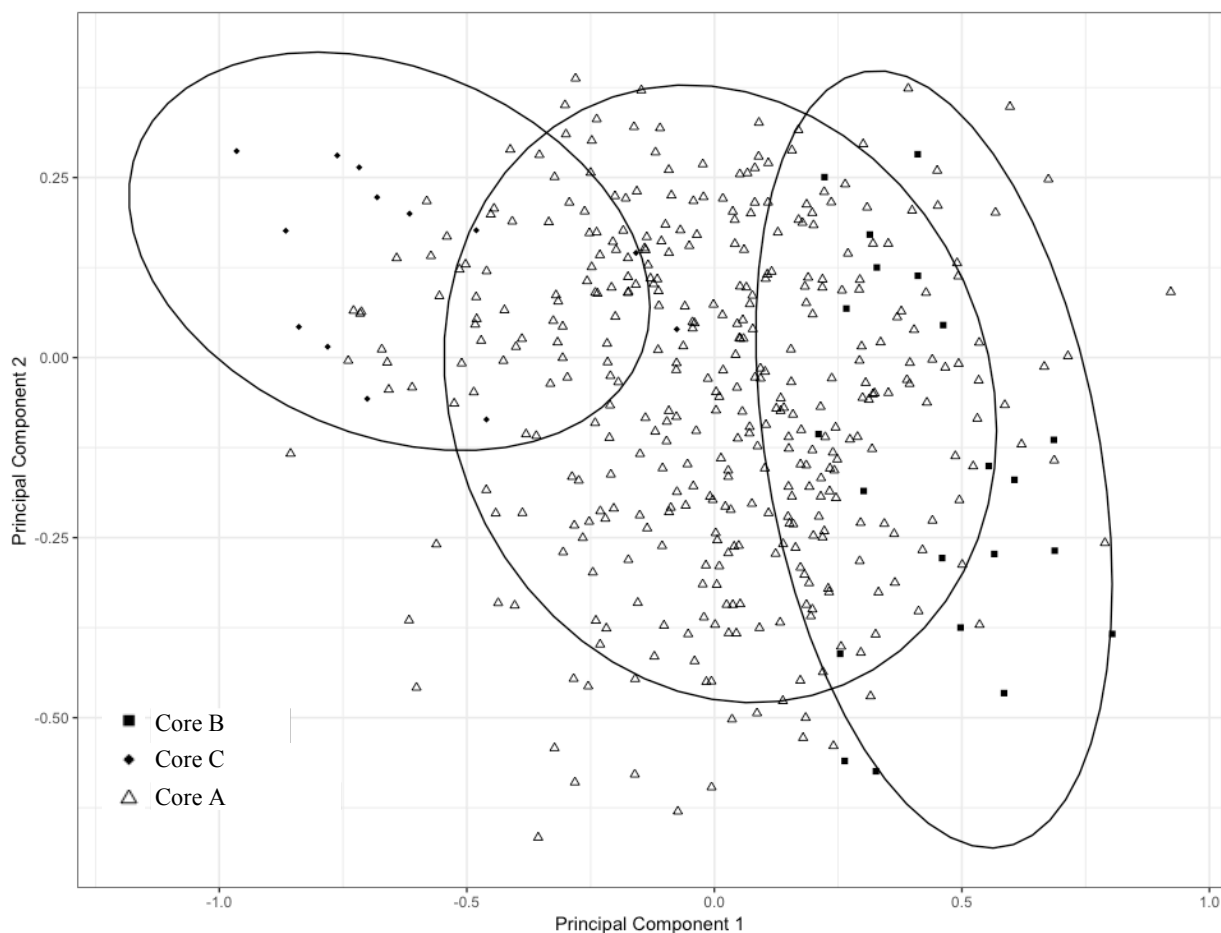


Figure 7.11 Principal components 1 and 2 biplot showing distinctions between the Core group, and core provisional groups – Core B and Core C. Ellipses demarcate 90% confidence intervals.

provisional groups on a principal component 1 and 2 bivariate plot. Membership probabilities for the Core B and Core C groups are provided in Table 7.6.

Core B and Core C groups are considered provisional due to their small sample sizes and the fact that they are probable statistical outliers to the Core A compositional group. In other words, as opposed to representing discrete chemical compositional distributions that may reflect the distribution of a given clay-source or ceramic production system, Core B and Core C are more likely outliers to the Core A chemical compositional distribution. Additional samples may

Sample #	Site	Core Sub-Group	Membership Probability		
			Core A	Core B	Core C
48	Orendorf C	Core B	0.340	34.973	0.167
268	Emmons	Core B	1.645	25.363	0.011
272	Emmons	Core B	5.743	12.613	0.039
533	Eveland	Core B	0.598	31.881	0.001
540	Eveland	Core B	9.740	57.217	0.024
541	Eveland	Core B	7.334	82.332	0.051
543	Eveland	Core B	0.829	66.191	0.014
585	Kingston Lake	Core B	4.542	56.195	1.491
741	Buckeye Bend	Core B	5.165	44.750	8.543
743	Buckeye Bend	Core B	6.248	35.512	1.931
760	Fouts Village	Core B	1.567	11.262	0.452
770	Larson	Core B	3.329	36.730	0.060
771	Larson	Core B	7.580	66.461	0.460
777	Larson	Core B	5.493	27.502	0.227
795	Larson	Core B	5.013	29.513	0.853
858	Morton Village	Core B	1.134	12.936	0.460
860	Morton Village	Core B	4.178	24.510	0.405
863	Morton Village	Core B	4.115	34.834	0.048
870	Morton Village	Core B	2.105	40.302	0.632
1173	Morton Village	Core B	9.071	33.763	0.914
1180	Morton Village	Core B	3.514	27.812	0.038
103	Crable	Core C	7.259	0.001	86.329
234	Lawrenz Gun Club	Core C	2.539	0.071	4.687
342	Myer-Dickson	Core C	4.390	0.019	38.463
428	Star Bridge	Core C	0.590	0.008	78.579
490	Ten Mile Creek	Core C	2.464	0.005	15.953
500	Ten Mile Creek	Core C	0.463	0.009	42.399
502	Ten Mile Creek	Core C	0.543	0.051	58.820
559	Eveland	Core C	3.496	0.007	58.748
664	Lawrenz Gun Club	Core C	8.216	0.060	29.085
878	Morton Village	Core C	5.128	0.279	51.190
958	Star Bridge	Core C	4.573	0.011	60.734
1206	Orendorf D	Core C	2.418	0.009	24.504
1236	Orendorf D	Core C	6.059	0.087	49.135

Table 7.6 Mahalanobis distance based probabilities of group membership in the Core A group and Core B and Core C provisional groups

confirm or refute their separation into provisional groupings. Out of the original 416 core sherds, 21 were assigned to Core B, 13 were assigned to Core C and 382 were assigned to Core A.

Analysis proceeded by examining the Core A compositional group for potentially meaningful group separation, disregarding non-core groups as well as provisional groups Core B and Core C. No obvious clusters emerged from biplots using *a priori* information such as geographic locations of the site of recovery, vessel class, temporal occupation of sites, or based on the presence/absence of Oneota material culture at sites. Statistical clustering methods

including k-means, k-medoids, and hierarchical clustering were thus applied to the Core A group. The k-medoid (or partitioning around medoids (Leonard Kaufman and Rousseeuw 1990b)) cluster solution for the presence of two groups was identified as the most likely candidate to hold up to membership probability assessment. A threshold of greater than 10% probability in the assigned group and less than 10% probability in any other group for initial iterations and greater than 3% probability in the assigned group and less than 2.5% probability of membership in any other group for subsequent iterations resulted in the identification of two quite distinct compositional groups within the Core A group. These appear to represent the primary statistically significant compositional groups within the entire CIRV ceramic chemical compositional data set. Figure 7.12 displays Core A1 and Core A2 group separation along principal components 1 and 2 while Figure 7.13 displays Core A sub-group separation along log base 10 magnesium (Mg) and nickel (Ni) parts per million concentrations. Membership probabilities for Core A1 and Core A2 sherds are presented in Appendix D.

While two sub-groups were able to be identified within the Core A group, a significant number of vessels within Core A were unable to be assigned to either the Core A1 or Core A2 sub-groups (42.1% or $n = 161$). This is not uncommon in compositional analysis studies (Cochrane and Neff 2006; Eerkens, et al. 2002; Fitzpatrick, et al. 2006; Golitko 2010; Hegmon, et al. 1997; Neff 2002, 2003; Niziolek 2013; Peeples 2011; Wallis, et al. 2010). For the present case, this is likely reflective of the refined geographic scale with which samples were derived (a single archaeological region along one major river valley spanning approximately 137 km), massive geologic parent features that extend across the study area, and the highly interconnected

nature of most of the communities sampled as demonstrated in other portions of this research, particularly during the Mississippian occupations prior to Oneota in-migration.

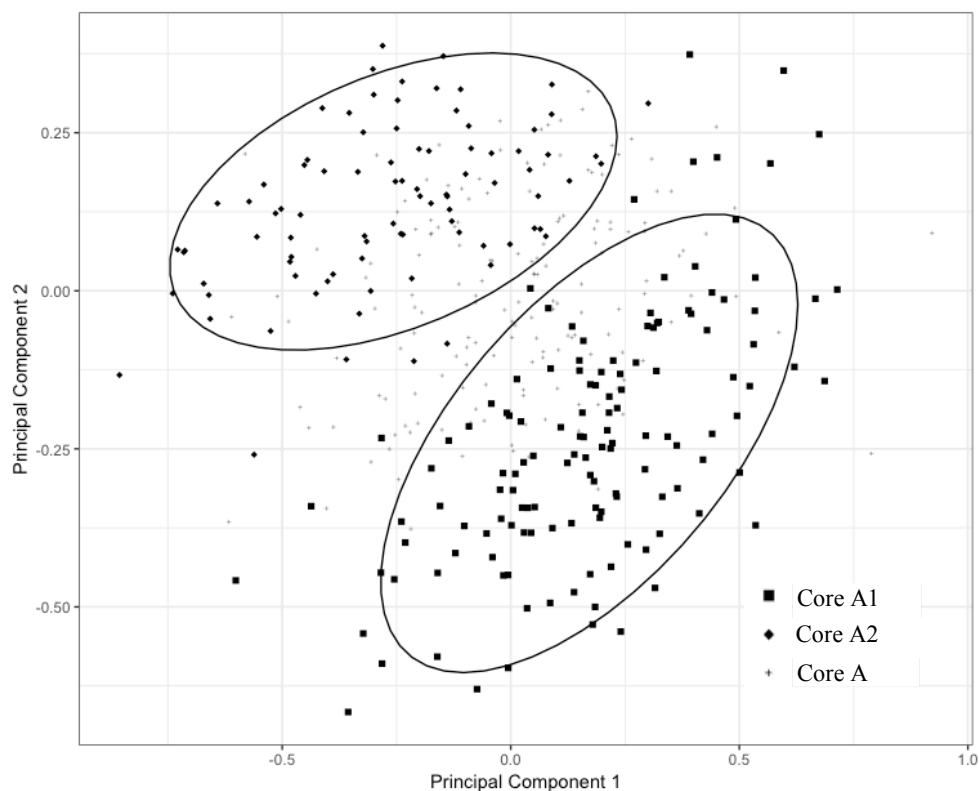


Figure 7.12 Principal components 1 and 2 biplot showing distinctions within the Core A group. Ellipses demarcate 90% confidence intervals.

Core A1 and Core A2 follow a similar trend of group separation primarily along principal components 1 and 2. Core A1 is dominated by sherds emanating from sites north, or in the vicinity, of the Spoon/Illinois River confluence (82% or $n = 109$). Recall that the chemical profile is one of enrichment in most elements along principal component 1 and general depletion along principal component 2 with the exception of molybdenum (Mo) and the HREEs (see Figure 7.7 or 7.15). Thus, the Core A2 sub-group is primarily distinguished by depletion in most elements relative to the Core A1 sub-group, again affirming the overarching trend seen in the clay analysis of down valley elemental diminution. Core A2 shows greater variability in the geographic location of the site of sherd origin, with only a simple majority of sherds originating

from a site located to the south of the Spoon/Illinois River confluence (58% or $n = 51$). However, two sites alone account for some 32 of the 51 sherds in Core A2. A total of 18 sherds in Core A2 were derived from Crable and 14 sherds in Core A2 were derived from Lawrenz Gun Club. Both of these sites are located well to the south of the Spoon/Illinois River confluence.

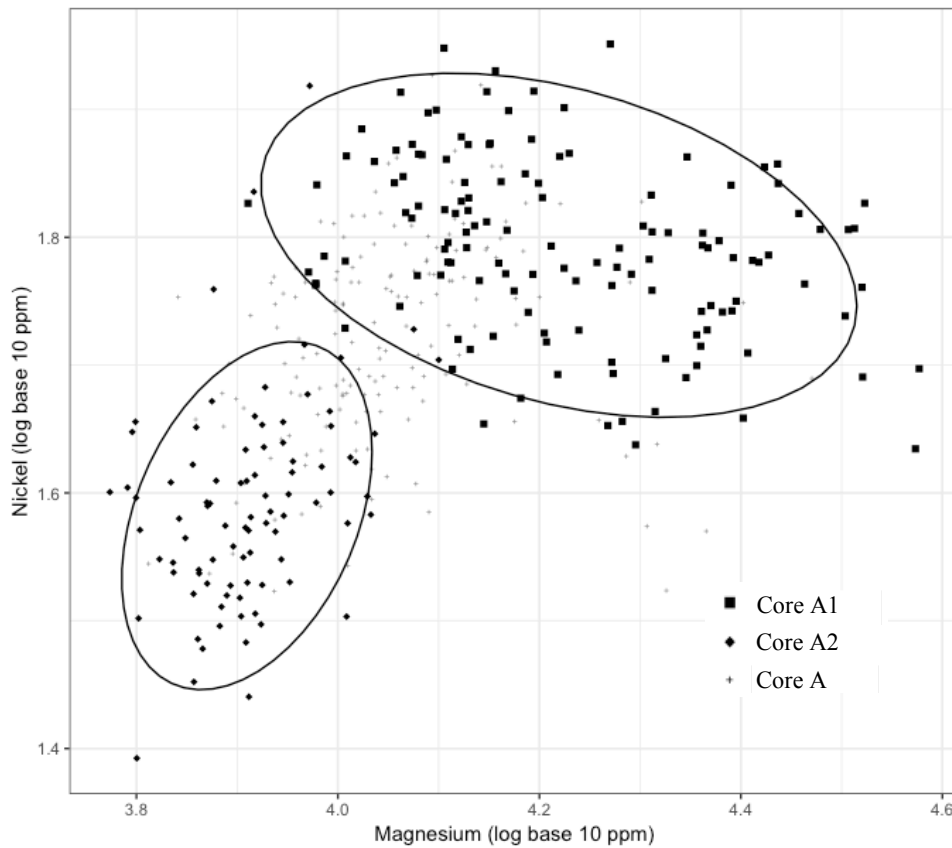


Figure 7.13 Bivariate plot of log base 10 magnesium and nickel concentrations of Core A1 and Core A2 sherds with 90% confidence ellipse boundaries.

In terms of individual elements, the partition in the Core A pottery sample is most readily viewed in a bivariate plot of magnesium (Mg) and nickel (Ni) because the distribution of these elements shows little overlap between the Core A1 and Core A2 sub-groups. As alkaline earth and transition metals respectively, it is likely that differences in these elements are the result of differences in clay parent materials. Leveraging the criterion of abundance (Bishop, et al. 1982), the preponderance of Core A2 group member sherds from northerly locales in the CIRV suggests

primarily Pennsylvanian bedrock or Pleistocene alluvium/lacustrine clay sources with a higher percentage of Mississippian geologic age bedrock clays perhaps being responsible for elemental diminution for Core A1 sherds. Figures 7.5 and 7.6 display these trends among clay materials for alkali, alkaline earth, and transition metals more broadly (e.g. elements Be, Li, Ce, Ni).

However, that there is a significant number of Core A sherds that were unable to be assigned to a sub-group indicates the likelihood of at least some overlap in elemental distributions between these different source materials, even at such a broad geographic scale.

All final group assignments are visualized in Figures 7.14 – 7.16 in biplots along principal components 1 and 2. Figure 7.14 emphasizes group separation boundaries and shows the outlier nature of Outgroups 1 and 2 for the entire data set and Core B and Core C for the Core A group. Figure 7.15 emphasizes elemental component loadings along principal component 1 and 2. Core A1, Core B, and Outgroup 1 show general enrichment along principal component 1, while the inverse is true for Core A2, Core C, and Outgroup 2. Figure 7.16 displays bivariate separation among all groups along molybdenum (Mo) and magnesium (Mg), showing the inherent difficulty in using individual elemental features to account for group separation among most groups. Final group assignments are summarized in Tables 7.7 and 7.8 as counts by site and by geographic location of site and by vessel class.

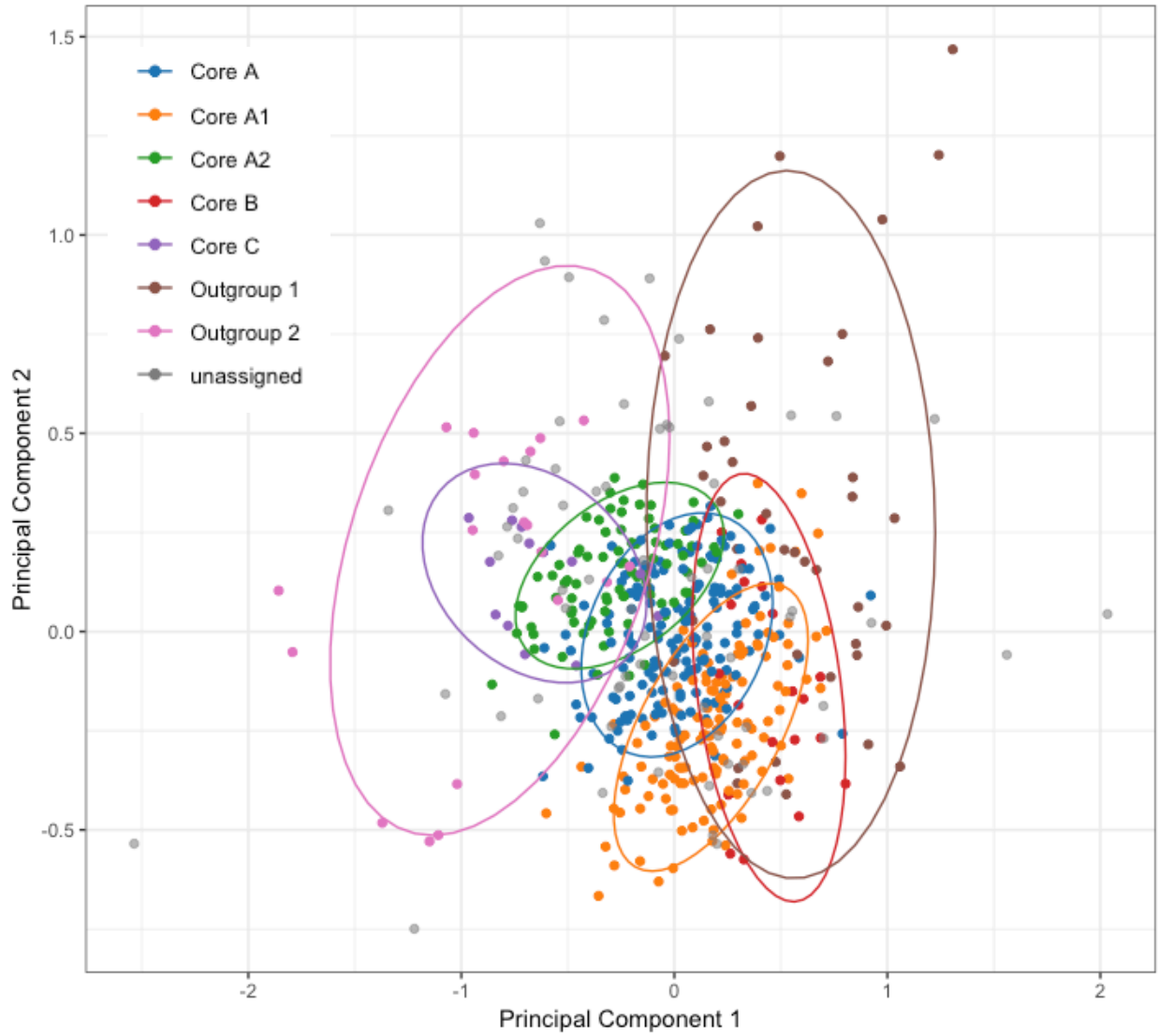


Figure 7.14 Principal component 1 and 2 bivariate plot of all group, sub-group, and provisional group assignments with 90% confidence ellipse boundaries.

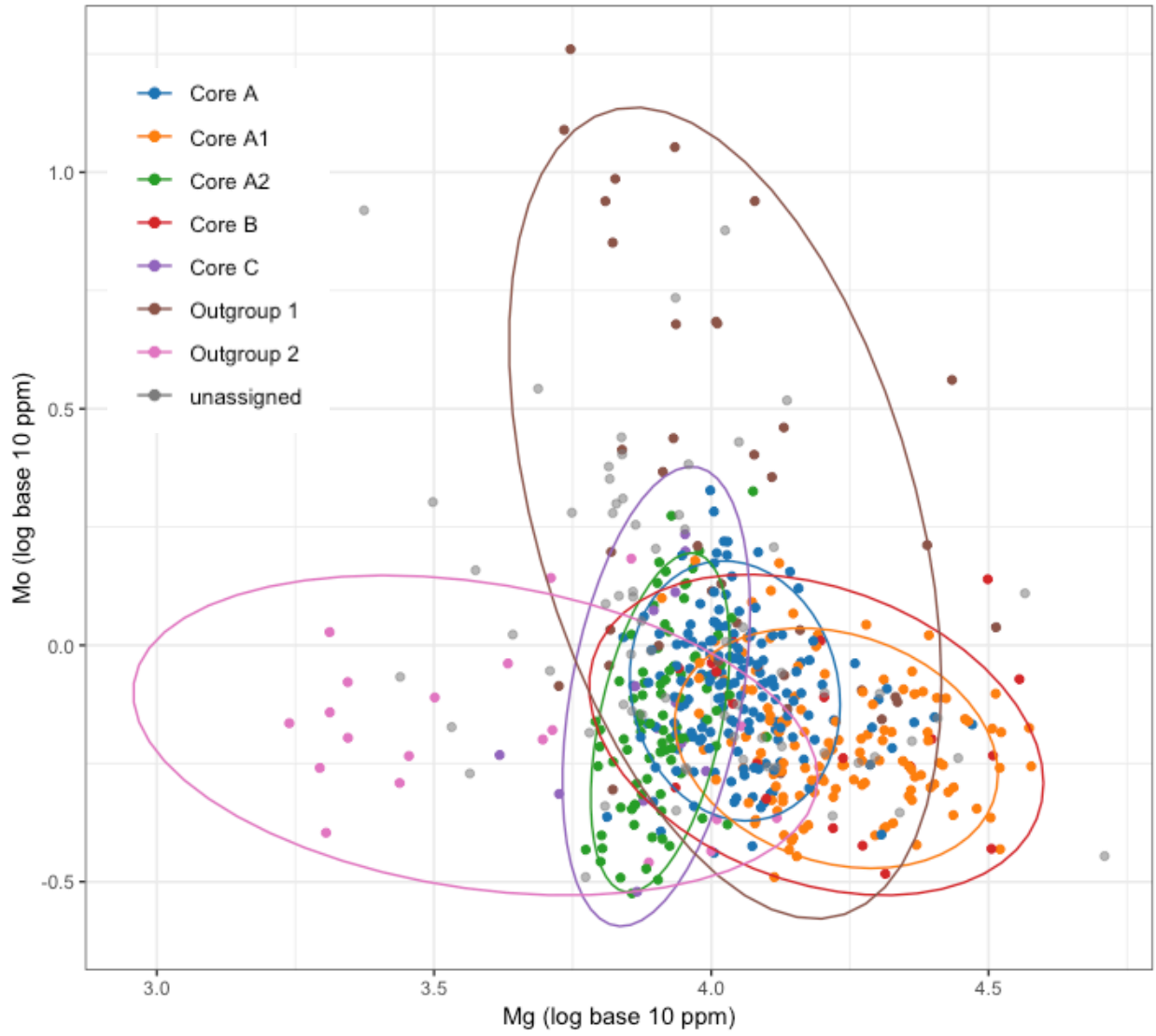


Figure 7.16 Bivariate plot of log base 10 magnesium and molybdenum concentrations of all group, sub-group, and provisional group assignments with 90% confidence ellipse boundaries.

Site	Core A	Core A1	Core A2	Core B	Core C	Outgroup 1	Outgroup 2	Unassigned
Baehr South (11Br47)	6	1	3	-	-	4	-	1
Buckeye Bend (11F310)	8	6	2	2	-	1	-	1
C.W. Cooper (11F11F15)	14	11	1	-	-	1	-	1
Crable (11F249)	8	8	18	-	1	1	11	8
Emmons Village (11F218)	7	12	6	2	-	2	-	1
Eveland (11F353)	6	9	5	4	1	1	2	2
Fouts Village 11F164)	5	11	1	1	-	2	-	-
Houston-Shryock (11F114)	10	12	4	-	-	3	-	1
Kingston Lake (11P11)	12	5	8	1	-	1	-	-
Larson (11F3)	12	16	1	4	-	2	-	5
Lawrenz Gun Club (11Cs4)	5	1	14	-	2	2	-	3
Morton Village (11F2)	17	12	4	6	1	3	2	13
Myer-Dickson (11F10)	6	6	2	-	1	-	-	-
Orendorf C (11F107)	3	6	1	1	-	6	1	12
Orendorf D (11F107)	10	12	4	-	2	2	-	-
Star Bridge (11Br105)	20	2	5	-	2	-	-	-
Ten Mile Creek (11T2)	5	3	4	-	3	2	2	10
Walsh (11Br11)	7	-	5	-	-	6	2	10
Total	161	133	88	21	13	39	20	68

Table 7.7 Compositional group assignments by site

Geography*	Vessel Class	Core A	Core A1	Core A2	Core B	Core C	Outgroup 1	Outgroup 2	Unassigned
North	Jar	63	64	19	14	6	22	3	28
North	Plate	45	45	18	5	2	2	4	17
South	Jar	19	9	26	2	4	7	4	12
South	Plate	34	15	25	-	1	8	9	11

Table 7.8 Compositional group assignments summarized by site geography and vessel class

* North indicates in vicinity, or north, of Spoon/Illinois River confluence at approximately 40.297141N latitude

7.8 Compositional Groups as Economic Social Networks

Using the Brainerd-Robinson coefficient of similarity, it is possible to create networks of economic relationships related to ceramic industry through community-based membership in compositional groups. The Brainerd-Robinson coefficient of similarity assesses how similar any two given sites are based on parallels in the number of individual sherd assignments from those sites in different compositional groups. The resulting similarity scores can be modeled as social networks, which are in turn able to be quantitatively analyzed to reveal insights related to network structure and any changes overtime therein. While this method provides a means to model relational economic interactions as gleaned from ceramic artifacts, it must be acknowledged that these models are highly oversimplified and generalized based on a fragmented archaeological record amidst a highly complex geologic backdrop. Furthermore, since compositional groups are a product of both cultural practice regarding raw material source selection and vessel circulation as well as geological constraints on source material variation, it must be acknowledged that the resulting network relationships are a product of both cultural and geological forces, neither of which may be controlled for in a rigorous way. In other words, relationships as modeled should be viewed, with some skepticism, as a foundational approach using a novel methodology to the analysis of geo-chemical compositional data. Additional sampling, greater geological contextual detail, or comparisons to other Mississippian or Oneota contexts may lend credence to or challenge the results presented herein.

For the purposes of this analysis, six of the eight defined compositional group accounting for 314 ceramic vessels from 18 sites were considered. Because of equivocal group membership probabilities in two or more groups, unassigned samples and samples assigned only to the Core A compositional group were not considered (see Table 7.8). A regression of the number of

compositional groups a site is present in as a function of sample size from that site indicates a statistically significant positive relationship at an alpha of 0.01 ($p = 0.007$) but with a limited explanation of variation in group membership as explained by sample size ($R^2 = 0.37$). This suggests a potential correlation between the number of compositional groups and sample size but with a significant amount of unexplained variability. Economic relationships modeled using the BR coefficient of similarity may therefore be negatively impacted by the vagaries of sampling. Economic relational ties were assigned between sites by defining a threshold similarity value for Brainerd-Robinson (BR) coefficient scores. The threshold value was chosen through an

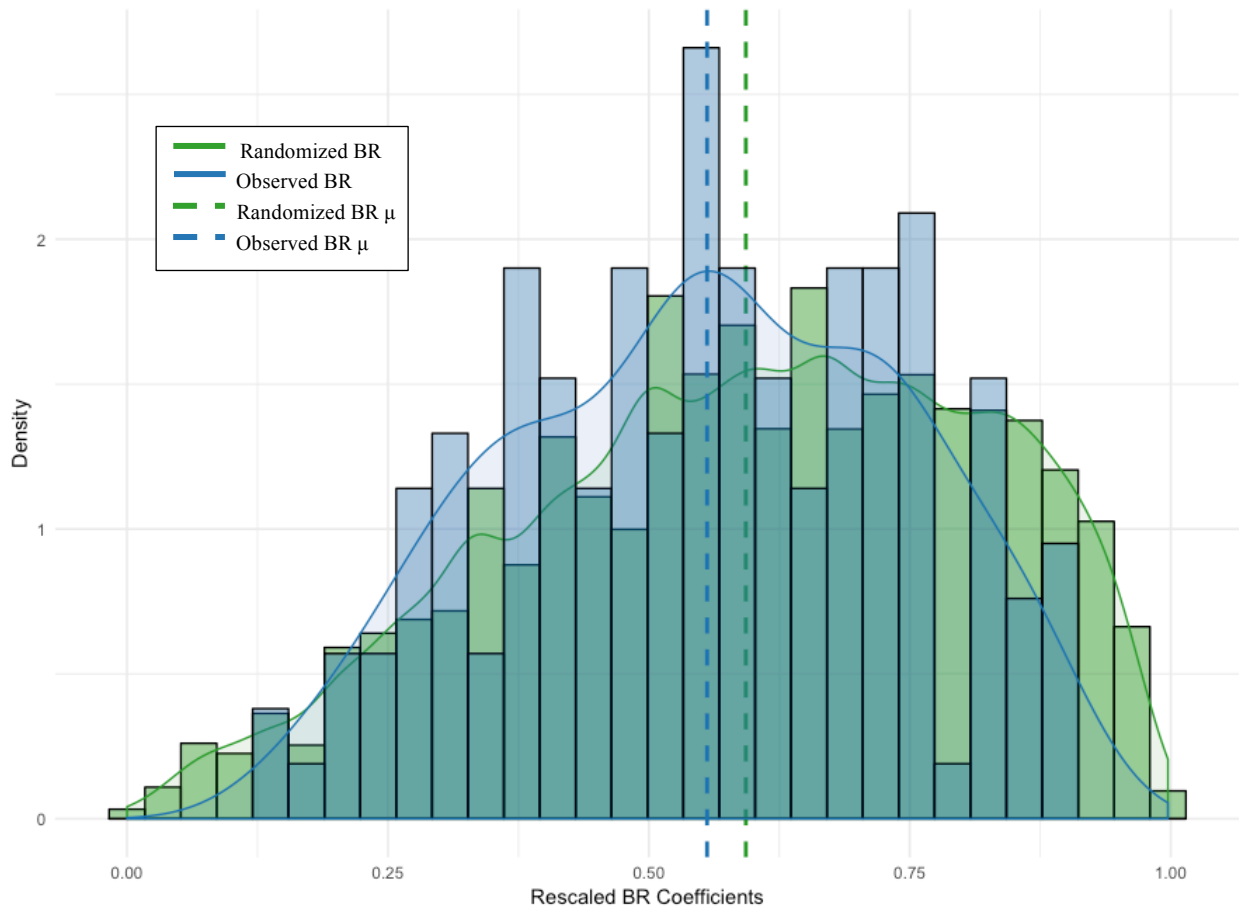


Figure 7.17 Distribution of Brainerd-Robinson coefficients for simulated (green) and observed (blue) compositional group membership matrices

evaluative framework that considers a Monte Carlo procedure that simulates BR scores from randomly generated matrices based on the actual proportions of membership in compositional groups present at each site. That is, the six-column matrix in Table 7.8 (e.g. Core A1 – Outgroup 2) was column and row randomized with replacement 10,000 times. The distribution of BR coefficient values for the randomized matrices provides an estimate of the overall range and frequency of BR scores that might be expected by chance given the number of sites and relative counts for each design category. The random distribution and observed distribution of rescaled BR coefficients are shown in Figure 7.17. The simulated and observed BR coefficients share similar distributions that both approximate normality. Put another way, the underlying structure of economic relationships among archaeological site-nodes is not markedly different from what might be expected by chance alone. This is likely a reflection of the limited number of compositional groups with which to model economic relationships and the fact that many samples were unable to be assigned to a compositional group due to equivocal membership probabilities. However, observed BR coefficients are nuanced in ways that suggest a deviation from random chance. Observed BR coefficients lack scores at the very high and low ends of the distribution, or greater or less than two standard deviations from the mean. Furthermore, significant peaks and valleys at various positions along the histogram presented in Figure 7.17 and a reduced central tendency among observed BR coefficients shows further separation between observed and simulated BR coefficient distributions. Ties between site-nodes are therefore given for all rescaled BR coefficient values greater than the mean BR value for the observed data set. This is an arbitrary value ($BR > 0.55$) but follows the heuristic used across this research of giving a tie between two site-nodes when economic, or other, relationships related to

ceramic industry among them are more similar than they are different in due consideration of the range and frequency of observed similarity scores.

Network data was handled in the R statistical package and exported to Gephi 0.9.2 (Bastian, et al. 2009) for visualization. Geographic network visualizations were rendered in Gephi and overlain on vectorized LiDAR maps using the open-source Inkscape program, version 0.92.2. Slight jittering of site geographic coordinates was applied to protect site locations. LiDAR maps are provided courtesy of the Illinois Geospatial Data Clearinghouse and the University of Illinois at Urbana Champaign. Network statistics were calculated using Gephi 0.9.2 and the R tidyverse and igraph package suites (Kolaczyk and Csárdi 2014; Wickham and Grolemund 2017).

Network statistical measures provide insight into the nature of network topology, or overall structure of the networks. Statistical measures assessed here include mean degree, or average number of edges among nodes in the network; mean weighted degree, or the average of the sum of edge weights among nodes in the network; diameter, or number of steps in the longest path from one node to another; mean path length, or average number of steps for each node to reach every other node; density, or proportion of observed ties compared to the number of possible ties; transitivity, which is also known as the global clustering coefficient, or proportion of transitive triples wherein all three nodes in a triad are connected (Wasserman and Faust 1994). Degree, betweenness, closeness, and eigenvector centralization indices quantify the range or variability of individual actor indices. Centralization indices extend the concept of individual node centrality to the entire network. Degree centralization assesses whether or not all nodes are only connected to a singular central node. Betweenness centralization evaluates the extent to which an individual actor is located ‘between’ other actor pairs – actors in this ‘between’ space

for many actor pairs are likely more critical information conduits. Closeness centralization considers how many actors are within one step, or are ‘close’, to a central node. Finally, eigenvector centralization gauges the degree to which central actors are connected to all other central actors.

In addition to relying on formal methods in the statistical analysis of network data, interpretations are based in part on conditional uniform graph tests through Monte Carlo simulation. Each observed network statistic was compared against the distribution of that statistic generated from 5,000 random graphs of the same order (or number of nodes) and probability of an edge being given between any two nodes (based on the observed graph’s density) or size (number of edges) using the Erdős-Rényi graph randomization technique (Erdős and Rényi 1959). Network randomization simulation enables formal hypothesis testing of whether the observed network statistics are unusually high or low given what might be expected if the same probability of edges (or number of edges) were connected to the same number of nodes as the observed network based on random chance alone.

Erdős-Rényi graph models place equal probability on all graphs of a given order and size. That is, a collection of graphs are considered based on the provided order and size and a probability is assigned to each, where the total number of distinct node pairs are considered (Kolaczyk and Csárdi 2014). An extension provided by Gilbert (1959) enables the random graph concept to be extended to graphs of a fixed order but where each pair of distinct nodes are independently assigned based on a given probability.

It is important to again emphasize that modeling membership in geochemical compositional groups as social networks of economic interaction related to ceramic industry subsumes both cultural *and* geological phenomenon. That is, glacial forces acting on surficial

features and the complex geology of bedrock features results in a lack of discrete patches or zones of geochemical distinctiveness that otherwise might lend itself to the identification of cultural choices made by potter communities in the central Illinois River valley archaeological region. Instead, a pattern of northeast-southwest trending geochemical continuum was shown to best describe the valley based on the sample of sediments and archaeological ceramics analyzed here. Geochemical compositional groups therefore rely on subtle differences in geochemical concentrations, resulting in boundaries between compositional groups that are a more a product of arbitrary statistical features as opposed to reflecting discrete geological source variation in clay resources. This is not uncommon in archaeometry studies (Garraty 2006; Glowacki 2006). Because compositional groups were recognized that had clear geographic trends in the specimens that comprised each group, however, it can be reasonably assumed that most pottery vessels from a given site were locally manufactured, lending to a theoretical approach of modeling networks of economic interaction related to ceramic industry.

7.9 Ceramic Industry Economic Network Analysis and Discussion

A general temporal trend is evident in economic relationships related to ceramic industry in CIRV in network graphs (Figures 7.19 – 7.23) as well as in their associated network statistical measures (Table 7.9; Figures 7.24 – 7.25). In short, ceramic industry economic relationships shift from being characterized as highly interconnected to highly dispersed across the pre-migration to post-migration transition. During both pre- and post-migration periods, there is a high tendency for sites to group together into triadic clusters. However, while these clusters show remarkable overlap in the cohesive pre-migration time period, clustering overlap becomes severely reduced following Oneota in-migration. In other words, the scale of parity in economic relationships

related to ceramic industry as modeled via membership in ceramic compositional groups is greatly reduced from the pre-migration to post-migration time periods. The likely driving force behind this change is a regional de-centralization away from the Spoon/Illinois River confluence and consolidation into fewer settlements at the northerly and southerly geographic extremes of the study region. This finding provides further support for the hypothesis proposed in Chapter 6 for the formation of a social and spatial internal frontier, or unoccupied interstice between settlements (Kopytoff 1987), among Mississippian communities that likely contributed to, or acted to structure, Oneota in-migration. The following discussion considers the context of the formation of an internal frontier from a perspective rooted in the analysis of economic networks related to ceramic industry wherein it is argued that increasing parallels of membership in chemical compositional groups gleaned from ceramic artifacts reflect increasing economic relationships among sites. That is, ceramic industry compositional groups are used as a proxy measure to assess behavioral economic interaction prior to and succeeding culture contact.

A correlation matrix of all rescaled Brainerd-Robinson (BR) coefficients is shown in Figure 7.18. There is a lack of scaled BR coefficient values above 0.91 or below 0.13. Economic network relationship values overall show a higher degree of variation among CIRV sites than those seen in categorical identification networks (see Chapter 6), but a lower degree of variation in models of social interaction through cultural transmission (see Chapter 5). Economic relationships derived from ceramic industry are modeled in network graphs only for sites that were occupied within the same general time period, either the Mississippian CIRV prior to Oneota in-migration (circa 1200 – 1300 A.D.) or following Oneota in-migration (circa 1300 –

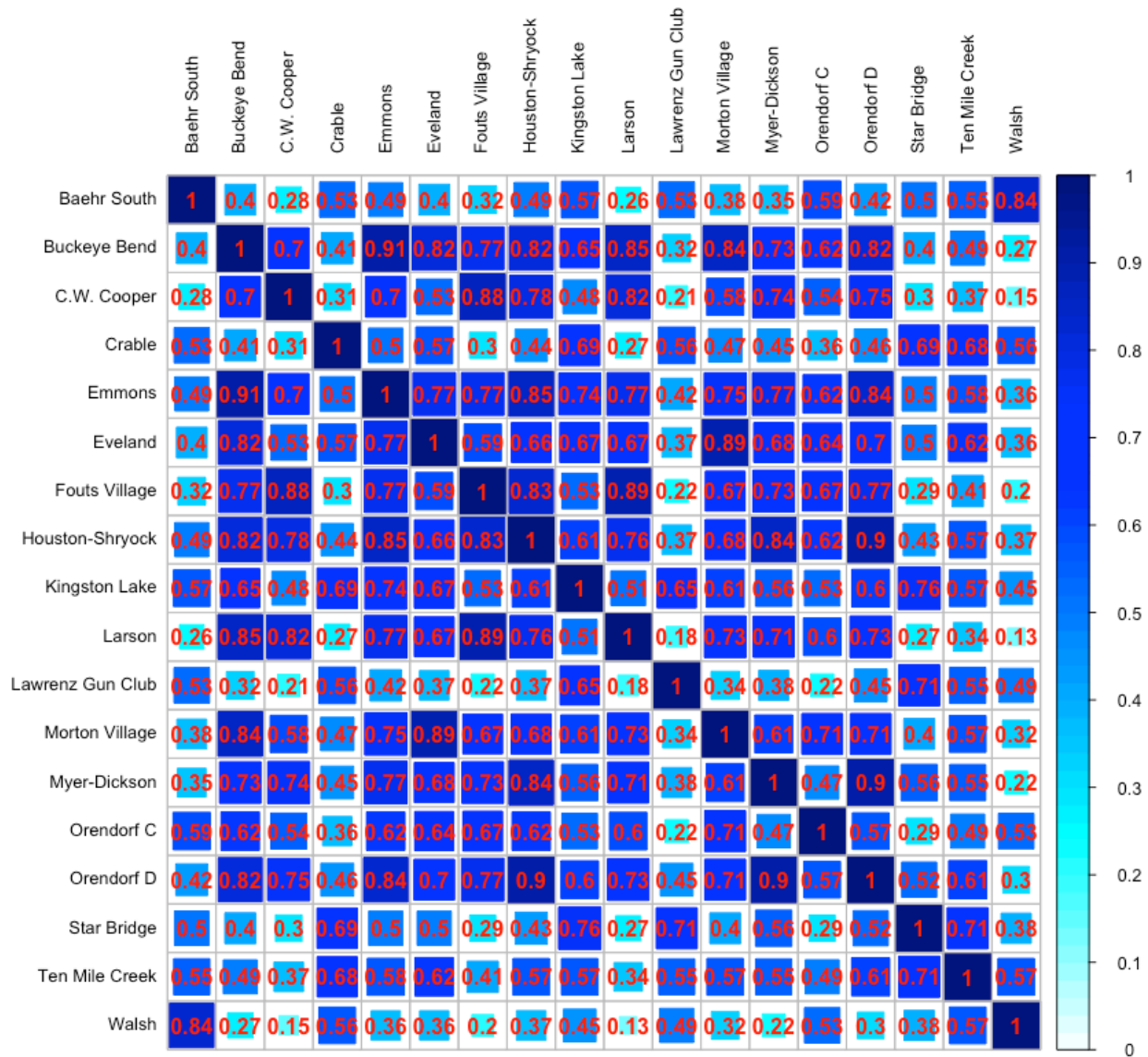


Figure 7.18 Correlation matrix heat-map of rescaled Brainerd-Robinson coefficients

1450 A.D.) and with a BR coefficient value greater than threshold value of 0.55. Because of extended or intermittent occupations that span across the circa 1300 A.D. Oneota in-migration point, Lawrenz Gun Club and Buckeye Bend are modeled in both the pre- and post-migration periods.

Network visualizations are presented, in Figures 7.19 –7.23, in one of two ways. First is through the use of a multilevel layout algorithm that finds a global optimal layout while

approximating short and long-range forces (Hu 2005). In other words, site-nodes with strong similarities in compositional group membership are laid out in closer proximity when all site-to-site relationships are considered. The second layout method uses randomly jittered, or modified, geographic coordinates of sites in a geographic network rendering. In each visualization, site-nodes are colored and sized based on weighted degree, which is the sum of relationship (edge) weights. The edges connecting nodes are colored and sized by weight, or the depth of ceramic industry economic relationship. That is, edges that are darker blue and larger reflect a higher degree of economic relationships among sites, and darker blue and larger site-nodes indicate that a given site is characterized by a high degree of proportional similarities in compositional group membership to many other sites.

	Pre-Migration	Post-Migration	Flattened Across Time
<u>Summary Statistics</u>			
Nodes	11	8	17
Edges	42	10	52
Mean Degree	7.636	2.5	6.118
Mean Weighted Degree	5.576	1.655	4.387
<u>Network Size Measures</u>			
Diameter	3	4	4
Mean Path Length	1.291	2.071	2.066
<u>Network Topology Measures</u>			
Network Density	76.4%	35.70%	38.20%
Mean Clustering Coefficient	90.2%	69.00%	74.30%
Degree Centralization	0.136	0.214	0.305
Betweenness Centralization	0.184	0.612	0.27
Closeness Centralization	0.242	0.492	0.363
Eigenvector Centralization	0.179	0.48	0.502

Table 7.9 Central Illinois River Valley Ceramic Industry Economic Network Statistics

Regressions showed no meaningful statistical relationship in the degree of economic interaction related to ceramic industry as a function of geographic distance between sites (pre-migration: $p = 0.69$, $R^2 = 0.004$; post-migration: $p = 0.55$, $R^2 = 0.046$). This is a somewhat surprising finding given that it would be expected that sites closer in proximity to one another would likely share similar resource catchment zones or engage in more frequent exchange relationships. That distance is not a delimiting factor in the strength of economic relationships among sites attests to the relatively high degree of ceramic compositional group diversity present at each site (Table 7.7), where an average of four compositional sub-groups, outgroups, or provisional groups are represented.

With two notable exceptions, the pre-migration time period CIRV is characterized as highly densely interconnected, cohesive, distributed, and with a statistically significant number of transitive triads, suggesting economic interaction related to ceramic industry at a broadly regional scale. Transitivity is a graph level measure of network cohesion. Also known as the global clustering coefficient, transitivity assesses the proportion of node triads in which all three nodes are connected (Scott and Carrington 2016), capturing the notion of whether or not a ‘friend of a friend is a friend’ (Collar, et al. 2015). In the pre-migration CIRV, this notion holds true some 76.4% of the time. Fully 100% of networks simulated based on the pre-migration economic network using the Erdős-Rényi graph randomization technique showed lower transitivity values, indicating a very highly interconnected network (see Figure 7.24). The average clustering coefficient (which is an aggregate of a node level statistic that assesses how complete the neighborhood of a network is) for the pre-migration period is 90.2%. Taken together, these network statistical measures portend a decidedly cohesive network structure for the pre-migration period. The cohesion of the pre-migration ceramic industry economic network is

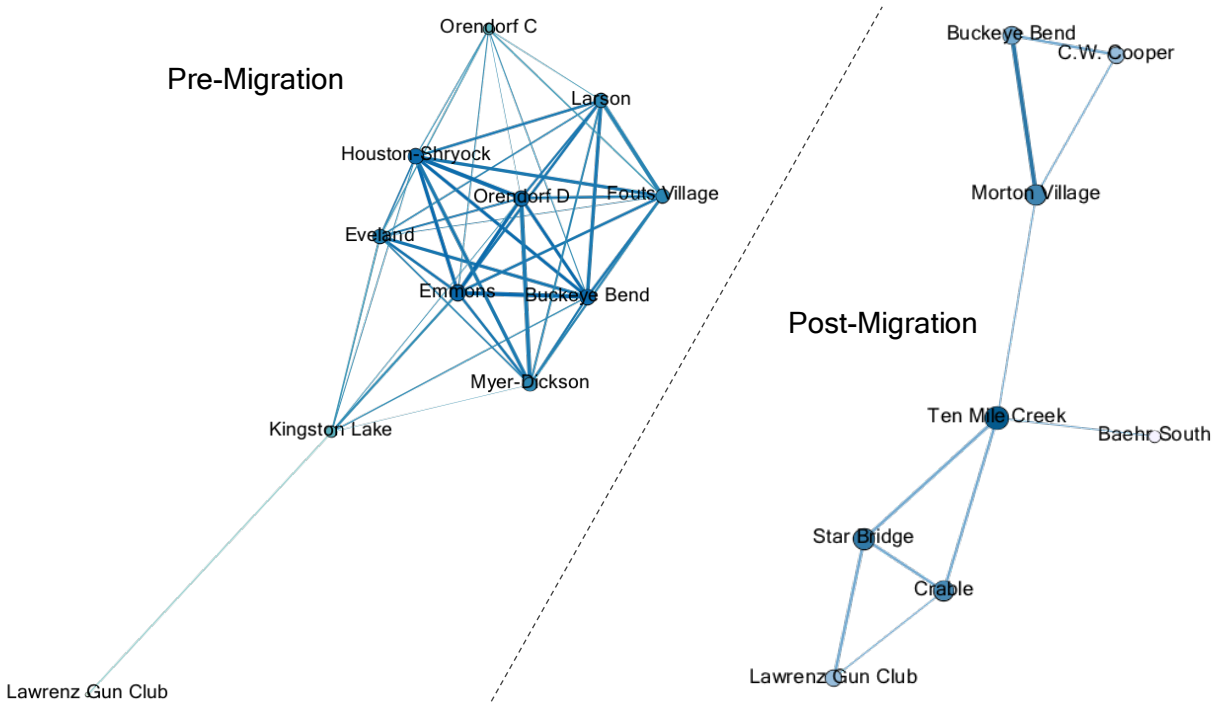


Figure 7.19 Yifan Hu multilevel network graph layout for the Pre-Migration Time Period (1200-1300 A.D.; left) and Post-Migration Time Period (1300-1450 A.D.; right)

illustrated in Figure 7.19, which shows one large cluster of highly interconnected sites with a single outlier – Lawrenz Gun Club. The dearth of edges to Lawrenz Gun Club is most readily explained by its unique geographic location along the Sangamon River within the southerly portion of the Illinois River floodplain as opposed to along the western bluff-tops above the floodplain. The second notable exception to pre-migration regional scale economic interaction is Walsh, the most southerly CIRV site included in this research. No ceramic industry economic relationship modeled with Walsh in the pre-migration period was characterized above the scaled BR threshold value of 0.55. However, Walsh did show meaningful relationships with southerly CIRV sites occupied in the post-migration period such as Baehr South and Crable (Figure 7.18), attesting to the regional foci in the pre-migration time period around the Spoon/Illinois River confluence and expansive occupational scale in the subsequent post-migration period (Figures

7.20 and 7.21 show the comparison). Low centralization scores across the pre-migration period (Table 7.9) indicate a distributed network structure where no single site or site cluster held a proportionally influential position relative to other sites when considering ceramic industry economic interaction.

Following Oneota in-migration, transitivity remained high but is no longer statistically significant (Figure 7.25). Coupled with significant reductions in network density, average degree, and average weighted degree and significant increases in the mean path length and network diameter, there is support for a contraction in the scale at which there is parity in economic relationships among sites from the pre-migration to post-migration time periods. Put another way, the post-migration period is characterized by many fewer relationships that are not only weaker on average but the network as a whole is also less efficient at transporting economic information related to ceramic industry, or vessels themselves, through it. Perhaps most significant is that while three fewer sites were occupied during the post-migration period in network models, network density is less than half of that seen in the post-migration period (76.4% to 35.7% density). Many fewer economic relationships related to ceramic industry were therefore pursued during the post-migration period. The relationships that were pursued were most often reciprocated, however. High average clustering coefficients indicate that the tendency for triads of site-actors to become fully economically interconnected seen in the pre-migration time period largely extends to the post-migration period. Yet, there is a stark shift from economic interaction at a global scale to a significantly reduced social scale. Therefore, a divergence is seen in exchange relationships, raw material catchment zones, and/or ceramic paste preparation methodologies in the CIRV following Oneota in-migration. This is best illustrated in Figure 7.22, which presents the entire ceramic industry economic network flattened across time periods and

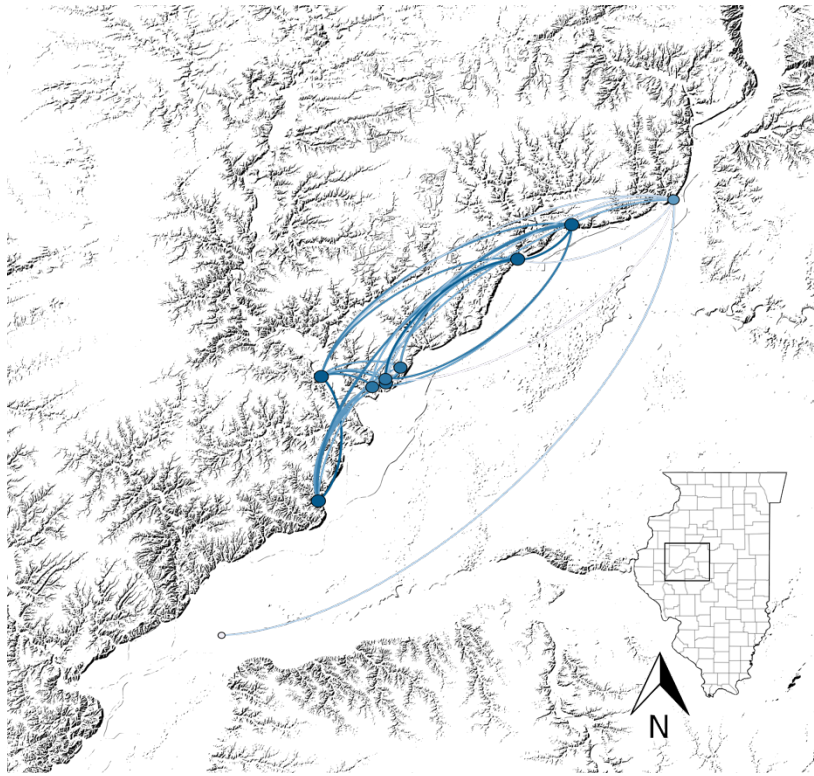


Figure 7.20 Geographic network graph layout for the Pre-Migration Time Period (1200-1300 A.D.)

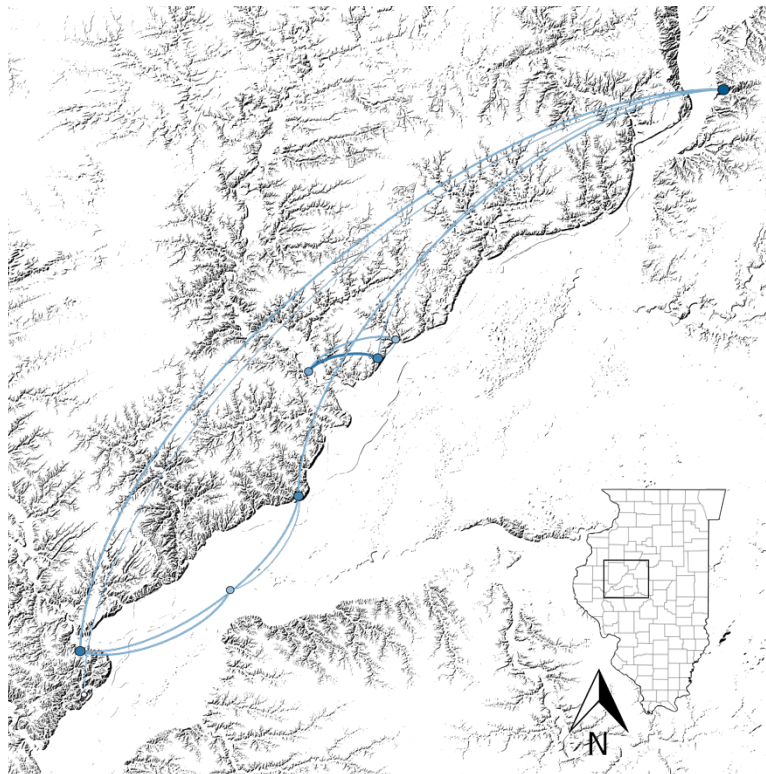


Figure 7.21 Geographic network graph layout for the Post-Migration Time Period (1300-1450 A.D.)

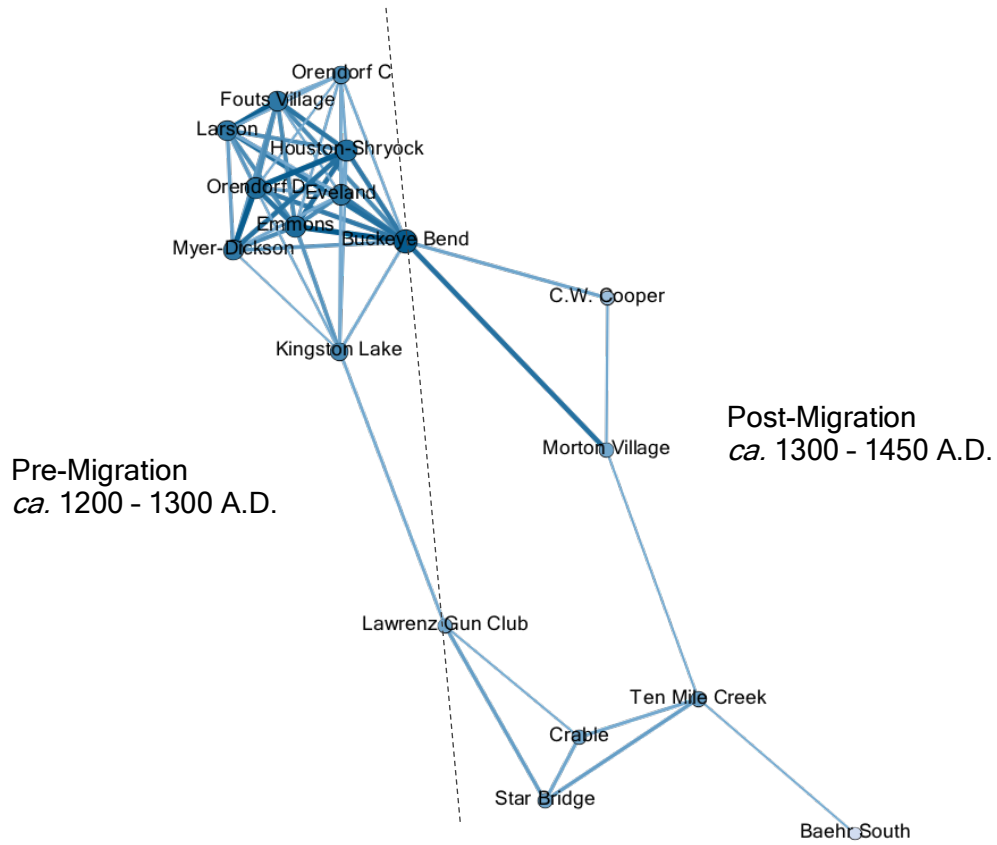


Figure 7.22 Yifan Hu multilevel network graph layout flattened across time (1200-1450 A.D.)

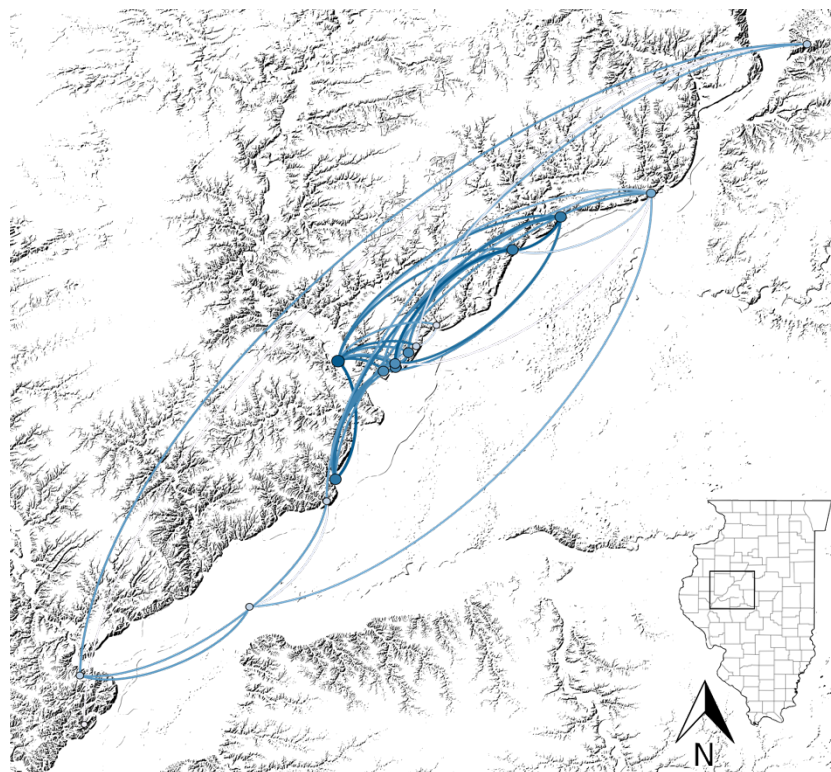


Figure 7.23 Geographic network graph layout flattened across time (1200-1450A.D.)

shows a tight-knit and strongly interconnected pre-migration network juxtaposed next to a splintered and dispersed post-migration period network. The three sites occupied in the Spoon/Illinois River confluence area in the post-migration period do show triadic transitive closure, and this is a significant finding because two of the three sites (Morton Village and C.W. Cooper) have a marked presence of Oneota material culture, suggesting that Oneota and Mississippian peoples not only used similar clay resources but also prepared ceramic paste in ways that led to similar geo-chemical profiles. For these sites, economic relationships are modeled primarily based on a significant presence in compositional sub-group Core A1. Finally, betweenness and closeness centralization scores increase significantly from the pre-migration to post-migration time periods, indicating a less distributed and likely more consolidated network structure (Table 7.9).

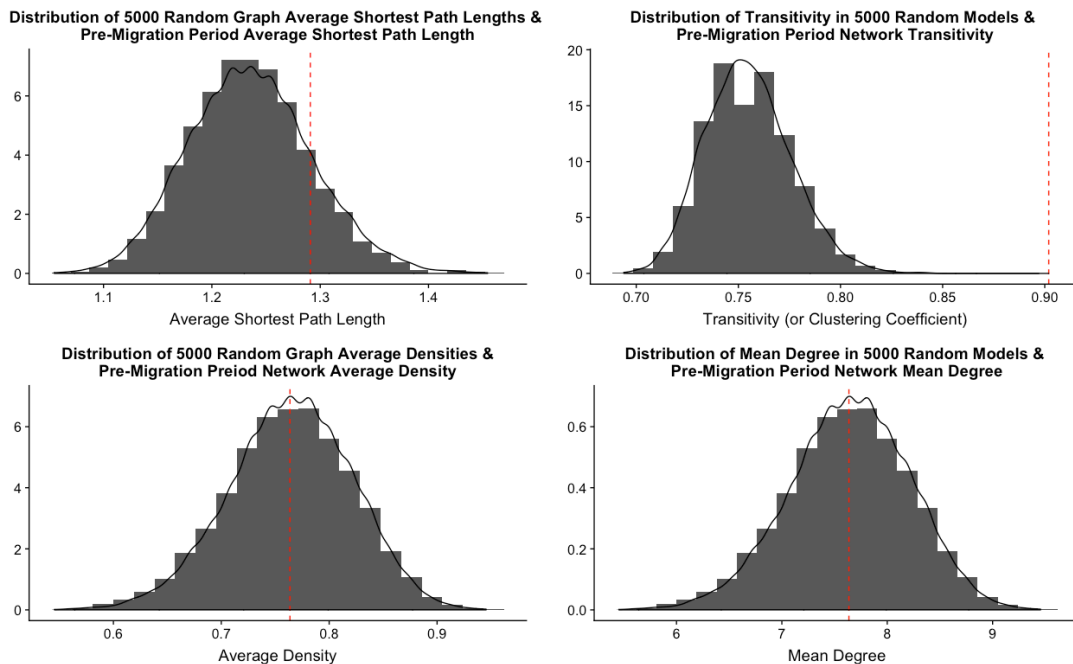


Figure 7.24 Network randomization results for pre-migration ceramic industry economic network. Observed statistic represents red line. Histogram shows distribution of statistic based on network randomization of 5000 random graphs using the Erdős–Rényi random network modeling technique.

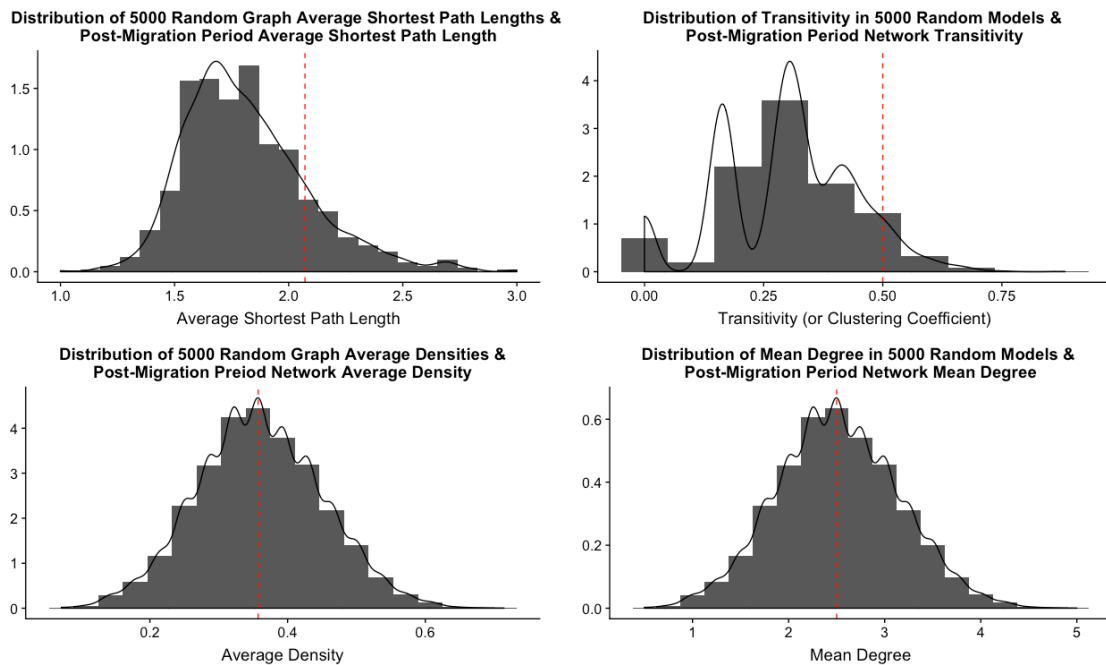


Figure 7.25 Network randomization results for post-migration ceramic industry economic network. Observed statistic represents red line. Histogram shows distribution of statistic based on network randomization of 5000 random graphs using the Erdős–Rényi random network modeling technique.

That such an evident shift is seen from highly cohesive to highly dispersed ceramic industry economic relationships suggests changes in the territorial component of Mississippian societies from the pre-migration to post-migration CIRV. Interacting communities in tribal and chiefly societies exist within recognized territory, in which local resources are often claimed by segments of society (Pugh 2010). Economic networks in the pre-migration period suggest that, in terms of its relation to ceramic industry, resource and exchange relationships were recognized at a broadly regional scale. This infers that a regional territory was likely recognized across the CIRV in the pre-migration period, but in particular in the Spoon/Illinois River confluence area of core Mississippian settlement. Efficient organization of territory and resource management can drive solidarity and downplay in-group social friction, reinforcing existing socio-political-economic power structures (Kowalewski 2006). Dispersal away from the Spoon/Illinois River

confluence and concomitant fracturing of economic network relationships related to ceramic industry indicates that part of the process of the emergence of an internal frontier in the post-migration CIRV was a divergence in economic interests and territorial social boundaries. Thus, perhaps the post-migration CIRV internal frontier burgeoned out of the establishment of buffer zones, which in turn could possibly be related to increasing conflict and violence (Fowles, et al. 2007; G. R. Milner, et al. 1991; G. D. Wilson 2012). However, the economic interconnectedness of Ten Mile Creek, the most northerly site in the post-migration CIRV, with sites such as Morton Village, Crable, and Star Bridge implies that models of antagonism should be nuanced. This is especially true given the complex relationship between war and peace and inter- and intra-group interactions seen in ethnographic contexts among the Santee Dakota and Ojibwa (Landes 1959, 1968), the Lakota (Walker 1982), and in the Mississippian ‘shatter zone’ following contact (Ethridge 2009b) for example.

7.10 Conclusion

The in-migration of Oneota peoples into the Mississippian central Illinois River valley provides a unique social context with which to demonstrate the role of networks of economic relationships as indicators of how both indigenous societies and migrant peoples approach intercultural social and economic relationships. Here, it was argued that increasing similarities of membership in chemical compositional groups among sites is a reflection of increasing economic interactions resulting from the exchange of finished vessels, overlapping resource exploitation areas, or shared paste preparation and ceramic production and refuse regimes. To that end, a number of findings were addressed.

First, ceramic vessels with distinctly Oneota stylistic decoration were unable to be geo-chemically differentiated from their Mississippian counterparts. As a result, it can be assumed that Mississippian and Oneota potters were utilizing similar or identical raw clay sources, engaging in similar paste preparation and production regimes, and discarding vessels in ways that did not result in diagenetic differentiation. Thus, while stylistic and morphological variation is evident among Oneota and Mississippian peoples in the Late Prehistoric CIRV, there is no support for variation in aspects of ceramic industry deemed here as primarily economic in nature.

Second, it has been argued that an observed shift in economic interaction patterns occurred concomitant with Oneota in-migration. Network analysis and simulation indicates that the Mississippian period showed unusually high cohesion in economic relationships related to ceramic industry compared to what might be expected by random chance, evidence supporting regional scale economic interaction patterns. The post-migration period of multi-cultural habitation, on the other hand, is characterized by a highly dispersed network structure where economic interaction was likely engaged in at a significantly reduced social and spatial scale. This was inferred to be reflective of intra-group divergences in economic interests and territorial boundaries related to the formation of an internal frontier. The presence of an internal frontier as a possible outgrowth of buffer zones is likely to have been impactful in structuring Oneota in-migration into the region.

The economic perspective to ceramic industry taken here provides an expansive view to the study of archaeological ceramics in that it considers aspects beyond style, form, and function. Coupled with relational methodologies, a focus on economic interactions such as vessel circulation or exchange, shared resource exploitation zones, and similar ceramic paste preparation methodologies highlights the transmutability of ceramic vessels in a way that cross-

cuts gendered divisions of labor and enables often under-emphasized aspects of the ceramic chaîne opératoire to provide insight into archaeological case studies of behavioral entanglement in multi-cultural social settings.

CHAPTER 8 TOWARD EXPLAINING SOCIAL INTERRELATIONSHIPS THROUGH CERAMIC INDUSTRY MULTILAYER SOCIAL NETWORKS

8.1 Introduction

This dissertation has employed an empirically focused approach to the construction and analysis of social networks in an archaeological case study region. Thus far, each analysis was concerned with a specific type of tie related to ceramic industry and how relations constructed from that type of tie may contribute to explanations of behavioral response trends to culture contact. Because social identities and relationships in human social systems are nuanced in multi-dimensional ways, this concluding chapter draws together each of the unique relational perspectives on ceramic industry discussed heretofore into a synthetic multilayer network. In this way, it is possible to access the influence and overlap of each individual network in structuring and being restructured by migration-induced culture contact in a Late Prehistoric west-central Illinois case study region. From these trends, I argue that patterns of *intercultural communal coexistence* may be revealed. I conclude by discussing the contributions of this study more broadly, caveats and assumptions built into the study, and future prospects for the use of the theoretical model used here in other archaeological contexts and beyond.

8.2 Culture Contact and Multi-dimensionality in Archaeological Social Networks

At the outset of this dissertation, I argued that social networks are conduits for culture. I also argued that networks shape culture (and vice versa), and that culture itself is organized into networks of cultural forms (Azarian 2005; Mische 2011; White 1992, 1993, 2008a, 2008b; White and Godart 2007). Network ties were argued to emerge out of the general chaos and uncertainty among identities. Social networks are informal and temporary patterns of the order that emerge

from such uncertainty and are composed of stories that link identities (White 1992:65). Stories and identities constitute the phenomenological reality of a network. Individual social actors are embedded between many, often divergent socio-cultural groups that each span a distinct network. Because of the plurality of roles across the multitudes of distinct networks, which are often divergent from one another, I further argued that an entire social system may only be approached when multiple relational layers are interconnected and parsed. Building on a recent formalism, I refer to the resulting models as multilayer networks. Using this framework, I argued that it is possible to access and explain behavioral response trends following culture contact under the rubric of *intercultural communal coexistence*. Here, I briefly recapitulate the theoretical and methodological underpinnings of multilayer networks and intercultural communal coexistence.

While social network analysis has surged in popularity in recent decades, it is increasingly being recognized that reducing a social system to a network in which actors are connected by a single type of relationship is often a rudimentary approximation of reality (Kivelä, et al. 2014). Social interactions, for example, seldom develop on a single conduit. Furthermore, pairs of actors can be bound by more than one relationship. Anthropologists and sociologists identified the need to represent social systems through multiple social networks that consider different types of relationships among the same set of individuals many decades ago (e.g. Breiger 1975; Gluckman 1967). It is only through recent breakthroughs in complex systems research, however, that has led to a mathematical formulation of multilayer networks that truly enables this type of analysis (Boccaletti, et al. 2014; De Domenico, Solé-Ribalta, Cozzo, et al. 2013; Dickison, et al. 2016; Kivelä, et al. 2014). Network science has shown that “the structure of the interactions among the constituents of the system plays a fundamental role in shaping the

emergence of complex behaviors, much more important than the role played by the specific properties of the single units of the system” (Battiston, et al. 2017:401-402). Methodologically, adjacency matrices used in monoplex (or single-layer) network analysis are incapable of coping with the challenges posed by networks that span multiple relational layers. Rather than reducing multiple types of tie into a single, all-encompassing tie known as a multiplex tie (Gluckman 1967), however, the mathematical formulation of multilayer networks considers network structure as consisting of multiple layers of connectivity using a tensorial approach (De Domenico, Solé-Ribalta, Cozzo, et al. 2013). This results in models that capture richer and fuller relationships between nodes and better represent the topology and dynamics of real-world social systems.

An apt application of multilayer network analysis is understanding behavioral response trends, or the creative refashioning of cultural forms, to culture contact following human migration (see also Danchev and Porter 2018; Vacca, et al. 2018). In Chapter 2, I argued that these trends may be understood as reflecting strategies of intercultural communal coexistence, or the synchronous habitation of lineally asymmetrical groups in proximity. A theoretical model of intercultural communal coexistence, which is not deterministic of peaceful or tolerant relations, proposes that communities may pursue four generalized behavioral strategies in multicultural environments based on evidence gleaned from relational and social identities: pluralistic coexistence, accommodative coexistence, integrative coexistence, or ethnogenesis (see Table 8.1). Multiple network layers that consider both the depth of interactions rooted in relational

<i>Communal Coexistence Trend</i>	<i>Depth of Relational Interaction</i>	<i>Categorical Identities Similarity</i>
Pluralistic Coexistence	Absent or Limited	Low
Accommodative Coexistence	Moderate to High	Low
Integrative Coexistence	Absent or Limited	Moderate to High
Ethnogenesis	Moderate to High	Moderate to High

Table 8.1 Matrix of expectations for intercultural communal coexistence strategies

identification and similarities in categorical identities are necessary to model intercultural communal coexistence. As a qualitative multilayer topological measure, intercultural communal coexistence characterizes trends across the layers of a multilayer network using insights regarding processes of collective action and social transformation (Peeples 2011, 2018; Tilly 1978).

Depth of relational interaction is evaluated through processes of relational identification, in which individuals identify themselves and others with larger collectives through their positions within networks of interpersonal interaction (Peeples 2018). Relational interaction was examined in this study through analysis of technological type-attributes on domestic cooking jars and serving plates as well as through analysis of ceramic geochemical compositional characterizations focused on identifying patterns of economic interaction through vessel exchange, overlapping resource exploitation areas, or shared paste preparation and ceramic production regimes.

Similarity in categorical identities is assessed through processes of categorical identification, in which individuals identify themselves and others as members in larger social units through similarities in socially defined roles or groups to which one can belong. Categorical identification relies on symbols or other forms of non-verbal communication in order to facilitate recognition among members and non-members of categorical social groups (Peeples 2018). Categorical identification was examined in this study through analysis of stylistic decoration on plates, which are vessels primarily used as serving or presentation pieces often in highly public and highly visible contexts.

Taken together, parity in relational and categorical identities is argued elsewhere to portend social transformations (Peeples 2018). That is, social settings characterized by a moderate to high degree of identities and a moderate to high depth of relational identities at a macro-scale are argued to be primed for collective social action and social transformations (Nexon 2009). As opposed to focusing on collective social action, the emphasis in this research are characterizations of behavioral responses to culture contact. Thus, instead of identifying the potential for collective social action to occur, relational and categorical identification are used here as sensitive indicators of intercultural communal coexistence trends. The trends outlined in Table 8.1 are assessed qualitatively based on quantitative network ties. That is, no attempt is made to define a function that may analyze network layers and provide an assessment of categorical and relational identities as they relate to intercultural communal coexistence trends. Instead, a host of structural and topological characteristics of individual network layers are considered in relation to each other in order to arrive at a value indicating the depth of relational interaction or an assessment of categorical identities similarity in a given social context.

8.3 Layers of Evidence – Results of the Individual Network Layers

The application of network analysis methodologies in archaeology is contingent upon the basic theoretical argument that similarities in material culture used and discarded at different sites can be used as a proxy measure of the degree of social connectedness between them, whether direct or indirect, material or informational (Peeples, et al. 2016:61). The most important aspect of a particular network layer is the type of connection used to construct relationships between nodes. Connections indicative of three types of relationships gleaned from ceramic industry are considered here. All three types of tie chosen for this research constitute

frameworks for constructing relationships between humans, wherein edges between sites act as statements of probability that a relationship existed. A recapitulation of the results of each monoplex network analysis is presented here prior to a presentation and discussion of the complete Late Prehistoric central Illinois River valley ceramic industry multilayer network in the following section.

8.3.1 Relational Interaction from Cultural Transmission

The topic of Chapter 5, the first two network layers assess relational interaction by means of relationships of descent or shared learning mechanisms based on relative technological similarity in type-attributes constrained by social, as opposed to engineering, forces (Eerkens and Bettinger 2008; Peeples 2011). Distinctive combinations of technological characteristics signal shared relationships of learning and the expression of social information among individuals and act as a proxy measure for the communities in which they were nested (Herbich 1987; Stark, et al. 1998). Distinct network layers were constructed for each of two vessel classes: domestic cooking jars and serving plates. From a suite of continuous type-attribute measurements, a quantitative model was applied to identify the specific artifact type-attributes that are free to vary from site to site, which is argued to indicate that social forces are more likely to be a contributing factor to that variation. Site assemblages are then compared to each other based on pairwise comparison of each artifact's socially mediated type-attributes. It was argued that as proportional similarities based on pairwise comparisons of type-attributes between two assemblages increases, so too does the probability that social interaction between those sites occurred as a result of shared learning mechanisms or homologous relationships. Network ties, representing statements of probability that a relationship rooted in relational identities existed between two

communities, were then modeled on only the type-attributes where moderate to high variation is observed across all communities relative to the amount of variation observed across all type-attributes.

Results of the jar and plate technological attribute network layers indicate that significant structural changes in relational interaction occur across the Middle to Late Mississippian transition concomitant with the circa 1300 A.D. in-migration of Oneota peoples into the CIRV. In particular, the scale at which attribute interaction networks form relational connections was shown to change across time. In the pre-migration context, technological similarity in jar attributes suggests cultural transmission across a regional interaction network. At the same time, spatial distance is argued to have acted as a major factor in influencing the degree of technological similarity in plate attributes, suggesting cultural transmission at a more nuanced scale of interaction. This trend inverses following Oneota in-migration and infusion of significant variation in jar technological norms by Oneota peoples, leading to networks of cultural transmission of jar attributes at reduced or nuanced scales of interaction largely based on spatial proximity. However, technological similarity in plate technology exhibits a pattern of creating regional scale relational connections among post-migration sites. Thus, neither the pre- nor post-migration CIRV is characterized by parity in the scale at which networks of interaction through cultural transmission formed strong relational connections across the different vessel classes under consideration.

The post-migration CIRV saw a significant infusion of variation related to jar attribute technology by Oneota peoples. That variation interrupted the regional scale relational interaction pattern seen in the pre-migration jar attribute interaction network. As a consequence, sites with an Oneota presence are weakly integrated into the post-migration jar attribute interaction

network. On the other hand, Oneota peoples did adopt the plate vessel class at two multi-cultural sites, Morton Village and Crable, likely as a result of the regional scale at which plate technological information spread in the post-migration CIRV. This suggests that the plate vessel class was adopted by Oneota peoples based on direct interaction through cultural transmission with Mississippian potters, and likely as a means to bridge extant cultural distinctions in the public sphere of life where a serving plate is most likely to have been utilized.

That both Oneota and Mississippian peoples did share information related to plate production techniques in limited contexts is an indication that cultural transmission patterns, and by extension patterns of relational interaction, were emphasized in certain spheres of material culture or daily life. Further, the expansion of the scale of interaction through cultural transmission of plate attributes suggests that in the public sphere of life in some Mississippian or multi-cultural contexts, attempts at inter-cultural mediation did occur among Oneota and Mississippian potters.

The lack of overlap between the jar and plate network layers presents a quandary when qualitatively assessing the depth of relational interaction gleaned from the cultural transmission of ceramic technological attributes as related to table 8.1. From a relational perspective, both the jar and plate post-migration technological attribute layers exhibit robust network densities (see Table 8.2). However, different sub-groups are apparent in network visualizations for the plate and jar attribute networks (e.g. Figures 5.35 and 5.37). This divergence of trends highlights an important issue when using material culture to model social interaction through relational identification – the social lives around objects often differ greatly, in particular as the social lives of those objects relate to the production contexts in which they are made and used (Appadurai 1986; Herbich 1987). Culture contact, furthermore, can have unpredictable effects on changes in

the social lives of different kinds of material culture. In any case, it is apparent that potters in the post-migration time period CIRV formed networks, directly or indirectly, through a specific kind of interpersonal bond: jar and plate production methodologies. During the multi-cultural post-migration period, networks formed through shared norms in the technological execution of plates spanned a regional scale, while jar attribute networks were likely formed at more nuanced spatial and social scales. However, because relatively dense networks were formed from both of these layers, it can be inferred that relational identities were likely stemmed from regional similarities among potters based on a common interest – producing vessels for the benefit of the community. As a result, under the rubric of Table 8.1, I hypothesize that the depth of relational interaction in the post-migration jar attribute network is moderate and in the post-migration plate attribute network is high, leading to an overall assessment as a moderate depth of relational interaction as seen in the cultural transmission of jar and plate technological attributes in the post-migration CIRV.

8.3.2 *Categorical Identities from Ceramic Design*

In Chapter 6, network layers were constructed that assess shared categorical identities as evidenced by proportions of stylistic decoration similarity (Borck, et al. 2015; Mills, Clark, et al. 2013; Mills, Roberts Jr., et al. 2013). Categorical identities are mechanisms for people to index ascription to common social units, express solidarity, and nonverbally communicate social information (Braun 1985; Wiessner 1990). Due to its highly visible and often symbolic nature, pottery decoration is posited as being an integral part of an active process to signal group membership. Categories of group membership may be related to ethnicity, gender, political status, religious affiliation, labor or craft expertise, or other social units at both hierarchical and

heterarchical levels. Regardless of the specific social grouping, symbolic communication and social identity are argued to interplay recursively. Active expression of identity is therefore intricately linked to the process of symbolization, a process also referred to in other contexts as emblematic style (Wiessner 1983, 1984, 1985, 1990). Consequently, it is argued that stylistic patterns gleaned from symbolic decoration on pottery vessels may reveal networks of shared categorical identities among groups of people in archaeological contexts.

Network models of categorical identities similarity were constructed based on patterns of proportional similarity in designs incised or trailed on the interior outflaring rims of ceramic plates. Plates are typically adorned with design motifs that would be highly visible during quotidian or ritualistic public gatherings. Results from analyses of the plate categorical design social identification network layers indicate that intra-regional mobility and shifting patterns in the scale of parity in networks of social identification during the Middle to Late Mississippian transition resulted in the formation of a spatial and social internal frontier. In many ways, this internal frontier likely structured networks of social identification following in-migration of Bold Counselor Oneota peoples into the CIRV. That is, the circa 1300 A.D. Oneota in-migration coincided with increasing regional diversity in social identification categories, a reduction in the scale of parity in social identification network relationships, and intra-regional mobility toward consolidation among Mississippian peoples. In turn, Oneota peoples likely contributed to increasing diversity in common categories of social identification through the permeation of distinctly Oneota design motif categories, thereby acting to disrupt and exacerbate ongoing restructuring of regional social identification networks and leading to weak integration of multicultural Oneota and Mississippian communities into the larger post-migration identification network.

Under the relational paradigm, social categories become entangled with stories about the nature and the difference of the groups involved. Social categories, in this way, constitute a lens that depicts in-group interaction as filled with solidarity and cross-group interaction as competitive (Fuhse 2015; Tilly 1998b). Increases in the diversity of social categories and the social and spatial fragmentation of those categories of identification in the multi-cultural post-migration CIRV strongly suggests that overall categorical identities similarity should be assessed as limited using the rubric presented in Table 8.1. In other words, the distribution of identities across the CIRV shifted from being homogenous across the population in the pre-migration time period to heterogeneous across the population in the post-migration time period. Forging and reinforcing shared categorical interests and identities in a heterogeneous distribution of identities is a major delimiter to collective action in such a context, even in cases of relatively dense relational social networks.

8.3.3 Economic Relationships as Relational Interaction

In Chapter 7, network layers assessed relational interaction through economic relationships related to ceramic industry through the analysis of pottery chemical composition. That is, increasing parallels of membership in chemical compositional groups was argued to reflect increasing economic relationships among communities (Gjesfjeld 2014, 2015; Golitko and Feinman 2014). Proportional similarities in chemical compositional groups reflect direct or indirect economic relational interaction through the exchange of finished vessels, the sharing of raw source material location information, or involvement in similar ceramic production processes (Brose 1994; Brown 2004; Zvelebil 2006).

Results of economic network analyses and simulation indicated that the Mississippian CIRV was characterized by economic network interrelationships related to ceramic industry of an unusually cohesive nature as opposed to what might be expected by random chance, supporting an interpretation of regional scale economic interaction patterns. This pattern changed dramatically in concert with the in-migration of an Oneota tribal group. Post-migration ceramic industry economic network structure was characterized as highly dispersed with many fewer and weaker relationships, suggesting a reduction in the spatial and social scale at which economic relationships related to ceramic industry were pursued. Furthermore, economic network structure in the post-migration period was shown to reflect the presence of a social and spatial internal frontier. The internal frontier was a possible outgrowth of buffer zone or other territorial boundary changes among Mississippian peoples in the CIRV and was argued to be likely impactful in structuring Oneota in-migration. Finally, Mississippian and Oneota pottery were shown to be chemically indistinguishable, indicating that potters from both cultural groups in the Late Prehistoric period CIRV were utilizing similar or identical raw clay sources, engaging in similar paste preparation and ceramic production regimes, and discarding vessels in ways that did not result in diagenetic differentiation.

Comparing the economic interaction networks across Figures 8.4 and 8.5 to the matrix of intercultural communal coexistence trends in Table 8.1 indicates that the depth of relational interaction through economic relationships should be assessed as absent or limited at the regional scale in the post-migration CIRV time period. In the prior pre-migration time period, dense social ties reflect regionally shared common interests around the procurement, circulation, production, and/or disposal of ceramic artifacts. The delimiting of those ties through processes involved in the formation of a social and spatial internal frontier indicates that inter-personal

bonds through economic processes were re-structured to emphasize local economic processes related to ceramic industry.

8.4 Building Late Prehistoric CIRV Ceramic Industry Multilayer Networks

Multilayer networks were constructed for two separate time periods – the pre-migration, or Mississippian, CIRV (circa 1200 – 1300 A.D.) and for the post-migration, or Cohabitation, CIRV (circa 1300 – 1450 A.D.). Each of the two multilayer networks consist of four separate layers. Individual network layers include 1) relational interaction as assessed through similarities in the cultural transmission of jar type-attributes; 2) relational interaction as assessed through similarities in the cultural transmission of plate type-attributes; 3) categorical identification as assessed through proportional similarities in plate style design groups; and 4) relational economic interaction as assessed through parallels of membership in ceramic compositional reference groups. The multilayer nature of these ceramic industry network models is a framework to understand the structuring and restructuring of economic, cultural, and identity politic interactions both prior to and following a circa 1300 A.D. in-migration of Oneota peoples into the Mississippian central Illinois River valley.

Multilayer network analysis was carried out using two distinct platforms – MuxViz 2.0 and multinet 2.0.0 (De Domenico, Porter, et al. 2015; Dickison, et al. 2016; Magnani 2017), both using the R statistical programming language. All R code for the multinet analysis is provided in Appendix C. No code is provided for the analyses performed using MuxViz, as it is a graphical user interface driven program. However, as it is open source, all code for the analytical measures is freely accessible.

A detailed discussion of methods used for the construction and analysis of multilayer networks is provided in Chapter 4 and as such will not be reiterated here. However, it is necessary to note an important caveat in the formation of ceramic industry multilayer networks for the pre-migration and post-migration time periods of the Late Prehistoric central Illinois River valley. Due to the complex tensorial approach used to construct multilayer networks (via rank-4 tensors (De Domenico, Solé-Ribalta, Cozzo, et al. 2013)), it was necessary to convert all network layers to a consistent format. Because the methods used to construct the economic networks related to ceramic industry and the categorical identification networks related to ceramic style result in undirected networks, it was necessary to convert the jar and plate attribute networks to a similar format. That is, the jar and plate attribute network layers were converted from directed networks to undirected networks. In cases where two directed connections existed among nodes in the attribute networks, the average of the two connections was taken as the undirected edge weight. While this results in a significant loss of nuanced information, the overarching patterns in these networks remain largely intact. However, as a result of the attribute networks' decomposition from directed to undirected, the multilayer networks that follow should be considered experimental in nature and to be used primarily as a means to provide heuristic insight into understandings of the individual network layers and their relationships to each other.

While the methods used to construct individual network layers differ (see Chapters 5 – 7), the methods used to visualize these layers in the figures below (Figures 8.1 – 8.5) were consistently applied across the layers. All visualizations were rendered in Gephi 0.9.2 (Bastian, et al. 2009), and are presented in two ways. The first method focuses on network structure in due consideration of the geographical positioning of site-nodes. Geographic network visualizations were rendered in Gephi and overlain on vectorized LiDAR maps using the open-source Inkscape

program, version 0.92.2. Slight jittering of site geographic coordinates was applied to protect site locations. LiDAR maps are provided courtesy of the Illinois Geospatial Data Clearinghouse and the University of Illinois at Urbana Champaign. The second method focuses on network structure disregarding the geographical location of nodes. A multilevel layout algorithm was used that finds a global optimal layout while approximating short and long-range forces (Hu 2005). In other words, site-nodes with strong relationships are laid out in closer proximity in consideration of all site-to-site relationships.

Within each visualization (Figures 8.1 – 8.5), a consistent format was applied to depict information about the relative influence of individual nodes as well as information about the edge relationships as modeled. Site-nodes are colored and sized based on weighted degree, which is the sum of relationship (edge) weights. The edges connecting nodes are colored and sized by the weight of the relationship as modeled. That is, edges that are darker in color and larger reflect stronger similarities in categorical identification or increased depth of relational interaction among sites, and darker and larger site-nodes indicate that a given site-node is characterized by a high degree of proportional similarities in categorical identification or significant depth of relational interaction to many other sites. Standard monoplex network statistical properties are provided in Table 8.2 for each of the network layers. For definitions of the measures, see Chapter 4.

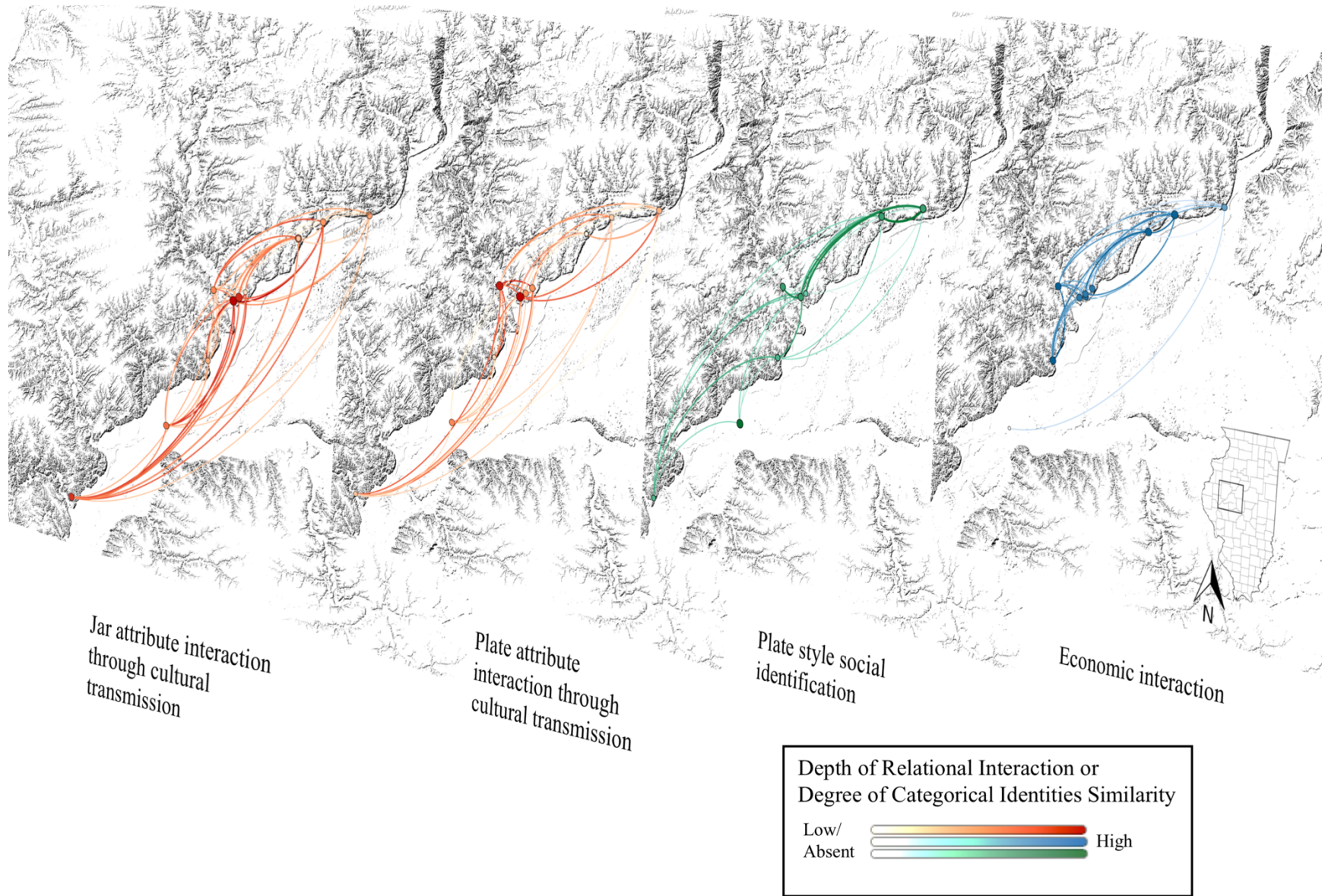


Figure 8.1 Pre-migration multilayer network (circa 1200 – 1300 A.D.)

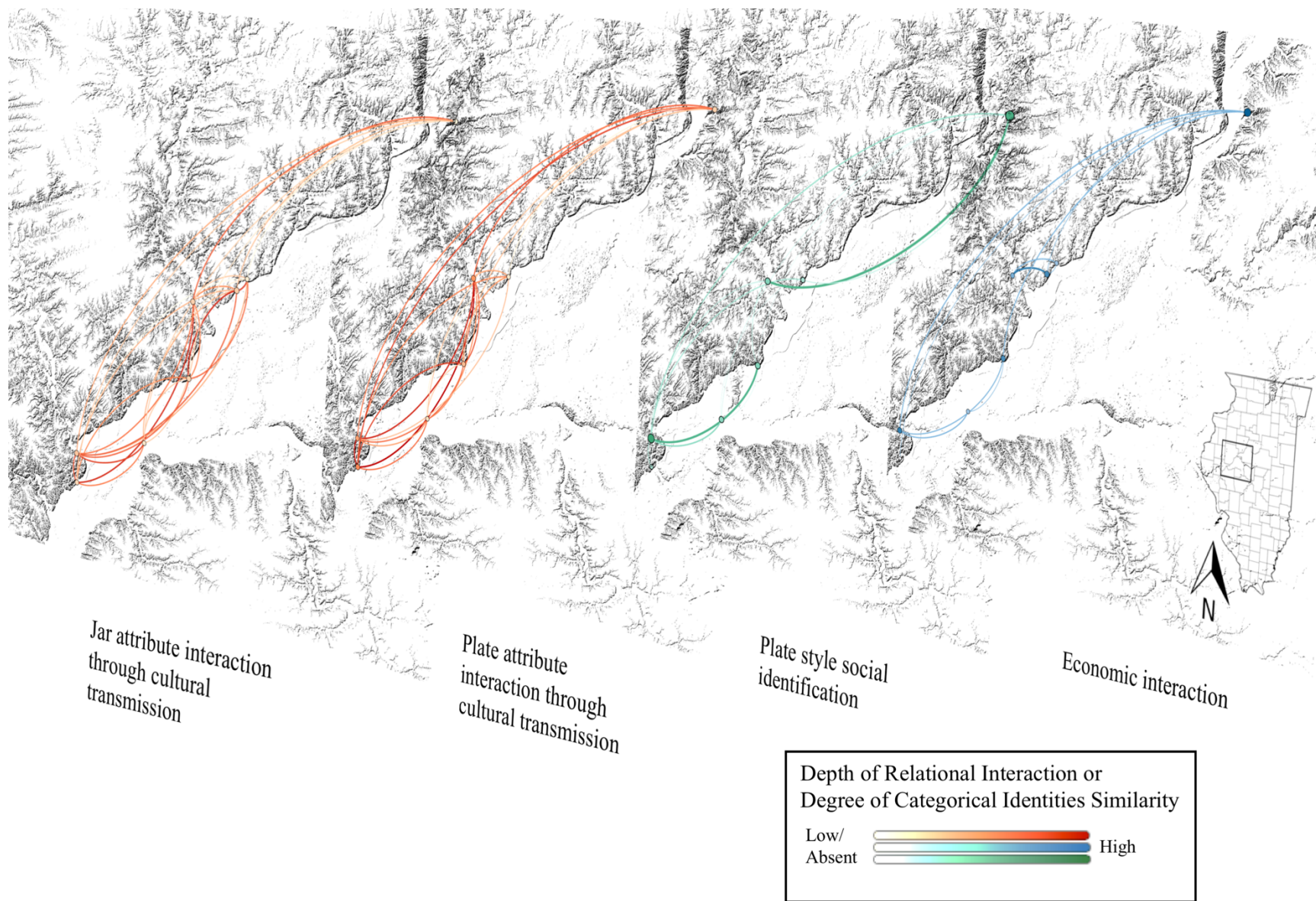


Figure 8.2 Post-migration multilayer network (circa 1300 - 1450 A.D.)

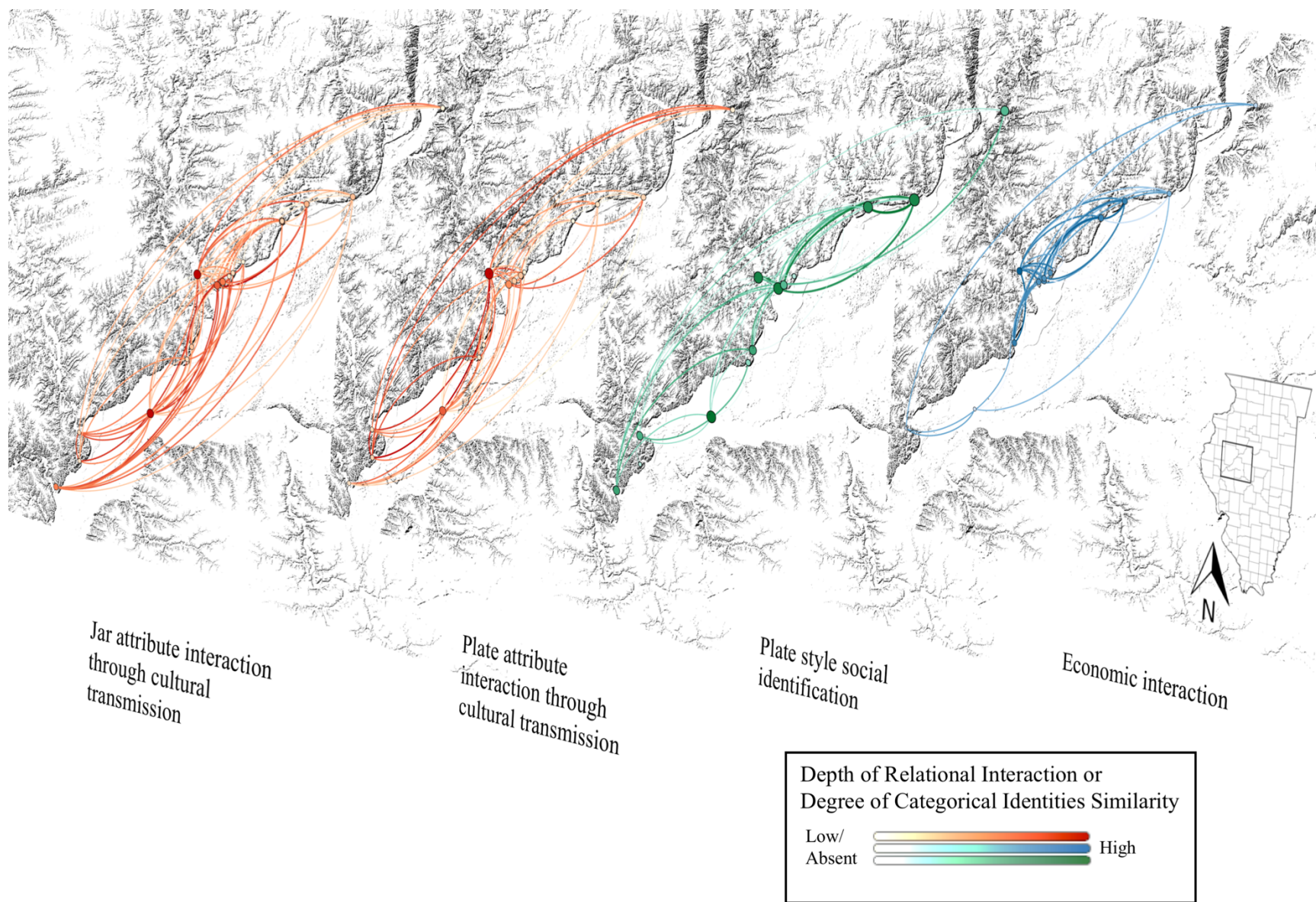


Figure 8.3 Flattened multilayer network (circa 1200 - 1450 A.D.)

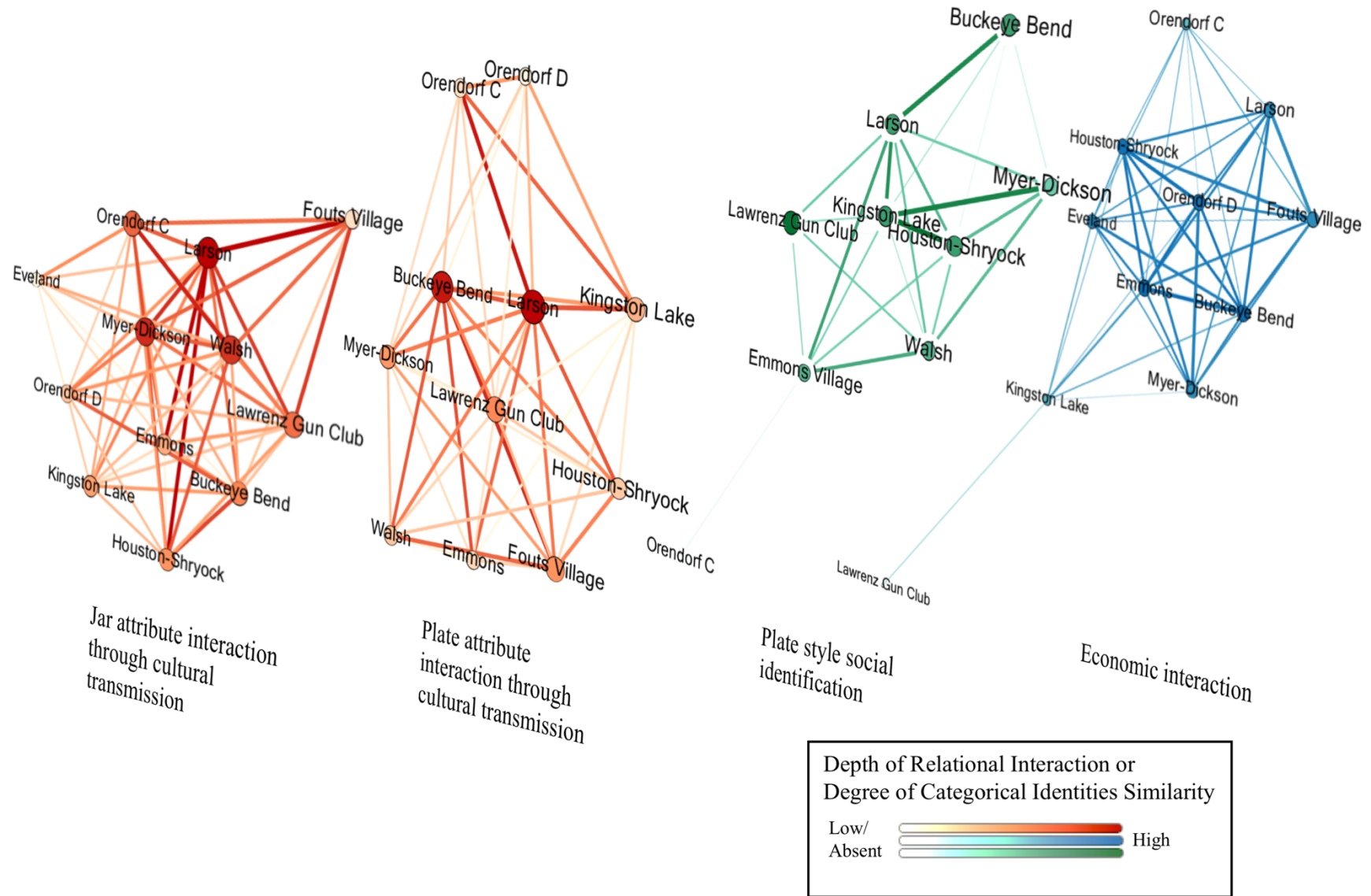


Figure 8.4 Multilevel graph layout for the pre-migration multilayer network (circa 1200 - 1300 A.D.)

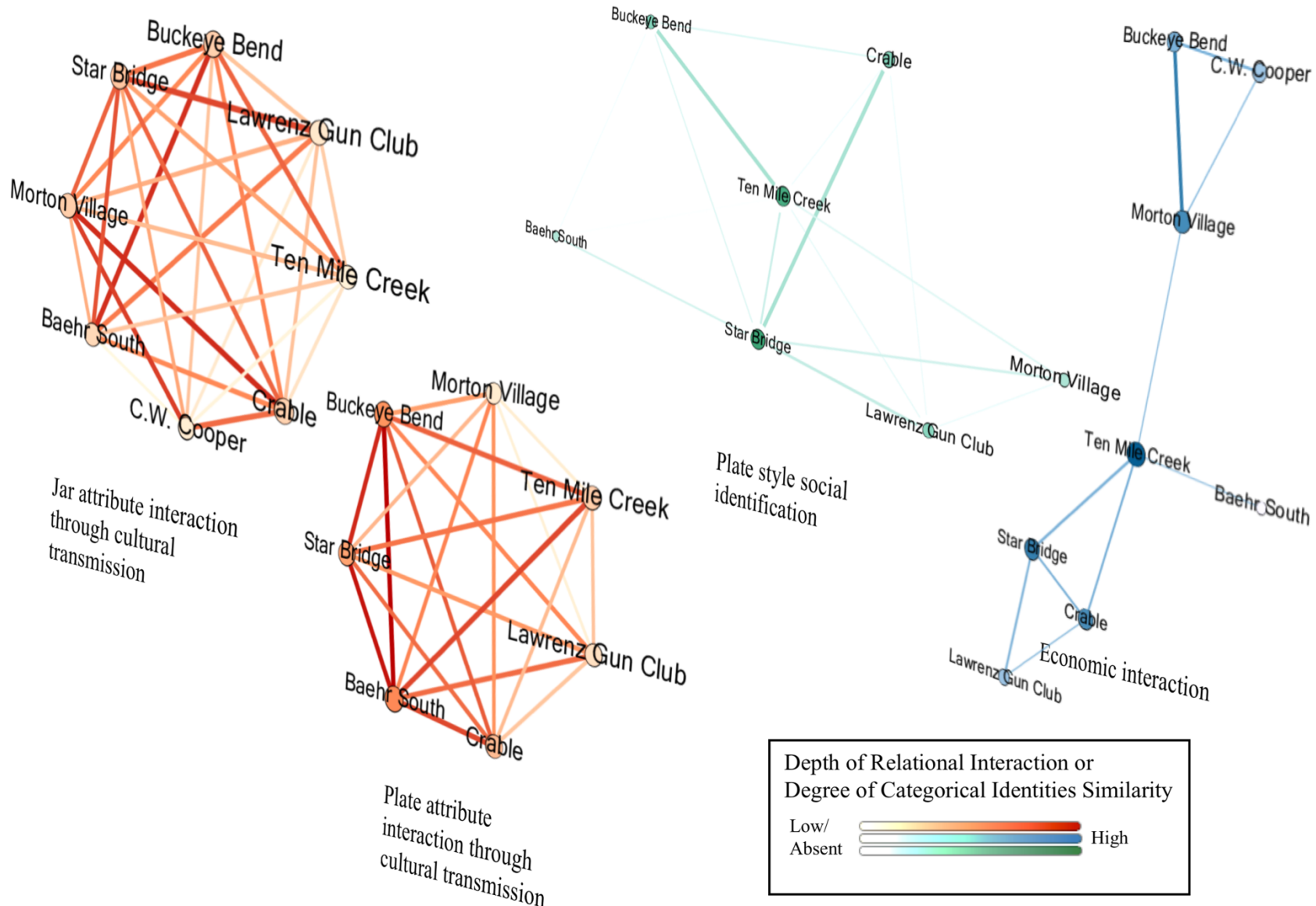


Figure 8.5 Multilevel graph layout for the post-migration multilayer network (circa 1300 - 1450 A.D.)

	Jar Attribute - Relational			Plate Attributes - Relational			Plate Style - Categorical			LA-ICP-MS Economic - Relational		
	Pre-Migration	Post-Migration	Flattened Across Time	Pre-Migration	Post-Migration	Flattened Across Time	Pre-Migration	Post-Migration	Flattened Across Time	Pre-Migration	Post-Migration	Flattened Across Time
Summary Statistics												
Nodes	12	8	18	11	7	16	9	7	14	11	8	17
Edges	56	28	83	44	21	64	24	15	39	42	10	52
Mean Degree	9.333	7	9.222	8	6	8	5.333	4.286	5.571	7.636	2.5	6.118
Mean Weighted Degree	7.042	5.129	6.903	5.503	4.585	5.694	2.922	2.057	2.901	5.576	1.655	4.387
Network Size Measures												
Diameter	2	1	2	1	1	2	3	2	4	3	4	4
Mean Path Length	1.152	1	1.458	1.2	1	1.467	1.389	1.286	1.692	1.291	2.071	2.066
Network Topology Measures												
Network Density	84.8%	100.0%	54.2%	80.0%	100.0%	53.3%	66.7%	71.40%	42.90%	76.4%	35.70%	38.20%
Mean Clustering Coefficient	87.7%	100.0%	87.9%	84.4%	100.0%	85.7%	68.6%	72.20%	64.60%	90.2%	69.00%	74.30%
Degree Centralization	0.152	0.036	0.397	0.200	0.048	0.467	0.208	0.286	0.264	0.136	0.214	0.305
Betweenness Centralization	0.014	0.002	0.215	0.028	0.004	0.215	0.219	0.128	0.237	0.184	0.612	0.270
Closeness Centralization	0.274	0.077	0.540	0.356	0.105	0.669	0.336	0.519	0.299	0.242	0.492	0.363
Eigenvector Centralization	0.146	0.038	0.340	0.198	0.052	0.441	0.277	0.299	0.386	0.179	0.480	0.502

Table 8.2 Network properties for individual undirected network layers

8.5 Overlap and Influence among Layers and Communities

In this section, I discuss the overlaps and influence among different network layers and among the communities within them from a quantitative perspective. Many monoplex network analytical measures have been extended to the analysis of multilayer networks (De Domenico, Porter, et al. 2015). These include analytical areas such as centrality (or node-level positioning), community detection, and connected components. However, there are two classes of measurements in particular that are unique to multilayer network analysis: overlap and influence. Influence in multilayer network analysis refers to the impact of a particular network layer on the full multilayer network. Overlap refers to the number of nodes and edges that are shared across different network layers. These measures may be applied to individual communities through inter-layer analyses of centrality, the degree to which node connectivity deviates across layers, and the redundancy of nodes connections across layers. In highlighting the convergence or divergence of individual network layers from one another, these measures emphasize a fundamental condition of human social reality, namely that individuals are embedded in multiple networks that may span very different or very similar architectures of relationships.

8.5.1 *Layer Interactions*

While most social network analyses tend to focus on the importance of individual nodes or seek to characterize network topology, the multilayer network formulation enables the comparative analysis of different network layers. Focus is placed here on assessing changes in the overlap of edges across the various Late Prehistoric CIRV ceramic industry networks. In particular, edge overlap assesses whether or not a node to node relationship present in one layer is also present in another layer (Munson and Macri 2009; Preiser-Kapeller 2011; Szell, et al.

2010). Edge overlap is measured in three ways: Jaccard similarity (or the intersection of edges present in both layers divided by the union of all possible edge relationships in both layers), Simple Matching (or whether or not an edge present in one layer is also present in another layer disregarding edge weight), and Edge Overlap (which is the same as Simple Matching but factors in edge weight). Edge overlap is a means to quantify inter-dependencies between the different network layers. Note, however, that no causal direction can be implied using these measures. Edge overlaps for the pre-migration CIRV time period are presented in Figure 8.6 and for the post-migration time period in Figure 8.7.

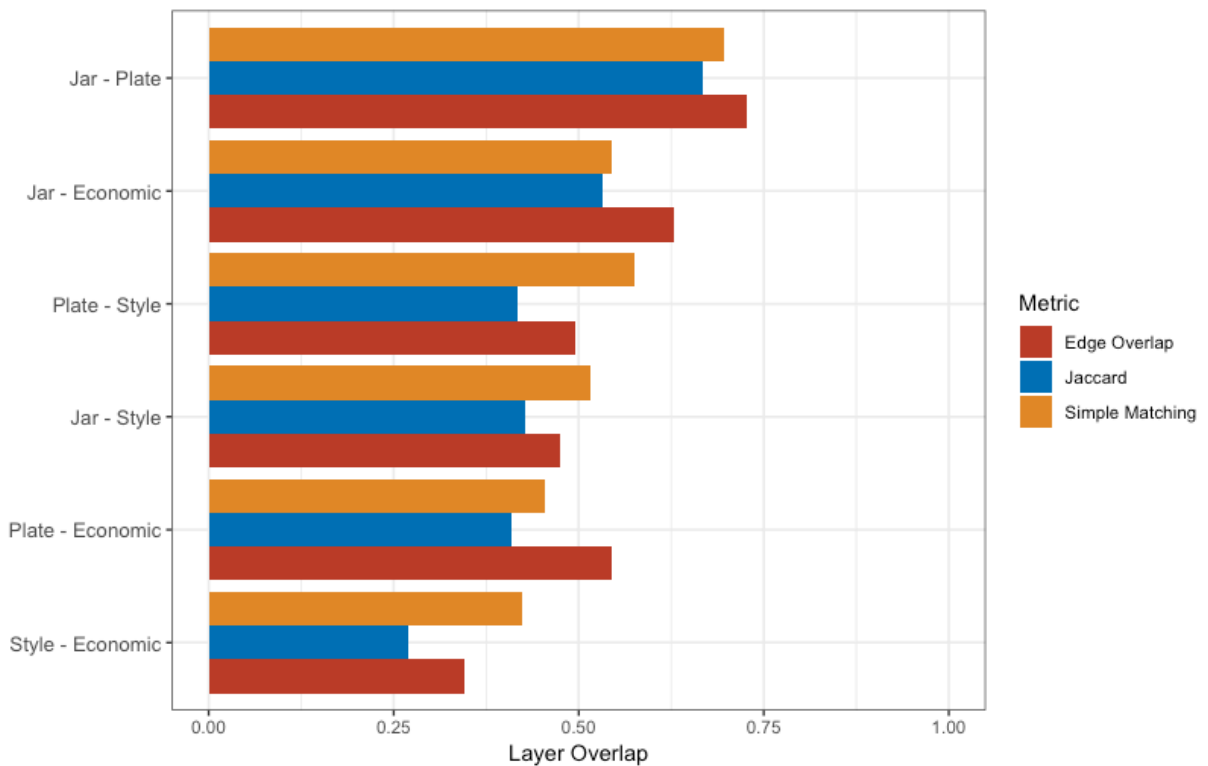


Figure 8.6 Edge overlap for the pre-migration time period

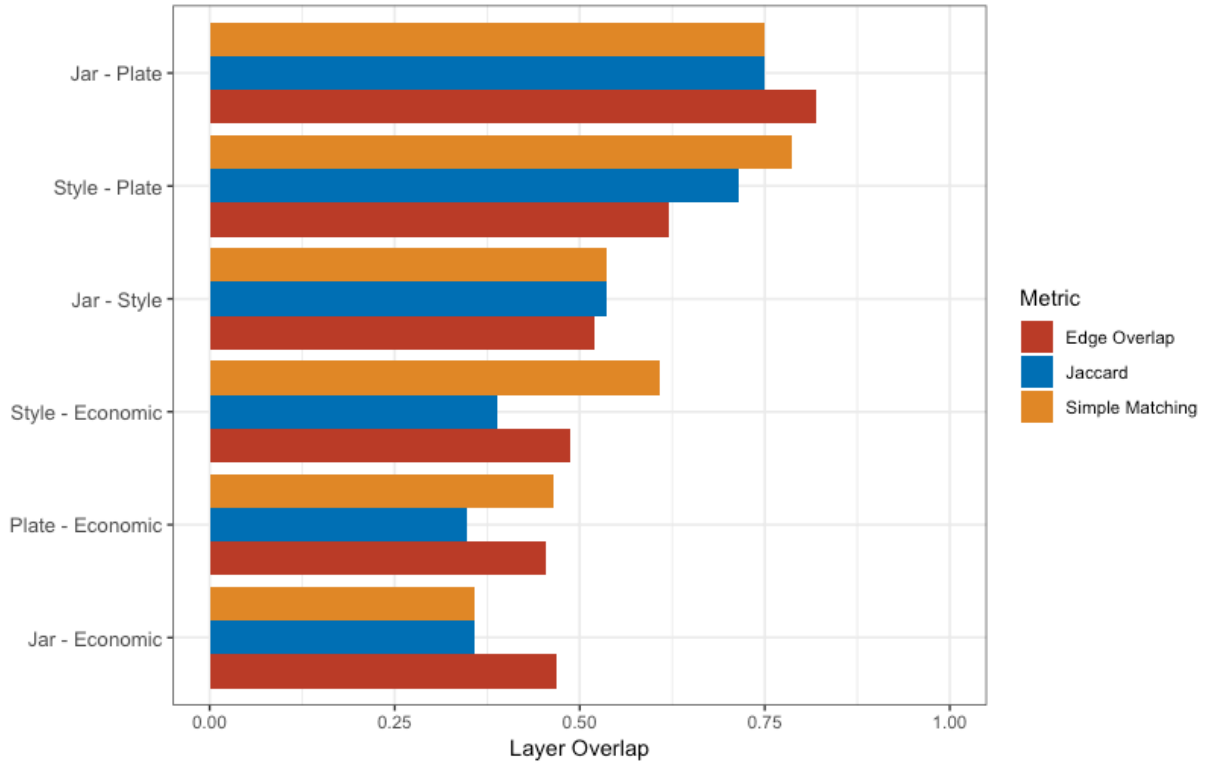


Figure 8.7 Edge overlap for the post-migration time period

The following interpretations are provided for each pair of layer interactions:

Jar attributes – Plate attributes. High edge overlap is exhibited for each of the three different metrics for jar and plate technological attribute network layers. That this trend is consistent across both the pre-migration and post-migration time periods indicates that communities of artisans developed strong channels for relational social interaction through the cultural transmission of ceramic technological information in the pre-migration period and maintained those channels following Oneota in-migration. Thus, relative to other layers of interactions, the cost of interaction through shared relational identification among potter communities was low throughout the Late Prehistoric CIRV with regard to the exchange of information related to socially mediated artifact attributes of pottery vessels used for quotidian tasks such as cooking and serving food. This highlights the importance of teaching, learning, emulation, and non-verbal communication through pottery technological characteristics among

Late Prehistoric CIRV communities. It is again important to note that this interpretation is based on undirected networks of jar and plate technological attribute similarity, see Chapter 5 for more nuanced interpretations of network layers constructed using directed relationships.

Plate attributes – Plate Style. Edge overlap across the plate technological attributes and plate stylistic categorical identification network layers shows the most significant numerical increase from the pre-migration to post-migration time periods. In other words, while categorical identity was less likely to influence plate technological characteristics in the pre-migration period (or *vice versa*), as the number of categorical identities present in plate stylistic designs increased concomitant with Oneota in-migration, so did the likelihood that sites sharing similar categorical identities produced plates with similar socially mediated technological attributes. This would suggest that while potters maintained relationships for the cultural transmission of artifact attributes, those relationships were more likely to be present among sub-groups that shared common social identities following Oneota in-migration, perhaps attesting to the increasing importance of exclusivity in categorical identities among Mississippian peoples in particular in the post-migration CIRV.

Jar attributes – Plate Style. Edge overlap in networks of jar technological attribute and plate stylistic categorical identification networks follow a similar but less pronounced increase as in the plate technological attribute and plate style layers edge overlap. This bolsters an interpretation that cultural transmission of artifact attributes was more likely practiced among sub-groups of communities whose potters indexed shared categorical identities (or *vice versa*) in the post-migration CIRV compared to the pre-migration CIRV.

Jar attributes – Economic interactions. Edge overlap measures between the jar attribute and economic interaction layers show the steepest drop from the pre-migration to post-migration

time periods (from the second highest layer edge overlap in the pre-migration to the lowest in the post-migration). The high edge overlap in the pre-migration period suggests that information about jar technological attributes flowed freely among communities who also utilized similar raw clay resources, had overlapping resource exploitation zones, or frequently exchanged ceramic vessels. The break-down in overlap among these relational channels following Oneota in-migration is likely related to the formation of a social and spatial internal frontier discussed in section 8.3. Late Prehistoric communities consolidated away from the Spoon/Illinois River confluence area, which decreased the likelihood of overlapping resource exploitation areas and increased the cost of vessel exchange due to longer travel distances. Territoriality perhaps increased as well. Channels of interaction through relational identification were thus unequal across the layers in the post-migration period.

Plate style – Economic interactions. Edge overlap in the plate stylistic categorical design layer and the economic interaction related to ceramic industry layer increases from being the lowest in the pre-migration period to being moderately high in the post-migration period. This indicates that overlapping resource exploitation areas, information related to raw clay resources, or the exchange of finished vessels was not limited to communities that indexed similar categorical identities using plate stylistic decoration in the Mississippian CIRV but that this trend changed following Oneota in-migration. This provides support for an interpretation that the post-migration CIRV likely saw an intensification of territoriality, which was related in some way to sub-groups who increasingly signaled membership in social sub-groups through plate stylistic decoration.

Plate attributes – Economic Interactions. Overlapping edges among the plate technological attribute transmission layer and the economic interaction related to ceramic

industry layer remain fairly low across the pre-migration to post-migration transition in the Late Prehistoric CIRV. This suggests that economic interaction related to ceramic industry did not go hand in hand with the cultural transmission of socially-mediated plate technological characteristics. In other words, communities that consistently transmitted information about socially mediated plate technological characteristics were not necessarily also sharing information related to raw clay resources, utilizing overlapping resource exploitation areas, or exchanging finished vessels and that this trend was consistent both prior to and following Oneota in-migration.

Comparing each of the individual layers of the Late Prehistoric CIRV multilayer network highlights the different network model architectures along which information, individuals, and material culture could flow and how those channels change following culture contact. There are some notable trends discussed in the network layer comparisons that are worth emphasizing. In particular, Late Prehistoric ceramic artisans appear to have been sensitive to changes in the technological characteristics of both jars and plates across the pre-migration and post-migration time periods. This suggests low interaction costs, relative to other layers, regarding the cultural transmission of socially-mediated artifact attribute information through teaching and learning, emulation, the likely exchange of individuals across communities, and the likely gathering of groups together for events to facilitate such transfers of information or individuals. Another significant finding is that categorical identities became a more influential predictor of interaction through relational identification following Oneota in-migration. It is possible that this trend predated culture contact to some extent, but nevertheless a key facet of behavioral response trends to culture contact in the multicultural CIRV was a disruption of prior regional inclusivity in the indexing of social categories toward increasing exclusivity through a proliferation of social

categories. Channels of economic interaction related to ceramic industry that were largely tenuous in the pre-migration CIRV appear to have waned following culture contact. This suggests increasing territoriality and the presence of an internal frontier inhibiting otherwise strong channels for interaction through relational identification related to the cultural transmission of ceramic technological attributes in the post-migration time period. Before turning to a discussion of how commonalities and divergences of individual network layers may relate to intercultural communal coexistence trends, it is pertinent to explore the role of individual site-actors through an analysis of community interactions across the multilayer network.

8.5.2 Community and Layer Influence

A key aim of network analysis studies is to examine the role(s) of individual nodes in a network. Identifying which nodes are most influential often provides a means toward interpreting network structure and explaining the social system as modeled (e.g. Mizoguchi 2009; Padgett and Ansell 1993). Using a multilayer network formulation, it is possible to explore how influential individual nodes are across different layers, providing a richer and fuller understanding of node influence on the entire social system. Toward this end, node influence is assessed using three measures of centrality: degree, eigenvector, and strength. Degree centrality and strength assess influence as a function of the overall connectedness of individual nodes. Whereas degree centrality only assesses the presence or absence of relationships, strength factors in the weight of those relationships. Eigenvector centrality characterizes nodes based on their connectiveness to other well-connected nodes (see Chapter 4 for an extended discussion of these measures). Results are presented in Figures 8.8 and 8.9.

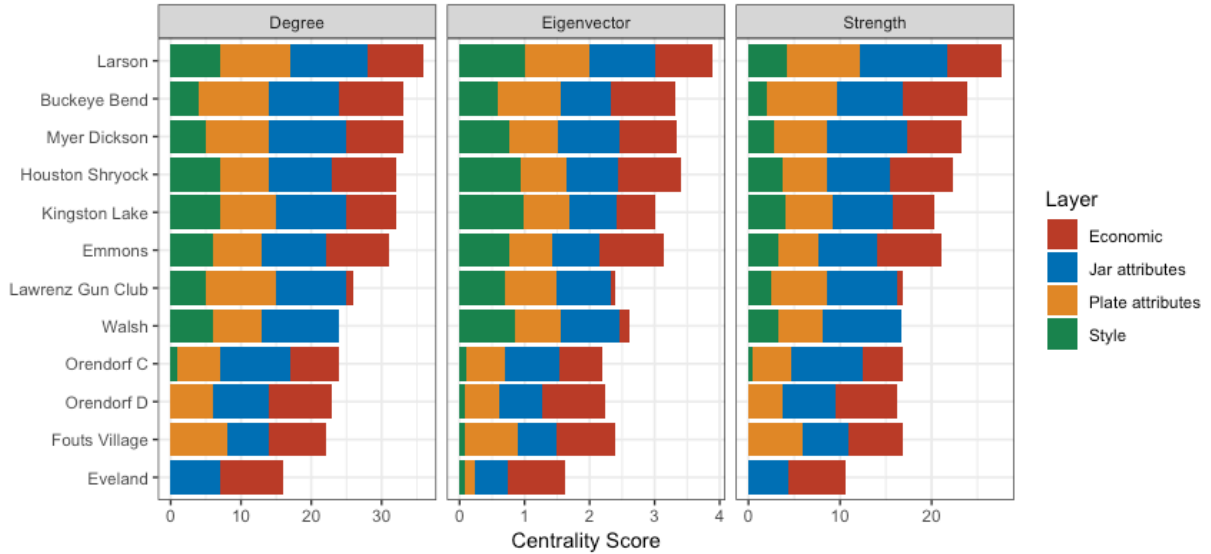


Figure 8.8 Node centrality measures for the pre-migration multilayer network

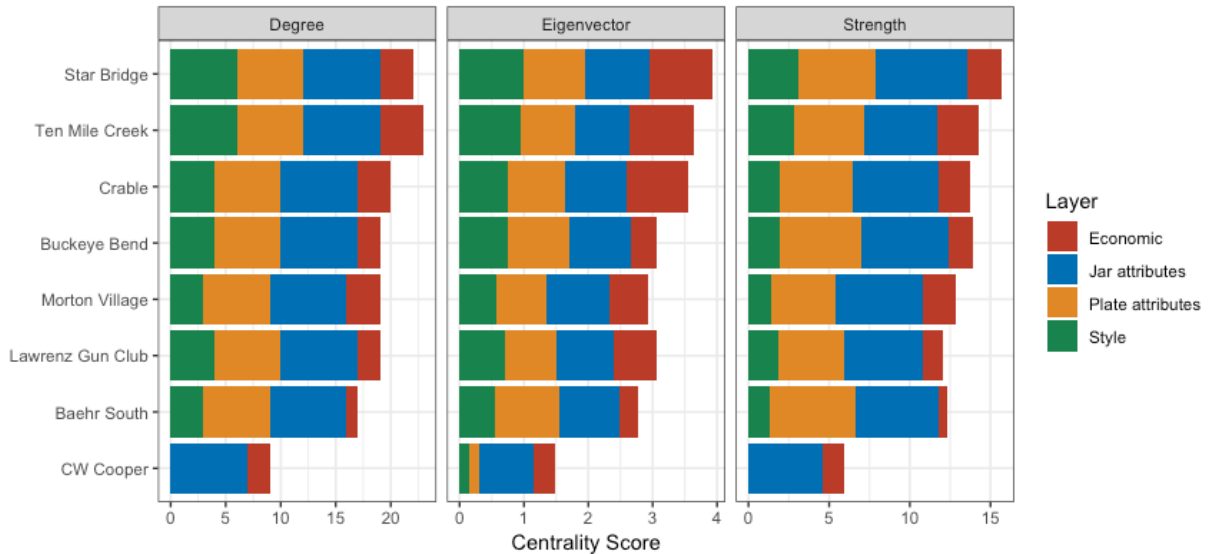


Figure 8.9 Node centrality measures for the post-migration multilayer network

Based on the ceramic industry multilayer network centrality measures, Larson appears to be the most influential node in the pre-migration time period, while Star Bridge and Ten Mile Creek appear most influential in the post-migration time period. However, both time periods do not have high centralization scores consistent across centralization metrics (see Table 8.2) nor are node centrality scores highly skewed. In other words, there is little support for individual

nodes or node clusters playing outsized roles in either any individual network layer nor across the multilayer network for either time period. There is, however, some support for nodes playing more peripheral roles in interaction and identification networks. As used here, influence refers primarily to the extent to which individual nodes are connected to other nodes. As a result, a number of communities are inhibited in their influence due to a lack of presence on a given layer, which is the case for sites such as C.W. Cooper and Eveland where the plate vessel class has not been recovered (see Chapter 3).

Some overarching trends are notable in measures of node centrality. First are the high centrality scores in the jar attribute layer in particular. Second are the high centrality scores in the plate attribute layer aside from a few notable exceptions. The influence of the economic network layer and the stylistic layer are both diminished from the pre-migration to post-migration period. However, the economic network layer appears to diminish in influence much more acutely than the plate stylistic layer. These trends are more apparent when summarizing all node degree centrality and strength measures, as presented in Figure 8.10 and 8.11.

While the jar and plate attribute layers remain relatively consistent in influencing relationships for both the pre-migration and post-migration multilayer networks, the plate stylistic categorical design layer increases in influence at the same time that the economic interaction related to ceramic industry layer significantly wanes in influence. Thus, despite regional scale parity in ascription to common social groups as seen in proportional similarities of plate style groups, indexing a categorical identity was of less influence to network relationships relative to other channels of interaction during the pre-migration time period. In other words, relationships formed through the indexing of shared categorical identities often contributed the least to the pre-migration multilayer network for each site relative to the other

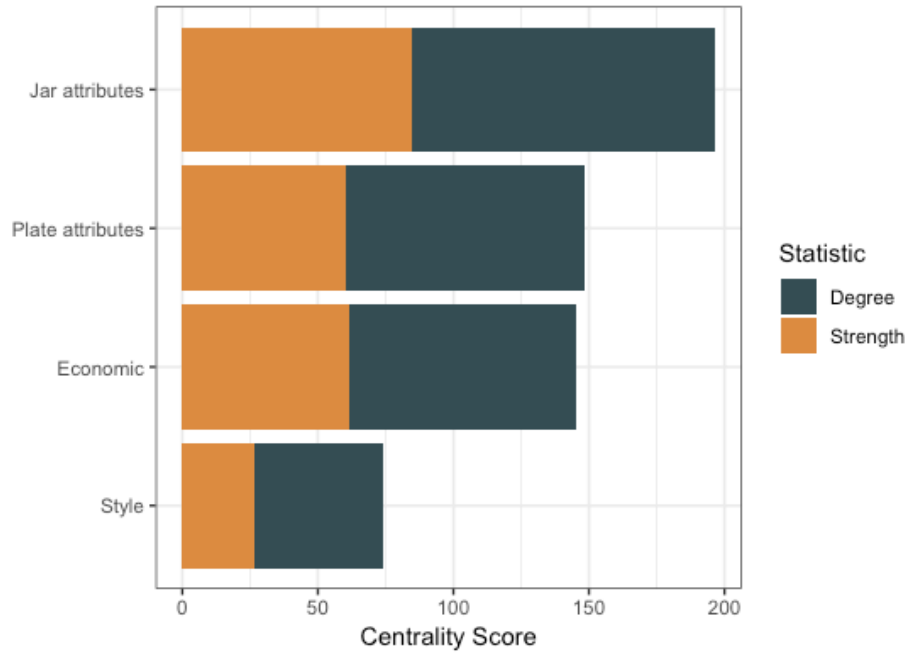


Figure 8.10 Summary of node degree centrality and strength for the pre-migration time period

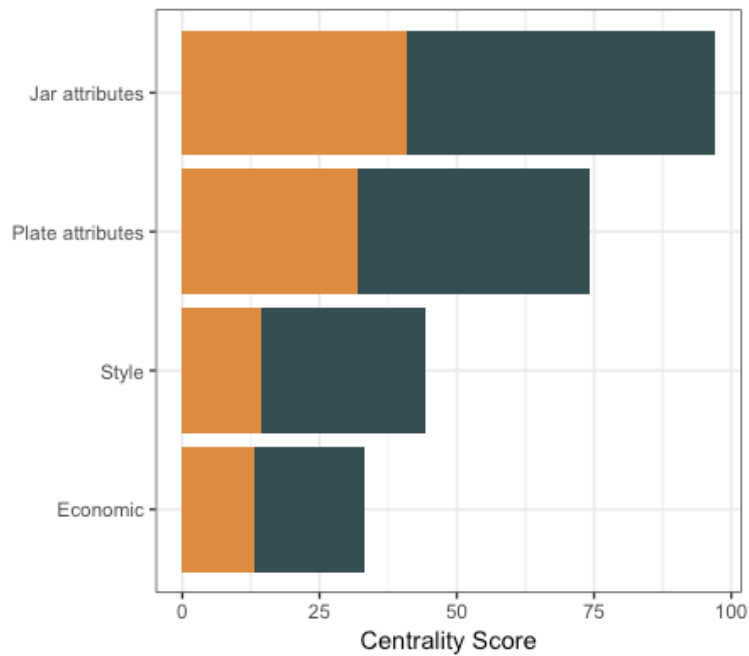


Figure 8.11 Summary of node degree centrality and strength for the post-migration time period

layers. This trend reversed following Oneota in-migration, where indexing categorical identity through stylistic designs on plates took on an increased role in community interactions. This attests to an active role of likely female potters in signaling membership in regional groups in the pre-migration time period and, increasingly, more localized groups in the post-migration time period. Furthermore, Mississippian sites are shown to be characterized by strong channels of economic interaction through ceramic industry that precipitously decrease in influence alongside the in-migration of Oneota peoples.

In looking at the differential role of site-node influence across ceramic industry network layers, it is pertinent to address site-node degree deviation. Degree deviation quantitatively assesses variation in the influence of site-nodes across different network layers. A site-node with the same degree of interconnectedness across different layers will have a degree deviation of 0, while a site-node with many relationships on some layers and only a few on other layers will have a very high degree deviation, which shows an uneven usage of the layers (or layers with different densities) (Dickison, et al. 2016; Magnani 2017). Comparing degree deviation in figures 8.12 and 8.13 with centrality measures indicates that there is an inverse relationship between site-node degree deviation and site-node centrality across both the pre-migration and post-migration time periods. In other words, sites that are consistently interconnected across network layers are more likely to have a higher influence overall in the Late Prehistoric CIRV. This is an unsurprising finding but does bolster an interpretation for a lack of hegemony or regional hierarchy among major CIRV sites over more peripheral CIRV sites. While the most influential sites based on centrality measures are also larger town or ceremonial sites (e.g. Larson, Ten Mile Creek, Star Bridge), neither site size nor assumed site complexity alone predict site influence in the pre-migration and post-migration ceramic industry multilayer networks.

High degree deviation scores and variation in strength and eigenvector centrality indicate that site-nodes play different roles in different relational and categorical social networks. This

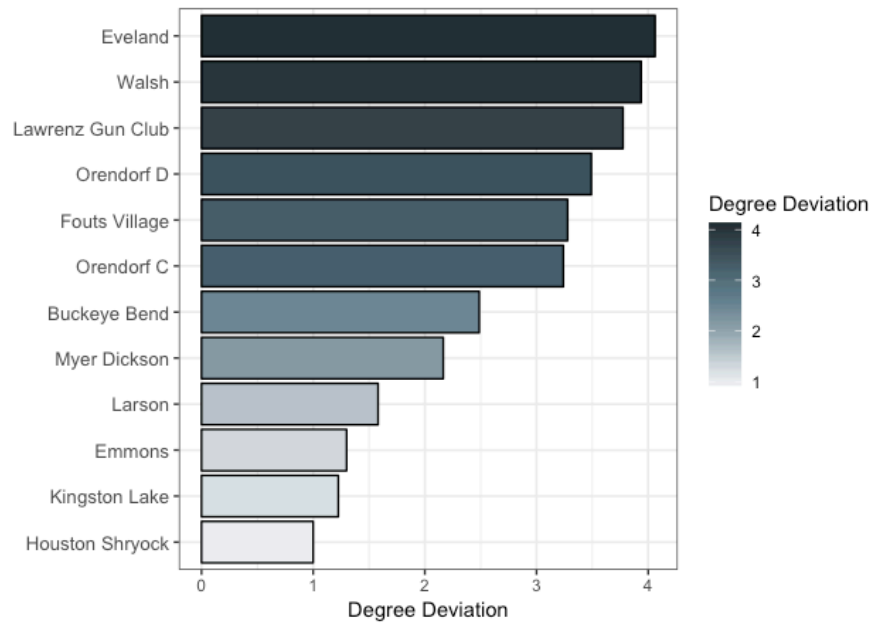


Figure 8.12 Site-node degree deviation for the pre-migration CIRV time period; lower scores indicate more even influence across layers

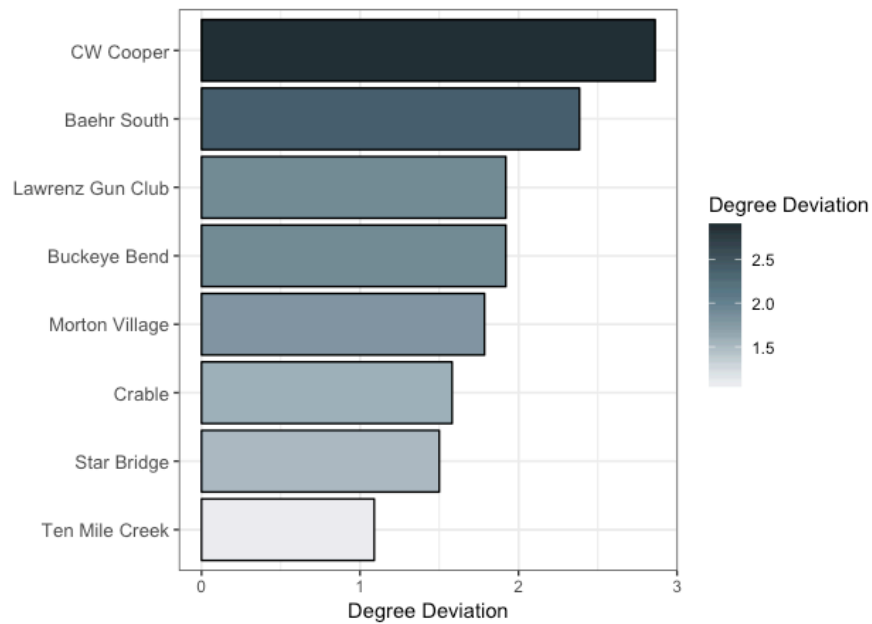


Figure 8.13 Site-node degree deviation for the post-migration CIRV time period; lower scores indicate more even influence across layers

highlights the value of a multi-measure quantitative approach to investigating community and layer influence in a multilayer network, and the value of a multidimensional approach more broadly. Additionally, the often contrasting nature of network relationships across different layers is highlighted. Finally, analyses of interlayer interactions and layer and community influence have shed light on regional scale structural changes that occurred concomitant with Oneota in-migration. In particular, relational network connections formed through the cultural transmission of socially-mediated jar and plate artifact attributes were maintained in the multicultural CIRV while network ties formed through economic relational interaction related to ceramic industry were relegated at the same time that the significance of indexing shared categorical identities amplified.

8.6 Intercultural Communal Coexistence in the Late Prehistoric CIRV

As the multilayer network graph visualizations and the preceding discussion summarizing individual network layer and community overlaps and influences shows, different types of interactions are characterized by distinct connectivity patterns. Exploring the inter-dependencies of the different network layers reveals how multiple relations shape the organization of the Late Prehistoric CIRV social system at different levels both prior to and succeeding circa 1300 A.D culture contact with Oneota immigrants. By qualitatively interpreting quantitative topological and statistical properties of relational network layers, it is possible to characterize regional behavioral response trends to intercultural communal coexistence. Here, I hypothesize that, based on a comparative analysis of the structure of multiple network layers of relational and categorical identification across the Middle to Late Mississippian transition, Oneota in-migration

into the CIRV resulted in a period of accommodative intercultural communal coexistence at the macro-regional scale. In social settings following culture contact characterized by accommodative coexistence, relational transaction costs are relatively moderate to low but heterogeneous or exclusive categorial identities delimit the extent of collective action or social movements. Collective action is therefore limited to sub-divisions within densely relational networks that do share common categorial identities as opposed to spreading across a broader array of actors (Peeples 2018).

Significant structural changes are apparent in the depth of relational interaction and in categorial identification among CIRV communities coinciding with Oneota in-migration. While channels of relational social interaction through the cultural transmission of jar and plate socially-mediated technological characteristics are largely maintained, parity in the scale network relationships formed through economic interaction related to ceramic industry is deeply reduced. As a result of the imbalance in relational interaction layers, where two layers are characterized by moderate or high depth of relational interaction and one layer is characterized by low depth of relational interaction, an overall trend of moderate depth of relational interaction is argued here to characterize the Mississippian and Oneota multicultural occupation of the Late Prehistoric CIRV.

Likewise, structural changes are apparent in categorial identities similarity paralleling culture contact among chiefly CIRV Mississippian peoples and exogenous Oneota peoples. The indexing of shared categorial identities using stylistic decorations on plates took on an increased role in community interactions in the post-migration relative to the pre-migration time period as seen in layer influence. However, analysis of network statistical properties indicates that global scale ascription to categorial identities in the Mississippian CIRV gave way to ascription to

categorical identities at a reduced social scale. Chapter 6 showed that the range and the number of design categories present at sites sharply increases from the pre-migration to post-migration time periods, which in part accounts for the degree of similarity in social identities on average being significantly reduced from that of the Mississippian period. As a result, using the rubric presented in Table 8.1, macro-scale categorical identities similarity in the post-migration CIRV time period are assessed as low.

These structural changes to networks of relational interaction and categorical identification had very real implications for Mississippian and Oneota potters and the communities in which they were nested more broadly. However, it is important to emphasize that an interpretation of accommodative intercultural communal coexistence *does not* presuppose peaceful or tolerant relationships. Rather, intercultural communal coexistence is used as a means to infer macro-scale behavioral response trends following culture contact. The Late Prehistoric CIRV was marked by multicultural accommodation at the macro-regional scale despite only limited evidence for intra-community multicultural cohabitation, which is only thus far present at two out of the eight sites with occupations dating between 1300 and 1450 A.D. – Crable and Morton Village. That these sites were interconnected to other sites in both the jar and plate technological attribute network layers attests to the accommodative nature of inter-community relationships in the post-migration time period. The breakdown of economic relationships and reduction in social scale of shared categorical identities among communities, however, were clear inflection points in delimiting collective action or social transformations to sub-groups within quasi-densely relational networks that did share common categorical identities, identities that may have cross-cut cultural boundaries.

Behavioral response trends toward inter-community cultural accommodation highlight a human capacity to habituate or acclimatize to novel social environments, sometimes unwillingly so. For example, Chapters 6 and 7 argued for the presence of a spatial and social internal frontier in the Late Prehistoric CIRV. The presence of an internal frontier was likely an outgrowth of deteriorating economic interrelationships and diverging social identities, both of which are likely to have structured Oneota in-migration.

Some degree of cultural pluralism is inherent in accommodative inter-cultural communal coexistence. What distinguishes accommodative and pluralistic coexistence, however, is an active willingness of communities to accommodate themselves to a new social setting through the creative refashioning of cultural forms that otherwise fit within the worldviews of each distinct cultural group. In the Late Prehistoric CIRV ceramic industry multilayer network, it is clear that Oneota and Mississippian potters developed cultural innovations in ceramic industry that reflect a multicultural region but that those innovations were largely rooted in social interaction through the cultural transmission of socially-mediated artifact attributes. Oneota potters adopted a unique vessel form, the plate, at two multicultural sites – Crable and Morton Village – but decorated their plates with uniquely Oneota stylistic patterns. This indicates potential broader accommodation to foodways indigenous to CIRV Mississippian communities by Oneota peoples but in such a way as to bridge them within their own worldviews. That both multicultural sites were integrated into regional relational networks of interaction attests to likely cultural innovations among Mississippian potters in how they made ceramic vessels of the jar and plate classes. As proxy evidence for the broader communal social milieu in which potters were nested, it can be assumed that these relational trends of the creative refashioning of cultural

forms toward accommodation best explains behavioral responses to culture contact in the Late Prehistoric CIRV.

8.7 Contributions of this Research

A significant theoretical contribution of this project involved a quantitative relational perspective to archaeological ceramics in the study region, as well as of culture contact more broadly. Studies of archaeological ceramics in the study region have traditionally focused on taxonomically defining vessels into mutually exclusive types. Work in this regard has resulted in a substantial amount of detail with which to understand the chronological and cultural positioning of Late Prehistoric CIRV sites. A relational perspective richly contributes to these studies by providing hypotheses that characterize community relationships to one another along certain relational and categorical dimensions, and how those relationships change overtime. That these hypotheses were generated from a multidimensional analysis of a single material culture class shows how very different perspectives and interpretations may be drawn depending on the artifactual evidence or theoretical underpinnings used in different models. The generalized nature of this theoretical model provides an accessible template for its application in archaeological contexts in other regions.

This dissertation has compiled a large amount of data from ceramic artifacts recovered from settlements across the Late Prehistoric central Illinois River valley. These data include systematic technological characterizations of two classes of ceramic artifacts, a coding schema for categorizing stylistic decorations on plate vessels, and a chemical compositional database. Many of the same ceramic vessels are included in each of these different data sets. All statistical and network analysis programming for this project on these data was performed in the R

statistical platform. Additionally, all code is provided in Appendix C as well as in various GitHub repositories (<https://github.com/ajupton>). As R is a free and open source programming language, the code enables all analyses and interpretations to be reproducible by any researcher and therefore to be testable. After an embargo period, all data will be digitally curated alongside the R code and interpretations produced through this study by the Digital Archaeological Record (tDAR). Providing both raw data and open-source code to analyze those data in an accessible manner replete with comments and extended discussions of methodology will hopefully encourage other archaeological researchers to do the same, leading to increased collaborations on open-source tools for archaeologists, a greater emphasis on reproducibility in archaeological science, and renewed focus on archaeological data as a component of shared human heritage.

A major methodological contribution of this dissertation stems from the vessel technological attribute data pre-processing steps necessary to develop networks of interaction through cultural transmission. A novel method was developed by adapting a model from cultural transmission theory that identifies which individual artifact attributes are free to vary from site to site, enabling attributes likely constrained by engineering principles to be differentiated from attributes that likely bear social information. A method is then provided for constructing and analyzing similarities in socially mediated artifact attribute among sites as network graph objects. This method is unique in that it produces weighted *and* directed network graphs, which provide significant nuance in understanding topological or structural patterns of interaction through cultural transmission. The method may be applied to any attribute measured on a continuous scale, making it generalizable to a host of other archaeological artifact or feature data. In developing this methodology, it was identified that burial jar technological attributes in the Late Prehistoric CIRV were not independent from each other. In other words, as one burial jar

attribute changes, so do all other measurable attributes change in a step-wise fashion. This may lead to fruitful hypothesis generation about the relationship between burial jar and the individual(s) it was interred alongside that are outside the scope of this study.

Another methodological contribution of this study is using geo-chemical data within a relational framework. Many geo-chemical compositional analysis studies focus largely on the exchange or circulation of vessels themselves as explaining parallels of membership in statistical chemical reference groups. The use of a relational framework rooted in economic interaction identifies the role that the sharing of raw material source information, overlapping resource exploitation areas, and similar production processes play in addition to exchange in explanations of geo-chemical patterning.

A component of this project was the creation of a public website, <https://andyupton.net>. The website houses hundreds of photographs of the ceramic vessels used in project analyses alongside blog posts that discuss the project in an accessible manner as well as an interactive tool for sherd continuous attribute measurement data to be explored from both a quantitative as well as relational perspective. This should be a trend that continues for all archaeological analyses funded by public sources because it increases public literacy and interest in archaeology and cultural heritage at multiple scales.

8.7.1 Contributions to Archaeology and CIRV Archaeology

This study provides the archaeological profession more broadly and archaeologists working in the central Illinois River valley more specifically with a number of valuable contributions. First, this study has shown how taxonomically defined cultural groups may be analyzed from a relational perspective. This provides a richer and fuller perspective on these

archaeologically defined cultures because it emphasizes social dimensions gleaned from artifacts, breathing life into the relationships among individuals and the unique social milieu in which archaeological artifacts were produced, used, and discarded. This research also shows how extant museum collections may be used to foster regional scale relational perspectives, thereby maximizing the value of museum collections and furthering arguments for long-term curation strategies.

This study provides CIRV archaeologists with a regional scale understanding of social structure prior to and succeeding a specific migration process of Oneota peoples into the Mississippian CIRV. In particular, those contributions emphasize regional scale organization among communities in the Mississippian period and the roles of deteriorating economic relationships related to ceramic industry and a proliferation of categorical social identities in structuring Oneota in-migration into the region as well as in explaining behavioral response trends to culture contact. In these ways, archaeologists and other researchers examining Late Prehistoric CIRV peoples have been provided with a regional synthesis from a relational perspective in order to provide a broader context on how individual sites are structurally situated vis-à-vis their relationships to other sites. That is, individual CIRV communities may now be placed into a broader social context, and future work in the region that considers other lines of evidence at various scales may validate or challenge many of the interpretations provided herein. In concert with interaction network layers based on the cultural transmission of jar and plate socially mediated technological attributes, this research highlights the value of a multidimensional, relational perspective to the analysis of culture contact.

A number of CIRV sites were able to be chronologically positioned using radiocarbon data in this project. Short-lived faunal and floral samples submitted from Morton Village (11F2),

Ten Mile Creek (11T2), Star Bridge (11Br105/11Br17), Buckeye Bend (11F310), Emmons Village (11F218), Kingston Lake (11P11), and Baehr South (11Br47) each returned usable radiocarbon dates. Importantly, the major sites of Star Bridge and Ten Mile Creek were able to be confidently dated to a 14th century occupation. An attempt to provide a radiocarbon date for Houston-Shryock (11F114) was unfortunately unsuccessful due to sample contamination. Calibrated probability ranges are provided for each of these dates in Appendix H.

On a broader level, this research contributes to an understanding of social structure during the Late Prehistoric period in the U.S. Eastern Woodlands. This critical period in American prehistory preceded the collapse and abandonment of fifteenth century chiefly polities in the central Illinois River valley (Esarey and Conrad 1998), the American Bottom (Cobb and Butler 2002, 2006), the lower Ohio valley and central Mississippi valley (Cobb 2005), and the lower Savannah River drainage (Anderson, et al. 1995). While many analyses of societal collapse focus on environmental factors (Bird, et al. 2017; Weiss and Bradley 2001) this research offers an alternative perspective by analyzing network models of social relations prior to abandonment and population displacement (Borck, et al. 2015). Problematizing and integrating social interaction and categorical identification with larger-scale political and social change is fundamental for understanding how culture is created, continued, and contested by people in the past and the present.

8.8 Future Directions

As with any archaeological research endeavor, the results presented in this dissertation must be considered as preliminary due in large part to the limitations and the vagaries of sampling a representative ceramic population from many sites across a fairly large study region

encompassing some 250 years of occupations. Invariably, this research will generate as many questions as it addresses, if not more. However, the present study shows the potential for a multidimensional relational perspective to the analysis of material culture data. Additionally, this study shows potential for chemical studies using LA-ICP-MS on shell tempered pottery, for a model of cultural transmission to be applied to ceramic technological attribute data, and for categorical identification to be explored on plate stylistic data sets in Mississippian and Upper Mississippian assemblages. Each of these data strands will hopefully be used in future inter-regional analyses across broader Mississippian and Upper Mississippian sampling universes. Eastern North America is primed for the emergence of big data approaches to understanding cultural contact and the spread of Mississippian and Upper Mississippian culture, among a host of other analytical avenues.

Multilayer network analysis is still largely in its infancy as a mathematical formulation, and applications in archaeological contexts have much to offer this fledgling analytical arena. Material culture lends itself to studies of the kinds of relationships that can be modeled in network analysis because it often encapsulates information about both inter-community or inter-regional interactions as well as information about the social identity of the artisan(s) or individual(s) responsible for its production. In addition, archaeology has a uniquely human timescale with which to apply problems longitudinally. Archaeology is therefore uniquely situated to explore how humans actually behaved as opposed to how they might say they behaved in written text or in a survey or interview – which are otherwise often the basis for network analysis studies.

As with any data-driven approach, additional data would improve the interpretations presented in this dissertation. In this regard, this dissertation has set up testable hypotheses about

the role of relations and categories in structuring Oneota in-migration and the re-structuring of social relationships in the multi-cultural CIRV following culture contact. Economic interactions can be further explored along other analytical dimensions such as foodways and the exchange of other material culture classes than pottery. Targeted excavations at sites such as Crable, Ten Mile Creek, and Lawrenz Gun Club hold promise for testing whether or not an accommodative intercultural communal coexistence framework is appropriate for explaining culture contact in the Late Prehistoric CIRV. Additionally, a number of sites with distinctly Oneota material culture present were unable to be included in this dissertation due to limited artifactual evidence. Sleeth and Otter Creek warrant additional sub-surface testing to enrich understanding of the Bold Counselor Oneota and their interactions with CIRV Mississippian peoples.

APPENDICES

APPENDIX A

Coding Sheet

Coding Sheet

This document provides a description of all variables collected on ceramic artifacts. Included are provenance information, taxonomic distinctions, continuous measurements, and categorical values. Stylistic categories for jar and plate decorations are provided detailing 72 distinct jar decorations and 7 jar decoration categories as well as 94 distinct plate decorations and 29 plate categories. Non-outlier maximal values were retained for continuous measurements using calipers.

Site Name:

- 1 Orendorf Settlement C (#1-79)
- 2 Crable (#80-189; 371-376; 1058-1100; 1300-1308)
- 3 Walsh (#190-220;)
- 4 Lawrenz Gun Club (#221-241; 660-711; 1133-1152)
- 5 C.W. Cooper (#242-250; 370; 723;1279-1299)
- 6 Emmons Village (#251-294; 764-767; 1024-1025)
- 7 Baehr South (#295-311)
- 8 Myer-Dickson (#312-346; 894)
- 9 Ester Berry (#347-362)
- 10* Fiedler (#363-365)
- 11* Gillette (#366-369; 377)
- 12 Star Bridge (#378-486; 952-974)
- 13 Ten Mile Creek (aka Hildemeyer) (#487-532; 712-722; 875)
- 14 Eveland (#533-565)
- 15 Kingston Lake (#567-659; 1022-1023)
- 16 Buckeye Bend (#724-743)
- 17 Fouts (#744-763)
- 18 Larson (#768-851)
- 19 Morton Village (#852-874; 876-893; 1153-1166; 1167-1194)

- 20 Houston-Shryock (#895-935; 1101-1132)
- 21 Orendorf Cemetery (11F414) (#936-951)
- 22 Vandeventer (#975-1021; 1026-1027)
- 23 Norris Farms #36 (1028-1057)
- 24 Orendorf D [courtesy Illinois State Archaeological Survey] (1195-1257; 1309-1310)
- 25 Dickson Mounds (1258-1278)

*Fielder and Gillette were not included in any analyses due to small sample sizes

Institutional Holding:

- 1 Dickson Mounds Museum, Lewistown, IL
- 2 Western Illinois University, Macomb, IL
- 3 Upper Mississippi Valley Archaeological Research Foundation/Western Illinois Archaeological Research Center, Macomb, IL (courtesy L. Conrad)
- 4 Indiana University Purdue University Indianapolis (courtesy, J. Wilson)
- 5 UMRV/IL Illinois State Archaeological Survey (courtesy L. Conrad and T. Emerson, K. Emerson, A. Zelin)

Provenience Sphere:

- 1 Domestic (e.g. feature, domestic structure)
- 2 Mortuary (e.g. burial mound, burial furniture, associated with burial)

- 3 Ritual (e.g. public structure, non-burial mound)
- 4 Unknown

- 17 Bold Counselor Oneota Jar
- 18 Indet. Trailed Jar
- 19 Sepo
- 20 Dickson Series

Specific Provenience:

- 1 Feature
- 2 Domestic Structure
- 3 Public Structure
- 4 Mound
- 5 Mound, with burial
- 6 Occupation Area
- 7 Surface, unknown
- 8 Unknown
- * Pilot Study Sherds

Residue (pottery char):

- 0 Absent
- 1 Present, interior only
- 2 Present, exterior only
- 3 Present, interior and exterior

Sherd Type General:

- 1 Probable Cooking Jar
- 2 Broad Rim Plate/Bowl
- 3 Probable Burial Jar

Tempering Agent:

- 1 Shell
- 2 Grit
- 3 Grit and Shell
- 4 Un-tempered

Sherd Type Specific (Traditional Taxonomic Type):

See (Conrad 1991; Conrad and Esarey 1983; Esarey and Conrad 1981, 1998; Harn 1971, 1978, 1980, 1991, 1994; Harn and McClure 2012; Santure, et al. 1990; Vogel 1975)

- 1 Mississippian Plain Globular
- 2 Cahokia Cordmarked
- 3 Powell Plain
- 4 Ramey Incised
- 5 Trotter Trailed
- 6 Dickson Cordmarked
- 7 Dickson Trailed (also cordmarked)
- 8 Crable Trailed
- 9 Lobed
- 10 Indeterminate Jar
- 11 Plate - Plain
- 12 Wells Incised Plate
- 13 Crable Deep Rimmed, Incised
- 14 Crable Deep Rimmed, Trailed
- 15 Plate - Indeterminate
- 16 Wells Broad Trailed Plate

Temper Maximum Grain Size Diameter:

- 1 Very Fine (0.0625-0.125 mm)
- 2 Fine (0.125-0.25 mm)
- 3 Medium (0.25-0.5 mm)
- 4 Coarse (0.5-1 mm)
- 5 Very Coarse (1-2 mm)
- 6 Granules (2-4 mm)
- 7 Gravel (4+ mm)

Percent Temper Occurrence:

- 1 Few (6%)
- 2 Little (12%)
- 3 Some (31%)

Jar Lip Decoration (e.g. scalloping, incising):

- 1 Present
- 2 Absent

Jar Handle Decoration (e.g. trailing):

- 1 Present
- 2 Absent
- 3 No handle present

Jar Orifice Diameter (measured on orifice diameter chart):

In cm

Jar Height (from the bottom of the globular base to the top of the vessel lip – only measured for complete or partially complete vessels):

In cm

- | | |
|---|--|
| 4 | Trailed and Impressed
(Includes Punctates & Stab
and Drag) |
| 5 | Trailed unidentified |
| 6 | Applique |

Jar Maximum Lip Thickness (lip refers to the extruded edge or margin of the orifice of the vessel (Rice 2005):

In mm

Jar Max cordmarking Thickness (measures the horizontal width of cordmarking):

In mm

Jar Maximum Shoulder Thickness (shoulder refers to the upper part of the body of a restricted vessel (Rice 2005) – for domestic jars, the shoulder was measured below the everted rim-globular body attachment and above where the vessel wall angle is 90° perpendicular to the vessel opening):

In mm

Jar Max Incising Thickness (measures the horizontal width of incised decoration):

In mm

Jar Maximum Wall Thickness (wall refers to within a few cm of the equator of the globular jar, or where the vessel wall angle is 90° perpendicular to the vessel opening):

In mm

Jar Max Trailing Thickness (measures the horizontal width of trailing decoration):

In mm

Jar Rim Height (rim refers to the area between the lip and the neck of the vessel (Rice 2005)):

In mm

Jar Shape of Elements (general trend of decoration elements):

- | | |
|----|-------------------------|
| -1 | Missing |
| 0 | Indeterminate |
| 1 | Horizontal |
| 2 | Vertical |
| 3 | Rectilinear |
| 4 | Curvilinear |
| 5 | One Repeating Motif |
| 6 | Two Repeating Motifs |
| 7 | Three+ Repeating Motifs |
| 8 | Horizontal and Vertical |

Jar Rim Angle (90° equates to a completely vertical rim, 360° equates to a completely unrestricted vessel opening):

In degrees

Jar Shoulder Decoration (each combination of elements received a distinct category – text descriptions were used in conjunction with high-resolution photographs during categorization):

Jar Primary Design Technique (see Chapter 6 for a description of incised and trailing/trail-impressed categorical distinctions):

- | | |
|---|------------|
| 0 | Plain |
| 1 | Incised |
| 2 | Cordmarked |
| 3 | Trailed |

- | | |
|----|---------------------------------|
| -1 | Missing |
| 0 | Indeterminate |
| 1 | One line Horizontal Trailing |
| 2 | Two lines Horizontal Trailing |
| 3 | Three lines Horizontal Trailing |
| 4 | Four lines Horizontal Trailing |
| 5 | Five lines Horizontal Trailing |
| 6 | Six+ lines Horizontal Trailing |
| 7 | Three Concentric Chevrons |

8	Inverse elongated chevrons, cutoff at rim	32	Three lines rectilinear trailing, not cutoff at rim like Code 8, forms continuous chevron
9	Trotter Trailed - curvilinear motif		
10	Two chevrons "V" above rectilinear trailing	33	Overlapping Code 8 motifs
11	Elongated Chevrons	34	Four lines curvilinear trailing
12	Four+ concentric chevrons	35	Two concentric chevrons
13	Ramey "trailed" eye motif	36	Two lines curvilinear trailing
14	Four Concentric chevrons	37	Concentric arc/curvilinear trailing flanked by vertical incising
15	Three lines Horizontal trailing with punctates below and stab and drag below punctates* (identical to 18)	38	Code 20 line filled triangles/rectilinear motif but incised instead of trailed
16	Trailed Concentric circle cross-in-sun motif, flanked by rectilinear trailing bordered by punctates	39	Three trailed lines forming a chevron but lines in between are curvilinear
17	Three lines horizontal trailing above stab-and-drag	40	Three trailed horizontal lines above a horizontal line of punctates above groups of five stab-and-drag trailing spaced apart roughly equal to their width (of five drags)
18	Three lines horizontal trailing above punctates above stab-and-drag* (need to fix same as 15)	41	Rectilinear line of punctates above three lines rectilinear trailing above stab and drag (code 27, three lines)
19	Two chevrons "V" above two lines of rectilinear trailing	42	Horizontal line of punctates above four lines horiz. trailing above stab and drag (same as 24?)
20	Trailed line filled triangles, triangle line forms rectilinear trailing	43	Five lines horizontal trailing above stab and drag
21	Three Trailed arcs on shoulder	44	Two lines horizontal trailing above stab and drag
22	Ramey Incised bi-shoulder vessel; each shoulder has a distinct Ramey design, see photo	45	Four lines horizontal trailing above punctates above stab and drag
23	Applique forms noded arc	46	Alternating concentric chevrons (either V shaped or the inverse) flanked by two lines diagonal trailing with punctates either above or below motif (V below, inverse above)
24	Horizontal punctate above four lines horizontal trailing above stab and drag	47	Alternating curvilinear trailing flanked by three diagonal lines with punctates either above or below trailing (same as 46, but curvilinear instead of chevron motif)
25	Code 21 Trailed arcs below arced punctates	48	Three lines horizontal trailing above stab and drag with punctates superimposed in horizontal linear groups of 6-9 on lines of trailing
26	Rectilinear line of punctates above two lines rectilinear trailing above stab and drag		
27	Code 26 but with punctate filled zones above rectilinear trailing		
28	Two lines arced punctates above three trailed arcs above stab and drag		
29	Three trailed concentric chevrons with a line of punctates on one side of lowest chevron		
30	Indeterminate ladder		
31	Sepo Collar Decoration		

- 49 Three lines arc trailing above stab and drag, trailing forms arcs with punctates flanking two lines of trailing between each arc-based motif
- 50 Three lines curvilinear trailing above stab and drag
- 51 Punctates above four lines arc trailing above stab and drag, lacks the motif between arcs like Code 49, also includes punctates below handles
- 52 Punctates above three lines rectilinear trailing above stab and drag, though punctates only appear on one side of the trailing (i.e. only on the right side of the “V”)
- 53 Code 10 but only one chevron above rectilinear trailing. Space between rectilinear trailing indicates this was made as a motif as opposed to interconnected trailing
- 54 Nested “U” shape, or U within a U; maybe a beaver tail or flower pedal?
- 55 Arc line of punctates above three lines arc trailing above stab and drag. In between arc motif is a smaller and similar arc motif with punctates above three lines arc trailing. Main motifs are quadripartite in corners, smaller motifs at main directions.
- 56 Code 44 but stab and drag occurs in groups of 4 eight times around the vessel
- 57 Two horizontal applique nodes
- 58 Arc of punctates above bifurcated arrow. Arrow consists of three vertical lines and three diagonal lines emanating from the upper/middle portion of the vertical lines (five total motifs)
- 59 Arcs punctates above two lines arc trailing above stab and drag. Motif is quadripartite in corners
- 60 Repeating motif of rectilinear arc of punctates above three diagonal lines of trailing above stab and drag. Trailing/stab and drag are cut off before a typical rectilinear trailing would descend. Only the ascending portion of the trailing is present (six total motifs)
- 61 Two motifs - on cardinal directions (including handles) are concentric inverse arc (“U”) trailing above an inverse arc of punctates. Second motif - on corners is a traileed spiral sun inside a circle of punctates. Line of punctates below inverse arcs is continuous around the vessel
- 62 Three lines rectilinear trailing above stab and drag
- 63 Two lines horizontal trailing above punctates above stab and drag
- 64 Rectilinear line of punctates above diagonal stab and drag trailing with nested vertical stab and drag trailing. Like Code 60, but there are four lines of trailing and they are executed via stab and drag below the rectilinear punctates. The stab is diagonal to the left and diagonal to the right (see photo!)
- 65 Code 61 traileed spiral sun motif repeating six times; second motif is two inverse arc “U” trailing and an inverse arc of punctates below handles
- 66 Vertical trailing in groups of 3 eight times around the vessel
- 67 Curvilinear punctates above three lines curvilinear trailing above stab and drag
- 68 Incised inverse line filled triangle nested in a triangle motif repeats 7 times. (Triangles point up)
- 69 Two incised arcs above incised stab and drag motif
- 70 Two lines curvilinear trailing above stab and drag
- 71 Three lines horizontal trailing above punctates above stab and drag but

- stab and drag only appears in groups of 3, 4, or 6 eight times total (similar to Code 40)
- 72 Two arcs of punctates above two inverse “V” trailed lines above stab and drag
- 73 Code 72 motif but three trailed “V” lines as opposed to two
- 74 Horizontal line of punctates above four lines horizontal trailing above a line of horizontal punctates
- 75 Code 52 but punctates only occur on the left side of the “V”
- 76 Four lines horizontal trailing above stab and drag
- 77 Code 27 and 41 but with four lines recliner trailing below punctates above stab and drag
- 78 Two lines of rectilinear punctates above four lines rectilinear trailing (likely stab and drag below, but not present)
- 79 Indeterminate trailing and punctates

Brainerd-Robinson Design Group - Jars
(Unique Designs were re-categorized into design groups in order to compute Brainerd-Robinson coefficients of agreement.)

- 1 =(isolate, will not be included) 14, 21, 27, 29, 30, 31, 33, 34, 36, 37
- 1 =7, 8, 10, 11, 12, 19, 32, 35, 39, 53
- 2 =9, 13
- 3 =17
- 4 =18, 40, 45, 48
- 5 =20, 38
- 6 =41
- 7 =42

Jar Shoulder Type:

- 1 Missing
- 1 Rounded (Globular)
- 2 Sub-angular (Shallow)
- 3 Lobed
- 4 Bi-shoulder

Jar Slip/Paint: (surface treatment)

- 0 Eroded
- 1 Absent
- 2 Present, Interior Rim Only
- 3 Present, Interior rim and body
- 4 Present, Exterior
- 5 Present, Exterior and Interior

Jar Lip Shape:

- 0 Indeterminate
- 1 Extruded
- 2 Flat
- 3 Rounded
- 4 Rolled
- 5 Flared
- 6 In-Curved
- 7 Interior Beveled
- 8 Exterior Beveled
- 9 Out-Curved

Plate Maximum Rim Diameter (measured using rim diameter chart):

In cm

Plate Height (height refers to the bottom of the vessel well (or globular bowl) to the opening plane of the vessel rim – see image below):

In mm

Plate Depth (depth refers to the bottom of the vessel well to the attachment between the well and the rim or flare):

In mm

Plate Flare Length (flare refers to the highly everted outflaring rim):

In mm

Plate Flare Angle (see image below):

In degrees

Plate Max Lip Thickness (before tapering):

In mm

Plate Max Thickness Below Lip (or max thickness of the outflaring rim):

In mm

Plate Max Incising Thickness:

In mm

Plate Max Trailing Thickness:

In mm

Plate Primary Design Technique:

- 0 Plain
- 1 Incised
- 2 Trailed
- 3 Trailed and Impressed
(Includes Punctates & Stab and Drag)

Plate Decoration (each combination received a distinct categorical value):

- 0 Indeterminate
- 1 Plain
- 2 Vertical line filled curvilinear trailing (lines below curves)
- 3 Line filled triangles, flares out, lines emanate from vertical line to rim
- 4 Repeating > (weeping eye?)
- 5 Vertical incised lines extending from curvilinear trailing (lines above curves)
- 6 Incised line filled triangles, flares out, triangles point to inside plate, lines follow triangle
- 7 Repeating Curvilinear >
- 8 Line filled triangle nested in triangle, points to well
- 9 Vertical Incising
- 10 Diagonal Incising above a horizontal line
- 11 Triangle filled with horizontal lines, points toward well
- 12 Triangles filled with vertical lines, points towards well

- 13 Code 6 Triangle on rim with vertical line filled triangles following bottom flare lip
- 14 Sun motif with concentric curvilinear incising composing sun body and triangles composing sun rays
- 15 Chevron incising points toward well, with nested arc
- 16 Concentric chevrons pointing out bordered by vertical trailing
- 17 Semi-circle filled with vertical lines nested within curvilinear ladder
- 18 Vertical incising with sun ray border
- 19 Incised concentric arcs point towards well
- 20 Code 6 on rim with horizontal line filled curvilinear chevrons following bottom flare lip
- 21 Cross hatched oblique triangle
- 22 Code 14 sun motif with vertical incising between suns
- 23 Code 14 sun motif with code 18 vertical incising/sun ray border between suns
- 24 Semi-circle filled with vertical lines
- 25 Code 6 line filled triangles but trailed instead of incised
- 26 Code 11 Horizontal Line Filled Triangles on rim with horizontal line filled triangles pointing out from base of rim, forms rectilinear chevron bordered by the line filled triangles
- 27 Rectilinear chevron trailing - O'Byam Incised?
- 28 Code 14 sun motif emanating from rim, points toward well
- 29 Code 11 Triangle filled with horizontal lines, points away from well
- 30 Concentric Rectilinear Chevrons, points towards well
- 31 Bifurcated Concentric Chevrons, points toward well

32	Line filled triangles point away from plate following bottom flare lip, lines follow triangle (inverse of Code 6)	45	Code 38 but with horizontal line filled triangles extending from rim
33	Code 6 Line Filled Triangles on rim with line filled triangles (following triangle) pointing out from base of rim, forms rectilinear chevron bordered by the line filled triangles	46	Indeterminate Cross Hatching
34	Cross inside sun motif, whole sun	47	Curvilinear chevron bordered by horizontal line filled arcs
35	Code 32 horizontal line filled triangles with sun motif pointing towards plate, cutoff by triangles	48	Nested cross hatched triangle points towards well
36	Code 34 cross inside sun motif with Code 18 vertical incising/sun ray border between suns	49	Alternating line filled triangles (pointing toward and away from well), lines follow triangles, no space between - Compound Triangles
37	Code 9 Vertical Incising with Cross in Circle motif appearance in b/t incising	50	Code 14 sun motif with indeterminate sun flare bordered design between suns
38	Code 20 alternating incised line filled triangles on rim but with horizontal triangles from well lip extend to plate rim (i.e. NOT Code 33), but with space b/t triangles	51	Vertical line filled triangle nested in two lines of rectilinear incising. Very reminiscent of Bold Counselor jar designs minus the punctates. Clearly incised
39	Bifurcated horizontal incised line filled triangles flare out and point to inside plate, incised line filled triangles point away from plate with lines following triangle - no space between triangles	52	Cross hatched Code 6
40	Small Code 6 diagonal line filled triangles on rim, with small diagonal line filled triangle on lip that point toward the plate and form sun rays emanating from the plate well	53	Code 49 alternating triangles but trailed instead of incised
41	Vertical incised line filled triangles point toward base, are bordered by punctates	54	Elongated and alternating incised oblique triangles
42	Curvilinear incising on rim and on base of rim	55	Incised elongated "X" shape
43	Code 34 Cross in circle sun motif with line filled triangles in between suns	56	Incised line Filled squares, diagonal lines alternate in directionality
44	Code 34 cross in circle sun, cross in circle is nested inside sun, surrounded by line filled triangles	57	Alternating code 6 triangles and code 12 vertical line filled triangles
		58	Alternating incised vertical lines (code 9) and incised line filled arcs
		59	Alternating? "Arrow feather" diagonal incising and horizontal incising
		60	Code 14 sun motif alternating with code 9 vertical incising
		61	Code 31 bifurcated concentric chevrons on both exterior and interior rim, forms negative space chevron
		62	Code 5 but trailed instead of incised
		63	O'Byam Incised-like curvilinear trailing/incising
		64	Indeterminate Cross-in-circle motif
		65	Diagonal (as opposed to vertical) trailing

- | | | | |
|----|--|----|---|
| 66 | Code 14 style sun but nested within arcs are indeterminate line filled triangles and other concentric arcs | 84 | Alternating trailed concentric arcs sun motif on exterior and interior rims |
| 67 | Sun ray triangles on upper and lower rim forming negative space chevron flanked by vertical incised lines | 85 | Motif on tab - Three lines inverse arc "U" shape trailing with one arc of punctates on the top and bottom of motif |
| 68 | Code 33-like chevron but triangles are filled with concentric triangles (or chevrons) instead of lines following triangle | 86 | Vertical trailed lines flanked by a vertical line of punctates alternating with likely trailed arcs bordered by a line of punctates on interior rim. Much like Code 23 but punctates replaces triangular sun rays |
| 69 | O'Byam incising flanked by Code 18 sun rays/vertical incising | 87 | Code 23 sun and vertical incised motif but the vertical lines are not flanked by triangular sun rays |
| 70 | Indeterminate ladder | 88 | Code 25 (trailed Code 6) nested in a line of rectilinear trailing and a rectilinear line of punctates. |
| 71 | Concentric chevron/triangle/"V" shape, points out or away from well | 89 | Curvilinear incised concentric arc sun motif point away from base sun rays formed not by triangles but by incised lines |
| 72 | Alternating arc, i.e. incomplete arc in between complete arcs | 90 | Code 25 (trailed Code 6) nested in three lines rectilinear trailing bordered by punctates |
| 73 | Code 47 curvilinear trailing/chevron but with vertical line filled arcs | 91 | Code 33 but Code 6 style triangles emanate from the rim to the lip, creating negative space triangles that are not connected |
| 74 | Inverse of Code 26 - triangles on base rim follow triangle while exterior rim are horizontal | 92 | Code 19 nested arcs but trailed instead of incised (like Code 85 but no punctates below arcs) |
| 75 | Four concentric chevrons | 93 | Alternating concentric chevrons, i.e. incomplete concentric chevrons bordered by chevrons. All point towards well. Main, complete, chevrons have punctates on outer border |
| 76 | Opposite of Code 13 - vertical incised line filled triangles on exterior rim and Code 6 on interior rim pointing out | 94 | Like Code 27 O'Byam incising but trailed and two lines, more rectilinear |
| 77 | Sun, moon?, and chevrons. Idiosyncratic and poorly executed | | |
| 78 | Concentric arcs or chevrons, inverse of Code 19 in that they point away from well | | |
| 79 | Code 40 but bottom lip triangles are horizontal line-filled | | |
| 80 | Code 6 on exterior rim with Code 63 O'Byam incising on interior rim | | |
| 81 | Concentric arc incising, arcs are filled with horizontal incising near interior rim and nested diagonal incising on exterior rim | | |
| 82 | "V" chevron points towards well, flanked by diagonal lines | | |
| 83 | Horizontal incised line filled arcs, arcs open away from well | | |

Brainerd-Robinson Design Group - Plates
(Unique Designs were re-categorized into
design groups in order to compute Brainerd-
Robinson coefficients of agreement.)

- 1 =(Isolate, will not be included in analysis)16, 17
- 1 = plain
- 2 =2, 5, 58, 62, 73
- 3 =3
- 4 =4, 7
- 5 = 6, 25, 70
- 6 =8
- 7 =9, 10
- 8 =11
- 9 =12, 24, 57
- 10 =13, 76
- 11 =14, 22, 23, 28, 50, 60, 66, 87
- 12 =15, 30, 75
- 13 =13, 69
- 14 =19
- 15 =20, 26, 38, 40, 45, 74, 79, 91
- 16 =21, 46, 48, 52
- 17 =27, 55, 63, 94
- 18 =29, 32, 68, 71
- 19 =31, 61
- 20 =33, 80
- 21 =34, 36, 43, 44
- 22 =39, 49, 53, 56, 81
- 23 =41, 83, 86, 88, 90
- 24 =47
- 25 =51
- 26 =54, 59, 67
- 27 =65, 82
- 28 =72, 78, 84, 89, 92
- 29 =85

Plate Lip Shape:

- 0 Indeterminate
- 1 Extruded
- 2 Flat
- 3 Rounded
- 4 Rolled
- 5 Flared
- 6 In-Curved
- 7 Interior Beveled
- 8 Exterior Beveled
- 9 Out-Curved

APPENDIX B

Ceramic Vessel Measurement Data Availability

All ceramic vessel technological attribute data are provided in electronic form through the Digital Archaeological Record (tDAR) at the following permanent link:

<https://core.tdar.org/project/447475>

After an embargo period lasting five years from the publication of this dissertation, electronic versions of LA-ICP-MS data presented in Chapter 7 will be available through the Field Museum Elemental Analysis Facility.

<https://www.fieldmuseum.org/science/labs/elemental-analysis-facility>

<https://www.fieldmuseum.org/>

APPENDIX C

All R Code for Statistical Analyses

Following an embargo period lasting six months after the publication of this dissertation, all code and individual data files will be presented on GitHub at the following link:

<https://github.com/ajupton>

Because GitHub is a private company whose policies may change unpredictably, all R code is presented in text form here. Note that the R code provided here has no warranty whatsoever and any kind of support is not guaranteed to be provided. You are free to do what you like with this code provided that you cite this dissertation document and/or any future publications out of which this dissertation data and methodologies are published. All stand-alone Shiny app software below may be freely redistributed and/or modified under the terms of the GNU General Public License as published by the Free Software Foundation, either version 3 of the License, or (at your option) any later version. See <http://www.gnu.org/licenses/>.

R Code from Chapter 5

Routines to generate and analyze networks of interaction through cultural transmission from continuous artifact attribute data

```
# Load the required libraries for analysis
library(tidyverse)
library(igraph)
library(cluster)
library(cowplot)
library(ggribbles)
library(readxl)
library(knitr)
library(readr)
library(colorRamps)
library(RColorBrewer)

# Read in data sets - domestic jars and serving plates
jars <- read_csv("jars_cont.csv", col_types = cols(Orifice = col_double(),
          RimAngle = col_double()))

# Read in sherd id information
jar_unique <- read_csv("jar_unique.csv")

# Set row names as the unique sherd id's
rownames(jars) <- jar_unique$`2`

# Do the same for plate data set
plates <- read_csv("plate_cont.csv", col_types = cols(FlareAngle = col_double(),
          MaxDiameter = col_double()))
plate_unique <- read_csv("plate_unique.csv")
rownames(plates) <- plate_unique$`1`

# Factorize site data for grouping
levels(as.factor(jars$Site))
levels(as.factor(plates$Site))

# Function to compute the length of the data set, ignoring NAs
my_length <- function(x){
  sum(!is.na(x))
}

# Function to compute number of vessels in total
n_vessels <- function(x){
  x %>%
  summarise_all(my_length)
}

# Function to computer number of vessels by "Site";
# This function can group the data by any factor or string column, "Site" is used here
n_vessels_by_site <- function(x){
  x %>% group_by(Site) %>%
```

```

    summarise_all(my_length)
  }

```

Functions from Eerkens and Bettinger (2008)

```

# Unbiased estimator of coefficient of variation
my_cv <- function(x){
  (sd(x, na.rm = TRUE)/mean(x, na.rm = TRUE)) * (1 + (1/(4*length(x[!is.na(x)]))))
}

# Standard Deviation, removing missing values by default
my_sd <- function(x){
  sd(x, na.rm = TRUE)
}

# Mean function, removing missing values by default
my_mean <- function(x){
  mean(x, na.rm = TRUE)
}

# Variation of Variation (VOV)
# Unbiased CV of assemblage CVs
VOV <- function(x){x %>%
  group_by(Site) %>%
  summarise_all(my_cv) %>%
  summarise_all(my_cv)
}

# Variation of the mean (VOM)
# Unbiased CV of assemblage means
VOM <- function(x){x %>%
  group_by(Site) %>%
  summarise_all(my_mean) %>%
  summarise_all(my_cv)
}

# Average variation (AV)
# Mean of assemblage CVs
AV <- function(x){x %>%
  group_by(Site) %>%
  summarise_all(my_cv) %>%
  summarise_all(my_mean)
}

```

Results of Eerkens and Bettinger (2008) analysis

```

# Sample size determination
# Gather sample means and standard deviations
all_mean_sd <- bind_rows(bj_mean_sd, j_mean_sd, p_mean_sd)
all_mean_sd_log <- all_mean_sd

# Take the Log base 10 of means/std in order to account for scalar effects across the
# different measurement scales (mm, cm, degrees)

```

```

all_mean_sd_log$my_mean <- log10(all_mean_sd_log$my_mean)
all_mean_sd_log$my_sd <- log10(all_mean_sd_log$my_sd)

# Plot with regression lines
all_mean_sd_log %>%
  ggplot(aes(x = my_mean, y = my_sd, color = Class)) +
  geom_point() +
  geom_smooth(method = "lm", se = FALSE) +
  theme_classic() +
  xlab("Mean of Log Base 10 Measurements") +
  ylab("Standard Deviation of Log Base 10 Measurements")

# Calculate VOV for jars and plates, add vessel class to attribute name
jarsVOV <- VOV(jars)
colnames(jarsVOV) <- paste("Jar", colnames(jarsVOV), sep = "_")
platesVOV <- VOV(plates)
colnames(platesVOV) <- paste("Plate", colnames(platesVOV), sep = "_")

# Calculate AV for jars and plates, add vessel class to attribute name
jarsAV <- AV(jars)
colnames(jarsAV) <- paste("Jar", colnames(jarsAV), sep = "_")
platesAV <- AV(plates)
colnames(platesAV) <- paste("Plate", colnames(platesAV), sep = "_")

# Calculate VOM for jars and plates, add vessel class to attribute name
jarsVOM <- VOM(jars)
colnames(jarsVOM) <- paste("Jar", colnames(jarsVOM), sep = "_")
platesVOM <- VOM(plates)
colnames(platesVOM) <- paste("Plate", colnames(platesVOM), sep = "_")

# Transpose scores to prepare for concatenating into a table
VOV_scores <- t(tbl_df(c(jarsVOV[-1], platesVOV[-1])))
VOM_scores <- t(tbl_df(c(jarsVOM[-1], platesVOM[-1])))
AV_scores <- t(tbl_df(c(jarsAV[-1], platesAV[-1])))

# Bind together different score metrics and provide column names
EB_scores <- as.data.frame(cbind(scale(VOV_scores), scale(VOM_scores), scale(AV_scores)))
colnames(EB_scores) <- c("VOV", "VOM", "AV")

# Add a column of the rownames and order the table by VOV
EB_scores <- EB_scores %>%
  rownames_to_column(var = "Metric") %>%
  arrange(desc(VOV))

# Plot VOV
pVOV <- EB_scores %>%
  gather(key = EB_Metric, value = Score, VOV:AV) %>%
  filter(EB_Metric == "VOV") %>%
  ggplot() + geom_point(aes(x = reorder(Metric, Score), y = Score),
                        shape = 18, size = 4) +
  ylab("VOV") + xlab("") +
  theme(axis.text.x = element_blank(), axis.ticks.x = element_blank(),
        axis.text.y = element_text(family = "Times", color = "gray5"),
        axis.title.y = element_text(family = "Times", color = "gray5"),

```

```

    legend.position = "none") + coord_cartesian(ylim = c(-2, 2)) +
    scale_y_continuous(breaks = c(-2, -1.5, -1, -0.5, 0, 0.5, 1, 1.5, 2))

# Plot AV
pAV <- EB_scores %>%
  gather(key = EB_Metric, value = Score, VOV:AV) %>%
  filter(EB_Metric == "AV") %>%
  ggplot() + geom_point(aes(x = reorder(Metric, Score), y = Score),
    shape = 18, size = 4) +
  ylab("AV") + xlab("") +
  theme(axis.text.x = element_blank(), axis.ticks.x = element_blank(),
    axis.text.y = element_text(family = "Times", color = "gray5"),
    axis.title.y = element_text(family = "Times", color = "gray5"),
    legend.position = "none") + coord_cartesian(ylim = c(-2, 2.2)) +
  scale_y_continuous(breaks = c(-2, -1.5, -1, -0.5, 0, 0.5, 1, 1.5, 2))

# Plot VOM
pVOM <- EB_scores %>%
  gather(key = EB_Metric, value = Score, VOV:AV) %>%
  filter(EB_Metric == "VOM") %>%
  ggplot() + geom_point(aes(x = reorder(Metric, Score), y = Score),
    shape = 18, size = 4) +
  ylab("VOM") + xlab("") +
  theme(axis.text.x = element_blank(), axis.ticks.x = element_blank(),
    axis.text.y = element_text(family = "Times", color = "gray5"),
    axis.title.y = element_text(family = "Times", color = "gray5"),
    legend.position = "none") + coord_cartesian(ylim = c(-2, 2)) +
  scale_y_continuous(breaks = c(-2, -1.5, -1, -0.5, 0, 0.5, 1, 1.5, 2))

# plot_grid(pVOV, pVOM, pAV, align = "hv")

```

Variables likely not constrained by engineering factors:

Plate:

flare angle, trailing thickness, incising thickness, and diameter

Jar

rim angle, trailing thickness, rim height, and wall thickness.

Assess variable distributions at sites through ridgeline plots

```

# Gather data for faceting. Faceting allows the graph to show each attribute's
# distribution across the different sites
pGathered <- gather(plates[, c(1, 2, 6, 7, 8)], Attribute, Value, MaxDiameter:MaxTrailing)
jGathered <- gather(jars[, c(1, 5, 6, 7, 9)], Attribute, Value, MaxWall:MaxTrailing)

# Read in node tables to add column to arrange by time period in ridgeline plots
jar_node_table <- read_csv("Jar_node_table.csv")
colnames(jar_node_table) <- c("Site", "Label", "Long", "Lat", "Time")
plate_node_table <- read_csv("Plate_node_table.csv")
colnames(plate_node_table) <- c("Site", "Label", "Long", "Lat", "Time")

```

```

# Join node table to allow for separating out sites by time in plots
pGathered <- pGathered %>% left_join(plate_node_table[c(1, 5)])
pGathered$Time1 <- as.factor(pGathered$Time) # Add Time column as factor for discrete color scale
jGathered <- jGathered %>% left_join(jar_node_table[c(1, 5)])
jGathered$Time1 <- as.factor(jGathered$Time)

# Create plate ridgeline plot
pRidge <- pGathered %>% group_by(Site) %>% arrange(Time, Site) %>%
  ggplot(aes(x = Value, y = reorder(Site, desc(Time)), fill = Time1)) +
  geom_density_ridges() +
  facet_wrap(~Attribute, scale = "free") +
  theme(axis.text.y = element_text(size=12)) +
  xlab("") +
  ylab("") + ggtitle("Plate Attributes") +
  scale_fill_brewer(palette = "Greens") +
  theme(legend.position = "none")

# Create jar ridgeline plot
jRidge <- jGathered %>% group_by(Site) %>% arrange(Site, Time) %>%
  ggplot(aes(x = Value, y = reorder(Site, desc(Time)), fill = Time1)) +
  geom_density_ridges() +
  facet_wrap(~Attribute, scale = "free") +
  theme(axis.text.y = element_text(size=12)) +
  xlab("") +
  ylab("") + ggtitle("Jar Attributes") +
  scale_fill_brewer(palette = "Greens") +
  theme(legend.position = "none")

# Show the jar ridgeline plot
# jRidge

# Show the plate ridgeline plot
# pRidge

```

Calculating proportional similarity from socially mediated artifact type-attributes

```

# Select the socially mediated variables from jars and plates
jar_social <- jars %>%
  select(Site, MaxWall, RimHeight, RimAngle, MaxTrailing)

plate_social <- plates %>%
  select(Site, MaxDiameter, FlareAngle, MaxIncising, MaxTrailing)

```

Assessing similarity

```

# Calculating Gower distance for jars
jdaisy <- as.matrix(daisy(jar_social[-1], metric = "gower", stand = TRUE))

# Convert matrix of distances to matrix of similarities
jdaisy_sim <- 1 - jdaisy

```

```

# Change from unique sherd i.d. to site name for column and row names
rownames(jdaisy_sim) <- as.matrix(jars[1])
colnames(jdaisy_sim) <- as.matrix(jars[1])

# Calculating Gower distance for plates
pdaisy <- as.matrix(daisy(plate_social[-1], metric = "gower", stand = TRUE))

# Convert matrix of distance to matrix of similarities
pdaisy_sim <- 1 - pdaisy

# Change from unique sherd i.d. to site name for column and row names
rownames(pdaisy_sim) <- as.matrix(plates[1])
colnames(pdaisy_sim) <- as.matrix(plates[1])

```

Turning similarity into social networks

```

# Graph object of jars
jg <- graph_from_adjacency_matrix(jdaisy_sim,
                                  mode = "directed", weighted = TRUE)

# Graph object of plates
pg <- graph_from_adjacency_matrix(pdaisy_sim,
                                  mode = "directed", weighted = TRUE)

# Construct jar weighted edgelist
jel <- as_edgelist(jg, names = TRUE)
jweights <- as.numeric(E(jg)$weight)
jwel <- tbl_df(cbind(jel, jweights))
colnames(jwel) <- c("Source", "Target", "weight")
jwel$weight <- as.numeric(jwel$weight)

# Construct plate weighted edgelist
pel <- as_edgelist(pg, names = TRUE)
pweights <- as.numeric(E(pg)$weight)
pwel <- tbl_df(cbind(pel, pweights))
colnames(pwel) <- c("Source", "Target", "weight")
pwel$weight <- as.numeric(pwel$weight)

# Proportional similarity of plates
plate_ps <- pwel %>%
  group_by(Source, Target) %>%
  summarise(sum = sum(weight, na.rm = TRUE), n = n()) %>%
  mutate(Prop_sim = sum/n)

# Proportional similarity of jars
jar_ps <- jwel %>%
  group_by(Source, Target) %>%
  summarise(sum = sum(weight, na.rm = TRUE), n = n()) %>%
  mutate(Prop_sim = sum/n)

# Function to range normalize the proportional similarity weights between 0 and 1
range01 <- function(x){

```

```

    (x-min(x))/(max(x)-min(x))
  }

# Range normalize the proportional similarity scores
range_norm_jar_ps <- jar_ps %>%
  na.omit() %>%
  group_by(Source) %>%
  mutate(Range_prop_sim = range01(Prop_sim))

range_norm_plate_ps <- plate_ps %>%
  na.omit() %>%
  group_by(Source) %>%
  mutate(Range_prop_sim = range01(Prop_sim))

# Filter to only include scores above 0.5 and remove recursive edges
# (i.e. node edges pointing to the node itself)
range_norm_jar_ps_filt <- range_norm_jar_ps %>%
  filter(Range_prop_sim > 0.5) %>%
  filter(Source != Target)

range_norm_plate_ps_filt <- range_norm_plate_ps %>%
  filter(Range_prop_sim > 0.5) %>%
  filter(Source != Target)

# Read in tables of jar site names, geographic coords., and time distinction
# For time, 1 is a primary occupation prior to Oneota in-migration
# and 2 is a primary occupation succeeding Oneota in-migration
jar_node_table <- read_csv("Jar_node_table.csv")
colnames(jar_node_table) <- c("Source", "Label", "Long", "Lat", "Time")
plate_node_table <- read_csv("Plate_node_table.csv")
colnames(plate_node_table) <- c("Source", "Label", "Long", "Lat", "Time")

# Join the node table columns to the edgelist, dropping the extra
# columns used to calculate the range normalized similarity
jar_t1 <- full_join(range_norm_jar_ps_filt[c(-3:-5)], jar_node_table[-2],
  by = "Source")
plate_t1 <- full_join(range_norm_plate_ps_filt[c(-3:-5)],
  plate_node_table[-2], by = "Source")

# Prepare node tables to join time designation for the target node
colnames(jar_node_table) <- c("Target", "Label", "Long", "Lat", "Time2")
colnames(plate_node_table) <- c("Target", "Label", "Long", "Lat", "Time2")

# Join Time 2 column to Target node
jar_edgelist_complete <- left_join(jar_t1, jar_node_table[c(-2:-4)],
  by = "Target")
plate_edgelist_complete <- left_join(plate_t1, plate_node_table[c(-2:-4)],
  by = "Target")

# Change "Range_prop_sim" column name to "weight" for Gephi/igraph
colnames(jar_edgelist_complete) <- c("Source", "Target", "weight", "Long",
  "Lat", "Time", "Time2")
colnames(plate_edgelist_complete) <- c("Source", "Target", "weight", "Long",

```

```

"Lat", "Time", "Time2")

# Write complete edgelists
# write_excel_csv(jar_edgelist_complete, "jar_edgelist_complete_March2018.csv")
# write_excel_csv(plate_edgelist_complete, "plate_edgelist_complete_March2018.csv")

# Create Pre- and Post-Migration Edgelists
jar_pre_el_need_dist <- jar_edgelist_complete %>%
  filter(Time == Time2) %>%
  filter(Time == 1)

jar_post_el_need_Law <- jar_edgelist_complete %>%
  filter(Time == Time2) %>%
  filter(Time == 2)

plate_pre_el_need_dist <- plate_edgelist_complete %>%
  filter(Time == Time2) %>%
  filter(Time == 1)

plate_post_el_need_Law <- plate_edgelist_complete %>%
  filter(Time == Time2) %>%
  filter(Time == 2)

# Two sites, Lawrenz Gun Club and Buckeye Bend, have occupations in both time periods,
# so we have to control for that
Law_jar_post <- jar_edgelist_complete %>%
  filter(Time == 2 & Target == "Lawrenz Gun Club" |
    Source == "Lawrenz Gun Club" & Time2 == 2 ) %>%
  mutate(Time = replace(Time, Time==1, 2)) %>%
  mutate(Time2 = replace(Time2, Time2==1, 2))

Law_plate_post <- plate_edgelist_complete %>%
  filter(Time == 2 & Target == "Lawrenz Gun Club" |
    Source == "Lawrenz Gun Club" & Time2 == 2 ) %>%
  mutate(Time = replace(Time, Time==1, 2)) %>%
  mutate(Time2 = replace(Time2, Time2==1, 2))

Buck_jar_post <- jar_edgelist_complete %>%
  filter(Time == 2 & Target == "Buckeye Bend" |
    Source == "Buckeye Bend" & Time2 == 2 ) %>%
  mutate(Time = replace(Time, Time==1, 2)) %>%
  mutate(Time2 = replace(Time2, Time2==1, 2))

Buck_plate_post <- plate_edgelist_complete %>%
  filter(Time == 2 & Target == "Buckeye Bend" |
    Source == "Buckeye Bend" & Time2 == 2 ) %>%
  mutate(Time = replace(Time, Time==1, 2)) %>%
  mutate(Time2 = replace(Time2, Time2==1, 2))

# Bind the Lawrenz Gun Club post-migration edges to the post-migration edgelists
jar_post_el_need_dist <- rbind(jar_post_el_need_Law, Law_jar_post,
  Buck_jar_post)

```

```

plate_post_el_need_dist <- rbind(plate_post_el_need_Law, Law_plate_post,
                                Buck_plate_post)

# Adding geographic coordinates
# Read in matrix of site distances
site_distances <- read_csv("Site Distances Matrix in km.csv")
site_distances <- column_to_rownames(site_distances, var = "X1") #first column of site names
to rownames
# Convert geographic distance matrix to graph object
distance_g <- graph_from_adjacency_matrix(as.matrix(site_distances),
                                         weighted = TRUE,
                                         mode = "directed")

# Convert geo distance graph object to edgelist
distance_el <- as_edgelist(distance_g)
distance_el_weight <- as.numeric(E(distance_g)$weight)
distance_el <- tbl_df(cbind(distance_el, distance_el_weight))
colnames(distance_el) <- c("Source", "Target", "weight")
distance_el$Distance <- as.numeric(distance_el$weight)

# Merge the geographic distance edgelist with jar and plate edgelists
jar_pre_el_complete <- merge(jar_pre_el_need_dist, distance_el[-3])
jar_post_el_complete <- merge(jar_post_el_need_dist, distance_el[-3])
plate_pre_el_complete <- merge(plate_pre_el_need_dist, distance_el[-3])
plate_post_el_complete <- merge(plate_post_el_need_dist, distance_el[-3])

# Combine the pre- and post-migration data sets into a single edgelist
# Each edgelist will become one layer in a multilayer network analysis
jar_el_all_time_complete <- rbind(jar_pre_el_complete,
                                  jar_post_el_complete)
plate_el_all_time_complete <- rbind(plate_pre_el_complete,
                                   plate_post_el_complete)

```

Analysis of Networks and Network Randomization

```

# Read in data file for jars
jel <- read_csv("Jar_complete_edgelist.csv")

# Mississippian period jars
jelpre <- jel %>% filter(Time == 1)

# Cohabitation period jars
jelpost <- jel %>% filter(Time == 2)

# Read in data file for plates
pel <- read_csv("Plate_complete_edgelist.csv")

# Mississippian period plates
pelpre <- pel %>% filter(Time == 1)

# Cohabitation period plates
pelpost <- pel %>% filter(Time == 2)

```

```

# Convert jar character columns to factor to enable plotting features
cols <- c(1, 2, 6, 7)
jel[cols] <- lapply(jel[cols], factor)
jelpre[cols] <- lapply(jelpre[cols], factor)
jelpost[cols] <- lapply(jelpost[cols], factor)

# Convert plate character columns to factor to enable plotting features
pel[cols] <- lapply(pel[cols], factor)
pelpre[cols] <- lapply(pelpre[cols], factor)
pelpost[cols] <- lapply(pelpost[cols], factor)

# Create igraph objects from jar data frames
jg <- graph_from_data_frame(jel, directed = TRUE)
jgpre <- graph_from_data_frame(jelpre, directed = TRUE)
jgpost <- graph_from_data_frame(jelpost, directed = TRUE)

# Create igraph objects from plate data frames
pg <- graph_from_data_frame(pel, directed = TRUE)
pgpre <- graph_from_data_frame(pelpre, directed = TRUE)
pgpost <- graph_from_data_frame(pelpost, directed = TRUE)

# Merge together graphs to create flattened multilayer graphs
mpre <- igraph::union(jgpre, pgpre)
mpost <- igraph::union(jgpost, pgpost)
plate_multilayer <- igraph::union(pgpre, pgpost)
jar_multilayer <- igraph::union(jgpre, jgpost)
full_multilayer <- igraph::union(plate_multilayer, jar_multilayer)

# igraph union does not combine edge weights so we have to manually mutate them
# first bind the weights from each graph together
mpre_weight <- cbind(E(mpre)$weight_1, E(mpre)$weight_2)
mpost_weight <- cbind(E(mpost)$weight_1, E(mpost)$weight_2)
plate_multi_weight <- cbind(E(plate_multilayer)$weight_1, E(plate_multilayer)$weight_2)
jar_multi_weight <- cbind(E(jar_multilayer)$weight_1, E(jar_multilayer)$weight_2)
full_multi_weight <- cbind(E(full_multilayer)$weight_1, E(full_multilayer)$weight_2)

# Sum across the rows removing NA's
mpre_weight <- rowSums(mpre_weight, na.rm = TRUE)
mpost_weight <- rowSums(mpost_weight, na.rm = TRUE)
plate_multi_weight <- rowSums(plate_multi_weight, na.rm = TRUE)
jar_multi_weight <- rowSums(jar_multi_weight, na.rm = TRUE)
full_multi_weight <- rowSums(full_multi_weight, na.rm = TRUE)

# Now we can append the flattened weights to the multilayer graph objects
E(mpre)$weight <- mpre_weight
E(mpost)$weight <- mpost_weight
E(plate_multilayer)$weight <- plate_multi_weight
E(jar_multilayer)$weight <- jar_multi_weight
E(full_multilayer)$weight <- full_multi_weight

# Explore jar igraph object
farthest_vertices(jg)      #which two vertices are farthest apart?
get_diameter(jg)          #shows the path sequence between two furthest apart vertices

```

```

degree(jg, mode = c("out")) #calculate out-degree of each vertex
jgd <- edge_density(jg)

#----- Analysis of HUBS and AUTHORITIES -----
# Developed by Jon Kleinberg, the authorities algorithm was initially
# used to examine web pages. The idea behind authorities is that these
# nodes would get many incoming links, and so it is a measure to look
# at which hubs receive the most connections.
# Algorithms by Jon Kleinberg

#-----PRE-MIGRATION HUB/AUTHORITY-----
hsjgpre <- hub_score(jgpre)$vector
hspgpre <- hub_score(pgpre)$vector
asjgpre <- authority_score(jgpre)$vector
aspgpre <- authority_score(pgpre)$vector

par(mfrow = c(2,2))
jgprel <- layout.kamada.kawai(jgpre)
pgprel <- layout.kamada.kawai(pgpre)
plot(jgpre, layout = jgprel, vertex.size = asjgpre*30,
     vertex.label.color = "gray0", vertex.frame.color = "gray88",
     vertex.color = "darkolivegreen2", edge.arrow.size = 0.15,
     edge.curved = 0.1,
     main = "Authorities in the \n Jar Pre-Migration Network")

plot(pgpre, layout = pgprel, vertex.size = aspgpre*30,
     vertex.label.color = "gray0", vertex.frame.color = "gray88",
     vertex.color = "darkolivegreen2", edge.arrow.size = 0.15,
     edge.curved = 0.1,
     main = "Authorities in the \n Plate Pre-Migration Network")

plot(jgpre, layout = jgprel, vertex.size = hsjgpre*30,
     vertex.label.color = "gray0", vertex.frame.color = "gray88",
     vertex.color = "darkolivegreen2", edge.arrow.size = 0.15,
     edge.curved = 0.1,
     main = "Hubs in the \n Jar Pre-Migration Network")

plot(pgpre, layout = pgprel, vertex.size = hspgpre*30,
     vertex.label.color = "gray0", vertex.frame.color = "gray88",
     vertex.color = "darkolivegreen2", edge.arrow.size = 0.15,
     edge.curved = 0.1,
     main = "Hubs in the \n Plate Pre-Migration Network")

# Pre-migration multilayer hubs and authorities
hspremulti <- hub_score(mpre)$vector
aspremulti <- authority_score(mpre)$vector

par(mfrow = c(1,2))
mprel <- layout.kamada.kawai(mpre)

plot(mpre, layout = mprel, vertex.size = hspremulti*30,
     vertex.label.color = "gray0", vertex.frame.color = "gray88",
     vertex.color = "darkolivegreen2", edge.arrow.size = 0.15,

```

```

    edge.curved = 0.1,
    main = "Hubs in the \n Multilayer Pre-Migration Network")

plot(mpre, layout = mprel, vertex.size = aspremulti*30,
     vertex.label.color = "gray0", vertex.frame.color = "gray88",
     vertex.color = "darkolivegreen2", edge.arrow.size = 0.15,
     edge.curved = 0.1,
     main = "Authorities in the \n Multilayer Pre-Migration Network")

#-----POST-MIGRATION HUB/AUTHORITY-----

hsjgpost <- hub_score(jgpost)$vector
hspgpost <- hub_score(pgpost)$vector
asjgpost <- authority_score(jgpost)$vector
aspgpost <- authority_score(pgpost)$vector

par(mfrow = c(2,2), family = "Times", font = 2)
jgpost1 <- layout.kamada.kawai(jgpost)
pgpost1 <- layout.kamada.kawai(pgpost)
plot(jgpost, layout = jgpost1, vertex.size = asjgpost*30,
     vertex.label.color = "gray0", vertex.frame.color = "gray88",
     vertex.color = "darkolivegreen2", edge.arrow.size = 0.15,
     edge.curved = 0.1,
     main = "Authorities in the \n Jar Post-Migration Network")

plot(pgpost, layout = pgpost1, vertex.size = aspgpost*30,
     vertex.label.color = "gray0", vertex.frame.color = "gray88",
     vertex.color = "darkolivegreen2", edge.arrow.size = 0.15,
     edge.curved = 0.1,
     main = "Authorities in the \n Plate Post-Migration Network")

plot(jgpost, layout = jgpost1, vertex.size = hsjgpost*30,
     vertex.label.color = "gray0", vertex.frame.color = "gray88",
     vertex.color = "darkolivegreen2", edge.arrow.size = 0.15,
     edge.curved = 0.1, main = "Hubs in the \n Jar Post-Migration Network")

plot(pgpost, layout = pgpost1, vertex.size = hspgpost*30,
     vertex.label.color = "gray0", vertex.frame.color = "gray88",
     vertex.color = "darkolivegreen2", edge.arrow.size = 0.15,
     edge.curved = 0.1,
     main = "Hubs in the \n Plate Post-Migration Network")

# Post-migration multilayer hubs and authorities
hspostmulti <- hub_score(mpost)$vector
aspostmulti <- authority_score(mpost)$vector

par(mfrow = c(1,2))
mpost1 <- layout.fruchterman.reingold(mpost)

plot(mpost, layout = mpost1, vertex.size = hspostmulti*30,
     vertex.label.color = "gray0", vertex.frame.color = "gray88",
     vertex.color = "darkolivegreen2", edge.arrow.size = 0.15,
     edge.curved = 0.1,

```

```

    main = "Hubs in the \n Multilayer Post-Migration Network")

plot(mpost, layout = mpostl, vertex.size = aspostmulti*30,
     vertex.label.color = "gray0", vertex.frame.color = "gray88",
     vertex.color = "darkolivegreen2", edge.arrow.size = 0.15,
     edge.curved = 0.1,
     main = "Authorities in the \n Multilayer Post-Migration Network")

#-----Centralization Analysis-----

# Calculate degree, betweenness, closeness, and eigenvector centrality
# for a graph and return a data frame with the scores

centr_all <- function(graph, g_name = "Score") {

  # Check that graph is an igraph object
  if (!is_igraph(graph)) {
    stop("Not a graph object")
  }

  # Prompt user for input on name of graph
  g_name <- as.character(g_name)

  # Degree centralization
  res_centr <- centr_degree(graph)$centralization

  # Betweenness centralization
  res_centr[2] <- centr_betw(graph)$centralization

  # Closeness centralization
  res_centr[3] <- centr_clo(graph)$centralization

  # Eigenvector centralization
  res_centr[4] <- centr_eigen(graph)$centralization

  res_centr <- t(as.data.frame(res_centr))

  # Table of scores
  colnames(res_centr) <- c("Degree", "Closeness", "Betweenness", "Eigenvector")
  rownames(res_centr) <- g_name

  res_centr
}

jprecentr <- centr_all(jgpre, g_name = "Jar Pre-Migration")
pprecentr <- centr_all(pgpre, g_name = "Plate Pre-Migration")
mprecentr <- centr_all(mpre, g_name = "Multilayer Pre-Migration")
jpostcentr <- centr_all(jgpost, g_name = "Jar Post-Migration")
ppostcentr <- centr_all(pgpost, g_name = "Plate Post-Migration")
mpostcentr <- centr_all(mpost, g_name = "Multilayer Post-Migration")
platecentr <- centr_all(plate_multilayer, g_name = "Plate Multilayer")
jarcentr <- centr_all(jar_multilayer, g_name = "Jar Multilayer")
fullcentr <- centr_all(full_multilayer, g_name = "Complete Multilayer")

```

```

rbind(jprecentr, pprecentr, mprecent, jpostcentr,
      ppostcentr, mpostcentr, platecentr, jarcentr, fullcentr)

#-----Weighted Degree (Strength) Distributions-----

# Pre-migration
jpredegree <- strength(jgpre)
hist(strength(jgpre), col = "lightblue", xlab = "Weighted Degree",
     ylab = "Frequency",
     main = "Jar Pre-Migration \n Degree Distribution")

hist(strength(pgpre), col = "lightgreen", xlab = "Weighted Degree",
     ylab = "Frequency",
     main = "Plate Pre-Migration \n Degree Distribution")

summary(strength(jgpre))
summary(strength(pgpre))

# Post-Migration
jpostdegree <- strength(jgpost, mode = "total")
par(mfrow = c(1, 2))
hist(strength(jgpost), col = "lightblue", xlab = "Weighted Degree",
     ylab = "Frequency",
     main = "Jar Post-Migration \n Degree Distribution")

hist(strength(pgpost), col = "lightgreen", xlab = "Weighted Degree",
     ylab = "Frequency",
     main = "Plate Post-Migration \n Degree Distribution")

summary(degree(jgpost))
summary(degree(pgpost))

#-----Edge Betweenness Community Detection-----

# Edge betweenness extends the concept of vertex betweenness centrality
# to edges by assigning each edge a score that reflects the number of
# shortest paths that move through that edge.
# You might ask the question, which ties in a social network are the
# most important in the spread of information?

# Some graphs are changed from directed to undirected to enable
# modularity features
jgpre_eb <- cluster_edge_betweenness(jgpre)
jgpost_eb <- cluster_edge_betweenness(jgpost)
pgpre_eb <- cluster_edge_betweenness(as.undirected(pgpre))
pgpost_eb <- cluster_edge_betweenness(pgpost)
mpre_eb <- cluster_edge_betweenness(as.undirected(mpre))
mpost_eb <- cluster_edge_betweenness(mpost)

# Pre-Migration community detection via edge betweenness in jar and
# plate layers
par(mfrow = c(1,2))
plot(jgpre_eb, jgpre, col = membership(jgpre_eb),

```

```

    vertex.label.cex = c(1.5), edge.arrow.size = .1, edge.curved = .1)
title(main = "Edge Betweenness Community Detection in the \n Pre-Migration Period Jar Attribute Network",
      cex.main = 1.5)

plot(pgpre_eb, pgpre, col = membership(pgpre_eb),
     vertex.label.cex = c(1.5), edge.arrow.size = .1, edge.curved = .1)
title(main = "Edge Betweenness Community Detection in the \n Pre-Migration Period Plate Attribute Network",
      cex.main = 1.5)

# Pre-migration multilayer community detection using edge betweenness
par(mfrow = c(1, 1))
plot(mpre_eb, mpre, col = membership(mpre_eb), vertex.label.cex = c(1.5),
     edge.arrow.size = .1, edge.curved = .1)
title(main = "Edge Betweenness Community Detection in the \n Pre-Migration Period Multilayer Jar and Plate Attribute Network",
      cex.main = 1.5)

# Post-migration jar and plate community detection via edge betweenness
par(mfrow = c(1,2))
plot(jgpost_eb, jgpost, col = membership(jgpost_eb),
     vertex.label.cex = c(1.5), edge.arrow.size = .1)
title(main = "Edge Betweenness Community Detection in the \n Post-Migration Period Jar Attribute Network",
      cex.main = 1.5)

plot(pgpost_eb, pgpost, col = membership(pgpost_eb),
     vertex.label.cex = c(1.5), edge.arrow.size = .1, edge.curved = .1)
title(main = "Edge Betweenness Community Detection in the \n Post-Migration Period Plate Attribute Network",
      cex.main = 1.5)

# Post-migration multilayer community detection via edge betweenness
par(mfrow = c(1, 1))
plot(mpost_eb, mpost, col = membership(mpost_eb),
     vertex.label.cex = c(1.5), edge.arrow.size = .1, edge.curved = .1,
     layout = mpostl)
title(main = "Edge Betweenness Community Detection in the \n Post-Migration Period Multilayer Jar and Plate Attribute Network",
      cex.main = 1.5)
#dev.off()

#-----Randomization for Pre-Migration Jar network-----
#-----PRE_MIGRATION_JAR-----
# Initiate empty List for assessing jar pre-migration average path length and transitivity
jglpre <- vector('list', 5000)

# Initiate empty List for assessing jar pre-migration density density and mean weighted degree
jglpre.d <- vector('list', 5000)

# Populate jglpre List with random graphs of same order and size
for(i in 1:5000){

```

```

jglpre[[i]] <- erdos.renyi.game(n = gorder(jgpre), p.or.m = gsize(jgpre), directed = TRUE, t
ype = "gnm")
}

# Populate jglpre.d list with random graphs of same order and approximate density. A separate
list
# of 5000 random graphs is necessary for density and mean degree because these statistics woul
d
# identical in random graphs of the same order and size as our observed graph. Instead, a prob
ability
# of edge creation equal to the observed density is used. Further, only mean degree (as oppose
d to
# mean weighted degree) is used because Erdos-Renyi random graphs do not support weights.
for(i in 1:5000){
  jglpre.d[[i]] <- erdos.renyi.game(n = gorder(jgpre), p.or.m = edge_density(jgpre), directed
= TRUE, type = "gnp")
}

# Calculate average path length, transitivity (lclustering coefficient), density, and degree a
cross
# the 5000 random jglpre graphs
jglpre.pl <- lapply(jglpre.d, mean_distance, directed = TRUE)
jglpre.trans <- lapply(jglpre, transitivity)
jglpre.density <- lapply(jglpre.d, edge_density)
jglpre.degree <- lapply(jglpre.d, function(x){
  y <- degree(x)
  mean(y)
})

# Unlist and change to a data frame for visualizations
jglpre.pl <- as.data.frame(unlist(jglpre.pl))
jglpre.trans <- as.data.frame(unlist(jglpre.trans))
jglpre.density <- as.data.frame(unlist(jglpre.density))
jglpre.degree <- as.data.frame(unlist(jglpre.degree))

# Plot the distribution of random graph's average shortest path lengths with the pre-migration

# jar network's ave. shortest path as line
p.jpre.pl <- ggplot(jglpre.pl, aes(x = jglpre.pl)) +
  geom_histogram(aes(y = ..density..)) +
  geom_vline(xintercept = (mean_distance(jgpre,
                                     directed = TRUE)),
            linetype = "dashed", color = "red") +
  geom_density() +
  ggtitle("Distribution of 5000 Random Graph Average Shortest Path Lengths & \nPre
-Migration Jar Attribute Network Average Shortest Path Length") +
  xlab("Average Shortest Path Length") +
  ylab("")

# Plot the distribution of random graph's transitivity with the pre-migration jar network's
# transitivity path as line
p.jpre.trans <- ggplot(jglpre.trans, aes(x = jglpre.trans)) +

```

```

    geom_histogram(aes(y = ..density..)) +
    geom_vline(xintercept = (transitivity(jgpre)),
              linetype = "dashed", color = "red") +
    geom_density() +
    ggtitle("Distribution of Transitivity in 5000 Random Models & \nPre-Migratio
n Jar Attribute Network Transitivity") +
    xlab("Transitivity (or Clustering Coefficient)") +
    ylab("")

# Plot the distribution of random graph's average density with the pre-migration jar network's
# ave. shortest path as line
p.jpre.density <- ggplot(jglpre.density, aes(x = jglpre.density)) +
  geom_histogram(aes(y = ..density..)) +
  geom_vline(xintercept = (edge_density(jgpre)),
            linetype = "dashed", color = "red") +
  geom_density() +
  ggtitle("Distribution of 5000 Random Graph Average Densities & \nPre-Migrat
ion Jar Attribute Network Average Density") +
  xlab("Average Density") +
  ylab("")

# Plot the distribution of random graph's mean degree with the pre-migration jar network's
# mean
# degree path as line
p.jpre.degree <- ggplot(jglpre.degree, aes(x = jglpre.degree)) +
  geom_histogram(aes(y = ..density..), bins = 10) +
  geom_vline(xintercept = (mean(degree(jgpre,
                                mode = "all"))),
            linetype = "dashed", color = "red") +
  geom_density() +
  ggtitle("Distribution of Mean Degree in 5000 Random Models & \nPre-Migration
Jar Attribute Network Mean Degree") +
  xlab("Mean Degree") +
  ylab("")

# Use plot_grid to plot all four graphs on the same grid
plot_grid(p.jpre.pl, p.jpre.trans, p.jpre.density, p.jpre.degree)

# Calculate the proportion of graphs with an average path length lower than observed
sum(jglpre.pl < mean_distance(jgpre, directed = TRUE))/5000*100

# Calculate the proportion of graphs with a transitivity (mean clustering coefficient) lower
# than our observed
sum(jglpre.trans < transitivity(jgpre))/5000*100

# Calculate the proportion of graphs with a density lower than our observed
sum(jglpre.density < edge_density(jgpre))/5000*100

# Calculate the proportion of graphs with a mean degree lower than observed
sum(jglpre.degree < mean(degree(jgpre)))/5000*100

#-----Randomizations for Pre-Migration PLATE network-----

```

```

#-----PRE_MIGRATION_PLATE-----

# Initiate empty list for assessing jar pre-migration average path length and transitivity
pglpre <- vector('list', 5000)

# Initiate empty list for assessing jar pre-migration density density and mean weighted degree
pglpre.d <- vector('list', 5000)

# Populate jglpre list with random graphs of same order and size
for(i in 1:5000){
  pglpre[[i]] <- erdos.renyi.game(n = gorder(pgpre), p.or.m = gsize(pgpre),
                                directed = TRUE, type = "gnm")
}

# Populate jglpre.d list with random graphs of same order and approximate density.
# A separate list of 5000 random graphs is necessary for density and mean degree because
# these statistics would be identical in random graphs of the same order and size as our observed
# graph. Instead, a probability of edge creation equal to the observed density is used.
# Further, only mean degree (as opposed to mean weighted degree) is used because Erdos-Renyi
# random graphs do not support weights.
for(i in 1:5000){
  pglpre.d[[i]] <- erdos.renyi.game(n = gorder(pgpre),
                                    p.or.m = edge_density(pgpre),
                                    directed = TRUE, type = "gnp")
}

# Calculate average path length, transitivity (clustering coefficient), density, and degree
across
# the 5000 random jglpre graphs
pglpre.pl <- lapply(pglpre.d, mean_distance, directed = TRUE)
pglpre.trans <- lapply(pglpre, transitivity)
pglpre.density <- lapply(pglpre.d, edge_density)
pglpre.degree <- lapply(pglpre.d, function(x){
  y <- degree(x)
  mean(y)
})

# Unlist and change to a data frame for visualizations
pglpre.pl <- as.data.frame(unlist(pglpre.pl))
pglpre.trans <- as.data.frame(unlist(pglpre.trans))
pglpre.density <- as.data.frame(unlist(pglpre.density))
pglpre.degree <- as.data.frame(unlist(pglpre.degree))

# Plot the distribution of random graph's average shortest path
# lengths with the pre-migration jar network's ave. shortest path as line
p.ppre.pl <- ggplot(pglpre.pl, aes(x = pglpre.pl)) +
  geom_histogram(aes(y = ..density..)) +
  geom_vline(xintercept = (mean_distance(pgpre, directed = TRUE)),
            linetype = "dashed", color = "red") +
  geom_density() +
  ggtitle("Distribution of 5000 Random Graph Average Shortest Path Lengths & \nPre-Migration P

```

```

late Attribute Network Average Shortest Path Length") +
  xlab("Average Shortest Path Length") +
  ylab("")

# Plot the distribution of random graph's transitivity with the pre-migration jar network's
# transitivity path as line
p.ppre.trans <- ggplot(pglpre.trans, aes(x = pglpre.trans)) +
  geom_histogram(aes(y = ..density..)) +
  geom_vline(xintercept = (transitivity(pgpre)), linetype = "dashed",
            color = "red") +
  geom_density() +
  ggtitle("Distribution of Transitivity in 5000 Random Models & \nPre-Migration Plate Attribute
Network Transitivity") +
  xlab("Transitivity (or Clustering Coefficient)") +
  ylab("")

# Plot the distribution of random graph's average density with the pre-migration jar network's
# density as line
p.ppre.density <- ggplot(pglpre.density, aes(x = pglpre.density)) +
  geom_histogram(aes(y = ..density..)) +
  geom_vline(xintercept = (edge_density(pgpre)), linetype = "dashed",
            color = "red") +
  geom_density() +
  ggtitle("Distribution of 5000 Random Graph Average Densities & \nPre-Migration Plate Attribute
Network Average Density") +
  xlab("Average Density") +
  ylab("")

# Plot the distribution of random graph's mean degree with the pre-migration jar network's
# mean degree path as line
p.ppre.degree <- ggplot(pglpre.degree, aes(x = pglpre.degree)) +
  geom_histogram(aes(y = ..density..), bins = 10) +
  geom_vline(xintercept = (mean(degree(pgpre, mode = "all"))),
            linetype = "dashed", color = "red") +
  geom_density() +
  ggtitle("Distribution of Mean Degree in 5000 Random Models & \nPre-Migration Plate Attribute
Network Mean Degree") +
  xlab("Mean Degree") +
  ylab("")

# Use plot_grid to plot all four graphs in the same grid
plot_grid(p.ppre.pl, p.ppre.trans, p.ppre.density, p.ppre.degree)

# Calculate the proportion of graphs with an average path length lower than observed
sum(pglpre.pl < mean_distance(pgpre, directed = TRUE))/5000

# Calculate the proportion of graphs with a transitivity (mean clustering coefficient) lower
# than our observed
sum(pglpre.trans < transitivity(pgpre))/5000

# Calculate the proportion of graphs with a density lower than our observed
sum(pglpre.density < edge_density(pgpre))/5000

```

```

# Calculate the proportion of graphs with a mean degree lower than observed
sum(pglpre.degree < mean(degree(pgppe)))/5000

#-----Randomization for Post-Migration Jar network-----
#-----POST_MIGRATION_JAR-----

# Initiate empty list for assessing jar pre-migration average path length and transitivity
jglpost <- vector('list', 5000)

# Initiate empty list for assessing jar pre-migration density density and mean weighted degree
jglpost.d <- vector('list', 5000)

# Populate jglpre list with random graphs of same order and size
for(i in 1:5000){
  jglpost[[i]] <- erdos.renyi.game(n = gorder(jgpost),
                                p.or.m = gsize(jgpost),
                                directed = TRUE, type = "gnm")
}

# Populate jglpre.d list with random graphs of same order and approximate density.
# A separate list of 5000 random graphs is necessary for density and mean degree because
# these statistics would be identical in random graphs of the same order and size as our
# observed graph. Instead, a probability of edge creation equal to the observed density is
# used.
# Further, only mean degree (as opposed to mean weighted degree) is used because Erdos-Renyi
# random graphs do not support weights.
for(i in 1:5000){
  jglpost.d[[i]] <- erdos.renyi.game(n = gorder(jgpost),
                                    p.or.m = edge_density(jgpost),
                                    directed = TRUE, type = "gnp")
}

# Calculate average path length, transitivity (Lclustering coefficient), density, and degree
# across the 5000 random jglpre graphs
jglpost.pl <- lapply(jglpost.d, mean_distance, directed = TRUE)
jglpost.trans <- lapply(jglpost, transitivity)
jglpost.density <- lapply(jglpost.d, edge_density)
jglpost.degree <- lapply(jglpost.d, function(x){
  y <- degree(x)
  mean(y)
})

# Unlist and change to a data frame for visualizations
jglpost.pl <- as.data.frame(unlist(jglpost.pl))
jglpost.trans <- as.data.frame(unlist(jglpost.trans))
jglpost.density <- as.data.frame(unlist(jglpost.density))
jglpost.degree <- as.data.frame(unlist(jglpost.degree))

# Plot the distribution of random graph's average shortest path lengths with the pre-migration
# jar network's ave. shortest path as line
p.jpost.pl <- ggplot(jglpost.pl, aes(x = jglpost.pl)) +
  geom_histogram(aes(y = ..density..), bins = 18) +

```

```

    geom_vline(xintercept = (mean_distance(jgpost,
                                          directed = TRUE)),
              linetype = "dashed", color = "red") +
    geom_density() +
    ggtitle("Distribution of 5000 Random Graph Average Shortest Path Lengths & \nPost-Migration Jar Attribute Network Average Shortest Path Length") +
    xlab("Average Shortest Path Length") +
    ylab("")

# Plot the distribution of random graph's transitivity with the pre-migration jar network's transitivity path as Line
p.jpost.trans <- ggplot(jglpost.trans, aes(x = jglpost.trans)) +
  geom_histogram(aes(y = ..density..), bins = 5) +
  geom_vline(xintercept = (transitivity(jgpost)),
            linetype = "dashed", color = "red") +
  geom_density() +
  ggtitle("Distribution of Transitivity in 5000 Random Models & \nPost-Migration Jar Attribute Network Transitivity") +
  xlab("Transitivity (or Clustering Coefficient)") +
  ylab("")

# Plot the distribution of random graph's average density with the pre-migration jar network's average shortest path as Line
p.jpost.density <- ggplot(jglpost.density, aes(x = jglpost.density)) +
  geom_histogram(aes(y = ..density..), bins = 11) +
  geom_vline(xintercept = (edge_density(jgpost)),
            linetype = "dashed", color = "red") +
  geom_density() +
  ggtitle("Distribution of 5000 Random Graph Average Densities & \nPost-Migration Jar Attribute Network Average Density") +
  xlab("Average Density") +
  ylab("")

# Plot the distribution of random graph's mean degree with the pre-migration jar network's mean degree path as Line
p.jpost.degree <- ggplot(jglpost.degree, aes(x = jglpost.degree)) +
  geom_histogram(aes(y = ..density..), bins = 10) +
  geom_vline(xintercept = (mean(degree(jgpost,
                                mode = "all"))),
            linetype = "dashed", color = "red") +
  geom_density() +
  ggtitle("Distribution of Mean Degree in 5000 Random Models & \nPost-Migration Jar Attribute Network Mean Degree") +
  xlab("Mean Degree") +
  ylab("")

# Use plot_grid to plot all four graphs on the same grid
plot_grid(p.jpost.pl, p.jpost.trans, p.jpost.density, p.jpost.degree)

# Calculate the proportion of graphs with an average path length Lower than observed
sum(jglpost.pl < mean_distance(jgpost, directed = TRUE))/5000

# Calculate the proportion of graphs with a transitivity (mean clustering coefficient) Lower

```

```

than our observed
sum(jglpost.trans < transitivity(jgpost))/5000

# Calculate the proportion of graphs with a density lower than our observed
sum(jglpost.density < edge_density(jgpost))/5000

# Calculate the proportion of graphs with a mean degree lower than observed
sum(jglpost.degree < mean(degree(jgpost)))/5000

#-----Randomizations for Post-Migration PLATE network-----
#-----POST_MIGRATION_PLATE-----

# Initiate empty list for assessing jar pre-migration average path length and transitivity
pglpost <- vector('list', 5000)

# Initiate empty list for assessing jar pre-migration density density and mean weighted degree
pglpost.d <- vector('list', 5000)

# Populate jglpre list with random graphs of same order and size
for(i in 1:5000){
  pglpost[[i]] <- erdos.renyi.game(n = gorder(pgpost),
                                p.or.m = gsize(pgpost),
                                directed = TRUE, type = "gnm")
}

# Populate jglpre.d list with random graphs of same order and approximate density.
# A separate list of 5000 random graphs is necessary for density and mean degree because
# these statistics would be identical in random graphs of the same order and size as our observed
# graph. Instead, a probability of edge creation equal to the observed density is used.
# Further, only mean degree (as opposed to mean weighted degree) is used because Erdos-Renyi
# random graphs do not support weights.
for(i in 1:5000){
  pglpost.d[[i]] <- erdos.renyi.game(n = gorder(pgpost),
                                    p.or.m = edge_density(pgpost),
                                    directed = TRUE, type = "gnp")
}

# Calculate average path length, transitivity (clustering coefficient), density, and degree
# across the 5000 random jglpre graphs
pglpost.pl <- lapply(pglpost.d, mean_distance, directed = TRUE)
pglpost.trans <- lapply(pglpost, transitivity)
pglpost.density <- lapply(pglpost.d, edge_density)
pglpost.degree <- lapply(pglpost.d, function(x){
  y <- degree(x)
  mean(y)
})

# Unlist and change to a data frame for visualizations
pglpost.pl <- as.data.frame(unlist(pglpost.pl))
pglpost.trans <- as.data.frame(unlist(pglpost.trans))

```

```

pglpost.density <- as.data.frame(unlist(pglpost.density))
pglpost.degree <- as.data.frame(unlist(pglpost.degree))

# Plot the distribution of random graph's average shortest path lengths with the pre-migration
# jar network's ave. shortest path as line
p.ppost.pl <- ggplot(pglpost.pl, aes(x = pglpost.pl)) +
  geom_histogram(aes(y = ..density..), bins = 10) +
  geom_vline(xintercept = (mean_distance(pgpost, directed = TRUE)),
            linetype = "dashed", color = "red") +
  geom_density() +
  ggtitle("Distribution of 5000 Random Graph Average Shortest Path Lengths & \nPost-Migration
Plate Attribute Network Average Shortest Path Length") +
  xlab("Average Shortest Path Length") +
  ylab("")

# Plot the distribution of random graph's transitivity with the pre-migration jar network's tr
ansitivity path as line
p.ppost.trans <- ggplot(pglpost.trans, aes(x = pglpost.trans)) +
  geom_histogram(aes(y = ..density..), bins = 10) +
  geom_vline(xintercept = (transitivity(pgpost)), linetype = "dashed",
            color = "red") +
  geom_density() +
  ggtitle("Distribution of Transitivity in 5000 Random Models & \nPost-Migration Plate Attribu
te Network Transitivity") +
  xlab("Transitivity (or Clustering Coefficient)") +
  ylab("")

# Plot the distribution of random graph's average density with the pre-migration jar network's
ave. shortest path as line
p.ppost.density <- ggplot(pglpost.density, aes(x = pglpost.density)) +
  geom_histogram(aes(y = ..density..), bins = 10) +
  geom_vline(xintercept = (edge_density(pgpost)), linetype = "dashed",
            color = "red") +
  geom_density() +
  ggtitle("Distribution of 5000 Random Graph Average Densities & \nPost-Migration Plate Attribu
te Network Average Density") +
  xlab("Average Density") +
  ylab("")

# Plot the distribution of random graph's mean degree with the pre-migration jar network's mea
n degree path as line
p.ppost.degree <- ggplot(pglpost.degree, aes(x = pglpost.degree)) +
  geom_histogram(aes(y = ..density..), bins = 10) +
  geom_vline(xintercept = (mean(degree(pgpost, mode = "all"))),
            linetype = "dashed", color = "red") +
  geom_density() +
  ggtitle("Distribution of Mean Degree in 5000 Random Models & \nPost-Migration Plate Attribu
te Network Mean Degree") +
  xlab("Mean Degree") +
  ylab("")

# Use plot_grid to plot all four graphs in the same grid

```

```

plot_grid(p.ppost.pl, p.ppost.trans, p.ppost.density, p.ppost.degree)

# Calculate the proportion of graphs with an average path length lower than observed
sum(pglpost.pl < mean_distance(pgpost, directed = TRUE))/5000

# Calculate the proportion of graphs with a transitivity (mean clustering coefficient) lower than our observed
sum(pglpost.trans < transitivity(pgpost))/5000

# Calculate the proportion of graphs with a density lower than our observed
sum(pglpost.density < edge_density(pgpost))/5000

# Calculate the proportion of graphs with a mean degree lower than observed
sum(pglpost.degree < mean(degree(pgpost)))/5000

#-----Randomization for Pre-Migration Multilayer network-----
#-----PRE_MIGRATION_MULTILAYER-----
# Initiate empty list for assessing jar pre-migration average path length and transitivity
mglpre <- vector('list', 5000)

# Initiate empty list for assessing jar pre-migration density density and mean weighted degree
mglpre.d <- vector('list', 5000)

# Populate jglpre list with random graphs of same order and size
for(i in 1:5000){
  mglpre[[i]] <- erdos.renyi.game(n = gorder(mpre), p.or.m = gsize(mpre), directed = TRUE, type = "gnm")
}

# Populate jglpre.d list with random graphs of same order and approximate density.
# A separate list of 5000 random graphs is necessary for density and mean degree because
# these statistics would be identical in random graphs of the same order and size as our
# observed graph. Instead, a probability of edge creation equal to the observed density
# is used. Further, only mean degree (as opposed to mean weighted degree) is used because
# Erdos-Renyi random graphs do not support weights.
for(i in 1:5000){
  mglpre.d[[i]] <- erdos.renyi.game(n = gorder(mpre),
                                   p.or.m = edge_density(mpre),
                                   directed = TRUE, type = "gnp")
}

# Calculate average path length, transitivity (clustering coefficient), density,
# and degree across the 5000 random jglpre graphs
mglpre.pl <- lapply(mglpre.d, mean_distance, directed = TRUE)
mglpre.trans <- lapply(mglpre, transitivity)
mglpre.density <- lapply(mglpre.d, edge_density)
mglpre.degree <- lapply(mglpre.d, function(x){
  y <- degree(x)
  mean(y)
})
)

# Unlist and change to a data frame for visualizations

```

```

mglpre.pl <- as.data.frame(unlist(mglpre.pl))
mglpre.trans <- as.data.frame(unlist(mglpre.trans))
mglpre.density <- as.data.frame(unlist(mglpre.density))
mglpre.degree <- as.data.frame(unlist(mglpre.degree))

# Plot the distribution of random graph's average shortest path lengths with the
# pre-migration multilayer network's ave. shortest path as Line
p.mpre.pl <- ggplot(mglpre.pl, aes(x = mglpre.pl)) +
  geom_histogram(aes(y = ..density..)) +
  geom_vline(xintercept = (mean_distance(mpre, directed = TRUE)),
            linetype = "dashed", color = "red") +
  geom_density() +
  ggtitle("Distribution of 5000 Random Graph Average Shortest Path Lengths & \nPre-Migration M
utilayer Attribute Network Average Shortest Path Length") +
  xlab("Average Shortest Path Length") +
  ylab("")

# Plot the distribution of random graph's transitivity with the pre-migration
# multilayer network's transitivity path as Line
p.mpre.trans <- ggplot(mglpre.trans, aes(x = mglpre.trans)) +
  geom_histogram(aes(y = ..density..)) +
  geom_vline(xintercept = (transitivity(mpre)), linetype = "dashed",
            color = "red") +
  geom_density() +
  ggtitle("Distribution of Transitivity in 5000 Random Models & \nPre-Migration Multilayer Att
ribute Network Transitivity") +
  xlab("Transitivity (or Clustering Coefficient)") +
  ylab("")

# Plot the distribution of random graph's average density with the pre-migration
# multilayer network's density as Line
p.mpre.density <- ggplot(mglpre.density, aes(x = mglpre.density)) +
  geom_histogram(aes(y = ..density..)) +
  geom_vline(xintercept = (edge_density(mpre)), linetype = "dashed",
            color = "red") +
  geom_density() +
  ggtitle("Distribution of 5000 Random Graph Average Densities & \nPre-Migration Multilayer Att
ribute Network Average Density") +
  xlab("Average Density") +
  ylab("")

# Plot the distribution of random graph's mean degree with the pre-migration
# multilayer network's meandegree path as Line
p.mpre.degree <- ggplot(mglpre.degree, aes(x = mglpre.degree)) +
  geom_histogram(aes(y = ..density..), bins = 10) +
  geom_vline(xintercept = (mean(degree(mpre, mode = "all"))),
            linetype = "dashed", color = "red") +
  geom_density() +
  ggtitle("Distribution of Mean Degree in 5000 Random Models & \nPre-Migration Multilayer Attr
ibute Network Mean Degree") +
  xlab("Mean Degree") +
  ylab("")

```

```

# Use plot_grid to plot all four graphs in the same grid
plot_grid(p.mpre.pl, p.mpre.trans, p.mpre.density, p.mpre.degree)

# Calculate the proportion of graphs with an average path length lower than observed
sum(mglpre.pl < mean_distance(mpre, directed = TRUE))/5000

# Calculate the proportion of graphs with a transitivity (mean clustering coefficient) lower
than our observed
sum(mglpre.trans < transitivity(mpre))/5000

# Calculate the proportion of graphs with a density lower than our observed
sum(mglpre.density < edge_density(mpre))/5000

# Calculate the proportion of graphs with a mean degree lower than observed
sum(mglpre.degree < mean(degree(mpre)))/5000

#-----Randomization for Post-Migration Multilayer network-----
#-----POST_MIGRATION_MULTILAYER-----

# Initiate empty list for assessing jar pre-migration average path length and transitivity
mglpost <- vector('list', 5000)

# Initiate empty list for assessing jar pre-migration density density and mean weighted degree
mglpost.d <- vector('list', 5000)

# Populate jglpost list with random graphs of same order and size
for(i in 1:5000){
  mglpost[[i]] <- erdos.renyi.game(n = gorder(mpost),
                                p.or.m = gsize(mpost),
                                directed = TRUE, type = "gnm")
}

# Populate jglpre.d list with random graphs of same order and approximate density.
# A separate list of 5000 random graphs is necessary for density and mean degree because
# these statistics would be identical in random graphs of the same order and size as our
# observed graph. Instead, a probability of edge creation equal to the observed density
# is used. Further, only mean degree (as opposed to mean weighted degree) is used because
# Erdos-Renyi random graphs do not support weights.
for(i in 1:5000){
  mglpost.d[[i]] <- erdos.renyi.game(n = gorder(mpost),
                                    p.or.m = edge_density(mpost),
                                    directed = TRUE, type = "gnp")
}

# Calculate average path length, transitivity (clustering coefficient), density, and degree
# across the 5000 random jglpre graphs
mglpost.pl <- lapply(mglpost.d, mean_distance, directed = TRUE)
mglpost.trans <- lapply(mglpost, transitivity)
mglpost.density <- lapply(mglpost.d, edge_density)
mglpost.degree <- lapply(mglpost.d, function(x){
  y <- degree(x)
  mean(y)
})

```

```

)

# Unlist and change to a data frame for visualizations
mglpost.pl <- as.data.frame(unlist(mglpost.pl))
mglpost.trans <- as.data.frame(unlist(mglpost.trans))
mglpost.density <- as.data.frame(unlist(mglpost.density))
mglpost.degree <- as.data.frame(unlist(mglpost.degree))

# Plot the distribution of random graph's average shortest path lengths with the
# pre-migration multilayer network's ave. shortest path as line
p.mpost.pl <- ggplot(mglpost.pl, aes(x = mglpost.pl)) +
  geom_histogram(aes(y = ..density..), bins = 10) +
  geom_vline(xintercept = (mean_distance(mpost, directed = TRUE)),
            linetype = "dashed", color = "red") +
  geom_density() +
  ggtitle("Distribution of 5000 Random Graph Average Shortest Path Lengths & \nPost-Migration
Multilayer Attribute Network Average Shortest Path Length") +
  xlab("Average Shortest Path Length") +
  ylab("")

# Plot the distribution of random graph's transitivity with the pre-migration
# multilayer network's transitivity path as line
p.mpost.trans <- ggplot(mglpost.trans, aes(x = mglpost.trans)) +
  geom_histogram(aes(y = ..density..), bins = 7) +
  geom_vline(xintercept = (transitivity(mpost)), linetype = "dashed",
            color = "red") +
  geom_density() +
  ggtitle("Distribution of Transitivity in 5000 Random Models & \nPost-Migration Multilayer At
tribute Network Transitivity") +
  xlab("Transitivity (or Clustering Coefficient)") +
  ylab("")

# Plot the distribution of random graph's average density with the pre-migration
# multilayer network's density as line
p.mpost.density <- ggplot(mglpost.density, aes(x = mglpost.density)) +
  geom_histogram(aes(y = ..density..), bins = 10) +
  geom_vline(xintercept = (edge_density(mpost)), linetype = "dashed",
            color = "red") +
  geom_density() +
  ggtitle("Distribution of 5000 Random Graph Average Densities & \nPost-Migration Multilayer At
tribute Network Average Density") +
  xlab("Average Density") +
  ylab("")

# Plot the distribution of random graph's mean degree with the pre-migration
# multilayer network's meandegree path as line
p.mpost.degree <- ggplot(mglpost.degree, aes(x = mglpost.degree)) +
  geom_histogram(aes(y = ..density..), bins = 10) +
  geom_vline(xintercept = (mean(degree(mpost, mode = "all"))),
            linetype = "dashed", color = "red") +
  geom_density() +
  ggtitle("Distribution of Mean Degree in 5000 Random Models & \nPost-Migration Multilayer Att
tribute Network Mean Degree") +

```

```

xlab("Mean Degree") +
ylab("")

# Use plot_grid to plot all four graphs in the same grid
plot_grid(p.mpost.pl, p.mpost.trans, p.mpost.density, p.mpost.degree)

# Calculate the proportion of graphs with an average path length lower than observed
sum(mglpost.pl < mean_distance(mpost, directed = TRUE))/5000

# Calculate the proportion of graphs with a transitivity (mean clustering coefficient) lower than our observed
sum(mglpost.trans < transitivity(mpost))/5000

# Calculate the proportion of graphs with a density lower than our observed
sum(mglpost.density < edge_density(mpost))/5000

# Calculate the proportion of graphs with a mean degree lower than observed
sum(mglpost.degree < mean(degree(mpost)))/5000

```

Function to plot results of Monte Carlo Network Randomization

```

# Function to plot Monte Carlo simulation distributions based on Erdos-Renyi Random Graphs

# Package dependencies
library(igraph)
library(cowplot)
library(ggplot2)

graph_mc_sim <- function(graph, sim = 5000){

  # Check that graph is an igraph object
  if (!is_igraph(graph)) {
    stop("Not a graph object")
  }

  # Check that graph is directed
  if(!is_directed(graph)){
    stop("Graph is not directed")
  }

  # Prompt user for input on name of graph
  g_name <- readline(prompt = "What name would you like to use for the graph in the plots?: ")
  g_name <- as.character(g_name)

  # Initiate empty List for housing transitivity simulations
  gl <- vector('list', sim)

  # Initiate empty List for housing density, average path length, and mean degree simulations
  gl.d <- vector('list', sim)

  # Populate List with random graphs of same order and size
  for(i in 1:sim){
    gl[[i]] <- erdos.renyi.game(n = gorder(graph), p.or.m = gsize(graph),

```

```

        directed = TRUE, type = "gnm")
}

# Populate gl.d List with random graphs of same order and approximate density.
# A separate list of random graphs is necessary for density, average path length, and
# mean degree because these statistics would be identical in random graphs of the same
# order and size as the observed graph.
# Instead, a probability of edge creation equal to the observed density is used.
# Further, only mean degree (as opposed to mean weighted degree) is used because
# Erdos-Renyi random graphs do not support weights.
for(i in 1:sim){
  gl.d[[i]] <- erdos.renyi.game(n = gorder(graph),
                              p.or.m = edge_density(graph),
                              directed = TRUE, type = "gnp")
}

# Calculate average path length, transitivity (clustering coefficient), density, and
# degree across the random graphs
gl.pl <- lapply(gl.d, mean_distance, directed = TRUE)
gl.trans <- lapply(gl, transitivity)
gl.density <- lapply(gl.d, edge_density)
gl.degree <- lapply(gl.d, function(x){
  y <- degree(x)
  mean(y)
})

# Unlist and change to a data frame for vizualizations
gl.pl <- as.data.frame(unlist(gl.pl))
gl.trans <- as.data.frame(unlist(gl.trans))
gl.density <- as.data.frame(unlist(gl.density))
gl.degree <- as.data.frame(unlist(gl.degree))

# Plot the distribution of random graph's average shortest path lengths with the
# input graphs's ave. shortest path as line
p.gl.pl <- ggplot(gl.pl, aes(x = gl.pl)) +
  geom_histogram(aes(y = ..density..)) +
  geom_vline(xintercept = (mean_distance(graph, directed = TRUE)),
            linetype = "dashed", color = "red") +
  geom_density() +
  ggtitle(paste0("Distribution of ", sim, " Random Graph Average Shortest Path Lengths & \n
Observed Average Shortest Path Length in ", g_name)) +
  xlab("Average Shortest Path Length") +
  ylab("")

# Plot the distribution of random graph's transitivity with the input graph's
# transitivity path as line
p.gl.trans <- ggplot(gl.trans, aes(x = gl.trans)) +
  geom_histogram(aes(y = ..density..)) +
  geom_vline(xintercept = (transitivity(graph)), linetype = "dashed",
            color = "red") +
  geom_density() +
  ggtitle(paste0("Distribution of Transitivity in ", sim, " Random Models & \n Observed Tran

```

```

sitivity in ", g_name)) +
  xlab("Transitivity (or Clustering Coefficient)") +
  ylab("")

# Plot the distribution of random graph's average density with the input graph's
# density as Line
p.gl.density <- ggplot(gl.density, aes(x = gl.density)) +
  geom_histogram(aes(y = ..density..)) +
  geom_vline(xintercept = (edge_density(graph)), linetype = "dashed",
            color = "red") +
  geom_density() +
  ggtitle(paste0("Distribution of ", sim, " Random Graph Average Densities &\n Observed Ave
rage Density in ", g_name)) +
  xlab("Average Density") +
  ylab("")

# Plot the distribution of random graph's mean degree with the input graph's mean
# degree path as Line
p.gl.degree <- ggplot(gl.degree, aes(x = gl.degree)) +
  geom_histogram(aes(y = ..density..), bins = 10) +
  geom_vline(xintercept = (mean(degree(graph, mode = "all"))),
            linetype = "dashed", color = "red") +
  geom_density() +
  ggtitle(paste0("Distribution of Mean Degree in ", sim, " Random Models & \n Observed Mean
Degree in ", g_name)) +
  xlab("Mean Degree") +
  ylab("")

# Use plot_grid to plot all four graphs in the same grid
plot_grid(p.gl.pl, p.gl.trans, p.gl.density, p.gl.degree)
}

```

Function to Calculate Centralization Scores

```

# Calculate degree, betweenness, closeness, and eigenvector centralization for a graph
# and return a data frame with the scores

centr_all <- function(graph, g_name = "Score") {

  # Check that graph is an igraph object
  if (!is_igraph(graph)) {
    stop("Not a graph object")
  }

  # Prompt user for input on name of graph
  g_name <- as.character(g_name)

  # Degree centralization
  res_centr <- centr_degree(graph)$centralization

  # Betweenness centralization
  res_centr[2] <- centr_betw(graph)$centralization
}

```

```

# Closeness centralization
res_centr[3] <- centr_clo(graph)$centralization

# Eigenvector centralization
res_centr[4] <- centr_eigen(graph)$centralization

res_centr <- t(as.data.frame(res_centr))

# Table of scores
colnames(res_centr) <- c("Degree", "Closeness", "Betweenness", "Eigenvector")
rownames(res_centr) <- g_name

res_centr
}

```

Multilayer Network Analysis of Directed Jar and Plate Attribute Layers

```

# Multilayer analysis of ceramic attribute interaction networks in the Late Prehistoric CIRV

library(tidyverse)
library(multinet)
library(igraph)

# Read in multilayer network into a multinet object
cnet <- read.ml("ceramicMultilayer_UPDATED_may-2018.csv")

#-----Pre-Migration Multilayer Analysis-----

# Checking to see node representation across the layers - degree.deviation.ml returns the
# standard deviation of the degree of an actor on the input layers. An actor with the same
# degree on all layers will have deviation 0, while an actor with a lot of neighbors on one
# layer and only a few on another will have a high degree deviation, showing an uneven usage
# of the layers (or layers with different densities).
degree.deviation.ml(cnet, layers = c("Jar_pre", "Plate_pre"))

# connective.redundancy.ml returns 1 minus neighborhood divided by degree and is a
# measure of how often actors are connected to the same neighbors across multiple layers
mean(connective.redundancy.ml(cnet, layers = c("Jar_pre", "Plate_pre")), na.rm = TRUE)

# Layer comparison
# Common edges divided by the union of all edges for all pairs of layers (jaccard)
layer.comparison.ml(cnet, layers = c("Jar_pre", "Plate_pre"), method="jaccard.edges")
# Simple matching edges comparison
layer.comparison.ml(cnet, layers = c("Jar_pre", "Plate_pre"), method="sm.edges")

layer.summary.ml(cnet, "Jar_pre", method = "mean.degree")

#-----Post-Migration Multilayer Analysis-----

degree.deviation.ml(cnet, layers = c("Jar_post", "Plate_post"))

mean(connective.redundancy.ml(cnet, layers = c("Jar_post", "Plate_post")),
      na.rm = TRUE)

```

```

# Layer comparison
# Common edges divided by the union of all edges for all pairs of layers (jaccard)
layer.comparison.ml(cnet, layers = c("Jar_post",
                                     "Plate_post"), method="jaccard.edges")

# Simple matching edges comparison
layer.comparison.ml(cnet, layers = c("Jar_post",
                                     "Plate_post"), method="sm.edges")

```

Linear Regression Models Assessing the Role of Geographic Distance on the Strength of Relational Connections

```

library(infer)
library(tidyverse)
library(igraph)
library(reshape2)
library(stringr)
library(cowplot)
library(broom)

# Import interaction networks
jar_el_all_time <- read_csv("Jar_complete_edgelist.csv")
plate_el_all_time <- read_csv("Plate_complete_edgelist.csv")

# Function to take a random sample from a data set a certain number of times
rep_sample_n <- function(tbl, size, replace = FALSE, reps = 1)
{
  n <- nrow(tbl)
  i <- unlist(replicate(reps, sample.int(n, size, replace = replace),
                       simplify = FALSE))

  rep_tbl <- cbind(replicate = rep(1:reps, rep(size, reps)), tbl[i,])

  dplyr::group_by(rep_tbl, replicate)
}

# Inference testing with linear models
# Take 100 samples of 50 each from the jar and plate data sets
# The idea is to explore regression trends on the slope coefficient using samples
# from each data set. Does the trend with the entire data hold true when
# sub-samples are taken from the data?
# This is a two-tailed test to see if a linear relationship (positive or negative) exists
# between distance (explanatory variable) and weight (response variable)
jarsamples <- rep_sample_n(jar_el_all_time[, c(8, 3, 6, 7)], size = 50,
                          reps = 100)
platesamples <- rep_sample_n(plate_el_all_time[, c(8, 3, 6, 7)],
                            size = 50, reps = 100)

# Add replicate col to align observed trends with random samples
jar_observed <- jar_el_all_time[, c(8, 3, 6, 7)] %>%
  mutate(replicate = 200)

plate_observed <- plate_el_all_time[, c(8, 3, 6, 7)] %>%

```

```

mutate(replicate = 200)

# Multilayer models showing relationships across time
jar_lm_multi <- ggplot(jarsamples, aes(x = Distance, y = weight,
                                     group = replicate)) +
  geom_point(size = 2, shape = 20) +
  stat_smooth(geom = "line", se = FALSE, alpha = 0.4, method = "lm") +
  ggtitle("Jar Attribute Interaction Network Across Time") +
  background_grid(major = 'y', minor = "none") +
  xlab("Distance (km)") +
  ylab("Strength of Relational Connection") +
  theme(strip.background = element_blank(),
        strip.text.x =element_blank()) +
  stat_smooth(data = jar_observed, aes(x = Distance, y = weight),
             color = "red3", linetype = "twodash", method = "lm",
             se = FALSE)

plate_lm_multi <- ggplot(platesamples, aes(x = Distance, y = weight,
                                           group = replicate)) +

  geom_point(size = 2, shape = 20) +
  stat_smooth(geom = "line", alpha = 0.4, method = "lm", se = FALSE) +
  ggtitle("Plate Attribute Interaction Network Across Time") +
  background_grid(major = 'y', minor = "none") +
  xlab("Distance (km)") +
  ylab("Strength of Relational Connection") +
  theme(strip.background = element_blank(),
        strip.text.x =element_blank())+
  stat_smooth(data = plate_observed, aes(x = Distance, y = weight),
             color = "red3", linetype = "twodash", method = "lm",
             se = FALSE)

lm_multi_grid_p <- plot_grid(jar_lm_multi, plate_lm_multi)

title <- ggdraw() +
  draw_label("Distribution of Linear Regression Lines of 100 random samples from the\n
  Multilayer Jar and Plate Attribute Networks Flattened Across Time", fontface = 'bold')

plot_grid(title, lm_multi_grid_p, ncol= 1, rel_heights = c(0.1, 1))

# How do the trends across time compare to the pre- and post-migration group trends?
jar_lms <- ggplot(jarsamples, aes(x = Distance, y = weight,
                                  group = replicate)) +
  geom_point(size = 2, shape = 20) +
  stat_smooth(geom = "line", se = FALSE, alpha = 0.4,
             method = "lm") +
  facet_wrap(Time ~ Time2) +
  ggtitle("Jar Attribute Interaction Networks\nPre-Migration
ost-Migration") +
  # extra space above accommodates the facet label separation
  background_grid(major = 'y', minor = "none") +
  xlab("Distance (km)") +
  ylab("Strength of Relational Connection") +
  theme(strip.background = element_blank(),

```

```

        strip.text.x =element_blank()) +
    stat_smooth(data = jar_observed, aes(x = Distance, y = weight),
               color = "red3",
               linetype = "twodash", method = "lm", se = FALSE) +
    facet_wrap(Time ~ Time2)

plate_lms <- ggplot(platesamples, aes(x = Distance, y = weight,
                                     group = replicate)) +
  geom_point(size = 2, shape = 20) +
  stat_smooth(geom = "line", alpha = 0.4, method = "lm",
             se = FALSE) +
  facet_wrap(Time ~ Time2) +
  ggtitle("Plate Attribute Interaction Networks\nPre-Migration
Post-Migration") +
  background_grid(major = 'y', minor = "none") +
  xlab("Distance (km)") +
  ylab("Strength of Relational Connection") +
  theme(strip.background = element_blank(),
        strip.text.x =element_blank())+
  stat_smooth(data = plate_observed, aes(x = Distance,
                                         y = weight),
             color = "red3", linetype = "twodash",
             method = "lm", se = FALSE) +
  facet_wrap(Time ~ Time2)

lm_grid_p <- plot_grid(jar_lms, plate_lms)

title <- ggdraw() + draw_label("Distribution of Linear Regression Lines of 100 random samples
from the Jar and Plate Attribute Networks",
                             fontface = 'bold')
plot_grid(title, lm_grid_p, ncol= 1, rel_heights = c(0.1, 1))

# Inference
# First, let's calculate the observed slope of the lm in the jar and plate attribute networks
jar_obs_slope <- lm(weight ~ Distance, data = jar_el_all_time) %>%
  tidy() %>%
  filter(term == "Distance") %>%
  pull(estimate)

plate_obs_slope <- lm(weight ~ Distance, data = plate_el_all_time) %>%
  tidy() %>%
  filter(term == "Distance") %>%
  pull(estimate)

# Simulate 500 slopes with a permuted dataset for jars and plates - this will allow us to
# develop a sampling distribution of the slop under the hypothesis that there is no
# relationship between the explanatory and response variables.
set.seed(1568)
jar_perm_slope <- jar_el_all_time %>%
  specify(weight ~ Distance) %>%
  hypothesize(null = "independence") %>%
  generate(reps = 500, type = "permute") %>%
  calculate(stat = "slope")

```

```

plate_perm_slope <- plate_el_all_time %>%
  specify(weight ~ Distance) %>%
  hypothesize(null = "independence") %>%
  generate(reps = 500, type = "permute") %>%
  calculate(stat = "slope")

ggplot(jar_perm_slope, aes(x = stat)) + geom_density() + theme_classic()
ggplot(plate_perm_slope, aes(x = stat)) + geom_density() + theme_classic()

mean(jar_perm_slope$stat)
mean(plate_perm_slope$stat)
sd(jar_perm_slope$stat)
sd(plate_perm_slope$stat)

# Calculate the absolute value of the slope
abs_jar_obs_slope <- lm(weight ~ Distance, data = jar_el_all_time) %>%
  tidy() %>%
  filter(term == "Distance") %>%
  pull(estimate) %>%
  abs()

abs_plate_obs_slope <- lm(weight ~ Distance, data = plate_el_all_time) %>%
  tidy() %>%
  filter(term == "Distance") %>%
  pull(estimate) %>%
  abs()

# Compute the p-value
jar_perm_slope %>%
  mutate(abs_jar_perm_slope = abs(stat)) %>%
  summarize(p_value = mean(abs_jar_perm_slope > abs_jar_obs_slope))

plate_perm_slope %>%
  mutate(abs_plate_perm_slope = abs(stat)) %>%
  summarize(p_value = mean(abs_plate_perm_slope > abs_plate_obs_slope))

# Linear models sans visualization
# First prep the data by splitting it into specific groups by time
plate_pre <- plate_el_all_time %>%
  filter(Time == 1) %>%
  select(Distance, weight)
plate_post <- plate_el_all_time %>%
  filter(Time == 2) %>%
  select(Distance, weight)
jar_pre <- jar_el_all_time %>%
  filter(Time == 1) %>%
  select(Distance, weight)
jar_post <- jar_el_all_time %>%
  filter(Time == 2) %>%
  select(Distance, weight)

# Plate attribute network Linear models - explore residuals

```

```

plate_pre_lm <- augment(lm(weight ~ Distance, data = plate_pre))
plate_post_lm <- augment(lm(weight ~ Distance, data = plate_post))

# Check SSE - how well does the model fit?
augment(lm(weight ~ 1, data = plate_pre)) %>% summarize(SSE = var(.resid))
plate_pre_lm %>% summarize(SSE = var(.resid))

# Breakdown of linear model results for plate attribute networks
summary(lm(weight ~ Distance, data = plate_pre)) # for each 1 km increase in distance, weight
drops 0.0014 and at 0 distance, a weight of 0.7463 is expected
summary(lm(weight ~ Distance, data = plate_pre))$coefficients # plate pre = p-value of 0.05796
, significant at alpha of 0.06, reject null, significant linear relationship between distance
and weight in plate pre
summary(lm(weight ~ Distance, data = plate_post)) # for each 1 km increase in distance, weight
drops 0.0001292 and at 0 distance, a weight of 0.7782248 is expected
summary(lm(weight ~ Distance, data = plate_post))$coefficients # plate post p-value of 0.86862
, fail to reject null hypothesis - no significant linear relationship between distance and wei
ght in plate post-migration network

# Check correlations
cor(plate_pre$Distance, plate_pre$weight)
cor(plate_post$Distance, plate_post$weight)

summary(lm(weight ~ Distance, data = jar_pre)) # for each 1 km increase in distance, weight in
creases 0.00005609 and at 0 distance, a weight of 0.7559 is expected
summary(lm(weight ~ Distance, data = jar_pre))$coefficients # jar pre = p-value of 0.925, fail
to reject null hypothesis - no significant linear relationship between distance and weight in
jar pre-migration network
summary(lm(weight ~ Distance, data = jar_post)) # for each 1 km increase in distance, weight d
rops 0.001697 and at 0 distance, a weight of 0.843158 is expected
summary(lm(weight ~ Distance, data = jar_post))$coefficients # jar post = p-value of 0.003207,
significant at alpha of 0.01, reject null, significant linear relationship between distance a
nd weight in jar post

cor(jar_pre$Distance, jar_pre$weight)
cor(jar_post$Distance, jar_post$weight)

```

R Code from Chapter 6 - Ceramic Design and Networks of Social Identification

Routines to generate and analyze networks of social identification from counts of artifact decoration categories

Brainerd Robinson Analysis

```

# Brainerd Robinson Analysis of Late Prehistoric central Illinois River
# valley (circa 1200 - 1450 A.D.) plate style groups

# The Brainerd-Robinson coefficient is a similarity metric that is unique

```

```

# to archaeology and is used to compare assemblages based on proportions
# of categorical data such as vessel or point types. The data used in the
# site to site proportional similarity comparison include 506 plate
# fragments, 94 unique stylistic designs, and 29 style groups.

# The Brainerd-Robinson coefficient has been coded in R by Matt Peeples
# (http://www.mattpeeples.net/BR.html) and by Gianmarco Alberti
# (http://cainarchaeology.weebly.com/r-function-for-brainerd-robinson-similarity-coefficient.h
# tml).
# Here, I follow Matt Peeples's BRsim implementation because it is
# substantially less resource intensive. However, I include a rescaling
# feature to rescale the BR coefficients from 0 - 200 to 0 - 1, which makes
# the output amenable for the construction of network graphs.

# The input for the function is a data frame with assemblages to be compared
# are found in the rows and the categorical variables
# (such as pottery/lithic types, objects, compositional groups, etc.)
# comprise the columns. Each variable is the numerical amount of a
# particular categorical variable found at each site/sample/discrete
# observation unit.

# Start by loading in some necessary packages
library(tidyverse)
library(igraph)
library(corrplot)
library(reshape2)

# Here is the BRsim function as coded by Gianmarco
BRsim <- function(x, correction, rescale) {
  if(require(corrplot)){
    print("corrplot package already installed. Good!")
  } else {
    print("trying to install corrplot package...")
    install.packages("corrplot", dependencies=TRUE)
    suppressPackageStartupMessages(require(corrplot))
  }
  rd <- dim(x)[1]
  results <- matrix(0,rd,rd)
  if (correction == T){
    for (s1 in 1:rd) {
      for (s2 in 1:rd) {
        zero.categ.a <-length(which(x[s1,]==0))
        zero.categ.b <-length(which(x[s2,]==0))
        joint.absence <-sum(colSums(rbind(x[s1,], x[s2,]))) == 0)
        if(zero.categ.a==zero.categ.b) {
          divisor.final <- 1
        } else {
          divisor.final <- max(zero.categ.a, zero.categ.b)-joint.absence+0.5
        }
        results[s1,s2] <- round((1 - (sum(abs(x[s1, ] / sum(x[s1,]) - x[s2, ] / sum(x[s2,])))
/2)/divisor.final, digits=3)
      }
    }
  }
}

```

```

} else {
  for (s1 in 1:rd) {
    for (s2 in 1:rd) {
      results[s1,s2] <- round(1 - (sum(abs(x[s1, ] / sum(x[s1,]) - x[s2, ] / sum(x[s2,]))) /
2, digits=3)
    }
  }
}
rownames(results) <- rownames(x)
colnames(results) <- rownames(x)
col1 <- colorRampPalette(c("#7F0000", "red", "#FF7F00", "yellow", "white", "cyan", "#007FFF"
, "blue", "#00007F"))
if (rescale == F) {
  upper <- 200
  results <- results * 200
} else {
  upper <- 1.0
}
corrplot(results, method="square", addCoef.col="red", is.corr=FALSE, cl.lim = c(0, upper), c
ol = col1(100), tl.col="black", tl.cex=0.8)
return(results)
}

```

*# Here is a more simplified version from Matt Peeples
Function for calculating Brainerd-Robinson (BR) coefficients
Note there is data pre-processing for Matt's script not included here

```

BR <- function(x) {
  rd <- dim(x)[1]
  results <- matrix(0,rd,rd)
  for (s1 in 1:rd) {
    for (s2 in 1:rd) {
      x1Temp <- as.numeric(x[s1, ])
      x2Temp <- as.numeric(x[s2, ])
      br.temp <- 0
      results[s1,s2] <- 200 - (sum(abs(x1Temp - x2Temp))))}
  row.names(results) <- row.names(x)
  colnames(results) <- row.names(x)
  return(results)}

```

My editing of the two

```

BR_au <- function(x, rescale = F, counts = T) {
  if (counts == T){
    x <- prop.table(as.matrix(x), 1) * 100
  } else {
  }
  rd <- dim(x)[1]
  results <- matrix(0,rd,rd)
  for (s1 in 1:rd) {
    for (s2 in 1:rd) {
      x1Temp <- as.numeric(x[s1, ])
      x2Temp <- as.numeric(x[s2, ])
      br.temp <- 0
      results[s1,s2] <- 200 - (sum(abs(x1Temp - x2Temp))))

```

```

    }
  }
  row.names(results) <- row.names(x)
  colnames(results) <- row.names(x)
  if (rescale == F) {
    return(results)
  } else {
    results <- results / 200
    return(results)
  }
}

# Now that we have the function constructed, let's bring in our data.
BRdata <- read.csv("BRsimdata.csv")

# Our first column is the name of the sites. In order for the function to
# run, we need to turn this first column into our row names and remove
# the first column so all data are numeric.
row.names(BRdata) <- BRdata[,1]
BRdata <- BRdata[, -1]

# Time to use Gianmarco's BRsim function, which produces a nice correlation
# matrix and corresponding heat map of the results of the Brainerd-Robinson
# analysis.
# First we filter out Fouts Village
BRdata_row_names <- rownames(BRdata)
BRdata_row_names <- filter(as.data.frame(BRdata_row_names),
                          BRdata_row_names != "Fouts Village")
colnames(BRdata_row_names) <- NULL
BRdata_no_fouts <- filter(BRdata, rownames(BRdata) != "Fouts Village")
rownames(BRdata_no_fouts) <- sapply(BRdata_row_names, as.character)
BRsim(BRdata_no_fouts, correction = F, rescale = T)

# Rather than dwelling on the results, let's implement the function using
# my own function, which is primarily drawn from Matt Peeples' implementation
# Since the data provides counts, we first need to convert to proportions
# for the BR coefficient
BRdata_prop <- prop.table(as.matrix(BRdata), 1) * 100
BRresults <- BR_au(BRdata_prop, rescale = T, counts = F)

# Now, let's turn the results into a social network graph.

# The results of the BRsim function come in the form of an adjacency matrix.
# igraph can easily handle this kind of data to create a network graph.
# Because the adjacency matrix is between 0 and 1, we need to tell igraph
# that the resulting network graph is weighted. Otherwise an edge will only
# be given for the relationship between each site and itself.
BRgraph <- graph_from_adjacency_matrix(BRresults, weighted = T)

# Now we can manipulate the graph object using igraph's functions and
# create a weighted edgelist for work in Gephi and multinet.

# Create edgelist

```

```

BRel <- as_edgelist(BRgraph)

# Create the weights and format as a data frame for column binding
BRw <- E(BRgraph)$weight
BRw <- as.data.frame(BRw)

# Add the weights, and viola we have a weighted, directed edgelist for
# proportional stylistic similarity between sites.
BRel <- cbind(BRel, BRw)

# Write out complete Brainerd Robinson edgelist
write_csv(BRel, "complete_BR_edgelist.csv")

# Assessing the distribution of the BR coefficients
BRel %>%
  filter(`1` != `2`) %>%
  ggplot(aes(x = BRw)) +
  geom_histogram(aes(y=..density..), binwidth=.05, colour="black",
                fill="white") +
  geom_density(alpha = 0.2) +
  geom_vline(aes(xintercept=mean(BRw, na.rm=T)), # Ignore NA values for mean
            color="red", linetype="dashed", size=1) +
  xlab("Rescaled BR Coefficients") +
  ylab("Density") +
  theme_minimal()

# Mean of BR coefficients (this will be used as a cutoff point for giving
# edges)
BRel %>%
  filter(`1` != `2`) %>%
  summarise(Mean = mean(BRw))

# Looks like the mean is 0.4132476. We'll round it down to 0.4 for an edge
# cutoff value

# But before we apply that cutoff, let's explore the range and frequency of
# BR scores if they were produced purely by chance based on our data set

# First, we will row and column randomize the BR input 10,000 times and
# create a list of the results
# This means that we'll shuffle the order of row and column data with
# replacement
BRdata_rand_list <- replicate(10000, BRdata[sample(1:nrow(BRdata),
                                                replace = T),
                                             sample(1:nrow(BRdata),
                                                replace = T)],
                             simplify = F)

# Setup an empty list to hold the BR coefficients for the randomized data
BR_rand_result <- list()

# Number of simulations
nsim <- 10000

```

```

# Now we can iterate the BR algorithm over the randomized lists
for (i in 1:nsim) {
  BR_rand_result[[i]] <- BR_au(BRdata_rand_list[[i]], rescale = T)
}

# Turn adjacency matrices into three column data frames
for (i in 1:nsim) {
  BR_rand_result[[i]] <- setNames(melt(BR_rand_result[[i]]),
                                c('1', '2', 'values'))
}

# Now we can extract the BR values from the data frames in the list
BR_rand_result_vals <- lapply(BR_rand_result, '[[', 3)

# And collapse that list into one long vector and turn into a
# tibble data frame
BR_rand_vals <- tbl_df(unlist(BR_rand_result_vals))

# Add a column to indicate these are simulated data
BR_rand_vals <- BR_rand_vals %>%
  mutate(Type = "Randomized BR")

# Append the actual data
BRrel <- tbl_df(BRrel)
BR_vals_all <- BRrel %>%
  select(BRw) %>%
  mutate(value = BRw) %>%
  select(value) %>%
  mutate(Type = "Actual BR") %>%
  bind_rows(., BR_rand_vals)

# Drop 0's and 1's since no sites are perfectly dissimilar or similar
BR_vals_final <- BR_vals_all %>%
  filter(value != 1) %>%
  filter(value != 0)

# Plot
ggplot(BR_vals_final, aes(x = value)) +
  geom_histogram(data = subset(BR_vals_final, Type == "Randomized BR"),
                aes(y=..density..), alpha = 0.5, bins = 25, colour="black",
                fill="green4") +
  geom_density(data = subset(BR_vals_final, Type == "Randomized BR"),
              alpha = 0.1, color = "green4", fill = "green4",
              adjust = 2.5) +
  geom_vline(data = subset(BR_vals_final, Type == "Randomized BR"),
            aes(xintercept=mean(value, na.rm=T)), # Ignore NA values for mean
            color="green4", linetype="dashed", size=1) +
  geom_histogram(data = subset(BR_vals_final, Type == "Actual BR"),
                aes(y=..density..), bins = 25, colour="black",
                fill="navy", alpha = 0.4) +
  geom_density(data = subset(BR_vals_final, Type == "Actual BR"),
              alpha = 0.1, color = "navy", fill = "navy") +

```

```

geom_vline(data = subset(BR_vals_final, Type == "Actual BR"),
           aes(xintercept=mean(value, na.rm=T)), color = "navy",
           linetype = "dashed", size = 1) +
xlab("Rescaled BR Coefficients") +
ylab("Density") +
theme_minimal()

# Looks Like the mean for the simulated data is well above that of our
# observed data BR values. Neither the observed nor simulated data closely
# approximate normal distributions. This suggests some underlying issues
# related to sampling, in particular the small sample sizes from a
# number of sites. Nevertheless, the > 0.4 cutoff indicates that edges
# will be given in situations where the proportional similarity between
# two assemblages is greater than the average proportional similarity
# across the Late Prehistoric CIRV.

# Let's now apply our threshold of > 0.4 so that we only give edges to the
# strongest proportional relationship. We can use dplyr to wrangle the
# edgelist and also drop recursive edges.
BRel_t <- BRel %>%
  filter(BRw > 0.4 & BRel[1] != BRel[2])

# Change column names to be suitable for Gephi
colnames(BRel_t) <- c("Source", "Target", "weight")

# Add columns with additional node information
# Read in tables of site names, geographic coords., and time distinction
# For time, 1 is a primary occupation prior to Oneota in-migration
# and 2 is a primary occupation succeeding Oneota in-migration
plate_node_table <- read_csv("Plate_node_table.csv")
colnames(plate_node_table) <- c("Source", "Label", "Long", "Lat", "Time")

# Join the node table columns to the edgelist by the Source node
plate_t1 <- left_join(BRel_t, plate_node_table[-2], by = "Source")

# Prepare node tables to join time designation for the target node
colnames(plate_node_table) <- c("Target", "Label", "Long", "Lat", "Time2")

# Join Time 2 column to Target node
plate_edgelist_complete <- left_join(plate_t1, plate_node_table[c(-2:-4)],
                                     by = "Target")

# Create Pre- and Post-Migration Edgelists
plate_pre_el_need_dist <- plate_edgelist_complete %>%
  filter(Time == Time2) %>%
  filter(Time == 1)

plate_post_el_need_Law <- plate_edgelist_complete %>%
  filter(Time == Time2) %>%
  filter(Time == 2)

# Two sites have extended or multi-component occupations in both time periods
# So we need to include their connections in both time periods

```

```

Law_plate_post <- plate_edgelist_complete %>%
  filter(Time == 2 & Target == "Lawrenz Gun Club" |
         Source == "Lawrenz Gun Club" & Time2 == 2) %>%
  mutate(Time = replace(Time, Time == 1, 2)) %>%
  mutate(Time2 = replace(Time2, Time2 == 1, 2))

Buck_plate_post <- plate_edgelist_complete %>%
  filter(Time == 2 & Target == "Buckeye Bend" |
         Source == "Buckeye Bend" & Time2 == 2) %>%
  mutate(Time = replace(Time, Time == 1, 2)) %>%
  mutate(Time2 = replace(Time2, Time2 == 1, 2))

# Bind the LCG & Buckeye post-migration edges to the post-migration edgelists
plate_post_el_need_dist <- rbind(plate_post_el_need_Law, Law_plate_post,
                                Buck_plate_post)

# Adding geographic coordinates
# Read in matrix of site distances
site_distances <- read_csv("Site Distances Matrix in km.csv")

#first column of site names to rownames
site_distances <- column_to_rownames(site_distances, var = "X1")

# Convert geographic distance matrix to graph object
distance_g <- graph_from_adjacency_matrix(as.matrix(site_distances),
                                         weighted = TRUE,
                                         mode = "directed")

# Convert geo distance graph object to edgelist
distance_el <- as_edgelist(distance_g)
distance_el_weight <- as.numeric(E(distance_g)$weight)
distance_el <- tbl_df(cbind(distance_el, distance_el_weight))
colnames(distance_el) <- c("Source", "Target", "weight")
distance_el$Distance <- as.numeric(distance_el$weight)

# Merge the geographic distance edgelist with directed plate edgelists
plate_pre_el_complete <- merge(plate_pre_el_need_dist, distance_el[-3])
plate_post_el_complete <- merge(plate_post_el_need_dist, distance_el[-3])

# Combine the pre- and post-migration data sets into a single edgelist
plate_el_BR_all_time_complete <- rbind(plate_pre_el_complete, plate_post_el_complete)

# Finally, we can export the complete edgelist for visualization in Gephi
write_csv(plate_el_BR_all_time_complete, "BR_edgelist_complete.csv")

###_____UNDIRECTED Network Creation_____###
###_____###
###_____###

# The edgelists created thus far have been directed. Since we are
# disregarding directionality, it is important to account for duplicate
# edges.
BRgraph_un <- graph_from_adjacency_matrix(BRresults, weighted = T,
                                         mode = "undirected")

```

```

# Create undirected edgelist
BRel_un <- as_edgelist(BRgraph_un)

# Create the weights and format as a data frame for column binding
BRw_un <- E(BRgraph_un)$weight
BRw_un <- as.data.frame(BRw_un)

# Add the weights, and viola we have a weighted, directed edgelist for
# proportional stylistic similarity between sites.
BRel_un <- cbind(BRel_un, BRw_un)

# Write out complete Brainerd Robinson edgelist
write_csv(BRel_un, "complete_BR_UNDIRECTED_edgelist.csv")

# Apply our threshold of > 0.4 so that we only give UNDIRECTED edges to the
# strongest proportional relationship. We can use dplyr to wrangle the
# edgelist and also drop recursive edges.
BRel_t_un <- BRel_un %>%
  filter(BRw_un > 0.4 & BRel_un[1] != BRel_un[2])

# Change column names to be suitable for Gephi
colnames(BRel_t_un) <- c("Source", "Target", "weight")

# Join the node table columns to the edgelist by the Source node
plate_t1_un <- left_join(BRel_t_un, plate_node_table[-2], by = "Source")

# Prepare node tables to join time designation for the target node
colnames(plate_node_table) <- c("Target", "Label", "Long", "Lat", "Time2")

# Join Time 2 column to Target node
plate_edgelist_complete_un <- left_join(plate_t1_un,
                                       plate_node_table[c(-2:-4)],
                                       by = "Target")

# Create Pre- and Post-Migration Edgelists
plate_pre_el_need_dist_un <- plate_edgelist_complete_un %>%
  filter(Time == Time2) %>%
  filter(Time == 1)

plate_post_el_need_Law_un <- plate_edgelist_complete_un %>%
  filter(Time == Time2) %>%
  filter(Time == 2)

# Two sites have extended or multi-component occupations in both time periods
# So we need to include their connections in both time periods
Law_plate_post_un <- plate_edgelist_complete_un %>%
  filter(Time == 2 & Target == "Lawrenz Gun Club" |
         Source == "Lawrenz Gun Club" & Time2 == 2) %>%
  mutate(Time = replace(Time, Time == 1, 2)) %>%
  mutate(Time2 = replace(Time2, Time2 == 1, 2))

Buck_plate_post_un <- plate_edgelist_complete_un %>%

```

```

filter(Time == 2 & Target == "Buckeye Bend" |
       Source == "Buckeye Bend" & Time2 == 2) %>%
mutate(Time = replace(Time, Time == 1, 2)) %>%
mutate(Time2 = replace(Time2, Time2 == 1, 2))

# Bind the LCG & Buckeye post-migration edges to the post-migration edgelists
plate_post_el_need_dist_un <- rbind(plate_post_el_need_Law_un,
                                   Law_plate_post_un, Buck_plate_post_un)

# Merge the geographic distance edgelist with undirected plate edgelists
plate_pre_el_complete_un <- merge(plate_pre_el_need_dist_un, distance_el[-3])
plate_post_el_complete_un <- merge(plate_post_el_need_dist_un,
                                  distance_el[-3])

# Combine the pre- and post-migration data sets into a single edgelist
plate_el_BR_all_time_complete_un <- rbind(plate_pre_el_complete_un,
                                          plate_post_el_complete_un)

# Finally, we can export the complete undirected edgelist for visualization
# in Gephi
write_csv(plate_el_BR_all_time_complete_un,
          "BR_UNDIRECTED_edgelist_complete.csv")
write_csv(plate_pre_el_complete_un,
          "BR_UNDIRECTED_edgelist_pre-migration.csv")
write_csv(plate_post_el_complete_un,
          "BR_UNDIRECTED_edgelist_post-migration.csv")

```

Plate continuous attribute ridgeline plots

```

# Plate Attributes Ridgeline plot

library(tidyverse)
library(ggribes)

# Read in plate attribute data
plates <- read_csv("plate_cont.csv",
                  col_types = cols(FlareAngle = col_double(),
                                  MaxDiameter = col_double()))

# Assign rownames to unique vessel i.d.
plate_unique <- read_csv("plate_unique.csv")
rownames(plates) <- plate_unique$`1`

# Gather data for faceting. Faceting allows the graph to show each
# attribute's distribution across the different sites
pGathered <- gather(plates, Attribute, Value, MaxDiameter:MaxTrailing)

# read in node tables to add column to arrange by time period in ridgeline
# plots
plate_node_table <- read_csv("Plate_node_table.csv")
colnames(plate_node_table) <- c("Site", "Label", "Long", "Lat", "Time")

# join node table to allow for separating out sites by time in plots

```

```

pGathered <- pGathered %>% left_join(plate_node_table[c(1, 5)])
# Add Time column as factor for discrete color scale
pGathered$Time1 <- as.factor(pGathered$Time)

# Add a new factor Level for Lawrenz and Buckeye, with occupations in both
# time periods Also factor the Site Levels for ordering in the plot
ppGathered <- pGathered %>%
  mutate(Time3 = ifelse(Site == "Buckeye Bend", 3, Time1)) %>%
  mutate(Time4 = ifelse(Site == "Lawrenz Gun Club", 3, Time3)) %>%
  mutate(Time4 = ifelse(Time4 == 2, 4, Time4)) %>%
  mutate(Time4 = as.factor(.$Time4)) %>%
  mutate(Site = as.factor(.$Site))

# Create vector of columns names to appear in the plot
attribute_names <- c(
  "FlareAngle" = "Flare Angle (°)",
  "FlareLength" = "Flare Length (mm)",
  "MaxDiameter" = "Diameter (cm)",
  "MaxIncising" = "Incising (mm)",
  "MaxTrailing" = "Trailing (mm)",
  "RimThick" = "Rim Thickness (mm)",
  "ThickBelowFlare" = "Flare-Well Joint (mm)"
)

# Create plate ridgeline plot of plate attributes
ppGathered %>%
  group_by(Site) %>%
  arrange(Site, Time4) %>%
  ggplot(aes(x = Value, y = reorder(fct_rev(Site), desc(Time4)),
            fill = Time4)) +
  geom_density_ridges() +
  facet_wrap(~Attribute, scale = "free",
            labeller = as_labeller(attribute_names)) +
  theme(axis.text.y = element_text(size=12)) +
  xlab("") +
  ylab("") + ggtitle("Plate Attributes") +
  scale_fill_brewer(palette = "Greens") +
  theme_minimal() +
  theme(strip.text.x = element_text(face = "bold"),
        panel.grid.major.y = element_blank())

```

Summary and Network Statistics

```

# Plate design summary and network statistics

library(tidyverse)
library(readxl)
library(broom)
library(igraph)
library(cowplot)

plate_all <- read_excel("Upton_Dis_Plates.xlsx")

```

```

# Count total number of plates by site with decoration data
plate_all %>%
  group_by(Site) %>%
  select(Site, `BR Design Group`) %>%
  na.omit() %>%
  summarise(`Decorated Plates` = n())

# Count how many indeterminate vessel designs are present by site
plate_all %>%
  group_by(Site) %>%
  select(Site, `BR Design Group`) %>%
  mutate(`BR Design Group` = as.numeric(`BR Design Group`)) %>%
  summarise(NAs = sum(is.na(`BR Design Group`)))

# and missing values overall
plate_all %>%
  group_by(Site) %>%
  select(Site, `BR Design Group`) %>%
  mutate(`BR Design Group` = as.numeric(`BR Design Group`)) %>%
  summarise(NAs = sum(is.na(`BR Design Group`))) %>%
  select(NAs) %>%
  summarise(sum = sum(.))

# Count the number of plates with decoration techniques AND identifiable
# motif by site
plate_all %>%
  select(Site, `Primary Design Technique`, `BR Design Group`) %>%
  group_by(Site) %>%
  mutate(Tech_BR = ifelse(!is.na(`Primary Design Technique`) & !is.na(`BR Design Group`)),
         1, 0) %>%
  summarise(`Decorated Plates` = sum(`Tech_BR`)) %>%
  write_csv(., "Decorated Plates by Site.csv")

# Add a table of the different decoration techniques
write.csv(table(plate_all$Site, plate_all$`Primary Design Technique`),
          "plate decoration technique summary.csv")

# Count the total number of decorated plates by site
plate_all %>%
  group_by(Site) %>%
  select(Site, `BR Design Group`) %>%
  mutate(`Decorated Plates` = ifelse(`BR Design Group` %in% c(-1, 1),
                                     0, `BR Design Group`)) %>%

  na.omit() %>%
  summarise(`Decorated Plates` = n()) %>%
  write_csv(., "count of decorated plates by site.csv")

# and total number of decorated plates overall
plate_all %>%
  group_by(Site) %>%
  select(Site, `BR Design Group`) %>%
  mutate(`Decorated Plates` = ifelse(`BR Design Group` %in% c(-1, 1),
                                     0, `BR Design Group`)) %>%

```

```

na.omit() %>%
summarise(`Decorated Plates` = n()) %>%
select(`Decorated Plates`) %>%
mutate(`Decorated Plates` = as.numeric(`Decorated Plates`)) %>%
summarise(sum = sum(.))

# Table for BR Design Groups
BR_table <- table(plate_all$Site, plate_all$`BR Design Group`)
table(plate_all$Site, plate_all$`Primary Design Technique`)
write.csv(BR_table, "Plate_BR_table.csv")

# Total number of plates (includes all plates, even those without
# design data)
plate_all %>%
  group_by(Site) %>%
  select(Site, `BR Design Group`) %>%
  mutate(`Decorated Plates` = ifelse(`BR Design Group` %in% c(-1, 1),
                                     0, `BR Design Group`)) %>%
  summarise(`Decorated Plates` = n()) %>%
  select(`Decorated Plates`) %>%
  mutate(`Decorated Plates` = as.numeric(`Decorated Plates`)) %>%
  summarise(sum = sum(.))

# Ceramic Diversity at sites
BR_table_t <- t(BR_table)
cer_div <- as.data.frame(colSums(BR_table_t != 0))
cer_div <- rownames_to_column(cer_div)
colnames(cer_div) <- c("Site", "Count of Design Categories")
ppGathered %>% group_by(Site) %>% filter(distinct(Site))
cer_div <- left_join(cer_div, unique(ppGathered[, c(1, 7)]))
levels(cer_div$Time4) <- c("Pre-Migration", "Pre- and Post",
                          "Post-Migration")

# Remove Orendorf D and Fouts and plot box and whisker plot
cer_div %>%
  filter(Site != "Orendorf D") %>%
  filter(Site != "Fouts Village") %>%
  ggplot() +
    geom_boxplot(aes(x = Time4, y = `Count of Design Categories`)) +
    xlab("") +
    theme_classic() +
    scale_y_continuous(expand = c(0, 0), limits = c(0, 20),
                      breaks = c(0, 5, 10, 15, 20)) +
    ylab("Count of Design Categories Present") +
    theme(text = element_text(size=20))

# Regression of number of design categories as explained by sample size
categories <- read_xlsx("Number of Categories and Sample Size from each site for regression.xlsx")

# Summary of regression
cat_lm <- lm(num_categories ~ sample_size, data = categories)
summary(cat_lm)

```

```

tidy(cat_lm)

# Regression plot - Looks strongly positive
categories %>%
  filter(Site != "Fouts Village")%>%
  ggplot(aes(x = sample_size, y = num_categories)) +
  geom_smooth(method = "lm", se = FALSE) +
  geom_point()

# Correlation of the number of categories as a function of sample size -
# indeed the larger the sample size, the more plate decoration categories
# are present
cor(categories$num_categories, categories$sample_size)

### _____ Plate BR Network Stats _____ ###

# Read in finalized, undirected plate BR edgelist
BR_el_un <- read_csv("BR_UNDIRECTED_edgelist_complete.csv")

# Read in finalized, undirected pre-migration BR edgelist
BR_el_un_pre <- read_csv("BR_UNDIRECTED_edgelist_pre-migration.csv")

# Read in finalized, undirected post-migration BR edgelist
BR_el_un_post <- read_csv("BR_UNDIRECTED_edgelist_post-migration.csv")

# Convert to igraph graph
BR_g <- graph_from_edgelist(as.matrix(BR_el_un[, c(1:2)]),
                           directed = FALSE)
BR_g_pre <- graph_from_edgelist(as.matrix(BR_el_un_pre[, c(1:2)]),
                               directed = FALSE)
BR_g_post <- graph_from_edgelist(as.matrix(BR_el_un_post[, c(1:2)]),
                                 directed = FALSE)

# Assign edge weights to graph
E(BR_g)$weight <- BR_el_un$weight
E(BR_g_pre)$weight <- BR_el_un_pre$weight
E(BR_g_post)$weight <- BR_el_un_post$weight

# Function to calculate degree, betweenness, closeness, and eigenvector
# centrality for a graph and return a data frame with the scores
centr_all <- function(graph, g_name = "Score") {

  # Check that graph is an igraph object
  if (!is_igraph(graph)) {
    stop("Not a graph object")
  }

  # Name of graph
  g_name <- as.character(g_name)

  # Degree centralization
  res_centr <- centr_degree(graph)$centralization

```

```

# Betweenness centralization
res_centr[2] <- centr_betw(graph)$centralization

# Closeness centralization
res_centr[3] <- centr_clo(graph)$centralization

# Eigenvector centralization
res_centr[4] <- centr_eigen(graph)$centralization

res_centr <- t(as.data.frame(res_centr))

# Table of scores
colnames(res_centr) <- c("Degree", "Betweenness", "Closeness",
                        "Eigenvector")
rownames(res_centr) <- g_name

res_centr
}

# Calculate centralization scores for each graph
all_centr <- centr_all(BR_g, g_name = "Flattened Across Time")
pre_centr <- centr_all(BR_g_pre, g_name = "Pre-Migration")
post_centr <- centr_all(BR_g_post, g_name = "Post-Migration")
rbind(pre_centr, post_centr, all_centr)

# Calculated Mean Weighted Degree (or strength)
mean(strength(BR_g))
mean(strength(BR_g_pre))
mean(strength(BR_g_post))

#-----Edge Betweenness Community Detection-----
# Edge betweenness extends the concept of vertex betweenness centrality to
# edges by assigning each edge a score that reflects the number of shortest
# paths that move through that edge.
# You might ask the question, which ties in a social network are the most
# important in the spread of information?

# Calculated edge betweenness score for each network
pre_eb <- cluster_edge_betweenness(BR_g_pre)
post_eb <- cluster_edge_betweenness(BR_g_post)
all_eb <- cluster_edge_betweenness(BR_g)

# Looks like the only interesting graph in terms of community detection is
# the graph that is flattened across time. It correctly assigns the pre-
# and post-migration sites to clusters, but with some interesting intricacies

# Community detection via edge betweenness plot
plot(all_eb, BR_g, col = membership(all_eb), vertex.label.cex = c(1.5),
      edge.arrow.size = .1, edge.curved = .1)
title(main = "Edge Betweenness Community Detection in \n the Categorical Identification Network",
      cex.main = 1.5)

```

```

#-----Randomization for Pre-Migration Period BR-----
#-----PRE_MIGRATION-----

# Initiate empty List for assessing BR pre-migration average path Length
# and transitivity
gpre <- vector('list', 5000)

# Initiate empty List for assessing BR pre-migration density density
# and mean degree
gpre.d <- vector('list', 5000)

# Populate gpre List with random graphs of same order and size
for(i in 1:5000){
  gpre[[i]] <- erdos.renyi.game(n = gorder(BR_g_pre), p.or.m = gsize(BR_g_pre),
                              directed = FALSE, type = "gnm")
}

# Populate gpre.d List with random graphs of same order and approximate
# density. A separate List of 5000 random graphs is necessary for density
# and mean degree because these statistics would be identical in random graphs
# of the same order and size as our observed graph.
# Instead, a probability of edge creation equal to the observed density is
# used. Further, only mean degree (as opposed to mean weighted degree) is
# used because Erdos-Renyi random graphs do not support weights.
# However, see the bottom of this chapter's code for a method on assigning
# random edge edgeweights to an Erdo-Renyi graph
for(i in 1:5000){
  gpre.d[[i]] <- erdos.renyi.game(n = gorder(BR_g_pre), p.or.m = edge_density(BR_g_pre), direc
ted = FALSE, type = "gnp")
}

# Calculate average path Length, transitivity (clustering coefficient),
# density, and degree across the 5000 random pre-migration graphs
pre.pl <- lapply(gpre.d, mean_distance, directed = FALSE)
pre.trans <- lapply(gpre, transitivity)
pre.density <- lapply(gpre.d, edge_density)
pre.degree <- lapply(gpre.d, function(x){
  y <- degree(x)
  mean(y)
})

# Unlist and change to a data frame for visualizations
pre.pl <- as.data.frame(unlist(pre.pl))
pre.trans <- as.data.frame(unlist(pre.trans))
pre.density <- as.data.frame(unlist(pre.density))
pre.degree <- as.data.frame(unlist(pre.degree))

# Plot the distribution of random graph's average shortest path Lengths
# with the pre-migration BR network's ave. shortest path as Line
p.pre.pl <- ggplot(pre.pl, aes(x = pre.pl)) +
  geom_histogram(aes(y = ..density..), bins = 28) +
  geom_vline(xintercept = (mean_distance(BR_g_pre, directed = FALSE)),

```

```

        linetype = "dashed", color = "red") +
  geom_density() +
  ggtitle("Distribution of 5000 Random Graph Average Shortest Path Lengths & \nPre-Migration P
eriod Average Shortest Path Length") +
  xlab("Average Shortest Path Length") +
  ylab("")

# Plot the distribution of random graph's transitivity with the pre-migration
# BR network's transitivity path as Line
p.pre.trans <- ggplot(pre.trans, aes(x = pre.trans)) +
  geom_histogram(aes(y = ..density..), bins = 20) +
  geom_vline(xintercept = (transitivity(BR_g_pre)), linetype = "dashed",
            color = "red") +
  geom_density() +
  ggtitle("Distribution of Transitivity in 5000 Random Models & \nPre-Migration Period Network
Transitivity") +
  xlab("Transitivity (or Clustering Coefficient)") +
  ylab("")

# Plot the distribution of random graph's average density with the
# pre-migration jar network's ave. shortest path as Line
p.pre.density <- ggplot(pre.density, aes(x = pre.density)) +
  geom_histogram(aes(y = ..density..), bins = 20) +
  geom_vline(xintercept = (edge_density(BR_g_pre)), linetype = "dashed",
            color = "red") +
  geom_density() +
  ggtitle("Distribution of 5000 Random Graph Average Densities & \nPre-Migration Preiod Network
Average Density") +
  xlab("Average Density") +
  ylab("")

# Plot the distribution of random graph's mean degree with the pre-migration
# BR network's mean degree path as Line
p.pre.degree <- ggplot(pre.degree, aes(x = pre.degree)) +
  geom_histogram(aes(y = ..density..), bins = 20) +
  geom_vline(xintercept = (mean(degree(BR_g_pre, mode = "all"))),
            linetype = "dashed", color = "red") +
  geom_density() +
  ggtitle("Distribution of Mean Degree in 5000 Random Models & \nPre-Migration Period Network
Mean Degree") +
  xlab("Mean Degree") +
  ylab("")

# Use plot_grid to plot all four graphs on the same grid
plot_grid(p.pre.pl, p.pre.trans, p.pre.density, p.pre.degree)

# Calculate the proportion of graphs with an average path length lower than
# observed
sum(pre.pl < mean_distance(BR_g_pre, directed = False))/5000*100

# Calculate the proportion of graphs with a transitivity (mean clustering
# coefficient) lower than our observed
sum(pre.trans < transitivity(BR_g_pre))/5000*100

```

```

# Calculate the proportion of graphs with a density lower than our observed
sum(pre.density < edge_density(BR_g_pre))/5000*100

# Calculate the proportion of graphs with a mean degree lower than observed
sum(pre.degree < mean(degree(BR_g_pre)))/5000*100

#-----Randomization for Post-Migration Period BR-----
#-----POST_MIGRATION-----

# Initiate empty List for assessing BR post-migration average path length and
# transitivity
gpost <- vector('list', 5000)

# Initiate empty List for assessing BR post-migration density and
# mean degree
gpost.d <- vector('list', 5000)

# Populate gpost List with random graphs of same order and size
for(i in 1:5000){
  gpost[[i]] <- erdos.renyi.game(n = gorder(BR_g_post),
                               p.or.m = gsize(BR_g_post),
                               directed = FALSE, type = "gnm")
}

# Populate gpost.d List with random graphs of same order and approximate
# density. A separate List of 5000 random graphs is necessary for density
# and mean degree because these statistics would identical in random graphs
# of the same order and size as our observed graph.
# Instead, a probability of edge creation equal to the observed density is
# used. Further, only mean degree (as opposed to mean weighted degree) is
# used because Erdos-Renyi random graphs do not support weights.
for(i in 1:5000){
  gpost.d[[i]] <- erdos.renyi.game(n = gorder(BR_g_post),
                                   p.or.m = edge_density(BR_g_post),
                                   directed = FALSE, type = "gnp")
}

# Calculate average path length, transitivity (clustering coefficient),
# density, and degree across the 5000 random post-migration graphs
post.pl <- lapply(gpost.d, mean_distance, directed = FALSE)
post.trans <- lapply(gpost, transitivity)
post.density <- lapply(gpost.d, edge_density)
post.degree <- lapply(gpost.d, function(x){
  y <- degree(x)
  mean(y)
})

# Unlist and change to a data frame for visualizations
post.pl <- as.data.frame(unlist(post.pl))
post.trans <- as.data.frame(unlist(post.trans))
post.density <- as.data.frame(unlist(post.density))

```

```

post.degree <- as.data.frame(unlist(post.degree))

# Plot the distribution of random graph's average shortest path Lengths
# with the post-migration BR network's ave. shortest path as Line
p.post.pl <- ggplot(post.pl, aes(x = post.pl)) +
  geom_histogram(aes(y = ..density..), bins = 18) +
  geom_vline(xintercept = (mean_distance(BR_g_post, directed = FALSE)),
            linetype = "dashed", color = "red") +
  geom_density() +
  ggtitle("Distribution of 5000 Random Graph Average Shortest Path Lengths & \nPost-Migration
Period Average Shortest Path Length") +
  xlab("Average Shortest Path Length") +
  ylab("")

# Plot the distribution of random graph's transitivity with the
# post-migration BR network's transitivity path as Line
p.post.trans <- ggplot(post.trans, aes(x = post.trans)) +
  geom_histogram(aes(y = ..density..), bins = 12) +
  geom_vline(xintercept = (transitivity(BR_g_post)), linetype = "dashed",
            color = "red") +
  geom_density() +
  ggtitle("Distribution of Transitivity in 5000 Random Models & \nPost-Migration Period Networ
k Transitivity") +
  xlab("Transitivity (or Clustering Coefficient)") +
  ylab("")

# Plot the distribution of random graph's average density with the
# post-migration BR network's ave. shortest path as Line
p.post.density <- ggplot(post.density, aes(x = post.density)) +
  geom_histogram(aes(y = ..density..), bins = 15) +
  geom_vline(xintercept = (edge_density(BR_g_post)), linetype = "dashed",
            color = "red") +
  geom_density() +
  ggtitle("Distribution of 5000 Random Graph Average Densities & \nPost-Migration Period Networ
k Average Density") +
  xlab("Average Density") +
  ylab("")

# Plot the distribution of random graph's mean degree with the post-migration
# BR network's mean degree path as Line
p.post.degree <- ggplot(post.degree, aes(x = post.degree)) +
  geom_histogram(aes(y = ..density..), bins = 16) +
  geom_vline(xintercept = (mean(degree(BR_g_post, mode = "all"))),
            linetype = "dashed", color = "red") +
  geom_density() +
  ggtitle("Distribution of Mean Degree in 5000 Random Models & \nPost-Migration Period Network
Mean Degree") +
  xlab("Mean Degree") +
  ylab("")

# Use plot_grid to plot all four graphs on the same grid
plot_grid(p.post.pl, p.post.trans, p.post.density, p.post.degree)

```

```

# Calculate the proportion of graphs with an average path length lower than
# observed
sum(post.pl < mean_distance(BR_g_post, directed = FALSE))/5000*100

# Calculate the proportion of graphs with a transitivity (mean clustering
# coefficient) lower than our observed
sum(post.trans < transitivity(BR_g_post))/5000*100

# Calculate the proportion of graphs with a density lower than our observed
sum(post.density < edge_density(BR_g_post))/5000*100

# Calculate the proportion of graphs with a mean degree lower than observed
sum(post.degree < mean(degree(BR_g_post)))/5000*100

#-----Randomization BR Across Time in the CIRV-----
#-----ACROSS TIME-----

# Initiate empty list for assessing BR across time average path length and
# transitivity
gall <- vector('list', 5000)

# Initiate empty list for assessing BR across time density density and mean
# degree
gall.d <- vector('list', 5000)

# Populate gpost list with random graphs of same order and size
for(i in 1:5000){
  gall[[i]] <- erdos.renyi.game(n = gorder(BR_g), p.or.m = gsize(BR_g),
                              directed = FALSE, type = "gnm")
}

# Populate gall.d list with random graphs of same order and approximate
# density. A separate list of 5000 random graphs is necessary for density
# and mean degree because these statistics would be identical in random graphs
# of the same order and size as our observed graph.
# Instead, a probability of edge creation equal to the observed density is used. Further, only
# mean degree (as opposed to mean weighted degree) is used
# because Erdos-Renyi random graphs do not support weights.
for(i in 1:5000){
  gall.d[[i]] <- erdos.renyi.game(n = gorder(BR_g),
                                 p.or.m = edge_density(BR_g),
                                 directed = FALSE, type = "gnp")
}

# Calculate average path length, transitivity (clustering coefficient),
# density, and degree across the 5000 random graphs
all.pl <- lapply(gall.d, mean_distance, directed = FALSE)
all.trans <- lapply(gall, transitivity)
all.density <- lapply(gall.d, edge_density)
all.degree <- lapply(gall.d, function(x){
  y <- degree(x)
  mean(y)
})

```

```

)

# Unlist and change to a data frame for visualizations
all.pl <- as.data.frame(unlist(all.pl))
all.trans <- as.data.frame(unlist(all.trans))
all.density <- as.data.frame(unlist(all.density))
all.degree <- as.data.frame(unlist(all.degree))

# Plot the distribution of random graph's average shortest path lengths
# with the BR network's ave. shortest path as line
p.all.pl <- ggplot(all.pl, aes(x = all.pl)) +
  geom_histogram(aes(y = ..density..), bins = 32) +
  geom_vline(xintercept = (mean_distance(BR_g, directed = FALSE)),
            linetype = "dashed", color = "red") +
  geom_density() +
  ggtitle("Distribution of 5000 Random Graph Average Shortest Path Lengths & \n Average Shorte
st Path Length Across Time in the CIRV") +
  xlab("Average Shortest Path Length") +
  ylab("")

# Plot the distribution of random graph's transitivity with the observed
# network's transitivity path as line
p.all.trans <- ggplot(all.trans, aes(x = all.trans)) +
  geom_histogram(aes(y = ..density..), bins = 25) +
  geom_vline(xintercept = (transitivity(BR_g)), linetype = "dashed",
            color = "red") +
  geom_density() +
  ggtitle("Distribution of Transitivity in 5000 Random Models & \n Transitivity Across Time in
the CIRV") +
  xlab("Transitivity (or Clustering Coefficient)") +
  ylab("")

# Plot the distribution of random graph's average density with the observed
# BR network's ave. shortest path as line
p.all.density <- ggplot(all.density, aes(x = all.density)) +
  geom_histogram(aes(y = ..density..), bins = 20) +
  geom_vline(xintercept = (edge_density(BR_g)), linetype = "dashed",
            color = "red") +
  geom_density() +
  ggtitle("Distribution of 5000 Random Graph Average Densities & \n Average Density Across Time
in the CIRV") +
  xlab("Average Density") +
  ylab("")

# Plot the distribution of random graph's mean degree with the post-migration BR network's
# mean
# degree path as line
p.all.degree <- ggplot(all.degree, aes(x = all.degree)) +
  geom_histogram(aes(y = ..density..), bins = 20) +
  geom_vline(xintercept = (mean(degree(BR_g, mode = "all"))),
            linetype = "dashed", color = "red") +
  geom_density() +
  ggtitle("Distribution of Mean Degree in 5000 Random Models & \n Mean Degree Across Time in th

```

```

e CIRV") +
  xlab("Mean Degree") +
  ylab("")

# Use plot_grid to plot all four graphs on the same grid
plot_grid(p.all.pl, p.all.trans, p.all.density, p.all.degree)

# Calculate the proportion of graphs with an average path length lower than
# observed
sum(all.pl < mean_distance(BR_g, directed = FALSE))/5000*100

# Calculate the proportion of graphs with a transitivity (mean clustering
# coefficient) lower than our observed
sum(all.trans < transitivity(BR_g))/5000*100

# Calculate the proportion of graphs with a density lower than our observed
sum(all.density < edge_density(BR_g))/5000*100

# Calculate the proportion of graphs with a mean degree lower than observed
sum(all.degree < mean(degree(BR_g)))/5000*100

```

BR-Geodesic distance regression

```

library(infer)
library(tidyverse)
library(igraph)
library(reshape2)
library(stringr)
library(cowplot)
library(broom)

# Read in finalized, undirected plate BR edgelist
BR_el_un <- read_csv("BR_UNDIRECTED_edgelist_complete_.csv")

# Read in finalized, undirected pre-migration BR edgelist
BR_el_un_pre <- read_csv("BR_UNDIRECTED_edgelist_pre-migration_.csv")

# Read in finalized, undirected post-migration BR edgelist
BR_el_un_post <- read_csv("BR_UNDIRECTED_edgelist_post-migration_.csv")

# Function from infer to take a random sample from a data set a certain number of times
rep_sample_n <- function(tbl, size, replace = FALSE, reps = 1)
{
  n <- nrow(tbl)
  i <- unlist(replicate(reps, sample.int(n, size, replace = replace), simplify = FALSE))

  rep_tbl <- cbind(replicate = rep(1:reps,rep(size,reps)), tbl[i,])

  dplyr::group_by(rep_tbl, replicate)
}

# Inference testing with linear models
# Take 100 samples of 50 each from the plate BR data sets

```

```

# The idea is to explore regression trends on the slope coefficient using
# samples from each data set. Does the trend with the entire data hold true
# when sub-samples are taken from the data?
# This is a two-tailed test to see if a linear relationship (positive or
# negative) exists between distance (explanatory variable) and weight
# (response variable)
BRpresamples <- rep_sample_n(BR_el_un_pre[, c(3, 8)], size = 12, reps = 100)
BRpostsamples <- rep_sample_n(BR_el_un_post[, c(3, 8)], size = 7, reps = 100)
BRallsamples <- rep_sample_n(BR_el_un[, c(3, 8)], size = 18, reps = 100)

# Add replicate col to align observed trends with random samples
pre_observed <- BR_el_un_pre[, c(3, 8)] %>%
  mutate(replicate = 200)

post_observed <- BR_el_un_post[, c(3, 8)] %>%
  mutate(replicate = 200)

all_observed <- BR_el_un[, c(3, 8)] %>%
  mutate(replicate = 200)

# Model showing proportional similarity across time
BR_lm_all <- ggplot(BRallsamples, aes(x = Distance, y = weight,
                                     group = replicate)) +
  geom_point(size = 2, shape = 20) +
  stat_smooth(geom = "line", se = FALSE, alpha = 0.4, method = "lm") +
  ggtitle("Social Categorical Identification Network Across Time") +
  background_grid(major = 'y', minor = "none") +
  xlab("Distance (km)") +
  ylab("Degree of Proportional Categorical Similarity") +
  theme(strip.background = element_blank(),
        strip.text.x = element_blank()) +
  stat_smooth(data = all_observed, aes(x = Distance, y = weight),
             color = "red3",
             linetype = "twodash", method = "lm", se = FALSE)

# Model showing proportional similarity in the pre-migration CIRV
BR_lm_pre <- ggplot(BRpresamples, aes(x = Distance, y = weight,
                                       group = replicate)) +
  geom_point(size = 2, shape = 20) +
  stat_smooth(geom = "line", se = FALSE, alpha = 0.4, method = "lm") +
  ggtitle("Pre-Migration Social Categorical Identification Network") +
  background_grid(major = 'y', minor = "none") +
  xlab("Distance (km)") +
  ylab("Degree of Proportional Categorical Similarity") +
  theme(strip.background = element_blank(),
        strip.text.x = element_blank()) +
  stat_smooth(data = pre_observed, aes(x = Distance, y = weight),
             color = "red3",
             linetype = "twodash", method = "lm", se = FALSE)

# Model showing proportional similarity in the post-migration CIRV
BR_lm_post <- ggplot(BRpostsamples, aes(x = Distance, y = weight,
                                         group = replicate)) +

```

```

geom_point(size = 2, shape = 20) +
stat_smooth(geom = "line", se = FALSE, alpha = 0.4, method = "lm") +
ggtitle("Post-Migration Social Categorical Identification Network") +
background_grid(major = 'y', minor = "none") +
xlab("Distance (km)") +
ylab("Degree of Proportional Categorical Similarity") +
theme(strip.background = element_blank(),
      strip.text.x =element_blank()) +
stat_smooth(data = post_observed, aes(x = Distance, y = weight),
           color = "red3",
           linetype = "twodash", method = "lm", se = FALSE)

# Inference
# First, Let's calculate the observed slope of the lm in the jar and plate
# attribute networks
BR_all_slope <- lm(weight ~ Distance, data = BR_el_un) %>%
  tidy() %>%
  filter(term == "Distance") %>%
  pull(estimate)

BR_pre_slope <- lm(weight ~ Distance, data = BR_el_un_pre) %>%
  tidy() %>%
  filter(term == "Distance") %>%
  pull(estimate)

BR_post_slope <- lm(weight ~ Distance, data = BR_el_un_post) %>%
  tidy() %>%
  filter(term == "Distance") %>%
  pull(estimate)

# Simulate 500 slopes with a permuted dataset for identification network -
# this will allow us to develop a sampling distribution of the slop under
# the hypothesis that there is no relationship between the explanatory
# (Distance) and response (weight) variables.
set.seed(1568)
BR_all_perm_slope <- BR_el_un %>%
  specify(weight ~ Distance) %>%
  hypothesize(null = "independence") %>%
  generate(reps = 500, type = "permute") %>%
  calculate(stat = "slope")

BR_pre_perm_slope <- BR_el_un_pre %>%
  specify(weight ~ Distance) %>%
  hypothesize(null = "independence") %>%
  generate(reps = 500, type = "permute") %>%
  calculate(stat = "slope")

BR_post_perm_slope <- BR_el_un_post %>%
  specify(weight ~ Distance) %>%
  hypothesize(null = "independence") %>%
  generate(reps = 500, type = "permute") %>%
  calculate(stat = "slope")

```

```

ggplot(BR_all_perm_slope, aes(x = stat)) + geom_density() + theme_classic()
ggplot(BR_pre_perm_slope, aes(x = stat)) + geom_density() + theme_classic()
ggplot(BR_post_perm_slope, aes(x = stat)) + geom_density() + theme_classic()

mean(BR_all_perm_slope$stat)
mean(BR_pre_perm_slope$stat)
mean(BR_post_perm_slope$stat)
sd(BR_all_perm_slope$stat)
sd(BR_pre_perm_slope$stat)
sd(BR_post_perm_slope$stat)

# Calculate the absolute value of the slope
abs_BR_all_obs_slope <- lm(weight ~ Distance, data = BR_el_un) %>%
  tidy() %>%
  filter(term == "Distance") %>%
  pull(estimate) %>%
  abs()

abs_BR_pre_obs_slope <- lm(weight ~ Distance, data = BR_el_un_pre) %>%
  tidy() %>%
  filter(term == "Distance") %>%
  pull(estimate) %>%
  abs()

abs_BR_post_obs_slope <- lm(weight ~ Distance, data = BR_el_un_post) %>%
  tidy() %>%
  filter(term == "Distance") %>%
  pull(estimate) %>%
  abs()

# Compute the p-value
BR_all_perm_slope %>%
  mutate(abs_BR_all_obs_slope = abs(stat)) %>%
  summarize(p_value = mean(abs_BR_all_obs_slope > BR_all_perm_slope))

BR_pre_perm_slope %>%
  mutate(abs_BR_pre_obs_slope = abs(stat)) %>%
  summarize(p_value = mean(abs_BR_pre_obs_slope > BR_pre_perm_slope))

BR_post_perm_slope %>%
  mutate(abs_BR_post_obs_slope = abs(stat)) %>%
  summarize(p_value = mean(abs_BR_post_obs_slope > BR_post_perm_slope))

# Linear models sans visualization
# explore residuals
BR_all_lm <- augment(lm(weight ~ Distance, data = BR_el_un))
BR_pre_lm <- augment(lm(weight ~ Distance, data = BR_el_un_pre))
BR_post_lm <- augment(lm(weight ~ Distance, data = BR_el_un_post))

# Check SSE - how well do the models fit?
augment(lm(weight ~ 1, data = BR_el_un)) %>%
  summarize(SSE = var(.resid)) # null
BR_all_lm %>% summarize(SSE = var(.resid))

```

```

augment(lm(weight ~ 1, data = BR_el_un_pre)) %>%
  summarize(SSE = var(.resid)) # null
BR_pre_lm %>% summarize(SSE = var(.resid))

augment(lm(weight ~ 1, data = BR_el_un_post)) %>%
  summarize(SSE = var(.resid)) # null
BR_post_lm %>% summarize(SSE = var(.resid))

# Looks like the models do fit well

# Breakdown of linear model results for plate attribute networks
summary(lm(weight ~ Distance, data = BR_el_un)) # for each 1 km increase in distance, weight d
rops 0.0006741 and at 0 distance, a weight of 0.5549 is expected
summary(lm(weight ~ Distance, data = BR_el_un))$coefficients # all = p-value of 0.0464, null
# hypothesis is rejected at alpha of 0.05. As distance increases, weight moderately decreases

summary(lm(weight ~ Distance, data = BR_el_un_pre)) # for each 1 km increase in distance, wei
ght drops 0.0006655 and at 0 distance, a weight of 0.5765 is expected
summary(lm(weight ~ Distance, data = BR_el_un_pre))$coefficients # pre p-value of 0.1776, fail
to
#reject the null hypothesis - no significant linear relationship b/t distance and weight in pr
e

summary(lm(weight ~ Distance, data = BR_el_un_post)) # for each 1 km increase in distance, wei
ght drops 0.0002517 and at 0 distance, a weight of 0.4949 is expected
summary(lm(weight ~ Distance, data = BR_el_un_post))$coefficients # post p-value of 0.5007, fa
il
# to reject null - no significant linear relationship b/t distance and weight in post

# Check correlations
cor(BR_el_un$Distance, BR_el_un$weight)
cor(BR_el_un_pre$Distance, BR_el_un_pre$weight)
cor(BR_el_un_post$Distance, BR_el_un_post$weight)

```

Experimental method to randomly assign edge weights to Erdos-Renyi random networks

```

# Randomly assigning weights to a network
# runif() is used to assign the weights based on a normal distribution of
# random weights between the max and min values in the observed data
# This could be used to assess any statistic that uses edge weights, however,
# none of these measures proved to be significant for the current analysis

for(i in 1:5000){
  gpost.d[[i]] <- erdos.renyi.game(n = gorder(BR_g_post), p.or.m = edge_density(BR_g_post),
                                directed = FALSE, type = "gnp")
}

# Assign random weights to edges based on the min/max in the observed network
for(i in 1:5000){
  E(gpost.d[[i]])$weight <- runif(length(E(gpost.d[[i]])), min = min(E(BR_g_post)$weight), max
= max(E(BR_g_post)$weight))
}

```

```

# Calculate the mean weighted degree (or strength) for each graph
post.weighted.degree <- lapply(gpost.d, function(x){
  y <- strength(x)
  mean(y)
})

# Unlist and change to a data frame for visualizations
post.weighted.degree <- as.data.frame(unlist(post.weighted.degree))

ggplot(post.weighted.degree, aes(x = post.weighted.degree)) +
  geom_histogram(aes(y = ..density..), bins = 16) +
  geom_vline(xintercept = (mean(strength(BR_g_post, mode = "all"))),
            linetype = "dashed", color = "red") +
  geom_density() +
  ggtitle("Distribution of Mean Weighted Degree in 5000 Random Models & \nPost-Migration Perio
d Network Mean Degree") +
  xlab("Mean Degree") +
  ylab("")

```

R Code from Chapter 7 Networks of Economic Relationships - Results of the Chemical Analyses

Create map of sites and clay samples

```

# Map of sites and clay resources

library(ggmap)
library(tidyverse)
library(ggrepel)

# Read in context data
cc_loc <- read_csv("Clay Ceramic lat long.csv")

# Set center for the map
lat_mid <- mean(cc_loc$lat)
lon_mid <- mean(cc_loc$lon)

# Get map from google map terrain without any labels (via the style argument)
b <- get_googlemap(center = c(lon = lon_mid, lat = lat_mid), zoom = 9,
                  maptype = "terrain", source = "google",
                  style = 'feature:all|element:labels|visibility:off')

# Create map of sites/clay samples and label to check for accuracy
ggmap(b) + geom_point(data = cc_loc, aes(x = lon, y = lat, shape = Type)) +
  geom_text_repel(data = cc_loc[c(1:17),], aes(x = lon, y = lat, label = Site_Sample))

# Create transparent background map to overlay on bedrock geology map

```

```

map <- ggplot() + geom_point(data = cc_loc, aes(x = lon, y = lat, shape = Type)) +
  theme(
    panel.background = element_rect(fill = "transparent"), # bg of the panel
    plot.background = element_rect(fill = "transparent"), # bg of the plot
    panel.grid.major = element_blank(), # get rid of major grid
    panel.grid.minor = element_blank(), # get rid of minor grid
    legend.background = element_rect(fill = "transparent"), # get rid of Legend bg
    legend.box.background = element_rect(fill = "transparent") # get rid of Legend panel bg
  ) +
  xlab("") + ylab("")

# Save map with transparent background
ggsave(map, filename = "site-clay map.png", bg = "transparent")

## After exporting, map of sites/clay samples was overlain on top of a bedrock geology map
# of the state of Illinois

```

Read in geochemical data from Excel sheets and convert from % Oxide to parts-per-million (ppm)

Also included in the following code chunk is a method to correct for the presence of shell tempering.

```

## Reading Geochemical data into R and converting from % Oxide to ppm

# Load packages
library(tidyverse)
library(readxl)
library(stringr)
library(magrittr)

# Determine path to file
path <- "all.xlsx"

# Use map to iterate read_excel over each worksheet in the workbook
ld <- path %>%
  excel_sheets() %>%
  set_names(., .) %>% # this was giving me problems, but the two dots is a workaround
  map(read_excel, path = path)

# Bind the columns in the Lists together to form one dataframe
df <- bind_cols(ld)

# Change name of first column to element
names(df)[names(df) == 'X_1'] <- 'element'

# Now, Let's get tidy!
# Grab the first column as rownames, which will become the variable names
rnames <- df[,1]

# Then grab the column names, which will become a new column "Sample" once transposed
Sample <- colnames(df[-1]) #we can drop the first name because it will become the rownames

# Transpose the dataframe

```

```

df <- t(df[, -1]) #have to drop the first column or it will convert the numbers to strings

# Set the column names
colnames(df) <- unlist(rnames) #rnames is stored as a list, so we have to unlist it

# Convert to tibble dataframe
df <- tbl_df(df)

# Add the date as a column to our data frame so we know when each sample was run
# first we need to figure out how many samples were run each day
ld_lengths <- lapply(ld, length)

# With that information we can create a simple for loop to replicate the dates the
# appropriate number of times for the number of samples run each day
res1 <- as.data.frame(NULL)
for(i in names(ld_lengths)) {
  res <- rep(i, ld_lengths[[i]])
  res1 <- c(res1, res)
}

# Create a dataframe of those dates and add it to our sample data
date_col <- tbl_df(sapply(res1, paste0, collapse = ""))
colnames(date_col) <- "Date"
df <- cbind(date_col[2:nrow(date_col),], df)

# Add column of samples names, which were the columns names before transposing
df <- cbind(Sample, df)

# Use stringr to get rid of repetitive element row names - which have an "X"
# in them by default since they don't have a column name
dfnames <- df$Sample
x_detect <- str_detect(dfnames, "X")
df <- df[!x_detect, ]

# One pesky column name has a note in it, let's get rid of it too
note <- str_detect(df$Sample, "High")
df <- df[!note, ]

# Convert the sample data to numeric to allow for calculations
df[, 3:ncol(df)] <- sapply(df[, 3:ncol(df)], as.numeric)

##-----Correction for Shell Tempering Here-----##

# In analysis, I need to correct the sherd samples for the presence of shell tempering.
# Shell is composed almost entirely of calcium which is in the same row in the periodic table
# as strontium and barium.

# First step is to drop the Ohio Red standard samples because they don't need correcting
orows <- str_detect(tolower(df$Sample), "red")
df_samples1 <- df[!orows, ]

# Add up all elements calculated in percent oxide aside from Ca and Ba
CaP_correction <- df_samples1 %>%

```

```

select(SiO2, Na2O, MgO, Al2O3, K2O, Sb2O5,
       MnO, Fe2O3, CuO, SnO2, Ti, PbO2, BaO, Bi, ZnO) %>%
rowSums() %>%
tbl_df()

# Correct the elements by dividing their amount by the corrected percent oxide
df_samples1[, c(3:length(df_samples1))] <- sapply(df_samples1[, c(3:length(df_samples1))],
         function(x){x/CaP_correction}) %>%
         bind_cols()

# Bind the shell corrected ceramic samples with the Ohio Reds
df_shell_corrected <- tbl_df(bind_rows(df_samples1, df[orows, ]))

####-----#####

# Converting from %oxide to ppm
# Each element has a unique coefficient to use when converting, so we'll make a
# function for each and apply them across the rows
sio2 <- function(x){
  x * 1000000/2.1393 #have to multiply by a million then divide by the coefficient
}

nao2 <- function(x){
  x * 1000000/1.348
}

mgo <- function(x){
  x * 1000000/1.6583
}

al2o3 <- function(x){
  x * 1000000/1.8895
}

p2o5 <- function(x){
  x * 1000000/2.2914
}

k2o <- function(x){
  x * 1000000/1.2046
}

cao <- function(x){
  x * 1000000/1.3992
}

mno <- function(x){
  x * 1000000/1.2912
}

fe2o3 <- function(x){
  x * 1000000/1.4298
}

```

```

ti <- function(x){
  x * 1000000/1.6681
}

bao <- function(x){
  x * 1000000/1.1165
}

# Apply these functions across the appropriate columns
df_shell_corrected$SiO2 <- sio2(df_shell_corrected$SiO2)
df_shell_corrected$Na2O <- nao2(df_shell_corrected$Na2O)
df_shell_corrected$MgO <- mgo(df_shell_corrected$MgO)
df_shell_corrected$Al2O3 <- al2o3(df_shell_corrected$Al2O3)
df_shell_corrected$P2O3 <- p2o5(df_shell_corrected$P2O3)
df_shell_corrected$K2O <- k2o(df_shell_corrected$K2O)
df_shell_corrected$CaO <- cao(df_shell_corrected$CaO)
df_shell_corrected$MnO <- mno(df_shell_corrected$MnO)
df_shell_corrected$Fe2O3 <- fe2o3(df_shell_corrected$Fe2O3)
df_shell_corrected$Ti <- ti(df_shell_corrected$Ti)
df_shell_corrected$BaO <- bao(df_shell_corrected$BaO)

# Since we've converted from %oxide, it's a good idea to change the element names
# Some "O's" are left to differentiate the elements measured as both %oxide and not
names(df_shell_corrected) <- c("Sample", "Date", "Si", "Na", "Mg", "Al", "P", "Cl", "K", "Ca",
  "SbO", "Mn", "Fe", "CuO", "Sn", "Ti", "Pb", "Ba", "Bi", "ZnO", "Li",
  "Be", "B", "P", "Cl1", "Sc", "Ti1", "V", "Cr", "Mn", "Fe", "Ni",
  "Co", "Cu", "Zn", "As", "Rb", "Sr", "Zr", "Nb", "Ag", "In", "Sn", "Sb",
  "Cs", "Ba", "La", "Ce", "Pr", "Ta", "Au", "Y", "Pb", "Bi1", "U", "W",
  "Mo", "Nd", "Sm", "Eu", "Gd", "Tb", "Dy", "Ho", "Er", "Tm", "Yb",
  "Lu", "Hf", "Th")

# Write the full dataframe to a csv
write_csv(df_shell_corrected,
  "Upton_results_samples_and_OhioRed_shell_corrected_all_elements_August_21_2018.csv")

# Drop the Ohio Red Samples
dfsamps <- tolower(df_shell_corrected$Sample)
orows <- str_detect(dfsamps, "red")
df_samples <- df_shell_corrected[!orows, ]
df_reds <- df_shell_corrected[orows, ]

# Write csv with samples only, Ohio Red standards removed
write_csv(df_samples, "Upton_results_samples_shell_corrected_August_21_2018.csv")

# Write csv with Ohio Reds only
write_csv(df_reds, "Upton_results_OhioRed_August_21_2018.csv")

```

Ohio Red extraction and analysis

New Ohio Red clay is the common standard used in the chemical analysis of clay and archaeological samples by LA-ICP-MS and INAA. Here, the standards run each day of LA-ICP-MS analysis are

extracted from the entire data set and analyzed in their own right to determine the accuracy of the different machines. Ultimately, it was decided to discard a number of sherds that were run on the old machine at the Field Museum's Elemental Analysis Facility (circa 2015) and only retain ceramic samples run on the new machine.

```
# Extract Ohio Reds and Calculate Relative Standard Deviation

library(tidyverse)
library(stringr)
library(plotly)

# Import data
dfall <- read_csv("Upton_results_OhioRed_August_21_2018.csv")

# Change Sample column to all lower case to ensure complete string detection
dfall$Sample <- tolower(dfall$Sample)

# Search the sample column for the word Ohio based on the abbreviation oh
ohio <- str_detect(dfall$Sample, "oh")

# Double check by searching same column for Red
red <- str_detect(dfall$Sample, "red")

# Check to see if the two detection methods are identical
sum(ohio == red) == nrow(dfall)

# Index to extract all Ohio Red Samples
ohioreds <- dfall[red,]

# Function to calculate RSD
RSD <- function(x){
  meann <- mean(x)
  relsd <- sd(x)/meann
  relsd
}

# Calculate RSD across the rows
redRSD <- apply(ohioreds[, 3:ncol(ohioreds)], RSD)

# Calculate average and standard deviation of values across each of the Ohio Reds
redAVG <- ohioreds %>%
  gather(element, sample, Si:Th) %>%
  group_by(element) %>%
  summarize(Avg = mean(sample), SD = sd(sample))

# Plot to check average values
ohioreds %>%
  gather(element, sample, Si:Th) %>%
  group_by(element, Date) %>%
  summarize(AVG = mean(sample)) %>%
  ggplot(aes(x = Date)) +
  geom_line(aes(y = AVG, color = element, group = element)) +
  theme_minimal() +
```

```

theme(axis.text.x = element_text(angle = 90, hjust = 1))

# Filter the plot to look at HREE and LREE average values
p <- ohioreds %>%
  gather(element, sample, Si:Th) %>%
  group_by(Date, element) %>%
  summarize(AVG = mean(sample)) %>%
  filter(AVG < 100) %>%
  ggplot(aes(x = Date)) +
  geom_line(aes(y = AVG, color = element, group = element)) +
  theme_minimal() +
  theme(axis.text.x = element_text(angle = 90, hjust = 1))

ggplotly(p)

# Check very high RSD elements
all_samples %>%
  gather(element, sample, Si:Th) %>%
  group_by(Date, element) %>%
  summarize(AVG = mean(sample)) %>%
  filter(element == "Bi") %>%
  ggplot(aes(x = Date)) +
  geom_line(aes(y = AVG, color = element, group = element)) +
  theme_minimal() +
  theme(axis.text.x = element_text(angle = 90, hjust = 1))

# Bind Ohio Red averages to relative standard deviations
redRSD <- data.frame(redRSD)
redRSD <- rownames_to_column(redRSD, var = "element")
OHred_avg_rsd <- left_join(redRSD, redAVG, by = "element")

# Add RSD to the Ohio Red Samples
red_with_RSD <- bind_rows(ohioreds, redRSD)

write_csv(OHred_avg_rsd, "Ohio Red Averages and RSD_Aug-21-2018.csv")
write_csv(red_with_RSD, "Ohio Reds with RSD_Aug-21-2018.csv")

# Now check for any differences between samples run on different machines
ohioreds$Date <- as.POSIXct(paste(ohioreds$Date), format = "%Y-%b-%d", tz = "UTC")
redAVG_group <- ohioreds %>%
  mutate(Machine = ifelse(Date > as.POSIXct('2016-01-01', tz = "UTC"),
                          "New", "Old")) %>%
  gather(element, sample, SiO2:Th) %>%
  group_by(Machine, element) %>%
  summarize(Avg = mean(sample), SD = sd(sample))

# Count the number of Ohio Red samples run on each machine
ohioreds %>%
  mutate(Machine = ifelse(Date > as.POSIXct('2016-01-01', tz = "UTC"),
                          "New", "Old")) %>%
  select(Machine) %>%
  group_by(Machine) %>%

```

```

summarize(num = n())

write_csv(redAVG_group, "Ohio Reds across Machines_Aug_22_2018.csv")

```

Analysis of CIRV clay sample

```

# Clay analysis

library(tidyverse)
library(stringr)
library(plotly)
library(shiny)
library(shinydashboard)
library(ggsci)
library(broom)
library(knitr)
library(ggfortify)
library(stats)
library(ICSNP)
library(factoextra)
library(dendextend)

# Read in full dataset
all_samples <- read_csv("Upton_results_samples_shell_corrected_August_21_2018.csv")

# Read in clay context data
clay_context <- read_csv("clay context data.csv")

# Each clay sample is named "C##_1"
# An expedient way of isolating the clay samples
clay <- arrange(all_samples[str_detect(all_samples$Sample, "C[:digit:]"), ], Sample)

# Clean up clay and clay context sample names
clay_context$Sample <- str_replace(clay_context$Sample, pattern = "_1" %R% END, "")
clay$Sample <- str_replace(clay$Sample, pattern = "_1" %R% END, "")

# Join clay data to clay context
clay <- left_join(clay_context, clay)

# Take the log of the elemental composition data since they are on very different
# scales
claylog <- log10(clay[,8:ncol(clay)])
claylog <- bind_cols(clay[, 1:7], claylog)

# Number of clay samples analyzed
claylog %>%
  summarise(num = n())

# Remove problem elements. Some elements are known to be unreliably measured using the ICP-MS
# at the EAF. Following Golitko (2010), these include the following elements.
problem_elements <- c("P", "Sr", "Ba", "Ca", "Hf", "As", "Cl")

```

```

# Other elements such as Ca and Sr are affected by shell tempering.
# Want to drop those as well.

# Overall these are the Elements retained - 44 in all.
elems_retained <- c("Al", "B", "Be", "Ce", "Co", "Cr", "Cs", "Dy", "Er", "Eu", "FeO",
  "Gd", "Ho", "In", "K", "La", "Li", "Lu", "Mg", "MnO", "Mo", "Na", "Nb",
  "Nd", "Ni", "Pb", "Pr", "Rb", "Sc", "Si", "Sm", "Sn", "Ta", "Tb", "Th",
  "Ti", "Tm", "U", "V", "W", "Y", "Yb", "Zn", "Zr")

names.use <- names(claylog)[(names(claylog) %in% elems_retained)]
# Length(names.use) == Length(elems_retained) # check that all elements are retained
claylog_good <- claylog[, names.use]

# Check to ensure the elements were removed are supposed to be removed
anti_join(data.frame(names(clay)),
  data.frame(names(claylog_good)), by = c("names.clay." = "names.claylog_good."))

# Need to drop the "O" for oxide after elements measured as %oxide composition since they
# have already been converted to ppm
names(claylog_good) <- c("Si", "Na", "Mg", "Al", "K", "Mn", "Fe", "Ti", "Li", "Be", "B", "Sc", "V",
  "Cr", "Ni", "Co", "Zn", "Rb", "Zr", "Nb", "In", "Sn", "Cs", "La", "Ce", "Pr",
  "Ta", "Y", "Pb", "U", "W", "Mo", "Nd", "Sm", "Eu", "Gd", "Tb", "Dy", "Ho",
  "Er", "Tm", "Yb", "Lu", "Th")

# Bind sample id and other data to the logged chemical concentrations
clay_pcaready <- bind_cols(claylog[,c(1:7)], claylog_good)

# Remove two non-clay sample
clay_pcaready <- filter(clay_pcaready, Sample != "C26") %>% filter(Sample != "C31")

#write_csv(clay_pcaready, "Clay PCA Ready.csv")

# Exploring PCA
clay_pca <- clay_pcaready %>%
  nest() %>%
  mutate(pca = map(data, ~ prcomp(.x %>% select(Si:Th))),
    pca_aug = map2(pca, data, ~augment(.x, data = .y)))

# Check variance explained by each model
var_exp <- clay_pca %>%
  unnest(pca_aug) %>%
  summarize_at(.vars = vars(contains("PC")), .funs = funs(var)) %>%
  gather(key = pc, value = variance) %>%
  mutate(var_exp = variance/sum(variance),
    cum_var_exp = cumsum(var_exp),
    pc = str_replace(pc, ".fitted", ""))

# Looks like we need to retain the first 7 PC's to hit 90% of the data's variability
# Graphing this out might help
var_exp %>%
  rename(`Variance Explained` = var_exp,
    `Cumulative Variance Explained` = cum_var_exp) %>%

```

```

gather(key = key, value = value,
       `Variance Explained`:`Cumulative Variance Explained`) %>%
mutate(pc = str_replace(pc, "PC", "")) %>%
mutate(pc = as.numeric(pc)) %>%
ggplot(aes(reorder(pc, sort(as.numeric(as.character(pc))))), value, group = key)) +
geom_point() +
geom_line() +
facet_wrap(~key, scales = "free_y") +
theme_bw() +
lims(y = c(0, 1)) +
labs(y = "Variance", x = "",
      title = "Variance explained by each principal component")

# Plot PCs 1 & 2 against each other
cp1p2_plot <- clay_pca %>%
  mutate(
    pca_graph = map2(
      .x = pca,
      .y = data,
      ~ autoplot(.x, loadings = TRUE, loadings.label = TRUE,
                 scale = FALSE,
                 #Loadings.Label.repel = TRUE,
                 loadings.label.colour = "black",
                 loadings.colour = "gray85",
                 loadings.label.alpha = 0.5,
                 loadings.label.size = 3,
                 loadings.label.hjust = 1.1,
                 frame = TRUE,
                 frame.type = "norm",
                 data = .y,
                 colour = "Geography_2",
                 shape = "Geography_2",
                 frame.level = .9,
                 frame.alpha = 0.001,
                 size = 2) +
      theme_bw() +
      #geom_text(Label = .y$Sample) +
      labs(x = "Principal Component 1",
           y = "Principal Component 2",
           title = "First two principal components of PCA on CIRV Clay dataset")
    )
  ) %>%
  pull(pca_graph)

# autoplot is lazy with color. In order to make this publication friendly, have to
# manually edit the color scales
cp1p2_plot[[1]] + scale_fill_manual(values = c("black", "black")) +
  scale_color_manual(values = c("black", "black", "black"))

# Plot PCs 1 & 3 against each other
cp1p3_plot <- clay_pca %>%
  mutate(

```

```

pca_graph = map2(
  .x = pca,
  .y = data,
  ~ autoplot(.x, x = 1, y = 3, loadings = TRUE, loadings.label = TRUE,
    loadings.label.repel = TRUE,
    loadings.label.colour = "black",
    loadings.colour = "gray85",
    loadings.label.alpha = 0.5,
    frame = TRUE,
    frame.type = "norm",
    data = .y,
    colour = "Geography_2",
    shape = "Geography_2",
    frame.level = .9,
    frame.alpha = 0.001,
    size = 2) +
  theme_bw() +
  #geom_text(Label = .y$Sample) +
  labs(x = "Principal Component 1",
    y = "Principal Component 3",
    title = "First two principal components of PCA on CIRV Clay dataset")
)
) %>%
pull(pca_graph)

# autoplot is lazy with color. In order to make this publication friendly, have to
# manually edit the color scales
cp1p3_plot[[1]] + scale_fill_manual(values = c("black","black")) +
  scale_color_manual(values = c("black","black","black"))

# Shiny app to biplot the various elements against one another
# With 44 elements, there are p(p-1)/2 or 946 biplots to investigate!
# Therefore, it's a lot easier to make an app to easily and quickly run through the options

#####
##  UI  ##
#####
ui <- fluidPage(
  pageWithSidebar (
    headerPanel('Bivariate Plotting'),
    sidebarPanel(
      selectInput('x', 'X Variable', names(clay_pcaready),
        selected = names(clay_pcaready)[[8]]),
      selectInput('y', 'Y Variable', names(claylog_good),
        selected = names(clay_pcaready)[[9]]),
      selectInput('color', 'Color', names(clay_pcaready)),
      #Slider for plot height
      sliderInput('plotHeight', 'Height of plot (in pixels)',
        min = 100, max = 2000, value = 550)
    ),
    mainPanel(
      plotlyOutput('plot1')
    )
  )
)

```

```

)
)

#####
## Server ##
#####

server <- function(input, output, session) {

  # Combine the selected variables into a new data frame
  selectedData <- reactive({
    claylog_good[, c(input$x, input$y, input$color)]
  })

  output$plot1 <- renderPlotly({

    #Build plot with ggplot syntax
    p <- ggplot(data = clay_pcaready, aes_string(x = input$x,
                                                y = input$y,
                                                color = input$color,
                                                shape = input$color)) +

      geom_point() +
      theme(legend.title = element_blank()) +
      stat_ellipse(level = 0.9) +
      scale_color_igv() +
      theme_bw() +
      xlab(paste0(input$x, " (log base 10 ppm)")) +
      ylab(paste0(input$y, " (log base 10 ppm)"))

    ggplotly(p) %>%
      layout(height = input$plotHeight, autosize = TRUE,
             legend = list(font = list(size = 12)))
  })
}

shinyApp(ui, server)

# Based on the biplots, it looks like there is good separation for the most part
# in the north and south portions of the valley when comparing Lithium to
# Vanadium or Beryllium

# Biplot of Li and V
ggplot(data = clay_pcaready, aes(x = Li, y = V,
                                color = Geography_2, shape = Geography_2)) +

  geom_point() +
  theme(legend.title = element_blank()) +
  stat_ellipse(level = 0.9) +
  scale_color_igv() +
  theme_bw() +
  xlab("Lithium (log base 10 ppm)") +

```

```

ylab("Vanadium (log base 10 ppm)") +
scale_fill_manual(values = c("black","black")) +
scale_color_manual(values = c("black","black","black"))

# Biplot of Li and Be
ggplot(data = clay_pcaready, aes(x = Li, y = Be,
                                color = Geography_2, shape = Geography_2)) +
  geom_point() +
  theme(legend.title = element_blank()) +
  stat_ellipse(level = 0.9) +
  scale_color_igv() +
  theme_bw() +
  xlab("Lithium (log base 10 ppm)") +
  ylab("Beryllium (log base 10 ppm)") +
  scale_fill_manual(values = c("black","black")) +
  scale_color_manual(values = c("black","black","black"))

# Biplot of Li and Be
ggplot(data = clay_pcaready, aes(x = Li, y = Be,
                                color = Geography_2, shape = Geography_2)) +
  geom_point() +
  theme(legend.title = element_blank()) +
  stat_ellipse(level = 0.9) +
  scale_color_igv() +
  theme_bw() +
  xlab("Lithium (log base 10 ppm)") +
  ylab("Beryllium (log base 10 ppm)") +
  scale_fill_manual(values = c("black","black")) +
  scale_color_manual(values = c("black","black","black"))

# Biplot of Ni and Cs
ggplot(data = clay_pcaready, aes(x = Ni, y = Cs,
                                color = Geography_2, shape = Geography_2)) +
  geom_point() +
  theme(legend.title = element_blank()) +
  stat_ellipse(level = 0.9) +
  scale_color_igv() +
  theme_bw() +
  xlab("Nickel (log base 10 ppm)") +
  ylab("Cesium (log base 10 ppm)") +
  scale_fill_manual(values = c("black","black")) +
  scale_color_manual(values = c("black","black","black"))

# A table of average element concentrations and standard deviations between the two
# groups may be instructive of their differences numerically as opposed to visually
clay_group_ave_std <- clay_pcaready %>%
  select(Geography_2, Si:Th) %>%
  gather(Element, Si:Th, -Geography_2) %>%
  mutate(`Si:Th` = 10^`Si:Th`) %>% # convert from Log 10
  group_by(Geography_2, Element) %>%
  summarize(mean = mean(`Si:Th`, na.rm = TRUE),
            std = sd(`Si:Th`, na.rm = TRUE))

```

```

# Count number of clay in the different groups
clay_pcaready %>%
  group_by(Geography_2) %>%
  summarize(count = n())

write_csv(clay_group_ave_std, "Clay group averages and stds.csv")

# Almost every element is enriched in northerly clays and as a result depleted in the
# southerly clays, taking a look at that via a histogram is instructive
clay_pcaready %>%
  select(Geography_2, Si:Th) %>%
  gather(Element, Si:Th, -Geography_2) %>%
  mutate(`Si:Th` = 10^`Si:Th`) %>%
  filter(Element == "Sn") %>%
  ggplot(aes(x = Element, group = Geography_2, y = `Si:Th`)) + geom_boxplot()

# It looks like there is a good deal of separation in the geochemistry of clays between the
# Northern portion of the central Illinois River Valley (including the Spoon/Illinois
# confluence) and the Southern portion of the CIRV, south of the Spoon River
# But let's check to see if statistical techniques come to a similar conclusion

###                               HCA                               ###
# First, we create a data frame for distance calculations including the elemental data only
clay_for_dist <- claylog_good
rownames(clay_for_dist) <- claylog$Sample

# Now let's perform some hierarchical clustering using Euclidean distance
clay_hca <- hclust(dist(clay_for_dist))

# Create dendrogram object
dend_clay <- as.dendrogram(clay_hca)

# Plot dendrogram object to look for good cut-off heights - 2.5 seems to be a good height
plot(dend_clay, nodePar = list(lab.cex = .75, pch = NA))

# Looks like the hierarchical clustering doesn't group precisely as the geographic/geologic
# prior knowledge would suggest. This is an indication of the heterogeneous nature of clay as
# well as the complex geological processes that have resulted in clay availability in the
# CIRV.

###                               Mahalanobis Distance                               ###
# Since HCA wasn't overly insightful, we can at least check membership probabilities between
# the north and south groups statistically. The standard method of doing this in
# archaeology is via Mahalanobis distance, which is commonly used for outlier detection.

# Extract the first 7 PC's (accounting for 90% of variability) and bind to
# sample/geography data
clay_pc1to7 <- clay_pca %>%
  unnest(pca_aug) %>%
  select(starts_with(".fitted")) %>%
  bind_cols(clay_pcaready[, c(1,3)], .) %>%

```

```

        select(c(1:9))

clay1to7_north <- clay_pc1to7 %>% filter(Geography_2 == "North")

clay1to7_south <- clay_pc1to7 %>% filter(Geography_2 == "South")

# Edit colnames
colnames(clay_pc1to7) <- str_remove(colnames(clay_pc1to7), ".fitted")

# Mahalanobis distance of North to North
mahalanobis(clay1to7_north[,3:9], colMeans(clay1to7_north[,3:9]), cov(clay1to7_north[,3:9]))

# With 7 predictor variables (PCs 1-7), the critical chi-square value is 24.32
# Given that the highest MD value among the northerly clays is 20.92, it doesn't
# Look like there are any outliers

# Have to pair down the number of predictors to 5 for the South, since there are only 7
# samples. The critical chi-square value is 20.52 for that many, Looking good for the south.
mahalanobis(clay1to7_south[,3:7], colMeans(clay1to7_south[,3:7]), cov(clay1to7_south[,3:7]))

# Let's now look at group membership probabilities. This function written by Matt Peeples
# allows for calculating group membership probabilities by chemical compositional
# distance using Mahalanobis distances and Hotellings T^2 statistic
group.mem.probs <- function(x2.l,attr1.grp,grps) {

  # x2.l = transformed element data
  # attr1 = group designation by sample
  # grps <- vector of groups to evaluate

  probs <- list()
  for (m in 1:length(grps)) {
    x <- x2.l[which(attr1.grp==grps[m]),]
    probs[[m]] <- matrix(0,nrow(x),length(grps))
    colnames(probs[[m]]) <- grps
    rownames(probs[[m]]) <- rownames(x)

    grps2 <- grps[-m]

    p.val <- NULL
    for (i in 1:nrow(x)) {p.val[i] <- HotellingsT2(x[i,],x[-i,])$p.value}
    probs[[m]][,m] <- round(p.val,5)*100

    for (j in 1:length(grps2)) {
      p.val2 <- NULL
      for (i in 1:nrow(x)) {p.val2[i] <- HotellingsT2(x[i,],x2.l[which(attr1.grp==grps2[j]),])
      $p.value}
      probs[[m]][,which(grps==grps2[j])] <- round(p.val2,5)*100}}
    return(probs)
  }

# But how do the samples compare to each other on the first 5 PCs
# (85% of observed variability)?
group.mem.probs(clay_pc1to7[3:5], clay_pc1to7$Geography_2, unique(clay_pc1to7$Geography_2))

```

```

# How about using some elements that show good separation between the groups?
group.mem.probs(clay_pcaready[, c("Ni", "Cs")], clay_pc1to7$Geography_2,
               unique(clay_pc1to7$Geography_2))

# In both cases, there is a marked lack of clear group separation in statistical space for
# samples in both groups. That is, there are samples defined as North that have a higher
# probability of grouping with the Southerly sherds and vice versa.
# To a certain degree, this is expected - this is an experimental analysis looking within a
# single river valley, and indeed there is not statistically significant separation between
# the groups as a result.
# Nevertheless, it is instructive that chemical differences do appear as one moves from the
# northeast to the southwest in the CIRV, conforming to geologic patterns of exposing parent
# material of older ages. As a result, an argument can be made that pottery would likely
# follow this patterning based on raw material availability.

## Exploratory cluster analysis

# Optimal number of clusters based on the elbow method using the total within sum of squares
fviz_nbclust(clay_pc1to7[3:9], kmeans, method = "wss")

clay_dist <- hclust(dist(clay_pc1to7[3:9]))

View(clay_pc1to7)

# Create dendrogram object
clay_dend_df_com <- as.dendrogram(clay_dist)

# Plot dendrogram object to look for good cut-off heights - 2.5 seems to be a good height
plot(clay_dend_df_com, nodePar = list(lab.cex = 0.15, pch = NA))

dend_2.5 <- color_branches(clay_dend_df_com, h = 1.950)
plot(dend_2.5, cex.axis = 0.75, cex.lab = 0.75, nodePar = list(lab.cex = .85, pch = NA))

```

Assignment of ceramic samples into geochemical compositional groups

The lengthy code chunk below is a linear sequence of unsupervised learning based statistical analysis of CIRV ceramic samples. The sequence below was cross referenced against MURRAP GAUSS routines, a standard statistical suite in the analysis of geochemical data in archaeology.

```

##' Analysis of ceramic LA-ICP-MS data

library(tidyverse)
library(infer)
library(broom)
library(stringr)
library(plotly)
library(rebus)
library(xlsx)
library(readxl)
library(plotly)

```

```

library(ggpubr)
library(cluster)
library(dendextend)
library(factoextra)
library(stats)
library(ICSNP)
library(shiny)
library(shinydashboard)
library(ggsci)

##### Data Import and Cleaning #####
samps <- read_csv("Upton_results_samples_shell_corrected_August_21_2018.csv")

# Remove samples that hit shell to the point of being unusable or four samples
# that were victim to a chamber leakage issue on 2017-Oct-06
removes <- str_detect(tolower(samps$Sample), "remove")
samples <- samps[!removes,]
rm_samps <- samps[removes,]

# Validate removed samples
rm_samps[,c(1:2)]

# Pull out clay samples (we'll add them back in later on)
clay_rows <- str_detect(tolower(samples$Sample), "c[:digit:][:digit:]")
clay_samps <- samples[clay_rows,]
samples <- samples[!clay_rows,]

# Clean up clay sample names
clay_samps$Sample <- str_replace(clay_samps$Sample, pattern = "_1" %R% END, "")

# Add clay i.d.'s to a separate column
clay_samps <- clay_samps %>%
  mutate(id = parse_number(clay$Sample)) %>%
  arrange(Sample)

##### Add features to ceramic samples #####
# Extract sample unique sherd i.d. number
# First remove the run information from sample names
samples$Sample <- str_replace(samples$Sample, pattern = "_1" %R% END, "")
samples$Sample <- str_replace_all(samples$Sample, c("_run[:digit:][:digit:]" = "",
  "_run[:digit:]" = "",
  "_" = "",
  "_run[:digit:]" = "",
  "run1" = "",
  "_r" = "",
  " run 1" = "",
  "_" = " "))

# Now extract the sample i.d.'s to a separate column
samples <- samples %>%
  mutate(id = parse_number(samples$Sample))

```

```

# Read in contextual data for the ceramic samples
ceramic_features_by_id <- read_xlsx(path = "ceramic features.xlsx", sheet = 1)
ceramic_features_by_site <- read_xlsx(path = "ceramic features.xlsx", sheet = 2)

# Join ceramic features to sample data
samples <- left_join(samples, ceramic_features_by_id)
samples <- left_join(samples, ceramic_features_by_site)

# Number of sherds by site and by vessel type
samples %>%
  group_by(Site, Vessel_Class) %>%
  summarise(num = n()) # %>%
  # write_csv("Number of sherds by site and by vessel type.csv")

# Number of sherds by site and by cultural group
samples %>%
  group_by(Site, Cultural_Group) %>%
  summarize(num = n())

# Check for any linear relationships between Calcium and the other elements
# Looks like there are some significant at a 0.05 alpha, but there is a significant
# amount of heteroscedasticity and residual variation in all but Sr, which
# expectedly does highly correlate with Ca
summary(lm(Ca ~ ., data = samples[,3:length(samples)]))

# Plotting to show how strong the linear relationships are for some elements
p <- ggplot(samples, aes(x = Sr, y = Ca)) + geom_smooth() + geom_point()
#ggplotly(p)

# Remove problem elements. Some elements are known to be unreliably measured using the
# ICP-MS at the EAF. Following Golitko (2010), these include the following elements.
problem_elements <- c("P", "Sr", "Ba", "Ca", "Hf", "As", "Cl")

# Other elements such as Ca and Sr are affected by shell tempering. Want to drop those
# as well.

# Overall these are the Elements retained - 44 in all.
elems_retained <- c("Al", "B", "Be", "Ce", "Co", "Cr", "Cs", "Dy", "Er", "Eu", "FeO",
  "Gd", "Ho", "In", "K", "La", "Li", "Lu", "Mg", "MnO", "Mo", "Na", "Nb",
  "Nd", "Ni", "Pb", "Pr", "Rb", "Sc", "Si", "Sm", "Sn", "Ta", "Tb", "Th", "T
i",
  "Tm", "U", "V", "W", "Y", "Yb", "Zn", "Zr")

ceramic.names.use <- names(samples)[(names(samples) %in% elems_retained)]
#length(ceramic.names.use) == length(elems_retained) # check that all elements are retained
samples_good <- samples %>% select(ceramic.names.use)

# Check to ensure the elements were removed are supposed to be removed
anti_join(data.frame(names(samples)),
  data.frame(names(samples_good)), by = c("names.samples." = "names.samples_good."))

# Need to drop the "O" for oxide after elements measured as %oxide composition since they
# have already been converted to ppm

```

```

names(samples_good) <- str_remove(names(samples_good), "0")

# Bind sample id and other data to the logged chemical concentrations
sample_pcaready <- bind_cols(samples[,c(1:2, 71:80)], samples_good)

# Some ceramic samples were run on an older ICP-MS machine during an initial pilot study.
# I need to tease these out pending quality control from Laure Dussubieux, a chemist at the
# Field Museum.
sample_old_machine <- sample_pcaready %>% filter(Date < 2016)
sample_new_pcaready <- sample_pcaready %>% filter(Date > 2016)

##### End of data cleaning, beginning of statistical analysis #####

# First step is to take the log base 10 of all samples to account for scalar differences
# in the magnitude of chemical compositions across the elements, from major to minor to trace
sample_new_pcaready[,13:56] <- log10(sample_new_pcaready[,13:56])

##### PCA #####

# Exploring PCA
sample_pca <- sample_new_pcaready %>%
  nest() %>%
  mutate(pca = map(data, ~ prcomp(.x %>% select(Si:Th))),
         pca_aug = map2(pca, data, ~augment(.x, data = .y)))

# Check variance explained by each model
var_exp_sample <- sample_pca %>%
  unnest(pca_aug) %>%
  summarize_at(.vars = vars(contains("PC")), .funs = funs(var)) %>%
  gather(key = pc, value = variance) %>%
  mutate(var_exp = variance/sum(variance),
         cum_var_exp = cumsum(var_exp),
         pc = str_replace(pc, ".fitted", ""))

# Check eigen values
get_eigenvalue(prcomp(sample_new_pcaready %>% select(Si:Th)))

# Looks like we need to retain the first 12 PC's to hit 90% of the data's variability
# Graphing this out might help
var_exp_sample %>%
  rename(`Variance Explained` = var_exp,
         `Cumulative Variance Explained` = cum_var_exp) %>%
  gather(key = key, value = value,
         `Variance Explained`:`Cumulative Variance Explained`) %>%
  mutate(pc = str_replace(pc, "PC", "")) %>%
  mutate(pc = as.numeric(pc)) %>%
  ggplot(aes(reorder(pc, sort(as.numeric(as.character(pc))))), value, group = key)) +
  geom_point() +
  geom_line() +
  facet_wrap(~key, scales = "free_y") +
  theme_bw() +
  lims(y = c(0, 1)) +
  labs(y = "Variance", x = "",

```

```

    title = "Variance explained by each principal component")

# Check number of PCs to retain to reach 90% of the variability in the original dataset
var_exp_sample %>% filter(cum_var_exp < 0.909) # Need to retain the first 12 PCs.
# 12 PCs is much less than 44 elements

# Plot the first two PCs with Geography_2 as group separation
geo2_pc1pc2 <- sample_pca %>%
  mutate(
    pca_graph = map2(
      .x = pca,
      .y = data,
      ~ autoplot(.x, loadings = TRUE, loadings.label = TRUE,
        loadings.label.repel = TRUE,
        loadings.label.colour = "black",
        loadings.colour = "gray45",
        loadings.label.alpha = 0.5,
        loadings.label.size = 3,
        #Loadings.Label.hjust = 1.1,
        frame = TRUE,
        frame.type = "norm",
        data = .y,
        colour = "Geography_2",
        shape = "Geography_2",
        frame.level = .9,
        frame.alpha = 0.001,
        size = 2) +
      theme_bw() +
      #geom_text(label = .y$Sample) +
      labs(x = "Principal Component 1",
        y = "Principal Component 2",
        title = "First two principal components of PCA on CIRV Ceramic dataset")
    )
  ) %>%
  pull(pca_graph)

geo2_pc1pc2[[1]] + scale_fill_manual(values = c("black","black")) +
  scale_color_manual(values = c("black","black","black")) +
  scale_shape_manual(values=c(18, 2))

# This shows significant overlap but a general trend that follows the clay:
# in general there is less elemental enrichment in clay resources in the
# southern portion of the CIRV compared to the northern part with the
# north-south line of demarcation being the Spoon-Illinois River confluence
# (clay along the Spoon is included in the north)

# Check the first two PCs with Sites as group separation
site_pc1pc2 <- sample_pca %>%
  mutate(
    pca_graph = map2(
      .x = pca,
      .y = data,
      ~ autoplot(.x, loadings = TRUE, loadings.label = TRUE,

```

```

    #Loadings.Label.repel = TRUE,
    loadings.label.colour = "black",
    loadings.colour = "gray85",
    loadings.label.alpha = 0.5,
    loadings.label.size = 3,
    loadings.label.hjust = 1.1,
    frame = TRUE,
    frame.type = "norm",
    data = .y,
    colour = "Site",
    shape = "Geography_2",
    frame.level = .9,
    frame.alpha = 0.001,
    size = 2) +
  theme_bw() +
  #geom_text(Label = .y$Sample) +
  labs(x = "Principal Component 1",
       y = "Principal Component 2",
       title = "First two principal components of PCA on CIRV Ceramic dataset")
)
) %>%
pull(pca_graph)

```

Interact with the chart above

```

ggplotly(site_pc1pc2[[1]]) # plotly drops the stat_ellipse frames for some reason
# This is a challenge to interpret, but it doesn't seem as though there is meaningful
# patterning when considering the different sites on PC1-PC2 aside from some outliers in
# Walsh/Crable.

```

Check the first two PCs with Vessel Class as group separation

```

vessel_pc1pc2 <- sample_pca %>%
  mutate(
    pca_graph = map2(
      .x = pca,
      .y = data,
      ~ autoplot(.x, loadings = TRUE, loadings.label = TRUE,
                 #Loadings.Label.repel = TRUE,
                 loadings.label.colour = "black",
                 loadings.colour = "gray85",
                 loadings.label.alpha = 0.5,
                 loadings.label.size = 3,
                 loadings.label.hjust = 1.1,
                 frame = TRUE,
                 frame.type = "norm",
                 data = .y,
                 colour = "Vessel_Class",
                 shape = "Vessel_Class",
                 frame.level = .9,
                 frame.alpha = 0.001,
                 size = 2) +
                 theme_bw() +
                 #geom_text(Label = .y$Sample) +
                 labs(x = "Principal Component 1",

```

```

      y = "Principal Component 2",
      title = "First two principal components of PCA on CIRV Ceramic dataset")
    )
  ) %>%
  pull(pca_graph)

ggplotly(vessel_pc1pc2[[1]])
# The vessel graph is interesting. At first glance, it doesn't seem as though there is much
# in the way of separation by vessel class, but there appears to be some nuances to that
# upon further consideration. There are some plates that are low on both PC1 and PC2 axes
# as well as jars that are significantly more enriched on PC1

# How about separation by time?
time_pc1pc2 <- sample_pca %>%
  mutate(
    pca_graph = map2(
      .x = pca,
      .y = data,
      ~ autoplot(.x, loadings = TRUE, loadings.label = TRUE,
        #Loadings.Label.repel = TRUE,
        loadings.label.colour = "black",
        loadings.colour = "gray85",
        loadings.label.alpha = 0.5,
        loadings.label.size = 3,
        loadings.label.hjust = 1.1,
        frame = TRUE,
        frame.type = "norm",
        data = .y,
        colour = "Time",
        shape = "Time",
        frame.level = .9,
        frame.alpha = 0.001,
        size = 2) +
      theme_bw() +
      #geom_text(label = .y$Sample) +
      labs(x = "Principal Component 1",
        y = "Principal Component 2",
        title = "First two principal components of PCA on CIRV Ceramic dataset")
    )
  ) %>%
  pull(pca_graph)

ggplotly(time_pc1pc2[[1]])
# Again, this appears similar to the prior PC biplot separated by vessel class - there is
# no general trend of group separation but some interesting insights when considering
# outliers.

# Perhaps Oneota presence may be more revealing
oneota_pc1pc2 <- sample_pca %>%
  mutate(
    pca_graph = map2(
      .x = pca,
      .y = data,

```

```

~ autoplot(.x, loadings = TRUE, loadings.label = TRUE,
  #Loadings.Label.repel = TRUE,
  loadings.label.colour = "black",
  loadings.colour = "gray85",
  loadings.label.alpha = 0.5,
  loadings.label.size = 3,
  loadings.label.hjust = 1.1,
  frame = TRUE,
  frame.type = "norm",
  data = .y,
  colour = "Oneota_Present",
  shape = "Oneota_Present",
  frame.level = .9,
  frame.alpha = 0.001,
  size = 2) +
  theme_bw() +
  #geom_text(Label = .y$Sample) +
  labs(x = "Principal Component 1",
    y = "Principal Component 2",
    title = "First two principal components of PCA on CIRV Ceramic dataset")
)
) %>%
pull(pca_graph)

```

```
ggplotly(oneota_pc1pc2[[1]])
```

```

# I certainly can't see any meaningful trends here. This suggests that Oneota and
# Mississippian otters are almost undoubtedly using similar (or the same) clay.
# However, more work is needed to confirm this hypothesis.

```

```
# Does temper percent matter?
```

```
tempperc_pc1pc2 <- sample_pca %>%
```

```

mutate(
  pca_graph = map2(
    .x = pca,
    .y = data,
    ~ autoplot(.x, loadings = TRUE, loadings.label = TRUE,
      #Loadings.Label.repel = TRUE,
      loadings.label.colour = "black",
      loadings.colour = "gray85",
      loadings.label.alpha = 0.5,
      loadings.label.size = 3,
      loadings.label.hjust = 1.1,
      frame = TRUE,
      frame.type = "norm",
      data = .y,
      colour = "Temper_Perc",
      shape = "Geography_2",
      frame.level = .9,
      frame.alpha = 0.001,
      size = 2) +
      theme_bw() +
      #geom_text(Label = .y$Sample) +
      labs(x = "Principal Component 1",

```

```

        y = "Principal Component 2",
        title = "First two principal components of PCA on CIRV Ceramic dataset")
    )
) %>%
pull(pca_graph)

ggplotly(tempperc_pc1pc2[[1]])
# Can't really discern anything here

# Does temper size matter?
tempsize_pc1pc2 <- sample_pca %>%
mutate(
  pca_graph = map2(
    .x = pca,
    .y = data,
    ~ autoplot(.x, loadings = TRUE, loadings.label = TRUE,
               #Loadings.Label.repel = TRUE,
               loadings.label.colour = "black",
               loadings.colour = "gray85",
               loadings.label.alpha = 0.5,
               loadings.label.size = 3,
               loadings.label.hjust = 1.1,
               frame = TRUE,
               frame.type = "norm",
               data = .y,
               colour = "Temper_Size",
               shape = "Geography_2",
               frame.level = .9,
               frame.alpha = 0.001,
               size = 2) +
    theme_bw() +
    #geom_text(Label = .y$Sample) +
    labs(x = "Principal Component 1",
         y = "Principal Component 2",
         title = "First two principal components of PCA on CIRV Ceramic dataset")
  )
) %>%
pull(pca_graph)

ggplotly(tempsize_pc1pc2[[1]])
# Interestingly, it appears that the smallest temper size only appears in
# the northern part of the valley.
# That might suggest that there is either a preference for smaller temper grains there
# or it is a response to the clay available in the north.

# Finally, Let's check Cultural Group
culture_pc1pc2 <- sample_pca %>%
mutate(
  pca_graph = map2(
    .x = pca,
    .y = data,
    ~ autoplot(.x, loadings = TRUE, loadings.label = TRUE,
               #Loadings.Label.repel = TRUE,

```

```

        loadings.label.colour = "black",
        loadings.colour = "gray85",
        loadings.label.alpha = 0.5,
        loadings.label.size = 3,
        loadings.label.hjust = 1.1,
        frame = TRUE,
        frame.type = "norm",
        data = .y,
        colour = "Cultural_Group",
        shape = "Cultural_Group",
        frame.level = .9,
        frame.alpha = 0.001,
        size = 2) +
  theme_bw() +
  #geom_text(Label = .y$Sample) +
  labs(x = "Principal Component 1",
       y = "Principal Component 2",
       title = "First two principal components of PCA on CIRV Ceramic dataset")
)
) %>%
pull(pca_graph)

ggplotly(culture_pc1pc2[[1]])
# Very little to no discernible patterning here. This again indicates that both cultural
# groups are likely to be using the same clays.

# Based on the initial inspection of PCs 1 and 2, it looks like three elements in particular
# are driving some of the group separation (subtle as it is): Mo, Mn, and Si
# Let's plot those three elements in a 3D scatter plot
Mo_Mn_Si <- plot_ly(sample_new_pcaready, x = ~Mo, y = ~Mn, z = ~Si, color = ~Geography_2)

# Explore Samples by date
ggplotly(ggplot(sample_new_pcaready, aes(x = Mo, y = Mg, color = Date)) +
  stat_ellipse(aes(color = Geography_2)) + geom_text(aes(label = Date), size = 2))

# All in all, only a general trend of the north-south distinction holds when considering
# prior information on PC1-PC2 biplots. That distinction is marked by significant overlap.
# We'll consider that when running group membership probabilities. But first, it's
# necessary to explore how a variety of statistical methods will group the data. We'll
# append that group information to our PC list such that we can consider both prior
# information and statistical information in groups before moving on to group refinement.

##### Cluster Analysis #####

##### Hierarchical Cluster Analysis #####

# Now that I have a sense of the structure of the ceramic data set based on PCA, the next
# step in compositional analysis is to see how the groups defined from prior
# information compare to groups constructed using statistical clustering methods such
# as HCA, kmeans, and kmedoids

# Let's start with some tree-based methods (aka Hierarchical cluster analysis or HCA)

```

```

# We'll use agglomerative methods here (bottom up) as opposed to divisive methods (top down)

# Prep the dataset
# Set rownames to aid in interpretations of dendrograms and other plots
rownames(sample_new_pcaready) <- sample_new_pcaready$Sample

# Drop the prior known information features
sample_new_distready <- sample_new_pcaready %>% select(c(-1:-12))

# First make a dissimilarity matrix based on Euclidean distance
euc_dist_ceramics <- dist(sample_new_distready, method = "euclidean")

# We can check agglomerative coefficients with agnes to see which method(s) might
# work best with the ceramic compositional dataset
clustmethods <- c("average", "single", "complete", "ward")
names(clustmethods) <- c("average", "single", "complete", "ward")

# function to compute agglomerative coefficient
ac <- function(x) {
  agnes(euc_dist_ceramics, method = x)$ac
}

map_dbl(clustmethods, ac)

# Looks like complete and Ward linkage methods will work best. We'll run those

# Hierarchical clustering using Ward's Linkage
wardhc1 <- hclust(euc_dist_ceramics, method = "ward.D")
wardhc1_dend <- as.dendrogram(wardhc1) # create dendrogram object

# Plot Ward dendrogram
plot(wardhc1_dend, nodePar = list(lab.cex = 0.15, pch = NA))
# Looks like there are three well defined clusters at a height of 20.
# We can color the dendrogram at that height
wardhc1_dend_20 <- color_branches(wardhc1_dend, h = 20)
plot(wardhc1_dend_20, cex.axis = 0.75, cex.lab = 0.75,
     nodePar = list(lab.cex = 0.15, pch = NA))

# This looks like a good hypothetical groupings to add to our original dataset
# We'll add all statistical clusters to a dataset sample_new_stat_clusters
ward_dist_groups <- cutree(wardhc1_dend_20, h = 20)
table(ward_dist_groups) # How many samples are in each cluster?

sample_new_stat_clusters <- sample_new_pcaready %>%
  select(Sample) %>%
  mutate(Ward_HCA_Cluster = ward_dist_groups)

# Visualize the clusters from HCA using Ward's Linkage
fviz_cluster(list(data = sample_new_distready, cluster = ward_dist_groups))

# Complete Linkage also has a high agglomerative coefficient, let's model it
completehc1 <- hclust(euc_dist_ceramics, method = "complete")
completehc1_dend <- as.dendrogram(completehc1)

```

```

# Plot Complete Linkage dendrogram cut at 2.4, which results in 6 clusters (3 main and 3 minor
)
completehc1_dend_2.4 <- color_branches(completehc1_dend, h = 2.4)
plot(completehc1_dend_2.4, cex.axis = 0.75, cex.lab = 0.75,
     nodePar = list(lab.cex = 0.15, pch = NA))
complete_dist_groups <- cutree(completehc1_dend, h = 2.4)
table(complete_dist_groups)
sample_new_stat_clusters <- sample_new_stat_clusters %>%
  mutate(Complete_HCA_Cluster = complete_dist_groups)

# Visualize the clusters from HCA using Complete Linkage
fviz_cluster(list(data = sample_new_distready, cluster = complete_dist_groups))

# Let's compare the Ward's and Complete Linkage dendrograms with a tanglegram
# (this is very resource intensive, so I'm commenting it out)
# tanglegram(wardhc1_dend, completehc1_dend)

# Now let's see how these HCA groups correspond to other clustering methods

##### K-means Cluster Analysis #####
# First, it's a good idea to use a few methods to assess the number of clusters to model
# Elbow Method
fviz_nbclust(sample_new_distready, kmeans, method = "wss") # 3-8 optimal clusters;
# 3-4 Looks good

# Silhouette Method
fviz_nbclust(sample_new_distready, kmeans, method = "silhouette") # 3 optimal clusters
# Gap Stat
#fviz_nbclust(sample_new_distready, kmeans, method = "gap_stat") # 1 optimal cluster

# Based on the optimal cluster methods, it looks like we should run kmeans twice, once with
# 3 clusters and once with 4 clusters

# 3 Cluster K-means
k3 <- kmeans(sample_new_distready,
             centers = 3, # number of clusters
             nstart = 50, # number of random initial configurations
             # out of which the best one is chosen
             iter.max = 500) # number of allowable iterations allowed

# Visualize 3 cluster kmeans
fviz_cluster(k3, data = sample_new_distready)

# Assign to clustering assignments data frame
sample_new_stat_clusters <- sample_new_stat_clusters %>%
  mutate(Kmeans_3 = k3$cluster)

# 4 Cluster K-means
k4 <- kmeans(sample_new_distready, centers = 4, nstart = 50, iter.max = 500)

# Visualize 4 cluster kmeans
fviz_cluster(k4, data = sample_new_distready)

```

```

# Assign to clustering assignments data frame
sample_new_stat_clusters <- sample_new_stat_clusters %>%
  mutate(Kmeans_4 = k4$cluster)

##### K-medoids Cluster Analysis #####

# For k-medoids, we'll be using the pam function from the cluster package. pam stands for
# "partitioning around medoids"

# As with k-means, it's a good idea to use a few methods to assess the number of clusters
# to model
# Elbow Method
fviz_nbclust(sample_new_distready, pam, method = "wss") # 5 Looks optimal here
# Silhouette Method
fviz_nbclust(sample_new_distready, pam, method = "silhouette") # 2 optimal clusters
# Gap Stat
#fviz_nbclust(sample_new_distready, pam, method = "gap_stat") # 1 optimal cluster

# We'll run two clusters - one with 2 and one with 5
# 2 cluster K-medoids
pam2 <- pam(sample_new_distready, 2)

# Plot 2 cluster k-medoids
fviz_cluster(pam2, data = sample_new_distready)

# 5 cluster K-medoids
pam5 <- pam(sample_new_distready, 5)

# Plot 5 cluster k-medoids
fviz_cluster(pam5, data = sample_new_distready)

# Assign k-medoids results to clustering assignments data frame
sample_new_stat_clusters <- sample_new_stat_clusters %>%
  mutate(Kmediods_2 = pam2$clustering,
         Kmediods_5 = pam5$clustering)

# One last exploratory metric would be to take the most often occurring group assignment
# number, the mode
# Little function to calculate the mode
Mode <- function(x) {
  ux <- unique(x)
  ux[which.max(tabulate(match(x, ux)))]
}

# Apply this row-wise to the data
mode_assignment <- apply(sample_new_stat_clusters, 1, Mode)

#####_____Begin Mahalanobis distance and membership assignments_____###

# First, create a data frame of the first 12 PC's, which account for 90% of the variability
# in the elemental data set. This will allow group membership probability assessments with a
# group as small as 14 (or perhaps 13)

```

```

pc1to12 <- sample_pca[['pca_aug']][[1]] %>%
  select(.fittedPC1, .fittedPC2, .fittedPC3, .fittedPC4, .fittedPC5, .fittedPC6, .fittedPC7,
        .fittedPC8, .fittedPC9, .fittedPC10, .fittedPC11, .fittedPC12)

# This function written by Matt Peebles allows for calculating group membership
# probabilities by chemical compositional distance using Mahalanobis distances and
# Hotellings T^2 statistic
# This is identical to the procedure used in MURRAP GAUSS routines for the same purpose
# and has been cross referenced against that routine to ensure accuracy for data
# presented in this analysis
group.mem.probs <- function(x2.l,attr1.grp,grps) {

  # x2.l = transformed element data
  # attr1 = group designation by sample
  # grps <- vector of groups to evaluate

  probs <- list()
  for (m in 1:length(grps)) {
    x <- x2.l[which(attr1.grp == grps[m]),]
    probs[[m]] <- matrix(0,nrow(x),length(grps))
    colnames(probs[[m]]) <- grps
    rownames(probs[[m]]) <- rownames(x)

    grps2 <- grps[-m]

    p.val <- NULL
    for (i in 1:nrow(x)) {p.val[i] <- HotellingsT2(x[i,], x[-i,])$p.value}
    probs[[m]][,m] <- round(p.val,5)*100

    for (j in 1:length(grps2)) {
      p.val2 <- NULL
      for (i in 1:nrow(x)) {p.val2[i] <- HotellingsT2(x[i,],
                                                    x2.l[which(attr1.grp == grps2[j]),])$p.v
      alue}
      probs[[m]][,which(grps == grps2[j])] <- round(p.val2, 5)*100}}
    return(probs)
  }

##### WARD HCA #####
# Calculate group membership probabilities for the HCA Ward group assignments based on PCA data
ward_group_mem <- group.mem.probs(pc1to12, sample_new_stat_clusters$Ward_HCA_Cluster,
                                unique(sample_new_stat_clusters$Ward_HCA_Cluster))

# Create list of data that is grouped the same as the group probability list
ward_samp_list <- split(sample_new_stat_clusters[, c(1:2)],
                       f = sample_new_stat_clusters$Ward_HCA_Cluster)

# Convert the list of matrices of group membership probabilities to data frames
# and bind rows into one data frame
ward_group_mem <- map(ward_group_mem, as.data.frame) %>% bind_rows()

# Convert the list of matrices of sample names to data frames and bind into one data frame

```

```

ward_samp_df <- map(ward_samp_list, as.data.frame) %>% bind_rows()

# Bind to initial sample id and group assignment from Ward HCA
# and convert to data frame for easier handling
ward_group_mem <- as.data.frame(bind_cols(ward_group_mem, ward_samp_df))

# New column of membership probability for initially assigned group
ward_group_mem$assigned_val <- ward_group_mem[1:3][cbind(seq_len(nrow(ward_group_mem)),
                                                         ward_group_mem$Ward_HCA_Cluster)]

# Set the initial group assignment value to zero to allow for comparisons
ward_group_mem[cbind(seq_len(nrow(ward_group_mem)), ward_group_mem$Ward_HCA_Cluster)] <- 0

# The heuristic I am using to assess group membership asks whether or not the probability of
# group membership in the original assigned cluster is greater than 10% and that the
# probability of membership in any other cluster is less than 10%. This follows
# Peeples (2010) in part and is a fairly conservative threshold.
ward_group_mem %>%
  # mutate(out_group_sum = `1` + `2` + `3`) %>%
  mutate(assigned_val = as.numeric(assigned_val)) %>%
  mutate(new_assign = ifelse(assigned_val > 10 & (`1` < 10 & `2` < 10 & `3` < 10),
                             Ward_HCA_Cluster, "unassigned")) %>%
# filter(new_assign != "unassigned")
  summarize(perc_unassigned = sum(new_assign == "unassigned")/n() * 100)
# Applying the heuristic to the initial group assignments for the Ward HCA clusters results
# in an 77.16% unassignment rate. This is quite high. Let's check other methods to
# see how they fair.

##### Kmeans 4 #####
# Group probabilities for the kmeans 4 cluster solution on transformed PCA data
kmean4_group_mem <- group.mem.probs(pc1to12, sample_new_stat_clusters$Kmeans_4,
                                   unique(sample_new_stat_clusters$Kmeans_4))

# Create list of data that is grouped the same as the group probability list
kmean4_samp_list <- split(sample_new_stat_clusters[, c("Sample", "Kmeans_4")],
                          f = sample_new_stat_clusters$Kmeans_4)

# Reorder list to match the group membership probs
kmean4_samp_list <- list(kmean4_samp_list$`1`, kmean4_samp_list$`3`, kmean4_samp_list$`4`,
                       kmean4_samp_list$`2`)

# Convert the matrices of group membership probabilities to data frames and bind
# rows into one data frame
kmean4_group_mem <- map(kmean4_group_mem, as.data.frame) %>% bind_rows()

# Convert the list of matrices of sample names to data frames and bind into one data frame
kmean4_samp_df <- map(kmean4_samp_list, as.data.frame) %>% bind_rows()

# Bind to initial sample id and group assignment from Kmean 4
# and convert to data frame for easier handling
kmean4_group_mem <- as.data.frame(bind_cols(kmean4_group_mem, kmean4_samp_df))

```

```

# Convert to tibble data frame for easier handling
kmean4_group_mem <- as.data.frame(kmean4_group_mem)

# New column of membership probability for initially assigned group
kmean4_group_mem$assigned_val <- kmean4_group_mem[1:4][cbind(seq_len(nrow(kmean4_group_mem)),
                                                             kmean4_group_mem$Kmeans_4)]

# Set the initial group assignment value to zero to allow for comparisons
kmean4_group_mem[cbind(seq_len(nrow(kmean4_group_mem)), kmean4_group_mem$Kmeans_4)] <- 0

# Assess membership probabilities using my heuristic
kmean4_group_mem %>%
  mutate(assigned_val = as.numeric(assigned_val)) %>%
  mutate(new_assign = ifelse(assigned_val > 10 & (`1` < 10 & `2` < 10 & `3` < 10 & `4` < 10),
                             Kmeans_4, "unassigned")) %>%
  # filter(new_assign != "unassigned")
  summarize(perc_unassigned = sum(new_assign == "unassigned")/n() * 100)
# At an 99.26%, it doesn't seem like kmeans 4 group clusters faired much better than Ward HCA
# In fact, this did not do well at all

##### Kmedoids (pam) 5 #####
# Group probabilities for the kmedoids (pam) 5 cluster solution on PC's 1 to 12
# (90% of variability)
kmed5_group_mem <- group.mem.probs(pc1to12, sample_new_stat_clusters$Kmediods_5,
                                  unique(sample_new_stat_clusters$Kmediods_5))

# Create list of data that is grouped the same as the group probability list
kmed5_samp_list <- split(sample_new_stat_clusters[, c("Sample", "Kmediods_5")],
                        f = sample_new_stat_clusters$Kmediods_5)

# Convert the matrices of group membership probabilities to data frames and bind
# rows into one data frame
kmed5_group_mem <- map(kmed5_group_mem, as.data.frame) %>% bind_rows()

# Convert the list of matrices of sample names to data frames and bind into one data frame
kmed5_samp_df <- map(kmed5_samp_list, as.data.frame) %>% bind_rows()

# Bind to initial sample id and group assignment from Kmed 5
# and convert to data frame for easier handling
kmed5_group_mem <- as.data.frame(bind_cols(kmed5_group_mem, kmed5_samp_df))

# New column of membership probability for initially assigned group
kmed5_group_mem$assigned_val <- kmed5_group_mem[1:5][cbind(seq_len(nrow(kmed5_group_mem)),
                                                             kmed5_group_mem$Kmediods_5)]

# Set the initial group assignment value to zero to allow for comparisons
kmed5_group_mem[cbind(seq_len(nrow(kmed5_group_mem)), kmed5_group_mem$Kmediods_5)] <- 0

# Assess membership probabilities using my heuristic
kmed5_group_mem %>%
  mutate(new_assign = ifelse(assigned_val > 10 & `1` < 10 & `2` < 10 & `3` < 10 &
                             `4` < 10 & `5` < 10,

```

```

      Kmedioids_5, "unassigned")) %>%
# filter(new_assign != "unassigned")
summarize(perc_unassigned = sum(new_assign == "unassigned")/n() * 100)
# Ouch, at 95.58% unassigned using the heuristic criteria, this doesn't hold up

##### Kmedoids (pam) 2 #####
# Group probabilities for the kmedoids (pam) 2 cluster solution on PC's 1 to 12
# (90% of variability)
kmed2_group_mem <- group.mem.probs(pc1to12, sample_new_stat_clusters$Kmedioids_2,
                                unique(sample_new_stat_clusters$Kmedioids_2))

# Create list of data that is grouped the same as the group probability list
kmed2_samp_list <- split(sample_new_stat_clusters[, c("Sample", "Kmedioids_2")],
                        f = sample_new_stat_clusters$Kmedioids_2)

# Convert the matrices of group membership probabilities to data frames and bind
# rows into one data frame
kmed2_group_mem <- map(kmed2_group_mem, as.data.frame) %>% bind_rows()

# Convert the list of matrices of sample names to data frames and bind into one data frame
kmed2_samp_df <- map(kmed2_samp_list, as.data.frame) %>% bind_rows()

# Bind to initial sample id and group assignment from Kmed 5
# and convert to data frame for easier handling
kmed2_group_mem <- as.data.frame(bind_cols(kmed2_group_mem, kmed2_samp_df))

# New column of membership probability for initially assigned group
kmed2_group_mem$assigned_val <- kmed2_group_mem[1:2][cbind(seq_len(nrow(kmed2_group_mem)),
                                                         kmed2_group_mem$Kmedioids_2)]

# Set the initial group assignment value to zero to allow for comparisons
kmed2_group_mem[cbind(seq_len(nrow(kmed2_group_mem)), kmed2_group_mem$Kmedioids_2)] <- 0

# Assess membership probabilities using my heuristic
kmed2_group_mem %>%
  mutate(new_assign = ifelse(assigned_val > 10 & `1` < 10 & `2` < 10,
                             Kmedioids_2, "unassigned")) %>%
  # filter(assigned_val < `1` | assigned_val < `2`)
  summarize(perc_unassigned = sum(new_assign == "unassigned")/n() * 100)
# A 79.01% unassigned using the heuristic criteria is better, but still doesn't hold up

# Since none of these clustering methods were successful when held against Mahalanobis
# Distance, we'll drop them from the augmented PCA data
sample_pca[['pca_aug']][[1]] <- sample_pca[['pca_aug']][[1]] %>%
  select(-Kmeans_2:-Kmedioids_5)

##### Mahalanobis-first route #####
##### Core and Unassigned Group Assignments #####
# Another common method used for constructing core chemical compositional groups in
# archaeology is to initially treat the entire data set as one large group and iteratively
# removing samples with a membership probability of less than 1%. A Core group can thus
# be defined and sub-groups may be identified within the Core.

```

```

# Double the PC data so the group can be compared to itself
pc1to12_twice <- bind_rows(pc1to12, pc1to12)

# Double the stat cluster assignment data
sample_new_stat_clusters_twice <- bind_rows(sample_new_stat_clusters,
                                             sample_new_stat_clusters)

# Create vector of group assignments
one_two <- c(rep(1, 543), rep(2, 543))

# Bind group assignments to cluster data
sample_new_stat_clusters_twice <- cbind(sample_new_stat_clusters_twice, one_two)

# Group probabilities for the group as one data set on PC's 1 through 12
one_group_mem <- group.mem.probs(pc1to12_twice, sample_new_stat_clusters_twice$one_two,
                                 unique(sample_new_stat_clusters_twice$one_two))

# Create list of data that is grouped the same as the group probability list
one_samp_list <- split(sample_new_stat_clusters_twice[, c("Sample", "one_two")],
                      f = sample_new_stat_clusters_twice$one_two)

# Convert the matrices of group membership probabilities to data frames
# and bind rows into one data frame
one_group_mem <- map(one_group_mem, as.data.frame) %>% bind_rows()

# Convert the list of matrices of sample names to data frames and bind into one data frame
one_samp_df <- map(one_samp_list, as.data.frame) %>% bind_rows()

# Bind to initial sample id and group assignment from
# and convert to data frame for easier handling
one_group_mem <- as.data.frame(bind_cols(one_group_mem, one_samp_df))

# Create data frame of sample to retain after first iteration
iter1 <- one_group_mem %>%
  filter(one_two == 1) %>%
  filter(`1` > 1) %>%
  select(Sample)

# Create data frame of unassigned samples after first iteration
iter1_unassigned <- one_group_mem %>%
  filter(one_two == 1) %>%
  filter(`1` < 1) %>%
  select(Sample)

# Subset initial groups
one_group_mem1 <- one_group_mem %>%
  filter(Sample %in% iter1$Sample)

### Iteration two
# Bind samples list to PCA data, filter out the unassigned samples after iteration one
# and select PC data only for group membership probability calculation
pc1to12_twice_iter2 <- bind_cols(sample_new_stat_clusters_twice[, c("Sample", "one_two")],

```

```

        pc1to12_twice) %>%
        filter(Sample %in% iter1$Sample) %>%
        select(-Sample, -one_two)

# Prep the sample names and assignments for iteration 2
sample_new_stat_clusters_twice_iter2 <- sample_new_stat_clusters_twice[, c("Sample",
                                                                           "one_two")] %>%
        filter(Sample %in% iter1$Sample)

# Group probabilities for iteration 2 of the group as one data set on PC's 1 through 12
one_group_mem_iter_2 <- group.mem.probs(pc1to12_twice_iter2,
                                       sample_new_stat_clusters_twice_iter2$one_two,
                                       unique(sample_new_stat_clusters_twice_iter2$one_two))

# Create list of data that is grouped the same as the group probability list
one_samp_list_iter2 <- split(sample_new_stat_clusters_twice_iter2,
                             f = sample_new_stat_clusters_twice_iter2$one_two)

# Convert the matrices of group membership probabilities to data frames
# and bind rows into one data frame
one_group_mem_iter2 <- map(one_group_mem_iter_2, as.data.frame) %>% bind_rows()

# Convert the list of matrices of sample names to data frames and bind into one data frame
one_samp_df_iter2 <- map(one_samp_list_iter2, as.data.frame) %>% bind_rows()

# Bind to initial sample id and group assignment from
# and convert to data frame for easier handling
one_group_mem_iter2 <- as.data.frame(bind_cols(one_group_mem_iter2, one_samp_df_iter2))

# Create data frame of sample to retain after first interaction
iter2 <- one_group_mem_iter2 %>%
        filter(one_two == 1) %>%
        filter(`1` > 1) %>%
        select(Sample)

# Create data frame of unassigned samples after first interaction
iter2_unassigned <- one_group_mem_iter2 %>%
        filter(one_two == 1) %>%
        filter(`1` < 1) %>%
        select(Sample)

# Subset initial groups
one_group_mem2 <- one_group_mem_iter2 %>%
        filter(Sample %in% iter2$Sample)

### Iteration 3
# Bind samples list to PCA data, filter out the unassigned samples after iteration two
# and select PC data only for group membership probability calculation
pc1to12_twice_iter3 <- bind_cols(sample_new_stat_clusters_twice_iter2,
                                pc1to12_twice_iter2) %>%
        filter(Sample %in% iter2$Sample) %>%
        select(-Sample, -one_two)

```

```

# Prep the sample names and assignments for iteration 3
sample_new_stat_clusters_twice_iter3 <- sample_new_stat_clusters_twice_iter2 %>%
  filter(Sample %in% iter2$Sample)

# Group probabilities for iteration 3 of the group as one data set on PC's 1 through 12
one_group_mem_iter_3 <- group.mem.probs(pc1to12_twice_iter3,
  sample_new_stat_clusters_twice_iter3$one_two,
  unique(sample_new_stat_clusters_twice_iter3$one_two))

# Create list of data that is grouped the same as the group probability list
one_samp_list_iter3 <- split(sample_new_stat_clusters_twice_iter3,
  f = sample_new_stat_clusters_twice_iter3$one_two)

# Convert the matrices of group membership probabilities to data frames
# and bind rows into one data frame
one_group_mem_iter3 <- map(one_group_mem_iter_3, as.data.frame) %>% bind_rows()

# Convert the list of matrices of sample names to data frames and bind into one data frame
one_samp_df_iter3 <- map(one_samp_list_iter3, as.data.frame) %>% bind_rows()

# Bind to initial sample id and group assignment
# and convert to data frame for easier handling
one_group_mem_iter3 <- as.data.frame(bind_cols(one_group_mem_iter3, one_samp_df_iter3))

# Create data frame of sample to retain after third interaction
iter3 <- one_group_mem_iter3 %>%
  filter(one_two == 1) %>%
  filter(`1` > 1) %>%
  select(Sample)

# Create data frame of unassigned samples after third interaction
iter3_unassigned <- one_group_mem_iter3 %>%
  filter(one_two == 1) %>%
  filter(`1` < 1) %>%
  select(Sample)

# Subset initial groups
one_group_mem3 <- one_group_mem_iter3 %>%
  filter(Sample %in% iter3$Sample)

### Iteration 4
# Bind samples list to PCA data, filter out the unassigned samples after iteration three
# and select PC data only for group membership probability calculation
pc1to12_twice_iter4 <- bind_cols(sample_new_stat_clusters_twice_iter3,
  pc1to12_twice_iter3) %>%
  filter(Sample %in% iter3$Sample) %>%
  select(-Sample, -one_two)

# Prep the sample names and assignments for iteration 4
sample_new_stat_clusters_twice_iter4 <- sample_new_stat_clusters_twice_iter3 %>%
  filter(Sample %in% iter3$Sample)

```

```

# Group probabilities for iteration 4 of the group as one data set on PC's 1 through 12
one_group_mem_iter_4 <- group.mem.probs(pc1to12_twice_iter4,
                                       sample_new_stat_clusters_twice_iter4$one_two,
                                       unique(sample_new_stat_clusters_twice_iter4$one_two))

# Create list of data that is grouped the same as the group probability list
one_samp_list_iter4 <- split(sample_new_stat_clusters_twice_iter4,
                             f = sample_new_stat_clusters_twice_iter4$one_two)

# Convert the matrices of group membership probabilities to data frames
# and bind rows into one data frame
one_group_mem_iter4 <- map(one_group_mem_iter_4, as.data.frame) %>% bind_rows()

# Convert the list of matrices of sample names to data frames and bind into one data frame
one_samp_df_iter4 <- map(one_samp_list_iter4, as.data.frame) %>% bind_rows()

# Bind to initial sample id and group assignment
# and convert to data frame for easier handling
one_group_mem_iter4 <- as.data.frame(bind_cols(one_group_mem_iter4, one_samp_df_iter4))

# Create data frame of sample to retain after fourth iteration
iter4 <- one_group_mem_iter4 %>%
  filter(one_two == 1) %>%
  filter(`1` > 1) %>%
  select(Sample)

# Create data frame of unassigned samples after fourth iteration
iter4_unassigned <- one_group_mem_iter4 %>%
  filter(one_two == 1) %>%
  filter(`1` < 1) %>%
  select(Sample)

# Subset initial groups
one_group_mem4 <- one_group_mem_iter4 %>%
  filter(Sample %in% iter4$Sample)

### Iteration 5
# Bind samples list to PCA data, filter out the unassigned samples after iteration four
# and select PC data only for group membership probability calculation
pc1to12_twice_iter5 <- bind_cols(sample_new_stat_clusters_twice_iter4,
                                pc1to12_twice_iter4) %>%
  filter(Sample %in% iter4$Sample) %>%
  select(-Sample, -one_two)

# Prep the sample names and assignments for iteration 5
sample_new_stat_clusters_twice_iter5 <- sample_new_stat_clusters_twice_iter4 %>%
  filter(Sample %in% iter4$Sample)

# Group probabilities for iteration 5 of the group as one data set on PC's 1 through 12
one_group_mem_iter_5 <- group.mem.probs(pc1to12_twice_iter5,
                                       sample_new_stat_clusters_twice_iter5$one_two,
                                       unique(sample_new_stat_clusters_twice_iter5$one_two))

```

```

# Create list of data that is grouped the same as the group probability list
one_samp_list_iter5 <- split(sample_new_stat_clusters_twice_iter5,
                             f = sample_new_stat_clusters_twice_iter5$one_two)

# Convert the matrices of group membership probabilities to data frames
# and bind rows into one data frame
one_group_mem_iter5 <- map(one_group_mem_iter_5, as.data.frame) %>% bind_rows()

# Convert the list of matrices of sample names to data frames and bind into one data frame
one_samp_df_iter5 <- map(one_samp_list_iter5, as.data.frame) %>% bind_rows()

# Bind to initial sample id and group assignment
# and convert to data frame for easier handling
one_group_mem_iter5 <- as.data.frame(bind_cols(one_group_mem_iter5, one_samp_df_iter5))

# Create data frame of sample to retain after fifth iteration
iter5 <- one_group_mem_iter5 %>%
  filter(one_two == 1) %>%
  filter(`1` > 1) %>%
  select(Sample)

# Create data frame of unassigned samples after fifth iteration
iter5_unassigned <- one_group_mem_iter5 %>%
  filter(one_two == 1) %>%
  filter(`1` < 1) %>%
  select(Sample)

# Subset initial groups
one_group_mem5 <- one_group_mem_iter5 %>%
  filter(Sample %in% iter5$Sample)

### Iteration 6
# Bind samples list to PCA data, filter out the unassigned samples after iteration five
# and select PC data only for group membership probability calculation
pc1to12_twice_iter6 <- bind_cols(sample_new_stat_clusters_twice_iter5,
                                 pc1to12_twice_iter5) %>%
  filter(Sample %in% iter5$Sample) %>%
  select(-Sample, -one_two)

# Prep the sample names and assignments for iteration 6
sample_new_stat_clusters_twice_iter6 <- sample_new_stat_clusters_twice_iter5 %>%
  filter(Sample %in% iter5$Sample)

# Group probabilities for iteration 6 of the group as one data set on PC's 1 through 12
one_group_mem_iter_6 <- group.mem.probs(pc1to12_twice_iter6,
                                         sample_new_stat_clusters_twice_iter6$one_two,
                                         unique(sample_new_stat_clusters_twice_iter6$one_two))

# Create list of data that is grouped the same as the group probability list
one_samp_list_iter6 <- split(sample_new_stat_clusters_twice_iter6,
                             f = sample_new_stat_clusters_twice_iter6$one_two)

```

```

# Convert the matrices of group membership probabilities to data frames
# and bind rows into one data frame
one_group_mem_iter6 <- map(one_group_mem_iter_6, as.data.frame) %>% bind_rows()

# Convert the list of matrices of sample names to data frames and bind into one data frame
one_samp_df_iter6 <- map(one_samp_list_iter6, as.data.frame) %>% bind_rows()

# Bind to initial sample id and group assignment
# and convert to data frame for easier handling
one_group_mem_iter6 <- as.data.frame(bind_cols(one_group_mem_iter6, one_samp_df_iter6))

# Create data frame of sample to retain after sixth iteration
iter6 <- one_group_mem_iter6 %>%
  filter(one_two == 1) %>%
  filter(`1` > 1) %>%
  select(Sample)

# Create data frame of unassigned samples after sixth iteration
iter6_unassigned <- one_group_mem_iter6 %>%
  filter(one_two == 1) %>%
  filter(`1` < 1) %>%
  select(Sample)

# Subset initial groups
one_group_mem6 <- one_group_mem_iter6 %>%
  filter(Sample %in% iter6$Sample)

### Iteration 7
# Bind samples list to PCA data, filter out the unassigned samples after iteration six
# and select PC data only for group membership probability calculation
pc1to12_twice_iter7 <- bind_cols(sample_new_stat_clusters_twice_iter6,
  pc1to12_twice_iter6) %>%
  filter(Sample %in% iter6$Sample) %>%
  select(-Sample, -one_two)

# Prep the sample names and assignments for iteration 6
sample_new_stat_clusters_twice_iter7 <- sample_new_stat_clusters_twice_iter6 %>%
  filter(Sample %in% iter6$Sample)

# Group probabilities for iteration 7 of the group as one data set on PC's 1 through 12
one_group_mem_iter_7 <- group.mem.probs(pc1to12_twice_iter7,
  sample_new_stat_clusters_twice_iter7$one_two,
  unique(sample_new_stat_clusters_twice_iter7$one_two))

# Create list of data that is grouped the same as the group probability list
one_samp_list_iter7 <- split(sample_new_stat_clusters_twice_iter7,
  f = sample_new_stat_clusters_twice_iter7$one_two)

# Convert the matrices of group membership probabilities to data frames
# and bind rows into one data frame
one_group_mem_iter7 <- map(one_group_mem_iter_7, as.data.frame) %>% bind_rows()

# Convert the list of matrices of sample names to data frames and bind into one data frame

```

```

one_samp_df_iter7 <- map(one_samp_list_iter7, as.data.frame) %>% bind_rows()

# Bind to initial sample id and group assignment
# and convert to data frame for easier handling
one_group_mem_iter7 <- as.data.frame(bind_cols(one_group_mem_iter7, one_samp_df_iter7))

# Create data frame of sample to retain after seventh iteration
iter7 <- one_group_mem_iter7 %>%
  filter(one_two == 1) %>%
  filter(`1` > 1) %>%
  select(Sample)

# Create data frame of unassigned samples after seventh iteration
iter7_unassigned <- one_group_mem_iter7 %>%
  filter(one_two == 1) %>%
  filter(`1` < 1) %>%
  select(Sample)

# Subset initial groups
one_group_mem7 <- one_group_mem_iter7 %>%
  filter(Sample %in% iter7$Sample)

### Iteration 8
# Bind samples list to PCA data, filter out the unassigned samples after iteration seven
# and select PC data only for group membership probability calculation
pc1to12_twice_iter8 <- bind_cols(sample_new_stat_clusters_twice_iter7,
                                pc1to12_twice_iter7) %>%
  filter(Sample %in% iter7$Sample) %>%
  select(-Sample, -one_two)

# Prep the sample names and assignments for iteration 7
sample_new_stat_clusters_twice_iter8 <- sample_new_stat_clusters_twice_iter7 %>%
  filter(Sample %in% iter7$Sample)

# Group probabilities for iteration 8 of the group as one data set on PC's 1 through 12
one_group_mem_iter_8 <- group.mem.probs(pc1to12_twice_iter8,
                                         sample_new_stat_clusters_twice_iter8$one_two,
                                         unique(sample_new_stat_clusters_twice_iter8$one_two))

# Create list of data that is grouped the same as the group probability list
one_samp_list_iter8 <- split(sample_new_stat_clusters_twice_iter8,
                             f = sample_new_stat_clusters_twice_iter8$one_two)

# Convert the matrices of group membership probabilities to data frames
# and bind rows into one data frame
one_group_mem_iter8 <- map(one_group_mem_iter_8, as.data.frame) %>% bind_rows()

# Convert the list of matrices of sample names to data frames and bind into one data frame
one_samp_df_iter8 <- map(one_samp_list_iter8, as.data.frame) %>% bind_rows()

# Bind to initial sample id and group assignment
# and convert to data frame for easier handling
one_group_mem_iter8 <- as.data.frame(bind_cols(one_group_mem_iter8, one_samp_df_iter8))

```

```

# Create data frame of sample to retain after fifth iteration
iter8 <- one_group_mem_iter8 %>%
  filter(one_two == 1) %>%
  filter(`1` > 1) %>%
  select(Sample)

# Create data frame of unassigned samples after fifth iteration
iter8_unassigned <- one_group_mem_iter8 %>%
  filter(one_two == 1) %>%
  filter(`1` < 1) %>%
  select(Sample)

# Subset initial groups
one_group_mem8 <- one_group_mem_iter8 %>%
  filter(Sample %in% iter8$Sample)

### Iteration 9
# Bind samples list to PCA data, filter out the unassigned samples after iteration eight
# and select PC data only for group membership probability calculation
pc1to12_twice_iter9 <- bind_cols(sample_new_stat_clusters_twice_iter8,
  pc1to12_twice_iter8) %>%
  filter(Sample %in% iter8$Sample) %>%
  select(-Sample, -one_two)

# Prep the sample names and assignments for iteration 8
sample_new_stat_clusters_twice_iter9 <- sample_new_stat_clusters_twice_iter8 %>%
  filter(Sample %in% iter8$Sample)

# Group probabilities for iteration 9 of the group as one data set on PC's 1 through 12
one_group_mem_iter_9 <- group.mem.probs(pc1to12_twice_iter9,
  sample_new_stat_clusters_twice_iter9$one_two,
  unique(sample_new_stat_clusters_twice_iter9$one_two))

# Create list of data that is grouped the same as the group probability list
one_samp_list_iter9 <- split(sample_new_stat_clusters_twice_iter9,
  f = sample_new_stat_clusters_twice_iter9$one_two)

# Convert the matrices of group membership probabilities to data frames
# and bind rows into one data frame
one_group_mem_iter9 <- map(one_group_mem_iter_9, as.data.frame) %>% bind_rows()

# Convert the list of matrices of sample names to data frames and bind into one data frame
one_samp_df_iter9 <- map(one_samp_list_iter9, as.data.frame) %>% bind_rows()

# Bind to initial sample id and group assignment
# and convert to data frame for easier handling
one_group_mem_iter9 <- as.data.frame(bind_cols(one_group_mem_iter9, one_samp_df_iter9))

# Create data frame of sample to retain after eighth iteration
iter9 <- one_group_mem_iter9 %>%
  filter(one_two == 1) %>%
  filter(`1` > 1) %>%

```

```

select(Sample)

# Create data frame of unassigned samples after eighth iteration
iter9_unassigned <- one_group_mem_iter9 %>%
  filter(one_two == 1) %>%
  filter(`1` < 1) %>%
  select(Sample)

# Subset initial groups
one_group_mem9 <- one_group_mem_iter9 %>%
  filter(Sample %in% iter9$Sample)

# Data frame of unassigned samples
maha_unassigned <- bind_rows(iter1_unassigned, iter2_unassigned, iter3_unassigned,
  iter4_unassigned, iter5_unassigned, iter6_unassigned,
  iter7_unassigned, iter8_unassigned) %>%
  arrange(Sample) %>%
  mutate(one_two = 2)

##### End of Core-Unassigned membership iterations #####

# Now that I have a core group and an unassigned group, it's important to assess whether or not
# any of the unassigned samples might warrant inclusion back into the core group.
# To do this, the unassigned samples will be projected against the core group as before.
# Defined PC Loadings for core and unassigned samples
pc1to12_core_unassigned <- sample_new_stat_clusters_twice_iter9 %>%
  filter(one_two == 1) %>%
  bind_rows(maha_unassigned) %>%
  left_join(sample_pca[['pca_aug']][[1]], by = "Sample") %>%
  select(.fittedPC1:.fittedPC12)

# Prep the sample names and assignments for core/unassigned evaluation
sample_core_unassigned_clusters <- sample_new_stat_clusters_twice_iter9 %>%
  filter(one_two == 1) %>%
  bind_rows(maha_unassigned)

# Group probabilities for iteration 9 of the group as one data set on PC's 1 through 12
core_unassigned_group_prob <- group.mem.probs(pc1to12_core_unassigned,
  sample_core_unassigned_clusters$one_two,
  unique(sample_core_unassigned_clusters$one_two))

# Create list of data that is grouped the same as the group probability list
core_unassigned_list <- split(sample_core_unassigned_clusters,
  f = sample_core_unassigned_clusters$one_two)

# Convert the matrices of group membership probabilities to data frames and bind rows
# into one data frame
core_unassigned_group_prob <- map(core_unassigned_group_prob, as.data.frame) %>% bind_rows()

# Convert the list of matrices of sample names to data frames and bind into one data frame
core_unassigned_df <- map(core_unassigned_list, as.data.frame) %>% bind_rows()

```

```

# Bind to initial sample id and group assignment
# and convert to data frame for easier handling
core_unassigned_group_prob <- as.data.frame(bind_cols(core_unassigned_group_prob,
                                                    core_unassigned_df))

# Check to see if there are any unassigned above the 1% threshold for membership in the core
core_unassigned_group_prob %>%
  filter(one_two == 2 & `1` > 1)
# Does not appear to be the case

# Check to see if there are any core samples below 1% threshold of being assigned to the core
core_unassigned_group_prob %>%
  filter(one_two == 1 & `1` < 1)
# Also does not appear to be the case. This confirms that we have statistically robust
# core and unassigned groups.

# Create interactive 3D scatter plot showing first three PC's and the core and unassigned samples
p <- sample_new_stat_clusters_twice_iter9 %>%
  filter(one_two == 1) %>%
  bind_rows(maha_unassigned) %>%
  left_join(sample_pca[['pca_aug']][[1]], by = "Sample") %>%
  mutate(one_two = factor(one_two, labels = c("Core", "Unassigned"))) %>%
  mutate(symbols1 = ifelse(one_two == "Core", "plus", "triangle-up")) %>%
  # ggplot(aes(x = .fittedPC1, y = .fittedPC3, color = one_two)) + geom_point()
  plot_ly(type = "scatter3d", x = ~.fittedPC1, y = ~.fittedPC2, z = ~.fittedPC3,
         color = ~as.factor(one_two), size = 3, colors = c('grey40', 'black'),
         alpha = 0.8,
         text = ~(paste("Sample ID", Sample, '<br>Site:', Site, "<br>Geography_2:",
                        Geography_2, "<br>Time:", Time,
                        "<br>Cultural Group:", Cultural_Group)),
         # marker = list(symbol = ~I(symbols1)), size = .3,
         symbol = ~one_two, #symbols = ~symbols1,
         mode = "markers") %>%
  layout(scene = list(xaxis = list(title = 'Principal Component 1'),
                      yaxis = list(title = 'Principal Component 2'),
                      zaxis = list(title = 'Principal Component 3'))

# Adjust plot features
pb <- plotly_build(p)
pb$x$data[[1]]$marker$symbol <- 'diamond-open'
pb$x$data[[2]]$marker$symbol <- 'circle-open'
pb # Display interactive 3D scattergram

# Table of core and unassigned group membership
sample_new_stat_clusters_twice_iter9 %>%
  filter(one_two == 1) %>%
  bind_rows(maha_unassigned) %>%
  left_join(sample_pca[['pca_aug']][[1]], by = "Sample") %>%
  mutate(one_two = factor(one_two, labels = c("Core", "Unassigned"))) %>%
  select(one_two) %>%
  table()

```

```

##### Unassigned Group Structure #####
# There are 127 unassigned samples (or 23.4% of the original ceramic sample)
unassigned <- maha_unassigned %>%
  left_join(sample_pca[['pca_aug']][[1]], by = "Sample") %>%
  select(-starts_with(".")) # Drop PC's from full data set PCA

# In taking a look at a table of the sites from where the outliers were recovered,
# it looks like five sites in particular have outlier vessels: Crable, Morton Village,
# Orendorf C, Ten Mile Creek, and Walsh
table(unassigned$Site)
# Looking through the other pieces of a prior information, there don't appear to be
# any "smoking-gun" trends that may help guide cluster analysis of the Unassigned group

# Prepare samples for distance and clustering methods, we'll consider the elemental data here
unassigned_distready <- unassigned %>%
  select(Si:Th)

##### Kmeans of Unassigned #####
# First, it's a good idea to use a few methods to assess the number of clusters to model
# Elbow Method
fviz_nbclust(unassigned_distready, kmeans, method = "wss") # 4 - 8 optimal clusters;
# 4-5 Looks good

# Silhouette Method
fviz_nbclust(unassigned_distready, kmeans, method = "silhouette") # 2 optimal clusters
# Gap Stat
#fviz_nbclust(unassigned_distready, kmeans, method = "gap_stat") # 1 optimal cluster

# Based on the optimal cluster methods, it looks like we should run kmeans twice, once with
# 2 clusters and once with 5 clusters

# 2 Cluster K-means
unassigned_k2 <- kmeans(unassigned_distready,
  centers = 2, # number of clusters
  nstart = 50, # number of random initial configs
  # out of which best is chosen
  iter.max = 500) # number of allowable iterations allowed

# Visualize 2 cluster kmeans
fviz_cluster(unassigned_k2, data = unassigned_distready)

# Assign to clustering assignments data frame
unassigned_stat_clusters <- maha_unassigned %>%
  select(Sample) %>%
  mutate(Kmeans_2 = unassigned_k2$cluster)

# 5 Cluster K-means
unassigned_k5 <- kmeans(unassigned_distready, centers = 5, nstart = 50, iter.max = 500)

# Visualize 5 cluster kmeans
fviz_cluster(unassigned_k5, data = unassigned_distready)

# Assign to clustering assignments data frame

```

```

unassigned_stat_clusters <- unassigned_stat_clusters %>%
  mutate(Kmeans_5 = unassigned_k5$cluster,
         Kmeans_2 = unassigned_k2$cluster)

##### K-medoids of Unassigned #####

# For k-medoids, we'll be using the pam function from the cluster package. pam stands for
# "partitioning around medoids"

# As with k-means, it's a good idea to use a few methods to assess the number of clusters to m
odel
# Elbow Method
fviz_nbclust(unassigned_distready, pam, method = "wss") # 5 Looks optimal here
# Silhouette Method
fviz_nbclust(unassigned_distready, pam, method = "silhouette") # 2 optimal clusters
# Gap Stat
#fviz_nbclust(unassigned_distready, pam, method = "gap_stat") # 1 optimal cluster

# We'll run two clusters - one with 2 and one with 5
# 2 cluster K-medoids
pam2_unassigned <- pam(unassigned_distready, 2)

# Plot 2 cluster k-medoids
fviz_cluster(pam2_unassigned, data = unassigned_distready)

# 5 cluster K-medoids
pam5_unassigned <- pam(unassigned_distready, 5)

# Plot 5 cluster k-medoids
fviz_cluster(pam5_unassigned, data = unassigned_distready)

# Assign k-medoids results to clustering assignments data frame
unassigned_stat_clusters <- unassigned_stat_clusters %>%
  mutate(Kmediods_2 = pam2_unassigned$clustering,
         Kmediods_5 = pam5_unassigned$clustering)

# There appears to be fairly broad agreement between kmeans and kmedoids about the different
# clusters present, but it is important to see how these hold up to comparison using
# visual inspection

# Convert all unassigned statistical cluster assignments to character for joining
unassigned_stat_clusters[,2:5] <- sapply(unassigned_stat_clusters[,2:5], as.character)

# Make data frame with core sample assignments and unassigned cluster assignments
core_and_unassigned_clusters <- sample_new_stat_clusters_twice_iter9 %>%
  filter(one_two == 1) %>%
  mutate(Kmeans_2 = "Core",
         Kmeans_5 = "Core",
         Kmediods_2 = "Core",
         Kmediods_5 = "Core") %>%
  select(-one_two) %>%
  bind_rows(unassigned_stat_clusters)

```

```

# Join the core assignments to the original PCA data, which is stored in a nested
# prcomp list object
sample_pca[["data"]][[1]] <- left_join(sample_pca[["data"]][[1]], core_and_unassigned_clusters
, by = "Sample")

# Join the core assignments to the augmented PCA data, which is stored in a nested
# prcomp list object
sample_pca[["pca_aug"]][[1]] <- left_join(sample_pca[["pca_aug"]][[1]],
                                         core_and_unassigned_clusters, by = "Sample")

# Create column to apply alpha to core group points in biplots for easier interpretation
# sample_pca[["data"]][[1]] <- sample_pca[["data"]][[1]] %>%
#                                     mutate(alpha = ifelse(Kmeans_5 == "Core", 0.25, 1)) %>%
#                                     mutate(alpha = as.vector(alpha))

# Vectorize the alpha column
# core_alpha <- as.vector(sample_pca[["data"]][[1]]$alpha)

# Create plot of PC 1 and PC 2 with the 90% conf intervals around the core and outgroups
unass_pc1pc2_kmean2 <- sample_pca %>%
  mutate(
    pca_graph = map2(
      .x = pca,
      .y = data,
      ~ autoplot(.x, loadings = TRUE, loadings.label = TRUE,
                 loadings.label.repel = TRUE,
                 loadings.label.colour = "black",
                 loadings.colour = "gray45",
                 loadings.label.alpha = 0.9,
                 loadings.label.size = 3.5,
                 loadings.label.hjust = -0.5,
                 frame = TRUE,
                 frame.type = "norm",
                 data = .y,
                 colour = "Kmeans_5",
                 shape = "Kmeans_5",
                 frame.level = .9,
                 frame.alpha = 0.001,
                 #alpha = core_alpha,
                 size = 2) +
      theme_bw() +
      # geom_text(Label = .y$Sample) +
      labs(x = "Principal Component 1",
           y = "Principal Component 2")
    )
  ) %>%
  pull(pca_graph)

unass_pc1pc2_kmean2[[1]] + scale_fill_manual(values = c("black","black", "black",
                                                       "black", "black", "black")) +
  scale_color_manual(values = c("black","black", "black", "black", "black", "black")) +
  scale_shape_manual(values=c(3, 18, 16, 2, 43, 1))

```

```

## Add final assignments to shiny app data
sample_pca[["pca_aug"]][[1]] <- sample_pca[["pca_aug"]][[1]] %>%
  left_join(pca_aug[, c("Sample", "Final_Assign")], by = "Sample")

##### Shiny app to biplot the various elements and PCs against one another #####
## UI ##
ui_sample <- fluidPage(
  pageWithSidebar (
    headerPanel('Bivariate Plotting'),
    sidebarPanel(
      selectInput('x', 'X Variable', names(sample_pca[["pca_aug"]][[1]]),
                 selected = names(sample_pca[["pca_aug"]][[1]])[[14]]),
      selectInput('y', 'Y Variable', names(sample_pca[["pca_aug"]][[1]]),
                 selected = names(sample_pca[["pca_aug"]][[1]])[[15]]),
      selectInput('color', 'Color', names(sample_pca[["pca_aug"]][[1]]),
                 selected = names(sample_pca[["pca_aug"]][[1]])[[103]]),
      #Slider for plot height
      sliderInput('plotHeight', 'Height of plot (in pixels)',
                 min = 100, max = 2000, value = 550)
    ),
    mainPanel(
      plotlyOutput('plot1')
    )
  )
)

## Server ##
server_sample <- function(input, output, session) {

  # Combine the selected variables into a new data frame
  selectedData <- reactive({
    sample_pca[["pca_aug"]][[1]][, c(input$x, input$y, input$color)]
  })

  output$plot1 <- renderPlotly({

    #Build plot with ggplot syntax
    p <- ggplot(data = sample_pca[["pca_aug"]][[1]], aes_string(x = input$x,
                                                               y = input$y,
                                                               color = input$color,
                                                               shape = input$color)) +

      geom_point() +
      theme(legend.title = element_blank()) +
      stat_ellipse(level = 0.9) +
      scale_color_igv() +
      theme_bw() +
      xlab(paste0(input$x, " (log base 10 ppm)")) +
      ylab(paste0(input$y, " (log base 10 ppm)"))

    ggplotly(p) %>%
      layout(height = input$plotHeight, autosize = TRUE,

```

```

        legend = list(font = list(size = 12)))
    })
}

shinyApp(ui_sample, server_sample)

## Membership probabilities for outgroup Kmeans 5 group assignments

# Assess membership probabilities of the outgroup samples
# Out-groups 2, 3, and 4 are large enough to be assessed for Mahalanobis
# distance probabilities
table(sample_pca[["pca_aug"]][[1]]$Kmeans_5)

# Pull sample data for the Kmeans_5 samples
kmeans234_samps <- sample_pca[["pca_aug"]][[1]] %>%
  filter(Kmeans_5 == 2 | Kmeans_5 == 3 | Kmeans_5 == 4) %>%
  select(Sample, Kmeans_5, .fittedPC1:.fittedPC12) %>%
  mutate(Kmeans_5 = as.numeric(Kmeans_5) - 1)

# Pull PC data for the Kmeans_5 samples
kmeans234_pcs <- kmeans234_samps %>%
  select(.fittedPC1:.fittedPC12)

# Group membership probabilities for the groups large enough to be assessed
kmeans234_mem <- group.mem.probs(kmeans234_pcs, kmeans234_samps$Kmeans_5,
  unique(kmeans234_samps$Kmeans_5))

# Create list of data that is grouped the same as the group probability list
kmeans234_samp_list <- split(kmeans234_samps,
  f = kmeans234_samps$Kmeans_5)

# Convert the matrices of group membership probabilities to data frames and bind
# rows into one data frame
kmeans234_mem <- map(kmeans234_mem, as.data.frame) %>% bind_rows()

# Convert the list of matrices of sample names to data frames and bind into one data frame
kmeans234_samp_df <- map(kmeans234_samp_list, as.data.frame) %>% bind_rows()

# Bind to initial sample id and group assignment from Kmed 5
# and convert to data frame for easier handling
kmeans234_mem <- as.data.frame(bind_cols(kmeans234_mem, kmeans234_samp_df))

# Reorder columns
kmeans234_mem <- kmeans234_mem[, c(3, 1, 2, 4, 5)]

# New column of membership probability for initially assigned group
kmeans234_mem$assigned_val <- kmeans234_mem[1:3][cbind(seq_len(nrow(kmeans234_mem)),
  as.numeric(kmeans234_mem$Kmeans_5))]

# Determine column with the maximum value and assign to new column
kmeans234_mem$max_value <- colnames(kmeans234_mem[1:3])[max.col(kmeans234_mem[1:3])]

```

```

# There is broad disagreement in group assignment between the Kmeans/Kmedoids 5 group methods
# and the group membership probabilities. This isn't surprising since there is much overlap
# between the groups on PC biplots. As a result, I'll take the maximum group membership
# probability as assessed via Mahalanobis/Hotelling's T2 and re-run the assignments to
# refine the non-core group membership assignments.

# Samples and PCs for maximum membership after iteration one
kmeans234_iter2_samps <- kmeans234_mem %>%
  select(Sample, max_value) %>%
  left_join(kmeans234_samps[-2], by = "Sample")

# PC data for iteration 2 of Kmeans assignments
kmeans234_iter2_pcs <- kmeans234_iter2_samps %>% select(.fittedPC1:.fittedPC12)

# Group membership probs for iteration 2 of Kmeans
kmeans234_mem_iter2 <- group.mem.probs(kmeans234_iter2_pcs, kmeans234_iter2_samps$max_value,
  unique(kmeans234_iter2_samps$max_value))

# Unfortunately, it appears that the groups as defined and refined from Kmeans do not
# hold up to statistical rigor. Let's try the Kmeans 2 group assignments

## Membership probabilities for outgroup Kmeans 2 group assignments

# Assess membership probabilities of the outgroup samples for Kmeans_2
table(sample_pca[["pca_aug"]][[1]]$Kmeans_2)

# Pull sample data for the Kmeans_2 samples
out_kmeans2_samps <- sample_pca[["pca_aug"]][[1]] %>%
  filter(Kmeans_2 != "Core") %>%
  select(Sample, Kmeans_2, .fittedPC1:.fittedPC12)

# Pull PC data for the Kmeans_2 samples
out_kmeans2_pcs <- out_kmeans2_samps %>%
  select(.fittedPC1:.fittedPC12)

# Group membership probabilities for the groups large enough to be assessed
out_kmeans2_mem <- group.mem.probs(out_kmeans2_pcs, out_kmeans2_samps$Kmeans_2,
  c("1", "2"))

# Create list of data that is grouped the same as the group probability list
out_kmeans2_samp_list <- split(out_kmeans2_samps[1:2],
  f = out_kmeans2_samps$Kmeans_2)

# Convert the matrices of group membership probabilities to data frames and bind rows into one
# data frame
out_kmeans2_mem <- map(out_kmeans2_mem, as.data.frame) %>% bind_rows()

# Reorder column to put them in the correct position
#out_kmeans2_mem <- data.frame(out_kmeans2_mem$`1`, out_kmeans2_mem$`2`)
#colnames(out_kmeans2_mem) <- c(1, 2)

# Convert the list of matrices of sample names to data frames and bind into one data frame
out_kmeans2_samp_df <- map(out_kmeans2_samp_list, as.data.frame) %>% bind_rows()

```

```

# Bind to initial sample id and group assignment and convert to data frame for easier handling
out_kmeans2_mem <- as.data.frame(bind_cols(out_kmeans2_mem, out_kmeans2_samp_df))

# New column of membership probability for initially assigned group
out_kmeans2_mem$assigned_val <- out_kmeans2_mem[1:2][cbind(seq_len(nrow(out_kmeans2_mem)),
                                                         as.numeric(out_kmeans2_mem$Kmeans_2))]

# Set the initial group assignment value to zero to allow for comparisons
out_kmeans2_mem[cbind(as.numeric(seq_len(nrow(out_kmeans2_mem))),
                      as.numeric(out_kmeans2_mem$Kmeans_2))] <- 0

# Assess membership probabilities using my heuristic
out_kmeans2_mem %>%
  mutate(assigned_val = as.numeric(assigned_val)) %>%
  mutate(`1` = as.numeric(`1`)) %>%
  mutate(`2` = as.numeric(`2`)) %>%
  mutate(new_assign = ifelse(assigned_val > 2.5 & `1` < 10 & `2` < 10,
                             Kmeans_2, "unassigned")) %>%
  # filter(new_assign != "unassigned")
  summarize(perc_unassigned = sum(new_assign == "unassigned")/n() * 100)
# 50.4% unassigned rate suggests that there is some support for a two group solution here
# Let's remove the unassigned samples and run another iteration to firm up the outgroups

#### Data frame of Outgroup Kmeans 2 assignments for group mem iteration 2
out_kmeans2_iter2 <- out_kmeans2_mem %>%
  mutate(assigned_val = as.numeric(assigned_val)) %>%
  mutate(`1` = as.numeric(`1`)) %>%
  mutate(`2` = as.numeric(`2`)) %>%
  mutate(new_assign = ifelse(assigned_val > 2.5 & `1` < 10 & `2` < 10,
                             Kmeans_2, "unassigned")) %>%
  filter(new_assign != "unassigned")

# Data frame of Outgroup Kmeans 2 unassigned sherds after group mem iteration 1
out_kmeans2_iter2_unassigned <- out_kmeans2_mem %>%
  mutate(assigned_val = as.numeric(assigned_val)) %>%
  mutate(`1` = as.numeric(`1`)) %>%
  mutate(`2` = as.numeric(`2`)) %>%
  mutate(new_assign = ifelse(assigned_val > 2.5 & `1` < 10 & `2` < 10,
                             Kmeans_2, "unassigned")) %>%
  filter(new_assign == "unassigned")

# Sample and PC data for Kmeans 2 iteration 2
out_kmeans2_iter2_samps <- out_kmeans2_iter2 %>%
  select(Sample, new_assign) %>%
  left_join(out_kmeans2_samps[-2], by = "Sample")

# PC data for Kmenas sample 2
out_kmeans2_iter2_pcs <- out_kmeans2_iter2_samps %>%
  select(.fittedPC1:.fittedPC12)

# Membership probabilities for iteration 2 - only two samples need to become unassigned
out_kmeans2_iter2_mem <- group.mem.probs(out_kmeans2_iter2_pcs,

```

```

        out_kmeans2_iter2_samps$new_assign,
        unique(out_kmeans2_iter2_samps$new_assign))

# Create list of data that is grouped the same as the group probability list
out_kmeans2_iter2_samps_list <- split(out_kmeans2_iter2_samps[1:2],
                                     f = out_kmeans2_iter2_samps$new_assign)

# Convert the matrices of group membership probabilities to data frames and bind rows
# into one data frame
out_kmeans2_iter2_mem <- map(out_kmeans2_iter2_mem, as.data.frame) %>% bind_rows()

# Convert the list of matrices of sample names to data frames and bind into one data frame
out_kmeans2_iter2_samps_df <- map(out_kmeans2_iter2_samps_list, as.data.frame) %>% bind_rows()

# Bind to initial sample id and group assignment and convert to data frame for easier handling
out_kmeans2_iter2_mem <- as.data.frame(bind_cols(out_kmeans2_iter2_mem, out_kmeans2_iter2_samps_df))

# New column of membership probability for initially assigned group
out_kmeans2_iter2_mem$assigned_val <- out_kmeans2_iter2_mem[1:3][cbind(seq_len(nrow(out_kmeans2_iter2_mem)),
                                                                    as.numeric(out_kmeans2_iter2_mem$new_assign))]

# Set the initial group assignment value to zero to allow for comparisons
out_kmeans2_iter2_mem[cbind(as.numeric(seq_len(nrow(out_kmeans2_iter2_mem))),
                           as.numeric(out_kmeans2_iter2_mem$new_assign))] <- 0

# Assess membership probabilities using my heuristic but reduced in-group membership to >2.5%
out_kmeans2_iter2_mem %>%
  mutate(assigned_val = as.numeric(assigned_val)) %>%
  mutate(`1` = as.numeric(`1`)) %>%
  mutate(`2` = as.numeric(`2`)) %>%
  mutate(iter2_assign = ifelse(assigned_val > 2.5 & `1` < 10 & `2` < 10,
                              new_assign, "unassigned")) %>%
  # filter(new_assign != "unassigned")
  summarize(perc_unassigned = sum(iter2_assign == "unassigned")/n() * 100)
# Great, only dropped 6.3% of the samples. Seems like we have statistically robust outgroups
# Let's go ahead and define those here.

# Data frame of assigned outgroup samples
outgroup_assignments <- out_kmeans2_iter2_mem %>%
  mutate(assigned_val = as.numeric(assigned_val)) %>%
  mutate(`1` = as.numeric(`1`)) %>%
  mutate(`2` = as.numeric(`2`)) %>%
  mutate(iter2_assign = ifelse(assigned_val > 2.5 & `1` < 10 & `2` < 10,
                              new_assign, "unassigned")) %>%
  filter(iter2_assign != "unassigned") %>%
  mutate(Outgroup = iter2_assign) %>%
  select(Sample, Outgroup)

# Table of outgroup sample assignments
table(outgroup_assignments$Outgroup)

```

```

# Data frame of unassigned outgroup samples
outgroup_unassigned <- out_kmeans2_iter2_mem %>%
  mutate(assigned_val = as.numeric(assigned_val)) %>%
  mutate(`1` = as.numeric(`1`)) %>%
  mutate(`2` = as.numeric(`2`)) %>%
  mutate(new_assign = ifelse(assigned_val > 2.5 & `1` < 10 & `2` < 10,
                            new_assign, "unassigned")) %>%
  filter(new_assign == "unassigned") %>%
  full_join(out_kmeans2_iter2_unassigned, by = "Sample") %>%
  mutate(Outgroup = "unassigned") %>%
  select(Sample, Outgroup)

# Data frame of all outgroup samples
outgroup_assignments <- bind_rows(outgroup_assignments, outgroup_unassigned)

# Change the Label of 1 to Outgroup 2 and 2 to Outgroup 1
outgroup_assignments <- outgroup_assignments %>%
  mutate(Outgroup = ifelse(Outgroup == 1, "Outgroup 2", Outgroup)) %>%
  mutate(Outgroup = ifelse(Outgroup == 2, "Outgroup 1", Outgroup))

### Visualize core and outgroup samples
# Make data frame with core sample assignments and unassigned cluster assignments
core_and_outgroup_assignments <- sample_new_stat_clusters_twice_iter9 %>%
  filter(one_two == 1) %>%
  mutate(Outgroup = "Core") %>%
  select(-one_two) %>%
  bind_rows(outgroup_assignments)

# Join the core assignments to the original PCA data, which is stored in a nested
# prcomp list object
sample_pca[["data"]][[1]] <- left_join(sample_pca[["data"]][[1]], core_and_outgroup_assignments, by = "Sample")

# Join the core assignments to the augmented PCA data, which is stored in a nested
# prcomp list object
sample_pca[["pca_aug"]][[1]] <- left_join(sample_pca[["pca_aug"]][[1]],
                                         core_and_outgroup_assignments, by = "Sample")

# Create column to apply alpha to core group points in biplots for easier interpretation
sample_pca[["data"]][[1]] <- sample_pca[["data"]][[1]] %>%
  mutate(core_alpha = ifelse(Outgroup == "Core", 0.25, 1)) %>%
  mutate(core_alpha = as.vector(core_alpha))

# Vectorize the alpha column
core_alpha <- as.vector(sample_pca[["data"]][[1]]$core_alpha)

# Create plot of PC 1 and PC 2 with the 90% conf intervals around the core and outgroups
core_outgroup_pc1pc2 <- sample_pca %>%
  mutate(
    pca_graph = map2(
      .x = pca,
      .y = data,

```

```

~ autoplot(.x, loadings = TRUE, loadings.label = TRUE,
  scale = 0,
  loadings.label.repel = TRUE,
  loadings.label.colour = "black",
  loadings.colour = "gray45",
  loadings.label.alpha = 0.9,
  loadings.label.size = 2.5,
  loadings.label.hjust = -0.5,
  #frame = TRUE,
  #frame.type = "norm",
  data = .y,
  colour = "Outgroup",
  shape = "Outgroup",
  frame.level = .9,
  frame.alpha = 0.001,
  size = 2,
  alpha = core_alpha) +
  theme_bw() +
  # geom_text(Label = .y$Sample) +
  labs(x = "Principal Component 1",
  y = "Principal Component 2")
)
)%>%
pull(pca_graph)

core_outgroup_pc1pc2[[1]] +
  scale_fill_manual(values = c("black", "black", "black",
  "black", "black", "black")) +
  scale_color_manual(values = c("black", "black", "black", "black", "black", "black")) +
  stat_ellipse(data = filter(sample_pca[["pca_aug"]][[1]], Outgroup != "unassigned"),
  aes(x = .fittedPC1, y = .fittedPC2, color = Outgroup)) +
  scale_shape_manual(values=c(2, 15, 18, 43))

# Group membership probabilities for Outgroup 1, 2, unassigned, and core
core_out_unass_samps <- sample_pca[["pca_aug"]][[1]] %>%
  select(Sample, Outgroup, .fittedPC1:.fittedPC12)

core_out_unass_pcs <- core_out_unass_samps %>% select(.fittedPC1:.fittedPC12)

core_out_unass_mem <- group.mem.probs(core_out_unass_pcs, core_out_unass_samps$Outgroup,
  unique(core_out_unass_samps$Outgroup))

# Create list of data that is grouped the same as the group probability list
core_out_samp_list <- split(core_out_unass_samps[, c("Sample", "Outgroup")],
  f = core_out_unass_samps$Outgroup)

# Reorder list to match the order of the group membership probs
core_out_samp_list <- list(core_out_samp_list$Core, core_out_samp_list$`Outgroup 1`,
  core_out_samp_list$unassigned, core_out_samp_list$`Outgroup 2`)

# Convert the matrices of group membership probabilities to data frames and bind rows

```

```

# into one data frame
core_out_unass_mem <- map(core_out_unass_mem, as.data.frame) %>% bind_rows()

# Convert the list of matrices of sample names to data frames and bind into one data frame
core_out_samp_df <- map(core_out_samp_list, as.data.frame) %>% bind_rows()

# Bind to initial sample id and group assignment from Kmed 5
# and convert to data frame for easier handling
core_out_unass_mem <- as.data.frame(bind_cols(core_out_unass_mem, core_out_samp_df))

# Create table for dissertation
outgroup_core_table <- core_out_unass_mem %>%
  right_join(sample_pca[["pca_aug"]][[1]][, c("Sample", "Site")]) %>%
  filter(Outgroup != "unassigned", Outgroup != "Core") %>%
  select(-unassigned) %>%
  arrange(Outgroup) %>%
  mutate(Sample = parse_number(Sample))

# Write table to csv
# write_csv(outgroup_core_table, "outgroups - core.csv")

# Create plot of PC 1 and PC 2 with the 90% conf intervals around the core and outgroups
core_outgroup_pc1pc2 <- sample_pca %>%
  mutate(
    pca_graph = map2(
      .x = pca,
      .y = data,
      ~ autoplot(.x, x = 1, y = 2, loadings = TRUE, loadings.label = TRUE,
        scale = 0,
        loadings.label.repel = TRUE,
        loadings.label.colour = "black",
        loadings.colour = "gray45",
        loadings.label.alpha = 0.9,
        loadings.label.size = 2.5,
        loadings.label.hjust = -0.5,
        #frame = TRUE,
        #frame.type = "norm",
        data = .y,
        colour = "Outgroup",
        shape = "Outgroup",
        frame.level = .9,
        frame.alpha = 0.001,
        size = 2,
        alpha = core_alpha) +
      theme_bw() +
      # geom_text(Label = .y$Sample) +
      labs(x = "Principal Component 1",
        y = "Principal Component 2")
    )
  ) %>%
  pull(pca_graph)

```

```

core_outgroup_pc1pc5[[1]] +
  scale_fill_manual(values = c("black","black", "black",
                               "black", "black", "black")) +
  scale_color_manual(values = c("black","black","black", "black", "black", "black")) +
  stat_ellipse(data = filter(sample_pca[["pca_aug"]][[1]], Outgroup != "unassigned"),
              aes(x = .fittedPC1, y = .fittedPC2, color = Outgroup)) +
  scale_shape_manual(values=c(2, 15, 18, 43))

# Create plot of PC 1 and PC 5 with the 90% conf intervals around the core and outgroups
core_outgroup_pc1pc5 <- sample_pca %>%
  mutate(
    pca_graph = map2(
      .x = pca,
      .y = data,
      ~ autoplot(.x, x = 1, y = 5, loadings = TRUE, loadings.label = TRUE,
                 scale = 0,
                 loadings.label.repel = TRUE,
                 loadings.label.colour = "black",
                 loadings.colour = "gray45",
                 loadings.label.alpha = 0.9,
                 loadings.label.size = 2.5,
                 loadings.label.hjust = -0.5,
                 #frame = TRUE,
                 #frame.type = "norm",
                 data = .y,
                 colour = "Outgroup",
                 shape = "Outgroup",
                 frame.level = .9,
                 frame.alpha = 0.001,
                 size = 2,
                 alpha = core_alpha) +
      theme_bw() +
      # geom_text(Label = .y$Sample) +
      labs(x = "Principal Component 1",
           y = "Principal Component 5")
    )
  ) %>%
  pull(pca_graph)

core_outgroup_pc1pc5[[1]] +
  scale_fill_manual(values = c("black","black", "black",
                               "black", "black", "black")) +
  scale_color_manual(values = c("black","black","black", "black", "black", "black")) +
  stat_ellipse(level = 0.9, data = filter(sample_pca[["pca_aug"]][[1]],
                                         Outgroup != "unassigned"),
              aes(x = .fittedPC1, y = .fittedPC5, color = Outgroup)) +
  scale_shape_manual(values=c(2, 15, 18, 43))

# Create plot of Mo and Sc for elemental separation
# Prep data
pca_aug <- sample_pca[["pca_aug"]][[1]]

```

```

# Plot of ytterbium and magnesium of core-outgroup separation
ggplot(pca_aug, aes(x = Yb, y = Mg, color = Outgroup, shape = Outgroup)) +
  geom_point() +
  stat_ellipse(level = 0.9, data = filter(sample_pca[["pca_aug"]][[1]], Outgroup != "unassigned"),
             aes(x = Yb, y = Mg, color = Outgroup)) +
  scale_shape_manual(values=c(2, 15, 18, 43)) +
  scale_fill_manual(values = c("black","black", "black",
                              "black", "black", "black")) +
  scale_color_manual(values = c("black","black","black", "black", "black", "black")) +
  xlab("Yb (log base 10 ppm)") +
  ylab("Mg (log base 10 ppm)") +
  theme_bw()

# Explore Outgroup 1 sherds
pca_aug %>%
  select(Sample, Site, Outgroup, Cultural_Group, Vessel_Class, Geography_2) %>%
  group_by(Outgroup, Site, Vessel_Class) %>%
  summarize(n = n()) %>% View()

pca_aug %>%
  select(Sample, Site, Outgroup, Cultural_Group, Vessel_Class) %>%
  mutate(Outgroup = factor(Outgroup),
         Site = factor(Site)) %>%
  group_by(Outgroup, Vessel_Class) %>%
  summarize(n = n()) %>% View()

pca_aug %>%
  select(Sample, Site, Outgroup, Cultural_Group, Vessel_Class, Time) %>%
  mutate(Outgroup = factor(Outgroup),
         Site = factor(Site)) %>%
  group_by(Time, Outgroup) %>%
  summarize(total = n()) %>% View()

##### Core Group Structure #####

# Let's explore here structure within the core group
# First, isolate the core group samples and their accompanying elemental and PC data
core_group_data <- sample_pca[["pca_aug"]][[1]] %>%
  filter(Outgroup == "Core")

# Let's run some cluster analyses to see if the core group can be sub-divided
# Prepare a data frame of the elemental data for distance calculations
core_distready <- core_group_data %>%
  select(Si:Th)

# Kmeans of Core #
# First, it's a good idea to use a few methods to assess the number of clusters to model
# Elbow Method
fviz_nbclust(core_distready, kmeans, method = "wss") # 4-6 optimal clusters; 4-5 Looks good
# Silhouette Method
fviz_nbclust(core_distready, kmeans, method = "silhouette") # 2 optimal clusters

```

```

# Gap Stat
#fviz_nbclust(core_distready, kmeans, method = "gap_stat") # 1 optimal cluster

# Based on the optimal cluster methods, it looks like we should run kmeans twice, once with
# 2 clusters and once with 5 clusters

# 2 Cluster K-means
core_k2 <- kmeans(core_distready,
                  centers = 2, # number of clusters
                  nstart = 50, # number of random initial configs
                           # out of which best is chosen
                  iter.max = 500) # number of allowable iterations allowed

# Visualize 2 cluster kmeans
fviz_cluster(core_k2, data = core_distready)

# Assign to clustering assignments data frame
core_stat_clusters <- core_group_data %>%
  select(Sample) %>%
  mutate(Kmeans_2 = core_k2$cluster)

# Let's compare the kmeans to kmedoids
core_kmed2 <- pam(core_distready, 2)
fviz_cluster(core_kmed2, data = core_distready)

fviz_cluster(core_kmed2, data = core_distready, geom = text, label = )

core_group_data %>%
  filter(Outgroup == "Core") %>%
  select(-Kmeans_2:-Kmedoids_5) %>%
  left_join(core_stat_clusters, by = "Sample") %>%
ggplot(aes(x = .fittedPC4, y = .fittedPC2, color = Geography_2, label = Site)) +
  stat_ellipse(level = 0.9) +
  geom_text(size = 2.5)

# It appears as though there is broad agreement between the two cluster methods about
# there being two clusters at approximately the same locations (with primary separation
# in the first PC).
# Kmeans seems to offer a more conservative solution. We'll use that and see how it fairs in
# mahalanobis distance calculations.

core_pc1to12_samps <- core_group_data %>%
  select(Sample, .fittedPC1:.fittedPC12) %>%
  left_join(core_stat_clusters, by = "Sample")

core_pc1to12 <- core_pc1to12_samps %>% select(.fittedPC1:.fittedPC12)

# Group probabilities for the core kmeans 2 cluster solution on PC's 1 to 12
# (90% of variability)
core_kmean2_group_mem <- group.mem.probs(core_pc1to12, core_pc1to12_samps$Kmeans_2,
                                         unique(core_pc1to12_samps$Kmeans_2))

```

```

# Create list of data that is grouped the same as the group probability list
core_kmean2_samp_list <- split(core_pc1to12_samps[, c("Sample", "Kmeans_2")],
                             f = core_pc1to12_samps$Kmeans_2)

# Convert the matrices of group membership probabilities to data frames and bind
# rows into one data frame
core_kmean2_group_mem <- map(core_kmean2_group_mem, as.data.frame) %>% bind_rows()

# Convert the list of matrices of sample names to data frames and bind into one data frame
core_kmean2_samp_df <- map(core_kmean2_samp_list, as.data.frame) %>% bind_rows()

# Bind to initial sample id and group assignment
# and convert to data frame for easier handling
core_kmean2_group_mem <- as.data.frame(bind_cols(core_kmean2_group_mem, core_kmean2_samp_df))

# New column of membership probability for initially assigned group
core_kmean2_group_mem$assigned_val <- core_kmean2_group_mem[1:2][cbind(seq_len(nrow(core_kmean2_group_mem)),
                                                                    core_kmean2_group_mem$Kmeans_2)]

# Set the initial group assignment value to zero to allow for comparisons
core_kmean2_group_mem[cbind(seq_len(nrow(core_kmean2_group_mem)), core_kmean2_group_mem$Kmeans_2)] <- 0

# Assess membership probabilities using an outlier heuristic of less than 1%
# probability in another group
core_kmean_iter1 <- core_kmean2_group_mem %>%
  mutate(new_assign = ifelse(assigned_val > 2.5 & `1` < 1 & `2` < 1,
                             Kmeans_2, "Core")) %>%
  #summarize(perc_unassigned = sum(new_assign == "Core")/n() * 100)
  mutate(Kmeans_2_iter2 = new_assign) %>%
  select(Sample, Kmeans_2_iter2)

# Results in a 81.97% remaining in Core and shaving off the difference

# Assign Core, Core1 and Core2 memberships after iteration 1
core_stat_clusters <- core_stat_clusters %>%
  left_join(core_kmean_iter1, by = "Sample")

# Append Kmeans_2 + Core groups to PC data
core_pc1to12_samps <- core_pc1to12_samps %>%
  left_join(core_stat_clusters[,c("Sample", "Kmeans_2_iter2")],
           by = "Sample")

## Iteration 2 of Core group structure
# Group probabilities for the core kmeans 2 cluster solution on PC's 1 to 12 (90% of variability)
core_kmean2_group_mem_iter2 <- group.mem.probs(core_pc1to12, core_pc1to12_samps$Kmeans_2_iter2,
                                              unique(core_pc1to12_samps$Kmeans_2_iter2))

# Create list of data that is grouped the same as the group probability list
core_kmean2_samp_list_iter2 <- split(core_pc1to12_samps[, c("Sample", "Kmeans_2_iter2")],

```

```

f = core_pc1to12_samps$Kmeans_2_iter2)

# Reorder list so it matches the order of the group probs
core_kmean2_samp_list_iter2 <- list(core_kmean2_samp_list_iter2$Core, core_kmean2_samp_list_iter2$`2`,
                                   core_kmean2_samp_list_iter2$`1`)

# Convert the matrices of group membership probabilities to data frames and bind rows
# into one data frame
core_kmean2_group_mem_iter2 <- map(core_kmean2_group_mem_iter2, as.data.frame) %>% bind_rows()

# Convert the list of matrices of sample names to data frames and bind into one data frame
core_kmean2_samp_df_iter2 <- map(core_kmean2_samp_list_iter2, as.data.frame) %>% bind_rows()

# Bind to initial sample id and group assignment
# and convert to data frame for easier handling
core_kmean2_group_mem_iter2 <- as.data.frame(bind_cols(core_kmean2_group_mem_iter2,
                                                       core_kmean2_samp_df_iter2))

# Change "Core" column name to "3" for data handling
colnames(core_kmean2_group_mem_iter2) <- c("3", "2", "1", "Sample", "Kmeans_2_iter2")

# Change "Core" assignments to the character "3" to match the new column name
# and reorder the columns
core_kmean2_group_mem_iter2 <- core_kmean2_group_mem_iter2 %>%
  mutate(Kmeans_2_iter2 = ifelse(Kmeans_2_iter2 == "Core", "3",
                                Kmeans_2_iter2)) %>%
  select(`1`, `2`, `3`, Sample, Kmeans_2_iter2)

# New column of membership probability for initially assigned group
core_kmean2_group_mem_iter2$assigned_val <- core_kmean2_group_mem_iter2[1:3][cbind(seq_len(nrow(
  core_kmean2_group_mem_iter2)), as.numeric(core_kmean2_group_mem_iter2$Kmeans_2_iter2))]

# Set the initial group assignment value to zero to allow for comparisons
core_kmean2_group_mem_iter2[cbind(seq_len(nrow(core_kmean2_group_mem_iter2)),
                                  as.numeric(core_kmean2_group_mem_iter2$Kmeans_2_iter2))] <- 0

# Assess membership probabilities using an outlier heuristic of less than 10% probability
# in another group
core_kmean_iter2 <- core_kmean2_group_mem_iter2 %>%
  mutate(new_assign = ifelse(assigned_val > 2.5 & `1` < 10 & `2` < 10 & `3` < 10,
                             Kmeans_2_iter2, 3)) %>%
  #summarize(perc_unassigned = sum(new_assign == Kmeans_2_iter2)/n()) * 100)
  mutate(Kmeans_2_iter3 = new_assign)#%>%
  #select(Sample, Kmeans_2_iter3)
# Results in a 90.14% remaining in their iteration 2 assignment

# Explore Core sub-group assignments
core_kmean_iter2 %>%
  filter(Kmeans_2_iter3 == 1 | Kmeans_2_iter3 == 2) %>%
  left_join(pca_aug[, c("Sample", "Site")]) %>%
  mutate(id = parse_number(Sample)) %>%
  write_csv("Core A B and C.csv")

```

```

# Assign Core, Core1 and Core2 memberships
core_stat_clusters <- core_stat_clusters %>%
  left_join(core_kmean_iter2, by = "Sample")

# Add group designations to the Sample PCA augmented data
sample_pca[["pca_aug"]][[1]] <- sample_pca[["pca_aug"]][[1]] %>%
  left_join(core_stat_clusters[, c("Sample", "Kmeans_2_iter3")]) %>%
  mutate(Kmeans_2_iter3 = ifelse(Kmeans_2_iter3 == 3, "Core A", Kmeans_2_iter3)) %>%
  mutate(Kmeans_2_iter3 = ifelse(Kmeans_2_iter3 == 1, "Core C", Kmeans_2_iter3)) %>%
  mutate(Kmeans_2_iter3 = ifelse(Kmeans_2_iter3 == 2, "Core B", Kmeans_2_iter3)) %>%
  mutate(Core_Outgroup = ifelse(Kmeans_2_iter3 %in% c("Core A", "Core B", "Core C"),
                                Kmeans_2_iter3, Outgroup))

pca_aug <- pca_aug %>%
  #select(-Kmeans_2:-Kmediods_5) %>%
  left_join(core_stat_clusters[, c("Sample", "Kmeans_2_iter3")]) %>%
  mutate(Kmeans_2_iter3 = ifelse(Kmeans_2_iter3 == 3, "Core A", Kmeans_2_iter3)) %>%
  mutate(Kmeans_2_iter3 = ifelse(Kmeans_2_iter3 == 1, "Core C", Kmeans_2_iter3)) %>%
  mutate(Kmeans_2_iter3 = ifelse(Kmeans_2_iter3 == 2, "Core B", Kmeans_2_iter3)) %>%
  mutate(Core_Outgroup = ifelse(Kmeans_2_iter3 %in% c("Core A", "Core B", "Core C"),
                                Kmeans_2_iter3, Outgroup))

pca_aug <- pca_aug %>%
  mutate(Core_ABC = Kmeans_2_iter3) %>%
  mutate(Kmeans_2_iter3 = NULL)

# Plot Core A, B, C
pca_aug %>%
  filter(!is.na(Core_ABC)) %>%
  ggplot(aes(x = .fittedPC1, y = .fittedPC2, color = Core_ABC, shape = Core_ABC)) +
  geom_point() +
  stat_ellipse(level = 0.9) +
  scale_shape_manual(values=c(2, 15, 18)) +
  scale_fill_manual(values = c("black", "black", "black",
                              "black", "black", "black")) +
  scale_color_manual(values = c("black", "black", "black", "black", "black", "black")) +
  xlab("Principal Component 1") +
  ylab("Principal Component 2") +
  theme_bw()

# Out of the original 416 Core sherds, we've now identified three sub-groups - Core A, B, & C
# Core B and C are quite small, but that they could be removed from the main Core group
# is instructive of variation within the core group.
# Next, we'll set about searching for structure within the Core A Sub-Group

##### Core A Sub-Group Structure #####

# Append Kmeans_2 + Core groups to PC data
core_pc1to12_samps <- core_pc1to12_samps %>%
  left_join(pca_aug[,c("Sample", "Core_ABC", "Site")], by = "Sample")

# Extract the Core A Sherds

```

```

core_A <- core_pc1to12_samps %>%
  filter(Core_ABC == "Core A")

# First 12 PCs of Core A sherds
core_A_pc1to12 <- core_A %>% select(.fittedPC1:.fittedPC12)

# No obvious structure by vessel class or by geography or by site
core_A %>%
  left_join(pca_aug[, c(2, 6, 9)], by = "Sample") %>%
  ggplot(aes(x = .fittedPC1, y = .fittedPC2, color = Geography_2, shape = Geography_2)) +
  #ggplot(aes(x = .fittedPC1, y = .fittedPC2, color = Vessel_Class, shape = Vessel_Class)) +
  #ggplot(aes(x = .fittedPC1, y = .fittedPC2, color = Site))
  geom_point() +
  stat_ellipse(level = .9)

# Explore Core sherds
pca_aug %>%
  select(Sample, Site, Outgroup, Cultural_Group, Vessel_Class,
         Geography_2, Core_Outgroup, Core_ABC) %>%
  group_by(Core_Outgroup, Site) %>%
  summarize(n = n()) %>% View()

# Elbow Method
fviz_nbclust(core_A_pc1to12, kmeans, method = "wss") # 4 - 6 optimal clusters; 4 Looks good
# Silhouette Method
fviz_nbclust(core_A_pc1to12, kmeans, method = "silhouette") # 2 optimal clusters

# Ward Linkage hierarchical agglomerative clustering
plot(as.dendrogram(hclust(dist(core_A_pc1to12), method = "ward.D")),
     cex.axis = 0.75, cex.lab = 0.75, nodePar = list(lab.cex = 0.5, pch = NA))
# Two or three primary clusters seems optimal here

# 2 Cluster K-means for Core A
coreAkmean2 <- kmeans(core_A_pc1to12,
  centers = 2, # number of clusters
  nstart = 50, # number of random initial configurations
  # out of which the best one is chosen
  iter.max = 500) # number of allowable iterations allowed

# Visualize 2 cluster kmeans
fviz_cluster(coreAkmean2, data = core_A_pc1to12)

# Visualize a two cluster kmedoids solution
fviz_cluster(pam(core_A_pc1to12, 2), data = core_A_pc1to12)

## From all of this cluster analysis, it seems to me that the kmedoids 2 cluster solution
# captures separation in the data that can be best refined via Mahalanobis distance
coreA_pam2 <- pam(core_A_pc1to12, 2)

# Record kmeans Core A clustering assignments
core_A <- core_A %>%
  mutate(Kmedoids_2 = coreA_pam2$cluster)

```

```

# Group probabilities for the core kmeans 2 cluster solution on PC's 1 to 12
# (90% of variability)
core_A_kmed2_group_prob <- group.mem.probs(core_A_pc1to12, core_A$Kmedoids_2,
                                         unique(core_A$Kmedoids_2))

# Create list of data that is grouped the same as the group probability list
core_A_kmed2_list <- split(core_A[, c("Sample", "Kmedoids_2")],
                          f = core_A$Kmedoids_2)

# Convert the matrices of group membership probabilities to data frames and bind rows
# into one data frame
core_A_kmed2_group_prob <- map(core_A_kmed2_group_prob, as.data.frame) %>% bind_rows()

# Convert the list of matrices of sample names to data frames and bind into one data frame
core_A_kmed2_df <- map(core_A_kmed2_list, as.data.frame) %>% bind_rows()

# Bind to initial sample id and group assignment
# and convert to data frame for easier handling
core_A_kmed2_group_prob <- as.data.frame(bind_cols(core_A_kmed2_group_prob,
                                                  core_A_kmed2_df))

# New column of membership probability for initially assigned group
core_A_kmed2_group_prob$assigned_val <- core_A_kmed2_group_prob[1:2][cbind(seq_len(nrow(core_A
_kmed2_group_prob)), as.numeric(core_A_kmed2_group_prob$Kmedoids_2))]

# Set the initial group assignment value to zero to allow for comparisons
core_A_kmed2_group_prob[cbind(seq_len(nrow(core_A_kmed2_group_prob)),
                              as.numeric(core_A_kmed2_group_prob$Kmedoids_2))] <- 0

# Assess membership probabilities using an outlier heuristic of less than 10% probability
# in another group
core_A_kmed2_group_prob_iter1 <- core_A_kmed2_group_prob %>%
  mutate(new_assign = ifelse(assigned_val > 10 & `1` < 10 & `2` < 10,
                             Kmedoids_2, "Core A")) %>%
  #summarize(perc_unassigned = sum(new_assign == Kmedoids_2)/n() * 100)
  mutate(Kmedoids_iter1 = new_assign) %>%
  select(Sample, Kmedoids_iter1)
# Results in a 57.85% remaining in their Kmedoids assignment - suggests a good
# cluster solution

### End Iteration 1 of Core A group structure membership probabilities

# Append retained Kmed_2 sherds to PC data
core_A <- core_A %>%
  left_join(core_A_kmed2_group_prob_iter1, by = "Sample")

# PC data for Core A group membership probabilities iteration 2
core_A_iter1pc1to12 <- core_A %>%
  filter(Kmedoids_iter1 != "Core A") %>%
  select(.fittedPC1:.fittedPC12)

# Group Membership data for kmeds iteration 2 Core A
core_A_iter2 <- core_A %>% filter(Kmedoids_iter1 != "Core A")

```

```

# Group probabilities for the core kmeans 2 cluster solution on PC's 1 to 12 (90% of
# variability)
core_A_kmed2_group_prob_iter2 <- group.mem.probs(core_A_iter1pc1to12, core_A_iter2$Kmedoids_ite
er1,
                                         unique(core_A_iter2$Kmedoids_iter1))

# Create list of data that is grouped the same as the group probability list
core_A_kmed2_iter_list <- split(core_A_iter2[, c("Sample", "Kmedoids_iter1")],
                               f = core_A_iter2$Kmedoids_2)

# Convert the matrices of group membership probabilities to data frames and bind rows into
# one data frame
core_A_kmed2_group_prob_iter2 <- map(core_A_kmed2_group_prob_iter2, as.data.frame) %>% bind_ro
ws()

# Convert the list of matrices of sample names to data frames and bind into one data frame
core_A_kmed2_group_prob <- map(core_A_kmed2_iter_list, as.data.frame) %>% bind_rows()

# Bind to initial sample id and group assignment
# and convert to data frame for easier handling
core_A_kmed2_group_prob_iter2 <- as.data.frame(bind_cols(core_A_kmed2_group_prob_iter2,
                                                         core_A_kmed2_group_prob))

# New column of membership probability for initially assigned group
core_A_kmed2_group_prob_iter2$assigned_val <- core_A_kmed2_group_prob_iter2[1:2][cbind(seq_len
(nrow(core_A_kmed2_group_prob_iter2)), as.numeric(core_A_kmed2_group_prob_iter2$Kmedoids_iter1
))]

# Set the initial group assignment value to zero to allow for comparisons
core_A_kmed2_group_prob_iter2[cbind(seq_len(nrow(core_A_kmed2_group_prob_iter2)),
                                     as.numeric(core_A_kmed2_group_prob_iter2$Kmedoids_iter1))] <- 0

# Assess membership probabilities using a tighter heuristic of less than 2.5% probability
# in another group and greater than 3% probability in-group
core_A_kmed2_group_prob_iter2 <- core_A_kmed2_group_prob_iter2 %>%
  mutate(new_assign = ifelse(assigned_val > 3 & `1` < 2.5 & `2` < 2.5,
                             Kmedoids_iter1, "Core A")) %>%
  #summarize(perc_assigned = sum(new_assign == Kmedoids_iter1)/n() * 100)
  mutate(Kmedoids_iter2 = new_assign) %>%
  #select(Sample, Kmedoids_iter2)
# Results in a 100% remaining in their Kmedoids iter1 assignment - suggests a great
# cluster solution

# Prep data for export
core_A_kmed2_group_prob_iter2_table <- core_A_kmed2_group_prob_iter2 %>%
  left_join(pca_aug[, c("Sample", "Site")]) %>%
  mutate(id = parse_number(Sample))

# Export csv of Core A1 and A2 Groups
write_csv(core_A_kmed2_group_prob_iter2_table, "Core A groups.csv")

```

```

# Make table of Core A1/A2 sherd assignments
core_A_kmed2_group_prob_iter2_table <- core_A_kmed2_group_prob_iter2_table %>%
  mutate(Core_A_Sub = paste0("Core A", Kmedoids_iter1))

# Bind the Core A1/A2 table to Core A PC data
core_A_subs <- core_A %>%
  left_join(core_A_kmed2_group_prob_iter2_table[, c("Sample", "Core_A_Sub")],
            by = "Sample") %>%
  mutate(Core_A_Sub = ifelse(is.na(Core_A_Sub), "Core A", Core_A_Sub)) %>%
  select(-Kmeans_2:-Kmeans_2_iter2, -Kmedoids_2)

# Plot of PC1 - PC2 of the Core A, A1, and A2 group assignments
core_A_subs %>%
  filter(Core_A_Sub == "Core A1" | Core_A_Sub == "Core A2") %>%
  ggplot(aes(x = .fittedPC1, y = .fittedPC2, color = Core_A_Sub, shape = Core_A_Sub)) +
  geom_point() +
  stat_ellipse(level = 0.9) +
  scale_shape_manual(values=c(43, 15, 18)) +
  scale_fill_manual(values = c("black", "black", "black",
                              "black", "black", "black")) +
  scale_color_manual(values = c("black", "black", "black",
                              "black", "black", "black")) +
  xlab("Principal Component 1") +
  ylab("Principal Component 2") +
  geom_point(data = filter(core_A_subs[, c(".fittedPC1", ".fittedPC2", "Core_A_Sub")],
                          Core_A_Sub == "Core A"),
            aes(x = .fittedPC1, y = .fittedPC2, alpha = 0.2)) +
  theme_bw()

# Add Core A sub-groups to pca data
sample_pca$data[[1]] <- sample_pca$data[[1]] %>%
  left_join(core_A_subs[, c("Sample", "Core_A_Sub")])

# Plot Core A and Core A sub-groups using autoplot
core_A_pc1pc2 <- sample_pca %>%
  mutate(
    pca_graph = map2(
      .x = pca,
      .y = data,
      ~ autoplot(.x, x = 1, y = 2, loadings = TRUE, loadings.label = TRUE,
                 scale = 0,
                 loadings.label.repel = TRUE,
                 loadings.label.colour = "black",
                 loadings.colour = "gray45",
                 loadings.label.alpha = 0.9,
                 loadings.label.size = 2.5,
                 loadings.label.hjust = -0.5,
                 #frame = TRUE,
                 #frame.type = "norm",
                 data = .y,
                 colour = "Core_A_Sub",
                 shape = "Core_A_Sub",
                 frame.level = .9,

```

```

        frame.alpha = 0.001,
        size = 2,
        alpha = .00001) +
    theme_bw() +
    # geom_text(Label = .y$Sample) +
    labs(x = "Principal Component 1",
         y = "Principal Component 2")
  )
) %>%
pull(pca_graph)

core_A_pc1pc2[[1]] +
  scale_fill_manual(values = c("black", "black", "black",
                              "black", "black", "black")) +
  scale_color_manual(values = c("black", "black", "black", "black", "black", "black")) +
  stat_ellipse(data = filter(sample_pca[["pca_aug"]][[1]],
                            !is.na(Core_A_Sub) | Core_A_Sub != "Core A"),
              aes(x = .fittedPC1, y = .fittedPC2, color = Core_A_Sub)) +
  scale_shape_manual(values=c(2, 15, 18, 43))

# Add Core A sub-group data to the augmented PCA data for Shiny app biplotting
# (using the above shiny app)
sample_pca[["pca_aug"]][[1]] <- sample_pca[["pca_aug"]][[1]] %>%
  left_join(core_A_subs[, c("Sample", "Core_A_Sub")],
            by = "Sample")

# Do the same to the non-list pca aug data object
pca_aug <- pca_aug %>%
  left_join(core_A_subs[, c("Sample", "Core_A_Sub")], by = "Sample") %>%
  mutate(Final_Assign = Core_A_Sub) %>%
  mutate(Final_Assign = ifelse(is.na(Core_A_Sub), Core_Outgroup, Core_A_Sub))

table(pca_aug$Final_Assign)

# Plot of Mg - Ni of the Core A, A1 and A2 group assignments
pca_aug %>%
  filter(Core_A_Sub == "Core A1" | Core_A_Sub == "Core A2") %>%
  ggplot(aes(x = Mg, y = Ni, color = Core_A_Sub, shape = Core_A_Sub)) +
  geom_point() +
  stat_ellipse(level = 0.9) +
  scale_shape_manual(values=c(43, 15, 18)) +
  scale_fill_manual(values = c("black", "black", "black",
                              "black", "black", "black")) +
  scale_color_manual(values = c("black", "black", "black",
                              "black", "black", "black")) +
  xlab("Magnesium (log base 10 ppm)") +
  ylab("Nickel (log base 10 ppm)") +
  geom_point(data = filter(pca_aug[, c("Mg", "Ni", "Mo", "Core_A_Sub")],
                          Core_A_Sub == "Core A"),
            aes(x = Mg, y = Ni, alpha = 0.2)) +
  theme_bw()

```

```

# Plot all assignments along PC1 and PC2
pca_aug %>%
  filter(Final_Assign != "unassigned") %>%
  ggplot(aes(x = .fittedPC1, y = .fittedPC2, color = Final_Assign)) +
  geom_point() +
  stat_ellipse(level = 0.9) +
  xlab("Principal Component 1") +
  ylab("Principal Component 2") +
  geom_point(data = filter(pca_aug, Final_Assign == "unassigned"),
             aes(x = .fittedPC1, y = .fittedPC2, color = Final_Assign, alpha = 0.4)) +
  theme_bw() +
  scale_color_d3()

# Plot all assignments along Mg and Mo
pca_aug %>%
  filter(Final_Assign != "unassigned") %>%
  ggplot(aes(x = Mg, y = Mo, color = Final_Assign)) +
  geom_point() +
  stat_ellipse(level = 0.9) +
  xlab("Mg (log base 10 ppm)") +
  ylab("Mo (log base 10 ppm)") +
  geom_point(data = filter(pca_aug, Final_Assign == "unassigned"),
             aes(x = Mg, y = Mo, color = Final_Assign, alpha = 0.4)) +
  theme_bw() +
  scale_color_d3()

# Append Final Assignments to PCA data
sample_pca$data[[1]] <- sample_pca$data[[1]] %>%
  left_join(pca_aug[, c("Sample", "Final_Assign")])

# Plot Core A and Core A sub-groups using autoplot
final_assign_pc1pc2 <- sample_pca %>%
  mutate(
    pca_graph = map2(
      .x = pca,
      .y = data,
      ~ autoplot(.x, x = 1, y = 2, loadings = TRUE, loadings.label = TRUE,
                 scale = 0,
                 loadings.label.repel = TRUE,
                 loadings.label.colour = "black",
                 loadings.colour = "gray25",
                 loadings.label.alpha = 0.9,
                 loadings.label.size = 3.5,
                 #Loadings.Label.hjust = -0.5,
                 frame = TRUE,
                 frame.type = "norm",
                 data = .y,
                 colour = "Final_Assign",
                 #shape = "Final_Assign",
                 frame.level = .9,
                 frame.alpha = 0.001,
                 size = 2,
                 alpha = .3) +

```

```

    theme_bw() +
    # geom_text(Label = .y$Sample) +
    labs(x = "Principal Component 1",
         y = "Principal Component 2")
  )
) %>%
pull(pca_graph)

final_assign_pc1pc2[[1]] +
  theme_bw() +
  scale_color_d3()

# Averages and standard deviations of each of the identified compositional groups
pca_aug %>%
  select(Final_Assign, Si:Th) %>%
  gather(Element, Si:Th, -Final_Assign) %>%
  mutate(`Si:Th` = 10^`Si:Th`) %>% # convert from Log 10
  group_by(Final_Assign, Element) %>%
  summarize(mean = mean(`Si:Th`, na.rm = TRUE), std = sd(`Si:Th`, na.rm = TRUE)) %>%
  write_csv("Ceramic final group assignment element ave and std.csv")

# Pickup here with a PCA graph of Core A1 and A2 sherds as well as a table of membership
# probs for both of these groups

# Next step is to start a new script that looks at constructing networks based on BR
# coefs of similarities in site-based representation in the different groups
# (Outgroup 1, Outgroup 2, Core A, Core A1, Core A1, Core B and Core C)

# Table of all group assignments by site
group_assign_by_site <- pca_aug %>%
  select(Sample, Site, Final_Assign) %>%
  group_by(Final_Assign, Site) %>%
  summarize(count = n()) %>%
  spread(Final_Assign, count)

# Table of all group assignments by site AND geography
group_assign_by_site_geo <- pca_aug %>%
  select(Sample, Site, Final_Assign, Geography_2, Time) %>%
  group_by(Final_Assign, Site, Geography_2, Time) %>%
  summarize(count = n()) %>%
  spread(Final_Assign, count)

group_assign_by_geo_class <- pca_aug %>%
  select(Sample, Final_Assign, Geography_2, Vessel_Class) %>%
  group_by(Final_Assign, Geography_2, Vessel_Class) %>%
  summarize(count = n()) %>%
  spread(Final_Assign, count)

# Confirm assignments
colSums(group_assign_by_site[, -1], na.rm = TRUE)
table(pca_aug$Final_Assign)

```

```

# Regression of the number of compositional groups as a function of sample size
# Also included are lines to look at potential differences in the average number of
# compositional groups by geography of site or time period of occupation
group_assign_by_site %>%
  select(1, 3:8) %>%
  mutate(group_count = rowSums(!is.na(.))) %>%
  mutate(group_count = group_count - 1) %>% # need to subtract the Site col
  #left_join(group_assign_by_site_geo[c(1:3)]) %>%
  #group_by(Geography_2, Time) %>%
  #summarize(avg_group = mean(group_count)) # check average group count
  mutate(sample_size = rowSums(.[2:7], na.rm = TRUE)) %>%
  #ggplot(aes(x = sample_size, y = group_count)) +
  #geom_point() +
  #geom_smooth(method = "lm")
  lm(group_count ~ sample_size, data = .) %>%
  glance()

# Write out csv file of group assignments
# write_csv(group_assign_by_site, "group assignments by site.csv")
# write_csv(group_assign_by_site_geo, "group assignments by site-geo.csv")
# write_csv(group_assign_by_geo_class, "group assignments by geo-vessel class.csv")

pca_aug %>%
  filter(Final_Assign == "Core A2") %>% View()

# Component loadings for first 12 principal components
pc_loadings <- sample_pca$pca[[1]]$rotation %>%
  as.data.frame() %>%
  rownames_to_column(var = "element") %>%
  select(element:PC12)

# write_csv(pc_loadings, "pc1 - 12 loadings.csv")

```

Creation of Economic Networks from Compositional Membership Data

```

## Turning membership in LA-ICP-MS compositional groups into networks of economic
# relationships

#' The basic idea here is that, leveraging the criterion of abundance (Bishop et al., 1982),
#' as similarities in membership in different compositional groups increases between
#' archaeological communities, so does the likelihood that individuals from those
#' communities are engaging in direct economic interactions. As used here, economic
#' interactions are built around the concept of weak ties (Granovetter 1973). In contrast
#' to ties that are built on deep affinity such as close friendships, family or marriage
#' relationships, weak ties might be acquaintances or a stranger with a common cultural
#' background. Weak ties emanating from economic relationships related to
#' ceramic industry are constructed through such behaviors as exchange relationships,
#' overlapping resource exploitation areas, or similar production regimes.
#'
#' Using the Brainerd Robinson coefficient of similarity, it is possible to create networks
#' of economic relationships through community-based membership in compositional groups.

```

```

#' That is, beginning with raw elemental data produced from LA-ICP-MS of 543 ceramic
#' artifacts, several compositional groups were identified in the Late Prehistoric central
#' Illinois River valley.
#' The Brainerd Robinson coefficient of similarity assesses how similar any two given sites
#' are based on similarities in the number of individual sherd assignments in different
#' compositional groups. This method provides means to model relational economic interactions
#' in an archaeological region.

# Statistically robust compositional groups were identified in `Ceramic Analysis.R`.
# Beginning with hose counts, we'll clean the data and apply the Brainerd Robinson
# coefficient of similarity.
# Networks are then constructed and analyzed to reveal changing patterns of economic
# relationships in Illinois' archaeological heritage.

# First, we'll load in some package libraries
library(tidyverse)
library(igraph)
library(corrplot)
library(reshape2)

# Then read in compositional group count data by site
comp_group <- read_csv("group assignments by site.csv")

# Two of the eight compositional groups are based on equivocal membership probabilities
# While a core group was extracted and refined, we need to drop the sherds that were
# unable to be assigned to a core sub-group as well as those that were not able to be
# assigned to any other group.
comp_group_refined <- comp_group %>%
  select(-`Core A`, -unassigned)

# Sum up all of the retained sherds for compositional group construction
comp_group_refined %>%
  gather(key = Site, value = `Core A1`:`Outgroup 2`) %>%
  rename(count = "`Core A1`:`Outgroup 2`") %>%
  summarize(total_count = sum(count, na.rm = TRUE))
# Total is 314 out of the original 543, or 63% of the original data set

# Look at total number of sherds from each site
comp_group_refined %>%
  gather(key = group, value = `Core A`:`Outgroup 2`, -Site) %>%
  rename(count = "`Core A`:`Outgroup 2`") %>%
  group_by(Site) %>%
  summarize(total = sum(count, na.rm = TRUE))
# Perhaps the most problematic site here is Star Bridge, which had a massive drop from
# ~30 or so sherds analyzed but only 9 placed within compositional groups.
# Nevertheless, all 18 sites are represented by at least 8 sherds - not too bad.

# The Brainerd-Robinson coefficient is a similarity metric that is unique to archaeology,
# and is used to compare assemblages based on proportions of categorical data such as
# vessel or point types.

# The Brainerd-Robinson coefficient has been coded in R by Matt Peeples
# (http://www.mattpeeples.net/BR.html) and by Gianmarco Alberti

```

```

# (http://cainarchaeology.weebly.com/r-function-for-brainerd-robinson-similarity-coefficient.h
# tml).
# Here, I follow Matt Peeples's BRsim implementation because it is substantially less resource
# intensive. However, I include a rescaling feature to rescale the BR coefficients
# from 0 - 200 to 0 - 1, which makes the output amenable for the construction
# of network graphs.

# The input for the function is a dataframe with assemblages to be compared are found in
# the rows and the categorical variables (such as pottery/lithic types, objects,
# compositional groups, etc.) comprise the columns. Each variable is the numerical
# amount of a particular categorical variable found at each site/sample/discrete
# observation unit.

# Here is the BRsim function as coded by Gianmarco
BRsim <- function(x, correction, rescale) {
  if(require(corrplot)){
    print("corrplot package already installed. Good!")
  } else {
    print("trying to install corrplot package..")
    install.packages("corrplot", dependencies=TRUE)
    suppressPackageStartupMessages(require(corrplot))
  }
  rd <- dim(x)[1]
  results <- matrix(0, rd, rd)
  if (correction == T){
    for (s1 in 1:rd) {
      for (s2 in 1:rd) {
        zero.categ.a <-length(which(x[s1,] == 0))
        zero.categ.b <-length(which(x[s2,] == 0))
        joint.absence <-sum(colSums(rbind(x[s1,], x[s2,])) == 0)
        if(zero.categ.a == zero.categ.b) {
          divisor.final <- 1
        } else {
          divisor.final <- max(zero.categ.a, zero.categ.b) - joint.absence+0.5
        }
        results[s1,s2] <- round(((1 - (sum(abs(x[s1,] / sum(x[s1,]) - x[s2,] / sum(x[s2,]))) / 2
)/divisor.final,
                                digits=3)
      )
    }
  } else {
    for (s1 in 1:rd) {
      for (s2 in 1:rd) {
        results[s1,s2] <- round(1 - (sum(abs(x[s1,] / sum(x[s1,]) - x[s2, ] / sum(x[s2,]))) / 2
, digits=3)
      )
    }
  }
  rownames(results) <- rownames(x)
  colnames(results) <- rownames(x)
  col1 <- colorRampPalette(c("#7F0000", "red", "#FF7F00", "yellow", "white", "cyan", "#007FFF"
, "blue", "#00007F"))
  if (rescale == F) {

```

```

upper <- 200
results <- results * 200
} else {
  upper <- 1.0
}
corrplot(results, method="square", addCoef.col="red", is.corr=FALSE, cl.lim = c(0, upper), c
ol = col1(100), tl.col="black", tl.cex=0.8)
return(results)
}

```

*# Here is a more simplified version from Matt Peeples
Function for calculating Brainerd-Robinson (BR) coefficients
Note there is data pre-processing for Matt's script not included here

```

BR <- function(x) {
  rd <- dim(x)[1]
  results <- matrix(0,rd,rd)
  for (s1 in 1:rd) {
    for (s2 in 1:rd) {
      x1Temp <- as.numeric(x[s1, ])
      x2Temp <- as.numeric(x[s2, ])
      br.temp <- 0
      results[s1,s2] <- 200 - (sum(abs(x1Temp - x2Temp))))}
  row.names(results) <- row.names(x)
  colnames(results) <- row.names(x)
  return(results)}

```

My editing of the two

```

BR_au <- function(x, rescale = FALSE, counts = TRUE) {
  if (counts == T){
    x <- prop.table(as.matrix(x), 1) * 100
  } else {
  }
  rd <- dim(x)[1]
  results <- matrix(0,rd,rd)
  for (s1 in 1:rd) {
    for (s2 in 1:rd) {
      x1Temp <- as.numeric(x[s1, ])
      x2Temp <- as.numeric(x[s2, ])
      br.temp <- 0
      results[s1,s2] <- 200 - (sum(abs(x1Temp - x2Temp)))
    }
  }
  row.names(results) <- row.names(x)
  colnames(results) <- row.names(x)
  if (rescale == F) {
    return(results)
  } else {
    results <- results / 200
    return(results)
  }
}

```

Before we run the BR functions, the data frame needs to have the Sites become a row name

```

# because the BR functions all take as inputs counts or percentages only.
rownames(comp_group_refined) <- comp_group_refined$Site
comp_group_refined <- comp_group_refined[, -1]

# Also need to change NAs into 0 (two methods provided below)
comp_group_refined <- comp_group_refined %>%
  mutate_all(funs(replace(., is.na(.), 0)))

#   comp_group_refined %>%
#     mutate_all(funs(coalesce(., 0L)))

# Lost the rownames during manipulation, need to add them again
rownames(comp_group_refined) <- comp_group$Site

# A big advantage of Gianmarco's BR function is a succinct correlation plot. It can be
# thought of as a "heat-map" for BR similarities.
BRsim(comp_group_refined, correction = FALSE, rescale = TRUE)

eco_BR <- BR_au(comp_group_refined, rescale = TRUE)

# The results of the BRsim function come in the form of an adjacency matrix. igraph
# can easily handle this kind of data to create a network graph. Because the adjacency
# matrix is between 0 and 1, we need to tell igraph that the resulting network graph is
# weighted. Otherwise an edge will only be given for the relationship between each site
# and itself.
ecoBRgraph <- graph_from_adjacency_matrix(eco_BR, weighted = T)
BRrel <- as_edgelist(ecoBRgraph) # convert to 2 column edgelist
BRw <- as.data.frame(E(ecoBRgraph)$weight) # extract edge weights
BRwel <- cbind(BRrel, BRw) # append edge weights to edgelist
BRwel <- rename(BRwel, weight = `E(ecoBRgraph)$weight`) # rename weight column

# Assessing the distribution of the BR coefficients
BRwel %>%
  filter(`1` != `2`) %>% # drop recursive edges
  ggplot(aes(x = weight)) +
  geom_histogram(aes(y = ..density..), bins = 25, colour = "black", fill = "white") +
  geom_density(alpha = 0.2) +
  geom_vline(aes(xintercept = mean(weight, na.rm = T)), # Ignore NA values for mean
             color = "red", linetype = "dashed", size = 1) +
  xlab("Rescaled BR Coefficients") +
  ylab("Density") +
  theme_minimal()

# Mean of BR coefficients (this will be used as a cutoff point for giving edges)
BRwel %>%
  filter(`1` != `2`) %>%
  filter(weight != 1) %>%
  filter(weight != 0) %>%
  summarise(Mean = mean(weight))
# Looks like the mean is 0.556. This can be round down to 0.55 for edge cutoffs

# But before we apply that cutoff, Let's explore the range and frequency of BR

```

```

# scores if they were produced purely by chance based on our data set

# First, we will row and column randomize the BR input 10,000 times and create a List
# of the results
# This means that we'll shuffle the order of row and column data with replacement
BReco_rand_list <- replicate(10000, comp_group_refined[sample(1:nrow(comp_group_refined),
                                                           replace = T),
                                                           sample(1:ncol(comp_group_refined),
                                                           replace = T)], simplify = F)

# Setup an empty List to hold the BR coefficients for the randomized data
BReco_rand_result <- list()

# Number of simulations
nsim <- 10000

# Now we can iterate the BR algorithm over the randomized Lists
for (i in 1:nsim) {
  BReco_rand_result[[i]] <- BR_au(BReco_rand_list[[i]], rescale = T)
}

# Turn adjacency matrices into three column data frames
for (i in 1:nsim) {
  BReco_rand_result[[i]] <- setNames(melt(BReco_rand_result[[i]]), c('1', '2', 'values'))
}

# Now we can extract the BR values from the data frames in the List
BReco_rand_result_vals <- lapply(BReco_rand_result, '[[', 3)

# And collapse that List into one long vector and turn into a tibble data frame
BReco_rand_vals <- tbl_df(unlist(BReco_rand_result_vals))

# Add a column to indicate these are simulated data
BReco_rand_vals <- BReco_rand_vals %>%
  mutate(Type = "Randomized BR")

# Append the actual data
BRwel <- tbl_df(BRwel)
BReco_vals_all <- BRwel %>%
  select(weight) %>%
  mutate(value = weight) %>%
  select(value) %>%
  mutate(Type = "Actual BR") %>%
  bind_rows(., BReco_rand_vals)

# Drop 0's and 1's since no sites are perfectly dissimilar or similar
BReco_vals_all <- BReco_vals_all %>%
  filter(value != 1) %>%
  filter(value != 0)

# Plot density histograms of the observed and simulated BR coefficients
ggplot(BReco_vals_all, aes(x = value)) +
  geom_histogram(data = subset(BReco_vals_all, Type == "Randomized BR"), aes(y=..density..),

```

```

    alpha = 0.5, bins = 30, colour = "black", fill = "#2ca02c") +
geom_density(data = subset(BReco_vals_all, Type == "Randomized BR"),
  alpha = 0.1, color = "#2ca02c" , fill = "#2ca02c" , adjust = 2.5) +
geom_vline(data = subset(BReco_vals_all, Type == "Randomized BR"),
  aes(xintercept = mean(value, na.rm = T)), # Ignore NA values for mean
  color = "#2ca02c" , linetype = "dashed", size = 1) +
geom_histogram(data = subset(BReco_vals_all, Type == "Actual BR"),
  aes(y = ..density..), bins = 30, colour = "black",
  fill = "#1f77b4" , alpha = 0.4) +
geom_density(data = subset(BReco_vals_all, Type == "Actual BR"),
  alpha = 0.1, color = "#1f77b4" , fill = "#1f77b4" ) +
geom_vline(data = subset(BReco_vals_all, Type == "Actual BR"),
  aes(xintercept = mean(value, na.rm = T)), color = "#1f77b4" ,
  linetype = "dashed", size = 1) +
xlab("Rescaled BR Coefficients") +
ylab("Density") +
theme_minimal()

# "#1f77b4" = d3 blue
# "#2ca02c" = d3 green

# Looks like the simulated and observed data actually share similar distributions.
# Nevertheless, there are significant nuances seen in the observed data, suggesting
# deviations from random chance and a slightly lower than expected mean BR
# coefficient. This could reflect the small number of compositional groups (6),
# limited number of samples from a few sites (some have 8 or 9 samples), or
# simply a reflection of the limited geological diversity present in the CIRV.
# However, applying the the > 0.55 cutoff indicates that edges will be
# given in situations where the proportional similarity between two assemblages is
# greater than the average proportional similarity across economic relationships in
# the Late Prehistoric CIRV.

# Let's apply the 0.55 threshold
BRel_t <- BRwel %>%
  filter(weight > 0.55 & `1` != `2`)

# Change column names to be suitable for Gephi
colnames(BRel_t) <- c("Source", "Target", "weight")

# Add columns with additional node information
# Read in tables of site names, geographic coords., and time distinction
# For time, 1 is a primary occupation prior to Oneota in-migration
# and 2 is a primary occupation succeeding Oneota in-migration
node_table <- read_csv("Jar_node_table.csv")
colnames(node_table) <- c("Source", "Label", "Long", "Lat", "Time")

# Join the node table columns to the edgelist by the Source node
econet_t1 <- left_join(BRel_t, node_table[-2], by = "Source")

# Prepare node tables to join time designation for the target node
colnames(node_table) <- c("Target", "Label", "Long", "Lat", "Time2")

# Join Time 2 column to Target node

```

```

econet_edgelist_complete <- left_join(econet_t1, node_table[c(-2:-4)], by = "Target")

# Create Pre- and Post-Migration Edgelist
econet_pre_el_need_dist <- econet_edgelist_complete %>%
  filter(Time == Time2) %>%
  filter(Time == 1)

econet_post_el_need_Law <- econet_edgelist_complete %>%
  filter(Time == Time2) %>%
  filter(Time == 2)

# Two sites have extended or multi-component occupations in both time periods
# So we need to include their connections in both time periods
Law_econet_post <- econet_edgelist_complete %>%
  filter(Time == 2 & Target == "Lawrenz Gun Club" |
         Source == "Lawrenz Gun Club" & Time2 == 2) %>%
  mutate(Time = replace(Time, Time == 1, 2)) %>%
  mutate(Time2 = replace(Time2, Time2 == 1, 2))

Buck_econet_post <- econet_edgelist_complete %>%
  filter(Time == 2 & Target == "Buckeye Bend" |
         Source == "Buckeye Bend" & Time2 == 2) %>%
  mutate(Time = replace(Time, Time == 1, 2)) %>%
  mutate(Time2 = replace(Time2, Time2 == 1, 2))

# Bind the LCG & Buckeye post-migration edges to the post-migration edgelist
econet_post_el_need_dist <- rbind(econet_post_el_need_Law, Law_econet_post, Buck_econet_post)

# Adding geographic coordinates
# Read in matrix of site distances
site_distances <- read_csv("Site Distances Matrix in km.csv")

#first column of site names to rownames
site_distances <- column_to_rownames(site_distances, var = "X1")

# Convert geographic distance matrix to graph object
distance_g <- graph_from_adjacency_matrix(as.matrix(site_distances), weighted = TRUE,
                                         mode = "directed")

# Convert geo distance graph object to edgelist
distance_el <- as_edgelist(distance_g)
distance_el_weight <- as.numeric(E(distance_g)$weight)
distance_el <- tbl_df(cbind(distance_el, distance_el_weight))
colnames(distance_el) <- c("Source", "Target", "weight")
distance_el$Distance <- as.numeric(distance_el$weight)

# Merge the geographic distance edgelist with directed plate edgelist
econet_pre_el_complete <- merge(econet_pre_el_need_dist, distance_el[-3])
econet_post_el_complete <- merge(econet_post_el_need_dist, distance_el[-3])

# Combine the pre- and post-migration data sets into a single edgelist
econet_el_BR_all_time_complete <- rbind(econet_pre_el_complete, econet_post_el_complete)

```

```

# Finally, we can export the complete edgelist for visualization in Gephi
write_csv(econet_el_BR_all_time_complete, "Economic_network_BR_edgelist_complete_.csv")

#### Undirected Economic Networks ####

# The edgelists created thus far have been directed. Since we are disregarding
# directionality, it is important to account for duplicate edges.
BRgraph_un <- graph_from_adjacency_matrix(eco_BR, weighted = T, mode = "undirected")

# Create undirected edgelist
BRel_un <- as_edgelist(BRgraph_un)

# Create the weights and format as a data frame for column binding
BRw_un <- E(BRgraph_un)$weight
BRw_un <- as.data.frame(BRw_un)

# Add the weights, and viola we have a weighted, directed edgelist for proportional
# stylistic similarity between sites.
BRel_un <- cbind(BRel_un, BRw_un)

# Write out complete Brainerd Robinson edgelist
write_csv(BRel_un, "complete_ECO_BR_UNDIRECTED_edgelist.csv")

# Apply our threshold of > 0.4 so that we only give UNDIRECTED edges to the strongest
# proportional relationship. We can use dplyr to wrangle the edgelist and also drop
# recursive edges.
BRel_t_un <- BRel_un %>%
  filter(BRw_un > 0.55 & BRel_un[1] != BRel_un[2])

# Change column names to be suitable for Gephi
colnames(BRel_t_un) <- c("Source", "Target", "weight")

colnames(node_table) <- c("Source", "Label", "Long", "Lat", "Time")

# Join the node table columns to the edgelist by the Source node
eco_t1_un <- left_join(BRel_t_un, node_table[-2], by = "Source")

# Prepare node tables to join time designation for the target node
colnames(node_table) <- c("Target", "Label", "Long", "Lat", "Time2")

# Join Time 2 column to Target node
econet_edgelist_complete_un <- left_join(eco_t1_un, node_table[c(-2:-4)], by = "Target")

# Create Pre- and Post-Migration Edgelists
econet_pre_el_need_dist_un <- econet_edgelist_complete_un %>%
  filter(Time == Time2) %>%
  filter(Time == 1)

econet_post_el_need_Law_un <- econet_edgelist_complete_un %>%
  filter(Time == Time2) %>%
  filter(Time == 2)

# Two sites have extended or multi-component occupations in both time periods

```

```

# So we need to include their connections in both time periods
Law_econet_post_un <- econet_edgelist_complete_un %>%
  filter(Time == 2 & Target == "Lawrenz Gun Club" |
         Source == "Lawrenz Gun Club" & Time2 == 2) %>%
  mutate(Time = replace(Time, Time == 1, 2)) %>%
  mutate(Time2 = replace(Time2, Time2 == 1, 2))

Buck_econet_post_un <- econet_edgelist_complete_un %>%
  filter(Time == 2 & Target == "Buckeye Bend" |
         Source == "Buckeye Bend" & Time2 == 2) %>%
  mutate(Time = replace(Time, Time == 1, 2)) %>%
  mutate(Time2 = replace(Time2, Time2 == 1, 2))

# Bind the LCG & Buckeye post-migration edges to the post-migration edgelists
econet_post_el_need_dist_un <- rbind(econet_post_el_need_Law_un,
                                     Law_econet_post_un, Buck_econet_post_un)

# Merge the geographic distance edgelist with undirected plate edgelists
econet_pre_el_complete_un <- merge(econet_pre_el_need_dist_un, distance_el[-3])
econet_post_el_complete_un <- merge(econet_post_el_need_dist_un, distance_el[-3])

# Combine the pre- and post-migration data sets into a single edgelist
econet_el_BR_all_time_complete_un <- rbind(econet_pre_el_complete_un,
                                           econet_post_el_complete_un)

# Finally, we can export the complete undirected edgelist for visualization in Gephi
write_csv(econet_el_BR_all_time_complete_un, "Econet_BR_UNDIRECTED_edgelist_complete.csv")
write_csv(econet_pre_el_complete_un, "Econet_BR_UNDIRECTED_edgelist_pre-migration.csv")
write_csv(econet_post_el_complete_un, "Econet_BR_UNDIRECTED_edgelist_post-migration.csv")

```

CIRV Economic Network Analysis

```

# Geochemical compositional group economic network statistics

library(tidyverse)
library(readxl)
library(broom)
library(igraph)
library(cowplot)

#-----Economic BR Network Stats-----####

# Read in finalized, undirected economic BR edgelist
BReco_el_un <- read_csv("Econet_BR_UNDIRECTED_edgelist_complete.csv")

# Read in finalized, undirected pre-migration BR edgelist
BReco_el_un_pre <- read_csv("Econet_BR_UNDIRECTED_edgelist_pre-migration.csv")

# Read in finalized, undirected post-migration BR edgelist
BReco_el_un_post <- read_csv("Econet_BR_UNDIRECTED_edgelist_post-migration.csv")

```

```

# Convert to igraph graph
BReco_g <- graph_from_edgelist(as.matrix(BReco_el_un[, c(1:2)]), directed = FALSE)
BReco_g_pre <- graph_from_edgelist(as.matrix(BReco_el_un_pre[, c(1:2)]), directed = FALSE)
BReco_g_post <- graph_from_edgelist(as.matrix(BReco_el_un_post[, c(1:2)]), directed = FALSE)

# Assign edge weights to graph
E(BReco_g)$weight <- BReco_el_un$weight
E(BReco_g_pre)$weight <- BReco_el_un_pre$weight
E(BReco_g_post)$weight <- BReco_el_un_post$weight

# Function to calculate degree, betweenness, closeness, and eigenvector centrality
# for a graph and return a data frame with the scores
centr_all <- function(graph, g_name = "Score") {

  # Check that graph is an igraph object
  if (!is_igraph(graph)) {
    stop("Not a graph object")
  }

  # Name of graph
  g_name <- as.character(g_name)

  # Degree centralization
  res_centr <- centr_degree(graph)$centralization

  # Betweenness centralization
  res_centr[2] <- centr_betw(graph)$centralization

  # Closeness centralization
  res_centr[3] <- centr_clo(graph)$centralization

  # Eigenvector centralization
  res_centr[4] <- centr_eigen(graph)$centralization

  res_centr <- t(as.data.frame(res_centr))

  # Table of scores
  colnames(res_centr) <- c("Degree", "Betweenness", "Closeness", "Eigenvector")
  rownames(res_centr) <- g_name

  res_centr
}

# Calculate centralization scores for each graph
all_centr <- centr_all(BReco_g, g_name = "Flattened Across Time")
pre_centr <- centr_all(BReco_g_pre, g_name = "Pre-Migration")
post_centr <- centr_all(BReco_g_post, g_name = "Post-Migration")
rbind(pre_centr, post_centr, all_centr)

# Calculated Mean Weighted Degree (or strength)
mean(strength(BReco_g))
mean(strength(BReco_g_pre))

```

```

mean(strength(BReco_g_post))

## The following network statistics were calculated in Gephi 0.9.2:
# Average Degree, Avg. Weighted Degree, Avg. Clustering Coefficient, Avg. Path Length,
# Graph Density, Network Diameter

#-----Edge Betweenness Community Detection-----####

# Edge betweenness extends the concept of vertex betweenness centrality to edges by
# assigning each edge a score that reflects the number of shortest paths that move
# through that edge.
# You might ask the question, which ties in a social network are the most important in
# the spread of information?

# Calculated edge betweenness score for each network
ecopre_eb <- cluster_edge_betweenness(BReco_g_pre)
ecopost_eb <- cluster_edge_betweenness(BReco_g_post)
ecoall_eb <- cluster_edge_betweenness(BReco_g)

# Edge betweenness correctly assigns the pre- and post-migration
# sites to clusters, but with some interesting intricacies - Buckeye in pre and
# Lawrenz in post

# The pre- and post-migration eb communities are interesting as well

# Community detection via edge betweenness plot_across time
plot(ecoall_eb, BReco_g, col = membership(ecoall_eb), vertex.label.cex = c(1),
     edge.arrow.size = .1, edge.curved = .1)
title(main = "Edge Betweenness Community Detection in \n the Economic Network",
      cex.main = 1.5)

# Community detection via edge betweenness plot_pre-migration
plot(ecopre_eb, BReco_g_pre, col = membership(ecopre_eb), vertex.label.cex = c(1),
     edge.arrow.size = .1, edge.curved = .1)
title(main = "Edge Betweenness Community Detection in \n the Economic Network",
      cex.main = 1.5)

# Community detection via edge betweenness plot_post-migration
plot(ecopost_eb, BReco_g_post, col = membership(ecopost_eb), vertex.label.cex = c(1),
     edge.arrow.size = .1, edge.curved = .1)
title(main = "Edge Betweenness Community Detection in \n the Economic Network",
      cex.main = 1.5)

#-----Pre Randomization for Pre-Migration Period Economic BR-----####
#-----PRE_MIGRATION-----#

# Initiate empty List for assessing BR pre-migration average path length and transitivity
gecopre <- vector('list', 5000)

# Initiate empty List for assessing BR pre-migration density density and mean degree
gecopre.d <- vector('list', 5000)

# Populate gpre List with random graphs of same order and size

```

```

for(i in 1:5000){
  gecopre[[i]] <- erdos.renyi.game(n = gorder(BReco_g_pre), p.or.m = gsize(BReco_g_pre),
                                directed = FALSE, type = "gnm")
}

# Populate gecopre.d list with random graphs of same order and approximate density.
# A separate list of 5000 random graphs is necessary for density and mean degree because
# these statistics would be identical in random graphs of the same order and size as our
# observed graph.
# Instead, a probability of edge creation equal to the observed density is used. Further,
# only mean degree (as opposed to mean weighted degree) is used because Erdos-Renyi
# random graphs do not support weights.
for(i in 1:5000){
  gecopre.d[[i]] <- erdos.renyi.game(n = gorder(BReco_g_pre),
                                    p.or.m = edge_density(BReco_g_pre),
                                    directed = FALSE, type = "gnp")
}

# Calculate average path length, transitivity (clustering coefficient), density, and degree across
# the 5000 random pre-migration graphs
ecopre.pl <- lapply(gecopre.d, mean_distance, directed = FALSE)
ecopre.trans <- lapply(gecopre, transitivity)
ecopre.density <- lapply(gecopre.d, edge_density)
ecopre.degree <- lapply(gecopre.d, function(x){
  y <- degree(x)
  mean(y)
})

# Unlist and change to a data frame for visualizations
ecopre.pl <- as.data.frame(unlist(ecopre.pl))
ecopre.trans <- as.data.frame(unlist(ecopre.trans))
ecopre.density <- as.data.frame(unlist(ecopre.density))
ecopre.degree <- as.data.frame(unlist(ecopre.degree))

# Plot the distribution of random graph's average shortest path lengths with the pre-migration
# BR network's ave. shortest path as line
p.ecopre.pl <- ggplot(ecopre.pl, aes(x = unlist(ecopre.pl))) +
  geom_histogram(aes(y = ..density..), bins = 24) +
  geom_vline(xintercept = (mean_distance(BReco_g_pre, directed = FALSE)),
            linetype = "dashed", color = "red") +
  geom_density() +
  ggtitle("Distribution of 5000 Random Graph Average Shortest Path Lengths & \nPre-Migration P
eriod Average Shortest Path Length") +
  xlab("Average Shortest Path Length") +
  ylab("")

# Plot the distribution of random graph's transitivity with the pre-migration BR network's
# transitivity path as line
p.ecopre.trans <- ggplot(ecopre.trans, aes(x = unlist(ecopre.trans))) +
  geom_histogram(aes(y = ..density..), bins = 22) +

```

```

geom_vline(xintercept = (transitivity(BReco_g_pre)), linetype = "dashed", color = "red") +
geom_density() +
ggtitle("Distribution of Transitivity in 5000 Random Models & \nPre-Migration Period Network
Transitivity") +
xlab("Transitivity (or Clustering Coefficient)") +
ylab("")

# Plot the distribution of random graph's average density with the pre-migration jar network's
# ave. shortest path as Line
p.ecopre.density <- ggplot(ecopre.density, aes(x = unlist(ecopre.density))) +
  geom_histogram(aes(y = ..density..), bins = 22) +
  geom_vline(xintercept = (edge_density(BReco_g_pre)), linetype = "dashed", color = "red") +
  geom_density() +
  ggtitle("Distribution of 5000 Random Graph Average Densities & \nPre-Migration Preiod Network
Average Density") +
  xlab("Average Density") +
  ylab("")

# Plot the distribution of random graph's mean degree with the pre-migration BR network's mean
# degree path as Line
p.ecopre.degree <- ggplot(ecopre.degree, aes(x = unlist(ecopre.degree))) +
  geom_histogram(aes(y = ..density..), bins = 22) +
  geom_vline(xintercept = (mean(degree(BReco_g_pre, mode = "all"))),
            linetype = "dashed", color = "red") +
  geom_density() +
  ggtitle("Distribution of Mean Degree in 5000 Random Models & \nPre-Migration Period Network
Mean Degree") +
  xlab("Mean Degree") +
  ylab("")

# Use plot_grid to plot all four graphs on the same grid
plot_grid(p.ecopre.pl, p.ecopre.trans, p.ecopre.density, p.ecopre.degree)

# Calculate the proportion of graphs with an average path length Lower than observed
sum(ecopre.pl < mean_distance(BReco_g_pre, directed = FALSE))/5000*100

# Calculate the proportion of graphs with a transitivity (mean clustering coefficient)
# Lower than our observed
sum(ecopre.trans < transitivity(BReco_g_pre))/5000*100

# Calculate the proportion of graphs with a density Lower than our observed
sum(ecopre.density < edge_density(BReco_g_pre))/5000*100

# Calculate the proportion of graphs with a mean degree Lower than observed
sum(ecopre.degree < mean(degree(BReco_g_pre)))/5000*100

#-----Post Randomization for Post-Migration Period Economic BR-----####
#-----POST_MIGRATION-----#

# Initiate empty List for assessing BR pre-migration average path length and transitivity
gecopost <- vector('list', 5000)

# Initiate empty List for assessing BR pre-migration density density and mean degree

```

```

gecopost.d <- vector('list', 5000)

# Populate gpre List with random graphs of same order and size
for(i in 1:5000){
  gecopost[[i]] <- erdos.renyi.game(n = gorder(BReco_g_post), p.or.m = gsize(BReco_g_post),
    directed = FALSE, type = "gnm")
}

# Populate gecopre.d list with random graphs of same order and approximate density.
# A separate list of 5000 random graphs is necessary for density and mean degree because
# these statistics would be identical in random graphs of the same order and size as our
# observed graph.
# Instead, a probability of edge creation equal to the observed density is used. Further,
# only mean degree (as opposed to mean weighted degree) is used because Erdos-Renyi
# random graphs do not support weights.
for(i in 1:5000){
  gecopost.d[[i]] <- erdos.renyi.game(n = gorder(BReco_g_post),
    p.or.m = edge_density(BReco_g_post),
    directed = FALSE, type = "gnp")
}

# Calculate average path length, transitivity (clustering coefficient), density, and
# degree across the 5000 random pre-migration graphs
ecopost.pl <- lapply(gecopost.d, mean_distance, directed = FALSE)
ecopost.trans <- lapply(gecopost, transitivity)
ecopost.density <- lapply(gecopost.d, edge_density)
ecopost.degree <- lapply(gecopost.d, function(x){
  y <- degree(x)
  mean(y)
})

# Unlist and change to a data frame for visualizations
ecopost.pl <- as.data.frame(unlist(ecopost.pl))
ecopost.trans <- as.data.frame(unlist(ecopost.trans))
ecopost.density <- as.data.frame(unlist(ecopost.density))
ecopost.degree <- as.data.frame(unlist(ecopost.degree))

# Plot the distribution of random graph's average shortest path lengths with the pre-migration
# BR network's ave. shortest path as Line
p.ecopost.pl <- ggplot(ecopost.pl, aes(x = unlist(ecopost.pl))) +
  geom_histogram(aes(y = ..density..), bins = 24) +
  geom_vline(xintercept = (mean_distance(BReco_g_post, directed = FALSE)),
    linetype = "dashed", color = "red") +
  geom_density() +
  ggtitle("Distribution of 5000 Random Graph Average Shortest Path Lengths & \nPost-Migration
Period Average Shortest Path Length") +
  xlab("Average Shortest Path Length") +
  ylab("")

# Plot the distribution of random graph's transitivity with the pre-migration BR network's
# transitivity path as Line

```

```

p.ecopost.trans <- ggplot(ecopost.trans, aes(x = unlist(ecopost.trans))) +
  geom_histogram(aes(y = ..density..), bins = 10) +
  geom_vline(xintercept = (transitivity(BReco_g_post)), linetype = "dashed", color = "red") +
  geom_density() +
  ggtitle("Distribution of Transitivity in 5000 Random Models & \nPost-Migration Period Network Transitivity") +
  xlab("Transitivity (or Clustering Coefficient)") +
  ylab("")

# Plot the distribution of random graph's average density with the pre-migration jar network's
# ave. shortest path as line
p.ecopost.density <- ggplot(ecopost.density, aes(x = unlist(ecopost.density))) +
  geom_histogram(aes(y = ..density..), bins = 19) +
  geom_vline(xintercept = (edge_density(BReco_g_post)), linetype = "dashed", color = "red") +
  geom_density() +
  ggtitle("Distribution of 5000 Random Graph Average Densities & \nPost-Migration Period Network Average Density") +
  xlab("Average Density") +
  ylab("")

# Plot the distribution of random graph's mean degree with the pre-migration BR network's mean
# degree path as line
p.ecopost.degree <- ggplot(ecopost.degree, aes(x = unlist(ecopost.degree))) +
  geom_histogram(aes(y = ..density..), bins = 19) +
  geom_vline(xintercept = (mean(degree(BReco_g_post, mode = "all"))),
    linetype = "dashed", color = "red") +
  geom_density() +
  ggtitle("Distribution of Mean Degree in 5000 Random Models & \nPost-Migration Period Network Mean Degree") +
  xlab("Mean Degree") +
  ylab("")

# Use plot_grid to plot all four graphs on the same grid
plot_grid(p.ecopost.pl, p.ecopost.trans, p.ecopost.density, p.ecopost.degree)

# Calculate the proportion of graphs with an average path length lower than observed
sum(ecopost.pl < mean_distance(BReco_g_post, directed = FALSE))/5000*100

# Calculate the proportion of graphs with a transitivity (mean clustering coefficient)
# lower than our observed
sum(ecopost.trans < transitivity(BReco_g_post))/5000*100

# Calculate the proportion of graphs with a density lower than our observed
sum(ecopost.density < edge_density(BReco_g_post))/5000*100

# Calculate the proportion of graphs with a mean degree lower than observed
sum(ecopost.degree < mean(degree(BReco_g_post)))/5000*100

# There is a change from the pre-migration to post-migration period centralization scores
# Let's check to see which site-nodes are driving that change
betweenness(BReco_g_post, directed = FALSE)
closeness(BReco_g_post)

```

```

#-----Across Time Randomization for Post-Migration Period Economic BR-----####
#-----ACROSS TIME-----#

# Initiate empty List for assessing BR pre-migration average path length and transitivity
gecoall <- vector('list', 5000)

# Initiate empty List for assessing BR pre-migration density density and mean degree
gecoall.d <- vector('list', 5000)

# Populate gpre List with random graphs of same order and size
for(i in 1:5000){
  gecoall[[i]] <- erdos.renyi.game(n = gorder(BReco_g), p.or.m = gsize(BReco_g),
                                directed = FALSE, type = "gnm")
}

# Populate gecopre.d List with random graphs of same order and approximate density.
# A separate List of 5000 random graphs is necessary for density and mean degree because
# these statistics would identical in random graphs of the same order and size as our
# observed graph.
# Instead, a probability of edge creation equal to the observed density is used. Further,
# only mean degree (as opposed to mean weighted degree) is used because Erdos-Renyi
# random graphs do not support weights.
for(i in 1:5000){
  gecoall.d[[i]] <- erdos.renyi.game(n = gorder(BReco_g), p.or.m = edge_density(BReco_g),
                                    directed = FALSE, type = "gnp")
}

# Calculate average path length, transitivity (clustering coefficient), density, and degree across
# the 5000 random pre-migration graphs
ecoall.pl <- lapply(gecoall.d, mean_distance, directed = FALSE)
ecoall.trans <- lapply(gecoall, transitivity)
ecoall.density <- lapply(gecoall.d, edge_density)
ecoall.degree <- lapply(gecoall.d, function(x){
  y <- degree(x)
  mean(y)
})

# Unlist and change to a data frame for visualizations
ecoall.pl <- as.data.frame(unlist(ecoall.pl))
ecoall.trans <- as.data.frame(unlist(ecoall.trans))
ecoall.density <- as.data.frame(unlist(ecoall.density))
ecoall.degree <- as.data.frame(unlist(ecoall.degree))

# Plot the distribution of random graph's average shortest path lengths with the pre-migration
# BR network's ave. shortest path as Line
p.ecoall.pl <- ggplot(ecoall.pl, aes(x = unlist(ecoall.pl))) +
  geom_histogram(aes(y = ..density..), bins = 24) +
  geom_vline(xintercept = (mean_distance(BReco_g, directed = FALSE)),
            linetype = "dashed", color = "red") +

```

```

geom_density() +
ggtitle("Distribution of 5000 Random Graph Average Shortest Path Lengths & \nAverage Shortes
t Path Length Across Time in the CIRV") +
xlab("Average Shortest Path Length") +
ylab("")

# Plot the distribution of random graph's transitivity with the pre-migration BR network's
# transitivity path as line
p.ecoall.trans <- ggplot(ecoall.trans, aes(x = unlist(ecoall.trans))) +
  geom_histogram(aes(y = ..density..), bins = 25) +
  geom_vline(xintercept = (transitivity(BReco_g)), linetype = "dashed", color = "red") +
  geom_density() +
  ggtitle("Distribution of Transitivity in 5000 Random Models & \nTransitivity Across Time in
the CIRV") +
  xlab("Transitivity (or Clustering Coefficient)") +
  ylab("")

# Plot the distribution of random graph's average density with the pre-migration jar network's
# ave. shortest path as line
p.ecoall.density <- ggplot(ecoall.density, aes(x = unlist(ecoall.density))) +
  geom_histogram(aes(y = ..density..), bins = 24) +
  geom_vline(xintercept = (edge_density(BReco_g)), linetype = "dashed", color = "red") +
  geom_density() +
  ggtitle("Distribution of 5000 Random Graph Average Densities & \nAverage Density Across Time
in the CIRV") +
  xlab("Average Density") +
  ylab("")

# Plot the distribution of random graph's mean degree with the pre-migration BR network's mean
# degree path as line
p.ecoall.degree <- ggplot(ecoall.degree, aes(x = unlist(ecoall.degree))) +
  geom_histogram(aes(y = ..density..), bins = 23) +
  geom_vline(xintercept = (mean(degree(BReco_g, mode = "all"))),
            linetype = "dashed", color = "red") +
  geom_density() +
  ggtitle("Distribution of Mean Degree in 5000 Random Models & \nMean Degree Across Time in th
e CIRV") +
  xlab("Mean Degree") +
  ylab("")

# Use plot_grid to plot all four graphs on the same grid
plot_grid(p.ecoall.pl, p.ecoall.trans, p.ecoall.density, p.ecoall.degree)

# Calculate the proportion of graphs with an average path length lower than observed
sum(ecoall.pl < mean_distance(BReco_g, directed = FALSE))/5000*100

# Calculate the proportion of graphs with a transitivity (mean clustering coefficient)
# lower than our observed
sum(ecoall.trans < transitivity(BReco_g))/5000*100

# Calculate the proportion of graphs with a density lower than our observed
sum(ecoall.density < edge_density(BReco_g))/5000*100

```

```
# Calculate the proportion of graphs with a mean degree lower than observed
sum(ecoall.degree < mean(degree(BReco_g)))/5000*100
```

Economic Network Distance Regressions

Is the strength or degree of economic network relationships related to the distance between sites? The following analyses show that there is no support for a linear relationship between these variables.

```
library(infer)
library(tidyverse)
library(igraph)
library(reshape2)
library(stringr)
library(cowplot)
library(broom)

# Read in finalized, undirected plate BR edgelist
BReco_el_un <- read_csv("Econet_BR_UNDIRECTED_edgelist_complete.csv")

# Read in finalized, undirected pre-migration BR edgelist
BReco_el_un_pre <- read_csv("Econet_BR_UNDIRECTED_edgelist_pre-migration.csv")

# Read in finalized, undirected post-migration BR edgelist
BReco_el_un_post <- read_csv("Econet_BR_UNDIRECTED_edgelist_post-migration.csv")

# Inference testing with linear models
# Take 100 samples of half the network size each from the economic BR data sets
# The idea is to explore regression trends on the slope coefficient using samples
# from each data set. Does the trend with the entire data hold true when
# sub-samples are taken from the data?
# This is a two-tailed test to see if a linear relationship (positive or negative) exists
# between distance (explanatory variable) and weight (response variable)
BRecopresamples <- rep_sample_n(BReco_el_un_pre[, c(3, 8)], size = 21, reps = 100)
BRecopostsamples <- rep_sample_n(BReco_el_un_post[, c(3, 8)], size = 5, reps = 100)
BRecoallsamples <- rep_sample_n(BReco_el_un[, c(3, 8)], size = 26, reps = 100)

# Add replicate col to align observed trends with random samples
ecopre_observed <- BReco_el_un_pre[, c(3, 8)] %>%
  mutate(replicate = 200)

ecopost_observed <- BReco_el_un_post[, c(3, 8)] %>%
  mutate(replicate = 200)

ecoall_observed <- BReco_el_un[, c(3, 8)] %>%
  mutate(replicate = 200)

# Model showing proportional similarity across time
BReco_lm_all <- ggplot(BRecoallsamples, aes(x = Distance, y = weight, group = replicate)) +
  geom_point(size = 2, shape = 20) +
  stat_smooth(geom = "line", se = FALSE, alpha = 0.4, method = "lm") +
  ggtitle("Ceramic Industry Economic Network Across Time") +
```

```

background_grid(major = 'y', minor = "none") +
xlab("Distance (km)") +
ylab("Degree of Proportional Similarity in Compositional Groups") +
theme(strip.background = element_blank(),
strip.text.x = element_blank()) +
stat_smooth(data = ecoall_observed, aes(x = Distance, y = weight),
color = "red3",
linetype = "twodash", method = "lm", se = FALSE)

# Model showing proportional similarity in the pre-migration CIRV
BReco_lm_pre <- ggplot(BRecopresamples, aes(x = Distance, y = weight, group = replicate)) +
geom_point(size = 2, shape = 20) +
stat_smooth(geom = "line", se = FALSE, alpha = 0.4, method = "lm") +
ggtitle("Pre-Migration Ceramic Industry Economic Network") +
background_grid(major = 'y', minor = "none") +
xlab("Distance (km)") +
ylab("Degree of Proportional Similarity in Compositional Groups") +
theme(strip.background = element_blank(),
strip.text.x = element_blank()) +
stat_smooth(data = ecopre_observed, aes(x = Distance, y = weight),
color = "red3",
linetype = "twodash", method = "lm", se = FALSE)

# Model showing proportional similarity in the post-migration CIRV
BReco_lm_post <- ggplot(BRecopostsamples, aes(x = Distance, y = weight, group = replicate)) +
geom_point(size = 2, shape = 20) +
stat_smooth(geom = "line", se = FALSE, alpha = 0.4, method = "lm") +
ggtitle("Post-Migration Ceramic Industry Economic Network") +
background_grid(major = 'y', minor = "none") +
xlab("Distance (km)") +
ylab("Degree of Proportional Similarity in Compositional Groups") +
theme(strip.background = element_blank(),
strip.text.x = element_blank()) +
stat_smooth(data = ecopost_observed, aes(x = Distance, y = weight),
color = "red3",
linetype = "twodash", method = "lm", se = FALSE)

# Inference
# First, let's calculate the observed slope of the lm in the jar and plate attribute networks
BReco_all_slope <- lm(weight ~ Distance, data = BReco_el_un) %>%
tidy() %>%
filter(term == "Distance") %>%
pull(estimate)

BReco_pre_slope <- lm(weight ~ Distance, data = BReco_el_un_pre) %>%
tidy() %>%
filter(term == "Distance") %>%
pull(estimate)

BReco_post_slope <- lm(weight ~ Distance, data = BReco_el_un_post) %>%
tidy() %>%
filter(term == "Distance") %>%
pull(estimate)

```

```
# Simulate 500 slopes with a permuted dataset for economic network - this will allow us to  
# develop a sampling distribution of the slop under the hypothesis that there is no  
# relationship between the explanatory (Distance) and response (weight) variables.
```

```
set.seed(1568)
```

```
BReco_all_perm_slope <- BReco_el_un %>%  
  specify(weight ~ Distance) %>%  
  hypothesize(null = "independence") %>%  
  generate(reps = 500, type = "permute") %>%  
  calculate(stat = "slope")
```

```
BReco_pre_perm_slope <- BReco_el_un_pre %>%  
  specify(weight ~ Distance) %>%  
  hypothesize(null = "independence") %>%  
  generate(reps = 500, type = "permute") %>%  
  calculate(stat = "slope")
```

```
BReco_post_perm_slope <- BReco_el_un_post %>%  
  specify(weight ~ Distance) %>%  
  hypothesize(null = "independence") %>%  
  generate(reps = 500, type = "permute") %>%  
  calculate(stat = "slope")
```

```
ggplot(BReco_all_perm_slope, aes(x = stat)) + geom_density() + theme_classic()  
ggplot(BReco_pre_perm_slope, aes(x = stat)) + geom_density() + theme_classic()  
ggplot(BReco_post_perm_slope, aes(x = stat)) + geom_density() + theme_classic()
```

```
mean(BReco_all_perm_slope$stat)  
mean(BReco_pre_perm_slope$stat)  
mean(BReco_post_perm_slope$stat)  
sd(BReco_all_perm_slope$stat)  
sd(BReco_pre_perm_slope$stat)  
sd(BReco_post_perm_slope$stat)
```

```
# Calculate the absolute value of the slope
```

```
abs_BRco_all_obs_slope <- lm(weight ~ Distance, data = BReco_el_un) %>%  
  tidy() %>%  
  filter(term == "Distance") %>%  
  pull(estimate) %>%  
  abs()
```

```
abs_BReco_pre_obs_slope <- lm(weight ~ Distance, data = BReco_el_un_pre) %>%  
  tidy() %>%  
  filter(term == "Distance") %>%  
  pull(estimate) %>%  
  abs()
```

```
abs_BReco_post_obs_slope <- lm(weight ~ Distance, data = BReco_el_un_post) %>%  
  tidy() %>%  
  filter(term == "Distance") %>%  
  pull(estimate) %>%  
  abs()
```

```

# Compute the p-value
BReco_all_perm_slope %>%
  mutate(abs_BReco_all_obs_slope = abs(stat)) %>%
  summarize(p_value = mean(abs_BReco_all_obs_slope > BReco_all_perm_slope))

BReco_pre_perm_slope %>%
  mutate(abs_BReco_pre_obs_slope = abs(stat)) %>%
  summarize(p_value = mean(abs_BReco_pre_obs_slope > BReco_pre_perm_slope))

BReco_post_perm_slope %>%
  mutate(abs_BReco_post_obs_slope = abs(stat)) %>%
  summarize(p_value = mean(abs_BReco_post_obs_slope > BReco_post_perm_slope))

# Linear models sans visualization
# explore residuals
BReco_all_lm <- augment(lm(weight ~ Distance, data = BReco_el_un))
BReco_pre_lm <- augment(lm(weight ~ Distance, data = BReco_el_un_pre))
BReco_post_lm <- augment(lm(weight ~ Distance, data = BReco_el_un_post))

# Check SSE - how well do the models fit?
augment(lm(weight ~ 1, data = BReco_el_un)) %>% summarize(SSE = var(.resid)) # null
BReco_all_lm %>% summarize(SSE = var(.resid))

augment(lm(weight ~ 1, data = BReco_el_un_pre)) %>% summarize(SSE = var(.resid)) # null
BReco_pre_lm %>% summarize(SSE = var(.resid))

augment(lm(weight ~ 1, data = BReco_el_un_post)) %>% summarize(SSE = var(.resid)) # null
BReco_post_lm %>% summarize(SSE = var(.resid))

# Looks like the models do fit very well

# Breakdown of linear model results for plate attribute networks
summary(lm(weight ~ Distance, data = BReco_el_un))
# for each 1 km increase in distance, weight drops 0.0007723 and at 0 distance,
# a weight of 0.7378 is expected
summary(lm(weight ~ Distance, data = BReco_el_un))$coefficients
# all = p-value of 0.1454, fail to
# reject null hypothesis - no significant linear relationship b/t distance and weight
# across time

summary(lm(weight ~ Distance, data = BReco_el_un_pre))
# for each 1 km increase in distance, weight drops 0.0003959 and at 0 distance, a weight of
# 0.7385 is expected
summary(lm(weight ~ Distance, data = BReco_el_un_pre))$coefficients
# pre p-value of 0.6918, fail to reject the null hypothesis - no significant linear
# relationship b/t distance and weight in pre

summary(lm(weight ~ Distance, data = BReco_el_un_post)) # for each 1 km increase in distance,
# weight drops 0.0004263 and at 0 distance, a weight of 0.6835 is expected
summary(lm(weight ~ Distance, data = BReco_el_un_post))$coefficients
# post p-value of 0.5499, fail to reject null - no significant linear relationship b/t
# distance and weight in post

```

```

# Check r.squared
glance(lm(weight ~ Distance, data = BReco_el_un))
glance(lm(weight ~ Distance, data = BReco_el_un_pre))
glance(lm(weight ~ Distance, data = BReco_el_un_post))

ggplot(BReco_el_un_post, aes(Distance, weight)) + geom_point() + geom_smooth()
ggplot(BReco_el_un_pre, aes(Distance, weight)) + geom_point() + geom_smooth()

# Check correlations
cor(BReco_el_un$Distance, BReco_el_un$weight)
cor(BReco_el_un_pre$Distance, BReco_el_un_pre$weight)
cor(BReco_el_un_post$Distance, BReco_el_un_post$weight)

### No relationship between distance and degree of economic interactions is able to be
# identified this is interesting, as it would be expected that sites closer in proximity
# would exhibit stronger economic relationships via a higher degree of exchange of
# finished vessels, overlapping resource exploitation areas, or similar paste preparation
# and production regimes.

```

R Code from Chapter 8 – Toward Explaining Social Interrelationships through a Ceramic Industry Multilayer Network

Network Data Pre-Treatment for Multilayer Network Construction

```

#' Data munging to convert network data into a form amenable
#' to the construction of multilayer networks using multinet
#' and muxViz.

library(tidyverse)
library(multinet)
library(igraph)

# First, read in the social identification network built based on
# proportional similarity in plate stylistic designs between sites
style_all <- read_csv("BR_UNDIRECTED_edgelist_complete.csv")
eco_all <- read_csv("Econet_BR_UNDIRECTED_edgelist_complete.csv")

# Multinet is implement in a variant of the C language and as such
# is bound by different rules. One of those is avoiding spaces in
# the actor (or in this case archaeological site) names

# Replace all spaces and dashes with an underscore for style layers
style_all$Source <- str_replace_all(style_all$Source, c(" " = "_", "-" = "_"))
style_all$Target <- str_replace_all(style_all$Target, c(" " = "_", "-" = "_"))

# Decompose edge table to edge vectors for style layers
style_all %>%

```

```

mutate(Layer = ifelse(Time == 1, "Style_pre", "Style_post")) %>%
select(Source, Target, Layer, weight) %>%
unite(Style, sep = ",") %>%
write_csv("style_edge_table_multinet.csv")

# Style node table
style_all %>%
mutate(Layer = ifelse(Time == 1, "Style_pre", "Style_post")) %>%
select(Source, Target, Layer) %>%
gather(Site, Source:Layer, -Layer) %>%
select(`Source:Layer`, Layer) %>%
distinct(`Source:Layer`, Layer) %>%
unite(Nodes_style, sep = ",") %>%
write_csv("style_node_table_multinet.csv")

# Economic network Layer node cleaning
# '\\.' matches a .
eco_all$Source <- str_replace_all(eco_all$Source,
                                c(" " = "_", "-" = "_", "\\." = ""))
eco_all$Target <- str_replace_all(eco_all$Target,
                                  c(" " = "_", "-" = "_", "\\." = ""))

# Decompose edge table to edge vectors for economic layers
eco_all %>%
mutate(Layer = ifelse(Time == 1, "Eco_pre", "Eco_post")) %>%
select(Source, Target, Layer, weight) %>%
unite(Economic, sep = ",") %>%
write_csv("economic_edge_table_multinet.csv")

# Economic networks node table
eco_all %>%
mutate(Layer = ifelse(Time == 1, "Eco_pre", "Eco_post")) %>%
select(Source, Target, Layer) %>%
gather(Site, Source:Layer, -Layer) %>%
select(`Source:Layer`, Layer) %>%
distinct(`Source:Layer`, Layer) %>%
unite(Nodes_style, sep = ",") %>%
write_csv("economic_node_table_multinet.csv")

# At this point, node and edge table information is combined using the RStudio
# content editor. It's easier working in the content editor because Excel and text
# editing software often append spaces, commas, or other unwanted characters to
# the data, which multinet cannot handle. For information on how to create
# multilayer or multiplex networks in multinet, see the documentation on CRAN
# or you can view the file below once it is posted.

test <- read.ml("ceramicMultilayer_complete_in progress.csv")
test
plot(test)

# Pre-Treatment for muxViz #####
# muxViz is a powerful tool for multilayer network analysis and visualization
# Here, I'll work with the network data I have to create files for use in muxViz

```

```

# Style network edge lists for muxViz
# Pre-migration
style_all %>%
  filter(Time == 1) %>%
  select(Source, Target, weight) %>%
  unite(sep = " ") %>%
  write.table("edge_list_style_pre.txt", row.names = FALSE,
             col.names = FALSE, quote = FALSE)

# Post-migration
style_all %>%
  filter(Time == 2) %>%
  select(Source, Target, weight) %>%
  unite(sep = " ") %>%
  write.table("edge_list_style_post.txt", row.names = FALSE,
             col.names = FALSE, quote = FALSE)

# Across time
style_all %>%
  select(Source, Target, weight) %>%
  unite(sep = " ") %>%
  write.table("edge_list_style_all.txt", row.names = FALSE,
             col.names = FALSE, quote = FALSE)

# Economic network edge lists for muxViz
# Pre-migration
eco_all %>%
  filter(Time == 1) %>%
  select(Source, Target, weight) %>%
  unite(sep = " ") %>%
  write.table("edge_list_eco_pre.txt", row.names = FALSE,
             col.names = FALSE, quote = FALSE)

# Post-migration
eco_all %>%
  filter(Time == 2) %>%
  select(Source, Target, weight) %>%
  unite(sep = " ") %>%
  write.table("edge_list_eco_post.txt", row.names = FALSE,
             col.names = FALSE, quote = FALSE)

# Across time
eco_all %>%
  select(Source, Target, weight) %>%
  unite(sep = " ") %>%
  write.table("edge_list_eco_all.txt", row.names = FALSE,
             col.names = FALSE, quote = FALSE)

# Interaction through cultural transmission network edge lists for muxViz

# Jars muxViz ####
# Import jar edgelist and munge the site names

```

```

jars <- read_csv('jar_complete_edgelist.csv')
jars$Source <- str_replace_all(jars$Source,
                              c(" " = "_", "-" = "_", "\\." = ""))
jars$Target <- str_replace_all(jars$Target,
                               c(" " = "_", "-" = "_", "\\." = ""))

# First, make directed graph txt files for muxZiv
# Jar directed all
jars %>%
  select(Source, Target, weight) %>%
  unite(sep = " ") %>%
  write.table("edge_list_jtech_directed_all.txt", row.names = FALSE,
             col.names = FALSE, quote = FALSE)

# Jar directed pre
jars %>%
  filter(Time == 1) %>%
  select(Source, Target, weight) %>%
  unite(sep = " ") %>%
  write.table("edge_list_jtech_directed_pre.txt", row.names = FALSE,
             col.names = FALSE, quote = FALSE)

# Jar directed post
jars %>%
  filter(Time == 2) %>%
  select(Source, Target, weight) %>%
  unite(sep = " ") %>%
  write.table("edge_list_jtech_directed_post.txt", row.names = FALSE,
             col.names = FALSE, quote = FALSE)

# Now, create UNDIRECTED graph txt files for jars
# To do this, any reciprocal edge weights will be the mean of the two
# directed edge weights

# Jar undirected all
jg <- graph.data.frame(jars, directed = TRUE)
jg_un <- as.undirected(jg, edge.attr.comb = "mean", mode = "collapse")

as.data.frame(as_edgelist(jg_un)) %>%
  mutate(weight = E(jg_un)$weight) %>%
  unite(sep = " ") %>%
  write.table("edge_list_jtech_undirected_all.txt", row.names = FALSE,
             col.names = FALSE, quote = FALSE)

# Jar undirected pre
jars %>%
  filter(Time == 1) %>%
  graph.data.frame(directed = TRUE) -> jg_pre
jg_un_pre <- as.undirected(jg_pre, edge.attr.comb = "mean",
                        mode = "collapse")

as.data.frame(as_edgelist(jg_un_pre)) %>%
  mutate(weight = E(jg_un_pre)$weight) %>%

```

```

unite(sep = " ") %>%
write.table("edge_list_jtech_undirected_pre.txt", row.names = FALSE,
           col.names = FALSE, quote = FALSE)

# Jar undirected post
jars %>%
  filter(Time == 2 |
         (Source == "Buckeye_Bend" & Target == "Lawrenz_Gun_Club") |
         (Source == "Lawrenz_Gun_Club" & Target == "Buckeye_Bend")) %>%
  graph.data.frame(directed = TRUE) -> jg_post
jg_un_post <- as.undirected(jg_post, edge.attr.comb = "mean",
                          mode = "collapse")

as.data.frame(as_edgelist(jg_un_post)) %>%
  mutate(weight = E(jg_un_post)$weight) %>%
  unite(sep = " ") %>%
  write.table("edge_list_jtech_undirected_post.txt", row.names = FALSE,
            col.names = FALSE, quote = FALSE)

# Plates muxViz #####
plates <- read_csv('plate_complete_edgelist.csv')
plates$Source <- str_replace_all(plates$Source,
                                c(" " = "_", "-" = "_", "\\." = ""))
plates$Target <- str_replace_all(plates$Target,
                                c(" " = "_", "-" = "_", "\\." = ""))

# Plates directed all
plates %>%
  select(Source, Target, weight) %>%
  unite(sep = " ") %>%
  write.table("edge_list_ptech_directed_all.txt", row.names = FALSE,
            col.names = FALSE, quote = FALSE)

# Plates directed pre
plates %>%
  filter(Time == 1) %>%
  select(Source, Target, weight) %>%
  unite(sep = " ") %>%
  write.table("edge_list_ptech_directed_pre.txt", row.names = FALSE,
            col.names = FALSE, quote = FALSE)

# Plates directed post
plates %>%
  filter(Time == 2 |
         (Source == "Buckeye_Bend" & Target == "Lawrenz_Gun_Club") |
         (Source == "Lawrenz_Gun_Club" & Target == "Buckeye_Bend")) %>%
  select(Source, Target, weight) %>%
  unite(sep = " ") %>%
  write.table("edge_list_ptech_directed_post.txt", row.names = FALSE,
            col.names = FALSE, quote = FALSE)

# Now, create UNDIRECTED graph txt files for plates
# To do this, any reciprocal edge weights will be the mean of the two

```

```

# directed edge weights

# Plate undirected all
pg <- graph.data.frame(plates, directed = TRUE)
pg_un <- as.undirected(pg, edge.attr.comb = "mean", mode = "collapse")

as.data.frame(as_edgelist(pg_un)) %>%
  mutate(weight = E(pg_un)$weight) %>%
  unite(sep = " ") %>%
  write.table("edge_list_ptech_undirected_all.txt", row.names = FALSE,
             col.names = FALSE, quote = FALSE)

# Plate undirected pre
plates %>%
  filter(Time == 1) %>%
  graph.data.frame(directed = TRUE) -> pg_pre
pg_un_pre <- as.undirected(pg_pre, edge.attr.comb = "mean",
                        mode = "collapse")

as.data.frame(as_edgelist(pg_un_pre)) %>%
  mutate(weight = E(pg_un_pre)$weight) %>%
  unite(sep = " ") %>%
  write.table("edge_list_ptech_undirected_pre.txt", row.names = FALSE,
             col.names = FALSE, quote = FALSE)

# Plate undirected post
plates %>%
  filter(Time == 2 |
         (Source == "Buckeye_Bend" & Target == "Lawrenz_Gun_Club") |
         (Source == "Lawrenz_Gun_Club" & Target == "Buckeye_Bend")) %>%
  graph.data.frame(directed = TRUE) -> pg_post
pg_un_post <- as.undirected(pg_post, edge.attr.comb = "mean",
                        mode = "collapse")

as.data.frame(as_edgelist(pg_un_post)) %>%
  mutate(weight = E(pg_un_post)$weight) %>%
  unite(sep = " ") %>%
  write.table("edge_list_ptech_undirected_post.txt", row.names = FALSE,
             col.names = FALSE, quote = FALSE)

## UNDIRECTED Edgelist for Gephi
# Here I take directed jar and plate technological attribute networks and
# decompose them into undirected networks based on the average edge weights
# among any two given sites (if there is no reciprocal edge, the present
# edge weight is used to define the relationship).
# Filtering can be applied in Gephi, so only one edge table is needed for
# each vessel class.

# Import jar/plate data again (no special modifications to site names is
# needed for Gephi)
p <- read_csv('plate_complete_edgelist.csv')
j <- read_csv('jar_complete_edgelist.csv')

```

```

# Jars for Gephi
j %>%
  graph.data.frame(directed = TRUE) %>%
  as.undirected(edge.attr.comb = "mean", mode = "collapse") %>%
  as_edgelist(.) %>%
  as.data.frame(.) %>%
  mutate(weight = E(as.undirected(graph.data.frame(j,directed = TRUE),
                                edge.attr.comb = "mean",
                                mode = "collapse"))$weight) %>%
  rename(Source = V1, Target = V2) %>%
  write_csv("Jars_tech_UN_across_time.csv")

# Plates for Gephi
p %>%
  graph.data.frame(directed = TRUE) %>%
  as.undirected(edge.attr.comb = "mean", mode = "collapse") %>%
  as_edgelist(.) %>%
  as.data.frame(.) %>%
  mutate(weight = E(as.undirected(graph.data.frame(p,directed = TRUE),
                                edge.attr.comb = "mean",
                                mode = "collapse"))$weight) %>%
  rename(Source = V1, Target = V2) %>%
  write_csv("Plates_tech_UN_across_time.csv")

# Function to calculate degree, betweenness, closeness, and eigenvector centrality
# for a graph and return a data frame with the scores
centr_all <- function(graph, g_name = "Score") {

  # Check that graph is an igraph object
  if (!is_igraph(graph)) {
    stop("Not a graph object")
  }

  # Name of graph
  g_name <- as.character(g_name)

  # Degree centralization
  res_centr <- centr_degree(graph)$centralization

  # Betweenness centralization
  res_centr[2] <- centr_betw(graph)$centralization

  # Closeness centralization
  res_centr[3] <- centr_clo(graph)$centralization

  # Eigenvector centralization
  res_centr[4] <- centr_eigen(graph)$centralization

  res_centr <- t(as.data.frame(res_centr))

  # Table of scores
  colnames(res_centr) <- c("Degree", "Betweenness", "Closeness", "Eigenvector")
  rownames(res_centr) <- g_name

```

```

res_centr
}

## Centralization values for undirected jar and plate networks

# Jar pre-migration, post-migration, and all
j %>%
  #filter(Time == 1) %>%
  #filter(Time == 2) %>%
  graph.data.frame(directed = TRUE) %>%
  as.undirected(edge.attr.comb = "mean", mode = "collapse") %>%
  centr_all(.)

# Plate pre-migration, post-migration, and all
p %>%
  #filter(Time == 1) %>%
  #filter(Time == 2) %>%
  graph.data.frame(directed = TRUE) %>%
  as.undirected(edge.attr.comb = "mean", mode = "collapse") %>%
  centr_all(.)

# Undirected networks for multinet #####

# First, correct site (node) names for the convention I used previously
j$Source <- str_replace_all(j$Source, c(" " = "_", "-" = "_", "\\." = ""))
j$Target <- str_replace_all(j$Target, c(" " = "_", "-" = "_", "\\." = ""))
p$Source <- str_replace_all(p$Source, c(" " = "_", "-" = "_", "\\." = ""))
p$Target <- str_replace_all(p$Target, c(" " = "_", "-" = "_", "\\." = ""))

# Jars undirected multinet
# Pre-migration
j %>%
  filter(Time == 1) %>%
  graph.data.frame(directed = TRUE) %>%
  as.undirected(edge.attr.comb = "mean", mode = "collapse") %>%
  as_edgelist(.) %>%
  as.data.frame(.) %>%
  mutate(weight = E(as.undirected(graph.data.frame(filter(j, Time == 1),
                                                    directed = TRUE),
                                                    edge.attr.comb = "mean",
                                                    mode = "collapse"))$weight) %>%
  mutate(Layer = "Jar_pre") %>%
  select(V1, V2, Layer, weight) %>%
  unite(sep = ",") %>%
  write_delim("jar_pre_multinet_el.txt", delim = "")

# Post-migration
j %>%
  filter(Time == 2 |
         (Source == "Buckeye_Bend" & Target == "Lawrenz_Gun_Club") |
         (Source == "Lawrenz_Gun_Club" & Target == "Buckeye_Bend")) %>%
  graph.data.frame(directed = TRUE) %>%

```

```

as.undirected(edge.attr.comb = "mean", mode = "collapse") %>%
as_edgelist(.) %>%
as.data.frame(.) %>%
mutate(weight = E(as.undirected(graph.data.frame(filter(j, Time == 2 |
      (Source == "Buckeye_Bend" &
        Target == "Lawrenz_Gun_Club") |
      (Source == "Lawrenz_Gun_Club" &
        Target == "Buckeye_Bend")), directed = TRUE),
      edge.attr.comb = "mean", mode = "collapse"))$weight) %>%
mutate(Layer = "Jar_post") %>%
select(V1, V2, Layer, weight) %>%
unite(sep = ",") %>%
write_delim("jar_post_multinet_el.txt", delim = "")

# Plates undirected multinet
# Pre-migration
p %>%
filter(Time == 1) %>%
graph.data.frame(directed = TRUE) %>%
as.undirected(edge.attr.comb = "mean", mode = "collapse") %>%
as_edgelist(.) %>%
as.data.frame(.) %>%
mutate(weight = E(as.undirected(graph.data.frame(filter(p, Time == 1),
      directed = TRUE),
      edge.attr.comb = "mean",
      mode = "collapse"))$weight) %>%
mutate(Layer = "Plate_pre") %>%
select(V1, V2, Layer, weight) %>%
unite(sep = ",") %>%
write_delim("plate_pre_multinet_el.txt", delim = "")

# Post-migration
p %>%
filter(Time == 2) %>%
graph.data.frame(directed = TRUE) %>%
as.undirected(edge.attr.comb = "mean", mode = "collapse") %>%
as_edgelist(.) %>%
as.data.frame(.) %>%
mutate(weight = E(as.undirected(graph.data.frame(filter(p, Time == 2),
      directed = TRUE),
      edge.attr.comb = "mean",
      mode = "collapse"))$weight) %>%
mutate(Layer = "Plate_post") %>%
select(V1, V2, Layer, weight) %>%
unite(sep = ",") %>%
write_delim("plate_post_multinet_el.txt", delim = "")

```

Multilayer Network Analysis Using Multinet and MuxViz

```

# Multilayer Network Analysis using Multinet (and MuxViz)

# Multilayer networks of ceramic industry from the Late Prehistoric central
# IllinoisRiver valley (1200-1450 A.D.) are analyzed here.
# There are four distinct layers in this multilayer network:
# 1) attributes likely constrained by social forces, or imbued with social information,
# on domestic cooking jars and 2) likely serving plates, 3) proportional stylistic
# similarity in design groups present at sites, and 4) economic networks related
# to ceramic industry as gleaned from geochemical compositional groups.
# Networks are considered both prior to and preceding a circa 1300 A.D. in-migration
# of an Oneota group into a Mississippian chiefly environment.

# ALL network ties are unweighted and undirected in Multinet analysis -
# it does not yet support these network attributes yet. Nevertheless, significant
# insight can be gained when exploring the multilayer nature of the networks
# based on the threshold values for giving an edge between two sites across
# the different network layers.

# Load multinet
library(multinet)
library(igraph)
library(tidyverse)
library(ggsci)
library(magrittr)

# Import Ceramic Industry Multilayer Network
cnet <- read.ml("ceramicMultilayer_complete_in progress_UNDIRECTED.csv")
cnet_pre <- read.ml("ceramicMultilayer_PRE_in progress_UNDIRECTED_2.0.0.csv")
cnet_post <- read.ml("ceramicMultilayer_POST_in progress_UNDIRECTED_2.0.0.csv")

# Let's take a look at some basic Network Analysis Measures for actors in the network

# Degree of all actors, considering edges on all layers
# This does not consider edge weights
degree.ml(cnet)
degree.ml(cnet_pre)
degree.ml(cnet_post)

# Degree deviation is an interesting measure. It is the standard deviation of the
# degree of an actor on the input layers. An actor with the same degree on all layers
# will have deviation 0, while an actor with a lot of neighbors on one layer and
# only a few on another will have a high degree deviation, showing an uneven usage
# of layers (or layers with different densities).
# The values are quite high because of the many layers on which many of the sites are
# not represented.
degree.deviation.ml(cnet)
deviation_pre <- cnet_pre %>%
  degree.deviation.ml() %>%
  as.data.frame() %>%
  rownames_to_column() %>%
  as_tibble() %>%
  set_colnames(c("Site", "Degree Deviation")) %>%
  mutate(Time = "Pre-Migration")

```

```

deviation_post <- cnet_post %>%
  degree.deviation.ml() %>%
  as.data.frame() %>%
  rownames_to_column() %>%
  as_tibble() %>%
  set_colnames(c("Site", "Degree Deviation")) %>%
  mutate(Time = "Post-Migration")

# Plotting degree deviation for pre-migration time period
deviation_pre %>%
  mutate(Site = str_replace_all(Site, "_", " ")) %>%
  ggplot() +
  geom_col(aes(x = reorder(Site, `Degree Deviation`), y = `Degree Deviation`,
    fill = `Degree Deviation`), color = "black") +
  theme_bw() +
  scale_fill_material("blue-grey") +
  labs(y = "Degree Deviation",
    x = "",
    fill = "Degree Deviation") +
  coord_flip() +
  theme(axis.text.y = element_text(size = 10))

# Plotting degree deviation for post-migration time period
deviation_post %>%
  mutate(Site = str_replace_all(Site, "_", " ")) %>%
  ggplot() +
  geom_col(aes(x = reorder(Site, `Degree Deviation`), y = `Degree Deviation`,
    fill = `Degree Deviation`), color = "black") +
  theme_bw() +
  scale_fill_material("blue-grey") +
  labs(y = "Degree Deviation",
    x = "",
    fill = "Degree Deviation") +
  coord_flip() +
  #scale_y_continuous(limits = c(0.0, 4.0)) +
  theme(axis.text.y = element_text(size = 10))

# Let's refine this to only look at specific layers - either before or after
# the migration
degree.deviation.ml(cnet, layers = c("Jar_pre", "Plate_pre"))
degree.deviation.ml(cnet, layers = c("Jar_post", "Plate_post"))

# Two sites are off the charts for these measures - Eveland and CW_Cooper
# This is because one of the vessel classes is not present at these sites
# Overall, there is significantly less degree deviation in the post-migration
# period, indicating a more even usage of the layers overall compared to the
# pre-migration period. This might indicate that social relationships became
# more developed (which doesn't necessary connote positive or negative) kinds
# of relationships, only that interaction perhaps became more routinized in
# some way. Perhaps this is related to the presence of an internal frontier,
# which could act to structure inter-site relationships in ways not possible
# in the pre-migration period.

```

```

# What about measures for the multiplexity of an actor's relationships?
# Connective redundancy assesses whether or not sites that share a relationship
# on one layer also share that same relationships across other layers
connective.redundancy.ml(cnet)
connective.redundancy.ml(cnet_pre)
connective.redundancy.ml(cnet_post)

# Storing connective redundancy as a tidy tibble
redundancy_pre <- cnet_pre %>%
  connective.redundancy.ml() %>%
  as.data.frame() %>%
  rownames_to_column() %>%
  as_tibble() %>%
  set_colnames(c("Site", "Connective Redundancy")) %>%
  mutate(Time = "Pre-Migration")

# Storing connective redundancy as a tidy tibble
redundancy_post <- cnet_post %>%
  connective.redundancy.ml() %>%
  as.data.frame() %>%
  rownames_to_column() %>%
  as_tibble() %>%
  set_colnames(c("Site", "Connective Redundancy")) %>%
  mutate(Time = "Post-Migration")

# Plotting connective redundancy in the pre-migration period
redundancy_pre %>%
  mutate(Site = str_replace_all(Site, "_", " ")) %>%
  ggplot() +
  geom_col(aes(x = reorder(Site, `Connective Redundancy`),
                y = `Connective Redundancy`,
                fill = `Connective Redundancy`,
                color = "black") +
  theme_bw() +
  labs(y = "Connective Redundancy",
        x = "",
        fill = "Connective Redundancy") +
  scale_fill_material("green") +
  coord_flip() +
  scale_y_continuous(limits = c(0.0, 0.7)) +
  theme(axis.text.y = element_text(size = 10))

# Plotting connective redundancy in the post-migration period
redundancy_post %>%
  mutate(Site = str_replace_all(Site, "_", " ")) %>%
  ggplot() +
  geom_col(aes(x = reorder(Site, `Connective Redundancy`),
                y = `Connective Redundancy`,
                fill = `Connective Redundancy`,
                color = "black") +
  theme_bw() +
  labs(y = "Connective Redundancy",

```

```

    x = "",
    fill = "Connective Redundancy") +
  scale_fill_material("green") +
  coord_flip() +
  scale_y_continuous(limits = c(0.0, 0.7)) +
  theme(axis.text.y = element_text(size = 10))

# Comparing layers - Looks at overlapping and distribution similarity (0 to 1)
layer.comparison.ml(cnet)
layer.comparison.ml(cnet_pre)
layer.comparison.ml(cnet_post)
layer.comparison.ml(cnet,method="jaccard.edges")
layer.comparison.ml(cnet,method="sm.edges")
jaccard_pre <- layer.comparison.ml(cnet_pre,method="jaccard.edges")
jaccard_post <- layer.comparison.ml(cnet_post,method="jaccard.edges")
sm_pre <- layer.comparison.ml(cnet_pre,method="sm.edges")
sm_post <- layer.comparison.ml(cnet_post,method="sm.edges")

# Let's plot the different layer comparisons as two barcharts for the
# pre- and post-migration periods respectively
# Make weighted, undirected graph from Pre-migration Jaccard coefficient
jac_pre_g <- jaccard_pre %>%
  as.matrix() %>%
  graph_from_adjacency_matrix(., weighted = TRUE,
                              mode = "undirected")

# Weighted, undirected pre-migration period simple matching coefficient graph
sm_pre_g <- sm_pre %>%
  as.matrix() %>%
  graph_from_adjacency_matrix(., weighted = TRUE,
                              mode = "undirected")

# Convert pre-migration graphs to tbl_dfs and combine
e_pre <- jac_pre_g %>%
  as_edgelist() %>%
  as_tibble() %>%
  mutate(Jaccard = E(jac_pre_g)$weight) %>%
  filter(V1 != V2) %>%
  left_join(as_tibble(as_edgelist(sm_pre_g)) %>%
            mutate(Simple_Matching = E(sm_pre_g)$weight)) %>%
  unite("layers", c("V1", "V2"), sep = "-") %>%
  # Add edge overlapping from MuxViz (edge weights are factored in)
  mutate(Edge_Overlap = c(0.727, 0.474, 0.629, 0.495, 0.544, 0.345))

# Make weighted, undirected graph from Post-migration Jaccard coefficient
jac_post_g <- jaccard_post %>%
  as.matrix() %>%
  graph_from_adjacency_matrix(., weighted = TRUE,
                              mode = "undirected")

# Weighted, undirected post-migration period simple matching coefficient graph
sm_post_g <- sm_post %>%

```

```

    as.matrix() %>%
    graph_from_adjacency_matrix(., weighted = TRUE,
                                mode = "undirected")

# Convert post-migration graphs to tbl_dfs and combine
e_post <- jac_post_g %>%
  as_edgelist() %>%
  as_tibble() %>%
  mutate(Jaccard = E(jac_post_g)$weight) %>%
  filter(V1 != V2) %>%
  left_join(as_tibble(as_edgelist(sm_post_g)) %>%
            mutate(Simple_Matching = E(sm_post_g)$weight)) %>%
  unite("layers", c("V1", "V2"), sep = "-") %>%
  # Add edge overlapping from MuxViz (edge weights factored in)
  mutate(Edge_Overlap = c(0.520, 0.819, 0.469, 0.620, 0.488, 0.454))

# Pre-migration edge correlation barplot
e_pre %>%
  gather(Metric, value, Jaccard:Edge_Overlap, -layers) %>%
  mutate(layers = str_replace(layers, "_pre", ""),
         layers = str_replace(layers, "_pre", ""),
         layers = str_replace(layers, "Eco", "Economic"),
         Metric = str_replace(Metric, "_", " "),
         layers = str_replace(layers, "-", " - ")) %>%
  arrange(layers) %>%
  ggplot() +
  geom_col(aes(x = reorder(layers, value), y = value, fill = Metric),
          position = "dodge") +
  theme_bw() +
  scale_fill_nejm() +
  labs(y = "Layer Overlap",
       x = "",
       subtitle = "Pre-migration period layer edge overlaps") +
  coord_flip() +
  scale_y_continuous(limits = c(0.0, 1.0)) +
  theme(axis.text.y = element_text(size = 10))

# Post-migration edge correlation barplot
e_post %>%
  gather(Metric, value, Jaccard:Edge_Overlap, -layers) %>%
  mutate(layers = str_replace(layers, "_post", ""),
         layers = str_replace(layers, "_post", ""),
         layers = str_replace(layers, "Eco", "Economic"),
         Metric = str_replace(Metric, "_", " "),
         layers = str_replace(layers, "-", " - ")) %>%
  arrange(layers) %>%
  ggplot() +
  geom_col(aes(x = reorder(layers, value), y = value, fill = Metric),
          position = "dodge") +
  theme_bw() +
  scale_fill_nejm() +
  labs(y = "Layer Overlap",
       x = "",

```

```

    subtitle = "Post-migration period layer edge overlaps") +
  coord_flip() +
  scale_y_continuous(limits = c(0.0, 1.0)) +
  theme(axis.text.y = element_text(size = 10))

# Plotting MuxViz Multilayer Centrality Measures
#' Three centrality measures were calculated in MuxViz 2.0 - strength,
#' degree, and eigenvector. These provide assessments of the influence of
#' individual nodes in a network Layer. Combining the results across the
#' Layers provides an indirect assessment of the influence of a Layer
#' on the entire multilayer network
pre_centr <- read_delim("pre-migration muxviz centrality.csv", ";",
  escape_double = FALSE, trim_ws = TRUE)
post_centr <- read_delim("post-migration muxviz centrality.csv", ";",
  escape_double = FALSE, trim_ws = TRUE)

# Plot pre-migration centrality scores across the Layers
pre_centr %>%
  filter(Layer != "Aggr") %>%
  select(Layer, Label, Degree, Strength, Eigenvector) %>%
  gather(key = Statistic, value = value, Degree:Eigenvector, -Layer) %>%
  mutate(Label = str_replace_all(Label, "_", " ")) %>%
  mutate(Layer = ifelse(Layer == "1", "Plate attributes",
    ifelse(Layer == "2", "Jar attributes",
    ifelse(Layer == "3", "Style",
    ifelse(Layer == "4", "Economic", 0)))) %>%
  rename(Site = Label) %>%
  ggplot() +
  geom_bar(aes(x = reorder(Site, value),
    y = value, fill = Layer), stat = "identity") +
  facet_wrap(~Statistic, scales = "free_x") +
  coord_flip() +
  scale_fill_nejm() +
  theme_bw() +
  xlab("") +
  ylab("Centrality Score") +
  facet_wrap(~Statistic, scales = "free_x")

# Plot post-migration centrality scores across the Layers
post_centr %>%
  filter(Layer != "Aggr") %>%
  select(Layer, Label, Degree, Strength, Eigenvector) %>%
  gather(key = Statistic, value = value, Degree:Eigenvector, -Layer) %>%
  mutate(Label = str_replace_all(Label, "_", " ")) %>%
  mutate(Layer = ifelse(Layer == "1", "Plate attributes",
    ifelse(Layer == "2", "Jar attributes",
    ifelse(Layer == "3", "Style",
    ifelse(Layer == "4", "Economic", 0)))) %>%
  rename(Site = Label) %>%
  ggplot() +
  geom_bar(aes(x = reorder(Site, value),

```

```

    y = value, fill = Layer), stat = "identity") +
  facet_wrap(~Statistic, scales = "free_x") +
  coord_flip() +
  scale_fill_nejm() +
  theme_bw() +
  xlab("") +
  ylab("Centrality Score") +
  facet_wrap(~Statistic, scales = "free_x")

# Summary of centrality scores, pre-migration
pre_centr %>%
  filter(Layer != "Aggr") %>%
  select(Layer, Label, Degree, Strength) %>%
  gather(key = Statistic, value = value, Degree:Strength, -Layer) %>%
  mutate(Label = str_replace_all(Label, "_", " ")) %>%
  mutate(Layer = ifelse(Layer == "1", "Plate attributes",
    ifelse(Layer == "2", "Jar attributes",
    ifelse(Layer == "3", "Style",
    ifelse(Layer == "4", "Economic", 0)))) %>%
  rename(Site = Label) %>%
  group_by(Layer, Statistic) %>%
  summarize(Total_Centrality = sum(value)) %>%
  ggplot() +
  geom_bar(aes(x = reorder(Layer, Total_Centrality), y= Total_Centrality,
    fill = Statistic),
    stat = "identity") +
  coord_flip() +
  scale_fill_jama() +
  theme_bw() +
  xlab("") +
  ylab("Centrality Score")

# Summary of centrality scores, post-migration
post_centr %>%
  filter(Layer != "Aggr") %>%
  select(Layer, Label, Degree, Strength) %>%
  gather(key = Statistic, value = value, Degree:Strength, -Layer) %>%
  mutate(Label = str_replace_all(Label, "_", " ")) %>%
  mutate(Layer = ifelse(Layer == "1", "Plate attributes",
    ifelse(Layer == "2", "Jar attributes",
    ifelse(Layer == "3", "Style",
    ifelse(Layer == "4", "Economic", 0)))) %>%
  rename(Site = Label) %>%
  group_by(Layer, Statistic) %>%
  summarize(Total_Centrality = sum(value)) %>%
  ggplot() +
  geom_bar(aes(x = reorder(Layer, Total_Centrality), y= Total_Centrality,
    fill = Statistic),
    stat = "identity") +
  coord_flip() +
  scale_fill_jama() +
  theme_bw() +
  xlab("") +

```

```

ylab("Centrality Score")

# Plotting
plot(cnet, vertex.labels.cex = .6)
plot(cnet_pre, vertex.labels.cex = .6)
plot(cnet_post, vertex.labels.cex = .6)

# Circular Layout
l <- layout.circular.ml(cnet)
plot(cnet, layout = l, vertex.labels.cex = .6)

# Community Detection
com <- clique.percolation.ml(cnet)
com_pre <- clique.percolation.ml(cnet_pre)
com_pre_4 <- clique.percolation.ml(cnet_pre, m = 4)
com_post <- clique.percolation.ml(cnet_post)
com_post_4 <- clique.percolation.ml(cnet_post, m = 4)
plot(cnet, com = com, layout = l, vertex.labels.cex = .6)
plot(cnet_pre, com = com_pre, vertex.labels.cex = .6)
plot(cnet_pre, com = com_pre_4, vertex.labels.cex = .6)
plot(cnet_post, com = com_post, vertex.labels.cex = .6)
plot(cnet_post, com = com_post_4, vertex.labels.cex = .6)

glouvain.ml(cnet_post)
com_lart_pre <- lart.ml(cnet_pre)
plot(cnet_pre, com = com_lart_pre, vertex.labels.cex = .6)
com_lart_post <- lart.ml(cnet_post)
plot(cnet_post, com = com_lart_post, vertex.labels.cex = .6)

```

APPENDIX D

LA-ICP-MS Data and Supplementary Statistical Documentation for Group Assignments

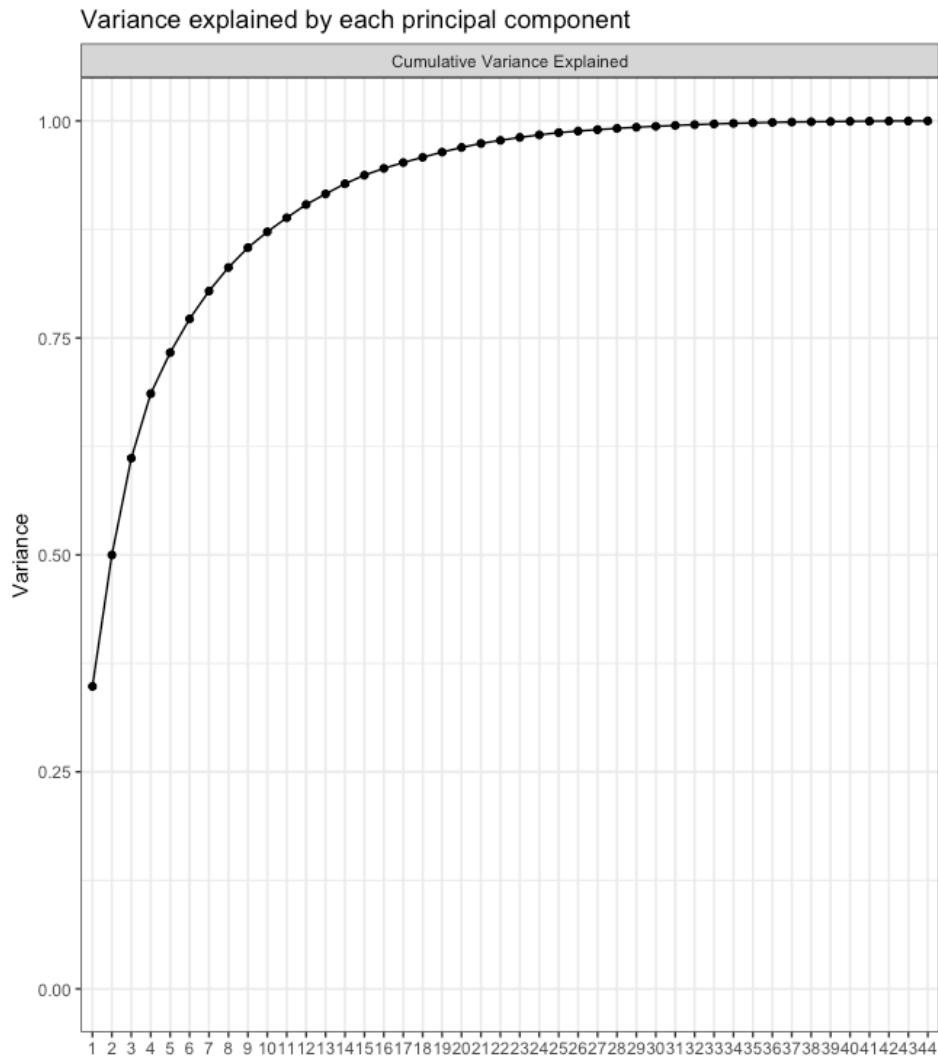


Figure D.1 Percent variance explained by each principal component for the sherds data set

Table D.1 Component loadings for the first 12 principal components, accounting for 90.4% of the variance in the 44 element data set

Element	PC1	PC2	PC3	PC4	PC5	PC6	PC7	PC8	PC9	PC10	PC11	PC12
Si	-0.033	0.026	0.016	-0.034	-0.024	0.011	-0.016	0.001	-0.029	0.009	-0.035	0.023
Na	0.021	-0.262	0.059	-0.160	-0.002	0.102	-0.015	0.450	0.359	0.035	-0.376	-0.345
Mg	0.175	-0.532	-0.085	0.226	0.241	0.567	-0.135	0.063	-0.215	0.293	0.041	0.213
Al	0.066	-0.030	0.045	0.120	0.079	-0.079	0.047	-0.034	0.117	-0.114	0.137	-0.055
K	0.055	-0.152	-0.019	0.087	0.043	0.024	-0.104	0.104	0.158	-0.198	-0.013	-0.342
Mn	0.282	-0.226	-0.582	-0.361	-0.350	-0.138	-0.207	0.109	-0.068	-0.133	0.251	0.058
Fe	0.081	0.018	-0.160	-0.001	0.056	-0.085	0.037	0.011	0.035	0.051	0.054	-0.192
Ti	0.058	-0.066	0.092	0.075	-0.035	0.101	0.043	-0.065	0.206	0.122	-0.004	-0.074

Table D.1 (cont.)

Li	0.079	-0.042	0.083	0.167	0.068	0.010	-0.129	-0.119	0.100	-0.106	0.344	-0.144
Be	0.088	-0.052	-0.026	0.120	0.051	-0.146	0.176	-0.190	0.032	0.020	0.065	-0.061
B	0.138	-0.187	0.023	0.288	0.106	-0.179	-0.259	-0.103	-0.317	-0.581	-0.449	0.028
Sc	0.097	0.031	0.083	-0.048	-0.136	0.067	-0.095	-0.357	-0.035	0.213	-0.116	-0.114
V	0.109	-0.043	-0.075	0.134	0.095	-0.060	0.051	-0.168	0.148	0.049	0.187	-0.009
Cr	0.103	-0.063	-0.002	0.185	0.086	-0.113	0.110	-0.114	0.111	-0.013	0.132	0.021
Ni	0.183	-0.138	-0.174	0.135	0.152	-0.203	0.338	-0.277	0.120	0.035	-0.179	-0.116
Co	0.195	-0.201	-0.218	-0.043	-0.024	-0.150	0.081	-0.104	0.288	0.097	-0.079	0.076
Zn	0.165	-0.068	0.036	0.277	-0.105	-0.416	-0.005	0.206	-0.347	0.476	-0.043	-0.178
Rb	0.073	-0.018	0.061	0.113	-0.071	-0.007	-0.226	0.037	0.040	-0.051	0.206	-0.257
Zr	0.098	-0.092	0.089	0.018	0.056	0.016	0.020	0.005	0.243	-0.021	-0.071	-0.045
Nb	0.085	0.002	0.114	0.050	-0.107	0.009	-0.052	-0.099	0.234	0.093	0.001	-0.037
In	0.136	0.003	0.019	0.068	-0.414	0.106	0.071	-0.079	-0.054	-0.068	-0.141	-0.100
Sn	0.158	-0.061	0.156	0.217	-0.539	0.287	0.517	0.094	-0.108	-0.223	0.098	-0.010
Cs	0.104	0.062	0.095	0.171	-0.097	0.007	-0.358	-0.103	0.001	-0.014	0.270	-0.123
La	0.190	0.025	0.084	-0.102	-0.008	0.070	-0.040	-0.186	0.020	-0.010	-0.089	0.152
Ce	0.187	0.021	0.018	-0.128	-0.065	0.010	-0.066	-0.175	0.183	0.017	-0.157	0.289
Pr	0.189	0.055	0.069	-0.109	0.005	0.057	-0.052	-0.122	0.029	-0.042	-0.083	0.116
Ta	0.106	0.059	0.166	0.015	-0.117	0.005	-0.197	-0.036	0.222	0.037	-0.099	0.013
Y	0.207	0.091	0.065	-0.184	0.037	0.082	0.038	-0.165	-0.200	0.151	-0.054	-0.221
Pb	0.169	0.103	0.032	0.184	-0.097	-0.278	-0.011	0.279	0.032	0.182	-0.166	0.332
U	0.152	0.140	0.129	0.110	-0.111	0.000	-0.174	0.162	0.101	0.095	0.002	0.179
W	0.084	0.065	0.137	0.155	-0.080	-0.080	-0.125	0.198	0.161	-0.084	0.122	0.158
Mo	0.117	0.569	-0.557	0.366	0.085	0.330	-0.034	0.087	0.100	0.011	-0.174	-0.098
Nd	0.178	0.019	0.045	-0.035	0.146	0.003	0.101	0.077	0.070	-0.131	0.081	0.190
Sm	0.174	0.044	0.039	-0.049	0.150	0.009	0.105	0.096	0.021	-0.109	0.078	0.140
Eu	0.196	0.062	0.087	-0.100	0.048	0.036	0.043	0.023	-0.031	0.023	-0.008	0.046
Gd	0.182	0.063	0.043	-0.082	0.160	-0.004	0.145	0.119	-0.040	-0.063	0.070	0.036
Tb	0.193	0.111	0.067	-0.158	0.048	0.040	0.005	-0.013	-0.118	0.018	-0.041	-0.078
Dy	0.184	0.062	0.055	-0.074	0.178	-0.020	0.116	0.144	-0.066	-0.079	0.108	-0.038
Ho	0.196	0.112	0.071	-0.159	0.060	0.033	-0.024	-0.005	-0.118	0.007	-0.024	-0.135
Er	0.184	0.054	0.073	-0.058	0.183	-0.021	0.115	0.160	-0.049	-0.057	0.111	-0.060
Tm	0.185	0.104	0.071	-0.133	0.031	0.050	-0.045	-0.002	-0.102	0.013	-0.057	-0.153
Yb	0.173	0.046	0.072	-0.033	0.168	-0.019	0.072	0.178	-0.027	-0.076	0.121	-0.041
Lu	0.180	0.105	0.087	-0.126	0.017	0.048	-0.066	-0.010	-0.088	0.028	-0.060	-0.142
Th	0.154	0.043	0.128	0.018	0.011	0.036	-0.173	-0.034	0.097	0.013	0.003	0.068

Table D.2 Posterior classification probabilities based on jackknifed Mahalanobis for Core A1 and Core A2 Sub-Groups

Sample #	Site	Core A Sub-Group	Membership Probability	
			Core A1	Core A2
5	Orendorf C	Core A1	37.3690	0.0000
23	Orendorf C	Core A1	42.4300	0.0000
50	Orendorf C	Core A1	18.7800	0.0000
67	Orendorf C	Core A1	8.2790	0.0000
68	Orendorf C	Core A1	48.9720	0.0080
70	Orendorf C	Core A1	14.1390	0.1430
145	Crabbe	Core A1	58.1420	0.0000
159	Crabbe	Core A1	27.1720	0.0000
166	Crabbe	Core A1	15.1250	0.0000
180	Crabbe	Core A1	9.2120	0.0000
245	C.W. Cooper	Core A1	91.1720	0.0000
246	C.W. Cooper	Core A1	78.0740	0.0000
252	Emmons	Core A1	74.8250	0.0000
	Emmons	Core A1	89.6390	0.0000

Table D.2 (cont.)

253				
254	Emmons	Core A1	91.7550	0.0000
261	Emmons	Core A1	83.7390	0.0030
263	Emmons	Core A1	59.3840	0.0000
266	Emmons	Core A1	80.6780	0.0000
276	Emmons	Core A1	95.6590	0.0000
277	Emmons	Core A1	35.5950	0.0000
279	Emmons	Core A1	17.2490	0.0000
280	Emmons	Core A1	28.3420	0.0000
281	Emmons	Core A1	90.3640	0.0000
291	Emmons	Core A1	43.1060	0.1650
307	Baehr South	Core A1	9.9830	0.0000
319	Myer-Dickson	Core A1	10.0350	0.0000
320	Myer-Dickson	Core A1	88.1220	0.0000
327	Myer-Dickson	Core A1	55.3070	0.0000
328	Myer-Dickson	Core A1	18.0850	0.0000
329	Myer-Dickson	Core A1	87.9720	0.0000
345	Myer-Dickson	Core A1	31.0480	0.0010
394	Star Bridge	Core A1	30.6000	0.0790
457	Star Bridge	Core A1	83.2690	0.0000
499	Ten Mile Creek	Core A1	79.3510	0.0000
508	Ten Mile Creek	Core A1	13.8100	0.2990
511	Ten Mile Creek	Core A1	83.6280	0.0000
535	Eveland	Core A1	69.5660	0.0110
537	Eveland	Core A1	44.0550	0.0330
544	Eveland	Core A1	57.0680	0.0180
545	Eveland	Core A1	13.6720	0.0050
552	Eveland	Core A1	28.6070	0.0160
561	Eveland	Core A1	37.8710	0.0000
562	Eveland	Core A1	42.6800	1.3380
563	Eveland	Core A1	67.0610	0.0080
564	Eveland	Core A1	64.9730	0.0260
580	Kingston Lake	Core A1	30.5190	0.0000
584	Kingston Lake	Core A1	53.6350	0.0000
630	Kingston Lake	Core A1	81.5830	0.0000
648	Kingston Lake	Core A1	10.1500	0.0000
655	Kingston Lake	Core A1	72.6500	0.0000
687	Lawrenz Gun Club	Core A1	12.3050	0.0290
728	Buckeye Bend	Core A1	31.3320	0.0010
729	Buckeye Bend	Core A1	17.1650	0.0000
737	Buckeye Bend	Core A1	19.6050	0.0000
738	Buckeye Bend	Core A1	64.7170	0.0330
740	Buckeye Bend	Core A1	29.1350	0.0020
742	Buckeye Bend	Core A1	6.0980	0.0680
745	Fouts Village	Core A1	86.6640	0.2640
746	Fouts Village	Core A1	34.3180	0.0500
748	Fouts Village	Core A1	88.9660	0.2800
749	Fouts Village	Core A1	42.8830	0.0000
750	Fouts Village	Core A1	75.3320	0.0010
751	Fouts Village	Core A1	63.9540	0.0100
755	Fouts Village	Core A1	44.7540	0.0320
756	Fouts Village	Core A1	45.2520	0.0660
757	Fouts Village	Core A1	88.4720	0.1320
758	Fouts Village	Core A1	34.2740	0.0000
763	Fouts Village	Core A1	60.3590	0.2340
773	Larson	Core A1	50.7510	0.0000

Table D.2 (cont.)

780	Larson	Core A1	8.9070	0.0030
786	Larson	Core A1	96.4890	0.0000
788	Larson	Core A1	29.3050	0.0000
793	Larson	Core A1	28.4760	0.0000
796	Larson	Core A1	65.5530	0.0110
797	Larson	Core A1	37.6950	0.0000
810	Larson	Core A1	24.9180	0.0010
815	Larson	Core A1	56.0440	0.0000
819	Larson	Core A1	66.0180	0.0000
822	Larson	Core A1	37.5620	0.0000
826	Larson	Core A1	98.4980	0.0000
838	Larson	Core A1	56.1790	0.0000
842	Larson	Core A1	23.8470	0.0000
843	Larson	Core A1	55.3470	0.0010
845	Larson	Core A1	54.5590	0.0000
867	Morton Village	Core A1	8.8500	0.0000
882	Morton Village	Core A1	14.2240	0.0000
884	Morton Village	Core A1	23.7390	0.0000
888	Morton Village	Core A1	61.5110	0.0040
895	Houston-Shryock	Core A1	32.0750	0.0010
896	Houston-Shryock	Core A1	77.4130	0.0000
898	Houston-Shryock	Core A1	63.5530	0.0000
900	Houston-Shryock	Core A1	35.0040	0.0000
908	Houston-Shryock	Core A1	30.7550	0.0000
910	Houston-Shryock	Core A1	98.3630	0.0000
915	Houston-Shryock	Core A1	25.8110	0.0330
918	Houston-Shryock	Core A1	87.0970	0.0000
920	Houston-Shryock	Core A1	3.9680	0.4320
921	Houston-Shryock	Core A1	53.5450	0.0000
927	Houston-Shryock	Core A1	82.8340	0.0000
930	Houston-Shryock	Core A1	61.6430	0.0000
1061	Crable	Core A1	30.3960	0.0000
1068	Crable	Core A1	21.5850	0.0000
1070	Crable	Core A1	81.4990	0.0000
1072	Crable	Core A1	64.6400	0.0000
1163	Morton Village	Core A1	61.4770	0.0000
1170	Morton Village	Core A1	63.4230	0.0390
1171	Morton Village	Core A1	23.8940	0.0030
1177	Morton Village	Core A1	71.1460	0.0000
1178	Morton Village	Core A1	15.5530	0.2160
1184	Morton Village	Core A1	20.1310	0.0260
1187	Morton Village	Core A1	25.9160	0.0010
1194	Morton Village	Core A1	30.8080	0.0000
1201	Orendorf D	Core A1	80.6520	0.0000
1202	Orendorf D	Core A1	50.4840	0.0000
1207	Orendorf D	Core A1	21.9190	0.0040
1211	Orendorf D	Core A1	6.4620	0.8890
1213	Orendorf D	Core A1	55.1570	0.0370
1223	Orendorf D	Core A1	42.9220	0.0110
1226	Orendorf D	Core A1	16.1780	0.0050
1235	Orendorf D	Core A1	36.6980	0.0110
1242	Orendorf D	Core A1	77.6970	0.0150
1251	Orendorf D	Core A1	18.4250	0.1340
1257	Orendorf D	Core A1	6.7060	0.0540
1282	C.W. Cooper	Core A1	60.1370	0.0000

Table D.2 (cont.)

1283	C.W. Cooper	Core A1	63.9300	0.0000
1284	C.W. Cooper	Core A1	47.1060	0.0000
1286	C.W. Cooper	Core A1	93.8340	0.0000
1291	C.W. Cooper	Core A1	83.6530	0.0000
1294	C.W. Cooper	Core A1	11.5030	0.0060
1296	C.W. Cooper	Core A1	68.0910	0.0000
1298	C.W. Cooper	Core A1	63.6830	0.0000
1299	C.W. Cooper	Core A1	53.0830	0.0000
1309	Orendorf D	Core A1	83.0500	0.3540
66	Orendorf C	Core A2	0.1010	11.8990
104	Crabbe	Core A2	0.0070	82.0550
105	Crabbe	Core A2	0.0450	91.9200
107	Crabbe	Core A2	0.0000	50.8880
118	Crabbe	Core A2	0.0000	54.1540
148	Crabbe	Core A2	0.0310	68.3250
162	Crabbe	Core A2	0.0020	31.3960
194	Walsh	Core A2	0.0000	94.4490
199	Walsh	Core A2	0.0000	77.8040
203	Walsh	Core A2	0.0310	27.7130
206	Walsh	Core A2	0.0010	55.3620
219	Walsh	Core A2	0.0100	82.0530
221	Lawrenz Gun Club	Core A2	0.0010	3.5200
231	Lawrenz Gun Club	Core A2	0.0000	41.7300
241	Lawrenz Gun Club	Core A2	0.0000	49.0670
243	C.W. Cooper	Core A2	0.0030	54.0250
257	Emmons	Core A2	0.2250	54.5390
262	Emmons	Core A2	0.0730	71.1940
270	Emmons	Core A2	0.3500	26.0490
275	Emmons	Core A2	0.0270	70.7010
285	Emmons	Core A2	0.1750	5.1830
294	Emmons	Core A2	0.0260	74.6740
298	Baehr South	Core A2	0.0240	27.7340
303	Baehr South	Core A2	0.0000	51.8190
310	Baehr South	Core A2	0.0470	49.1890
332	Myer-Dickson	Core A2	0.0380	10.8800
346	Myer-Dickson	Core A2	0.0010	64.6110
387	Star Bridge	Core A2	0.0090	59.4270
398	Star Bridge	Core A2	0.3380	8.6740
407	Star Bridge	Core A2	0.0240	67.7540
427	Star Bridge	Core A2	0.0540	26.5990
479	Star Bridge	Core A2	0.0510	4.0320
488	Ten Mile Creek	Core A2	0.0470	22.1940
515	Ten Mile Creek	Core A2	0.0000	20.9620
520	Ten Mile Creek	Core A2	0.0100	26.4740
531	Ten Mile Creek	Core A2	0.0020	60.0270
538	Eveland	Core A2	0.0010	38.5250
546	Eveland	Core A2	0.0000	10.6350
553	Eveland	Core A2	0.1270	9.7980
560	Eveland	Core A2	0.0450	9.3670
565	Eveland	Core A2	0.0000	19.0490
597	Kingston Lake	Core A2	0.0000	88.7310
600	Kingston Lake	Core A2	0.0040	16.4530
602	Kingston Lake	Core A2	0.0000	17.8080
608	Kingston Lake	Core A2	0.0050	67.1550
626	Kingston Lake	Core A2	0.0000	66.3040

Table D.2 (cont.)

631	Kingston Lake	Core A2	0.0000	77.4090
650	Kingston Lake	Core A2	0.1480	58.4460
652	Kingston Lake	Core A2	0.0000	55.7460
661	Lawrenz Gun Club	Core A2	0.0000	43.4560
662	Lawrenz Gun Club	Core A2	0.0000	91.4010
663	Lawrenz Gun Club	Core A2	0.0160	96.2420
665	Lawrenz Gun Club	Core A2	0.0010	79.5940
673	Lawrenz Gun Club	Core A2	0.0010	40.9220
677	Lawrenz Gun Club	Core A2	0.0000	75.7870
680	Lawrenz Gun Club	Core A2	0.0000	97.3340
681	Lawrenz Gun Club	Core A2	0.0000	47.3040
682	Lawrenz Gun Club	Core A2	0.0000	15.8450
683	Lawrenz Gun Club	Core A2	0.0000	59.8090
685	Lawrenz Gun Club	Core A2	0.0000	83.3410
724	Buckeye Bend	Core A2	0.0000	6.8130
739	Buckeye Bend	Core A2	0.0130	23.3610
762	Fouts Village	Core A2	0.2360	4.9930
850	Larson	Core A2	0.5420	22.2100
883	Morton Village	Core A2	0.1180	15.6590
901	Houston-Shryock	Core A2	0.0030	66.7800
902	Houston-Shryock	Core A2	0.0960	49.9000
913	Houston-Shryock	Core A2	0.1510	56.2730
919	Houston-Shryock	Core A2	0.0000	44.9240
1058	Crable	Core A2	0.0000	36.0610
1059	Crable	Core A2	0.0000	23.7950
1062	Crable	Core A2	0.0040	82.1710
1065	Crable	Core A2	0.0000	28.5450
1074	Crable	Core A2	0.0000	93.3400
1075	Crable	Core A2	0.0160	96.2150
1077	Crable	Core A2	0.0000	88.7430
1078	Crable	Core A2	0.0000	95.8950
1174	Morton Village	Core A2	0.0000	21.0460
1175	Morton Village	Core A2	0.0130	11.6420
1176	Morton Village	Core A2	1.4160	7.2310
1198	Orendorf D	Core A2	0.0030	88.9410
1229	Orendorf D	Core A2	0.0010	22.2370
1247	Orendorf D	Core A2	2.3470	27.6440
1302	Crable	Core A2	0.0000	45.4390
1303	Crable	Core A2	0.1030	98.0840
1305	Crable	Core A2	0.0130	39.6200
1306	Crable	Core A2	0.0180	98.5290
1310	Orendorf D	Core A2	0.0030	85.4870

Table D.3 Mean and standard deviation values for the ceramic geochemical compositional groups

	Core A (<i>n</i> = 161)		Core A1 (<i>n</i> = 133)		Core A2 (<i>n</i> = 88)	
	Average	Std Dev	Average	Std Dev	Average	Std Dev
Al	89977.7	± 7292.8	93785.0	± 7826.4	83861.7	± 8462.4
B	72.7	± 20.7	83.1	± 22.2	61.0	± 15.9
Be	2.5	± 0.3	2.7	± 0.4	2.4	± 0.3
Ce	91.4	± 15.6	97.4	± 16.7	82.0	± 13.9
Co	14.6	± 2.7	17.3	± 2.3	11.3	± 1.5
Cr	97.3	± 11.6	104.7	± 11.5	83.5	± 11.3
Cs	5.2	± 1.0	5.0	± 0.8	5.4	± 0.9
Dy	5.7	± 0.8	5.9	± 0.8	5.1	± 0.7
Er	3.2	± 0.4	3.3	± 0.5	2.9	± 0.5
Eu	1.8	± 0.3	1.9	± 0.3	1.7	± 0.3
Fe	53982.3	± 7132.0	55216.3	± 6394.8	46978.7	± 7554.3
Gd	6.4	± 0.9	6.6	± 0.9	5.8	± 0.8
Ho	1.3	± 0.2	1.3	± 0.3	1.2	± 0.2
In	0.1	± 0.0	0.1	± 0.0	0.1	± 0.0
K	21042.0	± 2361.0	22175.4	± 2369.6	18879.7	± 3005.5
La	47.3	± 8.6	50.9	± 8.9	41.8	± 7.0
Li	37.8	± 5.7	40.1	± 6.2	37.4	± 5.5
Lu	0.5	± 0.1	0.5	± 0.1	0.5	± 0.1
Mg	11606.3	± 3376.1	17914.7	± 6526.7	8250.3	± 1305.4
Mn	678.6	± 285.7	820.8	± 291.2	451.8	± 198.3
Mo	0.8	± 0.3	0.7	± 0.2	0.8	± 0.4
Na	6381.7	± 1223.8	6998.3	± 1043.8	5537.5	± 924.0
Nb	18.7	± 2.5	18.8	± 2.4	18.3	± 3.1
Nd	38.7	± 4.7	41.0	± 4.8	33.5	± 4.1
Ni	53.2	± 9.8	62.7	± 9.9	39.6	± 8.2
Pb	24.8	± 4.1	25.6	± 5.2	25.5	± 4.0
Pr	12.0	± 1.9	12.7	± 2.2	10.7	± 1.8
Rb	99.6	± 13.1	99.0	± 10.9	104.2	± 12.1
Sc	19.7	± 3.5	20.5	± 4.0	20.1	± 3.4
Si	321719.5	± 9731.1	311372.4	± 9357.3	336540.2	± 10783.4
Sm	7.7	± 0.9	8.0	± 1.0	6.8	± 0.9
Sn	2.5	± 0.5	2.6	± 0.4	2.4	± 0.4
Ta	1.3	± 0.2	1.3	± 0.2	1.3	± 0.2
Tb	1.0	± 0.2	1.1	± 0.2	1.0	± 0.2
Th	14.6	± 2.3	15.1	± 2.3	13.8	± 1.9
Ti	5225.7	± 563.0	5287.9	± 570.7	5049.6	± 628.1
Tm	0.5	± 0.1	0.5	± 0.1	0.5	± 0.1
U	3.2	± 0.6	3.1	± 0.5	3.4	± 0.6
V	150.9	± 24.2	153.5	± 19.2	122.2	± 22.8
W	1.5	± 0.2	1.4	± 0.2	1.6	± 0.2
Y	32.5	± 7.0	34.2	± 7.5	30.8	± 7.6
Yb	3.1	± 0.4	3.2	± 0.4	2.9	± 0.4
Zn	150.4	± 36.5	170.2	± 44.5	157.1	± 31.6
Zr	146.7	± 25.2	155.9	± 20.5	130.8	± 19.0

Table D.3 (cont.)

	Core B (<i>n</i> = 21)		Core C (<i>n</i> = 13)		Outgroup 1 (<i>n</i> = 39)	
	Average	Std Dev	Average	Std Dev	Average	Std Dev
Al	101189.3	± 8878.5	77825.0	± 5172.5	96053.4	± 13944.9
B	86.7	± 31.3	47.1	± 11.7	79.2	± 33.9
Be	3.1	± 0.4	2.2	± 0.3	3.0	± 0.5
Ce	109.6	± 14.1	65.6	± 14.4	106.3	± 20.8
Co	18.5	± 3.0	10.1	± 1.6	16.7	± 4.4
Cr	112.2	± 13.6	77.4	± 7.4	108.8	± 17.9
Cs	5.2	± 1.3	4.4	± 1.0	5.8	± 1.7
Dy	6.7	± 1.0	4.6	± 0.8	7.3	± 1.9
Er	3.8	± 0.6	2.6	± 0.4	4.1	± 1.0
Eu	2.1	± 0.2	1.5	± 0.3	2.3	± 0.6
Fe	58195.8	± 6574.8	48996.8	± 8966.9	66075.9	± 22711.5
Gd	7.5	± 1.0	5.3	± 0.9	8.4	± 2.3
Ho	1.4	± 0.1	1.0	± 0.2	1.7	± 0.5
In	0.1	± 0.0	0.1	± 0.0	0.1	± 0.0
K	22769.6	± 3066.7	16410.1	± 2662.9	20123.8	± 5145.7
La	58.4	± 7.5	33.6	± 6.6	58.3	± 13.9
Li	41.1	± 8.7	32.4	± 7.3	41.9	± 18.8
Lu	0.6	± 0.1	0.4	± 0.1	0.7	± 0.2
Mg	18059.4	± 8689.8	7792.6	± 1558.2	11976.4	± 6433.8
Mn	752.9	± 376.0	406.0	± 208.1	1258.6	± 972.3
Mo	0.7	± 0.3	0.8	± 0.5	3.4	± 4.0
Na	6789.3	± 1304.1	6971.0	± 1313.4	5273.9	± 2337.8
Nb	20.7	± 2.0	16.5	± 2.2	19.6	± 3.5
Nd	46.5	± 5.6	29.3	± 3.3	46.4	± 9.0
Ni	67.9	± 12.2	37.5	± 8.8	67.4	± 16.9
Pb	29.4	± 6.0	22.0	± 2.4	37.1	± 17.5
Pr	14.4	± 1.8	8.8	± 1.6	14.8	± 3.4
Rb	103.9	± 14.7	87.2	± 17.0	104.7	± 22.0
Sc	22.0	± 3.5	16.9	± 3.9	23.5	± 4.9
Si	301631.5	± 11596.5	341586.2	± 7977.0	308608.6	± 15673.1
Sm	9.0	± 1.1	6.0	± 0.6	9.5	± 2.1
Sn	3.3	± 0.7	2.0	± 0.2	5.3	± 6.1
Ta	1.5	± 0.2	1.2	± 0.2	1.3	± 0.2
Tb	1.2	± 0.1	0.8	± 0.2	1.4	± 0.5
Th	17.1	± 2.6	11.6	± 2.0	16.3	± 2.7
Ti	5848.9	± 512.1	4927.8	± 732.8	5268.8	± 1049.6
Tm	0.6	± 0.1	0.4	± 0.1	0.7	± 0.2
U	3.9	± 0.8	2.8	± 0.5	4.2	± 1.1
V	152.4	± 21.8	114.9	± 14.0	165.5	± 38.8
W	1.6	± 0.2	1.4	± 0.2	1.5	± 0.3
Y	39.1	± 4.7	25.7	± 6.8	47.3	± 17.4
Yb	3.7	± 0.6	2.5	± 0.3	3.8	± 0.7
Zn	229.1	± 77.4	129.3	± 31.5	226.0	± 100.3
Zr	172.0	± 21.2	112.5	± 19.4	144.7	± 33.3

Table D.3 (cont.)

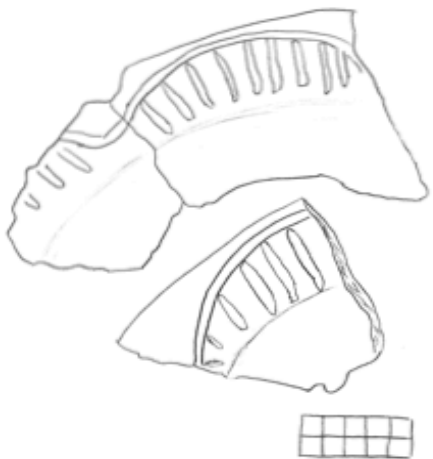
	Outgroup 2 ($n = 20$)		Unassigned ($n = 68$)	
	Average	Std Dev	Average	Std Dev
Al	78046.1	± 14533.7	83732.1	± 16282.0
B	46.6	± 9.3	61.2	± 24.1
Be	2.4	± 0.8	2.5	± 0.8
Ce	68.1	± 15.2	107.8	± 131.8
Co	11.1	± 2.7	22.7	± 65.4
Cr	78.3	± 11.9	93.7	± 53.8
Cs	4.0	± 0.9	5.0	± 1.7
Dy	3.8	± 1.2	5.1	± 1.6
Er	2.0	± 0.6	2.9	± 0.9
Eu	1.2	± 0.3	1.7	± 0.5
Fe	55708.7	± 12989.9	55436.1	± 14790.8
Gd	4.2	± 1.2	5.9	± 1.8
Ho	0.9	± 0.3	1.2	± 0.4
In	0.1	± 0.0	0.1	± 0.2
K	18096.4	± 4451.8	19804.1	± 5626.1
La	33.7	± 6.7	46.4	± 14.1
Li	29.9	± 5.7	33.4	± 7.9
Lu	0.4	± 0.1	0.5	± 0.1
Mg	5107.6	± 3595.6	11089.3	± 8066.7
Mn	574.3	± 309.4	1333.5	± 3842.3
Mo	0.7	± 0.3	1.4	± 1.5
Na	5138.9	± 1736.7	5818.7	± 1934.0
Nb	15.6	± 2.3	18.1	± 4.1
Nd	25.4	± 6.8	35.3	± 10.4
Ni	43.3	± 15.6	59.0	± 50.2
Pb	17.8	± 6.3	29.2	± 27.0
Pr	8.8	± 2.3	11.8	± 3.5
Rb	83.7	± 15.7	94.6	± 24.3
Sc	18.3	± 4.5	21.7	± 5.6
Si	339954.2	± 19989.5	327378.5	± 24369.5
Sm	5.2	± 1.4	7.0	± 2.0
Sn	1.8	± 0.4	3.9	± 3.7
Ta	1.0	± 0.3	1.2	± 0.3
Tb	0.8	± 0.2	1.0	± 0.3
Th	10.3	± 3.1	13.4	± 3.2
Ti	3980.7	± 903.0	5094.2	± 1315.8
Tm	0.4	± 0.1	0.5	± 0.1
U	2.3	± 0.8	3.3	± 1.7
V	119.6	± 25.1	141.9	± 49.1
W	1.1	± 0.3	1.4	± 0.4
Y	23.4	± 4.8	33.3	± 10.4
Yb	2.0	± 0.6	2.8	± 0.9
Zn	111.2	± 30.9	175.9	± 169.0
Zr	112.3	± 18.0	141.4	± 79.5

APPENDIX E

Plate Stylistic Design Group Sketches

Sketch-tracings or design sketches are provided for each of the plate style groups presented in Chapter 6. Sketch-tracings are denoted by the presence of 1 cm square scales and were sketched using a re-purposed computer monitor that was laid flat for accuracy of tracing. Certain design-only sketches appear without a scale. Unique Type numbers are provided that correspond to narrative descriptions of plate decoration presented in the Coding Sheet in Appendix A. These unique decoration categories total 94 across the 429 vessels with design techniques present. Additionally, a Brainerd Robinson (BR) group number is specified, which correspond to the 29 decoration motif grouping categories. Decoration categories were determined based on perceived similarities in decoration motifs alone (i.e. disregarding design technique) in order to focus solely on symbolism.

The term ‘share’ is used in sketches to denote unique types that share the decoration motif but were assessed as distinct in initial classification. The term ‘also’ is used below to denote vessels that were assessed as the same unique type number in initial classification. Sketches are ordered by BR group number and by unique decoration category.



Uniq. Type #2
P48
Orendorf C

BRG 67 #2
Shale #73, 562
Alm: P61, 62
(a. v. v. f. c.)

Uniq. Type #5
P55
Orendorf C



Shale #2
Isable

Unique Type #73
P757
Feds



Include
Re-classify sub-group
of Type #2
Shape #2, 5, 73, 62
BR Group #2

Unique Type #62
P675
Lawrence

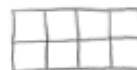
Include:
Shape Type #5, 2, 25,
BR Group #2

Unique Type #58
P 648
Kingsha Lake

Isolate
share #5, 2, 78, 62
BR Group #2

Unique Type #3
P49
Orenda & C

Also: P60, 176
(Ancient C)





Unique Type #4
P50
Dorsal C

Also: P122 Cribble
P842 Locom
Shore #7



Unique Type #7
P70
Dorsal C

Isolate
Shore #4?



Unique Type #6
P 828 Scribe?
Larson

BR Group #5
Also: 115 instances
Share #25

Unique Type #25

BR Group #5
See #6; #25 is tailed instead of incised

Share #6

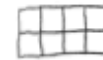
Also: 9 instances
Myer-Dickson: P333
Kingdon (see): P615, 622, 626, 649, 652
Larson: P319
Craib: P1071, 1071

Unique Type #70
P 719
Ten Mile



BR Group #5
Isolate
Re-classify as #63
or Share #6, 25

Unique Type #8
P 170
Cable



BR Group #6
Also: P123 Cable
P271 Emmons
P482 Star Bridge



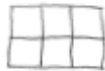
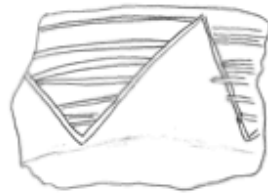
Unique Type #9
P124
Cobble

Share #10
BR Group #7
Also: P124 Cobble
P213 Walsh
P39, 311 Bache South
P627 Kingsda Linn
P954 Stone Bridge



Unique Type #10
P125
Cobble

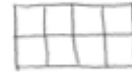
BR Group #7
Isolate
Share #9



Unique Type #11
P224
Larson

BR Group #8

Also: 11 instances
Coble, Laurens, Star Bridge,
Kingston Lake, Buckeye Bend,
Esomers, Larson



Unique Type #12
P650
Kingston Lake

BR Group #9

Also: 10 instances
Coble, Walsh, Myer-Dixon,
Star Bruce, Laurens,
Buckeye Bend, Larson
Shaw#24, 27



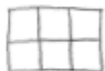
Unique Type #57
P 647
Kingston

BR Group #9
Isolate
Share #D, 24



Unique Type # 24
P 172
Cable

BR Group #9
Isolate
Share #D, 57



Unique Type #13
P146
Cable

BR Group #10

Also:
Cable: P150, 133, 157, 162, 173, 174, 178
Lowers: P241
Shore #76



Unique Type #14
P131
Cable

BR Group #11

Also: 16 instances
Cable (7), Star Bridge (9)
Shore # 23, 28, 50, 60, 66, 87
22



Unique Type #22
P 167
Cable



BR Group #11
Isolate
Share #60, 14, 23, 28,
50, 66, 27



Unique Type #23
P 169
Cable

BR Group #11
Isolate
Share #14, 28, 50, 60,
66, 27, 22



S. Makif

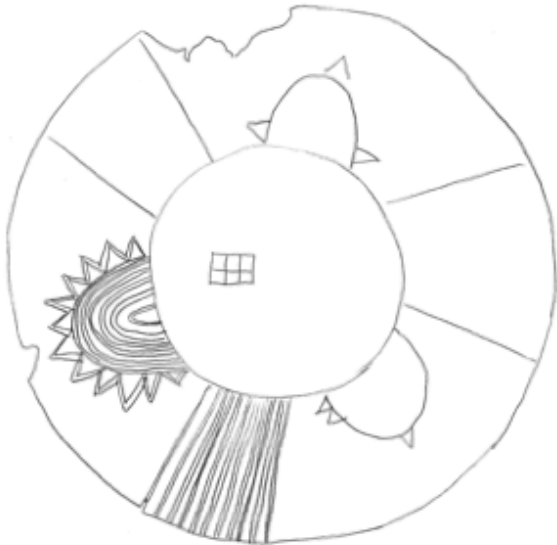
Unique Type #28
P209
Walsh

BR Group #11
Isolate
Share #14, 23, 50, 60,
66, 87, 22



Unique Type #50
P441
Ste Bridge

BR Group #11
Isolate
Share #23, 14, 20,
60, 66, 87, 22



Unique Type #60
P688
Lawrence

BR Group #11
4/ro
Lawrence P673
Cable P167 (Share #22)
Share #14, 23, 28, 50,
86, 87, 22



Unique Type #66
P687
Lawrence

BR Group #11
Isokite
Sub-type of #14/#23
Sub-variant of unique
hemispheric pattern
Share #14, 23, 28, 50, 60
87, 22

Unique Type #87
P 1075
Craie

BR Group #11
Isolate
Share # 25 (subgroup #)
20, 50, 60, 66, 22

Unique Type #30
P 628
Kingston Lake



BR Group #12
Share # 05, 25
Also:
Walsh P211
She Bridge P424
Kingston Lake P628
Lawrence P676, 709
Ten Mile P722

Unique Type #15
P139
Cable



BR Group #12
Isolate
Share #30, 15



Unique Type #75
P903
Husker Shoyard

BR Group #12
Share #30, 15
Also:
Emmons 7765
Lacina 1530, 251

Unique Type #19
P152
Cable

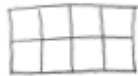


BR Group #13
Insulate
Share #69

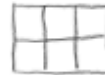
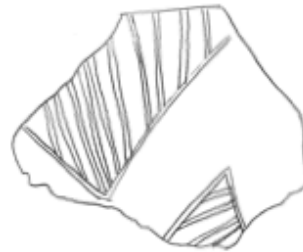
Unique Type #69
P715
Ten Mile



BR Group #13
Insulate
Share #18



Unique Type# 19
P153
Cable



BR Group# 17
Also:
P456 Star Bridge

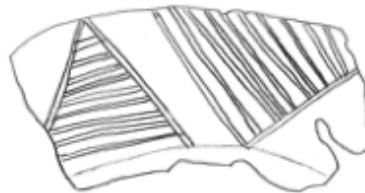
Unique Type# 20
P212
Walden

BR Group# 15
Also:
Cable P155
Share# 26, 38, 40, 74, 79+
2



Unique Type #26
P 313
Lacorn

BR Group # 15
Share # 20, 30, 40, 71, 79, 115
Also: 8 instances
Walsh P 202, 215
Evans P 211
Sto Bldg 1458
Fink P 741
Morton P 877, 1168



Unique Type #58
P 331
Myer-Dickson

Also:
Myer-Dickson P 339
BE Group # 15
Share # 20, 26, 40, 71, 79, 115, 11



Unique Type #45
P 427
Star Bridge

BR Group #15
Isolate
Shore # 20, 26, 35, 74, 77,
91



Unique Type #40
P 342
Myer-Dickson

Also: 8 Instances
Star Bridge P 425, 449,
455, 465, 466
Morden P 889, 1175
BR Group #15
Shore # 20, 26, 35, 74, 77,
91



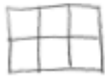
Unique Type #74
P 758
Fouls

Isolate
Re-classify as
sub-group of ? 26
Line-filled triangles
on rim and within
BE Group #15
Shore # 20, 26, 38, 40, 79, 45
71



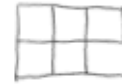
Unique Type #79
P 832
Lesson

Inhls
Shore # 40, 29, 26, 38, ?
BE Group #15 45,
71



Unique Type # 21
P 256
Cable

BR Group # 16
Also:
Star Bridge P434
Share # 46, 47, 50



Unique Type # 48
P 450
Star Bridge

BR Group # 16
Also:
Lawrence P 708
Share # 46, 47, 50

Unique Type #46
P 432
She Bridge

Cross-hatching, Ind

BR Group #16
Isolate
Share #48, #21, 52

Unique Type #52
P 737
Buckeye Bend



BR Group #16
Also:
Ten Mile P 531
Share # 21, 46, 48, 52



Unique Type *27, #63
P 275
Emmons

BR Group # 17

Abn:
With P 208
Emmons P 276
Shore # 63, 55, 94



BR Group # 17

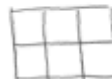
Imlate
Shore # 27, 63, 94



Unique Type #29
P899
Hoskin, Shiyek

BR Group #18

Also:
Wirth P210
Foks P752
Larson P838
Shore # 32, 68, 71



Unique Type #32
P480
Star Bridge

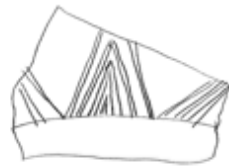
BR Group #18

Also:
Emmons P285
shore # 29, 68, 71

Unique Type #68
#713
Ten 1/16

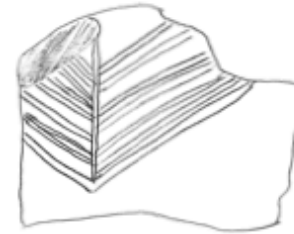


BR Group #11
Isolate
Shore ? #71, 29, 30



Unique Type # 71
P 738
Buckeye Bend

BR Group # 17
Isolate
Share? # 68, 29, 32



Unique Type # 31
P 219
Wabli

Also:
Kashin Shryack P 906
BR Group # 19
Share # 61



Unique Type #61
P 674
Lawrence

Isolate
BR Group #19
share 31

Unique Type #33
P 843
Larson

BR Group #20
share #8

Also: 26 Instances
Behr P 298, 310
Star Bridge P 420, 422, 423, 50, 157,
490, 413, 414, 417, 457,
459, 464, 471
Lawrence P 702
Ten Mile P 720
Buckeye P 754
Larkin P 87, 825, 843, 844
Cinyle P 1070
Floston P 1173, 1179



Unique Type #80
P 876
Morton

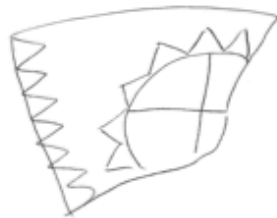
Isolate
Share #33 (rob-group)
BR Group #20

Unique Type #39
P 299
Bach



BR Group #21
Isolate
Share #36, #43, #44

Unique Type*36
P 306
Bachr



BR Group#21
Isolate
Shore # 34/43/44

Unique Type*43
P 415
Star Bridge



BR Group#21
Isolate
Shore # 34/43



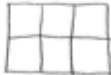
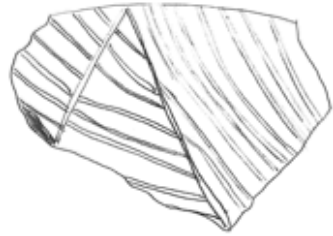
Unique Type #44
P416
Star Bridge

BR Group #21
Isolate
Share # 48, 54, 56



Unique Type #39
P336
Myer-Dickson

BR Group #22
Also
Star Bridge P445
Share # 47, 53, 58, 59



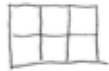
Unique Type # 49
 P 467
 Star Bridge

BR Group # 22
 Also:
 Kingston Lake P 629
 Lawrence P 696
 Larsen P 850
 Shore # 39, 53, 56, 81



Unique Type # 53
 P 623
 Kingston Lake

BR Group # 22
 Also:
 Kingston Lake P 617
 Shore # 39, 49, 56, 81



Unique Type #56
P693
Kingston Lake

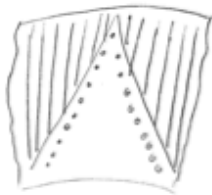
BR Group #22
Alto:
Kingston Lake P695
Share # 39, 49, 53, 54

Unique Type #81
P 992
Morden



BR Group #22
Isolate
Share w/
Compound?
Share # 39, 49, 53, 54

Unique Type #41
P 571
Cable



BIR Group # 23
Isolate
Share # 83, 84, 85, 90

Unique Type # 86
P 1074
Cable



Isolate
BIR Group # 23
Share # 41, 85, 87, 90



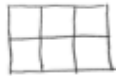
Unique Type #88
P1077
Crabbe

Isolate
Share #41, 86, 88, 90
BR Group #23



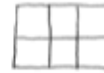
Unique Type #83
P1067
Crabbe

BR Group #23
Isolate
Share ? #41, 86, 88, 90



Unique Type #47
P705
Lawrence Gun Club

BR Group #24
Also:
Star Bridge P 448, 452



Unique Type #51
P486
Star Bridge

BR Group #25
Also:
Morton Village P1176



Unique Type #54
P621
Kingston Lake

BR Group #26
Isolate / Ind.
Share #59,67



Unique Type #59
P653
Kingston Lake

Isolate
BR Group #26
Share #59,67



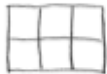
Unique Type #67
P 712
Ten Mile

Isolate
BR Group # 26
Shore # 54, 59



Unique Type #65
P 1023
Kingston Lake

BR Group # 27
Also:
Lawrence P 625
Hutchinson P 324
Shore # 82



Unique Type #82
P 908
Harden - Shryock

BR Group #27
Also:
Harden - Shryock P888
Share #65



Unique Type #72
P741
Buckeye Bend

BR Group #28
Isolate
?
Share ? #78, 84, 89
92

Unique Type #78
P 822
Larva



BR Group #28
Isolate
Share? # 72,
84, 89, 92

Unique Type #84
P 1072
Cable



BR Group #28
Isolate
Share *78 (cross-group),
? # 72, 84, 92



Unique Type #89
P1146
Lawrenz

BR Group #28
Isolate
Share # 72, 78, 84, 92



Unique Type #92
P1185
Markon

BR Group #28
Isolate:
Share # 72, 78, 84, 92

Unique Type #85
P1073
Cable



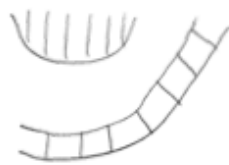
Alu
Mark. Village P167, 1181
BR Group #29

Unique Type #16
P147
Cable



BR Group # n/a
Isolate

Unique Type*17
P148
Centre



BR Group* n/a
Isolate

Unique Type*35
P335
Boehr

BR Group*-1
Isolate
Disynthetic

Unique Type #42
P413
Star Bridge



BR Group #1
Isolate

Unique Type #64
P682
Laurenz



BR Group #1
Isolate

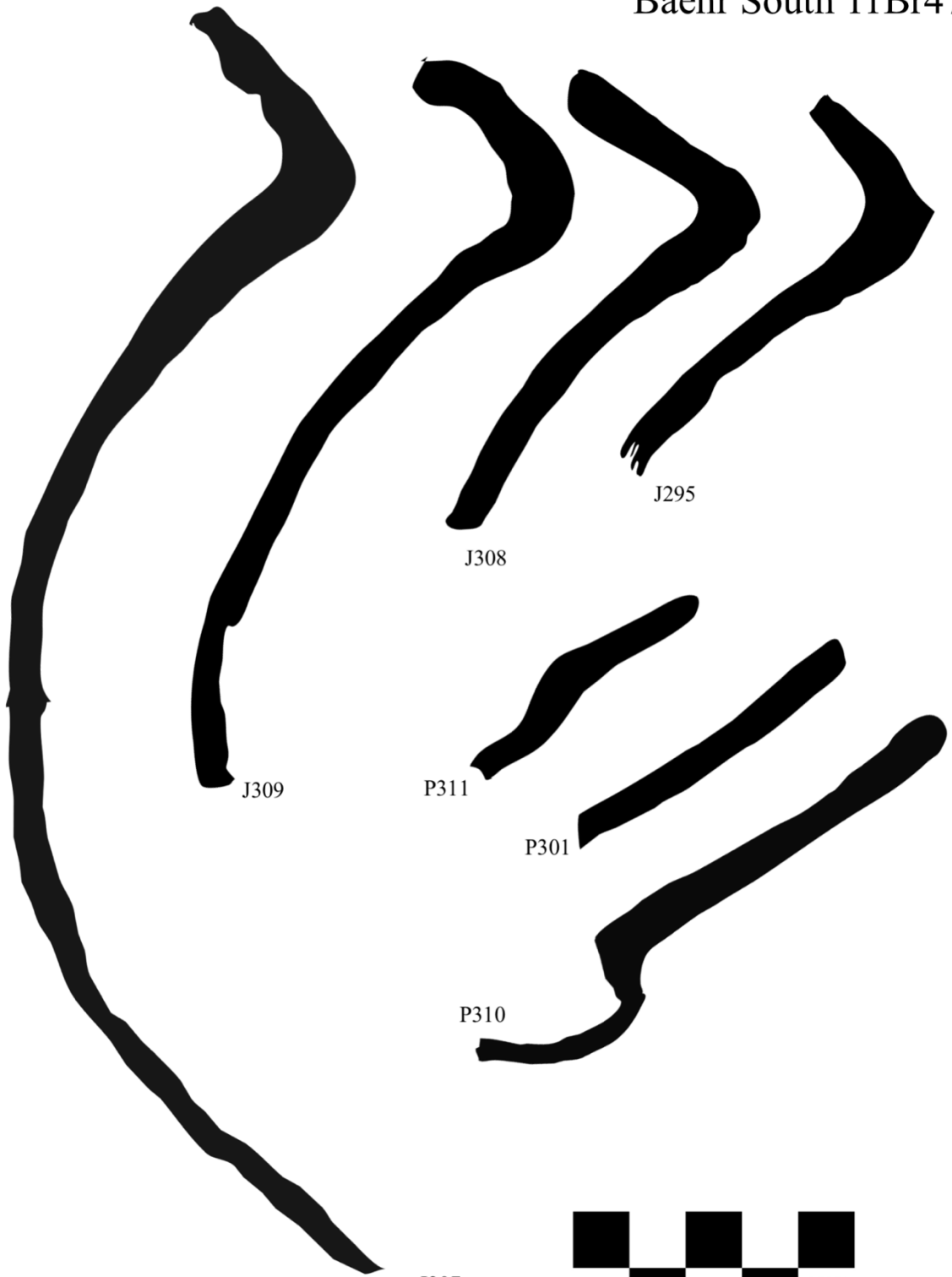
APPENDIX F

Jar and Plate Profile Sample

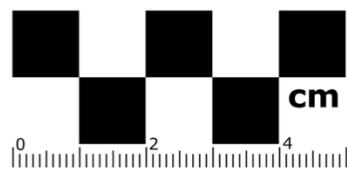
The following samples of jar and plate profiles are provided for heuristic purposes as well as to highlight the artifacts themselves that form the basis of the analyses and interpretations presented in this study. The sherds chosen for profiling follow no pre-defined sampling strategy but are meant to be representative of each assemblage. Profiles are scaled appropriately within a tolerance of approximately one cm, but no indications are provided for the presence of decoration or cord marking since detailed photographs of all vessels were taken and may be made available for research or teaching purposes by contacting the author. The orientations of vessels based on rim profiles are of course approximate. Numbering indicates the unique vessel identification number assigned to each vessel. A 'J' preceding a vessel number indicates a domestic jar, while a 'P' indicates a plate. Vessel identification numbers are sequential and do not consider the vessel class, which are provided here for ease of vessel type interpretation.

Jar and plate rim profiles from three sites are not presented here since they are already published elsewhere. See Conrad (1991) for profiles of vessels from Orendorf Settlement C and D (as well as for select other sites). See Conner (2016) for profiles of vessels from Myer-Dickson.

Baehr South 11Br47



J307



Buckeye Bend 11F310



J728



J726



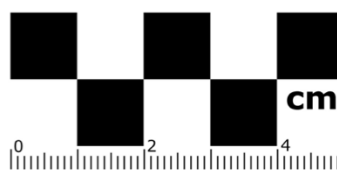
P730



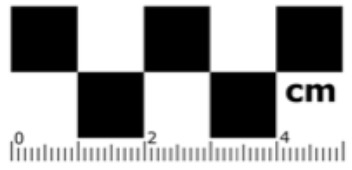
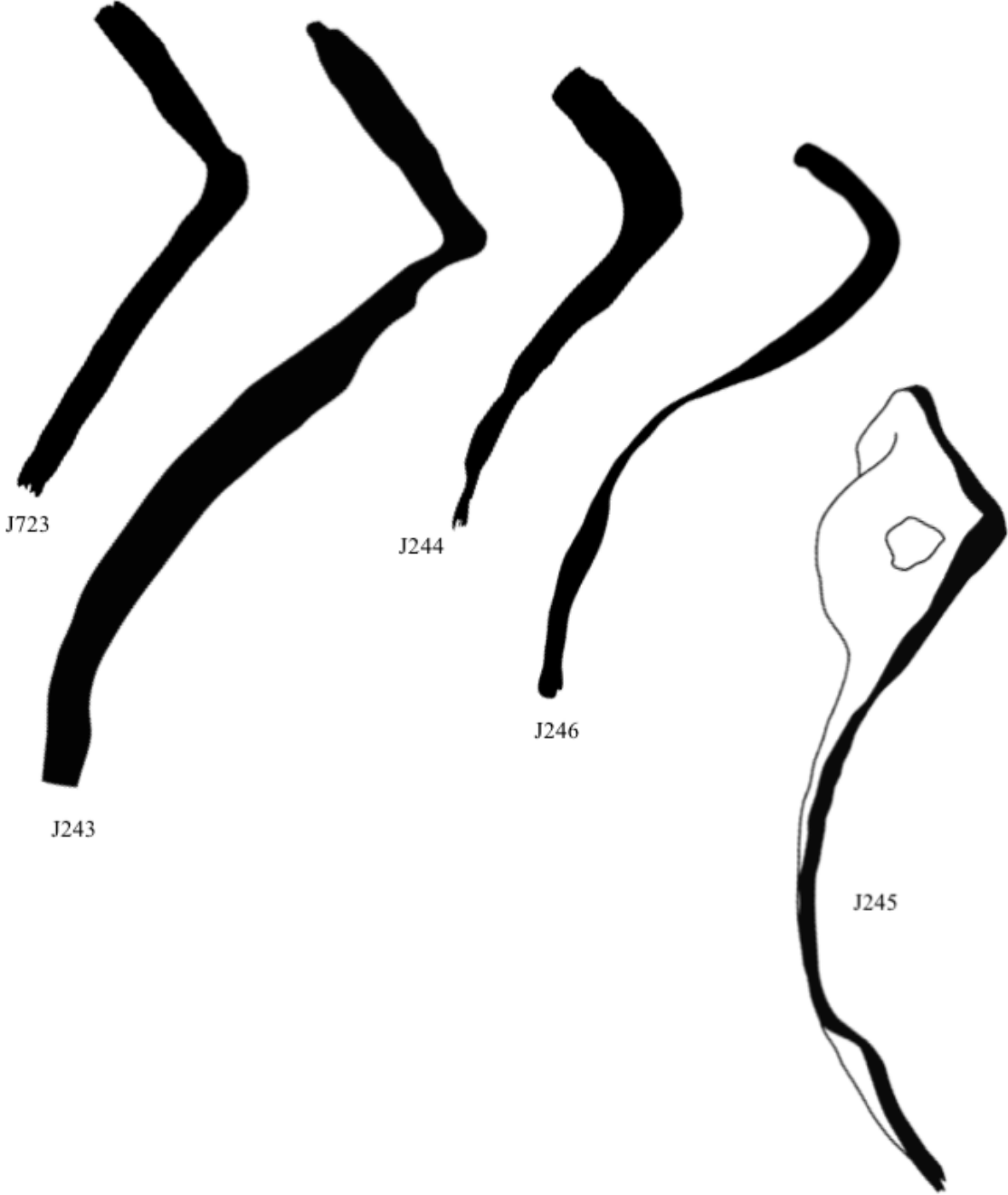
P731



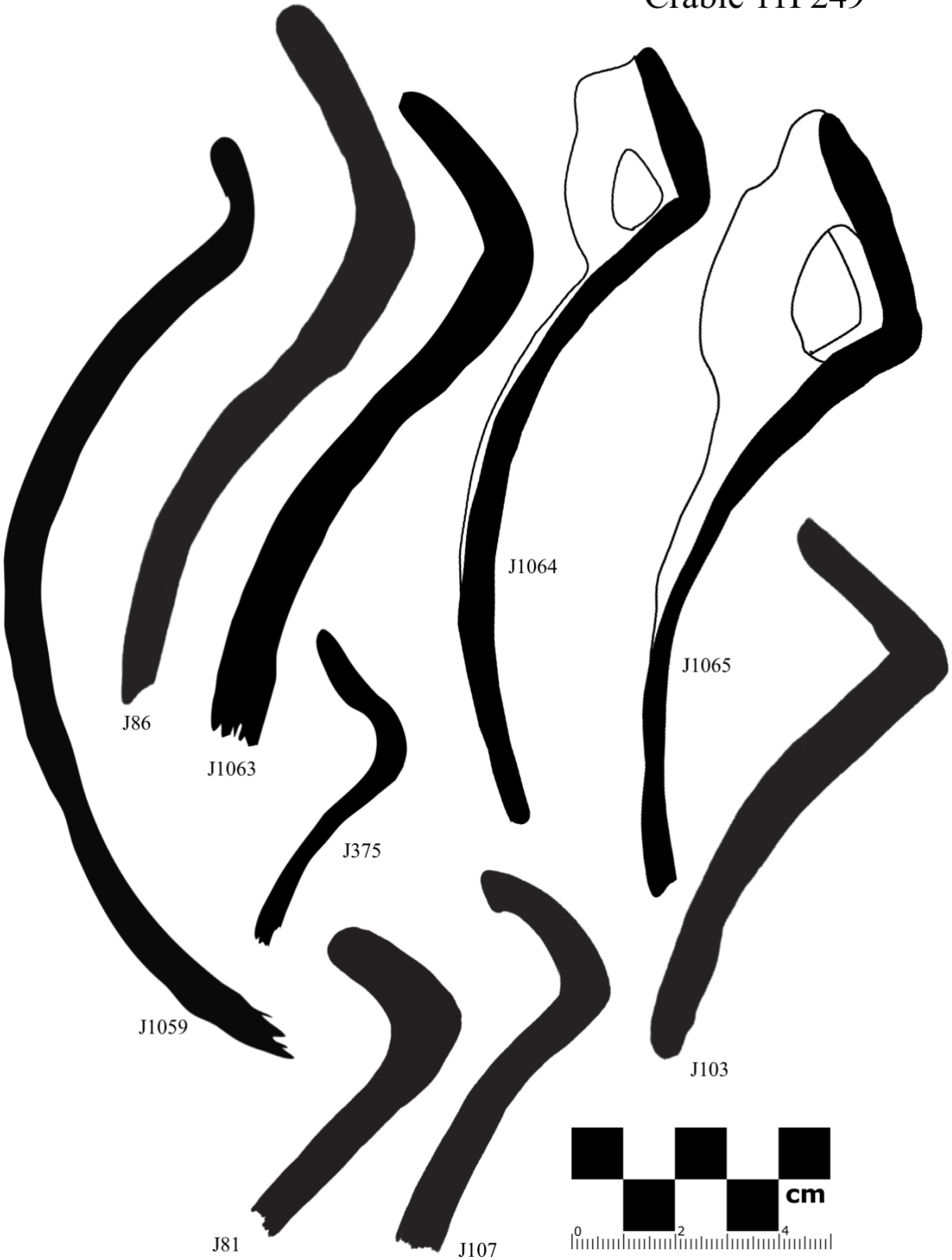
P741



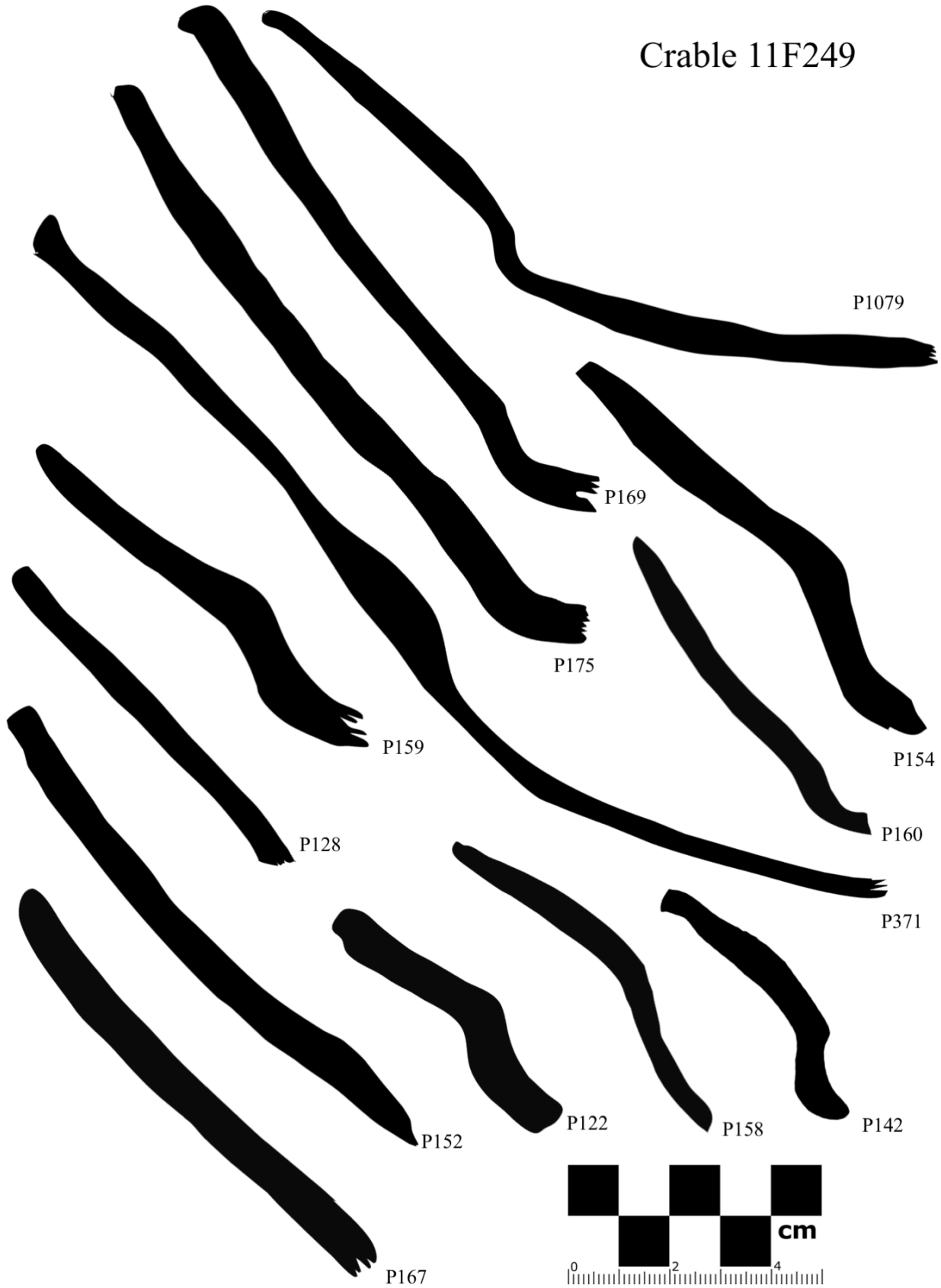
C.W. Cooper 11F15



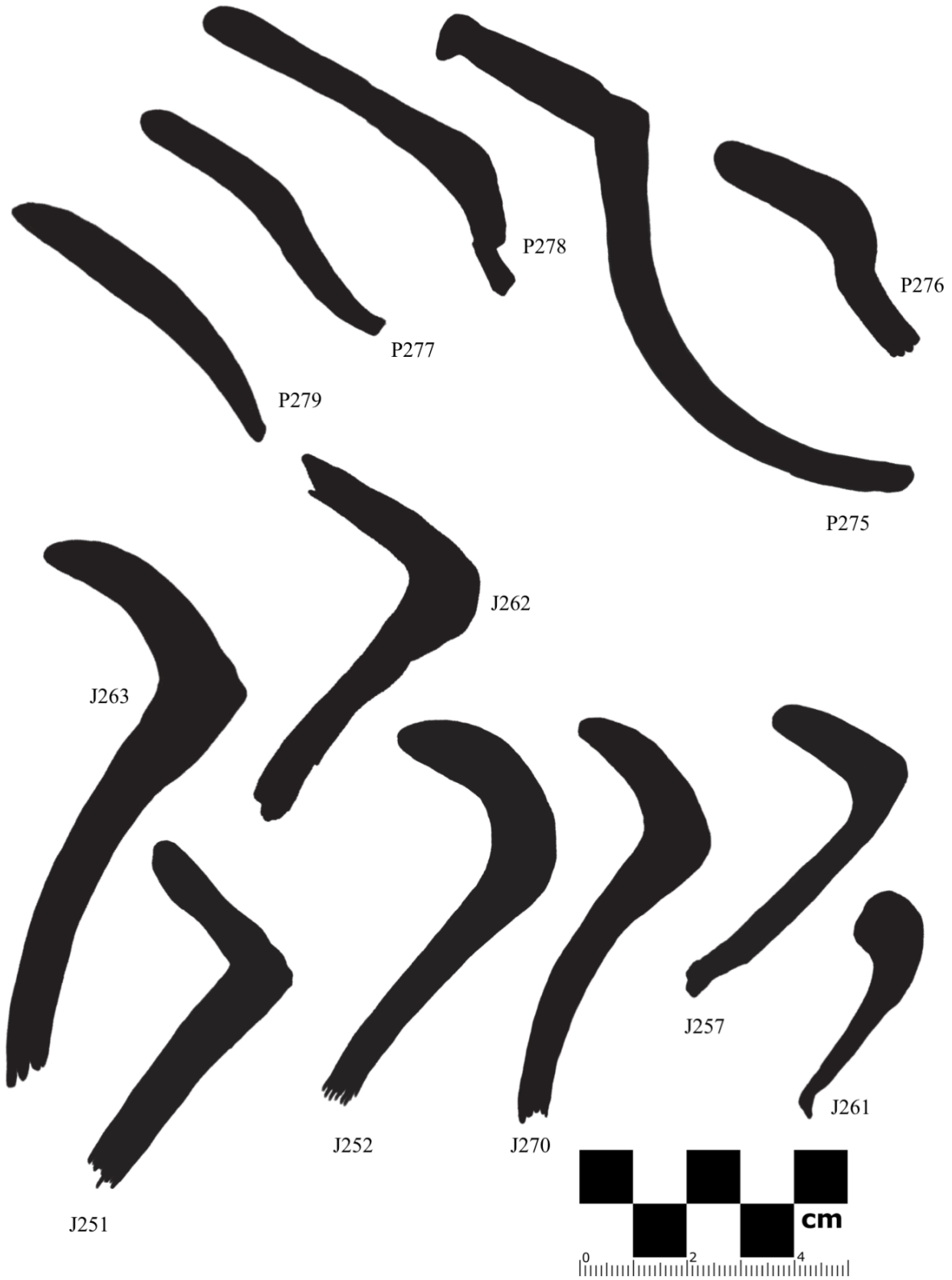
Crable 11F249



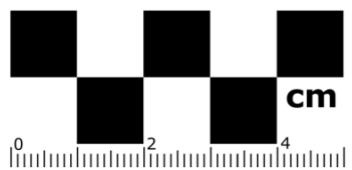
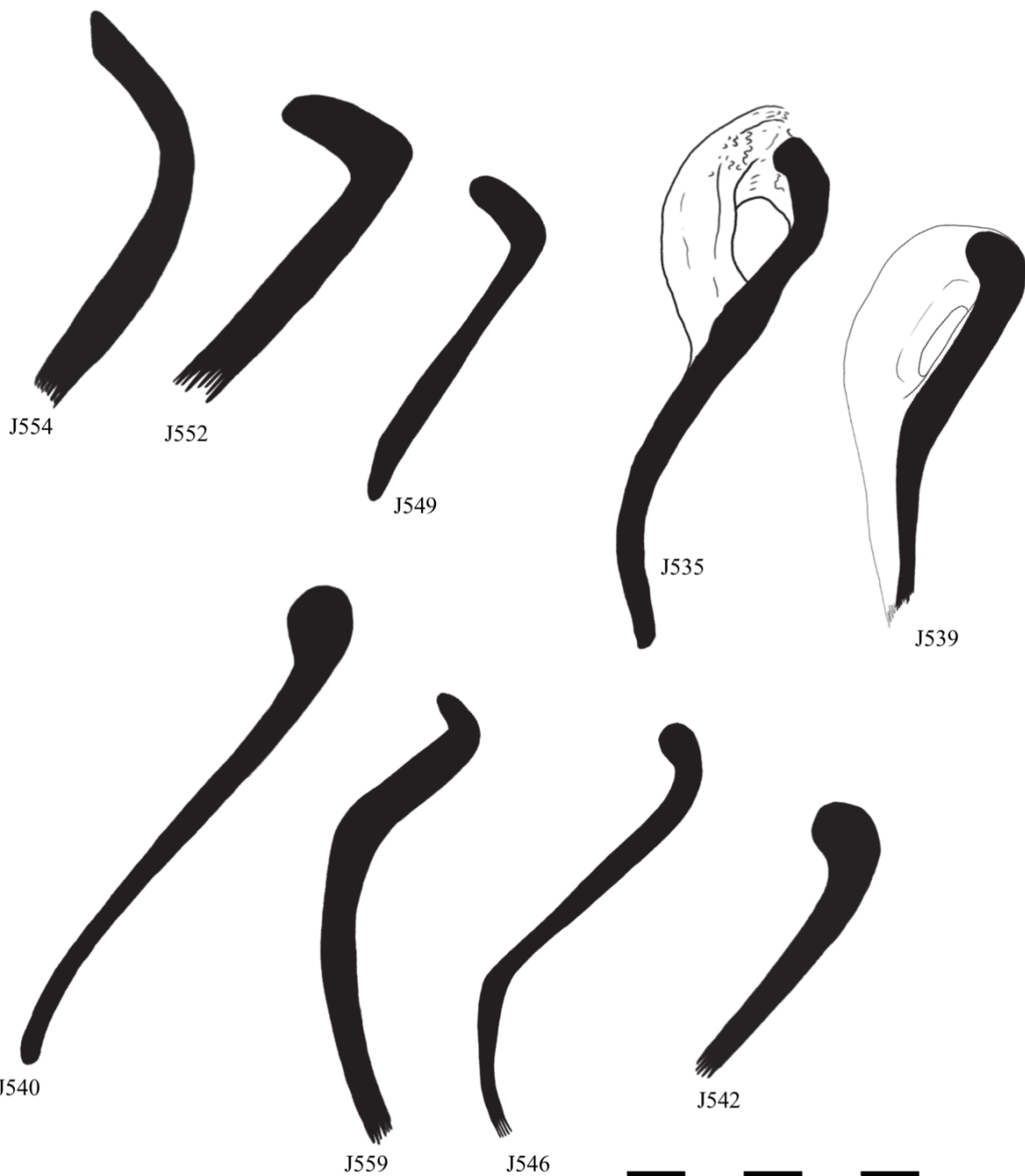
Crable 11F249



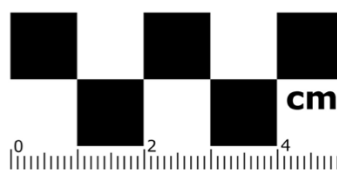
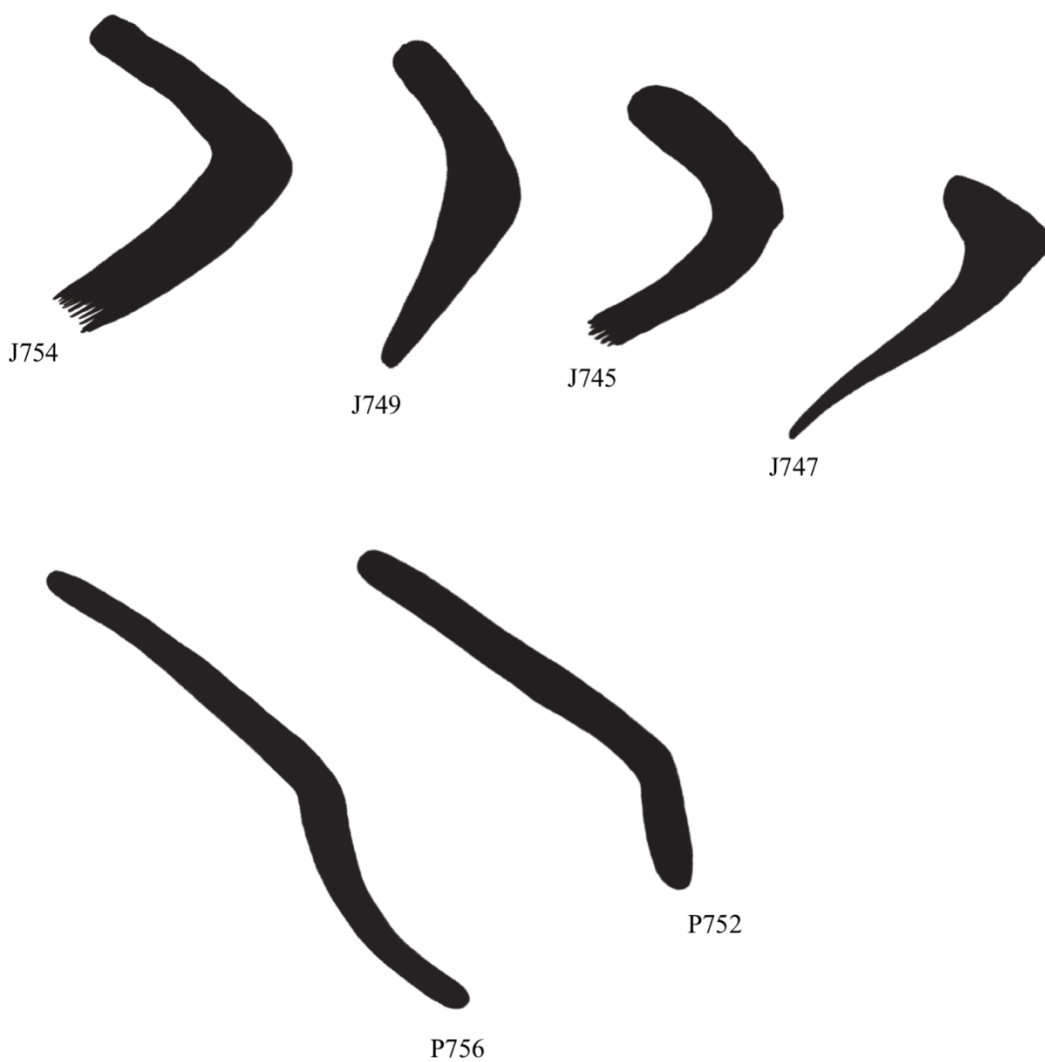
Emmons Village 11F218



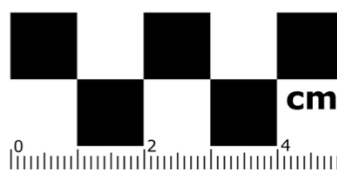
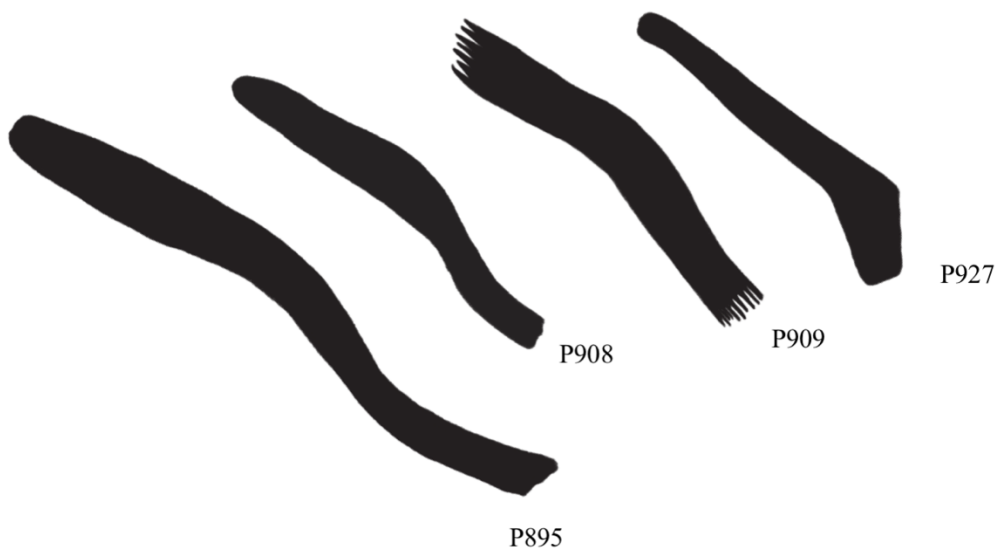
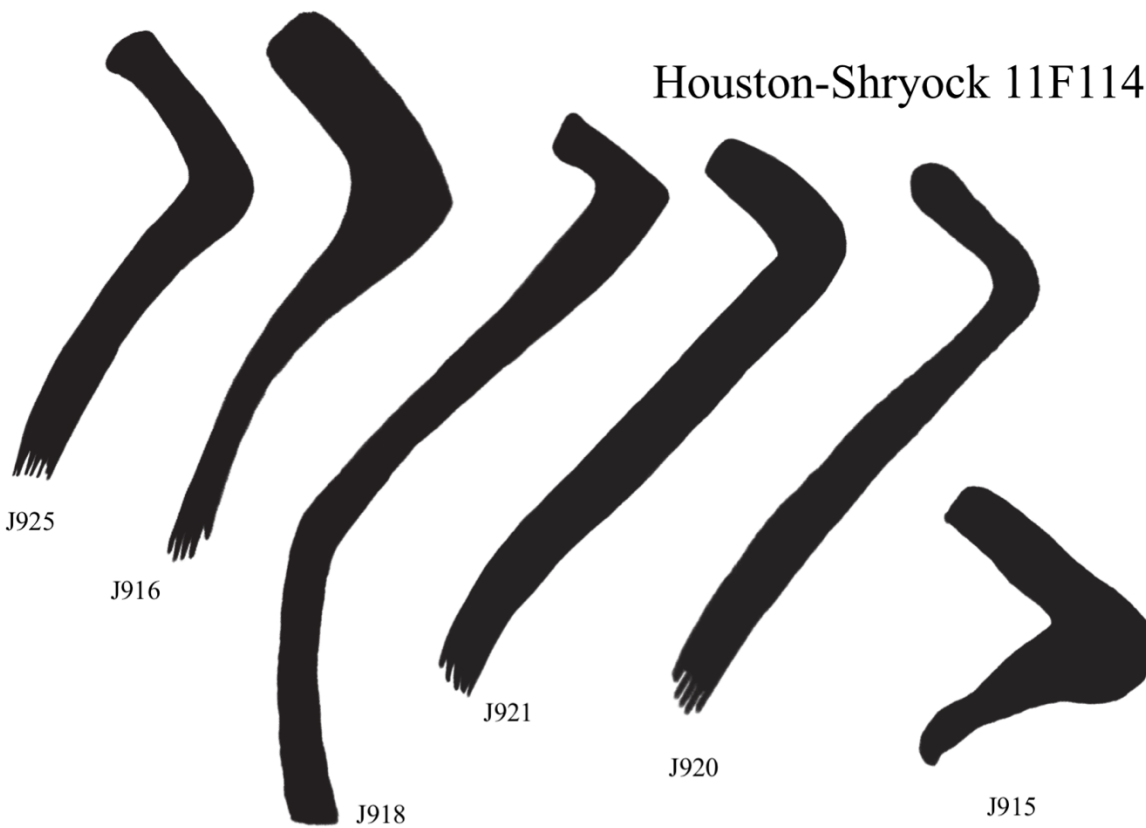
Eveland 11F353



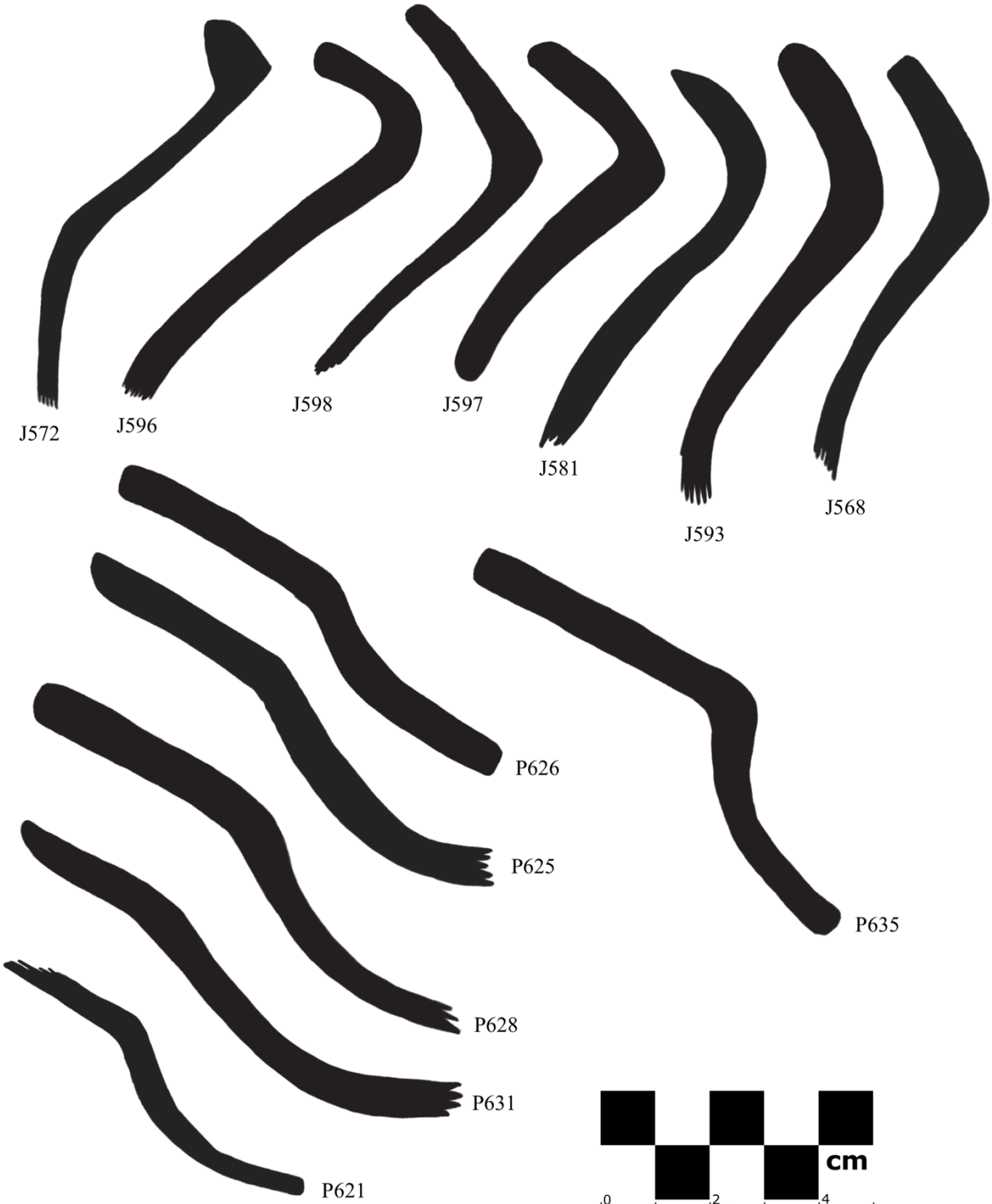
Fouts Village 11F164



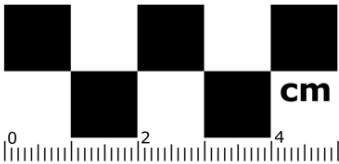
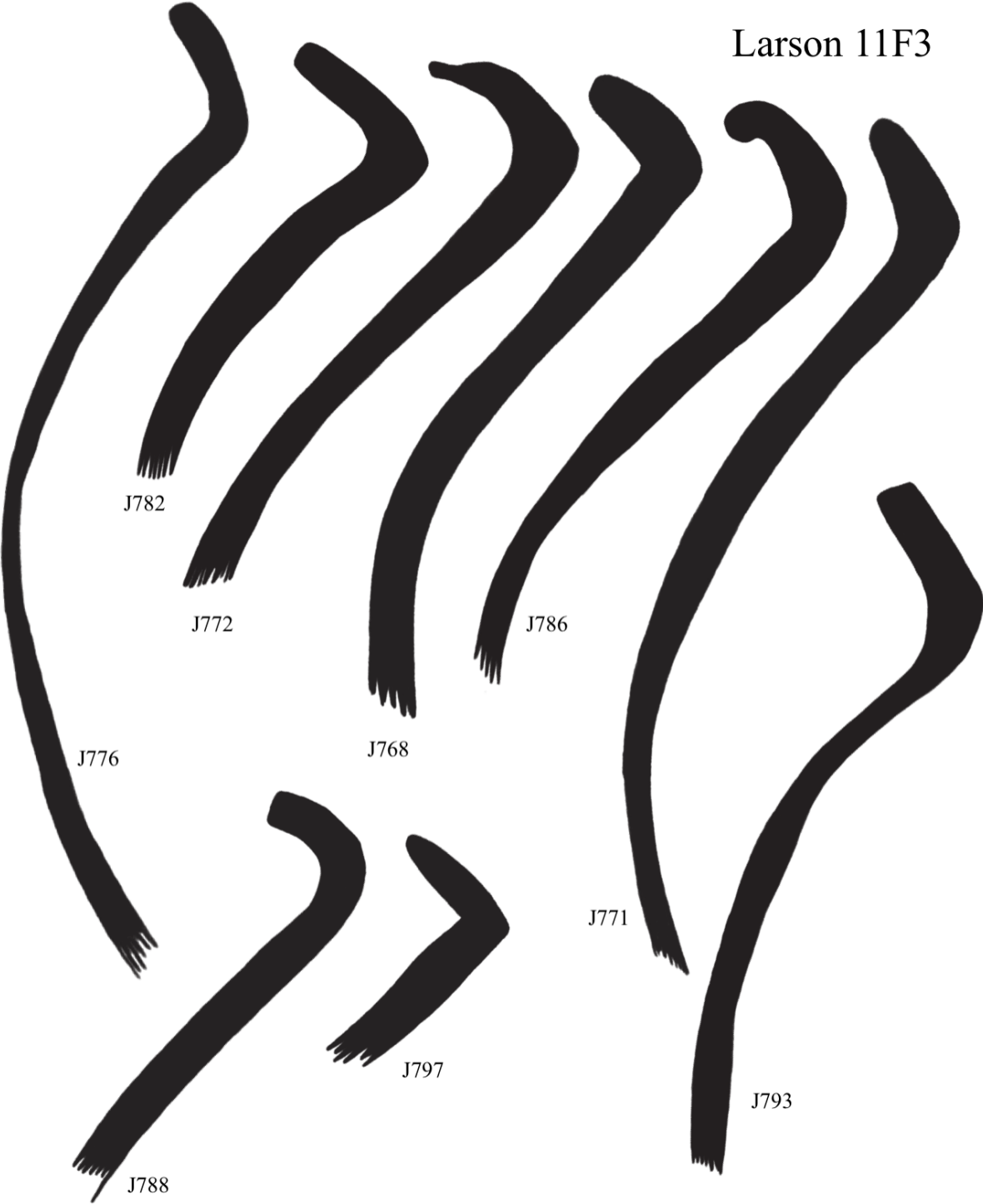
Houston-Shryock 11F114



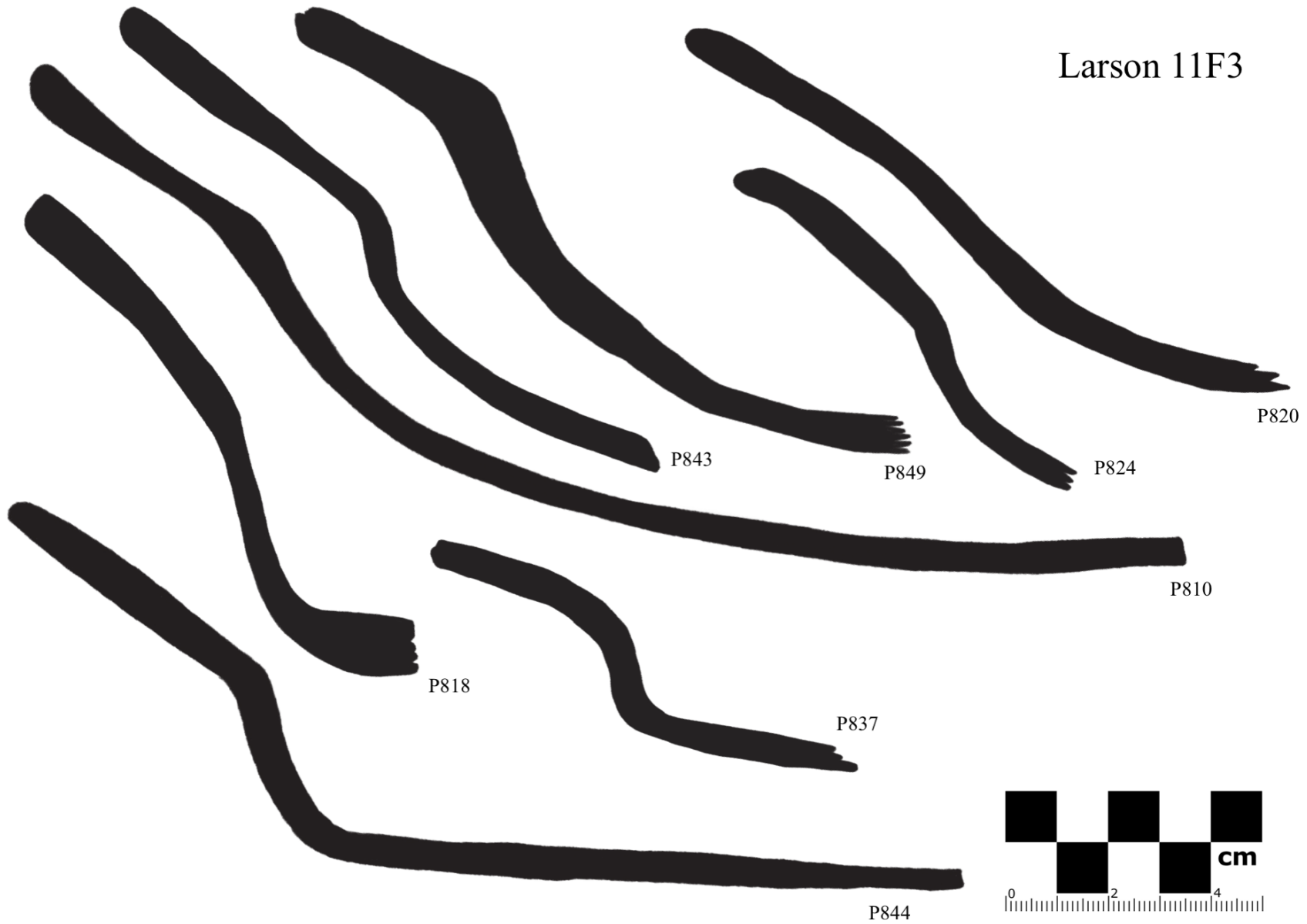
Kingston Lake 11P11



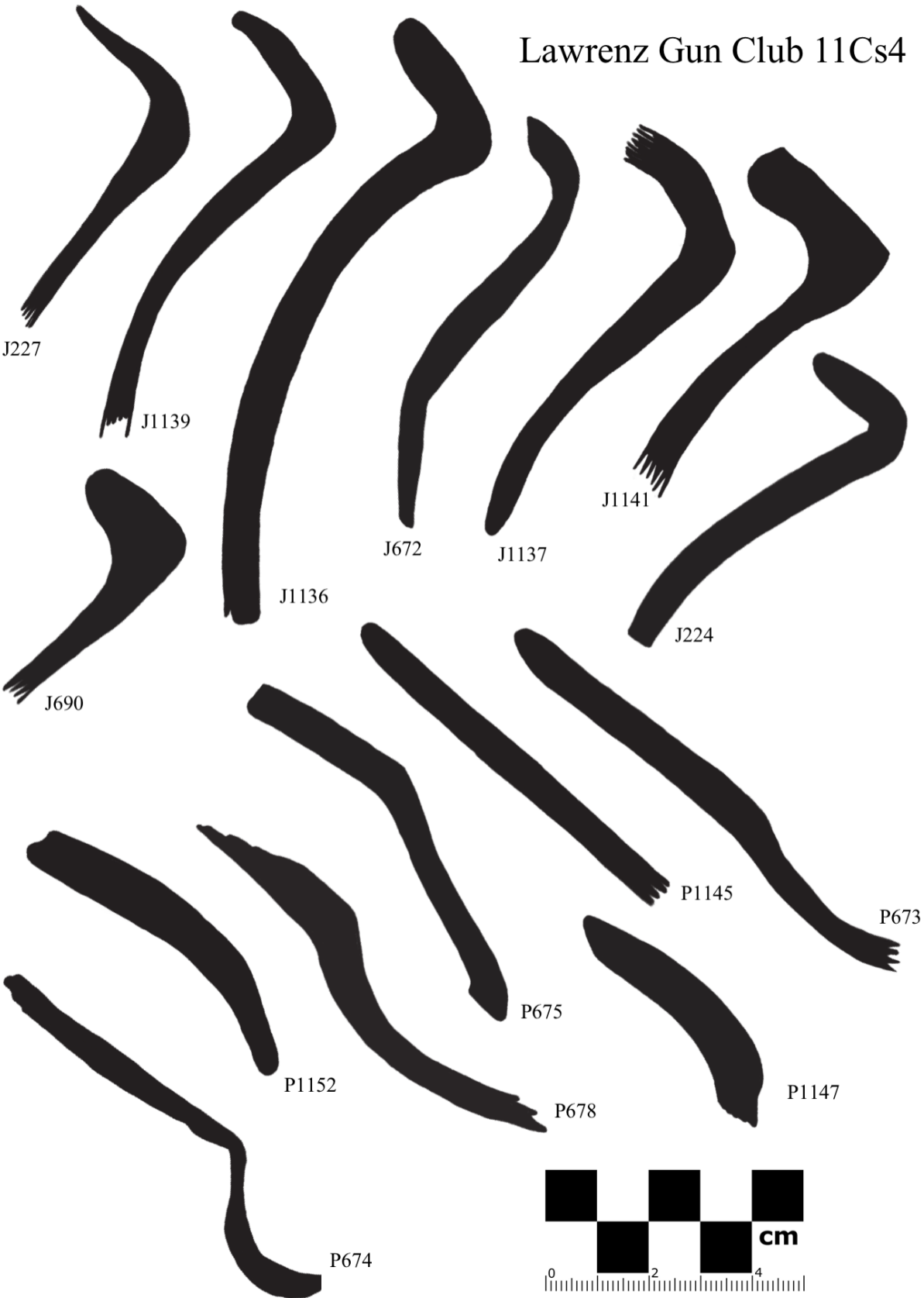
Larson 11F3



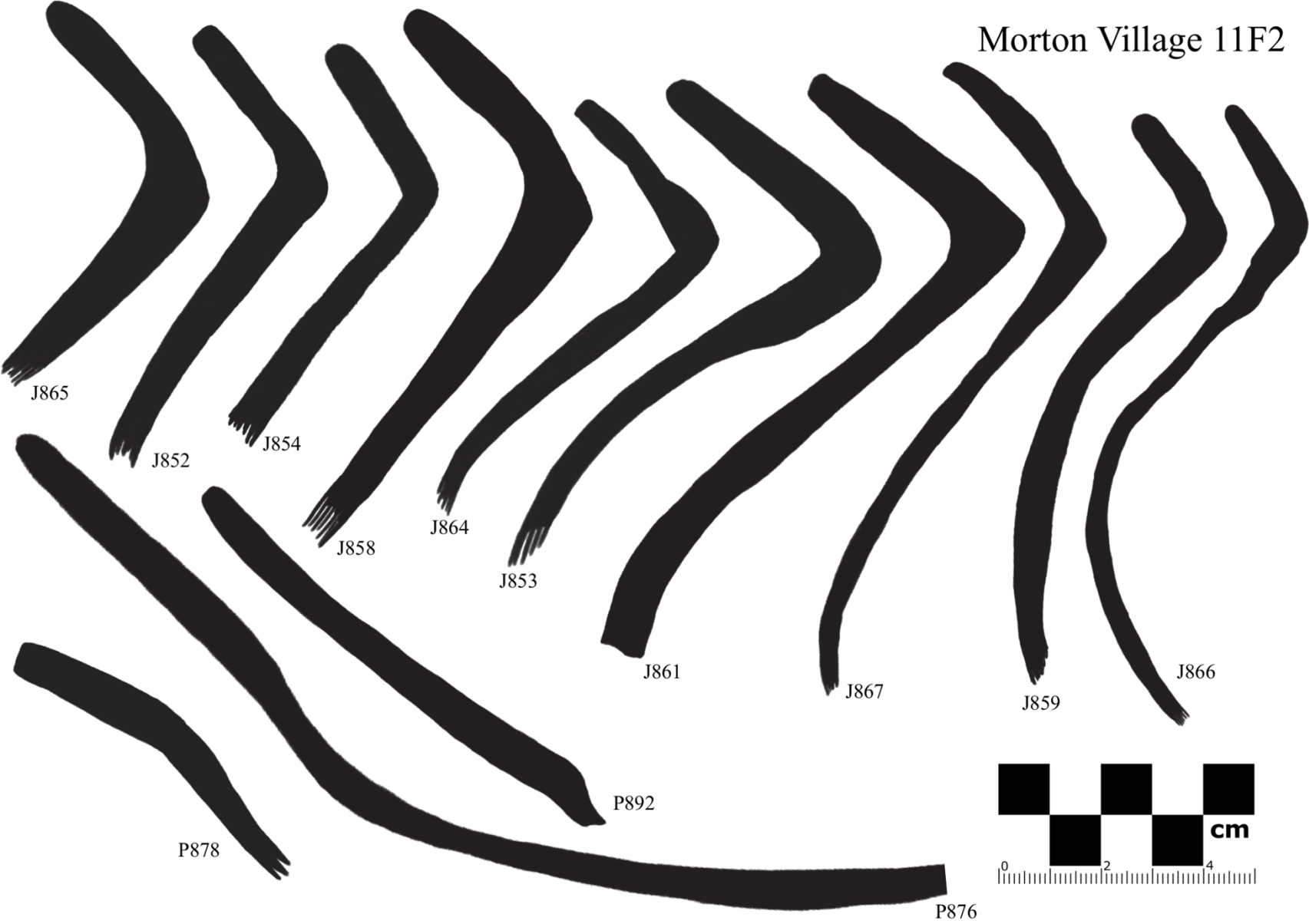
Larson 11F3



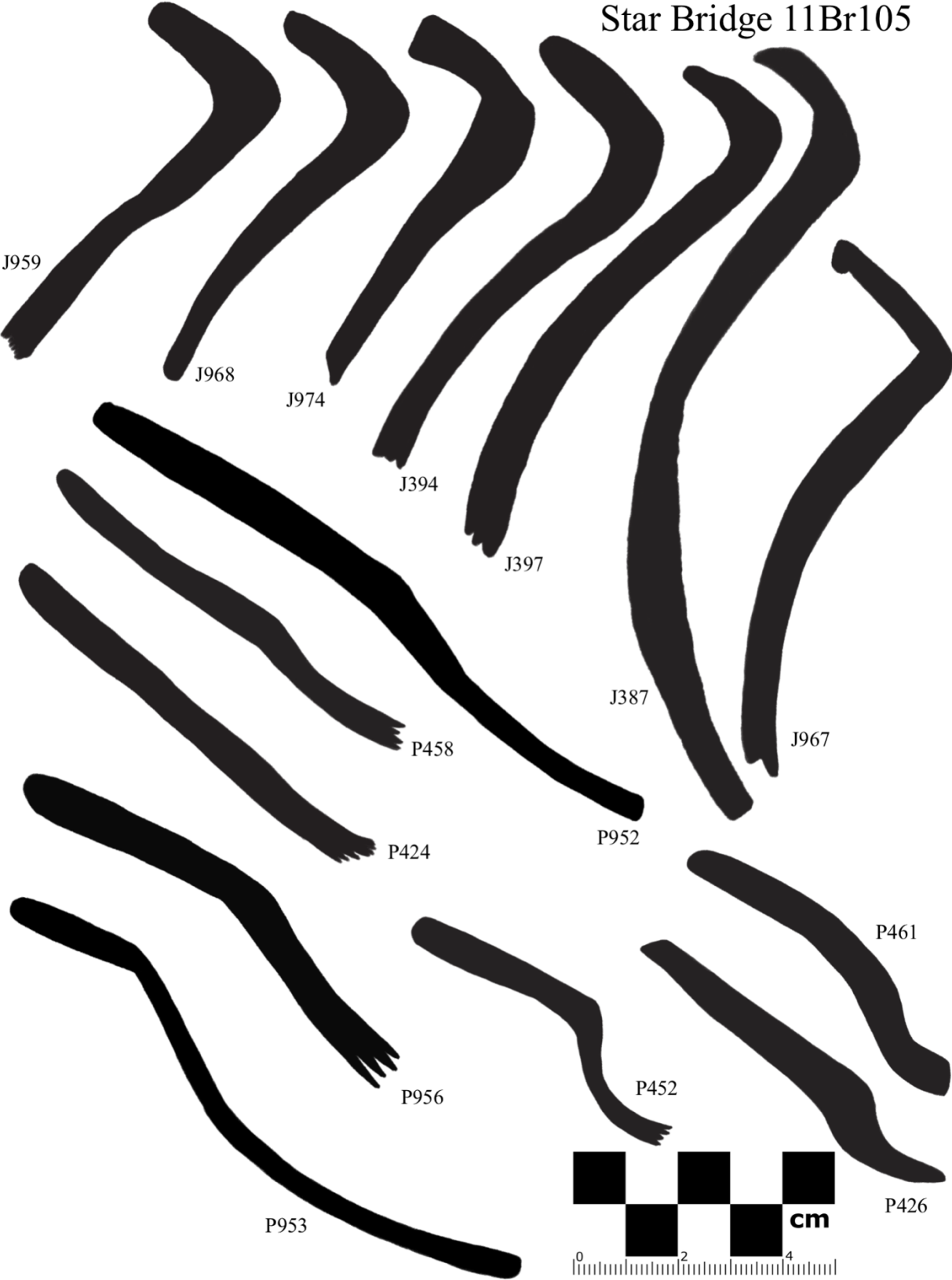
Lawrenz Gun Club 11Cs4



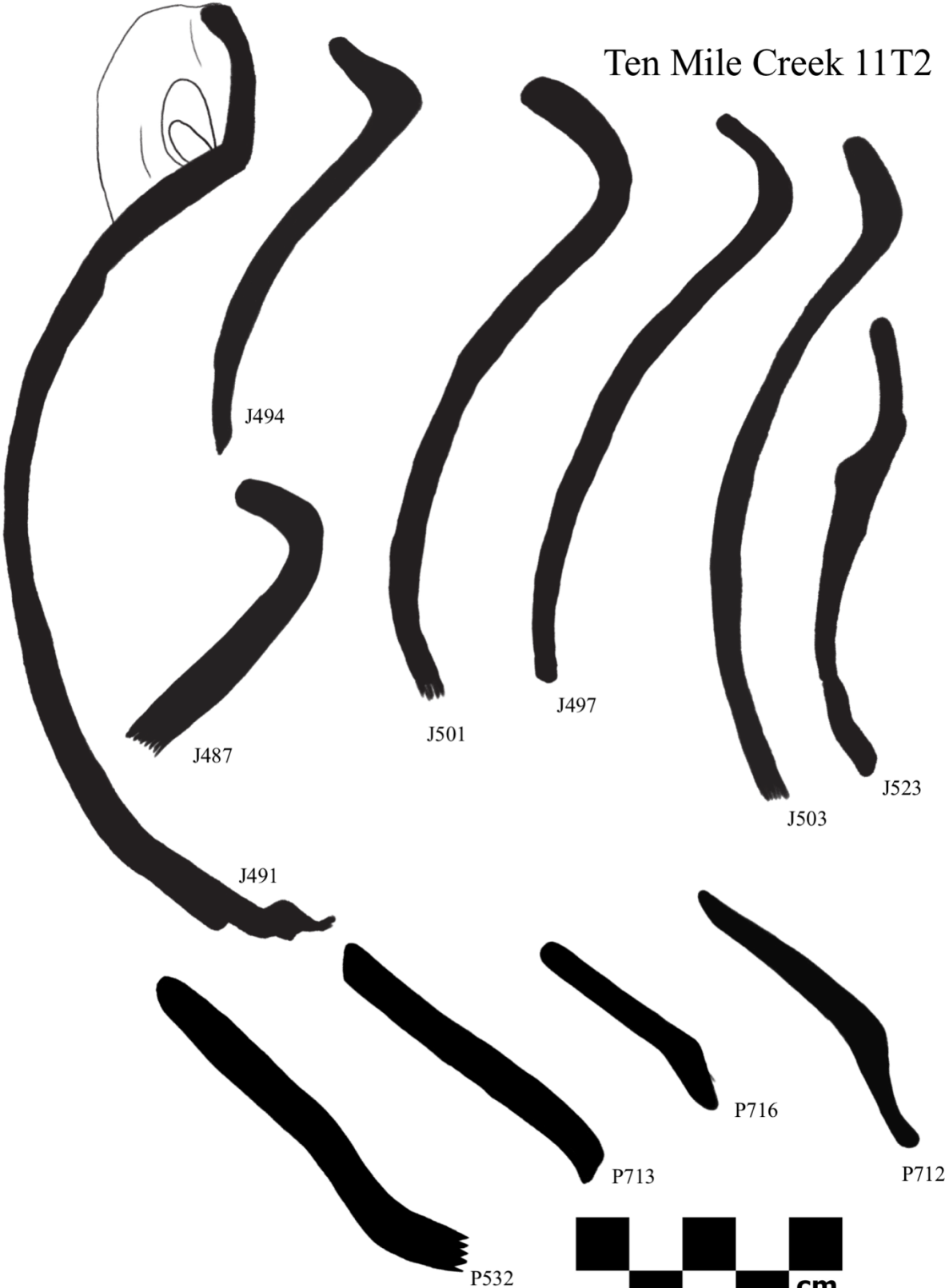
Morton Village 11F2



Star Bridge 11Br105



Ten Mile Creek 11T2



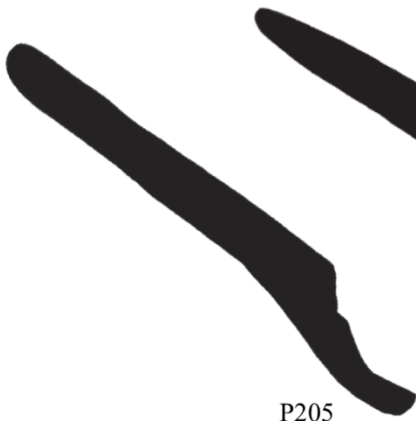
Walsh 11Br11



J192



J195



P205



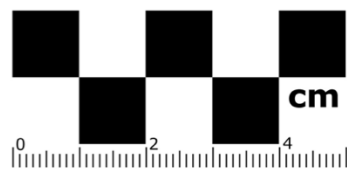
P200



P203



P207



APPENDIX G

Mineralogical Analysis Results

XRD #	Sample #	Type	Provenance/notes	Kaolinite	Illite	I/S	Calcite	dolomite	Quartz	Orthoclase	Plagioclase
1	1198	sherd	Jar sherd from Orendorf Settlement D; refired in village conflagration	0	18	0	0	0	74	3	5
2	1207	sherd	Jar sherd from Orendorf Settlement D; refired in village conflagration	0	60	0	0	0	34	0	6
3	1214	sherd	Jar sherd from Orendorf Settlement D; refired in village conflagration	0	49	0	0	0	42	1	8
4	1218	sherd	Jar sherd from Orendorf Settlement D; refired in village conflagration	0	29	0	0	0	51	10	10
5	776	sherd	F270 L2024; Jar sherd from Larson; un-refired	0	36	0	9	0	47	2	6
6	796	sherd	F137 L1491; Jar sherd from Larson; un-refired	0	51	0	0	0	43	1	5
7	810	sherd	H55; Plate sherd from Larson; un-refired	0	44	0	0	0	46	5	5
8	844	sherd	F71 L365; Plate sherd from Larson; un-refired	0	33	0	30	0	32	2	3
9	33	outcrop	East Creek outcrop, strata above lowest red layer above creek	20	6	0	0	0	55	7	12
10	34	outcrop	East Creek outcrop, red strata above Sample #33	35	10	0	3	0	42	2	8
11	36	outcrop	Manito sand pit; layers of sand above and below clay; collected with Ed	29	29	0	0	0	38	1	3
12	38	outcrop?	Recovered from pit at Lawrenz Gun Club at depth of 45-55 cmbd; manuport	0	7	0	85	0	7	1	0
13	16	outcrop	bottom of sand bank/river bend from Tenmile Creek near Caterpillar Peoria proving ground	15	11	0	0	25	39	3	7
14	18	outcrop	taken from bank of Coal Creek; iron? inclusion/coloration?	22	17	0	0	6	50	1	4
15	21	outcrop	taken from bank of West Branch LaMarsh Creek; red inclusions in matrix	13	13	0	0	0	64	5	5
16	25	outcrop	taken from creek that feeds La Moine River	13	12	0	0	0	61	1	13
17	EMQ-40	core	Illinois Valley, Emiquon 3.53 - 3.55 m	15	18	0	0	9	41	7	10
18	KMM-01	core	Kimmswick; 12.70 - 12.71 m	23	10	20	7	5	25	4	6
19	DPL-003	core	Illinois Valley, NW of Meredosia 3.78 - 3.85 m; 705926.959 4414752.135	29	39	0	0	0	37	1	3
20	32	outcrop	East Creek outcrop; red clay - lowest strata exposed by creek	18	25	0	0	0	54	1	2
21	37	core	Spunky Bottom - cored to 160-182cm; very low in the B-Horizon; collected with Ed	27	28	0	0	0	41	3	1
22	338	sherd	L2099/F345/H12; Plate sherd from Myer-Dickson	0	50	0	0	0	42	2	6
				Clays			Carbonates		Silicates		

Table G.1 X-ray Diffraction Results

XRD analysis was performed at University of Cincinnati College of Engineering and Applied Science Advanced Materials Characterization Center. See Chapter 4 for a discussion of methodology and interpretations.

Sample numbers for ceramic sherds are those used in artifact attribute recordings. Sample numbers for clay outcrop or cores are unique to this XRD analysis.

APPENDIX H

Site Identification Codes and Radiocarbon Probabilities

Table H.1 Site IAS and ISM Identification Numbers

Site Name	IAS Number(s)	ISM Number(s)
Baehr South	11Br47	11Br2?
Buckeye Bend	11F310	11Fv1079
C.W. Cooper	11F15	11Fv47
Crable	11F249	11Fv891-898
Emmons Village	11F218	11Fv962
Eveland	11F353	11Fv900
Fouts Village	11F164	11Fv664
Houston-Shryock	11F114	11Fb901-904 (11Fv902-903)
Kingston Lake	11P11	11Pv1-5
Larson	11F3	11Fv1109
Lawrenz Gun Club	11Cs4, Cs11 - 19	-
Morton Village	11F2	11Fv19
Myer-Dickson	11F10	11Fv33
Orendorf	11F1284	11Fv1284
Star Bridge	11Br105 or 11Br17	11Brv55
Ten Mile Creek	11T2	11Tv4
Walsh	11Br11	11Brv46

IAS - Illinois Archaeological Survey or Smithsonian Trinomial

ISM - Illinois State Museum

CIRV Site Radiocarbon assay probabilities

Table H.2 Radiocarbon assay probabilities and results

Site	ISM Site #	ISM Accession	Sample #	Sample Material	Provenience	Radiocarbon Age BP	1 σ error	DirectAMS code
Buckeye Bend	11F310	1975-0080	11F310 - 1	maize kernel	Pit 4	modern		D-AMS 026576
Buckeye Bend	11F310	1975-0080	11F310 - 2	deer astragalus	House 26	625	30	D-AMS 026579
Kingston Lake	11P11	1959-0025	11P11 - 1	maize kernels	unknown	880	25	D-AMS 026577
Houston-Shryock	11F114	1958-0100	11F114 - 1	thatch	House 2	failed in measurement		D-AMS 026578
Emmons Village	11F218	1960-0043	11F218 - 1	charred twig	house excavation	961	30	D-AMS 026575
Baehr South	11Br47	-	11Br47 - 1	bone (collagen)	unknown	651	23	D-AMS 027116
Fouts Village	11F164	-	11F164 - 1	bone (collagen)	unknown structure	insufficient collagen preservation		D-AMS 027296
Morton Village	11F2	-	F321-2	hazelnut	F321 Level 2	561	32	D-AMS 030550
Morton Village	11F2	-	Str 26-5SW PP286	willow twig	Str 26-5SW PP286	586	29	D-AMS 030535
Morton Village	11F2	-	Str 34 Bl18-1A	hazelnuts	Str34 Bl18-1A	620	28	D-AMS 030536
Ten Mile Creek	11T1	-	11T2 - 1	antler tine	Unknown feature	624	29	D-AMS 020156
Ten Mile Creek	11T2	-	11T2 - 2	elk long bone	Burned house w/cm jar	625	34	D-AMS 020157
Star Bridge	11Br105	-	11Br105 - 1	antler tine	unknown burnt structure	635	25	D-AMS 020158
Star Bridge	11Br105	-	11Br105 - 2	antler tine	unknown burnt structure	569	27	D-AMS 020159

Calibrated probability assessments for the 11 successful radiocarbon assays are presented below courtesy of OxCal.

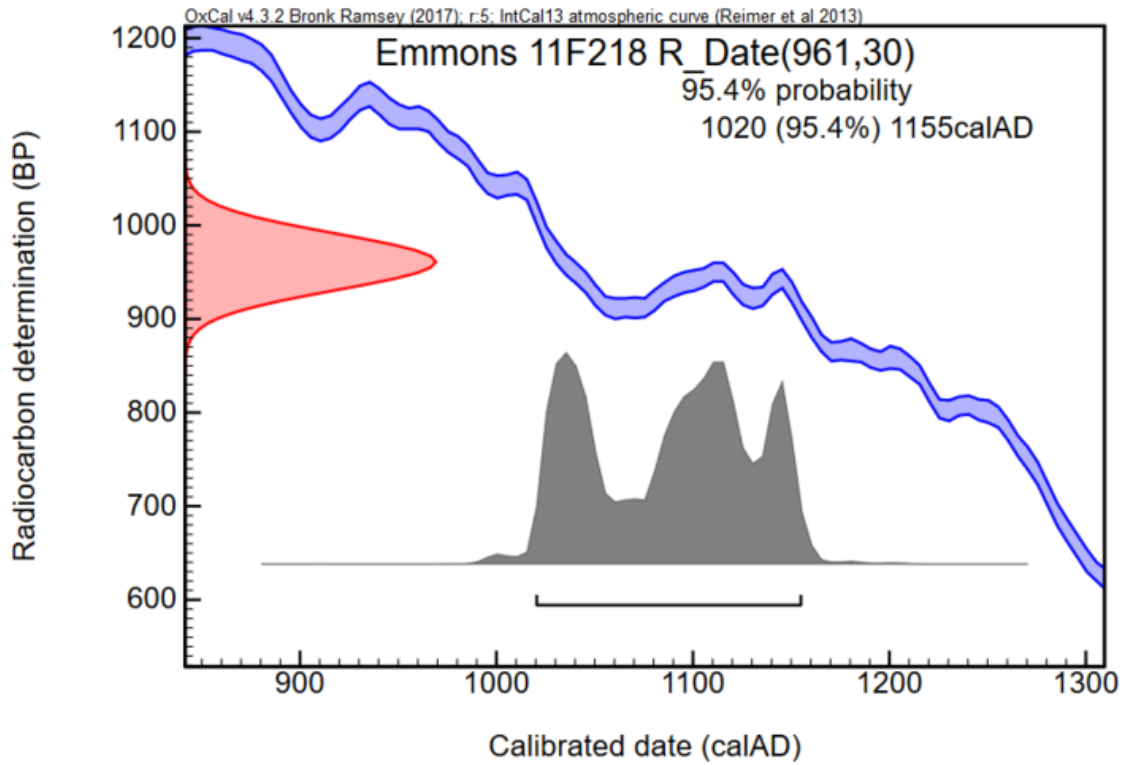


Figure H.1 Emmons Lake radiocarbon assay probability

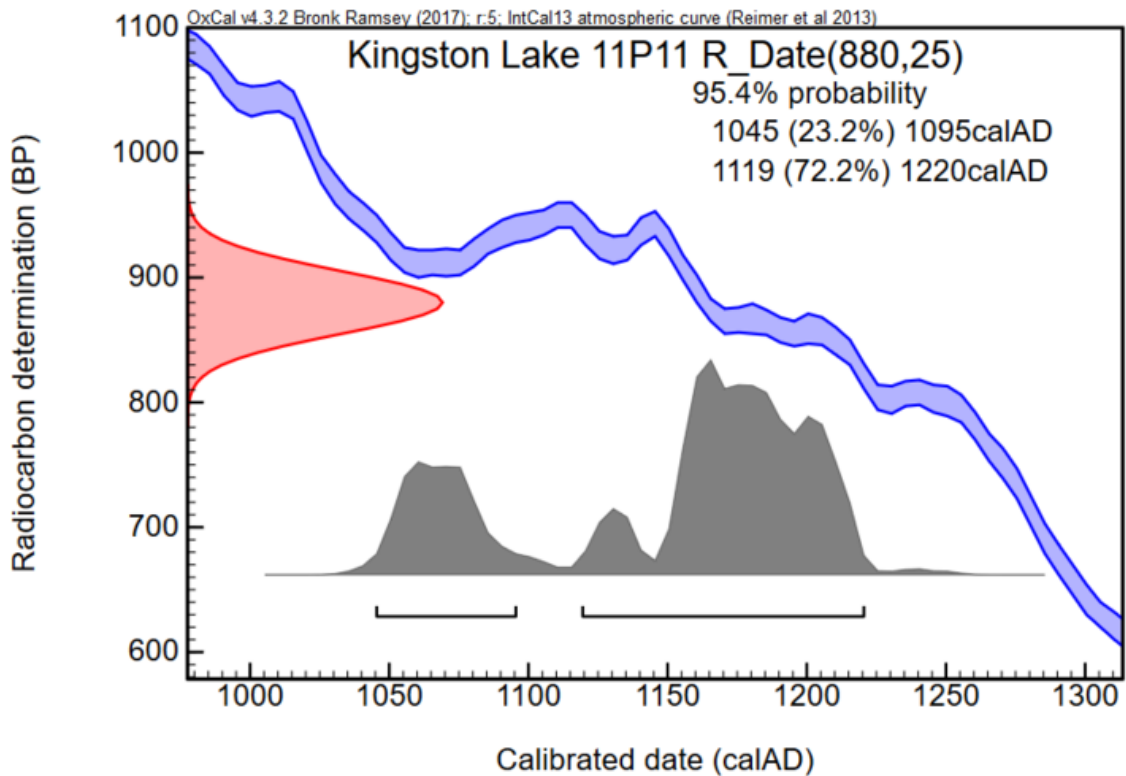


Figure H.2 Kingston Lake radiocarbon assay probability

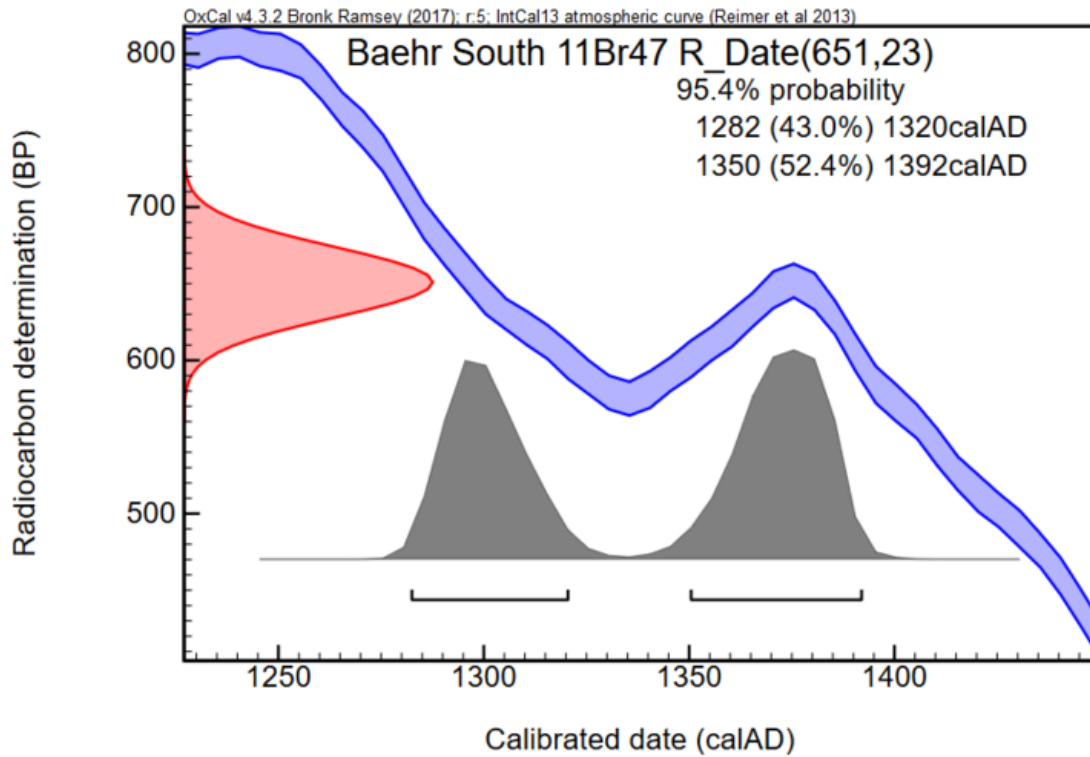


Figure H.3 Baehr South radiocarbon assay probability

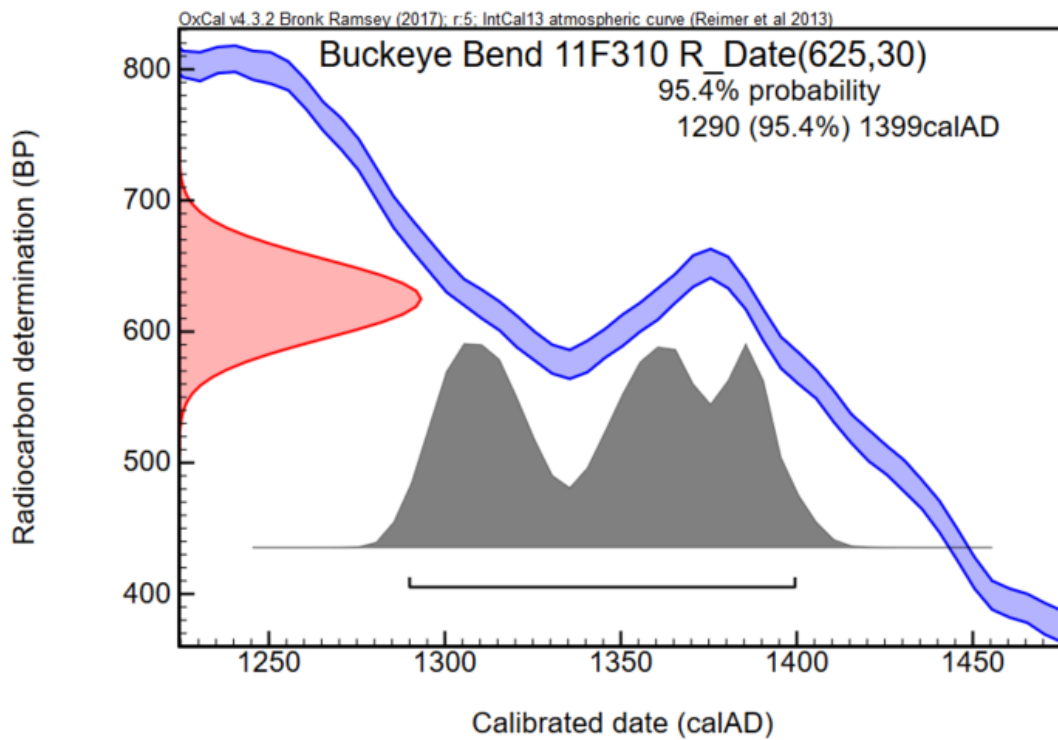


Figure H.4 Buckeye Bend radiocarbon assay probability

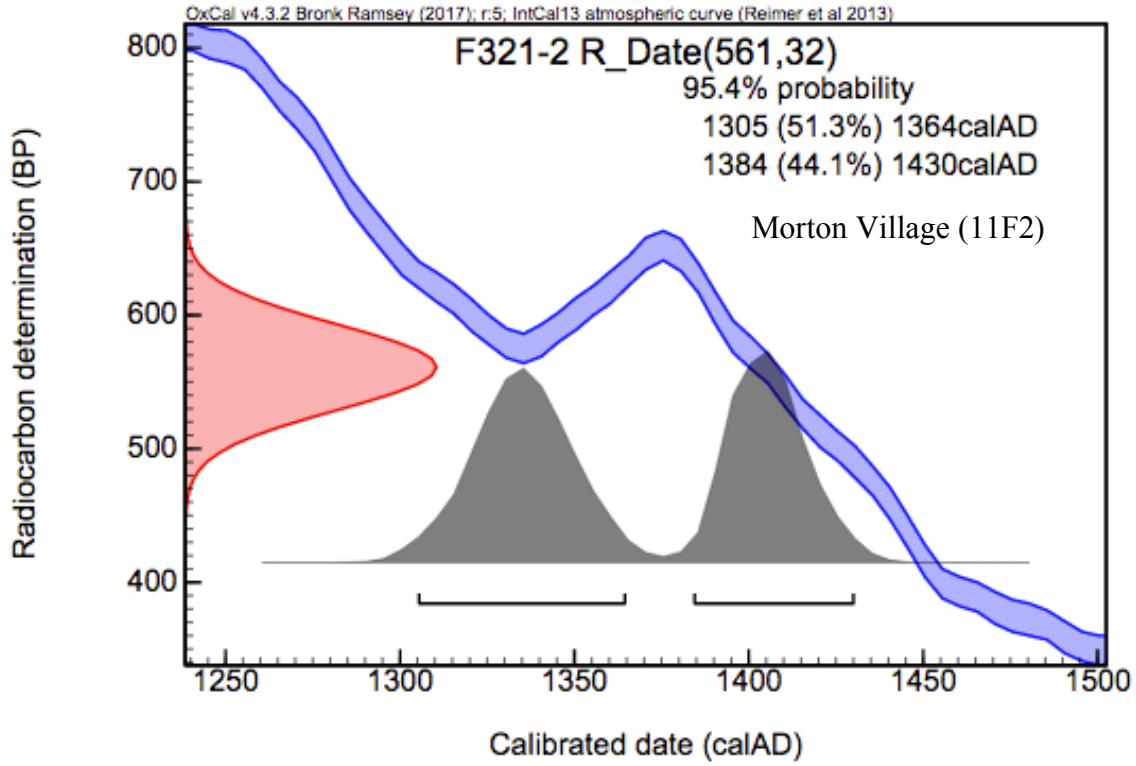


Figure H.5 Morton Village radiocarbon assay probability (1)

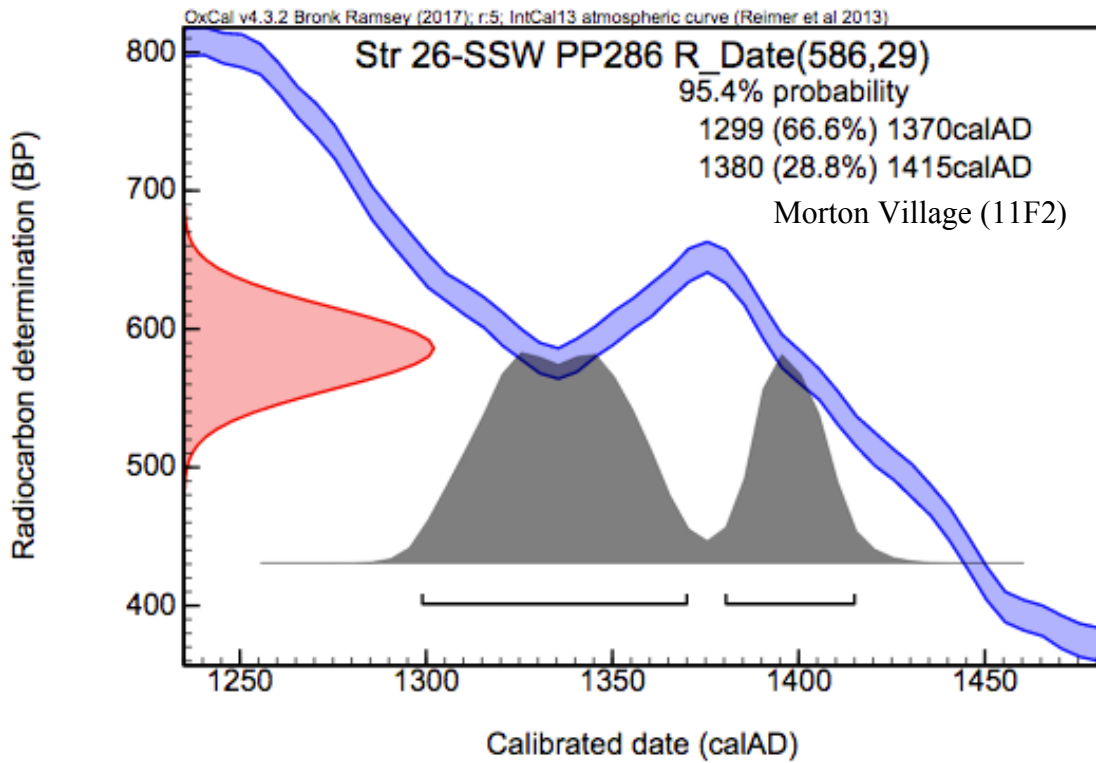


Figure H.6 Morton Village radiocarbon assay probability (2)

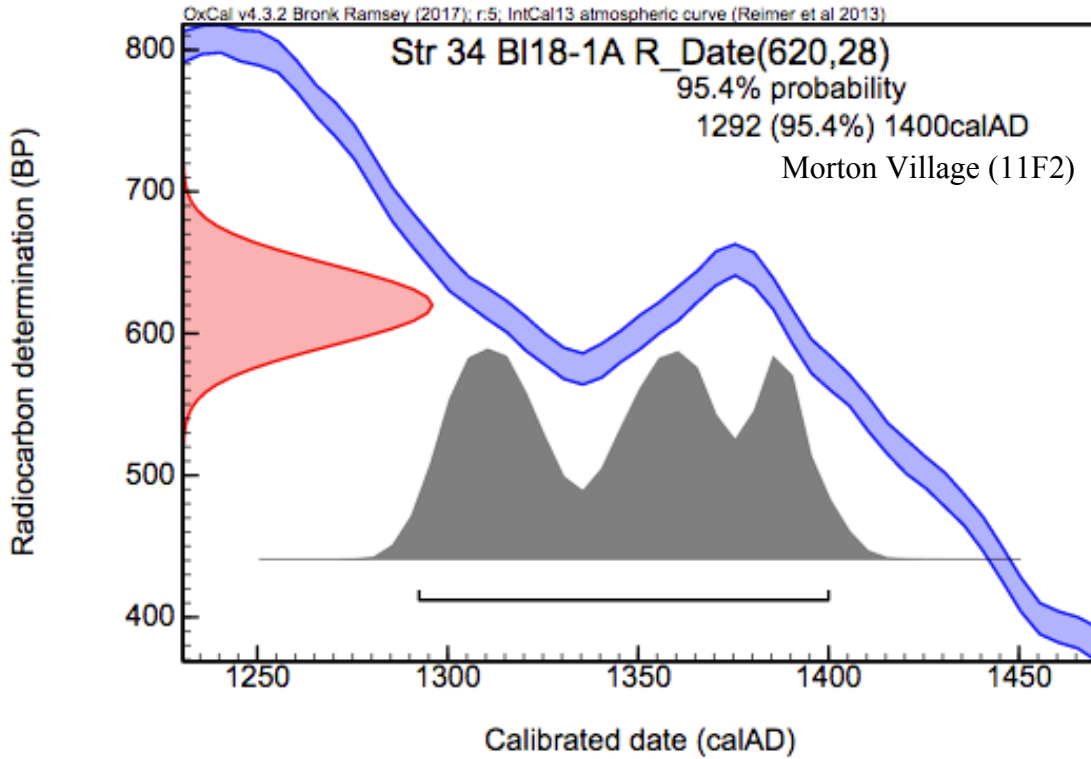


Figure H.7 Morton Village radiocarbon assay probability (3)

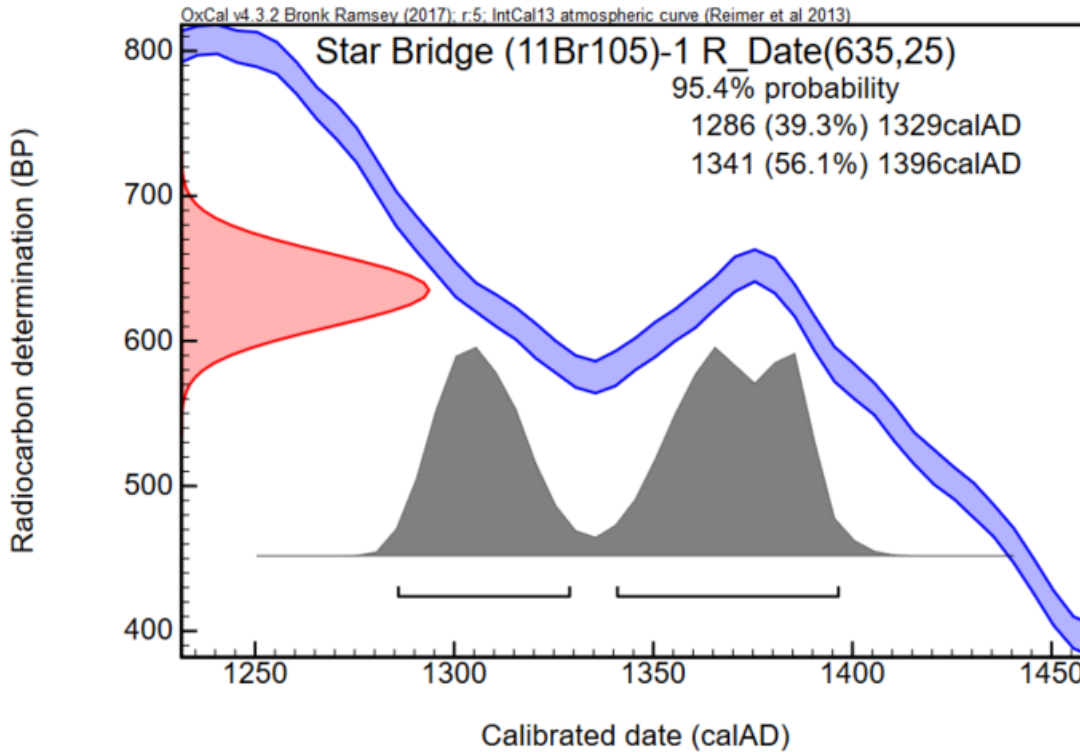


Figure H.8 Star Bridge radiocarbon assay probability (1)

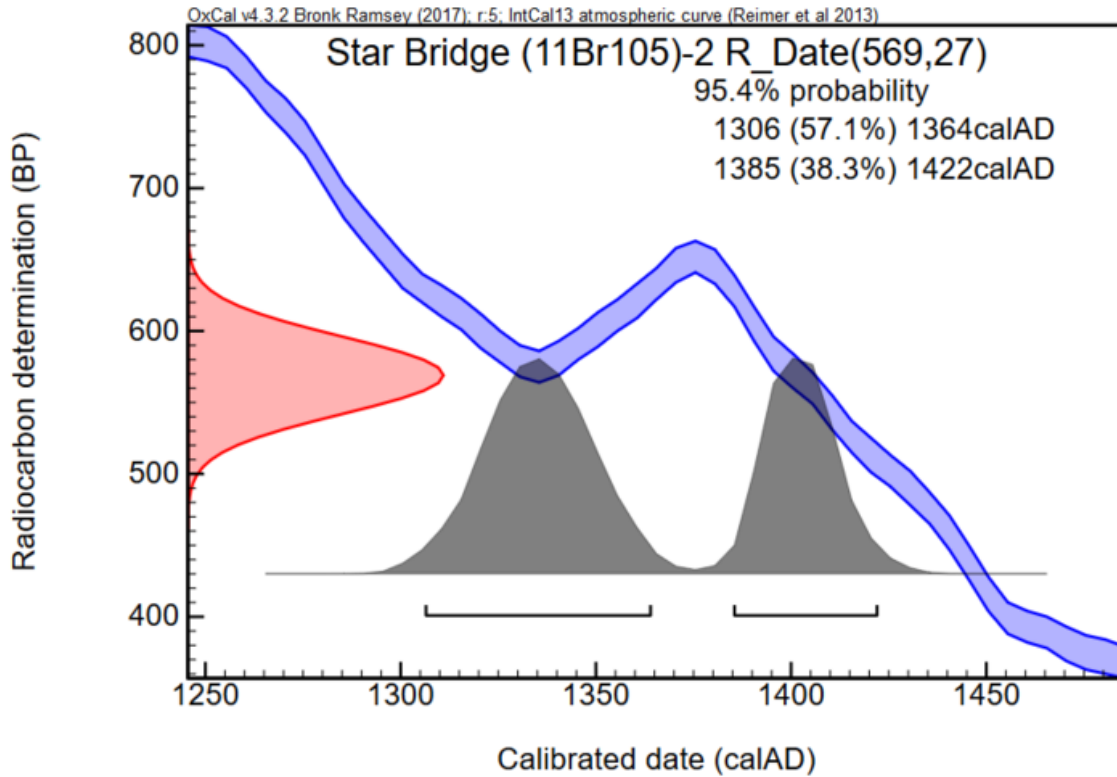


Figure H.9 Star Bridge radiocarbon assay probability (2)

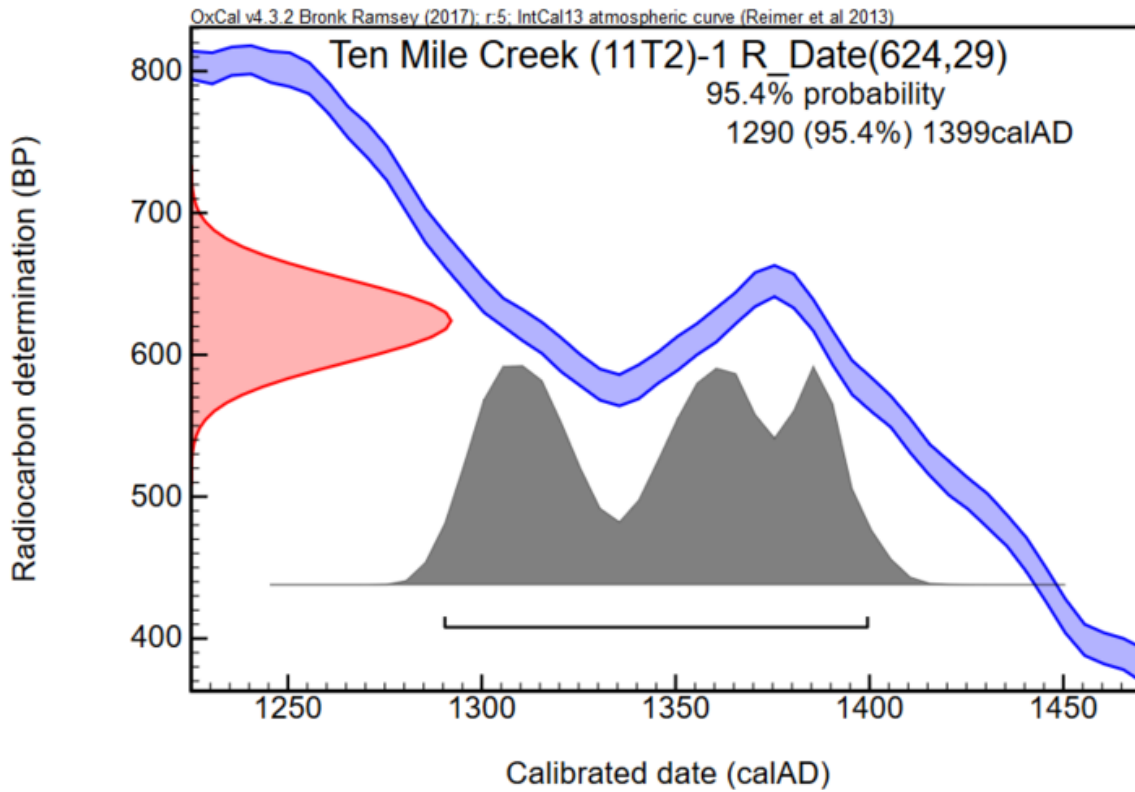


Figure H.10 Ten Mile Creek radiocarbon assay probability (1)

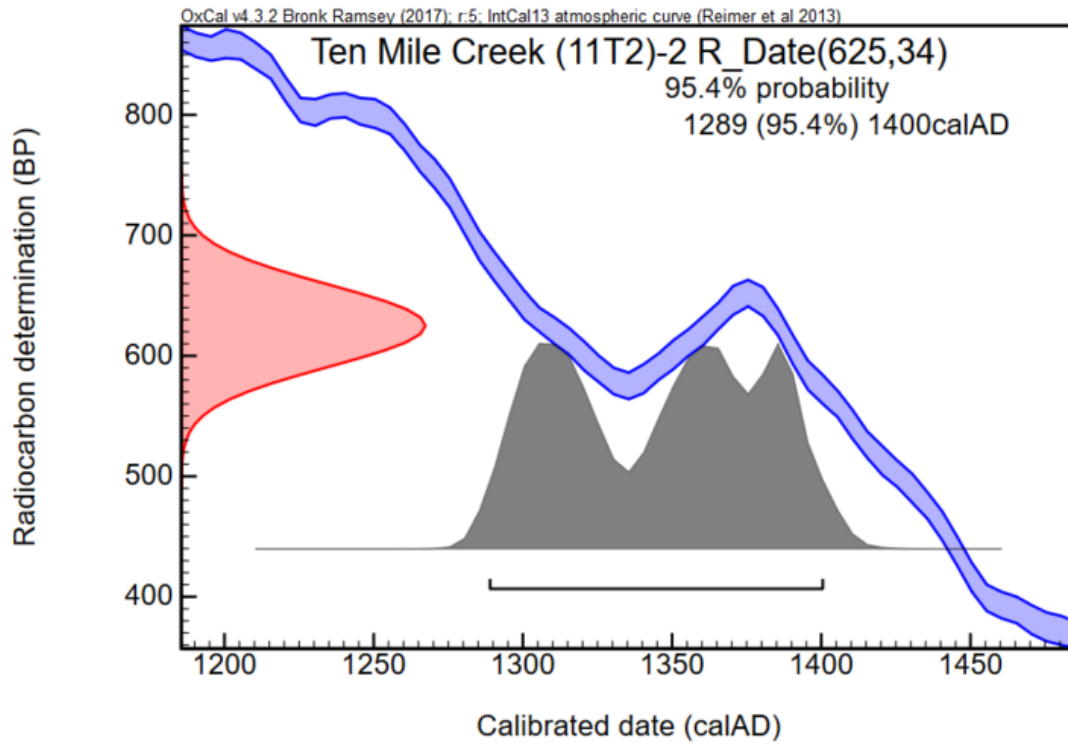


Figure H.11 Ten Mile Creek radiocarbon assay probability (2)

REFERENCES

REFERENCES

- Afsarmanesh, Nazanin and Matteo Magnani
2016 Finding overlapping communities in multiplex networks. *arXiv* 1602.03746:1-18.
- Albert, R. and A. L. Barabási
2002 Statistical mechanics of complex networks. *Reviews of Modern Physics* 74:47-97.
- Alt, Susan M.
2006 The Power of Diversity: The Roles of Migration and Hybridity in Culture Change. In *Leadership and Polity in Mississippian Society*, edited by B. M. Butler and P. D. Welch, pp. 289-308. Center for Archaeological Investigations, Southern Illinois University, Carbondale, IL.
- Anderson, David G.
1991 Examining Prehistoric Settlement Distribution in Eastern North America. *Archaeology of Eastern North America* 19:1-22.
- Anderson, David G., David W. Stahle and Malcolm K. Cleaveland
1995 Paleoclimate and the Potential Food Reserves of Mississippian Societies: A Case Study from the Savannah River Valley. *American Antiquity* 60(2):258-286.
- Anthony, David W.
1990 Migration in Archeology: The Baby and the Bathwater. *American Anthropologist* 92(4):895-914.
- Appadurai, Arjun (editor) 1986 *The Social Life of Things: Commodities in Cultural Perspective*. Cambridge University Press, Cambridge.
- Arnold, Dean E.
1985 *Ceramic Theory and Cultural Process*. Cambridge University Press, Cambridge.
- Azarian, G. Reza
2005 *The General Sociology of Harrison C. White: Chaos and Order in Networks*. Palgrave Macmillan, New York.
- Barabási, A. C. and R. Albert
1999 Emergence of scaling in random networks. *Science* 286(5439):509-512.
- Bardolph, Dana N.
2014 Evaluating Cahokian Contact and Mississippian Identity Politics in the Late Prehistoric Central Illinois River Valley. *American Antiquity* 79(1):69-89.
- Bardolph, Dana N. and Gregory D. Wilson

- 2015 The Lamb Site (11Sc24): Evidence of Cahokian Contact and Mississippianization in the Central Illinois River Valley. *Illinois Archaeology* 27:138-149.
- Barth, Frederick (editor) 1969 *Ethnic Groups and Boundaries*. Waveland Press, Prospect Heights, IL.
- Bastian, Mathieu, Sebastien Heymann and Mathieu Jacomy
2009 Gephi: an open source software for exploring and manipulating networks. *Proceedings of the Third International AAAI Conference on Weblogs and Social Media*.
- Battiston, Federico, Vincenzo Nicosia and Vito Latora
2017 The new challenges of multiplex networks: Measures and models. *European Physical Journal: Special Topics* 226(3):401-416.
- Baxter, Michael J.
1995 Standardization and Transformation in Principal Component Analysis, with Application to Archaeometry. *Journal of the Royal Statistical Society Series C (Applied Statistics)* 44(4):513-527.

2008 Mathematics, Statistics and Archaeometry: the Past 50 Years or So*. *Archaeometry* 50(6):968-982.

2015 *Notes on Quantitative Archaeology and R*, <http://www.mikemetrics.com/book-quantitative-archaeolog/4568129078>.
- Baxter, Michael J. and Caitlin E. Buck
2000 Data handling and statistical analysis. In *Modern Analytical Methods in Art and Archaeology*, edited by E. Ciliberto and G. Spoto, pp. 681-746. John Wiley and Sons, Inc., New York.
- Beck, Robin A.
2003 Consolidation and Hierarchy : Chiefdom Variability in the Mississippian Southeast. *American Antiquity* 68(4):641-661.
- Bender, Margaret M., Reid A. Bryson and David A. Baerreis
1975 University of Wisconsin Radiocarbon Dates XII17(1):121-134.
- Bengtson, Jennifer D.
2012 A Biocultural Perspective on Sex and Gender in Late Prehistoric West Central Illinois: Growth Patterns, Mississippianization, and Intracemetery Social Differentiation. Unpublished Ph.D. Dissertation, Michigan State University.
- Bengtson, Jennifer D. and Jodie A. O'Gorman
2017 War at the Door: Evolutionary Considerations of Warfare and Female Fighters. In *Bioarchaeology of Women and Children in Times of War: Case Studies from the Americas*, pp. 27-48. Springer International Publishing, Cham, Switzerland.

- Bengtson, Jennifer D. and Jodie A. O’Gorman
2017 Women’s Participation in Prehistoric Warfare: A Central Illinois River Valley Case Study. *International Journal of Osteoarchaeology* 27:230-244.
- Benn, David W.
1995 Woodland People and the Roots of Oneota. In *Oneota Archaeology: Past, Present and Future*, edited by W. Green, pp. 91-139. Office of the State Archaeologist, Iowa City, Iowa.

1998 Moon: A Fortified Mississippian-Period Village in Poinsett County, Arkansas. In *Changing Perspectives on the Archaeology of the Central Mississippi River Valley*, edited by M. J. O'Brien and R. C. Dunnell, pp. 225-257. The University of Alabama Press, Tuscaloosa, AL.
- Benson, Larry V., Timothy R. Pauketat and Edward R. Cook
2009 Cahokia's Boom and Bust in the Context of Climate Change. *American Antiquity* 74(3):467-483.
- Bentley, G. Carter
1987 Ethnicity and Practice. *Comparative Studies in Society and History* 29(1):24-55.
- Berkowitz, Steve
1982 *An Introduction to Structural Analysis: The Network Approach to Social Research*. Butterworth, Toronto.
- Bernardini, Wesley
2005 Reconsidering Spatial and Temporal Aspects of Prehistoric Cultural Identity: A Case Study from the American Southwest. *American Antiquity* 70(1):31-54.
- Berres, T. E.
2001 *Power and Gender in Oneota Culture: A Study of a Late Prehistoric People*. Northern Illinois University Press, DeKalb, IL.
- Bettinger, Robert L. and Jeltner Eerkens
2008 Evolutionary Implications of Metrical Variation in Great Basin Projectile Points. *Archeological Papers of the American Anthropological Association* 7(1):177-191.
- Bilodeau, Christopher
2001 “They honor our Lord among themselves in their own way” Colonial Christianity and the Illinois Indians. *The American Indian Quarterly* 25(3):352-377.
- Binford, Lewis R.
1962 Archaeology as Anthropology. *American Antiquity* 28(2):217-225.

- 1971 Mortuary practices: their study and their potential. *Memoirs of the Society for American Archaeology* (25):6-29.
- Birch, Jennifer
2010 Coalescence and Conflict in Iroquoian Ontario. *Archaeological Review from Cambridge* 25(1):29-48.
- Birch, Jennifer and John P. Hart
2018 Social Networks and Northern Iroquoian Confederacy Dynamics. *American Antiquity* 83(1):13-33.
- Bird, Broxton W., Jeremy J. Wilson, William P. Gilhooly III, Byron A. Steinman and Lucas Stamps
2017 Midcontinental Native American population dynamics and late Holocene hydroclimate extremes. *Scientific Reports* 7(December 2016):1-12.
- Bishop, Ronald L., Veletta Canouts, Suzanne P. De Atley, Alfred Qöyawayma and C.W. Aikins
1988 The Formation of Ceramic Analytic Groups: Hopi Pottery Production and Exchange, A.C. 1300-1600. *Journal of Field Archaeology* 15:317-337.
- Bishop, Ronald L. and Hector Neff
1989 Compositional data analysis in archaeology. In *Archaeological Chemistry IV. Advances in Chemistry Series*, edited by R. O. Allen, pp. 576-586. vol. 220. American Chemical Society, Washington, D.C.
- Bishop, Ronald L., R. L. Rands and G. R. Holley
1982 Ceramic compositional analysis in archaeological perspective. In *Advances in Archaeological Method and Theory*, edited by M. B. Schiffer, pp. 275-330. Academic Press, New York.
- Blanton, Richard E.
2010 Collective Action and Adaptive Socioecological Cycles in Premodern States. *Cross-Cultural Research* 44(1):41-59.

2011 Cultural Transformation, Art, and Collective Action in Polity Building. *Cross-Cultural Research* 45(2):106-127.

2015 Theories of ethnicity and the dynamics of ethnic change in multiethnic societies. *Proceedings of the National Academy of Sciences* 112(30):201421406-201421406.
- Blanton, Richard E. and Lane F. Fargher
2009 Collective Action in the Evolution of Pre-Modern States. *Social Evolution & History* 8(2):133-166.
- Bliege Bird, Rebecca and Eric Alden Smith

- 2005 Signaling Theory, Strategic Interaction, and Symbolic Capital. *Current Anthropology* 46(2):221-248.
- Blitz, John H.
 1999 Mississippian chiefdoms and the fission-fusion process. *American Antiquity* 64(4):577-592.
 2010 New perspectives in Mississippian archaeology. *Journal of Archaeological Research* 18(1):1-39.
- Boccaletti, S., G. Bianconi, R. Criado, C. I. del Genio, J. Gomez-Gardees, M. Romance, I. Sendiña-Nadal, Z. Wang and M. Zanin
 2014 The structure and dynamics of multilayer networks. *Physics Reports* 544(1):1-122.
- Borck, Lewis, Barbara J. Mills, Matthew A. Peeples and Jeffery J. Clark
 2015 Are Social Networks Survival Networks? An Example from the Late Pre-Hispanic US Southwest. *Journal of Archaeological Method and Theory* 22(1):33-57.
- Borgatti, Stephen P., Ajay Mehra, Daniel J. Brass and Giuseppe Labianca
 2009 Network analysis in the social sciences. *Science* 323(April):892-895.
- Boulanger, Matthew T. and Michael D. Glascock
 2015 Elemental variation in prehistoric Unionoida shell: Implications for ceramic provenance. *Journal of Archaeological Science: Reports* 1(1):2-7.
- Bourdieu, Pierre
 1977 *Outline of a Theory of Practice*. Cambridge University Press, Cambridge, U.K.
 1990 *The Logic of Practice*. Stanford University Press.
- Bowser, Brenda J.
 2000 From Pottery to Politics: An Ethnoarchaeological Study of Political Factionalism, Ethnicity, and Domestic Pottery Style in the Ecuadorian Amazon. *Journal of Archaeological Method and Theory* 7(3):219-248.
- Boyd, Robert and Peter J. Richerson
 1985 *Culture and the Evolutionary Process*. University of Chicago Press, Chicago, Illinois.
 1987 The Evolution of Ethnic Markers. *Cultural Anthropology* 2:65-79.
- Brainerd, George W.
 1951 The Place of Chronological Ordering in Archaeological Analysis. *American Antiquity* 16:301-313.

- Braun, David P.
1985 Ceramic Decorative Diversity and Illinois Regional Intergration. In *Decoding Prehistoric Ceramics*, edited by B. A. Nelson, pp. 128-153. Southern Illinois University Press, Carbondale, IL.
- Braun, David P. and Stephen Plog
1982 Evolution of "Tribal" Social Networks: Theory and Prehistoric North American Evidence. *American Antiquity* 47(3):504-525.
- Breiger, Ronald L.
1975 Dual and Multiple Networks of Social Structures: A Study of Affiliation and Interaction. Unpublished Ph.D. Dissertation, Sociology, Harvard.
- Brettell, Caroline B.
2000 Theorizing Migration in Anthropology: The Social Construction of Networks, Identities, Communities, and Globalscapes. In *Migration Theory: Talking across Disciplines*, pp. 97-135. Routledge, New York.
- Broch, Harald B.
1987 Ethnic Differentiation and Integration: Aspects of Inter-ethnic Relations at the Village Level on Bonerate. *Ethnic Groups* 7:19-37.
- Brose, David S.
1994 Trade and Exchange in the Midwestern United States. In *Prehistoric Exchange Systems in Eastern North America*, edited by T. G. Baugh and J. E. Ericson, pp. 215-240. Plenum Press, New York.
- Brown, James A.
1965 The Prairie Peninsula: An Interaction Area of the Eastern United States.

1995 On Mortuary Analysis - With Special Reference to the Saxe-Binford Research Program. *Regional Approaches to Mortuary Analysis*:3-26.

1996 *The Spiro Ceremonial Center: The Archaeology of Arkansas Valley Caddoan Culture in Eastern Oklahoma*. University of Michigan Museum of Anthropology, Ann Arbor, MI.

2004 Exchange and Interaction Until 1500. In *Handbook of North American Indians (v. 14 Southeast)*, edited by W. C. Sturtevant, pp. 677-685. Smithsonian Institution, Washington D.C.

2006 Where's the Power in Mound Building? An Eastern Woodlands Perspective. In *Leadership and Polity in Mississippian Society*, edited by B. M. Butler and P. D. Welch, pp. 197-213. Center for Archaeological Investigations, Southern Illinois University, Carbondale, IL.

- Brown, James A. and John E. Kelly
2000 Cahokia and the Southeastern Ceremonial Complex. In *Mounds, Modoc and Mesoamerica: Papers in Honor of Melvin L. Fowler*, edited by S. R. Ahler, pp. 469-510. Volume XXV ed. Illinois State Museum Scientific Papers, Springfield, IL.
- Brown, James A. and Robert F. Sasso
2001 Prelude to History on the Eastern Praries. In *Societies in Eclipse: Archaeology of the Eastern Woodlands, A.D. 1400-1700*, edited by D. S. Brose, C. W. Cowan and R. C. Mainfort, pp. 205-228. Smithsonian Institution, Washington D.C.
- Brughmans, Tom
2010 Connecting the dots: Towards archaeological network analysis. *Oxford Journal of Archaeology* 29(3):277-303.

2013 Thinking Through Networks: A Review of Formal Network Methods in Archaeology. *Journal of Archaeological Method and Theory* 20(4):623-662.
- Buchanan, Briggs, Marcus J. Hamilton, J. David Kilby and Joseph A. M. Gingerich
2016 Lithic networks reveal early regionalization in late Pleistocene North America. *Journal of Archaeological Science* 65:114-121.
- Buchanan, Meghan
2014 Making War, Making Pots: Mississippian Plate Iconography in the Midcontinent. Paper presented at the 71st Annual Southeastern Archaeological Conference, Greenville, SC.
- Burmeister, Stefan
2000 Archaeology and Migration: Approaches to an Archaeological Proof of Migration. *Current Anthropology* 41(4):539-567.
- Calhoun, Craig
1993 "New Social Movements" of the Early Nineteenth Century. *Social Science History* 17:385-427.
- Carneiro, Robert L.
1970 A Theory of the Origin of the State: Traditional theories of state origins are considered and rejected in favor of a new ecological hypothesis. *Science (New York, N.Y.)* 169(3947):733-738.
- Carr, Christopher
1995a Mortuary practices: Their social, philosophical-religious, circumstantial, and physical determinants. *Journal of Archaeological Method and Theory* 2(2):105-200.

1995b A Unified Middle-Range Theory of Artifact Design. In *Style, Society, and Person: Archaeological and Ethnological Perspectives*, edited by C. Carr and J. E. Nietzel, pp. 171-258. Plenum, New York.

- Childe, V. Gordon
1936 *Man makes himself*. Watts & Co., London.
- Clark, Jeffery J.
2001 *Tracking Prehistoric Migrations: Pueblo Settlers among the Tonto Basin Hohokam* Anthropological Papers No. 65. University of Arizona Press, Tuscon.
- Clarke, David L.
1968 *Analytical Archaeology*. Methuen, London.
- Clay, R. Berle
1976 *A Mississippian Cultural Sequence from the Lower Tennessee-Cumberland and Its Significance*. Office of State Archaeology, University of Kentucky, Lexington.
- Cobb, Charles R.
2000 *From Quarry to Cornfield: the Political Economy of Mississippian Hoe Production*. University of Alabama Press, Tuscaloosa, AL.

2003 Mississippian Chiefdoms: How Complex ? *Annual Review of Anthropology* 32(1):63-84.

2005 Archaeology and the "Savage Slot": Displacement and Emplacement in the Premodern World. *American Anthropologist* 107(4):563-574.
- Cobb, Charles R. and Brian M. Butler
2002 The Vacant Quarter Revisited: Late Mississippian Abandonment of the Lower Ohio Valley. *American Antiquity* 67(4):625-641.

2006 Mississippian Migration and Emplacement in the Lower Ohio Valley. In *Leadership and Polity in Mississippian Society*, edited by B. M. Butler and P. D. Welch, pp. 328-347. Southern Illinois University, Carbondale.
- Cochrane, Ethan E. and Hector Neff
2006 Investigating compositional diversity among Fijian ceramics with laser ablation-inductively coupled plasma-mass spectrometry (LA-ICP-MS): Implications for interaction studies on geologically similar islands. *Journal of Archaeological Science* 33(3):378-390.
- Cogswell, James W., Hector Neff, Michael D. Glascock, W. Cogswell and Michael D. Glascock
2015 Analysis of Shell-Tempered Pottery Replicates: Implications for Provenance Studies. *American Antiquity* 63(1):63-72.
- Cole, Fay-Cooper and Thorne Deuel
1937 *Rediscovering Illinois: Archaeological Explorations in and around Fulton County*. University of Chicago Press, Chicago, Illinois.

- Collar, Anna, Fiona Coward, Tom Brughmans and Barbara J. Mills
 2015 Networks in Archaeology: Phenomena, Abstraction, Representation. *Journal of Archaeological Method and Theory* 22(1).
- Conkey, Margaret W.
 1990 Experimenting with Style in Archaeology: Some Historical and Theoretical Issues. In *The Uses of Style in Archaeology*, edited by M. W. Conkey and C. Hastorf, pp. 5-17. Cambridge University Press, Cambridge.
- Conner, Michael D.
 2016 Mississippian Habitation Components at Dickson Mounds in the Central Illinois River Valley. *Midcontinental Journal of Archaeology* 41(1):67-92.
- Conrad, Lawrence A.
 1989 The Southeastern Ceremonial Complex on the Northern Middle Mississippian Frontier: Late Prehistoric Politico-religious Systems in the Central Illinois River Valley. In *The Southeastern Ceremonial Complex: Artifacts and Analysis*, edited by P. Galloway, pp. 93-113. University of Florida Press.
 1991 The Middle Mississippian Cultures of the Central Illinois Valley. In *Cahokia and the Hinterlands: Middle Mississippian Cultures of the Midwest*, edited by T. E. Emerson and R. B. Lewis, pp. 119-156. University of Illinois Press, Urbana, IL.
- Conrad, Lawrence A. and Duane Esarey
 1983 Oneota in West-Central Illinois. Paper presented at the 28th Midwest Archaeological Conference, Iowa City, Iowa.
- Cook, Robert A.
 2007 *Sunwatch: Fort Ancient Development in the Mississippian World*. University of Alabama Press, Tuscaloosa, AL.
- Cook, Robert A. and Lane F. Fargher
 2007 Fort Ancient-Mississippian Interaction and Shell-Tempered Pottery at SunWatch Village, Ohio. *Journal of Field Archaeology* 32(2):149-160.
- Cozzo, Emanuele, Mikko Kivelä, Manlio De Domenico, Albert Solé, Alex Arenas, Sergio Gómez, Mason a Porter and Yamir Moreno
 2013 Clustering Coefficients in Multiplex Networks. *arXiv* 1307.6780:1-10.
- Crowe, Jessica A.
 2007 In Search of a Happy Medium: How the Structure of Interorganizational Networks Influence Community Economic Development Strategies. *Social Networks* 29:469-488.
- Curry, B. Brandon, David A. Grimley and E. Donald McKay III

- 2011 Quaternary Glaciations in Illinois. *Developments in Quaternary Sciences* 15:467-487.
- Curry, B. Brandon, Edwin R. Hajic, James A. Clark, Kevin M. Befus, Jennifer E. Carrell and Steven E. Brown
2014 The Kankakee Torrent and other large meltwater flooding events during the last deglaciation, Illinois, USA. *Quaternary Science Reviews* 90:22-36.
- Danchev, Valentin and Mason A. Porter
2018 Neither global nor local: Heterogeneous connectivity in spatial network structures of world migration. *Social Networks* 53:4-19.
- De Domenico, Manlio, Vincenzo Nicosia, Alexandre Arenas and Vito Latora
2015 Structural reducibility of multilayer networks. *Nature communications* 6:6864-6864.
- De Domenico, Manlio, Mason A. Porter and Alex Arenas
2015 MuxViz: A tool for multilayer analysis and visualization of networks. *Journal of Complex Networks* 3(2):159-176.
- De Domenico, Manlio, Albert Solé-Ribalta, Emanuele Cozzo, Mikko Kivelä, Yamir Moreno, Mason A. Porter, Sergio Gómez and Alex Arenas
2013 Mathematical Formulation of Multilayer Networks. *Physical Review X* 3(4):041022-041022.
- De Domenico, Manlio, Albert Solé-Ribalta, Elisa Omodei, Sergio Gómez and Alex Arenas
2013 Centrality in Interconnected Multilayer Networks. *arXiv* 1311.2906:1-12.
- DeBoer, Warren R., Keith Kintigh and Arthur G. Rostoker
1996 Ceramic Seriation and Site Reoccupation in Lowland South America. *Latin American Antiquity* 7(3):263-278.
- Delaney-Rivera, Colleen M.
2007 Examining Interaction and Identity in Prehistory: Mortuary Vessels from the Schild Cemetery. *North American Archaeologist* 28(4):295-331.
- Diani, Mario
2007 The relational element in Charles Tilly's recent (and not so recent) work. *Social Networks* 29(2):316-323.
- Dickison, Mark E., Mark Magnani and Luca Rossi
2016 *Multilayer social networks*. Cambridge University Press, Cambridge.
- Dietler, M. and I. Herbich
1998 Habitus, techniques, style: An integrated approach to the social understanding of material culture and boundaries. *The Archaeology of Social Boundaries*:232-263.

- Dussubieux, Laure, Mark L. Golitko, Patrick Ryan Williams and Robert J. Speakman
2007 Laser Ablation-Inductively Coupled Plasma-Mass Spectrometry Analysis Applied to the Characterization of Peruvian Wari Ceramics. *Archaeological Chemistry: Analytical Techniques and Archaeological Interpretation*:349-363.
- Dussubieux, Laure and Thomas Oliver
2016 Myanmar's role in Iron Age interaction networks linking Southeast Asia and India: Recent glass and copper-base metal exchange research from the Mission Archéologique Française au Myanmar. *Journal of Archaeological Science: Reports* 5:598-614.
- Dye, David H.
2013 Trends in Cooperation and Conflict in Native Eastern North America. *War, Peace, and Human Nature: The Convergence of Evolutionary and Cultural Views*:132-150.
- Earle, Timothy
1989 The Evolution of Chiefdoms. *Current Anthropology* 30(1):84-88.
- Edler, Daniel and Martin Rosvall
2014 The MapEquation software package (InfoMap).
- Eerkens, Jelmer W. and Robert L. Bettinger
2008 Cultural Transmission and the Analysis of Stylistic and Functional Variation. In *Cultural Transmission and Archaeology: Issues and Case Studies*, edited by M. J. O'Brien, pp. 21-38. The Society for American Archaeology, Washington D.C.
- Eerkens, Jelmer W., Robert L. Bettinger and Peter J. Richerson
2013 *Cultural Transmission Theory and Hunter-Gatherer Archaeology*. Oxford University Press, Oxford.
- Eerkens, Jelmer W. and Carl P. Lipo
2005 Cultural transmission, copying errors, and the generation of variation in material culture and the archaeological record. *Journal of Anthropological Archaeology* 24(4):316-334.
- 2007 Cultural Transmission Theory and the Archaeological Record : Providing Context to Understanding Variation and Temporal Changes in Material Culture. *Journal of Archaeological Research* 15(3):239-274.
- Eerkens, Jelmer W., Hector Neff and Michael D. Glascock
2002 Ceramic production among small-scale and mobile hunters and gatherers: a case study from the Southwestern Great Basin. *Journal of Anthropological Archaeology* 21:200-229.

- Elliot, Shane, Michael Knowles and Iouri Kalinitchenko
2004 A new direction in ICP-MS. *Spectroscopy* 19:30-38.
- Emberling, Geoff
1997 Ethnicity in Complex Societies: Archaeological Ethnicity Perspectives. *Journal of Archaeological Research* 5(4):295-344.

1999 The Value of Tradition: The Development of Social Identities in Early Mesopotamian States. In *Material Symbols: Culture and Economy in Prehistory*, edited by J. E. Robb, pp. 277-301. Southern Illinois University Center for Archaeological Investigations Occasional Paper No. 26, Carbondale.
- Emberling, Geoff and Leah Minc
2016 Ceramics and long-distance trade in early Mesopotamian states. *Journal of Archaeological Science: Reports* 7:819-834.
- Emerson, Thomas E.
1991 The Apple River Mississippian Culture of Northwestern Illinois. In *Cahokia and the Hinterlands: Middle Mississippian Cultures of the Midwest*, edited by T. E. Emerson and R. B. Lewis, pp. 164-182. University of Illinois Press, Urbana, IL.

1999 The Langford Tradition and the Process of Tribalization on the Middle and the the of Process Tradition Middle on the Mississippian Borders. *Midcontinental Journal of Archaeology* 24(1):3-56.

2012 Cahokia Interaction and Ethnogenesis in the Northern Midcontinent. *The Oxford Handbook of North American Archaeology* (Chapter 33):398-409.
- Emerson, Thomas E. and James A. Brown
1992 The Late Prehistory and Protohistory of Illinois. In *Calumet and Fleu-de-Lys: Archaeology of Indian and French Contact in the Midcontinent I*, edited by J. A. Walthall, pp. 77-128. Smithsonian Institution Press, Washington D.C.
- Emerson, Thomas E. and R. Barry Lewis (editors)
1991 *Cahokia and the Hinterlands: Middle Mississippian Cultures of the Midwest*. University of Illinois Press, Urbana, IL.
- Emirbayer, M. and J. Goodwin
1994 Network Analysis, Culture and the Problem of Agency. *American Journal of Sociology* 99(1411-1454).
- Erdős, Paul and Alfréd Rényi
1959 On random graphs. *Publicationes Mathematicae* 6:290-297.
- Esarey, Duane

- 2000 The Late Woodland Maples Mills and Mossville Phase Sequence in the Central Illinois River Valley. In *Late Woodland Societies: Tradition and Transformation across the Midcontinent*, edited by T. E. Emerson, D. L. McElrath and A. C. Fortier, pp. 387-412. University of Nebraska, Lincoln.
- Esarey, Duane and Lawrence A. Conrad (editors)
 1981 *The Orendorf Site Preliminary Working Papers*. Western Illinois University, Archaeological Research Laboratory, Macomb, IL.
- 1998 The Bold Counselor Phase of the Central Illinois River Valley: Oneota's Middle Mississippian Margin. *The Wisconsin Archeologist* 79(2):38-61.
- Ethridge, Robbie
 2009a Introduction: Mapping the Mississippian Shatter Zone. In *Mapping the Mississippian Shatter Zone: The Colonial Indian Slave Trade and Regional Instability in the American South*, edited by R. Ethridge and S. M. Shuck-Hall, pp. 1-62. University of Nebraska Press, Lincoln.
- 2009b *Mapping the Mississippian Shatter Zone: The Colonial Indian Slave Trade and Regional Instability in the American South*. University of Nebraska Press, Lincoln, NE.
- Falabella, F., L. Sanhueza, I. Correa, M. D. Glascock, T. J. Ferguson and E. Fonseca
 2013 Studying technological practices at a local level: Neutron activation and petrographic analyses of early ceramic period pottery in central Chile. *Archaeometry* 55(1).
- Feathers, James K.
 1989 Effects of Temper on Strength of Ceramics: Response to Bronitsky and Hamer. *American Antiquity* 54(3):579-588.
- 2006 Explaining Shell-Tempered Pottery in Prehistoric Eastern North America Eastern Shell-Tempered America Pottery in Prehistoric North. *Journal of Archaeological Method and Theory* 13(2):89-133.
- Fie, Shannon M.
 2006 Visiting the Interaction Sphere: Ceramic Exchange and Interaction in the Lower Illinois Valley. In *Recreating Hopewell*, edited by D. K. Charles and J. E. Buikstra. University of Florida, Gainesville.
- Fisher, Alton K.
 1997 Origins of the Midwestern Taxonomic Method. *Midcontinental Journal of Archaeology* 22(1):1-5.
- Fitzpatrick, Scott M., Hiroto Takamiya, Hector Neff and William R. Dickinson
 2006 Compositional Analysis of Yayoi-Heian Period Ceramics From Okinawa: Examining the Potential for Provenance Study. *Geoarchaeology* 21(8):803-822.

- Flannery, Kent V.
1968 Archaeological systems theory and early Mesoamerica. In *Anthropological archaeology in the Americas*, pp. 67-87. Anthropological Society of Washington, Washington D.C. .
- Foley-Winkler, Kathleen M.
2011 Oneota and Langford mortuary practices from eastern Wisconsin and northeast Illinois. Unpublished Ph.D. Dissertation, University of Wisconsin-Milwaukee.
- Ford, Richard I.
1972 Barter, Gift, or Violence: An Analysis of Tewa Intertribal Exchange. In *Social Exchange and Interaction*, edited by E. N. Wilmsen, pp. 21-46. vol. 46. University of Michigan, Ann Arbor.
- Fowler, Melvin L.
1974 *Cahokia: Ancient Capital of the Midwest*. Addison-Wesley Module in Anthropology, No. 48.
- Fowles, Severin M., Leah Minc, Samuel Duwe, David V. Hill and Leah Mine
2007 Clay, Conflict, and Village Aggregation: Compositional Analyses of Pre-Classical Pottery. *American Antiquity* 72(1):125-152.
- Frangipane, Marcella
2015 Different types of multiethnic societies and different patterns of development and change in the prehistoric Near East. *Proceedings of the National Academy of Sciences of the United States of America* 112(30):9182-9189.
- Friberg, Christina M.
2018 Cosmic negotiations: Cahokian religion and Ramey Incised pottery in the northern hinterland. *Southeastern Archaeology* 37(1):39-57.
- Fuhse, Jan A.
2012 Embedding the Stranger: Ethnic Categories and Cultural Differences in Social Networks. *Journal of Intercultural Studies* 33(6):639-655.

2015 Theorizing social networks: the relational sociology of and around Harrison White. *International Review of Sociology* 25(1):15-44.
- Garcea, Elena A. A. and Elisabeth A. Hildebrand
2009 Shifting social networks along the Nile : Middle Holocene ceramic assemblages from Sai Island , Sudan. *Journal of Anthropological Archaeology* 28(3):304-322.
- Garraty, Christopher P.
2006 The Politics of Commerce: Aztec Pottery Production and Exchange in the Basin of Mexico, A.D. 1200-1650. Unpublished Ph.D. Dissertation, Arizona State University.

- Geary, Patrick
1983 Ethnic Identity as a Situational Construct in the Early Middle Ages. *Mitteilungen der Anthropologischen Gesellschaft in Wien* 113(15-26).
- Geertz, Clifford
1963 The integrative revolution: primordial sentiments and politics in the new states. In *Old societies and new states: the quest for modernity in Asia and Africa*, edited by C. Geertz, pp. 107-113. Free Press, New York.
- Gibbon, Guy E.
1972 Cultural Dynamics and the Development of the Oneota Life-Way in Wisconsin. *American Antiquity* 37(2):166-185.

1995 Oneota at the Periphery: Trade, Political Power, and Ethnicity in Northern Minnesota and on the Northeastern Plains in the Late Prehistoric Period. In *Oneota Archaeology: Past, Present and Future*, edited by W. Green, pp. 175-199. Report 20, Office of the State Archaeologist, University of Iowa, Iowa City, IA.

2002 Oneota. In *Encyclopedia of Prehistory*, pp. 389-407. Springer.
- Gilbert, E.
1959 Random graphs. *Annals of Mathematical Statistics* 30(4):1141-1144.
- Gjesfjeld, Erik W.
2014 Of Pots and People: Investigating Hunter-Gatherer Pottery Production and Social Networks in the Kuril Islands. Unpublished Ph.D. Dissertation, University of Washington.

2015 Network Analysis of Archaeological Data from Hunter-Gatherers: Methodological Problems and Potential Solutions. *Journal of Archaeological Method and Theory* 22(1):182-205.

2018 The compositional analysis of hunter-gatherer pottery from the Kuril Islands. *Journal of Archaeological Science: Reports* 17:1025-1034.
- Glascok, Michael D.
1992 Characterization of Archaeological Ceramics at MURR by Neutron Activation Analysis and Multivariate Statistics. In *Chemical Characterization of Ceramic Pastes in Archaeology*, edited by H. Neff, pp. 11-26. Prehistory Press, Madison.

2002 Obsidian Provenance Research in the Americas. *Accounts of Chemical Research* (35):611-617.

2016 Compositional Analysis in Archaeology. *Oxford Handbooks Online*.
- Glowacki, Donna M.

- 2006 The Social Landscape of Depopulation: The Northern San Juan, A.D. 1150-1300. Unpublished Ph.D. Dissertation, Arizona State University.
- Gluckman, Max
1967 *The Judicial Process among the Barotse of Northern Rhodesia*. Manchester University Press, Manchester.
- Goldstein, Lynne G.
1981 One-dimensional archaeology and multi-dimensional people: spatial organization and mortuary analysis. In *Archaeology of Death*, edited by R. W. Chapman, I. Kinnes and K. Randsborg, pp. 535-569. Cambridge University Press, Cambridge.
- 2000 Mississippian Ritual as Viewed Through the Practice of Secondary Disposal of the Dead. In *Mounds, Modoc and Mesoamerica: Papers in Honor of Melvin L. Fowler*, edited by S. R. Ahler, pp. 193-205. Illinois State Museum Scientific Papers Vol. 28, Springfield, IL.
- 2006 Mortuary Analysis in Bioarchaeology. In *Bioarchaeology: A Contextual Approach*, edited by L. Beck and J. E. Buikstra, pp. 375-387. Academic Press, Inc., New York.
- Goldstein, Lynne G. and John D. Richards
1991 Ancient Aztalan: The Cultural and Ecological Context of a Late Prehistoric Site in the Midwest. In *Cahokia and the Hinterlands: Middle Mississippian Cultures of the Midwest*, edited by T. E. Emerson and R. B. Lewis, pp. 193-206. University of Illinois Press, Urbana, IL.
- Goldstein, Paul S.
2015 Multiethnicity, pluralism, and migration in the south central Andes: An alternate path to state expansion. *Proceedings of the National Academy of Sciences* 112(30):9202-9209.
- Golitko, Mark L.
2010 Warfare and Alliance Building during the Belgian Early Neolithic, Late Sixth Millennium BC. Unpublished Ph.D. Dissertation, University of Illinois - Chicago.
- Golitko, Mark L. and Gary M. Feinman
2014 Procurement and Distribution of Pre-Hispanic Mesoamerican Obsidian 900 BC-AD 1520: a Social Network Analysis. *Journal of Archaeological Method and Theory*:206-247.
- Golitko, Mark L. and John Edward Terrell
2012 Mapping prehistoric social fields on the Sepik coast of Papua New Guinea: Ceramic compositional analysis using laser ablation-inductively coupled plasma-mass spectrometry. *Journal of Archaeological Science* 39(12):3568-3580.

- Goodby, Robert G.
1998 Technological Patterning and Social Boundaries: Ceramic Variability in Southern New England. In *The Archaeology of Social Boundaries*, edited by M. T. Stark, pp. 161-182. Smithsonian Institution Press, Washington D.C.
- Gosselain, O. P. and A. Livingstone Smith
2005 The Source. Clay selection and processing practices in Sub-Saharan Africa. In *Pottery Manufacturing Processes : Reconstruction and Interpretation*, edited by A. Livingstone Smith, D. Bosquet and R. Martineau, pp. 33-47.
- Gower, J. C.
1971 A General Coefficient of Similarity and Some of Its Properties. *Biometrics* 27:857-871.
- Granovetter, Mark S.
1973 The Strength of Weak Ties. *The American Journal of Sociology* 78:1360-1380.

2001 Economic Action and Social Structure: The Problem of Embeddedness. In *The Sociology of Economic Life*, edited by M. S. Granovetter and R. Swedberg. Westview Press, Boulder.
- Gratuze, Bernard, M. Blet-Lemarquand and J. N. Barrandon
2001 Mass Spectrometry with Laser Sampling: A New Tool to Characterize Archaeological Materials. *Journal of Radioanalytical and Nuclear Chemistry* 247(3):645-656.
- Graves, Michael W.
1981 Ethnoarchaeology of Kalinga Ceramic Design. Unpublished Ph.D. Dissertation, Anthropology, University of Arizona.

1994 Kalinga Social and Material Culture Boundaries: A Case Study of Spatial Convergence. In *Kalinga Ethnoarchaeology: Expanding Archaeological Method and Theory*, edited by W. A. Longacre and J. M. Skibo, pp. 13-49. Smithsonian Institution Press, Washington D.C.
- Green, William B. and Roland L. Rodell
1994 The Mississippian Presence and Cahokia Interaction at Trempealeau, Wisconsin. *American Antiquity* 59:334-359.
- Green, William and David J. Nolan
2000 Late Woodland Peoples in West-Central Illinois. In *Late Woodland Societies: Tradition and Transformation across the Midcontinent*, edited by T. E. Emerson and D. L. McElrath, pp. 345-386. University of Nebraska, Lincoln.
- Griffin, James B.

1949 The Cahokia Ceramic Complexes. In *Proceedings of the Fifth Plains Conference for Archaeology*, edited by J. L. Champe, pp. 44-58. University of Nebraska, Lincoln.

1960 A Hypothesis for the Prehistory of the Winnebago. In *Culture in History*, edited by S. Diamond, pp. 809-865. Columbia Press, New York.

Hajic, Edwin R.

1990 Late Pleistocene and Holocene landscape evolution, depositional subsystems, and stratigraphy in the lower Illinois River Valley and adjacent central Mississippi River Valley. Unpublished Ph.D. Dissertation, Geology, University of Illinois at Urbana-Champaign.

2006 *Geomorphology, Geoarchaeology, and Landscape and Wetland Evolution of the Emiquon Basins, Lower-Middle Illinois River Valley*. Report submitted to The Nature Conservancy.

Hally, David J.

2006 The Nature of Mississippian Regional Systems. In *Light on the Path: The Anthropology and History of the Southeastern Indians*, edited by R. Ethridge, T. J. Pluckhahn and C. Hudson, pp. 26-42. University of Alabama Press, Tuscaloosa, AL.

Harbottle, G.

1976 Activation Analysis in Archaeology. In *Radiochemistry*, edited by G. W. A. Newton, pp. 33-72. vol. 3. The Chemical Society, London.

Hargrave, Michael L., Charles R. Cobb and Paul A. Webb

1991 Late Prehistoric Ceramic Style Zones in Southern Illinois. In *Stability, Transformation and Variation: The Late Woodland Southeast*, edited by M. S. Nassaney and C. R. Cobb, pp. 149-176. Plenum Press, New York.

Harn, Alan D.

1971 *The Prehistory of Dickson Mounds: A Preliminary Report*. Dickson Mounds Museum Anthropological Studies. Illinois State Museum, Springfield, IL.

1978 Mississippian Settlement Patterns in the Central Illinois River Valley. In *Mississippian Settlement Patterns*, pp. 233-268. Academic Press, Inc., New York.

1980 *The Prehistory of Dickson Mounds: the Dickson Excavation*. Illinois State Museum Reports of Investigations #35. Illinois State Museum, Springfield, IL.

1991 The Eveland Site: Inroad to Spoon River Mississippian Society. In *New Perspectives on Cahokia: Views from the Periphery*, edited by J. B. Stoltman, pp. 129-153. Prehistory Press, Madison, WI.

1994 *The Larson Settlement System in the Central Illinois River Valley*. Illinois State Museum Reports of Investigations, No. 50, Springfield, IL.

- Harn, Alan D. and Sally McClure
2012 *Six Hundred Generations There: Archaeological and Historical Perspectives on Life at Emiquon The Nature Conservancy and U.S. Fish and Wildlife Services Properties Fulton County, Illinois*. Illinois State Museum Reports of Investigations, No. 57.
- Hart, John P.
1990 Modeling Oneota Agricultural Production: A Cross-Cultural Evaluation. *Current Anthropology* 31(5):569-577.
- Hart, John P. and William Engelbrecht
2012 Northern Iroquoian Ethnic Evolution: A Social Network Analysis. *Journal of Archaeological Method and Theory* 19(2):322-349.
- Hatch, Mallorie A.
2015 The Social Costs of War: Investigating the Relationship between Warfare and Intragroup Violence during the Mississippian Period of the Central Illinois Valley. Unpublished Ph.D. Dissertation, Arizona State University.

2017 Politics and Social Substitution in Total War: Exploring the Treatment of Combatants and Noncombatants During the Mississippian Period of the Central Illinois Valley. In *Bioarchaeology of Women and Children in Times of War*, pp. 49-69. Springer International Publishing, Cham.
- Hazen, Robert M., Dimitri A. Sverjensky, David Azzolini and David L. Bish
2013 Clay mineral evolution. *American Mineralogist* 98:2007-2029.
- Hegmon, Michelle
2000 Advances in Ceramic Ethnoarchaeology. *Journal of Archaeological Method and Theory* 7(3):129-137.
- Hegmon, Michelle, James R. Allison, Hector Neff and Michael D. Glascock
1997 Production of San Juan Red Ware in the Northern Southwest: Insights into Regional Interaction in Early Puebloan Prehistory. *American Antiquity* 62(3):449-463.
- Henning, Dale R.
1995 Oneota Evolution and Interactions: A Perspective from the Wever Terrace, Southeast Iowa. In *Oneota Archaeology: Past, Present and Future I*, edited by W. B. Green, pp. 65-88. Office of the State Archaeologist The University of Iowa, Iowa City, IA.

1998 The Oneota Tradition. In *Archaeology on the Great Plains*, edited by W. R. Wood, pp. 345-414. University Press of Kansas.

- 2005 The Evolution of the Plains village tradition. In *North American Archaeology*, edited by T. R. Pauketat and D. D. Loren, pp. 161-186. Blackwell Publishing, Malden, MA.
- Herbich, Ingrid
1987 Learning Patterns, Potter Interaction and Ceramic Style among the Luo of Kenya. *The African Archaeological Review* 5:193-204.
- Hilgeman, Sherri
2000 *Pottery and Chronology at Angel*. University of Alabama Press.
- Hill, Jonathan D.
2013 Long-Term Patterns of Ethnogenesis in Indigenous Amazonia. In *The Archaeology of Hybrid Material Culture*, edited by J. Card, pp. 165-184. Center for Archaeological Investigations, Southern Illinois University, Carbondale, IL.
- Hollinger, R. Eric
1995 Residence Patterns and Oneota Cultural Dynamics. In *Oneota Archaeology: Past, Present and Future*, edited by W. Green, pp. 141-174. Report 20 ed. Office of the State Archaeologist The University of Iowa, Iowa City, Iowa.

2005 Conflict and Culture Change in the Late Prehistoric and Early Historic American Midcontinent. Unpublished Ph.D. Dissertation, University of Illinois at Urbana-Champaign.
- Horberg, Leland
1950 *Bedrock topography of Illinois*. Illinois State Geologic Survey Bulletin 73, Urbana.
- Hu, Yifan
2005 Efficient, High-Quality Force-Directed Graph Drawing. *Mathematica Journal* 10(1):37-71.
- Hudson, Charles
1976 *The Southeastern Indians*. The University of Tennessee Press, Knoxville.
- Jackson, Doug
1992 Oneota in the American Bottom. In *The Sponemann Site 2: The Mississippian and Oneota Occupations*, edited by C. E. Bareis and J. H. Walthall, pp. 383-392. University of Illinois Press, Urbana, IL.
- Jenkins, Richard
2000 Categorization: Identity, Social Process and Epistemology. *Current Sociology* 48(3):7-25.

2004 *Social Identity*. Routledge, London.

- Jones, Sian
 1997 *The Archaeology of Ethnicity: Constructing Identities in the Past and Present*. Routledge, London.
- Kaufman, L. and Pj Rousseeuw
 1990a Clustering Large Applications (Program CLARA). *Finding Groups in Data: An introduction to Cluster Analysis*:126-163.
- Kaufman, Leonard and Peter J. Rousseeuw
 1990b *Finding groups in data: an introduction to cluster analysis*. Wiley Series in Probability and Statistics. Wiley.
- Keeley, Lawrence H.
 2014 War Before Civilization - 15 Years On. In *The Evolution of Violence*, pp. 23-31.
- Keller, W. D.
 1964 Processes of origin and alteration of clay minerals. In *Soil clay mineralogy: A symposium*, edited by C. I. Rich and G. W. Kunze, pp. 3-76. University of North Carolina Press, Chapel Hill.
- Kelly, John E.
 1984 Wells Incised Or O'Byam Incised, variety Wells, and Its Context in the American Bottom. Paper presented at the 1985 Paducah Ceramic Conference, Paducah, Kentucky.
- 1991a The Evidence for Prehistoric Exchange and Its Implications for the Development of Cahokia. In *New Perspectives on Cahokia: Views from the Periphery*, edited by J. B. Stoltman, pp. 65-92. Prehistory Press, Madison, WI.
- 1991b Wells Incised Plates: Symbolic Antecedents and Spatial Affinities. Paper presented at the 36th Annual Midwest Archaeological Conference, LaCrosse, WI.
- Kent, Susan
 2002 Interethnic Encounters of the First Kind: An Introduction. In *Ethnicity, Hunter-Gatherers, and the "Other": Association or Assimilation in Africa*, edited by S. Kent, pp. 1-27. Smithsonian Institution Press, Washington D.C.
- Keyes, Charles F. (editor) 1979 *Ethnic Adaptation and Identity*. Institute for the Study of Human Issues, Philadelphia, PA.
- King, Adam
 2002 Creek Chiefdoms at the Temporal Edge of the Mississippian World. *Southeastern Archaeology* 21(2):221-226.
- King, Frances B.

- 1990 Geographic Setting, Past and Present Physiography, Potential Subsistence Resources. In *Archaeological Investigations at the Morton Village and Norris Farms 36 Cemetery*, edited by S. K. Santure, D. Esarey and A. D. Harn, pp. 3-5. No. 45 ed. Illinois State Museum Reports of Investigations, Springfield, IL.
- Kivelä, Mikko, Alex Arenas, Marc Barthelemy, James P. Gleeson, Yamir Moreno and Mason A. Porter
 2014 Multilayer networks. *Journal of Complex Networks* 2(3):203-271.
- Kleinberg, Jon
 1999 Authoritative sources in a hyperlinked environment. *Journal of the ACM* 46(5):1-33.
- Knappett, Carl (editor) 2013 *Network Analysis in Archaeology: New Approaches to Regional interaction*. Oxford University Press, Oxford.
- Knight Jr, Vernon J.
 1986 The Institutional Organization of Mississippian Religion. *American Antiquity* 51(4):675-687.
 1990 Social Organization and the Evolution of Hierarchy in Southeastern Chiefdoms. *Journal of Anthropological Research* 46(1):1-23.
- Knoke, D. and J. Kuklinski
 1982 *Network Analysis*. Sage Publications, Newbury Park.
- Knox, Hannah, Mike Savage and Penny Harvey
 2006 Social networks and the study of relations: networks as method, metaphor and form. *Economy and Society* 35(1):113-140.
- Kolaczyk, Eric D. and Gábor Csárdi
 2014 *Statistical Analysis of Network Data with R*. Use R! 65. Springer, New York.
- Kolata, Dennis R.
 2005 Bedrock geology of Illinois. Illinois State Geologic Survey, Department of Natural Resources, <http://hdl.handle.net/2142/55796>.
- Kopytoff, Igor
 1987 The Internal African Frontier: The Making of African Political Culture. In *The African Frontier: The Reproduction of Traditional African Societies*, edited by I. Kopytoff, pp. 3-84. University of Indiana Press, Bloomington.
- Kossinna, Gustaf
 1911 *Der Herkunft der Germanen*. Kabitzsch, Leipzig.
- Kowalewski, Stephen A.

- 2006 Coalescent Societies. In *Light on the Path: The Anthropology and History of the Southeastern Indians*, edited by R. Ethridge, T. J. Pluckhahn and C. Hudson, pp. 94-122. University of Alabama Press, Tuscaloosa, AL.
- Kramer, Carol
1985 Ceramic Ethnoarchaeology. *Annual Review of Anthropology* 14:77-102.
- Kreisa, Paul P.
1993 Oneota Burial Practices in Eastern Wisconsin. *Midcontinental Journal of Archaeology* 18(1):35-60.
- Landes, Ruth
1959 Dakota Warfare. *Southwestern Journal of Anthropology* 15(1):43-52.

1968 *The Mystic Lake Sioux: Sociology of the Mdewakantonwan*. University of Wisconsin Press, Madison.
- Lankford, George E. (editor) 2011 *Native American Legends of the Southeast: Tales from the Natchez, Caddo, Biloxi, Chickasaw, and Other Nations*. The University of Alabama Press, Tuscaloosa.
- Lazzari, Marisa, Lucas Pereyra Domingorena, Wesley D. Stoner, María Cristina Scattolin, María Alejandra Korstanje and Michael D. Glascock
2017 Compositional data supports decentralized model of production and circulation of artifacts in the pre-Columbian south-central Andes. *Proceedings of the National Academy of Sciences* 114(20):E3917-E3926.
- LeBlanc, Stephen A.
2000 Regional Interaction and Warfare in the Late Prehistoric Southwest. In *The Archaeology of Regional Interaction: Religion, Warfare and Exchange Across the American Southwest and Beyond*, edited by M. Hegmon, pp. 41-70. University of Colorado Press, Boulder, CO.
- Leighton, M. M., G. E. Ekblaw and C. L. Horberg
1948 Physiographic divisions of Illinois. *Journal of Geology* 56:16-33.
- Lesmeister, Cory
2015 *Mastering Machine Learning with R*. Packt Publishing, Birmingham, UK.
- Liebmann, Matthew
2013 Parsing Hybridity: Archaeologies of Amalgamation in Seventeenth-Century New Mexico. In *The Archaeology of Hybrid Material Culture*, edited by J. Card, pp. 25-31. Center for Archaeological Investigations, Southern Illinois University, Carbondale, IL.
- Lieto, Josh and Jodie A. O’Gorman

- 2014 A Preliminary Analysis of Oneota and Mississippian Serving Vessels at the Morton Village Site *North American Archaeologist* 35(3):243-255.
- Lightfoot, Kent G.
1995 Culture Contact Studies: Redefining the Relationship Between Prehistoric and Historical Archaeology. *American Antiquity* 60(2):199-217.
- Lightfoot, Kent G. and Antoinette Martinez
1995 Frontiers and Boundaries in Archaeological Perspective. *Annual Review of Anthropology* 24(1):471-492.
- Lightfoot, Kent G., Antoinette Martinez and Ann M. Schiff
1998 Daily Practice and Material Culture in Pluralistic Social Settings: An Archaeological Study of Culture Change and Persistence from Fort Ross, California. *American Antiquity* 63(2):199-222.
- Lipo, Carl P.
2001 Community Structures among Late Mississippian Populations of the central Mississippi River valley. In *Posing Questions for a Scientific Archaeology*, edited by T. L. Hunt, C. P. Lipo and S. L. Sterling, pp. 175-216. Bergin & Garvey, Westport, CT.
- Longacre, William A.
1991 *Ceramic Ethnoarchaeology*. University of Arizona Press, Tucson.
- Lyman, R. Lee, Michael J. O'Brien and Robert C. Dunnell
1997 *The Rise and Fall of Culture History*. Springer US, Boston, MA.
- Magnani, Matteo
2017 Package 'multinet' Version 1.0. CRAN Repository.
- Maschner, Herbert D. G. and Katherine L. Reedy-Maschner
1998 Raid, Retreat, Defend (Repeat): The Archaeology and Ethnohistory of Warfare on the North Pacific Rim. *Journal of Anthropological Archaeology* 17:19-51.
- McElreath, Richard, Robert Boyd and Peter J. Richerson
1993 Shared Norms and the Evolution of Ethnic Markers. *Current Anthropology* 44(1):122-130.
- McKern, Will C.
1939 The Midwest Taxonomic Method as an aid to archaeological culture study. *American Antiquity* 3:138-143.
- McPherson, Miller, Lynn Smith-Lovin and James M Cook
2001 Birds of a Feather: Homophily in Social Networks. *Annual Review of Sociology* 27:415-444.

Mills, Barbara J.

1999 The reorganization of Silver Creek communities from the 11th to the 14th centuries. In *Living on the Edge of the Rim, Excavations and Analysis of the Silver Creek Archaeological Research Project 1993-1998*, edited by B. J. Mills, S. A. Herr and S. Van Keuren, pp. 505-512. Arizona State Museum Archaeological Series 192, University of Arizona, Tuscon.

2011 Themes and Models for Understanding Migration in the Southwest. In *Movement, Connectivity, and Landscape Change in the Ancient Southwest*, edited by M. C. Nelson and C. Strawhacker, pp. 345-362. University of Colorado Press, Boulder.

Mills, Barbara J., Jeffery J. Clark and Matthew A. Peeples

2016 Migration, skill, and the transformation of social networks in the pre-Hispanic Southwest. *Economic Anthropology* 3(2):203-215.

Mills, Barbara J., Jeffery J. Clark, Matthew A. Peeples, W. Randall Haas Jr., John M. Roberts Jr. and J. Brett Hill

2013 Transformation of social networks in the late pre-Hispanic US Southwest. *Proceedings of the National Academy of Sciences of the United States of America* 110(15):5785-5790.

Mills, Barbara J., Matthew A. Peeples, W. Randall Haas Jr., Lewis Borck, Jeffery J. Clark and John M. Roberts Jr.

2015 Multiscalar Perspectives on Social Networks in the Late Prehispanic Southwest. *American Antiquity* 80(01):3-24.

Mills, Barbara J., John M. Roberts Jr., Jeffery J. Clark, W. Randall Haas Jr., Deborah L. Huntley, Matthew A. Peeples, Lewis Borck, Susan C. Ryan, Meaghan Trowbridge and Ronald L. Breiger

2013 The Dynamics of Social Networks in the Late Prehispanic US Southwest. In *Network Analysis in Archaeology: New Approaches to Regional Interaction*, edited by C. Knappett, pp. 185-206. Oxford University Press.

Milner, Claire McHale and Miriam T. Stark

1999 The Archaeology of Social Boundaries. *American Antiquity* 64(3):548-548.

Milner, George R.

1986 Mississippian Period Population Density in a Segment of the Central Mississippi River Valley. *American Antiquity* 51(2):227-238.

1990 The Late Prehistoric Cahokia Cultural System of the Mississippi River valley: Foundations, Forescence, and Fragmentation. *Journal of World Prehistory* 4(1):1-43.

1999 Warfare in Prehistoric and Early Historic Eastern North America. *Journal of Archaeological Research* 7(2):105-151.

Milner, George R., Eve Anderson and Virginia G. Smith

- 1991 Warfare in Late Prehistoric West-Central Illinois. *American Antiquity* 56(4):581-603.
- Mische, Ann
2011 Relational Sociology, Culture, and Agency. In *The SAGE Handbook of Social Network Analysis*, edited by J. P. Scott and P. Carrington, pp. 80-98. SAGE Publications, London.
- Mizoguchi, Koji
2009 Nodes and edges : A network approach to hierarchisation and state formation in Japan. *Journal of Anthropological Archaeology* 28(1):14-26.
- Moerman, Michael
1965 Ethnic Identification in a Complex Civilization: Who Are the Lue? *American Anthropologist* 67:1215-1230.
- Moore, D.M. and R.C. Reynolds
1997 *X-Ray Diffraction and the Identification and Analysis of Clay Minerals*. Oxford University Press, Oxford.
- Mucha, Peter J., Thomas Richardson, Kevin Macon, Mason A. Porter and Jukka-Pekka Onnela
2010 Community Structure in Time-Dependent, Multiscale and Multiplex Networks. *Science* 328:876-879.
- Munson, Jessica L. and Martha J. Macri
2009 Sociopolitical network interactions: A case study of the Classic Maya. *Journal of Anthropological Archaeology* 28(4):424-438.
- Neff, Hector
1993 Theory, Sampling, and Analytical Techniques in the Archaeological Study of Prehistoric Ceramics. *American Antiquity* 58(1):23-44.

1994 RQ-Mode Principal Components Analysis of Ceramic Compositional Data. *Archaeometry* 36(July 1993):115-130.

2002 Quantitative Techniques for Analyzing Ceramic Compositional Data. In *Ceramic Production and Circulation in the Greater Southwest: Source Determination by INAA and Complementary Mineralogical Investigations*, edited by D. M. Glowacki and H. Neff, pp. 15-36. Cotsen Institute of Archaeology Monograph 44, Los Angeles.

2003 Analysis of Mesoamerican plumbate pottery surfaces by laser ablation-inductively coupled plasma-mass spectrometry (LA-ICP-MS). *Journal of Archaeological Science* 30:21-35.

- 2008 Review of Ceramic Compositional Studies from In and Around the Mississippi Valley. In *Time's River: Archaeological Syntheses from the Lower Mississippi Valley*, pp. 223-242.
- 2012 Comment: Chemical and mineralogical approaches to ceramic provenance determination. *Archaeometry* 54(2):244-249.
- Neff, Hector, Ronald L. Bishop and E. Sayre
 1989 More observations on the problem of tempering in compositional studies of archaeological ceramics. *Journal of Archaeological Science* 16(1):57-69.
- Neff, Hector, James W. Cogswell and Michael Ross
 2003 Supplementing Bulk Chemistry in Archaeological Provenance Investigations. In *Patterns and Process: A Festschrift in honor of Dr. Edward V. Sayre*, pp. 200-224, L. van Zelst, general editor. Smithsonian Center for Materials Research and Education, Suitland.
- Nelson, Margaret C., Michelle Hegmon, Stephanie R. Kulow, Matthew A. Peeples, Keith Kintigh and Ann P. Kinzig
 2011 Resisting Diversity: a Long-Term Archaeological Study. *Ecology and Society* 16(1):<http://www.ecologyandsociety.org/vol16/iss11/art25/>.
- Neupert, Mark A.
 2000 Clays of Contention: An Ethnoarchaeological Study of Factionalism and Clay Composition. *Journal of Archaeological Method and Theory* 7(3):249-272.
- Newman, M. and M. Girvan
 2004 Finding and evaluating community structure in networks. *Physical Review E - Statistical, Nonlinear, and Soft Matter Physics* 69(026113).
- Nexon, Daniel H.
 2004 Sovereignty, Religion, and the Fate of Empires in Early Modern Europe. Unpublished Ph.D. Dissertation, Columbia University.
- 2009 *The Struggle for Power in Early Modern Europe: Religious Conflict, Dynastic Empires, and International Change*. Princeton University Press, Princeton, NJ.
- Niziolek, Lisa C.
 2013 Earthenware production and distribution in the prehispanic Philippine polity of Tanjay: results from laser ablation-inductively coupled plasma-mass spectrometry (LA-ICP-MS). *Journal of Archaeological Science* 40:2824-2839.
- Nolan, David J. and Lawrence A. Conrad
 1993 Oneota Occupations Along the Mississippi Valley in West Central Illinois. *Proceedings of the Midwest Archaeological Conference*. Milwaukee, WI.

- O'Gorman, Jodie A.
 1996 Domestic Economics and Mortuary Practices: A Gendered View of Oneota Social Organization. Unpublished Ph.D. Dissertation, University of Wisconsin, Milwaukee.
- 2010 Exploring the Longhouse and Community in Tribal Society. *American Antiquity* 75(3):571-597.
- O'Gorman, Jodie A. and Michael D. Conner
 2016 Variability in Ritual at the Intersection of Oneota and Mississippian Worlds. *Proceedings of the 60th Annual Midwest Archaeological Conference*. Iowa City, Iowa.
- Odess, Daniel
 1998 The Archaeology of Interaction: Views from Artifact Style and Material Exchange in Dorest Society. *American Antiquity* 63(3):417-425.
- Oemig, Alexandria M.
 2016 Troubled times in late prehistoric Wisconsin: Violent skeletal trauma among the Winnebago phase Oneota. *American Journal of Physical Anthropology* 159:244-244.
- Opsahl, Tore, Filip Agneessens and John Skvoretz
 2010 Node centrality in weighted networks: Generalizing degree and shortest paths. *Social Networks* 32(3):245-251.
- Orr, Kenneth
 1951 Change at Kincaid: A Study of Cultural Dynamics. In *Kincaid: A Prehistoric Illinois Metropolis*, edited by F.-C. Cole, R. Bell, J. Bennett, J. Caldwell, N. Emerson, R. MacNeish, K. Orr and R. Willis, pp. 293-359. University of Chicago Press, Chicago.
- Östborn, Per and Henrik Gerding
 2014 Network analysis of archaeological data: A systematic approach. *Journal of Archaeological Science* 46(1):75-88.
- Overstreet, David F.
 1997 Oneota Prehistory and History. *The Wisconsin Archaeologist* 78(1-2):250-296.
- Padgett, John F. and Christopher K. Ansell
 1993 Robust Action and the Rise of the Medici, 1400-1434. *American Journal of Sociology* 98(6):1259-1319.
- Painter, Jeffrey M.
 2014 Sharing More than Spaces: Oneota and Mississippian Social and Cultural Interaction at the Crable Site, Fulton Co., Illinois. Unpublished M.S. thesis, Illinois State University.
- Parkinson, William A.

- 2006 Tribal Boundaries: Stylistic Variability and Social Boundary Maintenance during the Transition to the Copper Age on the Great Hungarian Plain. *Journal of Anthropological Archaeology* 25(1):33-58.
- Pauketat, Timothy R.
 1989 Monitoring Mississippian Homestead Occupation Span and Economy Using Ceramic Refuse. *American Antiquity* 54(2):288-310.
- 1994 *The Ascent of Chiefs: Cahokia and Mississippian Politics in North America*. University of Alabama Press, Tuscaloosa, AL.
- 2003 Resettled Farmers and the Making of a Mississippian Polity. *American Antiquity* 68(1):39-66.
- Pauketat, Timothy R., Robert F. Boszhardt and Danielle M. Benden
 2015 Trempealeau Entanglements: An Ancient Colony's Causes and Effects. *American Antiquity* 80(2):260-289.
- Pauketat, Timothy R. and Thomas E. Emerson
 1991 The Ideology of Authority and the Power of the Pot. *American Anthropologist* 93(4):919-941.
- 1997 *Cahokia: Domination and Ideology in the Mississippian World*. University of Nebraska, Lincoln.
- 1999 Representations of Hegemony as Community at Cahokia. In *Material Symbols: Culture and Economy in Prehistory*, edited by J. E. Robb. Southern Illinois University Center for Archaeological Investigations Occasional Paper No. 26, Carbondale, IL.
- Peacock, Evan, Hector Neff, Janet Rafferty and Thomas Meaker
 2007 Using Laser Ablation-Inductively Coupled Plasma-Mass Spectrometry in Shell Tempered Pottery: A Pilot Study from North Mississippi. *Southeastern Archaeology* 26(2):319-329.
- Pearce, Eiluned and Theodora Moutsiou
 2014 Using obsidian transfer distances to explore social network maintenance in late Pleistocene hunter-gatherers. *Journal of Anthropological Archaeology* 36(1):12-20.
- Peoples, Matthew A.
 2011 Identity and Social Transformation in the Prehispanic Cibola World: A.D. 1150-1325. Unpublished Ph.D. Dissertation, Arizona State University.
- 2018 *Connected Communities: Networks, Identity, and Social Change in the Ancient Cibola World*. The University of Arizona Press, Tucson, AZ.
- Peoples, Matthew A. and W. Randall Haas Jr.

- 2013 Brokerage and Social Capital in the Prehispanic U.S. Southwest. *American Anthropologist* 115(2):232-247.
- Peebles, Matthew A., Barbara J. Mills, W. Randall Haas Jr., Jeffrey J. Clark and John M. Roberts Jr.
 2016 Analytical Challenges for the Application of Social Network Analysis in Archaeology. In *The Connected Past: Challenging Networks in Archaeology and History*, edited by T. Brughmans, A. Collar and F. Coward, pp. 59-84. Oxford University Press, Oxford.
- Peebles, Matthew A. and John M. Roberts Jr.
 2013 To binarize or not to binarize: Relational data and the construction of archaeological networks. *Journal of Archaeological Science* 40(7):3001-3010.
- Phillips, S. Colby and Erik W. Gjesfjeld
 2013 Evaluating Adaptive Network Strategies with Geochemical Sourcing Data: A Case Study from the Kuril Islands. In *Network Analysis in Archaeology: New Approaches to Regional Interaction*, edited by C. Knappett, pp. 583-605. Oxford University Press, Oxford.
- Pollack, David, A. Gwynn Henderson and Christopher T. Begley
 2002 Fort Ancient/Mississippian Interaction on the Northeastern Periphery. *Southeastern Archaeology* 21(2):206-220.
- Preiser-Kapeller, Johannes
 2011 Networks of Border Zones: Multiplex Relations of Power, Religion and Economy in South-Eastern Europe, 1250-1453 AD. *Proceeding of the 39th Conference on Computer Applications and Quantitative Methods in Archaeology. Beijing, 12-16 April 2011*:381-393.
- Pugh, Daniel C.
 2010 The Swantek Site: Late Prehistoric Oneota Expansion and Ethnogenesis. Unpublished Ph.D. Dissertation, University of Michigan.
- Reimer, P. J., Edouard Bard, A. Bayliss, J. W. Beck, P. G. Blackwell, M. Bronk, P. M. Grootes, T. P. Guilderson, H. Haflidason, Hajdas, C. Hatte, T. J. Heaton, D. L. Hoffman, A. G. Hogg, K. A. Hughhen, J. F. Kaiser, B. Kromer, S. W. Manning, M. Niu, R. W. Reimer, D. A. Richards, E. M. Scott, J. R. Southon, R. A. Staff, C. S. M. Turney and J. van der Plicht
 2013 IntCal 13 and Marine 13 radiocarbon age calibration curves 0–50,000 years cal BP. *Radiocarbon* 55:1869-1887.
- Renfrew, Colin
 1984 Trade as Action at a Distance. In *Approaches to Social Archaeology*. Harvard University Press, Cambridge, MA.

- 1994 The Archaeology of Identity. *The Tanner Lectures on Human Values vol 15* 15:283-348.
- Rice, Prudence M.
 1998 Contexts of Contact and Change: Peripheries, Frontiers, and Boundaries. In *Studies in Culture Contact: Interaction, Culture Change, and Archaeology*, edited by J. G. Cusick, pp. 44-66. Center for Archaeological Investigations, Southern Illinois University, Carbondale.
- 2005 *Pottery Analysis: A Sourcebook*. The University of Chicago Press, Chicago.
- Robinson, W. S.
 1951 A Method for Chronologically Ordering Archaeological Deposits. *American Antiquity* 16:293-301.
- Rockman, Mary
 2003 Knowledge and learning in the archaeology of Colonization. In *Colonization of Unfamiliar Landscapes: The Archaeology of Adaptation*, edited by M. Rockman and J. Steele, pp. 3-24. Routledge, New York.
- Rowe, Sarah M.
 2016 Ceramic variation and negotiated communities in the Late Valdivia phase of coastal Ecuador. *Journal of Anthropological Archaeology* 43:69-82.
- Rumbaut, R. G.
 2015 Assimilation of Immigrants. In *International Encyclopedia of the Social & Behavioral Sciences*, edited by J. D. Wright, pp. 81-87. vol. 2. Elsevier, Oxford.
- Sampson, C. Garth
 1988 *Stylistic Boundaries Between Mobile Hunter-Foragers*. Smithsonian Institution Press, Washington D.C.
- Sampson, Kelvin
 2000 *The Crable Site: Reassembling a Shattered Past*. Manuscript on File, Dickson Mounds Museum.
- Santoro, M.
 2008 Framing Notes. An Introduction to "Catnets". *Sociologica* (1):1-23.
- Santure, Sharon K., Alan D. Harn and Duane Esarey
 1990 *Archaeological Investigations at the Morton Village and Norris Farms 36 Cemetery*. Illinois State Museum Reports of Investigations No. 45, Springfield, IL.
- Saxe, Arthur A.
 1970 Social Dimensions of Mortuary Practices. Unpublished Ph.D. dissertation, University of Michigan.

- Sayre, E., R. W. Dodson and D. Burr Thompson
1957 Neutron Activation Study of Mediterranean Potsherds. *American Journal of Archaeology* 61(1):35-41.
- Scarry, John F.
1999 Elite Identities in the Apalachee Province: The Construction of Identity and Cultural Change in a Mississippian Polity. In *Material Symbols: Culture and Economy in Prehistory*, edited by J. E. Robb, pp. 342-361. Occasional ed. Center for Archaeological Investigations, Southern Illinois University, Carbondale.
- Schneider, Seth A.
2015 Oneota Ceramic Production and Exchange: Social, Economic, and Political Interactions In Eastern Wisconsin Between A.D. 1050 - 1400. Unpublished Ph.D. Dissertation, University of Wisconsin-Milwaukee.
- Scholnick, Jonathan B., Jessica L. Munson and Martha J. Macri
2013 Positioning Power in a Multi-relational Framework. In *Network Analysis in Archaeology: New Approaches to Regional Interaction*, pp. 95-124.
- Schortman, Edward M. and Patricia A. Urban
1992 Current Trends in Interaction Research. In *Resources, Power, and Interregional Interaction*, edited by E. M. Schortman and P. A. Urban, pp. 235-255. Plenum Press, New York.
- Schortman, Edward M., Patricia A. Urban and Marne Ausec
2001 Politics with Style: Identity Formation in Prehispanic Southeastern Mesoamerica. *American Anthropologist* 103(2):312-330.
- Schroeder, Sissel
2004 Current Research on Late Precontact Societies of the Midcontinental United States. *Journal of Archaeological Research* 12(4):311-372.
- Schwartz, Saul and William B. Green
2013 Middle Ground or Native Ground? Material Culture at Iowaville. *Ethnohistory* 60(4):537-565.
- Scott, John
2000 *Social network analysis*. Sage, London.
- Scott, John and Peter J. Carrington (editors)
2016 *The SAGE Handbook of Social Network Analysis*. SAGE Publications Ltd, London.
- Sharratt, Nicola, Mark L. Golitko, P. Ryan Williams and Laure Dussubieux

- 2009 Ceramic production during the middle horizon: Wari and Tiwanaku clay procurement in the Moquegua Valley, Peru. *Geoarchaeology* 24(6):792-820.
- Sharratt, Nicola, Mark L. Golitko and P. Ryan Williams
2015 Pottery production , regional exchange , and state collapse during the Middle Horizon Tiwanaku pottery in the Moquegua Valley , Peru:397-412.
- Shaw, Ben, Mathieu Leclerc, William Dickinson, Matthew Spriggs and Glenn R. Summerhayes
2016 Identifying prehistoric trade networks in the Massim region, Papua New Guinea: Evidence from petrographic and chemical compositional pottery analyses from Rossel and Nimowa Islands in the Louisiade Archipelago. *Journal of Archaeological Science: Reports* 6:518-535.
- Shennan, Stephen J.
1989 Introduction: Archaeological Approaches to Cultural Identity. In *Archaeological Approaches to Cultural Identity*, pp. 1-32. Unwin-Hyman, London.

1997 *Quantifying Archaeology*. Edinburgh University Press, Edinburgh.
- Simpson, Edward H.
1951 The Interpretation of Interaction in Contingency Tables. *Journal of the Royal Statistical Society Series B*(13):238-241.
- Sindbæk, Søren
2013 Broken links and black boxes: material affiliations and contextual network synthesis in the Viking world. In *Network Analysis in Archaeology: New Approaches to Regional interaction*, edited by C. Knappett, pp. 71-94. Oxford University Press, Oxford.
- Skibo, James M. and Michael B. Schiffer
1995 The Clay Cooking Pot: An Exploration of Women's Technology. In *Expanding Archaeology*, edited by J. M. Skibo, W. H. Walker and A. E. Nielsen. University of Utah Press, Salt Lake City.
- Skibo, James M., Michael B. Schiffer and Nancy Kowalski
1989 Ceramic style analysis in archaeology and ethnoarchaeology: Bridging the analytical gap. *Journal of Anthropological Archaeology* 8(4):388-409.
- Smith, Bruce D. (editor) 1978 *Mississippian Settlement Patterns*. Academic Press, Inc., New York.

1995 The Analysis of Single-Household Mississippian Settlements. In *Mississippian Communities and Households*, edited by J. D. Rogers and B. D. Smith, pp. 224-250. University of Alabama Press, Tuscaloosa, AL.
- Smith, Hale G.

- 1951 *The Crable Site, Fulton County, Illinois*. Anthropological Papers No. 7. University of Michigan Museum of Anthropology Ann Arbor, MI.
- Smith, Kevin E., Daniel Brock and Christopher Hogan
2004 Interior Incised Plates and Bowls from the Nashville Basin of Tennessee. *Tennessee Archaeology* 1(1):49-57.
- Snead, James E. and Robert W. Preucel
1999 The Ideology of Settlement : Ancestral Keres Landscapes in the Northern Rio Grande. *Archaeologies of landscape*:169-197.
- Speakman, Robert J., Michael D. Glascock and Vincas P. Steponaitis
2008 Geochemistry. In *Woodland Pottery Sourcing in the Carolina Sandhills*, edited by J. M. Herbert and T. E. McReynolds, pp. 56-72. Report No. 29 Research Laboratories of Archaeology, The University of North Carolina at Chapel Hill.
- Speakman, Robert J., Michael D. Glascock, Robert H. Tykot, Christophe Descantes, Jennifer J. Thatcher, Craig E. Skinner and K. M. Lienhop
2007 Selected applications of laser ablation ICP-MS to archaeological research. *Archaeological Chemistry: Analytical Techniques and Archaeological Interpretation* (October):275-296.
- Spencer, C.
1993 Human agency, biased transmission, and the cultural evolution of chiefly authority. *Journal of Anthropological Archaeology* 12:41-74.
- Spier, Leslie
1921 *The sun dance of the Plains Indians: Its development and diffusion* 16. Anthropological Papers of the American Museum of Natural History.
- Stark Miriam, T., Ronald L. Bishop and Elizabeth Miksa
2000 Ceramic Technology and Social Boundaries: Cultural Practices in Kalinga Clay Selection and Use. *Journal of Archaeological Method and Theory* 7(4):295-331.
- Stark, Miriam T., Jeffrey J. Clark and Mark D. Elson
1995 Social Boundaries and Cultural Identity in the Tonto Basin. In *The Roosevelt Community Development Study: New Perspectives on Tonto Basin Prehistory*, pp. 343-368.

1998 Social Boundaries and Technical Choices in Tonto Basin Prehistory. In *The Archaeology of Social Boundaries*, edited by M. T. Stark, pp. 208-231. Smithsonian Institution Press, Washington D.C.
- Steadman, Dawnie Wolfe
1998 The Population Shuffle in the central Illinois Valley: a diachronic model of Mississippian biocultural interactions. *World Archaeology* 30(2):306-326.

- 2001 Mississippians in motion? A population genetic analysis of interregional gene flow in west-central Illinois. *American Journal of Physical Anthropology* 114(1):61-73.
- 2008 Warfare related trauma at Orendorf, a middle Mississippian site in west-central Illinois. *American Journal of Physical Anthropology* 136(1):51-64.
- Steponaitis, Vincas P.
- 1983 *Ceramics, Chronology, and Community Patterns: an Archaeological Study of Moundville*. Academic Press, New York.
- 1984 Technological Studies of prehistoric pottery from Alabama: physical properties and vessel function. In *The Many Dimensions of Pottery*, edited by S. E. van der Leeuw and A. C. Pritchard, pp. 79-127. University of Amsterdam, Amsterdam.
- Stokke, Hugo and Marit Tjomsland
- 1996 *Collective Identities and Social Movements*. Chr. Michelsen Institut, Bergen, Norway.
- Stoltman, James B.
- 1991 Ceramic petrography as a technique for documenting cultural interaction: An example from the upper Mississippi Valley. *American Antiquity* 56(1):103-120.
- 2000 A Reconsideration of the Cultural Processes Linking Cahokia to its Northern Hinterlands during the period A.D. 1000–1200. In *Mounds, Modoc and Mesoamerica: Papers in Honor of Melvin L. Fowler*, edited by S. A. Ahler, pp. 439-454. Scientific ed. Illinois State Museum, Springfield, IL.
- Stoltman, James B., Joyce Marcus, Kent V. Flannery, James H. Burton and Robert G. Moyle
- 2005 Petrographic evidence shows that pottery exchange between the Olmec and their neighbors was two-way. *Proceedings of the National Academy of Sciences* 102(32):11213-11218.
- Stone, Tammy
- 2003 Social Identity and Ethnic Interaction in the Western Pueblos of the American Southwest. *Journal of Archaeological Method and Theory* 10(1):31-67.
- Stoner, Wesley D. and Michael D. Glascock
- 2012 The forest or the trees? Behavioral and methodological considerations for geochemical characterization of heavily-tempered ceramic pastes using NAA and LA-ICP-MS. *Journal of Archaeological Science* 39(8):2668-2683.
- Stoner, Wesley D., Christopher A. Pool, Hector Neff and Michael D. Glascock
- 2008 Exchange of coarse orange pottery in the middle classic Tuxtla Mountains, Southern Veracruz, Mexico. *Journal of Archaeological Science* 35(14):12-1426.

- Strezewski, Michael
2003 Mississippian Mortuary Practices in the Central Illinois River Valley: A Region-Wide Survey and Analysis. Unpublished Ph.D. Dissertation, Indiana University.
- Sullivan, Lynne P. and Michaelyn S. Harle
2009 Mortuary Practices and Cultural Identity at the Turn of the Sixteenth Century in Eastern Tennessee..pdf. In *Mississippian Mortuary Practices: Beyond Hierarchy and the Representationist Perspective*, edited by L. P. Sullivan and R. C. Mainfort, pp. 234-249. University Press of Florida.
- Swanton, John R.
1928 Sun Worship in the Southwest. *American Anthropologist* 30:206-213.
- Swartz, B. K., Jr.
1996 The McKern "Taxonomic" System and Archaeological Cultural Classification in the Midwestern United States: A History and Evaluation. *Bulletin of the History of Archaeology* 6(1):3-9.
- Szell, Michael, Renaud Lambiotte and Stefan Thurner
2010 Multirelational organization of large-scale social networks in an online world. *Proceedings of the National Academy of Sciences of the United States of America* 107(31):13636-13641.
- Terrell, John Edward
2013 Social Network Analysis and the Practice of History. In *Network Analysis in Archaeology*, pp. 16-41. Oxford University Press.
- Theler, James L. and Robert F. Boszhardt
2006 Collapse of crucial resources and culture change: A model for the woodland to Oneota transformation in the Upper Midwest. *American Antiquity* 71(3):433-472.
- Thwaites, Reuben Gold (editor) 1897 *The Jesuit relations and allied documents travels and explorations of the Jesuit missionaries in New France, 1610-1791 : the original French, Latin, and Italian texts, with English translations and notes*. Burrows, Cleveland.
- Tilly, Charles
1978 *From Mobilization to Revolution*. Addison-Wesley, Reading, MA.

1998a *Durable inequality*. University of California Press, Berkeley, CA.

1998b Social movements and (all sorts of) other political interactions ^ local , national , and international ^ including identities Several divagations from a common path , beginning with British struggles over Catholic Emancipation , 1780 ^ 1829 , and endin. *Theory and Society* 27(4):453-480.

- 2001a Historical analysis of political processes. *Handbook of sociological theory* (November):567-588.
- 2001b Relational origins of inequality. *Anthropological Theory* 1(3):355-372.
- 2002 *Stories, Identities, and Political Change*. Rowman and Littlefield, Lanham, MD.
- 2004 Social Boundary Mechanisms. *Philosophy of the Social Sciences* 34(2):211-236.
- Tite, M. S., V. Kilikoglou and G. Vekinis
 2001 Strength, Toughness and Thermal Shock Resistance of Ancient Ceramics, and Their Influence on Technological Choice. *Archaeometry* 43(3):301-324.
- Trigger, Bruce G.
 2006 *A History of Archaeological Thought*. Cambridge University Press, Cambridge.
- Trubowitz, Neal L.
 1992 Native Americans and French on the Central Wabash. In *Calumet and Fleu-de-Lys: Archaeology of Indian and French Contact in the Midcontinent*, edited by J. Walthall and T. E. Emerson, pp. 241-264. Smithsonian Institution, Washington D.C.
- Tubbs, Ryan M.
 2013 Ethnic Identity and Diet in the Central Illinois River Valley. Unpublished Ph.D. Dissertation, Michigan State University.
- Tubbs, Ryan M. and Jodie A. O'Gorman
 2005 Assessing Oneota Diet And Health: A Community And Lifeway Perspective. *Midcontinental Journal of Archaeology* 30(1):119-163.
- Upton, Andrew J.
 2016 Function or Style? Cultural Transmission and Artifact Variation in Late Prehistoric West-Central Illinois. *Proceedings of the 60th Annual Midwest Archaeological Conference*. Iowa City, Iowa.
- Upton, Andrew J., William A. Lovis and Gerald R. Urquhart
 2015 An empirical test of shell tempering as an alkaline agent in the nixtamalization process. *Journal of Archaeological Science* 62:39-44.
- Upton, Dell
 1996 Ethnicity, Authenticity, and Invented Traditions. *Historical Archaeology* 30(2):1-7.
- Vacca, Raffaele, Giacomo Solano, Miranda Jessica Lubbers, José Luis Molina and Christopher McCarty
 2018 A personal network approach to the study of immigrant structural assimilation and transnationalism. *Social Networks* 53:72-89.

- Vanderwarker, Amber M. and Gregory D. Wilson
 2016 War, Food, and Structural Violence in the Mississippian Central Illinois Valley. In *The Archaeology of Food and Warfare*, edited by A. M. Vanderwarker and G. D. Wilson, pp. 75-105. Springer.
- Vanderwarker, Amber M., Gregory D. Wilson and Dana N. Bardolph
 2013 Maize Adoption and Intensification in the Central Illinois River Valley : an Analysis of Archaeobotanical Data From the Late Woodland to Early Mississippian Periods (A.D. 600-1200). *Southeastern Archaeology* 32(2):147-168.
- VanPool, Christine S.
 2008 Agents and Cultural Transmission. In *Cultural Transmission and Archaeology: Issues and Case Studies*, edited by M. J. O'Brien, pp. 190-200. The Society for American Archaeology, Washington D.C.
- Vaughn, K. J. , Laure Dussubieux and P. Ryan Williams
 2011 A Pilot Compositional Analysis of Nasca Ceramics from the Kroeber Collection. *Journal of Archaeological Science* 31(11):1577-1586.
- Veit, Ulrich
 1989 Ethnic Concepts in Prehistory: A Case Study on the Relationship between Cultural Identity and Archaeological Objectivity. In *Archaeological Approaches to Cultural Identity*, edited by S. J. Shennan, pp. 35-56. Unwin-Hyman, London.
- Velde, B. and J. C. Druc
 1999 *Archaeological Ceramic Materials: Origin and Utilization*. Springer, Berlin.
- Vogel, Joseph O.
 1975 Trends in Cahokia Ceramics: Preliminary Study of the Collections from Tracts 15A & 15B. In *Perspectives in Cahokia Archaeology*, edited by J. A. Brown, pp. 32-125. Illinois Archaeological Survey Bulletin, No. 10, Urbana.
- Walker, James R.
 1982 *Lakota Society*. University of Nebraska Press, Lincoln, NE.
- Wallis, Neill J.
 2009 Locating the Gift: Swift Creek Exchange on the Atlantic Coast (A.D. 200-800).
- Wallis, Neill J., Matthew T. Boulanger, Jeffrey R. Ferguson and Michael D. Glascock
 2010 Woodland period ceramic provenance and the exchange of Swift Creek Complicated Stamped vessels in the southeastern United States. *Journal of Archaeological Science* 37(10):2598-2611.
- Wallis, Neill J. and G. D. Kamenov

- 2013 Challenges in the analysis of heterogeneous pottery by LA-ICP-MS: A comparison with INAA. *Archaeometry* 55(5):893-909.
- Wallis, Neill J., Thomas J. Pluckhahn and Michael D. Glascock
2016 Sourcing Interaction Networks of the American Southeast: Neutron Activation Analysis of Swift Creek Complicated Stamped Pottery. *American Antiquity* 81(4):717-736.
- Wanless, Harold R.
1957 *Geology and mineral resources of the Beardstown, Glasford, Havana, and Vermont Quadrangles*. Illinois State Geologic Survey Bulletin 82, Urbana.
- Wasserman, Stanley and Katherine Faust
1994 *Social Network Analysis: Methods and Applications*. Cambridge University Press, New York.
- Wasserman, Stanley and J. Galaskiewicz (editors)
1994 *Advances in Social Network Analysis: Research in the Social and Behavioral Sciences*. Sage, London.
- Watts, Duncan J. and Steven H. Strogatz
1998 Collective dynamics of 'small-world' networks. *Nature* 393(6684):440-442.
- Weidele, Daniel, Mereke van Garderen, Mark L. Golitko and Gary Feinman
2016 On graphical representations of similarity in geo-temporal frequency data. *Journal of Archaeological Science* 72:105-116.
- Weigand, P., G. Harbottle and E. Sayre
1977 Turquoise Sources and Source Analysis: Mesoamerican and the Southwestern U.S.A. In *Exchange Systems in Prehistory*, edited by T. K. Earle and J. E. Ericson, pp. 15-34. Academic Press, Inc., New York.
- Weiss, Harvey and Raymond S. Bradley
2001 What Drives Societal Collapse? *Science* 291(5504):609-610.
- Wellman, Barry
1983 Network Analysis: Some Basic Principles. In *Sociological Theory*, edited by R. Collins. Joessey-Bass Publishers, San Francisco.

1988 Structural Analysis: From Method and Metaphor to Theory and Substance. In *Social Structures a Network Approach*, edited by B. Wellman and S. Berkowitz. Cambridge University Press, Cambridge.
- White, Harrison C.
1973 Everyday Life in Stochastic Networks. *Sociological Inquiry* 43:43-49.

- 1992 *Identity and control; a structural theory of action*. Princeton University Press, Princeton, NJ.
- 1993 Values come in styles, which mate to change. In *The origin of values*, edited by M. Hechter, L. Nadel and R. Michael, pp. 63-91. de Gruyter, New York.
- 2008a *Identity and Control: How Social Formations Emerge*. Princeton University Press, Princeton, NJ.
- 2008b Notes on the constituents of social structure. *Sociologica* 2(1):1-15.
- 2008c Preface:“Catnets” Forty Years Later. *Sociologica* 1:1-4.
- White, Harrison C. and Frederic C. Godart
2007 Stories from Identity and Control. *Sociologica. Italian Journal of Sociology Online* (3):1-17.
- White, Harrison C. and Francois Lorrain
1971 Structural Equivalence of Individuals in Social Networks. *Journal of Mathematical Sociology* 1(49-80).
- Wickham, Hadley and Garret Golemund
2017 *R for Data Science: Import, Tidy, Transform, Visualize, and Model Data*. O’Reilly Media, Inc.
- Wiessner, Polly
1983 Style and Social Information in Kalahari San Projectile Points. *American Antiquity* 48(2):253-276.
- 1984 Reconsidering the behavioral basis for style: A case study among the Kalahari San. *Journal of Anthropological Archaeology* 3(3):190-234.
- 1985 Style or Isochrestic Variation? A Reply to Sackett. *American Archaeology* 50(1):160-166.
- 1990 Is There a Unity to Style? In *The Uses of Style in Archaeology*, edited by M. W. Conkey and C. Hastorf, pp. 105-112. Cambridge University Press, Cambridge.
- Wiggers, Ray
1997 *Geology Underfoot in Illinois*. Mountain Press Publishing.
- Wilson, Gregory D.
2012 Living with War: the Impact of Chronic Violence in the Mississippian-Period Central Illinois River Valley. In *The Oxford Handbook of North American Archaeology*, edited by T. R. Pauketat, pp. 523-533. Oxford University Press.

- 2013 Incinerated Villages in the North. In *The Medieval Mississippians*, edited by T. R. Pauketat and S. M. Alt. School for Advanced Research Press, Santa Fe, NM.
- Wilson, Gregory D., Mallory A. Melton and Amber M. Vanderwarker
2018 Reassessing the chronology of the Mississippian Central Illinois River Valley using Bayesian analysis. *Southeastern Archaeology* 37(1):22-38.
- Wilson, Jeremy J.
2010 Modeling Life Through Death in Late Prehistoric West-Central Illinois: An Assessment of Paleodemographic and Paleoepidemiological Variability. Unpublished Ph.D. Dissertation, SUNY Binghamton.
- Wobst, Martin
1977 Stylistic Behavior and Information Exchange. In *For the Director: Research Essays in Honor of James B. Griffin*, pp. 317-339.
- Wolf, Eric R.
1982 *Europe and the People Without History*. University of California Press, Los Angeles.
- Wolfe, Eric R.
1982 *Europe and the people without history*. University of California Press, Berkeley.
- Zvelebil, Marek
2006 Mobility, contact, and exchange in the Baltic Sea basin 6000–2000 BC. *Journal of Anthropological Archaeology* 25(2):178-192.